PALYNOSTRATIGRAPHIC AND PALYNOFACIES INVESTIGATIONS OF THE MIOCENE UNITS IN THE ADANA BASIN (EASTERN MEDITERRANEAN, TURKEY)

A THESIS SUBMITTED TO
THE GRADUATE SCHOOL OF NATURAL AND APPLIED SCIENCES
OF
MIDDLE EAST TECHNICAL UNIVERSITY

BY

AKSEL TUĞBA TÜRKECAN

IN PARTIAL FULFILLMENT OF THE REQUIREMENTS
FOR
THE DEGREE OF DOCTOR OF PHILOSOPHY
IN
GEOLOGICAL ENGINEERING

JUNE 2017

Approval of the thesis:

PALYNOSTRATIGRAPHIC AND PALYNOFACIES INVESTIGATIONS OF THE NEOGENE UNITS IN THE ADANA BASIN (EASTERN MEDITERRANEAN, TURKEY)

submitted by **Aksel Tuğba Türkecan** in partial fulfillment of the requirements for the degree of **Doctor of Philosophy in Geological Engineering Department, Middle East Technical University** by,

Prof. Dr. Canan ÖZGEN
Dean, Graduate School of **Natural and Applied Sciences** _____

Prof. Dr. Erdin BOZKURT
Head of Department, **Geological Engineering** _____

Prof. Dr. Demir ALTINER
Supervisor, **Geological Engineering Dept., METU** _____

Dr. Dirk MUNSTERMAN
Co-Supervisor, **TNO, Holland** _____

Examining Committee Members:

Prof. Dr. F. Bora ROJAY
Geological Engineering Dept., METU _____

Prof. Dr. Demir ALTINER
Geological Engineering Dept., METU _____

Prof. Dr. Cemal TUNOĞLU
Geological Engineering Dept., Hacettepe University _____

Prof. Dr. İ.Ömer YILMAZ
Geological Engineering Dept., METU _____

Prof. Dr. Veysel IŞIK
Geological Engineering Dept., Ankara University _____

Date: June 5, 2017

I hereby declare that all information in this document has been obtained and presented in accordance with academic rules and ethical conduct. I also declare that, as required by these rules and conduct, I have fully cited and referenced all material and results that are not original to this work.

Name, Last Name: Aksel Tuğba TÜRKECAN

Signature:

ABSTRACT

PALYNOSTRATIGRAPHIC AND PALYNOFACIES INVESTIGATIONS OF THE MIOCENE UNITS IN THE ADANA BASIN (EASTERN MEDITERRANEAN, TURKEY)

Türkecan, Aksel Tuğba
Ph.D., Department of Geological Engineering
Supervisor: Prof. Dr. Demir Altıner
Co-Supervisor: Drs. Dirk Munsterman

June 2017, 555 pages

The main purpose of this study is to investigate the palynostratigraphy and palynofacies of the Miocene Units in the Adana Basin (Eastern Mediterranean) and to establish a biostratigraphic framework for future studies. This study is a pioneering work in the Adana Basin, regarding the dinoflagellate cyst biostratigraphy.

In this study, seven stratigraphic sections comprising the Köpekli, Cingöz, and Güvenç formations were measured and 482 samples were analyzed based on palynomorphs. According to the first and last occurrences and the acme of some selected taxa, nine biozones were identified from the late Burdigalian to earliest Tortonian. In order to apply a worldwide biostratigraphic correlation based on dinoflagellates, the biozones defined in this study have been compared with previously published dinocyst zonations in Denmark, Germany, Netherlands, NW Europe and the eastcoast U.S. The palynological analysis reveals that the recorded dinocyst events (e.g. *Labyrinthodinium truncatum, Cerebrocysta poulsenii, Unipontidinium aquaeductus*) occurred chronostratigraphically older in Turkey than those in Denmark, Germany, Netherlands, NW Europe and the eastcoast U.S.

A paleo-environmental model was created for Köpekli, Cingöz and Güvenç formations based on proximal-distal trends of dinoflagallates. Based on the

quantitative distribution patterns of dinocysts, a relative sea level curve is constructed and correlated with the eustatic sea level curve of Haq et al. (1987). The curve plotted for Miocene dinocysts in this study reflects striking similarities to the general trend of the eustatic sea level curve of Haq et al. (1987).

Keywords: Adana, Miocene, palynology, dinoflagellate, Mediterranean

ÖZ

ADANA BASENİ MİYOSEN BİRİMLERİNİN PALİNOSTRATİGRAFİ VE PALİNOFASİYES ÖZELLİKLERİ (DOĞU AKDENİZ, TÜRKİYE)

Türkecan, Aksel Tuğba
Doktora, Jeoloji Mühendisliği Bölümü
Tez Yöneticisi: Prof. Dr. Demir Altıner
Ortak Tez Yöneticisi: Dr. Dirk Munsterman

Haziran 2017, 555 sayfa

Bu çalışmanın esas amacı, Adana Baseni'nde (Doğu Akdeniz) yer alan Miyosen birimlerin palinostratigrafik ve palinofasiyes özelliklerini ortaya koymak ve daha sonraki çalışmalar için bir biyostratigrafik çatı oluşturmaktır. Çalışma Adana Baseni'nde dinoflagellat biyostratigrafisi kapsamında yapılan öncü bir çalışmadır.

Amaca uygun olarak Köpekli, Cingöz ve Güvenç formasyonlarını kapsayan 7 stratigrafik kesit ölçülmüş ve kesitler boyunca toplanan 482 adet örnek palynomorflara dayanılarak analiz edilmiştir. Seçili taksonların ilk ve son ortaya çıkışları ve bollukları göz önüne alınarak geç Burdugaliyen'den en erken Tortoniyen'e kadar 9 adet biyozon ayırtlanmıştır. Dinoflagellatlara dayanılarak evrensel bir biyostratigrafik korelasyon uygulayabilmek için, çalışmada tanımlanan biyozonlar daha önce Danimarka, Almanya, Hollanda, Kuzeybatı Avrupa ve Doğu Amerika sahillerinde yayınlanan dinokist zonları ile karşılaştırılmıştır. Yapılan karşılaştırmalar, çalışmada kaydedilen dinokist olaylarının (örneğin; *Labyrinthodinium truncatum, Cerebrocysta poulsenii, Unipontidinium aquaeductus*) Danimarka, Almanya, Hollanda, Kuzeybatı Avrupa ve Doğu Amerika sahillerinde ortaya konulanlara göre kronostratigrafik olarak daha erken oluştuğunu göstermektedir.

Dinoflagellatların proksimal-distal trendlerine göre, Köpekli, Cingöz ve Güvenç formasyonları için bir paleo-ortamsal model oluşturulmuştur. Dinokistlerin

sayısal dağılımlarına göre göreceli bir deniz seviyesi değişim grafiği oluşturulmuş ve Haq ve diğ. (1987)'nin küresel deniz seviyesi değişim grafiği ile karşılaştırılmıştır. Miyosen dinoflagellatları için bu çalışmada çizilen grafik, Haq ve diğ. (1987)'de yeralan küresel deniz seviyesi değişim grafikleri ile büyük oranda benzerlik göstermektedir.

Anahtar kelimeler: Adana, Miyosen, palinoloji, dinoflagellat, Akdeniz

To my husband…

ACKNOWLEDGEMENTS

This PhD Thesis was supported by Turkish Petroleum Corporation (TPAO) Research Center. I would like to thank for the permission and financial support.

I feel most grateful to my supervisor Prof. Dr. Demir Altıner who always encouraged me at every stage of this study and accomplishment of this thesis. His guidance over 11 years is invaluable for me to fulfill my academic career.

Special thanks to Dirk Munsterman for his contributions; especially for his criticisms on palynology and for his help during my taxonomy studies.

I would like to thank to all the jury members, namely Prof. Dr. Bora Rojay, Prof. Dr. Cemal Tunoğlu, Prof. Dr. Veysel Işık and Prof. Dr. İ. Ömer Yılmaz, who spared valuable time for this study. I am greatly thankful for their comments and criticisms which highly improve this thesis.

I am grateful to Uğraş Işık for her valuable contributions during my field studies and her suggestions and encouragement during the progress of this thesis. Her advice always motivated me. I also thank to Uğraş Işık, Mehtap Pınar, Zeynep Alay and Tuğba Çevik for helping me to correlate my data with their foraminiferal micropaleontology and nannoplankton analyses.

I am most grateful to my co-workers R. Hayrettin Sancay, Berkin Oktay, Tuba Aydın Özbek, Sinem Tanrıkulu and Işıl Akyüz for their suggestions and critisms on palynology during the progress of this thesis.

I would like to thank to technicians Serdar Şahin and Adem Sarı for helping me in the preparation of my samples.

I would like to thank Nihal Akça, Ayşegül Gürgey, Aslı Elmacı, Alev Güray, Seher Ünlü and Aylin Kocatürk for their friendships and endless encouragements during my studies.

I would like to thank my dear friends Meral Bacanak, Arzu Aktosun, Elif Medetoğulları, Yonca Toker, Pınar Kasımoğlu, Ahmet Sönmez, Ulvi Yazıcı and Gökçe Güven for their patience and tolerance during my studies.

I would like to express my eternal thanks to my parents Hamide Dinç, Yaşar Dinç, Nurcan Türkecan and Ahmet Türkecan, my brothers Cem and Özgür, my sister Pınar, my cousins Aylin Akçabayırlı and Serhat Akçabayırlı, my aunt Zeliha Akdemir and my uncle Ali Akdemir for their lifetime support and love.

Finally, I would like to express my deepest gratitude to my husband Onur Türkecan for his presence and great help during the realization of this thesis.

TABLE OF CONTENTS

ABSTRACT v
ÖZ vii
ACKNOWLEDGEMENTS x
TABLE OF CONTENTS xii
LIST OF TABLES xv
LIST OF FIGURES xvi
EXPLANATION OF SYMBOLS xxi
ABBREVIATIONS xxiii

CHAPTERS 1
1. INTRODUCTION 1
1.1. PURPOSE AND SCOPE 1
1.2. GEOGRAPHIC SETTING 3
1.3. METHOD OF STUDY 3
1.3.1. Sample Processing 5
1.4. PREVIOUS WORK 8
1.5. REGIONAL GEOLOGICAL SETTING 14
2. LITHOSTRATIGRAPHY 21
2.1. CENOZOIC FORMATIONS IN THE ADANA BASIN 22
2.1.1. Karsanti Formation 22
2.1.2. Gildirli Formation 23
2.1.3. Kaplankaya Formation 24
2.1.4. Karaisalı Formation 24
2.1.5. Köpekli Formation 25
2.1.6. Cingöz Formation 25
2.1.7. Güvenç Formation 26
2.1.8. Kuzgun Formation 27

2.1.9. Handere Formation 28
2.2. LITHOSTRATIGRAPHY OF THE MEASURED SECTIONS 29
2.2.1. Çukurköy Section 29
2.2.2. Köpekli Section 29
2.2.3. Sofular Section 30
2.2.4. Çorlu Section 30
2.2.5. Koruklu Section 41
2.2.6. Bekirli Section 45
2.2.7. Güvenç Section 45
3. BIOSTRATIGRAPHY 53
3.1. PALYNOMORPH BIOSTRATIGRAPHY 54
3.1.1. Dinocyst Zonation 54
3.2. BIOSTRATIGRAPHY OF THE MEASURED STRATIGRAPHIC SECTIONS 64
3.2.1. Çukurköy Section 64
3.2.2. Köpekli Section 68
3.2.3. Sofular Section 72
3.2.4. Çorlu Section 76
3.2.5. Koruklu Section 88
3.2.6. Bekirli Section 92
3.2.7. Güvenç Section 96
3.3. BIOSTRATIGRAPHIC CORRELATION WITH WELL-KNOWN DINOCYST EVENTS 100
4. TAXONOMY 111
4.1. POLLEN 111
4.2. SPORES 118
4.3. ORGANIC-WALLED GREEN ALGAE 121
4.4. DINOFLAGELLATES 122
4.5. CHITINOUS FORAMINIFERAL LININGS 146
5. PALEOCLIMATE AND PALEOENVIRONMENT 147

5.1. PRODUCTIVITY TRENDS 148
5.2. TEMPERATURE TRENDS 149
5.3. SALINITY TRENDS 151
5.4. PROXIMAL-DISTAL TRENDS 155
5.4.1. The *Spiniferites* group 156
5.4.2. The *Operculodinium* group 157
5.4.3. The *Cleistosphaeridium* group 158
5.4.4. The *Homotryblium* spp. group 158
5.4.5. The *Impagidinium* spp. group 162
5.4.6. Other taxa 162
5.5. RECOGNITION OF SEA-LEVEL FLUCTUATIONS BASED ON PALYNOLOGICAL DATA 165
6. PALYNOFACIES ANALYSIS 187
7. DISCUSSION AND CONCLUSION 203
7.1. DISCUSSION 203
7.2. CONCLUSION 208
REFERENCES 211
APPENDICES 247
A. 1-19. DIGITAL IMAGES OF THE PALYNOMORPHS AND EXPLANATIONS. 247
B. MEASURED SECTIONS IN THE ADANA BASIN 285
C. ORGANIC MATTER DISTRIBUTION THROUGH THE MEASURED SECTIONS 537
CURRICULUM VITAE 555

LIST OF TABLES

TABLES

Table 1. Location, GPS coordinates, total thickness and number of samples of all stratigraphic sections. 5

Table 2. Distribution of palynomorph associations along proximal-distal transect during the latest Burdigalian to earliest Tortonian within the Köpekli, Cingöz and Güvenç formations in the Adana Basin. 161

Table 3. The organic matter distribution through the Köpekli Formation in the Çukurköy Section..... 537

Table 4. The organic matter distribution through the Köpekli Formation in the Köpekli Section..... 538

Table 5. The organic matter distribution through the Köpekli Formation in the Sofular Section..... 539

Table 6. The organic matter distribution through the Köpekli Formation in the Çorlu Section..... 540

Table 7. The organic matter distribution through the Cingöz Formation in the Çorlu Section..... 542

Table 8. The organic matter distribution through the Güvenç Formation in the Çorlu Section..... 546

Table 9. The organic matter distribution through the Güvenç Formation in the Koruklu Section..... 548

Table 10. The organic matter distribution through the Güvenç Formation in the Bekirli Section..... 549

Table 11. The organic matter distribution through the Güvenç Formation within the Güvenç Section. 552

LIST OF FIGURES

FIGURES

Figure 1. Geographic location of stratigraphic sections (red lines show the measured stratigraphical sections). (A) Çukurköy Section; (B) Köpekli, Sofular and Çorlu sections; (C) Koruklu, Bekirli and Güvenç sections; (D) Location map of the study area. 4

Figure 2. Palynological sample processing diagram (Ediger, 1986a). 6

Figure 3. Location map of the study area in the Adana Basin (Eastern Mediterranean, Turkey). (Modified from Kozlu, 1987). 16

Figure 4. Geological map of the Adana Basin. (Red rectangular and lines show the study area and location of the measured sections, respectively; A: Çukurköy Section; B: Köpekli Section; C: Sofular Section; D: Çorlu Section; E: Koruklu Section, F: Bekirli Section; G: Güvenç Section) (modified from Geological Map of MTA (1: 500.000)). 19

Figure 5. Generalized stratigraphic section of the Adana Basin showing the measured sections (modified from Gürbüz, 1999). (A: Çukurköy Section; B: Köpekli Section; C: Sofular Section; D: Çorlu Section; E: Koruklu Section, F: Bekirli Section; G: Güvenç Section). 22

Figure 6. Köpekli Formation in the measured Çukurköy Section. 31

Figure 7. “a” and “c” show the field photos of the samples collected through the Köpekli Formation in the Çukurköy Section. “b” show the boundary between the Kaplankaya and Köpekli formations in the Çukurköy Section. 32

Figure 8. Köpekli Formation in the measured Köpekli Section. 33

Figure 9. Field photos show the samples (a: TD-160; b: TD-165; c: TD-166) collected through the Köpekli Section. 34

Figure 10. Köpekli Formation in the measured Sofular Section. 35

Figure 11. Field photos show the samples (a: TD-124; b: TD-126; c: TD-127 and TD-128) collected through the Köpekli Formation in the Sofular Section. 36

Figure 12. Köpekli, Cingöz and Güvenç formations in the measured Çorlu Section (red arrows show the collected sandstone samples). 37

Figure 13. Field photos show the samples (a: TD-184; b: TD-213; c: TD-231) collected through the Köpekli Formation in the Çorlu Section..... 39

Figure 14. Field photos “show the boundary between the Köpekli and Cingöz formations in the Çorlu Section. (‘b’ shows the close up view of TD-245).40

Figure 15. Field photos show the samples (a: TD-325; b: TD-364; c: TD-406) collected through the Cingöz Formation in the Çorlu section..... 42

Figure 16. Field photos show the bottom sedimentary structures recognized in the sandstone beds within the Çorlu Section (‘a’ and ‘b’ show the close up view of the sandstone bed overlying the sample TD-284; ‘c’ show the close up view of the sample TD-315). 43

Figure 17. Field photos show the samples (a: TD-428; b: TD-464; c: TD-480) collected through the Güvenç Formation in the Çorlu section..... 44

Figure 18. Güvenç Formation in the measured Koruklu Section (red arrows show the collected sandstone samples). 46

Figure 19. Field photos show the samples (a: Ripple marks were recognized on the surface of the sandstone bed overlying the sample ATD-60; b: ATD-65; c: ATD-71) collected through the Güvenç Formation in the Koruklu Section. 47

Figure 20. Güvenç Formation in the measured Bekirli Section (red arrows show the collected sandstone samples). 48

Figure 21. Field photos show the samples (a: ATD-1; b: ATD-7 and ATD-8 c: ATD-12) collected through the Güvenç Formation in the Bekirli Section. 49

Figure 22. Güvenç Formation in the measured Güvenç Section (red arrow shows the collected sandstone sample)..... 50

Figure 23. Field photos show the samples (a: Ripple marks were recognized on the surface of the sandstone bed overlying the sample ATD-85; b: ATD-100; c: ATD-115, ATD-116, ATD-117 and ATD-118) collected through the Güvenç Formation in the Güvenç Section. “c” also shows the boundary between the Güvenç and Kuzgun formations in the Güvenç Section. 51

Figure 24. Bio-chronostratigraphic chart and stratigraphic occurrences of selected taxa (D: dinoflagellate; PF: planktonic foraminifer; CA: calcareous nannoplankton). 55

Figure 25. Correlation of the biozonations along each measured section..... 57

Figure 26. Stratigraphic range chart of palynomorphs and biostratigraphy in the Çukurköy Section. 65
Figure 27. Correlation of the biozones based on palynomorphs, planktonic foraminifera and calcareous nannoplankton in the Çukurköy Section. 67

Figure 28. Stratigraphic range chart of palynomorphs and biostratigraphy in the Köpekli Section. 69

Figure 29. Correlation of the biozones based on palynomorphs, planktonic foraminifera and calcareous nannoplankton in the Köpekli Section. 71

Figure 30. Stratigraphic range chart of palynomorphs and biostratigraphy in the Sofular Section. 73

Figure 31. Correlation of the biozones based on palynomorphs, planktonic foraminifera and calcareous nannoplankton in the Sofular Section..... 75

Figure 32. Stratigraphic range chart of palynomorphs and biostratigraphy in the Çorlu Section (red arrows show the collected sandstone samples)..... 77

Figure 33. Correlation of the biozones based on palynomorphs, planktonic foraminifera and calcareous nannoplankton in the Çorlu Section. 85

Figure 34. Stratigraphic range chart of palynomorphs and biostratigraphy in the Koruklu Section (red arrows show the collected sandstone samples). 89

Figure 35. Correlation of the biozones based on palynomorphs, planktonic foraminifera and calcareous nannoplankton in the Koruklu Section. 91

Figure 36. Stratigraphic range chart of palynomorphs and biostratigraphy in the Bekirli Section (red arrows show the collected sandstone samples)..... 93

Figure 37. Correlation of the biozones based on palynomorphs, planktonic foraminifera and calcareous nannoplankton in the Bekirli Section. 95

Figure 38. Stratigraphic range chart of palynomorphs and biostratigraphy in the Güvenç Section (red arrow shows the collected sanstone sample)..... 97

Figure 39. Correlation of the biozones based on palynomorphs, planktonic foraminifera and calcareous nannoplankton in the Güvenç Section. 99

Figure 40. The biozonation defined in this study have been compared with previously published dinocyst zonations from Denmark, Germany, Netherlands, NW Europe and USA Eastcoast (modified from Dybkjaer & Piasecki). 101

Figure 41. Variation of distal process termination in Spiniferites cf. andalousiensis (Strauss et al., 2001)..... 123
Figure 42. Model for the response of cyst-forming dinoflagellate populations to climate-induced oceanographic changes in the lower Oligocene of southern Germany. (A) High sea-surface salinity is caused by reduced runoff and strong evaporation during relatively dry periods (dominance of *Homotryblium tenuispinosum*). (B) Increased nutrient input, salinity stratification and a decrease in bottom water oxygenation is caused by high freshwater discharge during relatively humid periods (dominance of *Thalassiphora pelagica*) (Pross and Schmiedl (2002) *in* Sluijs et al., 2005). 151

Figure 43. Schematic model for the distribution of dinocyst associations along a proximal –distal transect during the Langhian to Tortonian in the Adana Basin. 159

Figure 44. Diversity chart of Çukurköy Section plotted on the basis of quantitative distribution patterns of palynomorph groups. 167

Figure 45. Diversity chart of Köpekli Section plotted on the basis of quantitative distribution patterns of palynomorph groups. 171

Figure 46. Diversity chart of Sofular Section plotted on the basis of quantitative distribution patterns of palynomorph groups. 173

Figure 47. Diversity chart of Çorlu Section including Köpekli Formation plotted on the basis of quantitative distribution patterns of palynomorph groups. 175

Figure 48. Diversity chart of the Güvenç Formation within Çorlu Section plotted on the basis of quantitative distribution patterns of palynomorph groups. 177

Figure 49. Diversity chart of Koruklu Section plotted on the basis of quantitative distribution patterns of palynomorph groups. 179

Figure 50. Diversity chart of Bekirli Section plotted on the basis of quantitative distribution patterns of palynomorph groups. 181

Figure 51. Diversity chart of Güvenç Section plotted on the basis of quantitative distribution patterns of palynomorph groups. 183

Figure 52. Relative changes in sea level were plotted s based on the quantitative distribution patterns of dinocysts in this study and these curves were correlated with the eustatic sea level curves of the Haq et al., 1987 (red line shows the finilized relative sea level curve pollted in this study)..... 185

Figure 53. Organic matter classifications in different studies (Tekin, 2002). 189

Figure 54. The organic matter distribution chart for the Köpekli Formation in the Çukurköy Section. 191

Figure 55. The organic matter distribution chart for the Köpekli Formation in the Köpekli Section. 192

Figure 56. The organic matter distribution chart for the Köpekli Formation in the Sofular Section. 193

Figure 57. The organic matter distribution chart for the Köpekli Formation in the Çorlu Section. 195

Figure 58. The organic matter distribution chart for the Cingöz Formation in the Çorlu Section. 196

Figure 59. The organic matter distribution chart for the Güvenç Formation in the Çorlu Section. 198

Figure 60. The organic matter distribution chart for the Güvenç Formation in the Koruklu Section. 199

Figure 61. The organic matter distribution chart for the Güvenç Formation in the Bekirli Section. 200

Figure 62. The organic matter distribution chart for the Güvenç Formation in the Bekirli Section. 201

Figure 63 Çukurköy Measured Stratigraphic Section. 285

Figure 64. Köpekli Measured Stratigraphic Section. 292

Figure 65. Sofular Measured Stratigraphic Section. 300

Figure 66. Çorlu Measured Stratigraphic Section. 303

Figure 67. Koruklu Measured Stratigraphic Section. 480

Figure 68. Bekirli Measured Stratigraphic Section. 490

Figure 69. Güvenç Measured Stratigraphic Section. 524

EXPLANATION OF SYMBOLS

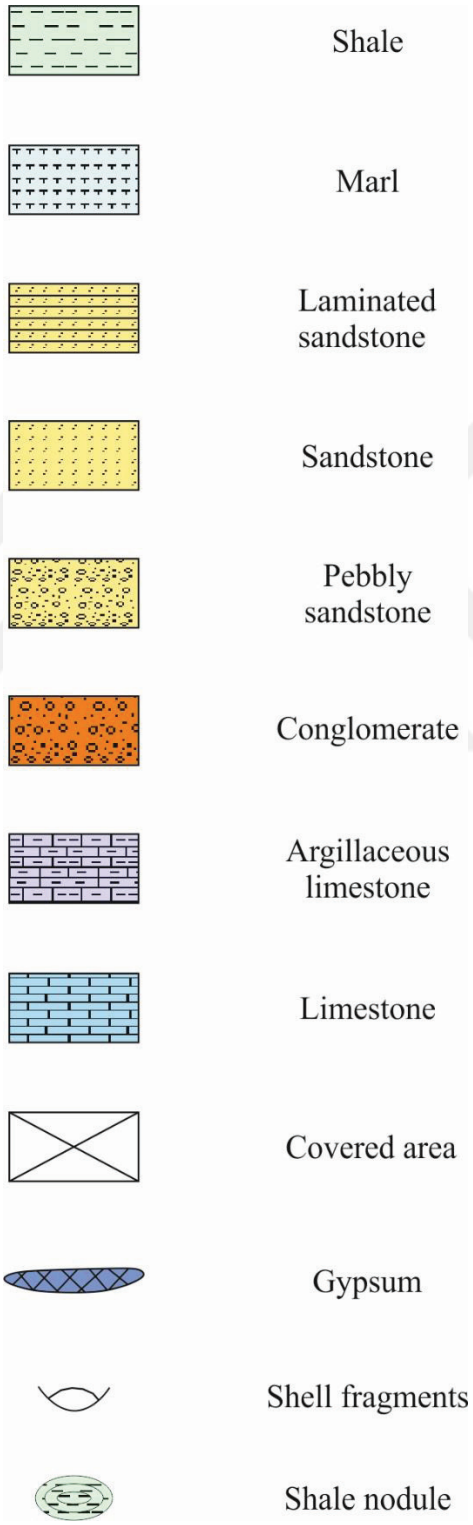

ABBREVIATIONS

Explanation of the abbreviations which are used in the PhD thesis:

FO: First occurrence datum

LO: Last occurrence datum

aa: very abundant (more than 100 specimens)

a: abundant (for 20 to 100 specimens)

c: common (for 6 to 20 specimens)

r: rare (for 2 to 6 specimens)

rr: very rare (for only 1 specimen)

CHAPTER 1

INTRODUCTION

1.1. PURPOSE AND SCOPE

The fundamental aim of this study is to investigate the palynostratigraphy and palynofacies of the Miocene Units in the Adana Basin (Eastern Mediterranean). The Adana Basin is one of the major Neogene basins located in the Eastern Mediterranean area, and its sedimentary fill provide essential records of the paleoenvironmental changes that affected the Mediterranean during the Neogene times.

All of the paleontological framework performed in this region was based on foraminiferal micropaleontology and nannopaleontology whereas palynological framework has not been properly established in this region yet. By means of this study, a detailed biozonation based on palynology has been documented in the study area for the first time. Furthermore, the established biozones were correlated with the zonations based on planktonic foraminifera and calcareous nannoplankton established on the same samples collected for this palynological study. Palynological analysis was based on not only terrestrial palynomorphs, but also marine palynomorphs such as dinoflagellates and acritarchs. According to Stover and Hardenbol (1994), dinoflagellates provide promising information for stratigraphic correlation due to their presence in neritic and deeper marine depositional conditions. Unlike planktonic foraminifera and calcareous nannoplankton, dinoflagellates are not affected by post-depositional decalcification processes. Dinoflagellates have very high tolerance to chemical dissolution and can reach high abundance in both coastal and oceanic settings and they may occur in all aquatic environments from fresh water to hypersaline conditions (Stover and Hardenbol, 1994). Thus, dinoflagellates are very useful indicators of paleoecological conditions and they yield important information about

the surface water temperature, salinity, paleobathymetry and productivity (Wall et al., 1977; Köthe, 1990; Brinkhuis, 1994; Stover and Hardenbol, 1994; Dale, 1996; Powell et al., 1996; Marret and Zonnoveld, 2003; Van Simaeys, 2004; Van Simaeys et al., 2004).

In order to identify sea level fluctuation patterns in the Köpekli, Cingöz and Güvenç formations, relative sea level curve was constructed based on the quantitative distribution patterns of dinocysts. This curve was correlated with the eustatic sea level curve of the Haq et al. (1987). Additionally, to understand depositional environmental changes and ensuring the facies control on biostratigraphy, palynofacies studies were carried out through the measured sections. Palynofacies studies aim to recognize changing patterns of depositional environments that reflect the history of sediment infills, by means of a thorough examination of their paleontological characteristics. Palynofacies characteristics may vary considerably within beds, both laterally and vertically. Vertical changes may indicate shallowing-up or deeping-up trends and may reveal facies dynamics (e.g. regressive/ transgressive events). Lateral changes may indicate differences in water depths and hydrodynamics. Especially, palynomorphs and organic matter constituents are significant proxies for paleoenvironmental conditions. Therefore, proximal-distal trends of dinocysts were studied in detail to construct a model for paleo-depositional environments of the Miocene deposits of the Adana Basin.

In order to investigate palynostratigraphic and palynofacies studies of the Miocene Units in the Adana Basin (Eastern Mediterranean), palynological and palynofacies analysis were carried out. By means of this study, a biozonation based on important dinocyst events was documented for the first time. To apply a worldwide biostratigraphic correlation, the dinocyst zonation constructed in this study was compared with previously published dinocyst zonations from Denmark, Germany, Netherlands, NW Europe and USA Eastcoast. Consequently, the evaluation of the data in this study will be enable to construct more accurate stratigraphical frameworks in the Mediterranean Region for future studies.

1.2. GEOGRAPHIC SETTING

The study area is located approximately 40 km northwest of the city of Adana. The sample material of this study was collected from 7 stratigraphical sections, namely Köpekli, Çorlu, Sofular, Çukurköy, Güvenç, Bekirli and Koruklu sections. All detailed information on the stratigraphic sections including GPS coordinates, thicknesses, numbers of samples are given in the Table 1.

1.3. METHOD OF STUDY

In this study, both field and laboratory works were carried out. Field studies were carried out in three steps from 2013 to 2015. The first field study was done for 2 weeks in September 2013. The main purpose of the first field study was to recognize the study area and to determine the locations of measured sections in the Adana Basin.

The second field work was arranged for 2 weeks in August 2014 for measuring and sampling the Köpekli and the Çorlu sections within the Adana Basin (Figure 1). A total number of 325 samples were collected along these two measured sections (Table 1).

The third field study was carried out for 2 weeks in September 2015. According to the biostratigraphical analysis of collected samples from the previous field works, additional sections have been measured in the Adana Basin during the last field trip. 5 stratigraphic sections, namely Bekirli, Koruklu, Güvenç, Sofular and Çukurköy sections, were measured to complete the missing parts of the Güvenç and Köpekli Formations measured in the previous field work (Figure 1). A total number of 161 samples were collected along these measured sections (Table 1).

This study is supported by the Turkish Petroleum (TP) in terms of permission and financial support for the field studies and the preparation of samples. Samples were prepared for palynological, micropaleontological and nannopaleontological analyses in the TPAO laboratories. All of the collected samples were analyzed in terms of faunal content semiquantitavely. Relative abundance of the palynomorphs have been documented by the following terms: “very abundant (aa)” for more than 100 specimens, “abundant (a)” for 20 to 100 specimens, “common (c)” for 6-20 specimens,

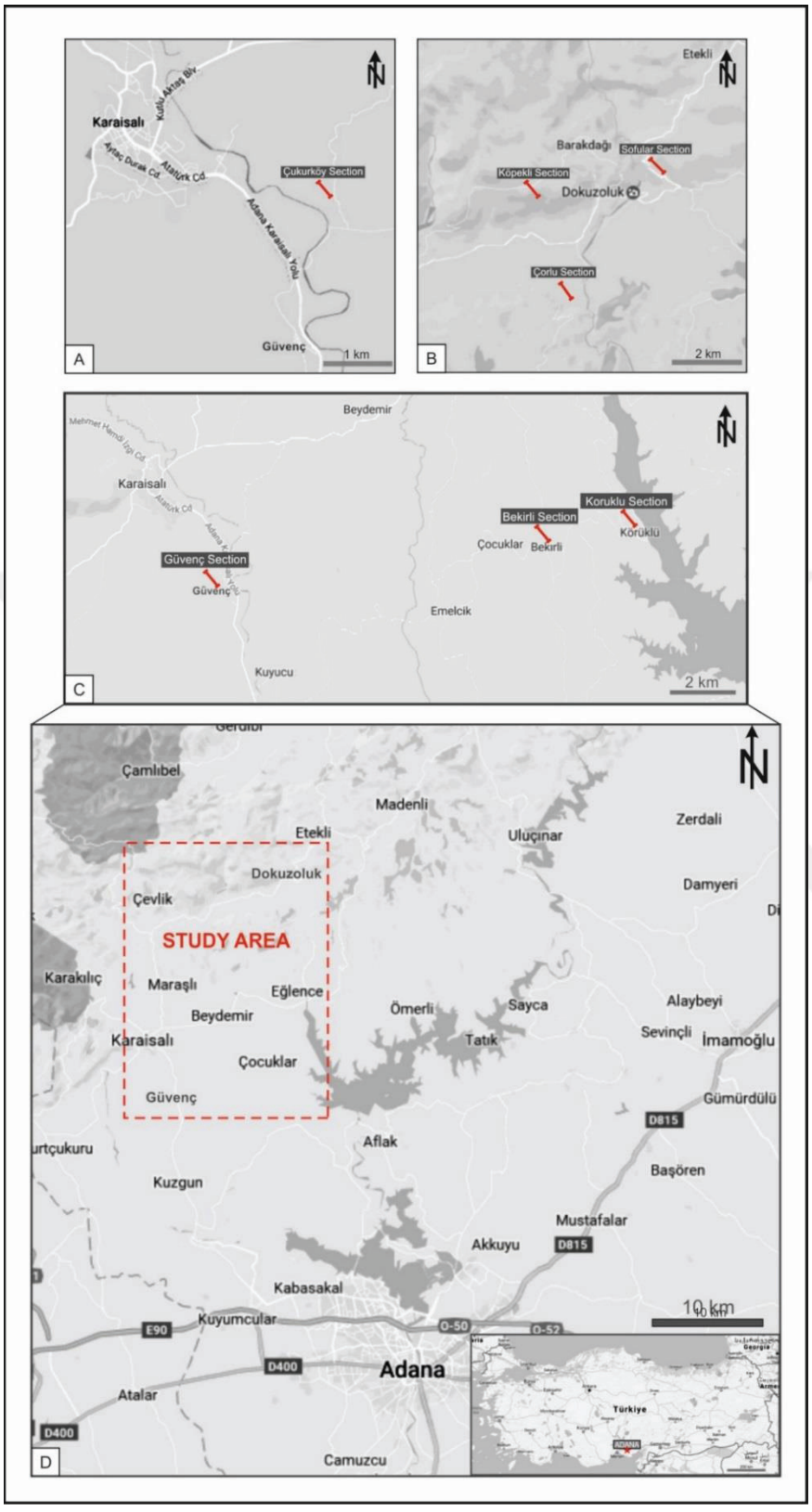

Figure 1. Geographic location of stratigraphic sections (red lines show the measured stratigraphical sections). (A) Çukurköy Section; (B) Köpekli, Sofular and Çorlu sections; (C) Koruklu, Bekirli and Güvenç sections; (D) Location map of the study area.

rare (r) for 2 to 6 specimens and "very rare (rr)" for only 1 specimen. Based on taxonomically well studied populations, a detailed biozonation was documented in the study area and the established biozones were correlated with each other on a bio-chronostratigraphic chart. Moreover, digital images of the palynomorphs recognized through the studied sections were taken and taxonomically organized plates were prepared (App. A).

Table 1. Location, GPS coordinates, total thickness and number of samples of all stratigraphic sections.

NAME OF SECTION	STARTING COORDINATE	ENDING COORDINATE	TOTAL THICKNESS	SAMPLE NO
KÖPEKLİ	36/ 695648 E, 4140344 N 273 m	36/ 695581 E 4140132 N 278 m	78	19 (TD-156 – TD-174)
ÇORLU	36/694001 E 4137366 N 220 m	36/ 692631 E 4129828 E 261 m	1766,1 m	306 (TD-175 – TD-480)
SOFULAR	36/ 695977 E 4140245 N 321 m	36/ 695899 E 4140186 N 332 m	21,8	14 (ATD-119 – ATD-132)
ÇUKURKÖY	36/ 686644 E 4136618 N 316 m	36/687377 E 4136490 N 268 m	70,8	25 (ATD-133 – ATD-161)
GÜVENÇ	36/ 685365 E, 4116244 N 155 m	36/ 686212 E 4113415 N 134 m	118,5	36 (ATD-83 – ATD-118)
BEKİRLİ	36/268761 E 4538905 N 128 m	36/ 694502 E 4127385 N 361 m	333	58 (ATD-1 – ATD-58)
KORUKLU	36/ 695912 E 4124263 N 233 m	36/695770 E 4122825 N 185 m	92,4	24 (ATD-59 – ATD-82)

1.3.1. Sample Processing

All of the collected samples have been prepared for palynological analyses with standard palynological processing techniques suggested by Ediger (1984, 1986a, b). The technique illustrated on Figure 2 is the standard procedure which is generally used for sedimentary rocks rather than coal. According to Ediger (1986a), initial Processes, demineralization, maceration and final processes are the four stages which should be followed during a palynological sample processing (Figure 2). Initial processes are

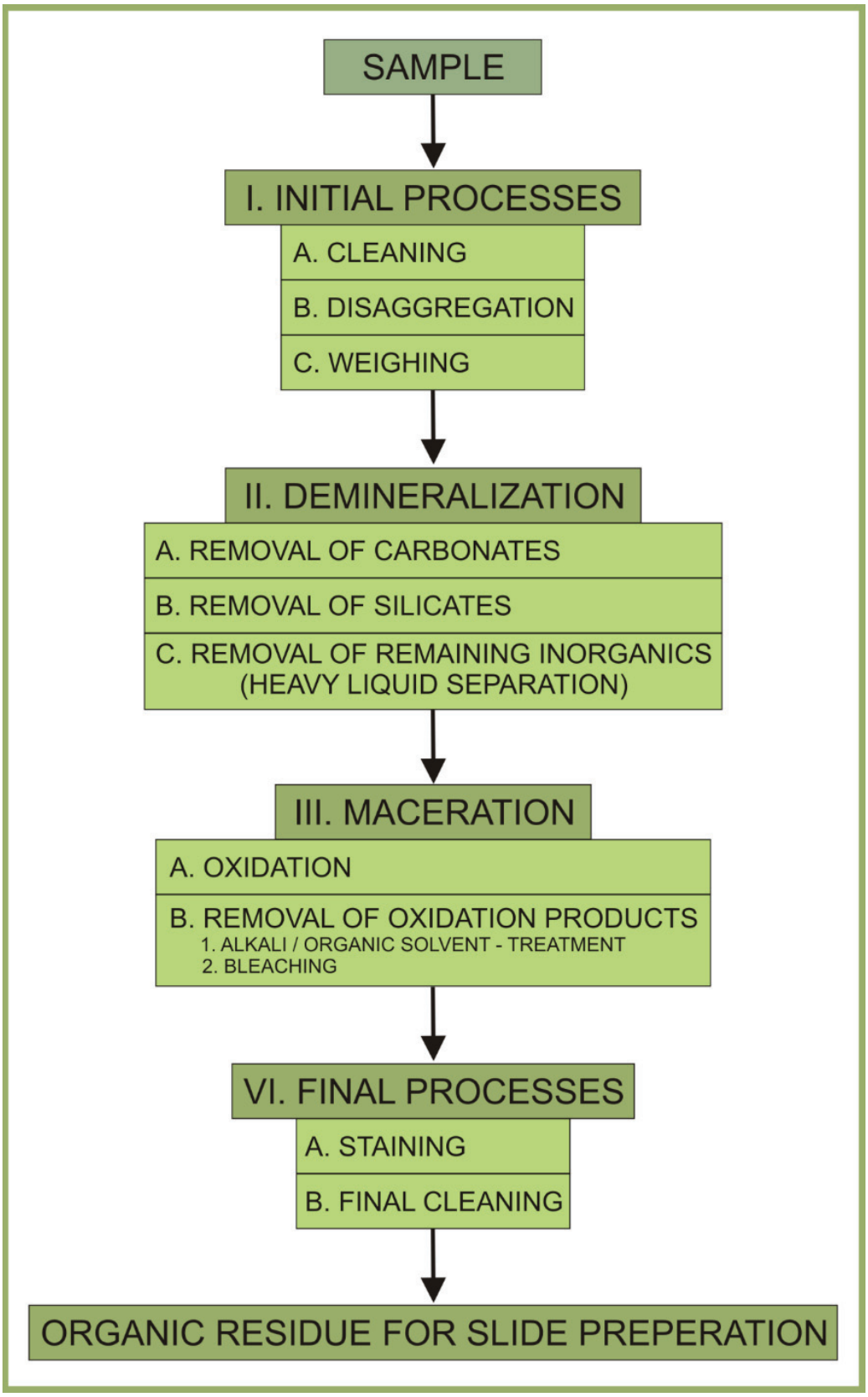

Figure 2. Palynological sample processing diagram (Ediger, 1986a).

composed of three main stages as weighing, disaggregation and cleaning. Amount of the sample used in the initial process depends on the type of the lithology. For example, coal is very rich in organic matter and 5 g of sample is suitable to get enough palynomorphs, whereas at least 10-20 g of sample is needed for marls and shales and 20-50 g of samples for coarser grained lithology (Traverse, 1988; Batı, 1996; Sancay, 2000; Sancay, 2005). After deciding the amount of samples used within the process, samples have to be crushed and pulverized in a hard-steel cup down to a size of less than 1 mm for coals and less than 2 mm for shales and marls (Batı, 1996; Sancay, 2005). This process helps to increase the reaction rate of the sample during the acid treatments.

Demineralization is the second and the most important stage for the palynological sample preparation. Removal of carbonates, removal of silicates and removal of remaining inorganics are the three substages belonging to demineralization. This process is mainly carried out to dispose of all the minerals such as carbonates and silicates within the sample. To remove carbonates, 50 ml of HCL (33 %) is added to the 300 ml beaker and stirred. After the chemical reaction is completely finished, the samples are decanted for two or three times. To remove the silicates, 30-40 ml of HF (40 %) is added to the beakers and it is put on a hot plate at approximately 50^0C for three hours until the chemical reaction is completely finished. Then, the sample is centrifuged in 50 ml of plastic tube for two minutes in 2500 rpm. This centrifuge process is repeated for three times. After centrifuge process is finished, oxidation might be necessary. For understanding the oxidation necessity, a small amount of residue is taken on a slide with water, and it is examined under the microscope. Since the residue consists of organics and heavy minerals, heavy density separation should be performed. Then the sample is centrifuged for 7-8 minutes at 2500 rpm. Centrifuge process will help to differentiate the organic matter from the heavy minerals. The floating organic matters at the top of the glass tube are taken to another glass tube by the help of pipette and filled up with water. These glass tubes are centrifuged at least two times until all the $ZnCl_2$ is removed.

The third stage is Maceration which is composed of two substages as oxidation and removal of oxidation products. In order to understand if oxidation is needed, a small amount of residue is taken on a slide with water, and the color of the

palynomorphs are examined under the microscope. If the color of the palynomorphs are very dark, oxidation should be performed. Oxidation stage helps palynomorphs to be lighter in color. HNO_3 (65 %) is used for marls and shales and Schulze solution is used for coals. Schulze solution is a mixture of 1 g of $KClO_3$ and 10-15 ml of HNO_3. 0.5-1 ml of water and 10-15 ml of HNO_3 or Schulze solution are put into the organic residue and the residue should be instantly centrifuged. Ediger (1984) mentioned that regenerated humic acids have to be removed after the oxidation. After KOH (5 %) or dilute NH_4OH treatment is performed for 15-20 seconds, the residue is washed with water and centrifuged to remove regenerated humic acid (Ediger, 1984).

Final processes consists of two substages as staining and final cleaning. A small amount of residue taken in previous stage is examined under the microscope to figure out whether some undesired particles of 1-2 micron-size are still present or not. If such particles still exist in the organic residue, alcohol is added to glass tube containing the residue and it is centrifuged for 15-20 minutes in 1500 rpm. After the centrifuge process finishes, undesired particles will be seen floating in the tube and the palynomorph will be located at the bottom of the tube. Then, the floating undesired particles are removed and the remaining residue is washed with water. The residue is ready for palynological preparation as soon as it is placed in a glass tube filled with water and 2-3 drops of alcohol.

In order to prepare a palynological slide, cellocise and elvacite are preferred to use. A drop of cellocise and approximately 4 ml organic residue and water are stirred at the center of a cover slip on a hot plate. After the sample get dried, it is mounted onto a glass slide (25x75 mm) and about 2-3 drops of elvacite are applied on the organic residue and the glass slide together. Finally, the glass slide with organic residue was held on the hot plate for about 8 hours.

1.4. PREVIOUS WORK

Eastern Mediterranean has been studied by various researchers during the last century. Most of the studies performed in this region were focused on the stratigraphical and the tectonic frameworks of the region (e.g. Kirk, 1935; Foley, 1937;

Blumenthal, 1941, 1944, 1947, 1951, 1952, 1955 and 1956; Ternek, 1957; Schimidt, 1961; Özer et al., 1974; İlker, 1975; Görür, 1977, 1979, 1985, 1992; Şengör, 1980; Şengör and Yılmaz, 1981; Robertson and Dixon, 1984; Yalçın and Görür, 1984; Lagap, 1985; Şengör et. al., 1985; Covey, 1986; Dewey et al., 1986; Yetiş and Demirkol, 1986; Yetiş et al., 1986; Kelling et al., 1987; Kozlu, 1987; Gökçen et al., 1988; Ünlügenç and Demirkol, 1988; Yetiş, 1988, Ünlügenç et al., 1990; Ünlügenç and Demirkol, 1991; Nazik and Gürbüz, 1992; Şafak and Ünlügenç, 1992; Gürbüz, 1993; Gürbüz and Kelling, 1993; Ünlügenç, 1993; Williams et al., 1995; Yetiş et al., 1995; Gürbüz et al. 1998; Robertson, 1998; Cronin et al., 2000; Satur et al., 2000; Burton, 2003; Aksu et al., 2005; Burton et al., 2005; Büyükutku and Bağcı, 2005; Derman and Gürbüz, 2007; McCay and Robertson, 2012).

Among these studies, Kirk (1935) and Foley (1937) defined the basic geological and geomorphological features of the Adana Basin. In the following years, Blumenthal (1941, 1944, 1947, 1951, 1952, 1955 and 1956) carried out detailed studies related with the stratigraphical framework of the Taurides and published maps illustrating the tectonic structure of the Taurides. These studies played an important role to understand the evolution of the Adana Basin. Ternek (1957) studied the Lower Miocene formations of the Adana Basin in detail and explained the petroleum possibilities of the basin. The first chart of the generalized stratigraphy of the Adana Basin was published by Mobil in the Bulletin of the Petroleum Administration Publications (1960). In these studies, Schimidt (1961) carried out very significant studies related to the structural evolution of the Adana Basin and defined 47 lithostratigraphical units within the Adana Basin. By the help of these detailed stratigraphical researches of Schimidt (1961), the Bulgurdağ Petroleum area was discovered. Özer et al. (1974) studied the geological and structural evolution of the Antalya, Mut and Adana basins. After Özer et al. (1974), İlker (1975) carried out geological studies to explain the petroleum potential of the Adana Basin. Most of the studies of Görür (1977, 1979, 1985 and 1992) were concerned with the stratigraphy and sedimentological evolution of the basin. Görür (1977) tried to explain the depositional history of Miocene sediments within the Adana Basin. The Karaisalı Limestone was divided into six facies. According to Görür (1977, 1979 and 1985), the Karaisalı Formation is predominantly a carbonate reefal sequence developed on

isolated highs. Görür (1979, 1992) also studied the Gildirli Formation within the Adana Basin in detail and divided this formation into two members as the Çakmak Member and the Kabalaktepe Member. Şengör (1980), Robertson and Dixon (1984) and Şengör et al. (1985) performed a very detailed framework including the tectonic evolution of the SE Turkey. According to these authors the structural evolution of SE Turkey was described in terms of the interaction of several major wrench faults in the Kahramanmaraş triple junction. These major structures are the Dead Sea fault zone, Bitlis suture and the Hellenic trench. Şengör and Yılmaz (1981) and Dewey et al. (1986) mentioned that the Adana Basin is located on the Anatolian Plate which is bound by the Bitlis suture to the south. Yalçın and Görür (1984), studied the sedimentological evolution of the Adana Basin and then, Lagap (1985) established the lithostratigraphic and chronostratigraphic framework of the Kıralan-Karakılıç-Karaisalı and within the northwestern part of the Adana Basin. In order to explain the Neogene tectonics and the kinematic evolution of the Adana Basin, Kelling et al. (1987) and Dewey et al. (1986) presented a model about the Adana Basin. They proposed that the Adana Basin formed by NW-directed lithospheric extension as the result of an incompatibility gap created by the evolution of a triple junction near the town of Maraş in eastern Turkey. Then, Kelling et al. (1987) and Gökçen et al. (1988) created a new model in which they proposed that the Miocene basinal successions in the central and eastern portion of the Misis Mountains were deposited in an elongate foreland basin in response to southwestward overthrusting along the southern border of the newly assembled Anatolian orogen. Moreover, they stated that these successions were affected by sinistral strike-slip faulting related to post-Miocene inception of motion along Eastern Anatolian Fault system. Yetiş et al. (1995) reported a detailed stratigraphic framework for the Late Cenozoic sequences in the northeastern Mediterranean region. According to these authors the basement of the Tertiary succession in the Adana Basin consists of the tectonically deformed and eroded Paleozoic and Mesozoic limestone. They defined that the oldest Tertiary rocks in the area belong to the Karsanti Formation (Oligocene) and the Gildirli Formation (Burdigalian). Williams et al. (1995) studied seismic stratigraphy to realize the tectonic controls on the stratigraphic evolution of the Adana Basin. According to the seismic character and the identification of the unconformities, three megasequences and two

megasequence boundaries were identified by Williams et al. (1995). They mentioned that their study was an attempt to integrate the tectonic evolution of the Adana Basin with the filling of the basin in Neogene times. Then, Robertson (1998) studied the tectonic evolution of the Adana-Cilicia Basin and suggested that the Oligocene sedimentation started within fault-controlled depo-centres in the Adana-Cilicia Basin and the Misis Mountains which occurred following the southeast emplacement of allochthonous units over carbonate platforms of the Taurides during the Late Eocene. Burton (2003, 2005) studied seismic stratigraphy to explain structural and sedimentary evolution of the Adana Basin. According to Burton (2003), the Miocene-Recent successions within the Adana Basin are divided into three seismic stratigraphic megasequences, MS1, MS2 and MS3, separated by two prominent regional unconformities, M and B1, respectively. Burton et al. (2005) studied the detailed interpretation and mapping of multi-channel seismic reflection profiles from the Adana Basin. The Megasequences defined in the study of Burton et al. (2005) were different from those described in Williams et al. (1995). According to Burton et al. (2005), the base of the succession was also characterized by a very prominent regional unconformity (B2) above pre-Miocene acoustic basement. Moreover, Burton et al. (2005) mentioned that the stratigraphic and structural architecture of the early to middle Miocene successions in the Adana Basin represents a significant phase of tectonic subsidence, followed by the deposition of a thick deep water succession in an underfilled basin. They noticed that a relatively rapid uplift gave rise to basin inversion and erosion prior to or during the early Tortonian and the upper Miocene global eustatic sea-level fall initiated in the Tortonian. Derman and Gürbüz (2007) studied the sedimentology of the Early Miocene paleovalley fills in the northern Adana Basin and explained their significance for sediment-bypassing on a carbonate platform. They measured stratigraphic sections within the Gildirli Formation in Gildirli, Çevlik, Nergizlik villages. They defined that the Gildirli Formation was the oldest Neogene rock unit in the Adana Basin and deposited during latest Oligocene- earliest Miocene. Moreover, they mentioned that Gildirli formation was formed by two different alluvial fan systems based on all the stratigraphical and sedimentological data obtained from the study area.

The paleontological studies play an important role mainly in the investigation of stratigraphic features and fossil associations of Neogene deposits within the Adana Basin. Erünal-Erentöz (1956) studied the Neogene sediments of the Karaman, Adana and Hatay Basins and defined the Güvenç Formation as "bottom shales" for the first time. Moreover, Erünal-Erentöz (1956) mentioned that the Güvenç Formation was deposited during the Helvetian. After Erünal-Erentöz (1956), Schmidt (1961) named these "bottom shales" as "Güvenç Formation". According to Schmidt (1961), Güvenç Formation was deposited in the deeper parts of the basin in early-middle Miocene time based on fossil data. Then, Öztümer et al. (1974) measured a section near the town of Kraisalı and established a biozonation scheme based on microfossils. They stated that the Güvenç Formation was deposited during the Langhian-Serravallian interval based on fossil fauna. Moreover, İlker (1975) studied the Güvenç Formation within the Adana Basin in detail and introduced a new biostratigraphical framework. According to the micropaleontological analysis, he defined that the Güvenç Formation was deposited during middle Miocene. Then, Nazik and Toker (1986) performed a detailed biostratigraphical study based on planktonic foraminifera within the Langhian-Serravallian time interval. Nazik and Gürbüz (1991, 1992) documented planktonic foraminifera within the turbidites of the Cingöz Formation which is well exposed around Karaisalı-Çatalan-Eğner region. They defined 3 biozones based on planktonic foraminifera within early-middle Miocene. Şafak (1993 a, b) performed biostratigraphical studies on Miocene sediments of Işıktepe-Dalakdere in Mersin based on planktonic foraminifera and ostracods. Based on planktonic foraminifera, they distinguished 2 zones and 2 subzones within the Burdigalian-Serravallian interval. After Şafak (1993 a,b), Şafak and Nazik (1994) studied the biostratigraphy and paleoecology of the Neogene sediments in Eshab-ı Kehf (north of Tarsus) at the western part of the Adana Basin based on planktonic foraminifera and ostracods. Özçelik and Yetiş (1994) studied the Güvenç Formation within the Adana Basin. They measured sections near Güvenç, Kuzgun and Çukurköy villages around the town of Karaisalı in Adana for the purpose of a biostratigraphic study and assigned a Burdigalian-Serravallian age to the Güvenç Formation. Öğrünç and Nazik (1998) studied the sedimentology and biostratigraphy of the Kuzgun Formation which is well exposed around Yenice (Tarsus) within the Adana Basin. They defined that the

Kuzgun Formation is composed of conglomerates, sandstones, siltstone and claystones. The biostratigraphical studies based on ostracods helped to assign a late Miocene-Pliocene interval for the Kuzgun Formation. Öğrünç et al. (2000) studied the evidence about Messinian Salinity Crisis in the Upper Miocene-Pliocene sediments of the Adana Basin by using the sedimentological and paleontological data. It is known that the salinity crisis that affected the Mediterranean is one of the major paleocenographic events during the Messinian. According to Öğrünç et al. (2000), the Upper Miocene-Pliocene units of the Adana Basin also has geological records of this catastrophic event occurred as a result of desiccation of the Mediterranean approximately 6 million years ago. They noticed that the identified species were numerous particularly during Tortonian, but these species started to decline in diversity and some of them disappeared at the Miocene-Pliocene boundary. This shows that this unusual environmental change negatively affected the biota. Sınacı and Toker (2010) studied Miocene (Langhian-Messinian) sediments within the Adana Basin based on the nannoplankton flora. In order to make a detailed biostratigraphical framework, they collected samples from two wells and they determined 7 nannoplankton biozones from Langhian to Messinian. Later, Darbaş and Nazik (2010) analyzed the stratigraphical features and fossil associations (ostracod and planktonic foraminifera) of the late Miocene deposits in the Adana Basin. In addition, they studied the paleoecology of the Neogene units in the Adana Basin. In order to understand the paleoenviromental changes during the Messinian salinity crisis, they analyzed the samples collected from the sediments below and above the Messinian evaporitic layers in the Adana Basin. They measured 3 stratigraphic sections located the middle and western part of the Adana Basin. They mentioned that the sediments below the gypsum layers are characterized by upper Tortonian to lower Messinian fine-grained deposits of the Kuzgun Formation based on the fossil fauna (ostracod and planktonic foraminifera). They concluded that all the gathered data are indicative of gradual environmental changes from humid to subarid climatic conditions during the latest Tortonian-earliest Messinian time interval. After Darbaş and Nazik (2010), Faranda et al. (2013) presented detailed Messinian paleoenviromental reconstructions for the Adana Basin based on multidisciplinary approach which documents the fossil content of Kuzgun and

Handere Formation. In order to reconstruct the paleoenviromental changes that affected the Adana Basin during the Messinian, they analyzed mollusks, ostracod, planktonic and benthonic foraminifera and calcareous nannofossil assemblages from two stratigraphic sections (Adana section and Semiramis section) near Kabasakal village in Adana. In order to understand whether the environmental changes were local or global in oceanic circulation impacted the Mediterranean sedimentary basins, they compared their results with those of Messinian sections from other locations; such as, northern Italy, southern Italy, Cyprus and Algeria. The first studies in the Adana Basin (Eastern Mediterranean) were aimed to describe the evolution of the basin including stratigraphy, structural geology and biostratigraphy. The basin has a complex basement structure and stratigraphy, and the nature and relations of all the basement units have not been fully resolved yet. The previous paleontological studies helped mainly in the investigation of stratigraphic features and fossil associations of Neogene deposits within the Adana basin. Furthermore, all of the paleontological studies carried out in Neogene sediments within the Adana Basin based on planktonic foraminifera, nannoplanktons and ostracods. Since the palynological framework has not been properly established in the Adana Basin yet, this study will be the first investigation carried out in this region.

1.5. REGIONAL GEOLOGICAL SETTING

Turkey and its surroundings comprise a series of accreted continental fragments and associated suture zones showing Laurasian and Gondwanan affinities (e.g. Şengör and Yılmaz, 1981; Robertson and Dixon, 1984; Okay and Tüysüz, 1999). Tauride mountain belt of southern Turkey comprises one, or several, continental fragments that rifted from the Gondwanan (northern African) margin and were later accreted to Eurasia as the intervening Tethys closed (e.g., Şengör and Yılmaz, 1981 and Dercourt et al., 1993). According to Şengör and Yılmaz (1981), the southern branch Tethyan Ocean opened during the Middle–Late Triassic time. Şengör and Yılmaz (1981) and Robertson (2002) discussed that Tauride continental fragments were bordered by Mesozoic ocean crust, formed by sea-floor spreading, both to the north and south. This

ocean is known as the Intra-Tauride Ocean. The northern branches of Neotethys, to the north of the Taurides, was completely closed by Oligocene time and followed by the development of post-collisional sedimentary basins above a regional unconformity (Şengör and Yılmaz, 1981 and Williams et al., 1995). The belt includes several tectono-stratigraphic rock units with distinctive stratigraphical, structural and metamorphic features (Özgül, 1976). Tertiary sedimentary basins cover these rock units of the Tauride mountain belt. One of these basins is the Adana Basin which lies to the south of the central part of the Tauride mountain belt along the Turkish Mediterranean coast (Figure 3). The basin, bounded by the Ecemiş Fault Zone to the west, the Misis Structural High to the southeast and overthrust Tauride Orogenic Belt to the north, was formed entirely on the Anatolian Micro-Plate (Şengör and Yılmaz, 1981; Dewey *et al*., 1986). NE–SW trending Adana Basin extends from the Tauride Orogenic Belt of southern Turkey towards the Mediterranean Sea. The morphology of the sea-floor of the northeast Mediterranean Sea is largely controlled by major tectonic features (e.g. the Misis–Kyrenia fault zone, Cyprus Arc). The structural and stratigraphical evolution history of the Adana Basin which is one of the major Neogene basins was initiated after the Late Eocene to Oligocene emplacement of an ophiolitic complex and associated melanges in the Taurides (Williams et al., 1995). The sedimentary fill of the Adana Basin, bounded by the Mut Basin to the west and the İskenderun Basin to the north in the Central Taurides, reflect striking similarities to the stratigraphy of these adjacent basins (Yalçın and Görür, 1984; Kozlu, 1987; Yılmaz et al., 1988; Uffenorde et al., 1990, Aksu et al., 2005). The Adana and Manavgat basins also represent a similar sedimentation pattern during the Miocene times (Yılmaz et al., 1988; Aksu et al., 2005).

Basement rocks of the Adana Basin consists of Paleozoic and Mesozoic clastics and carbonate sequences and this basement is unconformably overlain by Cenozoic sedimentary successions (Yetiş and Demirkol, 1986). Cenozoic sediments of the Adana Basin are composed of nine formations namely, Karsanti, Gildirli, Kaplankaya, Karaisalı, Köpekli, Cingöz, Güvenç, Kuzgun and Handere from bottom to top. The succession in this basin begins with the Oligocene-Miocene alluvial fan and lacustrine siliciclastic sediments of the Karsanti Formation (e.g. Schimidt, 1961; Ünlügenç and

Demirkol, 1988; Yetiş, 1988; Ünlügenç and Demirkol, 1991, Williams et al., 1995; Yetiş et al., 1995). Gildirli

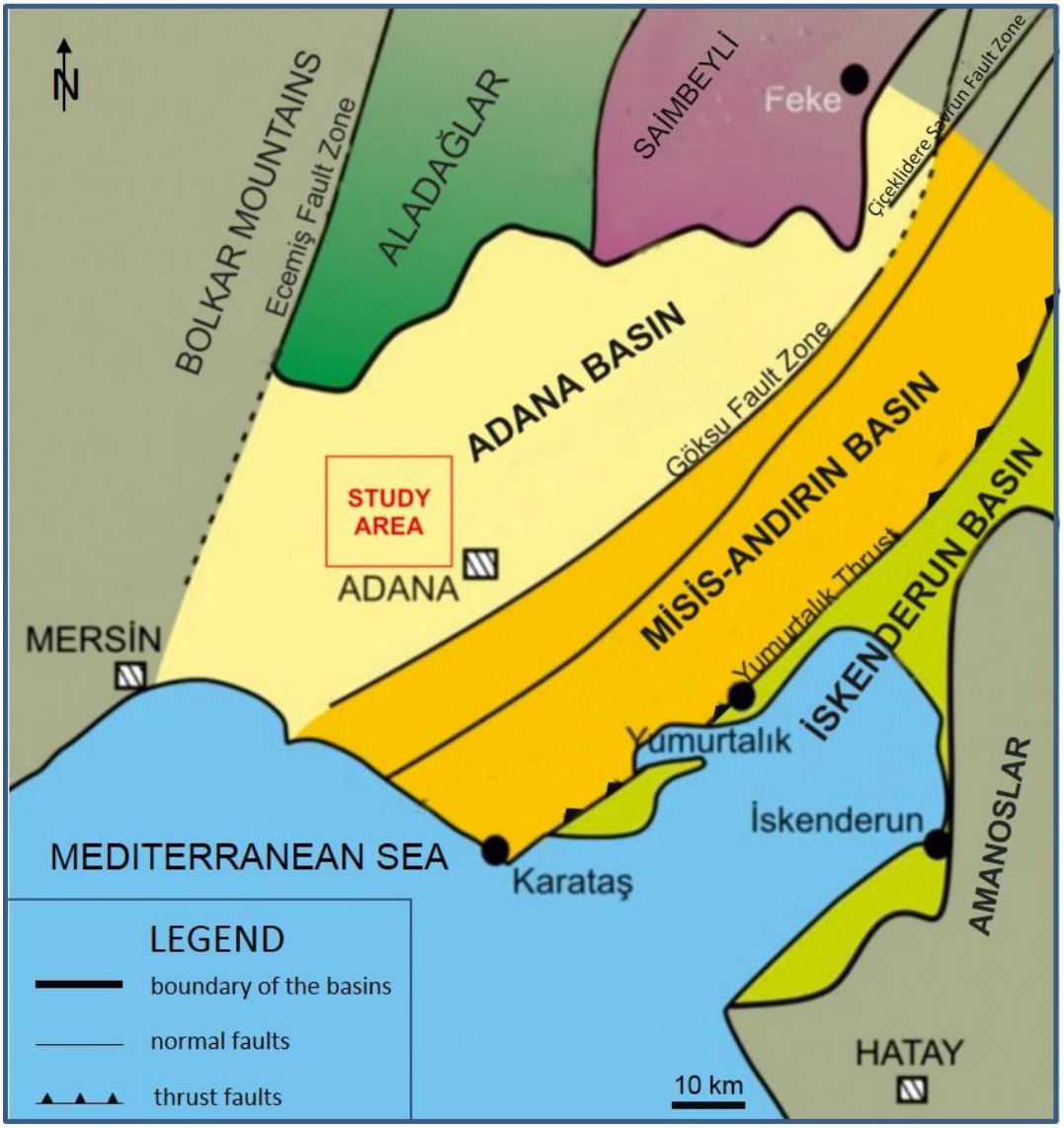

Figure 3. Location map of the study area in the Adana Basin (Eastern Mediterranean, Turkey). (Modified from Kozlu, 1987).

Formation characterized by the boulder to pebble conglomerates derived from the Paleozoic and Mesozoic carbonates and the ophiolite complex overlies the Karsanti Formation during Early Miocene (e.g. Schimidt, 1961; Görür, 1979; Görür, 1985; Yetiş and Demirkol, 1986; Ünlügenç et al., 1990; Yetiş et al., 1995; Williams et al.,

1995). Gildirli Formation passes upwards and laterally into the Kaplankaya Formation which has vertical and lateral transitional contacts with Gildirli, Karaisalı and Köpekli formations. Kaplankaya Formation is composed of reefal carbonates indicating the first input of marine clastics in the basin during the late Burdigalian-earliest Langhian (e.g. Schimidt, 1961; Ünlügenç et al., 1990; Nazik and Gürbüz, 1992; Gürbüz and Kelling, 1993; Görür, 1994; Williams et al., 1995). The overlying Karaisalı Formation consists of carbonate reefal sequence developed on isolated highs in the basin during the Early-Middle Miocene (Schimidt, 1961; Görür, 1977, 1979 and 1985; Büyükutku, 2009). Köpekli Formation characterized by a thick sequence of shale intercalated with subordinate thin sandstone beds is recognized between the Karaisalı and Cingöz formations (Kozlu, 1991). This formation was deposited during the late Burdigalian-Langhian (Türkecan et al., submitted). Due to a rapid and tectonically controlled subsidence during the early Langhian–Serravallian interval, more than 3 km thickness of both coarse and fine-grained, deep marine clastics were deposited in the northern part of the basin (e.g. Williams et al, 1995; Görür, 1994). The Cingöz Formation characterized by the turbidite sequence of the Adana Basin is composed of two distinct coeval submarine fans (Gürbüz and Kelling, 1992, 1993; Yetiş et al., 1995; Gürbüz, 1999; Satur et al., 2000). The Cingöz Formation consisting of poorly bedded, channelized conglomerates, pebbly sandstones followed by a thick succession of sandstone-shale alternations was deposited during the Langhian- Serravallian (Nazik and Gürbüz, 1992; Yetiş et al., 1995). The overlying Güvenç Formation composed of shales was deposited in the deeper parts of the basin in the Burdigalian-Serravallian time interval (Schimidt, 1961; Özçelik, 1993). The Kuzgun Formation characterized by shallow marine, fluvial and deltaic sediments overlies the Güvenç Formation with a low angle discordance (Schimidt, 1961; Kerey et al., 1985; Yetiş and Demirkol, 1986; Yetiş, 1988). The Kuzgun Formation deposited during the Late Miocene (Tanar, 1985; Gürbüz and Gökçen, 1985; Yetiş, 1988) overlies the Handere Formation consisting of fluvial sediments and shallow marine sediments (Schimidt, 1961; Yetiş, 1988; Yalçın and Görür, 1984; Yetiş et al., 1995). Regression and tectonic reorganization culminated in localised accumulation of Messinian evaporates in this Formation (Yalçın and Görür, 1984; Williams et al., 1995; Yetiş et al., 1995). Handere Formation was deposited during the Messinian- early Pliocene (Gürbüz and Gökçen,

1985; Yetiş, 1988; Yetiş et al., 1995) and it is unconformably capped by Quaternary deposits. Among these formations, the Köpekli, Cingöz and Güvenç formations constitute the main subject of this thesis. Within this general stratigraphic frame, the sections that we studied correspond to the exposures of the Köpekli, Cingöz and Güvenç formations that are the major Miocene clastic deposits of the Adana Basin (Figure 4).

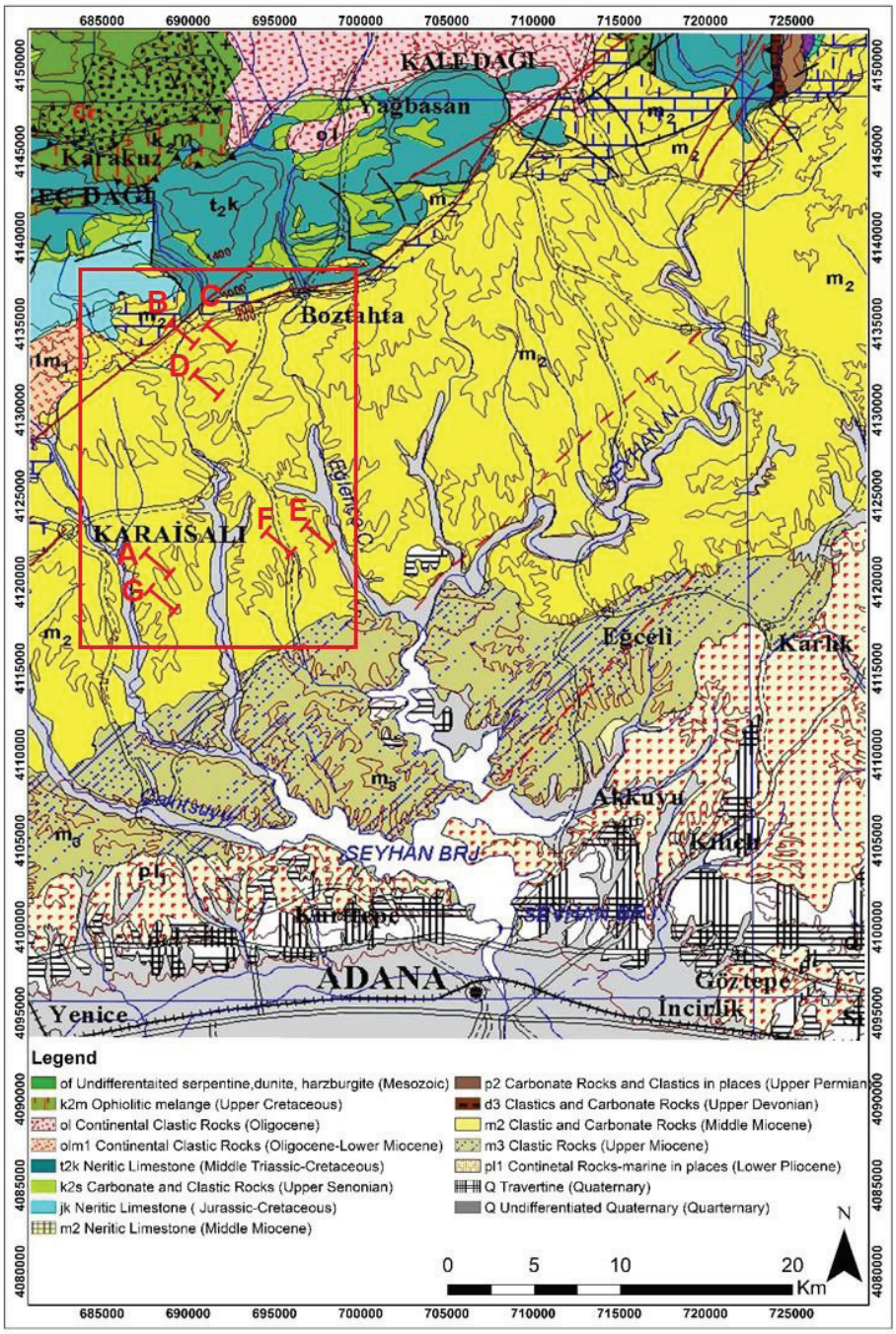

Figure 4. Geological map of the Adana Basin. (Red rectangular and lines show the study area and location of the measured sections, respectively; A: Çukurköy Section; B: Köpekli Section; C: Sofular Section; D: Çorlu Section; E: Koruklu Section, F: Bekirli Section; G: Güvenç Section) (modified from Geological Map of MTA (1: 500.000)).

CHAPTER 2

LITHOSTRATIGRAPHY

The study area is located on the exposures of the Neogene units of the Adana Basin (Eastern Mediterranean). Most of the studies performed in this region were concerned with the stratigraphical, sedimentological and structural evolution of the Adana Basin (e.g. Kirk, 1935; Foley, 1937; Blumenthal, 1941, 1944, 1947, 1951, 1952, 1955 and 1956; Ternek, 1957; Schimidt, 1961; İlker, 1975; Görür, 1977, 1979, 1985, 1992; Yalçın and Görür, 1984; Lagap, 1985; Covey, 1986; Yetiş and Demirkol, 1986; Yetiş et al., 1986; Kozlu, 1987; Ünlügenç and Demirkol, 1988; Yetiş, 1988, Ünlügenç et al., 1990; Ünlügenç and Demirkol, 1991; Nazik and Gürbüz, 1992; Şafak and Ünlügenç, 1992; Gürbüz, 1993; Gürbüz and Kelling, 1993; Ünlügenç, 1993; Williams et al.,1995; Yetiş et al., 1995; Gürbüz et al., 1998; Cronin et al., 2000; Satur et al., 2000; Aksu et al., 2005; Büyükutku and Bağcı, 2005; Derman and Gürbüz, 2007). Among these studies, Schimidt (1961) carried out the first significant studies related to the structural evolution of the Adana Basin and defined 47 lithostratigraphic units. According to Yetiş and Demirkol (1986), the basement of Adana Basin consists of Paleozoic and Mesozoic clastics and carbonate sequences and this basement is unconformably overlain by the Cenozoic sedimentary successions. Cenozoic sediments of the Adana Basin is composed of nine formations namely, Karsanti, Gildirli, Kaplankaya, Karaisalı, Köpekli, Cingöz, Güvenç, Kuzgun and Handere formations from bottom to top (Figure 5).

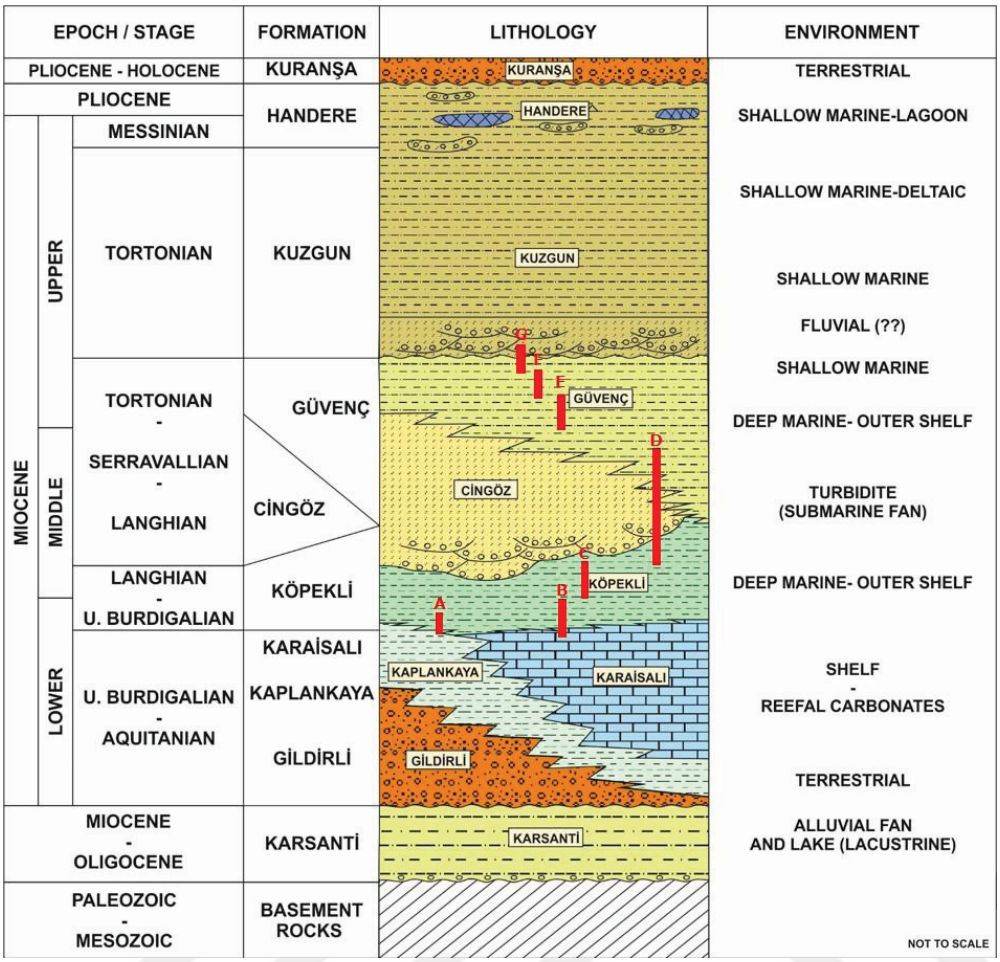

Figure 5. Generalized stratigraphic section of the Adana Basin showing the measured sections (modified from Gürbüz, 1999). (A: Çukurköy Section; B: Köpekli Section; C: Sofular Section; D: Çorlu Section; E: Koruklu Section, F: Bekirli Section; G: Güvenç Section).

2.1. CENOZOIC FORMATIONS IN THE ADANA BASIN

2.1.1. Karsanti Formation

The oldest Tertiary rocks in the Cenozoic units of the Adana Basin are represented by the Karsanti Formation (Miocene-Oligocene) (Yetiş et al., 1995). Schmidt (1961) described a group of redbeds developed in the Karsanti basin and named these beds as Karsanti, Meydan and Garajtepe formations. After Schmidt (1961), Ünlügenç and Demirkol (1988) and Yetiş (1988) combined these lithostratigraphic units into the Karsanti Formation. It is mainly composed of alluvial fan, fluvial, lagoonal and lacustrine deposits (Schimidt, 1961; Ünlügenç and Demirkol,

1991). According to Williams et al. (1995), these sediments were deformed by a compressional event during the Oligocene. The thickness of the formation ranges from 880 m to 1500 m (Schmidt, 1961). The age span of the Karsanti Formation was determined as Oligocene-Miocene (Abacı, 1985; Yurtmen, 198). Karsanti Formation unconformably overlies the Tauride ophiolitic rocks which were eroded and derived into the Karsanti Formation sediments and it is overlain unconformably by the Gildirli Formation (Ünlügenç and Demirkol, 1991) (Figure 5).

2.1.2. Gildirli Formation

Schmidt (1961) named the coarse clastic, continental to estuarine units along the northwest flank of the Adana Basin as the Gildirli Formation. According to Schmidt (1961), the Gildirli Formation filled the canyons and bays of the pre-Miocene paleotopography in the Adana Basin. The Gildirli Formation is composed of boulder to pebble conglomerate mainly derived from Paleozoic and Mesozoic carbonates and the ophiolite complex, mostly non-sorted and poorly bedded, interbedded with thick units of red shale, red and variegated siltstone, red sandstone (Schmidt, 1961). Schimidt (1961) noticed that thin lignite beds were seen within the Gildirli Formation locally. Moreover, he recognized that the redbeds disappeared in the upper part of the formation, and brackish to marine gray shales appeared in the succession. Görür (1979) divided the Gildirli Formation into two members, namely Çakmak Member and Kabalaktepe Member. Çakmak Member is composed of red colored and non-fossiliferous conglomerates, sandstones and siltstones. Çakmak Member is overlain by the Kabalaktepe Member which consists of yellowish grey colored, fossiliferous, marine conglomerates, sandstones and siltstones. Yetiş and Demirkol (1986) defined the Kaplankaya Formation and included the Kabalaktepe Member of Görür (1979) into the Kaplankaya Formation. Yetiş et al. (1995) defined the lowermost Miocene succession, Gildirli Formation, consisting of stacked, conglomerate dominant deposits. According to Williams et al. (1995), Gildirli Formation comprises a thick sequence of fluvio-lacustrine sediments and consists of conglomerates, sandstones, siltstones and mudstones. The succession is thickest in the structural depressions, but decreases in thickness substantially toward the basement high. Görür (1985)

recognized that clast compositions in the coarse lithologies give clues about the source. He defined that this succession is mainly sourced from the Taurus Mountains. Gildirli Formation is restricted to the northern part of the Adana Basin. It conformably passes into younger sediments in the NW part of the Adana Basin. Ünlügenç et al. (1990) defined that terrestrial redbeds belonging to the Gildirli Formation began to subside into a foreland basin in the Early Miocene period. Thus, relatively rapid subsidence resulted in the deposition of clastics of the Kaplankaya and reefal carbonates of the Karaisalı formations in the northern margin of the basin during Burdigalian- early Langhian time and resulted in the deposition of deeper marine clastics in the southern margin of the basin as the Güvenç Formation during Langhian- Serravallian time (Ünlügenç et al., 1990; Williams et al, 1995).

2.1.3. Kaplankaya Formation

Gildirli Formation grades upwards and laterally into the Kaplankaya Formation which marks the first input of marine clastics in the basin (Schimidt, 1961; Ünlügenç et al., 1990; Williams et al, 1995) (Figure 5). According to Schimidt (1961), it was deposited in a paleotopographic high and in the marginal parts of the Adana Basin and the thickness of the formation ranges from 35 m to 60 m. This succession was deposited during the late Burdigalian- earliest Langhian time (Nazik and Gürbüz, 1992; Gürbüz and Kelling, 1993). Kaplankaya Formation has vertical and lateral transitional contacts with the Gildirli, Karaisalı and Köpekli formations (Figure 5).

2.1.4. Karaisalı Formation

Karaisali Formation which is well exposed around Karaisalı region was first described by Schmidt (1961). According to this author, the Karaisalı Formation was deposited on a paleotopographic high and in the marginal parts of the basin and the thickness of the formation reaches up to 600 m. Görür (1977, 1979 and 1985) defined that the Karaisali Formation is predominantly characterized by a carbonate reefal sequence and this succession is mainly developed on isolated highs (Figure 5). According to Büyükutku (2009), the Lower-Middle Miocene Karaisali carbonate succession was deposited either under the control of local tectonism and/or eustatic

sea level fluctuations. Since the Karaisali Formation is very important for hydrocarbon exploration, it has been studied for years. According to Büyükutku (2009), the Karaisali limestones have intermediate to good reservoir characteristics.

2.1.5. Köpekli Formation

Köpekli Formation was first defined by Schmidt (1961) as a member of the Cingöz Formation, namely the Köpekli shale member. Schmidt (1961) described the Köpekli shale member as silty and argillaceous, fossiliferous limestone at the base, followed by a thick sequence of shale, gray to blue-gray, silty, fissile, with subordinate thin sandstone beds and fossiliferous limestone. He also mentioned that some of the shale intervals are very carbonaceous to lignitic. According to Schimidt (1961), the total thickness of the Köpekli shale member ranges from 25 to 650 meters. Yetiş and Demirkol (1986) suggested that the Köpekli shale member of Schimidt (1961) should be a part of the Güvenç Formation. Therefore, Yetiş and Demirkol (1986) analyzed the Köpekli shale member of Schimidt (1961) together with the Güvenç shale and mapped these two shale units as the Güvenç Formation. According to Yetiş and Demirkol (1986), these shale units gradually overlie the Karaisalı Formation and have lateral contacts with the Karaisalı Formation. Kozlu (1991) defined the Köpekli shale member of Schimidt (1961) as a formation, namely the Köpekli Formation. In this study, we also consider that the shaly intervals exposed between the Karaisalı and Cingöz Formations should be raised to a formation rank. In order to cover the whole formation, four stratigraphic sections, namely Çukurköy, Köpekli, Çorlu and Sofular Sections, are measured within the Adana Basin in this study

2.1.6. Cingöz Formation

Cingöz Formation was described as the turbidite sequence within the Adana Basin by Schmidt (1961), Yetiş (1988) and Ünlügenç and Demirkol (1988). Schmidt (1961) defined three members, namely Ayva, Topallı and Köpekli, within the Cingöz Formation. According to this auther, the thickness of the Cingöz Formation reaches up to 3500 m. Yetiş (1988) redefined the Cingöz Formation and divided it into two members (Ayva and Topallı). He assigned the Köpekli member consisting of shales to

the Güvenç Formation. Unlike Kaplankaya and Karaisalı formations, the Cingöz Formation was deposited in deeper parts of the basin in the Early- Middle Miocene period (Schmidt, 1961) (Figure 5). According to Gürbüz and Kelling (1992, 1993), Gürbüz (1999), Cronin et al. (2000) and Satur et al. (2000), the Cingöz Formation consists of two distinct coeval submarine fans characterized by a large eastern lobe and a smaller western lobe. According to Yetiş et al. (1995), these submarine fans are retrogradational in style and correspond to turbidite system types I and II of Mutti (1985). Cingöz Formation starts with poorly bedded, channelized conglomerates, pebbly sandstones at the base and grades upwards into a thick succession of turbidite sandstone-shale alternations (Yetiş et al., 1995). The intervening shale layers are fissile, calcareous and carbonaceous and become dominant towards the upper parts of the Cingöz succession (Yetiş et al., 1995). Gürbüz (1993) measured the thickness of the Cingöz Formation 1000 m in the west and 3200 m in the east. The age of the formation is determined as Langhian- Serravallian based on foraminiferal micropaleontological surveys (Nazik and Gürbüz; 1992). The Cingöz Formation with 1031.7 m thickness has been studied within the Çorlu Section in this study.

2.1.7. Güvenç Formation

The Güvenç Formation consisting of fine grained siliciclastics overlies the submarine fan deposits of the Cingöz Formation and overlain by fluvial sediments of the Kuzgun Formation with a truncation surface (Figure 5). According to Schmidt (1961), the Güvenç Formation consisting of shales was deposited in the deeper parts of the basin in the Early- Middle Miocene period. The thickness of the Güvenç Formation ranges from 20 to 3230 m (Schmidt, 1961; İlker, 1975). Yetiş (1988) redefined the Güvenç Formation and combined the Güvenç Formation of Schimidt (1961) and the Köpekli shale member of the Cingöz Formation. According to Özçelik (1993), Özçelik and Yetiş (1993) and Yetiş et al. (1995), the decreasing number and thickness of sandy layers, the decrease in assemblage of benthic foraminifera and increasing amounts of planktonic foraminifera and Discoaster-type nannofossils show that bathymetry is increasing from middle parts to upper parts of the Güvenç Formation. While, increasing amount of sandy detritus, the increase in assemblage of

benthic foraminifera and increasing amounts of *Braarudosphaera discula*, *Braarudosphaera bigelowii* type nannofossils indicate relatively shallow marine conditions in the uppermost part of the succession (Özçelik 1993; Özçelik and Yetiş; 1993 and Yetiş et al., 1995). The uppermost part of the Güvenç Formation marks by a transition from storm dominated shelf deposits to shallow marine clastics representing the transition to the upper regressive succession (Yalçın and Görür, 1984). Güvenç Formation was deposited during the Burdigalian-Serravallian interval based on planktonic foraminifera and nannofossils (Özçelik, 1993). In order to cover the whole formation, four stratigraphic sections, namely Çorlu, Koruklu, Bekirli and Güvenç Sections, were measured in the Adana Basin in this study.

2.1.8. Kuzgun Formation

Kuzgun Formation, which is one of the youngest succession in the Adana Basin, overlies the Güvenç Formation with a low-angle discordance (Figure 5). Kuzgun Formation consisting of coarse redbeds and shallow marine sediments was firstly defined by Schmidt (1961). Schmidt (1961) divided Kuzgun Formation into six members, namely Kocaveliler, Çaparlı, Kepez, Kurbanlı, Çirbiklar and Sarneli Members, to illustrate the different facies recognized within the Kuzgun Formation. Afterwards, Schmidt (1961), Kerey et al. (1985) and Yetiş and Demirkol (1986) described the distribution of the main facies within the Kuzgun Formation. They mentioned that there was a regional increase in the proportion of the carbonate sediments towards the western part of the Adana Basin. Yetiş and Demirkol (1986) and Yetiş (1988), Kuzgun Formation is subdivided into three members, namely Kuzgun, Salbaş Tuff and Memişli members. The Kuzgun Member grades into the Salbaş Member through a transitional unit consisting of light gray volcanoclastic sandstones, gray siltstones and pebbly sandstones, the sub-rounded pebbles including pale colored tuffites (Yetiş et. al., 1995). The thickness of the Kuzgun Member ranges from 200 m to 1600 m (İlker, 1975). Salbaş siltstones were deposited during Tortonian based on vertebrate teeth (*Hipparion* sp.) and gastrapods (Yetiş, 1988). The lithology of Memişli Member is very similar to Kuzgun Member. Yetiş et al (1995) defined the Memişli Member as a sandstone dominated unit consisting of fluvial, deltaic, lagoonal

and shallow marine deposits. The succession of Memişli Member starts with channelized conglomerates, through cross-bedded, poorly sorted pebbly sandstones, coarsed grained sandstones and continues upward with thickening upwards sequence of siltstones and fine grained sandstones exhibiting marked bioturbation and parallel and cross laminations (Yetiş et al., 1995). The thickness of this member was measured as 850 m by Schmidt (1961). The Memişli Member was deposited during Tortonian-Messinian based on Ostrea, gastropods, ostracods and planktonic foraminifera (Tanar, 1985; Gürbüz and Gökçen, 1985; Yetiş, 1988).

Ünlügenç (1993) recognized that there is a facies change from outer marine shelf to continental fluvio-deltaic deposits at the boundary between the Güvenç Formation and the Kuzgun Formation. A regionally extensive middle- upper Miocene unconformity forms the base of the Kuzgun Formation and is exposed in the northern part of the basin (Burton-Ferguson, 2005). The Miocene to Plio-Quaternary successions (Kuzgun and Handere formations) in the Adana Basin starts with regressive deposits at the base and continues upward with transgressive deposits. The lower unit consisting of primarily of Serravallian to Tortonian prograded alluvial deltaic, beach bar, lagoonal and shallow water deposits of the Kuzgun Formation (Yetiş et al., 1995). The upper portion of this regressive deposit is located in the southern part of the Adana Basin (Burton-Ferguson, 2005). The Kuzgun Formation was overlain by the Handere Formation.

2.1.9. Handere Formation

The Handere Formation consisting of fluvial sediments and shallow marine sediments overlies the Kuzgun Formation (Figure 5). Schmidt (1961) firstly defined the Handere Formation consisting of yellow and beige sandstones, conglomerates, subordinate siltstones and some mappable gypsiferous layers. According to this auther, the thickness of this formation ranges from 120 m to 700 m. Yetiş (1988) mapped these gypsum levels and named them as the Gökkuyu Gypsum Member of the Handere Formation. Yalçın and Görür (1984) and Yetiş et al. (1995) recognized that the Messinian evaporite and siliciclastic succession are overlain by the Handere Formation as the upper transgressive unit consisting of Pliocene shallow marine and lagoonal

deposits. The Handere Formation was deposited during the Messinian-Early Pliocene based on gastrapods, ostracods and planktonic foraminifera (Gürbüz and Gökçen, 1985; Yetiş, 1988; Yetiş et al., 1995). It is unconformably capped by Quaternary deposits consisting of alluvium, terrace conglomerates and caliche deposits (Yetiş and Demirkol, 1986; Yetiş, 1988).

2.2. LITHOSTRATIGRAPHY OF THE MEASURED SECTIONS

2.2.1. Çukurköy Section

Çukurköy Section was measured in Çukurköy Village located northwestern part of Adana. A considerable part of the measured section in this study comprises the uppermost part of the Kaplankaya Formation and lowermost part of the Köpekli formation (Figure 6, App. B). The measured part of the Kaplankaya Formation consists of limestone- argilllaceous limestone- marl alternations (layers from sample ATD-137 to ATD-140) (Figure 6 and Figure 7). A 70 cm thick limestone bed is recognized within the base of the section corresponding to the level of Kaplankaya Formation. The boundary between the Kaplankaya Formation and the Köpekli Formation is recognized with argilllaceous limestone and marl alternation (Figure 6). Shaly intervals overlying the Kaplankaya Formation, which has vertical and lateral relationship with the Karaisalı Formation, was considered as the Köpekli Formation in the Çukurköy Section (Figure 5). Köpekli Formation within this section starts with shell fragments bearing argillaceous limestone-marl alternation (layers from sample ATD-141 to ATD-145 (Figure 6 and Figure 7)) and grades into a thick succession of marls (layers from sample ATD-146 to ATD-161, (Figure 6)).

2.2.2. Köpekli Section

Köpekli Section comprising the uppermost part of the Karaisalı Formation and lowermost part of the Köpekli Formation was measured closed to Köpekli Village located in the northwestern part of Adana (Figure 1). The boundary between the Köpekli Formation and the Karaisalı Formation has been drawn at the top of the limestone deposits of the Karaisalı Formation comprising a carbonate reefal sequence

(Figure 8, Figure 9 and App. B). A fossiliferous limestone and shale alternation is observed at this boundary. The studied part of the Köpekli Formation in this measured section is characterized by silty and argillaceous, very fossiliferous limestone at the base (layers from sample TD-157 to TD-160 (Figure 8, App. B)) and it continues upwards with a thick sequence of shale (layers from sample TD-161 to TD-174 (Figure 8, Figure 9 and App. B)). The lower part of the shale part contains shale nodules (layers from sample TD-160 to TD-163 (Figure 8, Figure 9, App. B)). A 15 m thick covered area is also recognized between the level corresponding to the samples TD- 170 and TD-171 within the section (Figure 7, Figure 8, App. B).

2.2.3. Sofular Section

Sofular Section was measured close to Sofular Village located in the northwestern part of Adana (Figure 1). This section partly covers the Köpekli Formation characterized by a shale and marl alternation (Figure 10, Figure 11 and App. B). A few argillaceous limestone beds measuring 20-40 cm in thickness were recognized at the middle part of the section and it continues upwards with shale and marl alternations (Figure 10, Figure 11 and App. B). The thicknesses of these shale and marl beds vary from 80 cm to 120 cm and from 20 cm to 40 cm, respectively (Figure 10, Figure 11 and App. B).

2.2.4. Çorlu Section

Çorlu Section comprising the uppermost part of the Köpekli Formation, the Cingöz Formation from bottom to top and lowermost part of the Güvenç Formation was measured in Çorlu Village located northwestern part of Adana (Figure 1). This section starts in the Köpekli Formation with shale and sandstone alternations (layers from sample TD-175 to TD-245 (Figure 12, Figure 13 and App. B). The thicknesses of the shale sequences and sandstone beds vary from 5 m to 9 m and from 2 cm to 10 cm, respectively (Figure 12 and App. B). The level corresponding to the sample TD-245 characterized by the first appearance of pebbly sandstone bed in the measured section marks the boundary between the Köpekli Formation and the Cingöz Formation (Figure 12, Figure 14 and App. B).

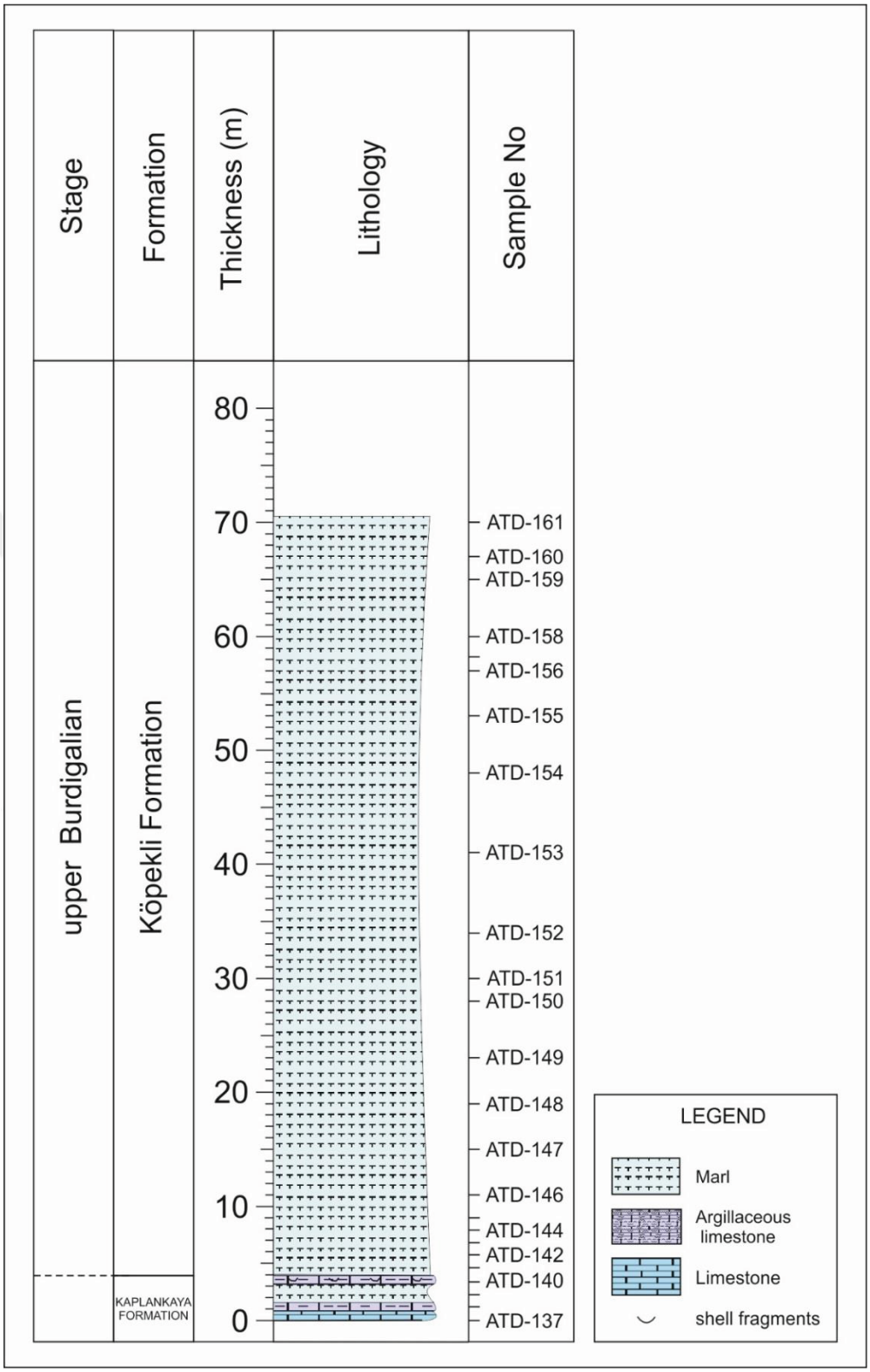

Figure 6. Köpekli Formation in the measured Çukurköy Section.

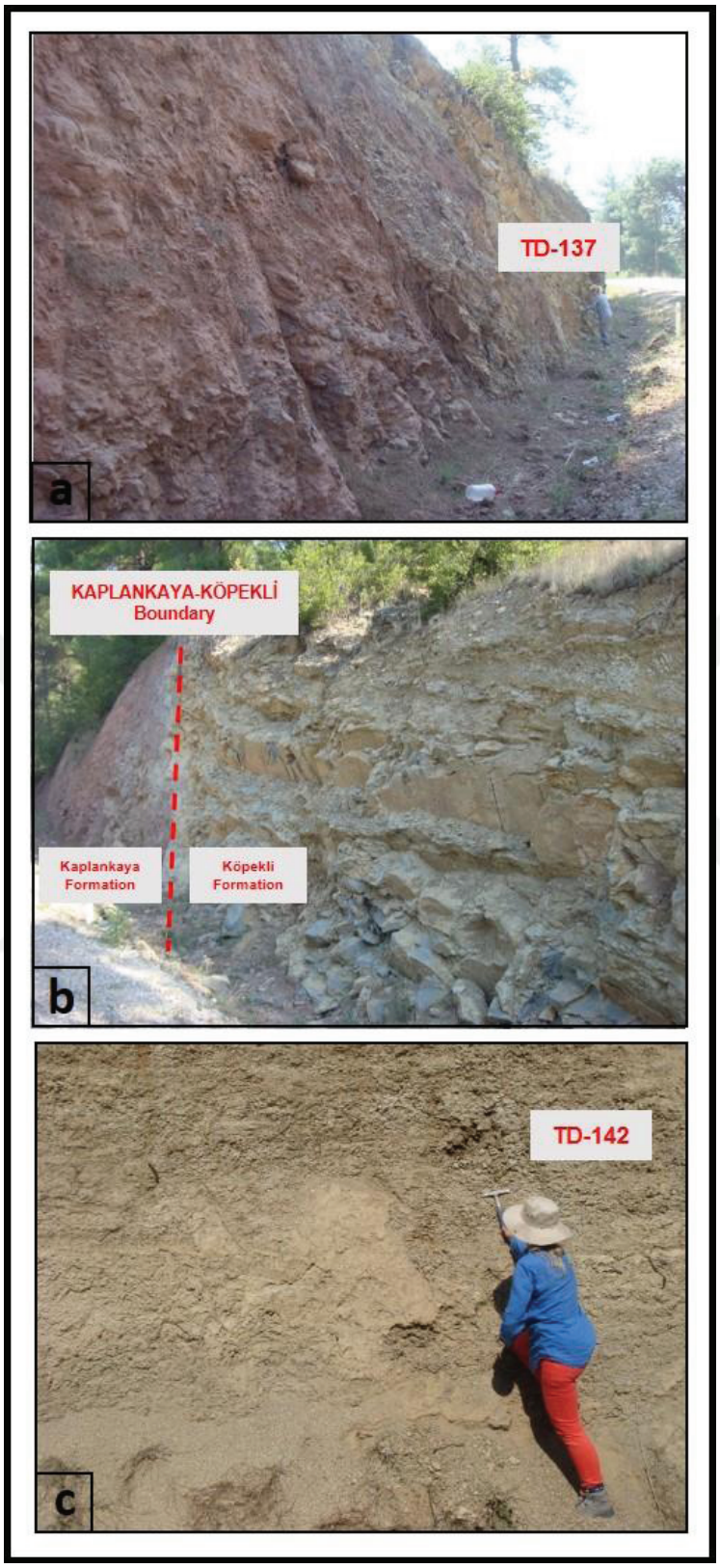

Figure 7. “a” and “c” show the field photos of the samples collected through the Köpekli Formation in the Çukurköy Section. “b” show the boundary between the Kaplankaya and Köpekli formations in the Çukurköy Section.

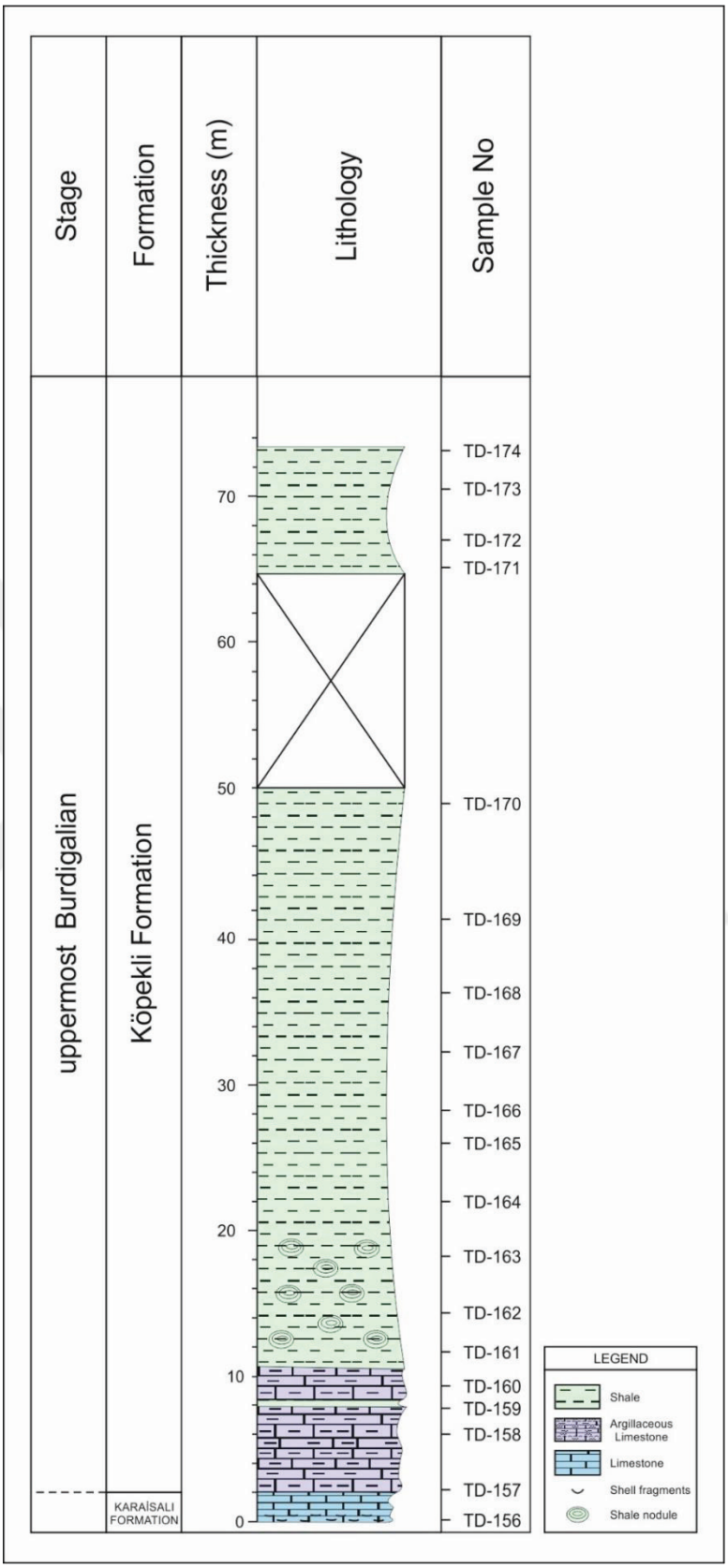

Figure 8. Köpekli Formation in the measured Köpekli Section.

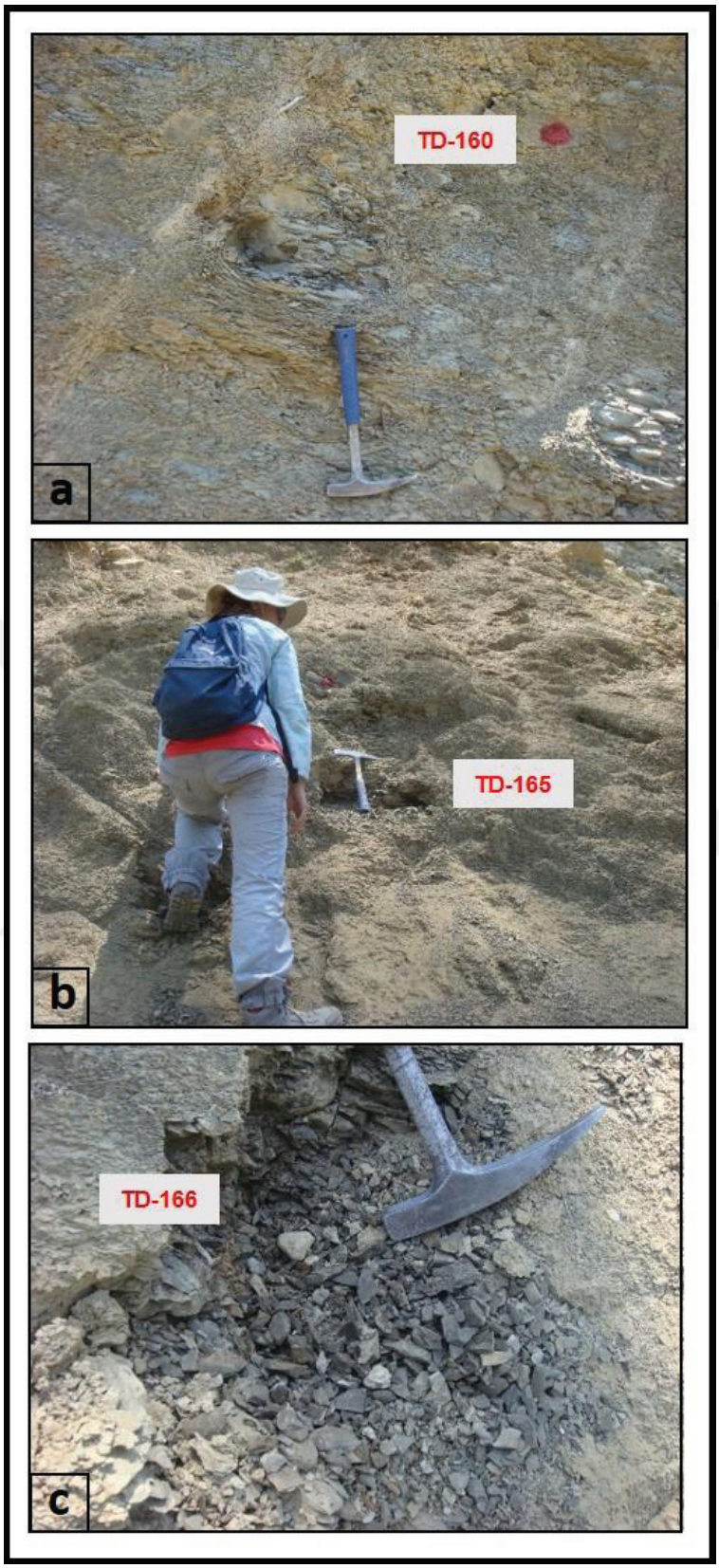

Figure 9. Field photos show the samples (a: TD-160; b: TD-165; c: TD-166) collected through the Köpekli Section.

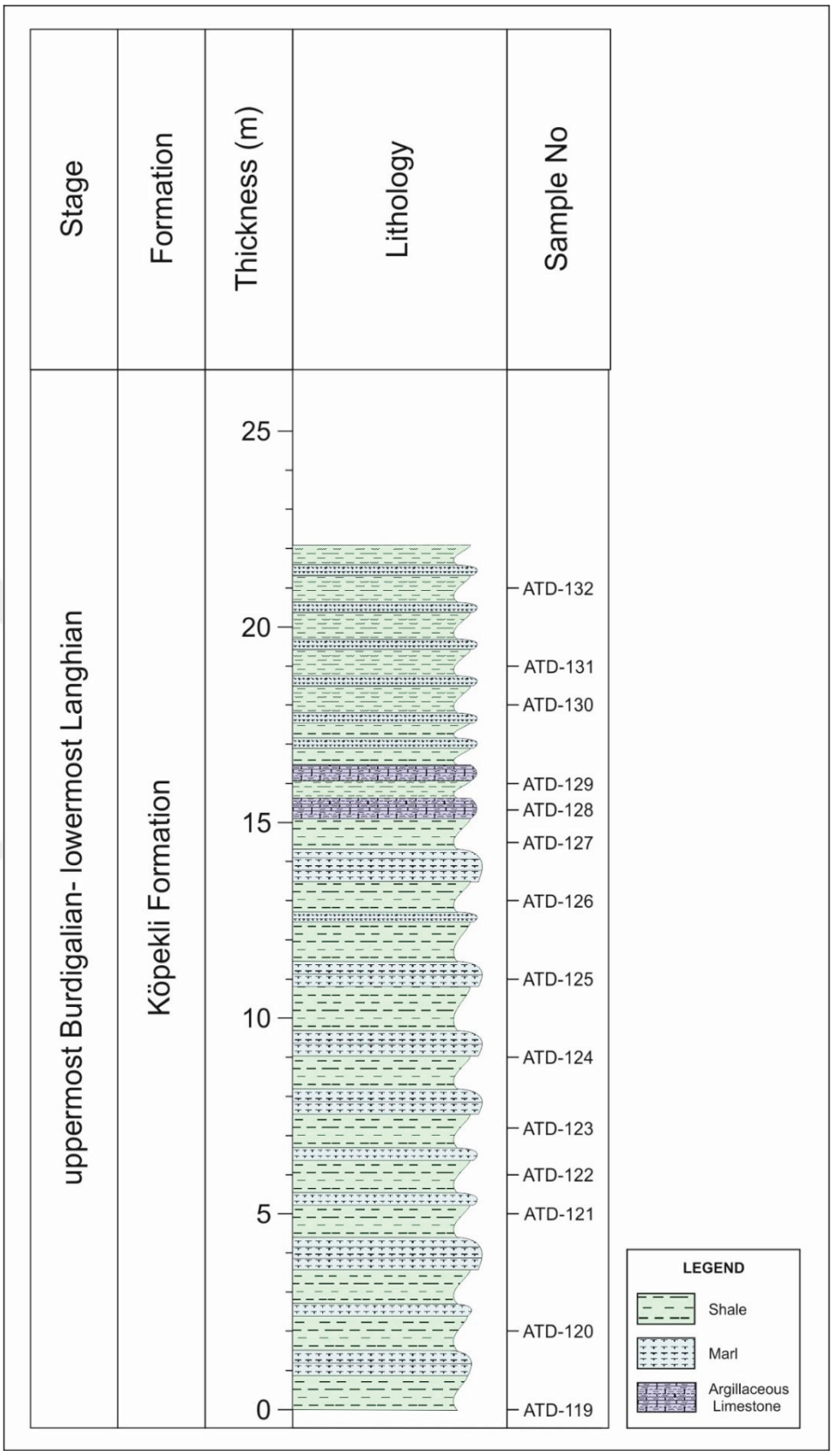

Figure 10. Köpekli Formation in the measured Sofular Section.

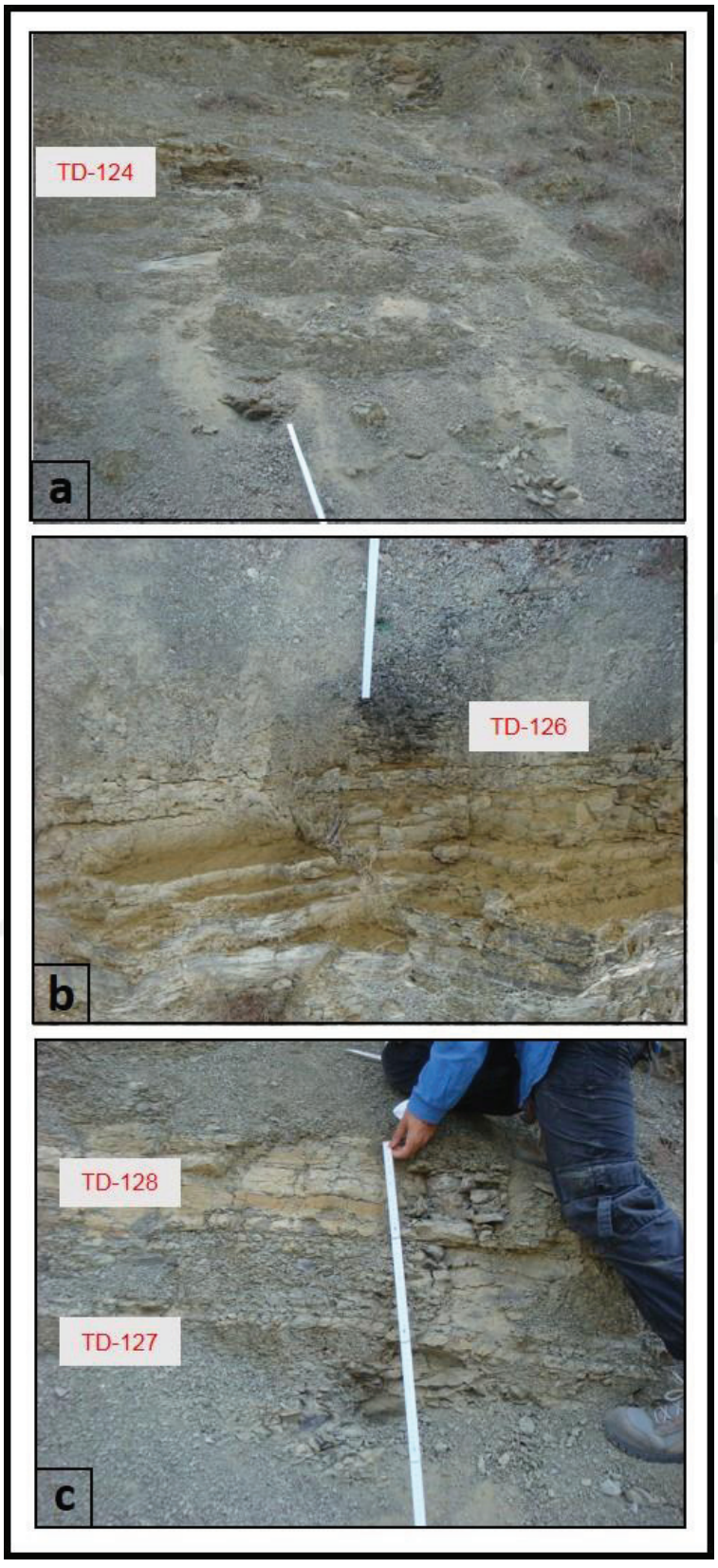

Figure 11. Field photos show the samples (a: TD-124; b: TD-126; c: TD-127 and TD-128) collected through the Köpekli Formation in the Sofular Section.

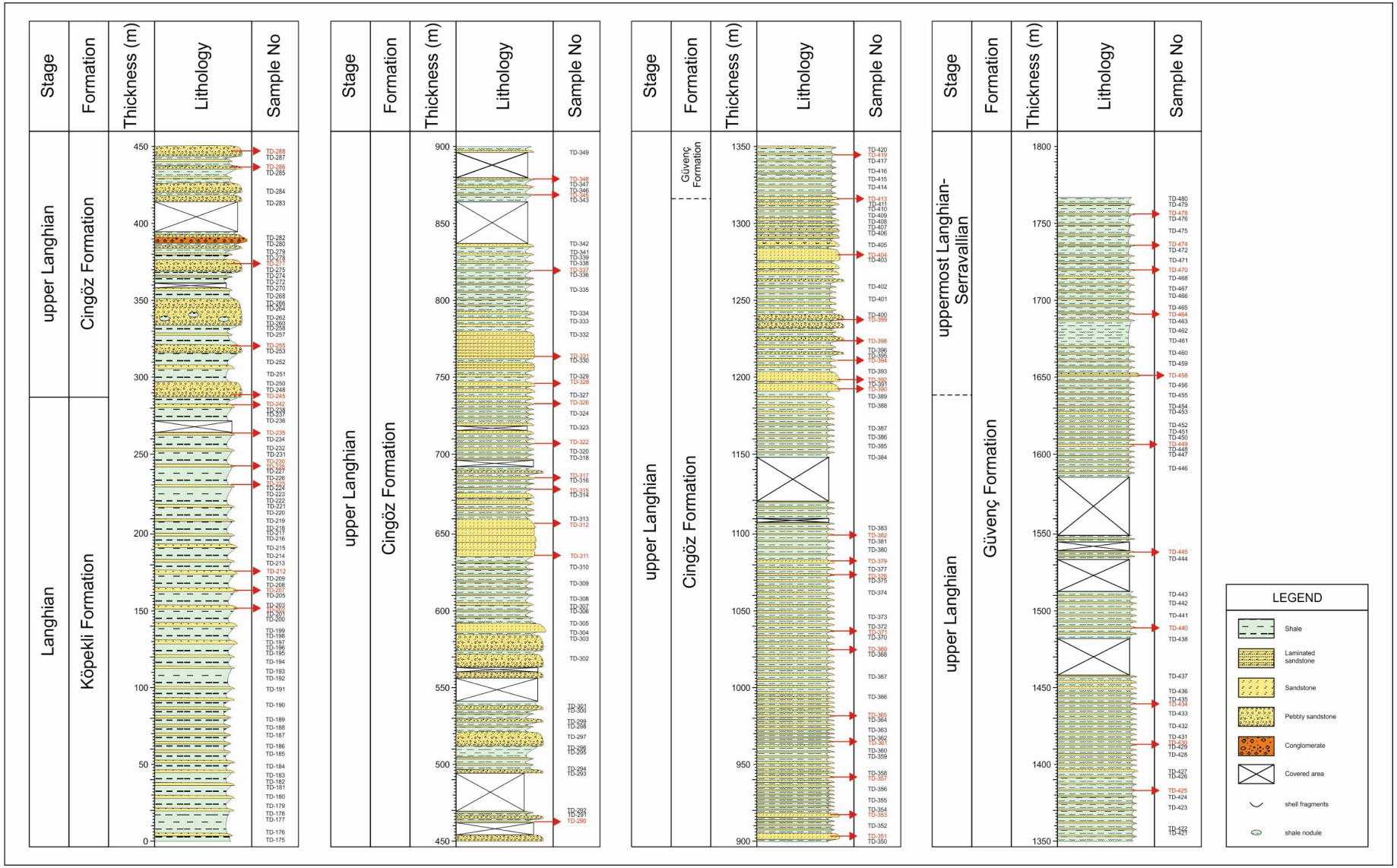

Figure 12. Köpekli, Cingöz and Güvenç formations in the measured Çorlu Section (red arrows show the collected sandstone samples).



Figure 13. Field photos show the samples (a: TD-184; b: TD-213; c: TD-231) collected through the Köpekli Formation in the Çorlu Section.

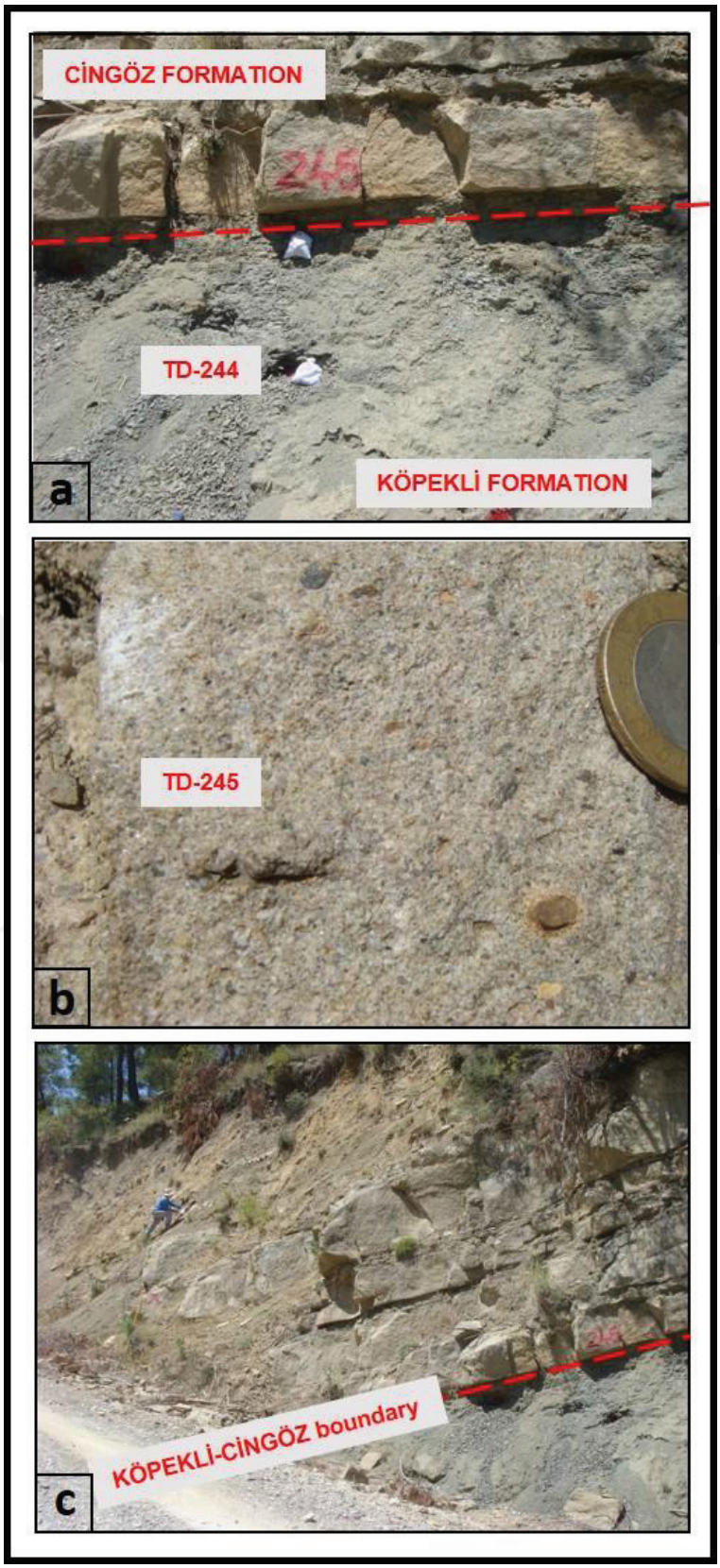

Figure 14. Field photos "show the boundary between the Köpekli and Cingöz formations in the Çorlu Section. ('b' shows the close up view of TD-245).

The Cingöz Formation with 1031.7 m thickness overlies the Köpekli Formation with a sharp contact and it is overlain by Güvenç Formation (Figure 12 and App. B). Above this level, poorly bedded, channelized conglomerates- pebbly sandstones- shale alternation representing a significant change in sedimentation pattern is recognized (layers from sample TD-245 to sample TD-305 (Figure 12 and App. B). The intervening shale layers are fissile, calcareous and carbonaceous. The level consisting of pebbly sandstone and shale alternations was first defined as the Ayva Member of the Cingöz Formation by Schimidt (1961). The thickness of the pebbly sandstone and shale sequences in this level varies from 40 cm to 400 cm and 10 cm to 150 cm, respectively. Some sedimentary structures (e.g. flute casts, groove casts, bioturbation) were also recognized in the sandstone beds within the measured section (Figure 15 and Figure 16). The section continues upwards with a thick succession of turbiditic sandstone-shale alternations (layers from sample TD-305 to sample TD-413 (Figure 12 and App. B)). Sand dominated sandstone-shale alternations were first defined as the Topallı Member of the Cingöz Formation by Schimidt (1961). The thickness of sandstone and shale sequences in this level varies from 10 cm to 600 cm and 5 cm to 90 cm, respectively. Laminated sandstone beds were also recognized at the level corresponding to the sample TD-406 and TD-407 (Figure 12, Figure 15 and App. B).

In the Çorlu Section, the Güvenç Formation overlies the Cingöz Formation at the level corresponding to the sample TD-413 (Figure 12, App. B). Above this level, intervening shale layers become dominant and the thickness and the number of the layers decrease (layers from sample TD-413 to sample TD-480 (Figure 12, Figure 17 and App. B)). Such an evidence shows that sedimentation is taking place at the deeper parts of the basin and the bathymetry is increasing. This level is considered as the Güvenç Formation that overlies the submarine fan deposits of the Cingöz Formation. The thickness of shale sequences and sandstone beds in this level varies from 20 cm to 5 m and 2 cm to 25 cm, respectively (Figure 12 and App. B).

2.2.5. Koruklu Section

Koruklu Section comprising the Güvenç Formation, was measured near the Koruklu Village located northwestern part of Adana (Figure 1). Koruklu Section is

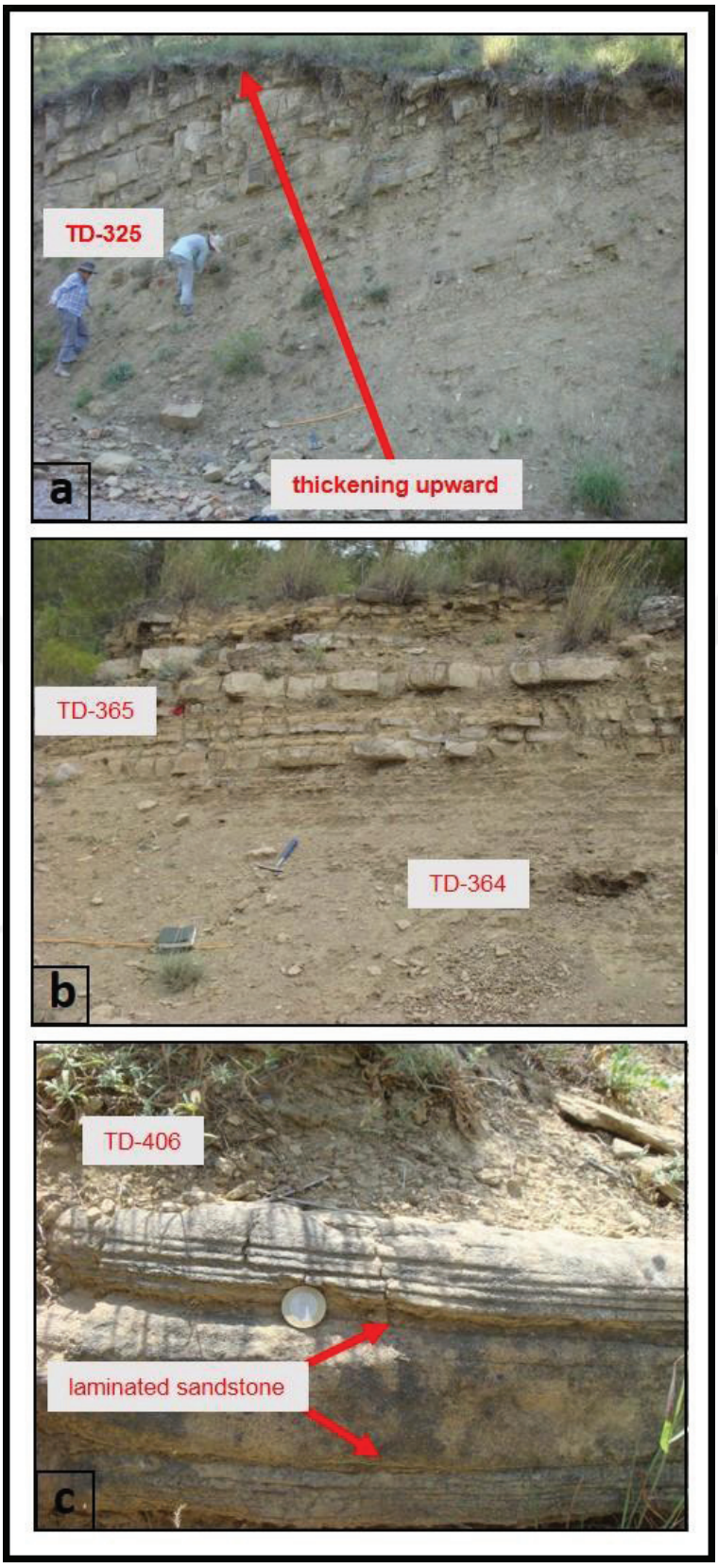

Figure 15. Field photos show the samples (a: TD-325; b: TD-364; c: TD-406) collected through the Cingöz Formation in the Çorlu section.

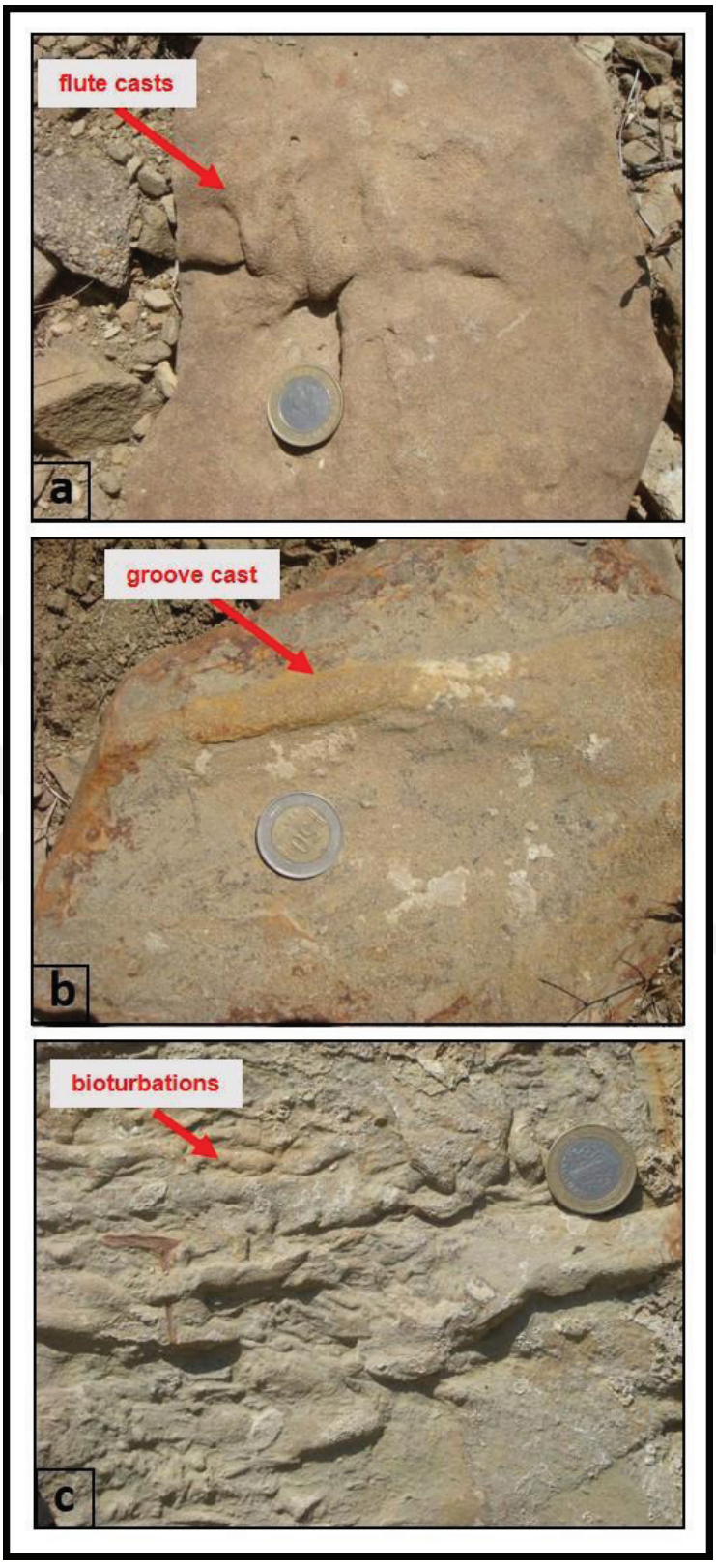

Figure 16. Field photos show the bottom sedimentary structures recognized in the sandstone beds within the Çorlu Section ('a' and 'b' show the close up view of the sandstone bed overlying the sample TD-284; 'c' show the close up view of the sample TD-315).

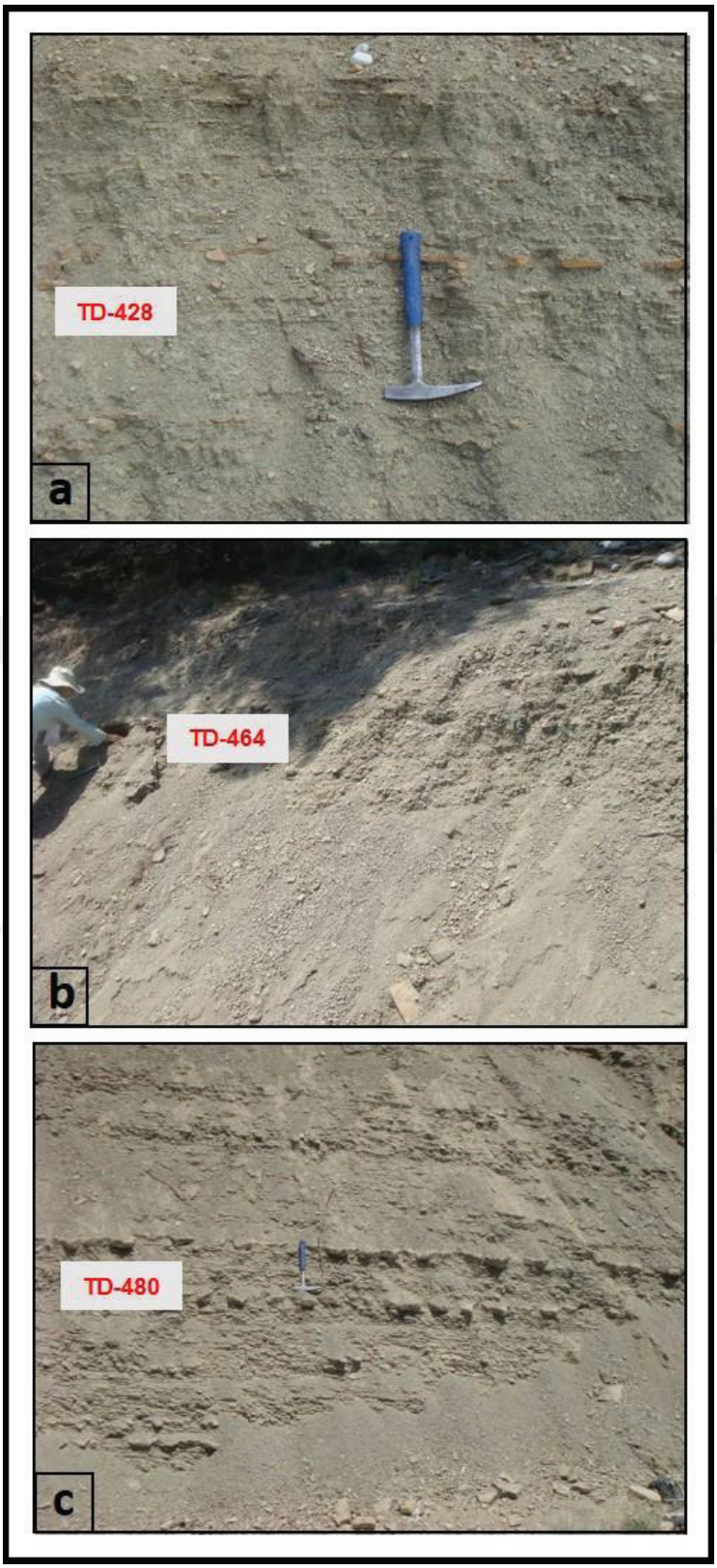

Figure 17. Field photos show the samples (a: TD-428; b: TD-464; c: TD-480) collected through the Güvenç Formation in the Çorlu section.

mainly characterized by shale and sandstone alternations (layers from sample ATD-59 to ATD-82 (Figure 18, Figure 19 and App. B)). In the lower part of the section (layers from sample ATD-59 to TD-61 (Figure 18 and App. B)), the thicknesses of the shale sequences and sandstone beds vary from 5 cm to 100 cm and from 5 cm to 20 cm, respectively. At the level corresponding to the samples from ATD-61 to ATD-62, laminated sandstone beds (measuring 35 cm) intercalated with thin shale layers were recognized (Figure 18, Figure 19 and App.B). It continues upwards with a shale dominated shale and sandstone alternations up to the level corresponding to sample ATD-71 (Figure 18 and App. B). A level characterized by the stacking pattern of thick sandstone sequences, measuring 8 m, was recognized (layers from sample ATD-71 to 2.5 m above the layer ATD-72 (Figure 18, Figure 19 and App. B). Then, the section continues upward with shale layers intercalated with thin sandstone beds (layers from sample ATD-72 to ATD-82 (Figure 18, Figure 19 and App. B).

2.2.6. Bekirli Section

Bekirli Section was measured close to the Bekirli Village located in the northwestern part of Adana (Figure 1). This section partly covers the Güvenç Formation characterized by shale and sandstone alternation (layers from ATD-1 to ATD-58 (Figure 20, Figure 21 and App. B)). The thicknesses of sandstone and shale sequences vary from 2 cm to 20 cm and 200 cm to 600 cm, respectively (Figure 20). The decrease in the number and thickness of sandy layers and becoming shale dominated lithology indicate a deposition in the deeper parts of the basin.

2.2.7. Güvenç Section

Güvenç Section was measured in the upper part of the Güvenç Formation and the lowermost part of the Kuzgun Formation close to the Güvenç Village located in the northwestern part of Adana (Figure 1). It mainly consists of shale layers intercalated with thin sandstone beds (Figure 22, Figure 23 and App. B). The thicknesses of the shale and sandstone sequence generally vary from 100 cm to 120 cm and from 2 cm to 10 cm, respectively (Figure 22 and App. B). Thick sandstone beds, measuring 20-25 cm in thickness, were recognized at only few levels (ATD-98 and ATD-104 (Figure

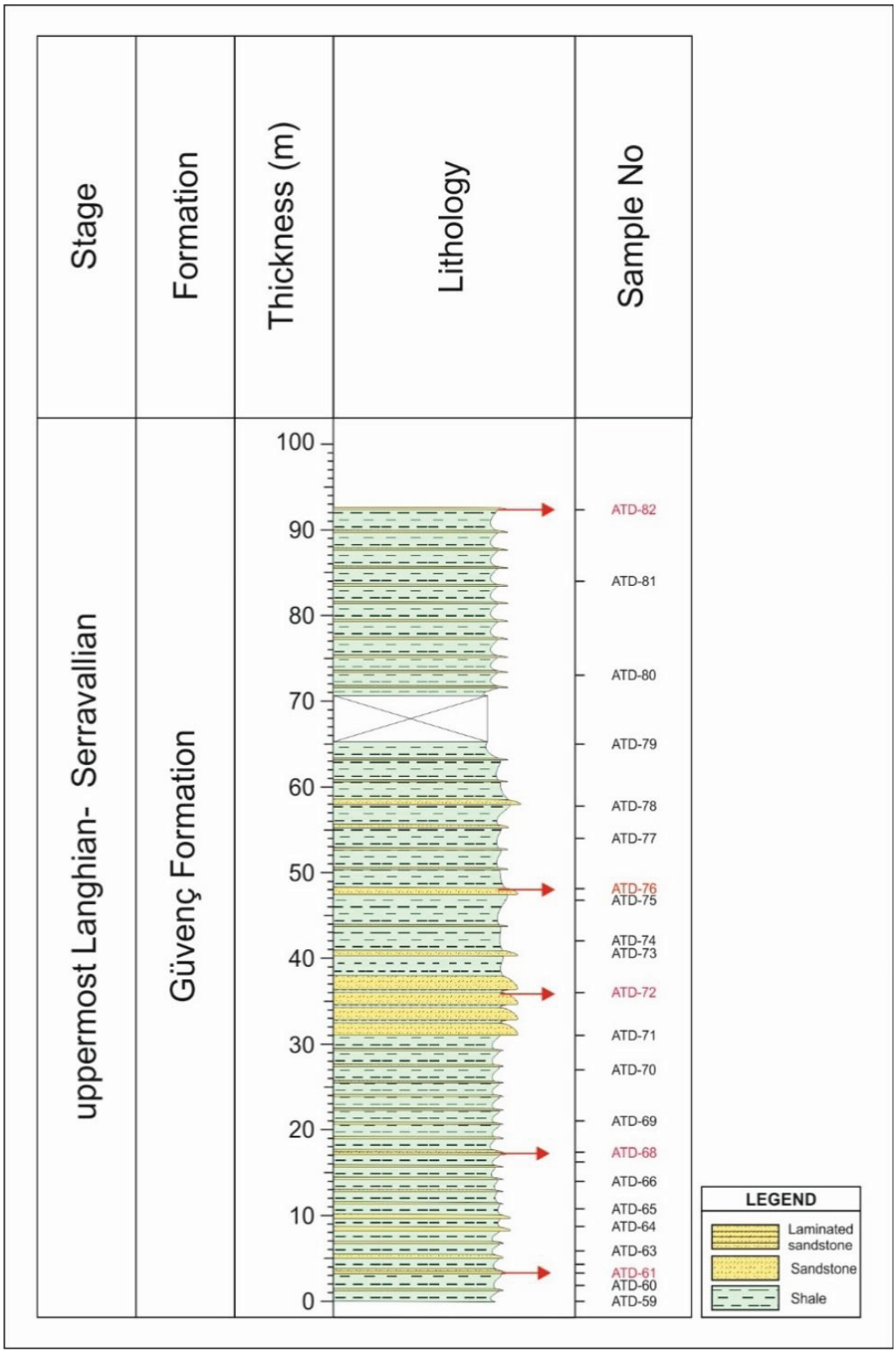

Figure 18. Güvenç Formation in the measured Koruklu Section (red arrows show the collected sandstone samples).

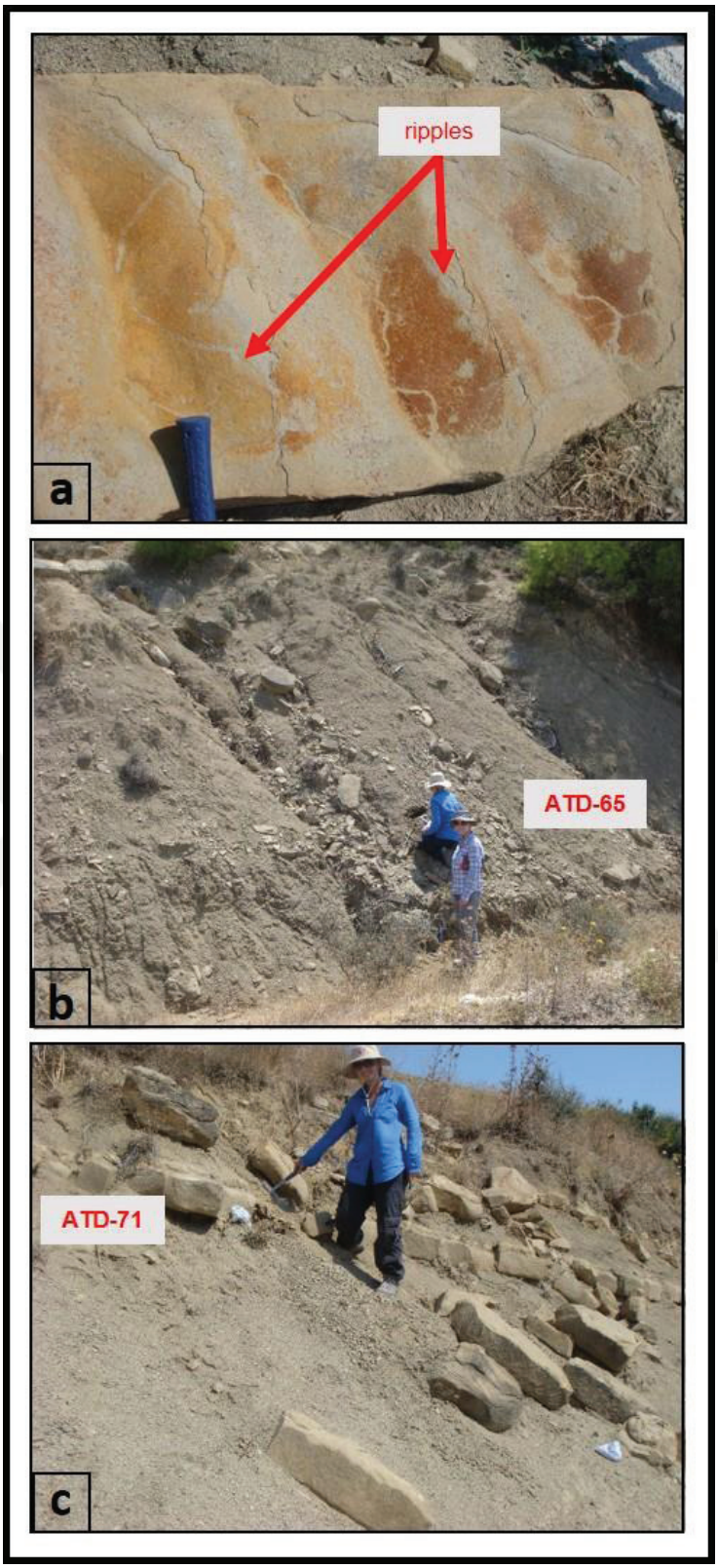

Figure 19. Field photos show the samples (a: Ripple marks were recognized on the surface of the sandstone bed overlying the sample ATD-60; b: ATD-65; c: ATD-71) collected through the Güvenç Formation in the Koruklu Section.

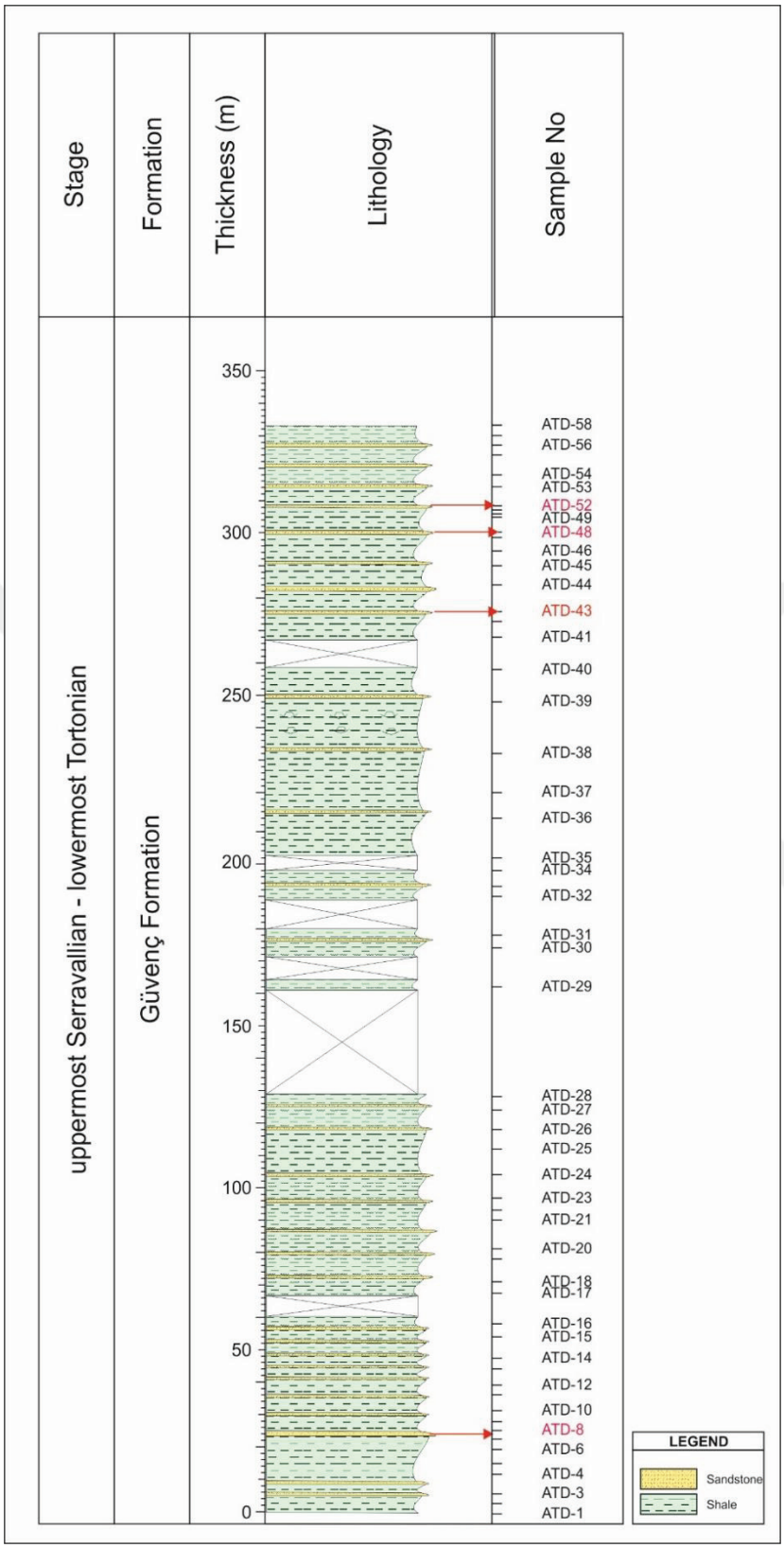

Figure 20. Güvenç Formation in the measured Bekirli Section (red arrows show the collected sandstone samples).

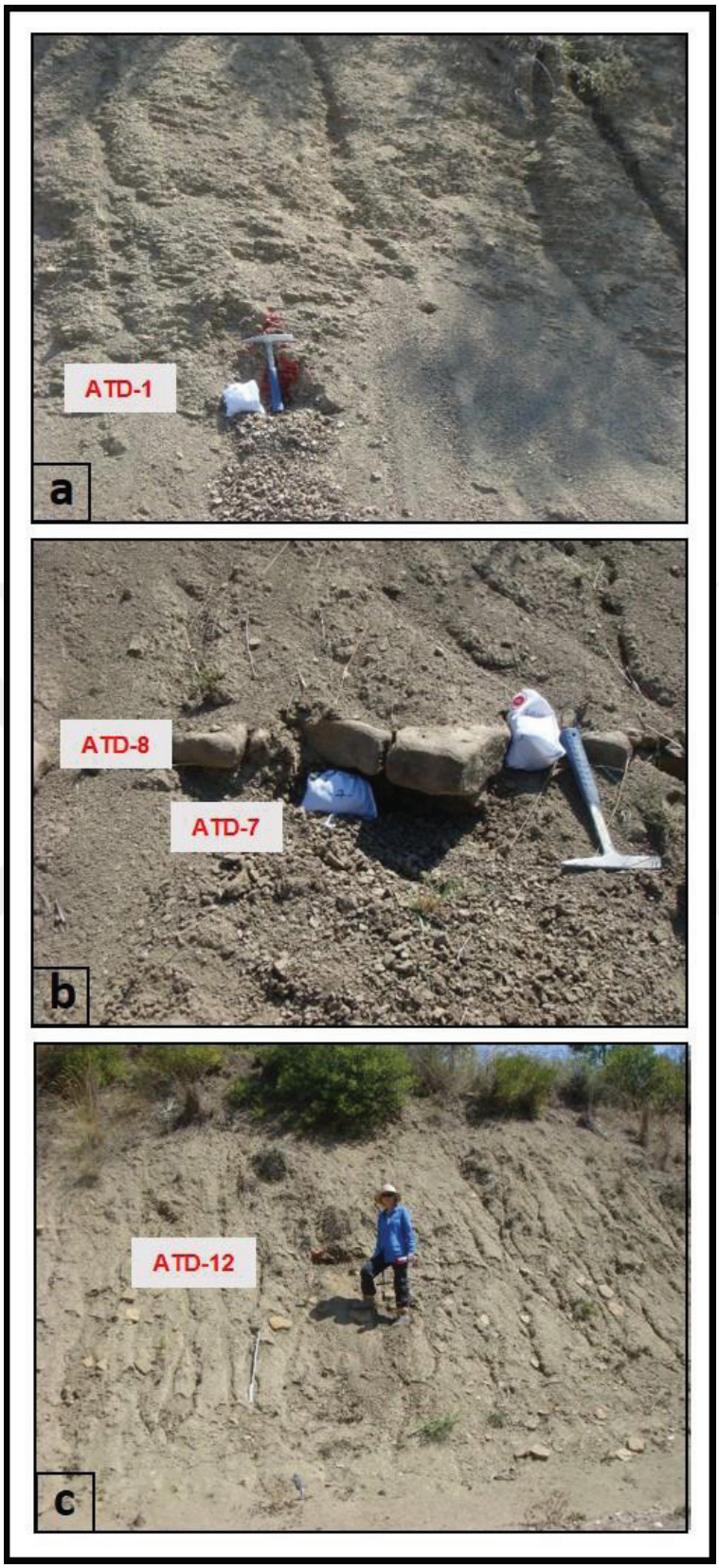

Figure 21. Field photos show the samples (a: ATD-1; b: ATD-7 and ATD-8 c: ATD-12) collected through the Güvenç Formation in the Bekirli Section.

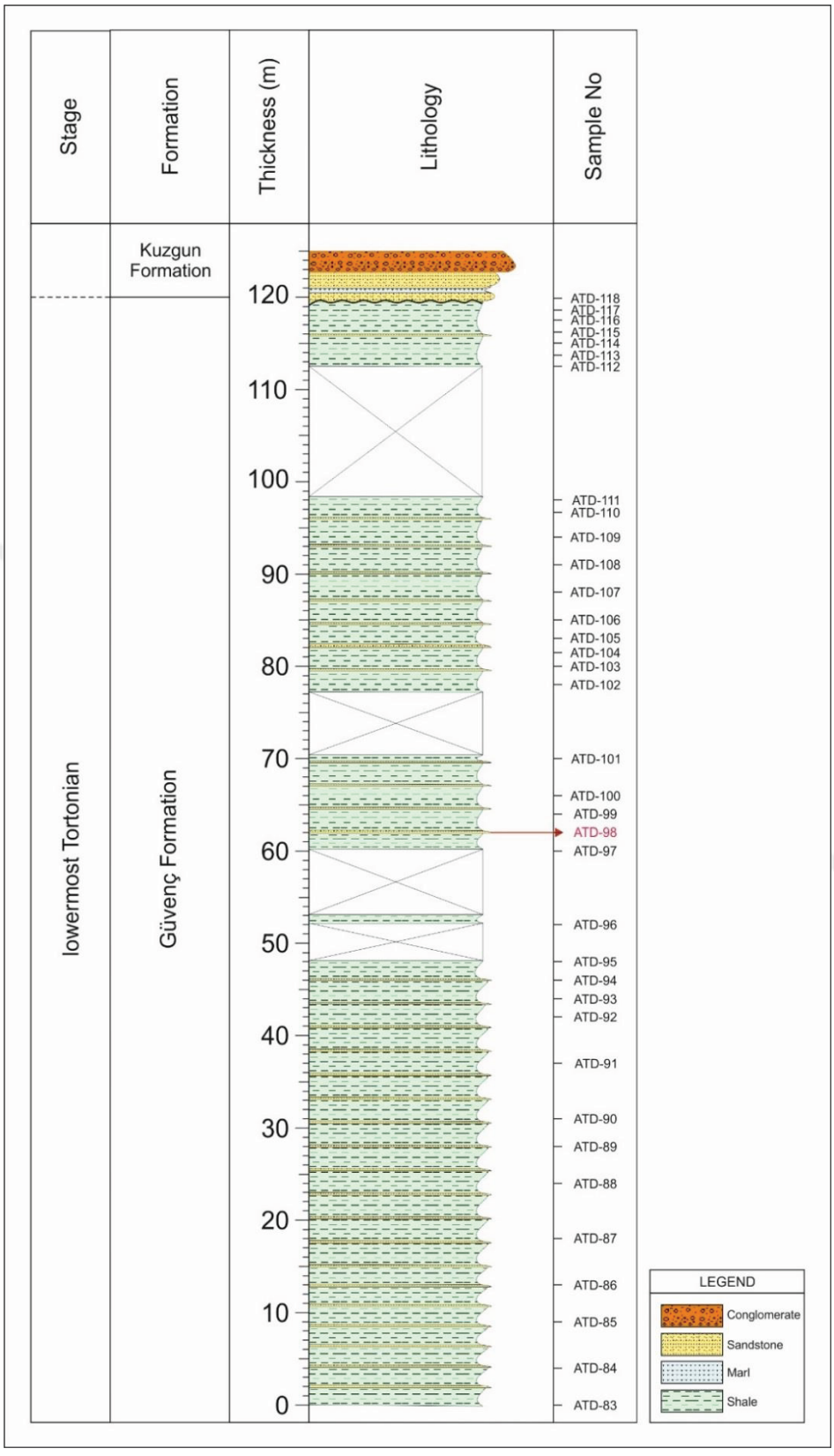

Figure 22. Güvenç Formation in the measured Güvenç Section (red arrow shows the collected sandstone sample).

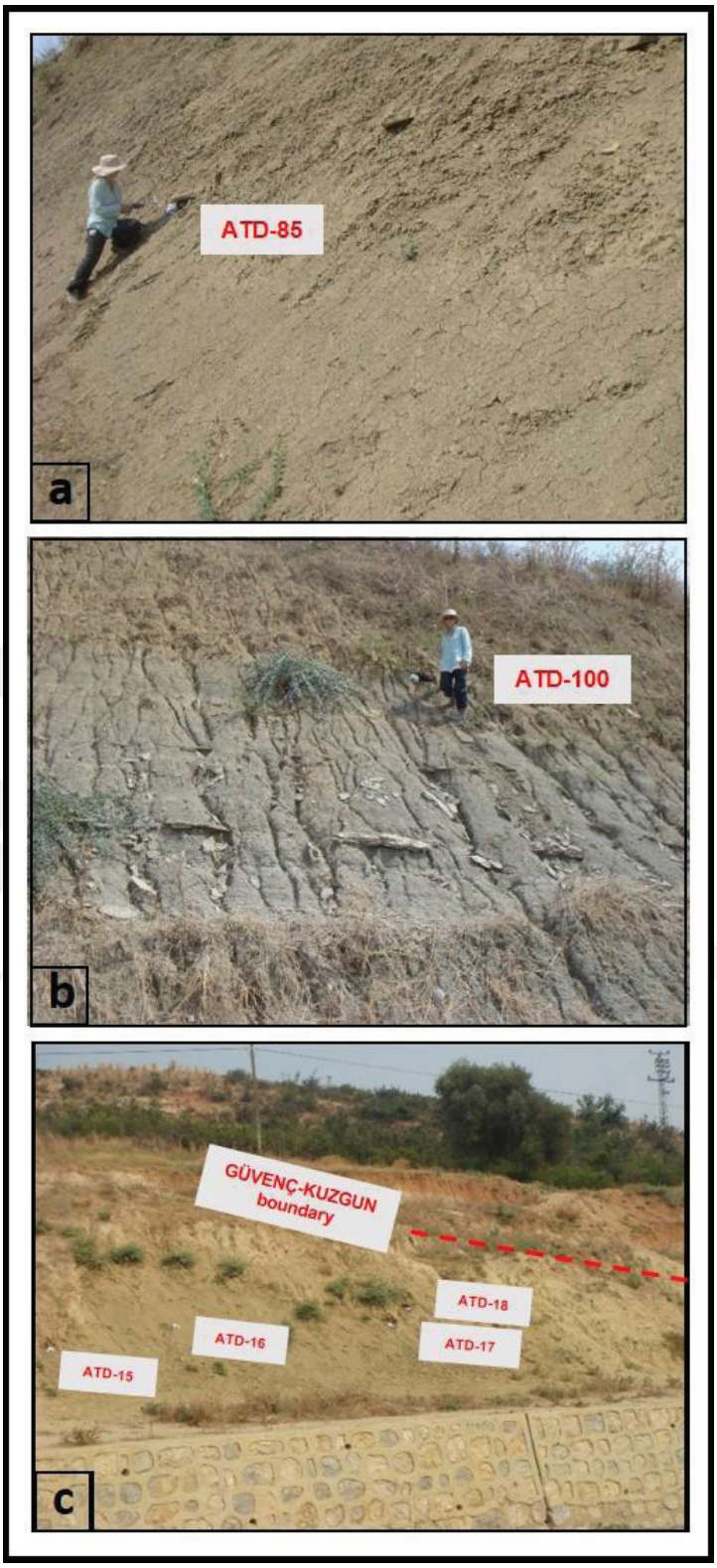

Figure 23. Field photos show the samples (a: Ripple marks were recognized on the surface of the sandstone bed overlying the sample ATD-85; b: ATD-100; c: ATD-115, ATD-116, ATD-117 and ATD-118) collected through the Güvenç Formation in the Güvenç Section. “c” also shows the boundary between the Güvenç and Kuzgun formations in the Güvenç Section.

22, Figure 23 and App. B). Güvenç Formation grades into the Kuzgun Formation by a thick conglomerate bed above the level corresponding to the sample ATD-118 and this boundary was also recognized by an erosional truncation (Figure 22, Figure 23 and App. B).

CHAPTER 3

BIOSTRATIGRAPHY

Neogene period began about 23 million years ago with the Miocene and it extends up to Pleistocene. Neogene palynology is increasingly attracting the attention of the scientific community due to the lack of data to construct a detailed dinocyst zonation for the Neogene clastic deposits all over the world and it represents one of the most climatically and evolutionary dynamic periods in the Earth history.

The paleontological studies played an important role in the investigation of the chronostratigraphic frame of Neogene deposits in the Adana basin. (e.g., Erünal-Erentöz, 1956; Schmidt, 1961; Öztümer et al., 1974; İlker, 1975; Nazik and Toker, 1986; Nazik and Gürbüz, 1991; Nazik and Gürbüz, 1992; Şafak, 1993 a,b; Şafak and Nazik, 1994; Özçelik and Yetiş, 1994; Nazik et al., 1997; Öğrünç and Nazik, 1998; Öğrünç et al., 2000; Fidancı, 2006; Sınacı and Toker, 2010; Darbaş and Nazik, 2010; Faranda et al., 2013). Nearly, all of these paleontological studies carried out in the Neogene sediments of the Adana Basin are based on planktonic foraminifera, nannoplankton and ostracods. The palynological framework has not been properly established in the Adana Basin yet and this study will be the first investigation carried out in this region. The potential of palynomorphs as a biostratigraphical tool for the Neogene interval has been well documented to construct the dinocyst zonation within the North Sea Basin, North Atlantic, North Western and South Western Europe in many studies (e.g., Piasecki, 1980; Powell, 1986; Herngreen, 1987; Biffi and Manum, 1988; Head et al., 1989; Daniels et al., 1990; Strauss, 1991; Brinkhuis et al., 1992; Powell, 1992; Rusbült and Straus, 1992; Strauss and Lund, 1992; Zevenboom, 1995; De Verteuil and Norris, 1996; Head, 1998; Laursen et al., 1998; Dybkjaer and Rasmussen, 2000; Strauss et al., 2001; Köthe, 2003; Munsterman and Brinkhuis, 2004; Powell and Brinkhuis, 2004; Rasmussen, 2004a, b; Dybkjaer, 2004a, b; Rasmussen et al., 2004; Piasecki, 2005; Rasmussen, 2005; Rasmussen and Dybkjaer, 2005;

Rasmussen et al., 2006; Dybkjaer and Rasmussen, 2007; Dybkjaer and Piasecki, 2008; Dybkjaer and Piasecki, 2010). In this study, a detailed biozonation based on palynomorphs has been constructed in the Miocene deposits of the Adana Basin for the first time. The established palynomorph biostratigraphy is documented in detail as below.

3.1. PALYNOMORPH BIOSTRATIGRAPHY

In order to investigate a detailed biozonation in Miocene deposits of the Adana Basin (Eastern Mediterranean), collected samples along the measured sections (Çukurköy Section, Köpekli Section, Sofular Section, Çorlu Section, Bekirli Section, Koruklu Section and Güvenç Section) were studied based on palynomorphs. A total number of 482 samples have been studied in terms of their palynomorph content. According to the first occurrences (FOs), the last occurrences (LOs) and the acme of selected taxa, 9 biozones, namely *Polysphaeridium zoharyi* Partial Range Zone (P-1), *Labyrinthodinium truncatum* Interval Zone (P-2), *Cerebrocysta poulsenii* Interval Zone (P-3), *Unipontidinium aquaeductus* Total Range Zone (P-4), *Paleocystodinium ventricosum* Interval Zone (P-5), *Cleistosphaeridium placacanthum* Interval Zone (P-6), *Operculodinium centrocarpum* Partial Range Zone (P7), *Achomosphaera* cf. *andalousiensis* Interval Zone (P-8) and *Homotryblium* Acme Zone (P-9), were established through Köpekli, Cingöz and Güvenç formations deposited during Miocene (Figure 24, Figure 25). Moreover, the established biozones were correlated with those of planktonic foraminifera and calcareous nannofossils.

3.1.1. Dinocyst Zonation

P-1. *Polysphaeridium zoharyi* Partial Range Zone

Assigned Age: late Burdigalian

Equivalent Planktonic Foraminiferal Zone: lower part of M4a Zone

Equivalent Nannoplankton Zone: NN4 Zone

Samples: from ATD-142 to ATD-146 (Çukurköy Section)

Definition: This interval is defined between the LO of ?*Cordosphaeridium cantharellus* and the FO of *Labyrinthodinium truncatum* and occurrence of

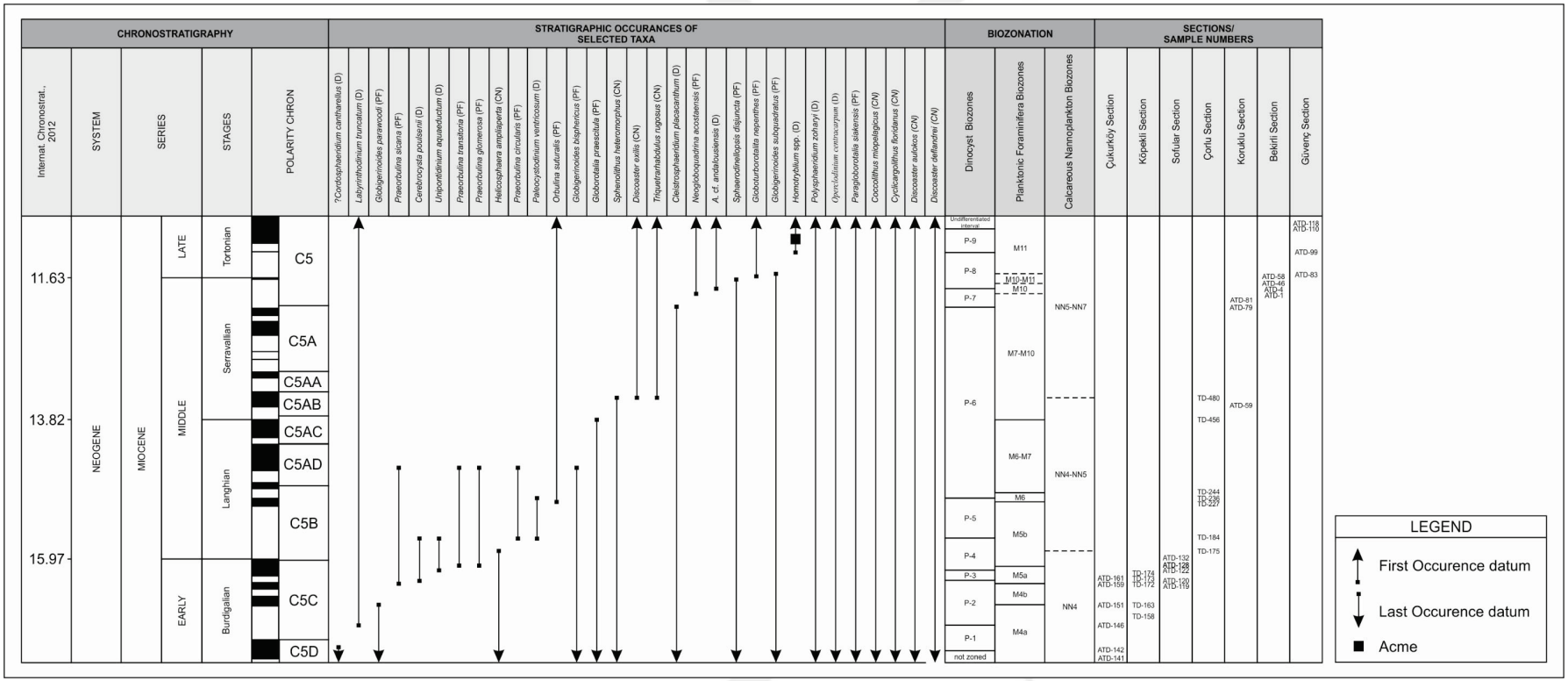

Figure 24. Bio-chronostratigraphic chart and stratigraphic occurrences of selected taxa (D: dinoflagellate; PF: planktonic foraminifer; CA: calcareous nannoplankton).

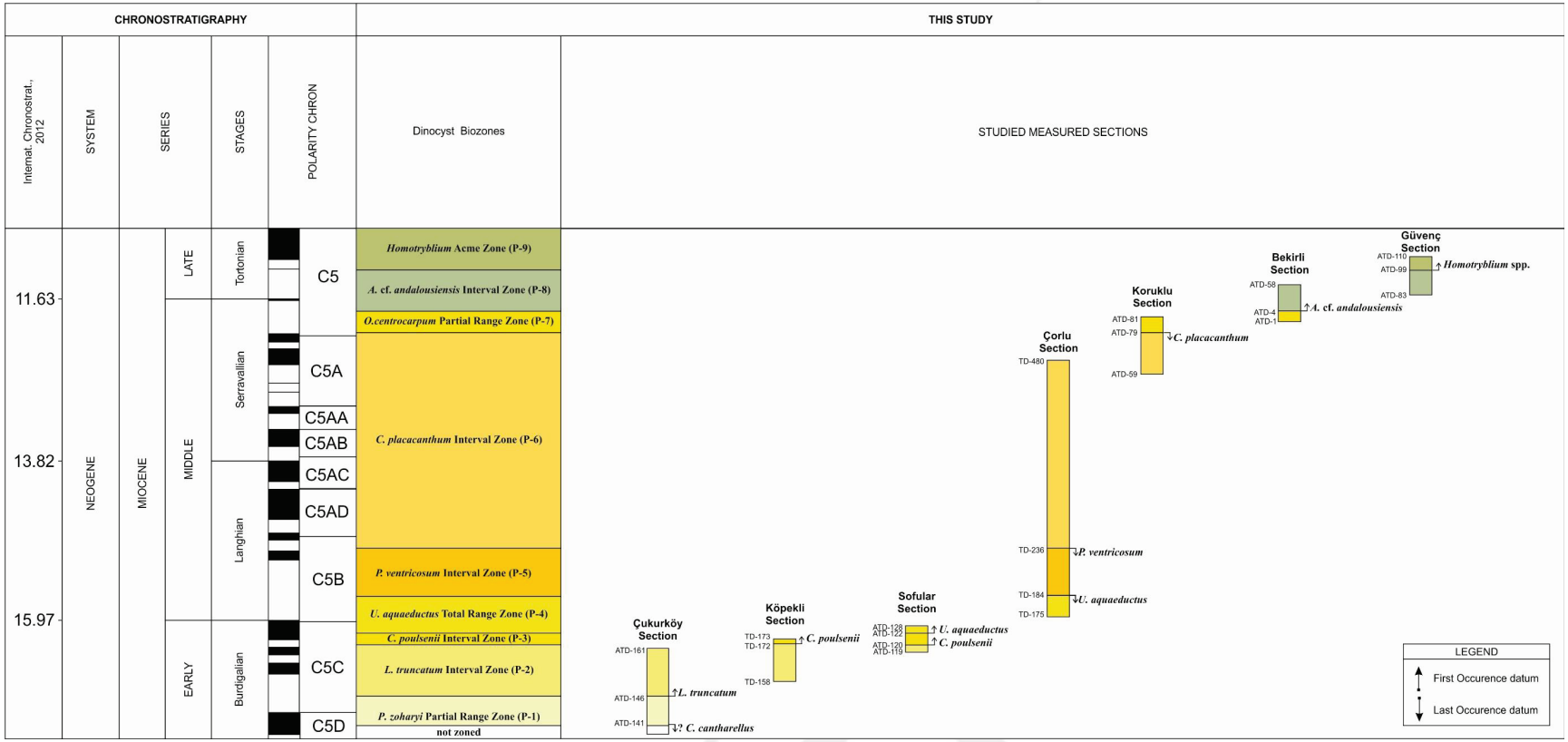

Figure 25. Correlation of the biozonations along each measured section.

Polysphaeridium zoharyi (Figure 24 and Figure 25). *Cleistrosphaeridium placacanthum* and *Lingulodinium machaerophorum* are some of the important dinocysts recognized within this zone. This zone is also characterized by a poor palynomorph assemblage. Türkecan *et al.* (submitted) have identified M4a Zone based on foraminifers in this interval. The top of this zone is defined by the LO of *Globigerinoides parawoodi* (Figure 24). *Globigerinoides bisphericus, Globorotalia praescitula*, *Sphaerodinellopsis disjuncta*, *Globigerinoides subquadratus* and *Paragloborotalia siakensis* are the main taxa defined within this zone (Figure 24). They have also distinguished NN4 Zone based on calcareous nannoplanktons in this interval. The top of this calcareous nannoplankton zone is defined by the LO of *Helicosphaera ampliaperta* (Figure 24). Based on biostratigraphical data, a late Burdigalian age is assigned for this interval.

P-2. *Labyrinthodinium truncatum* Interval Zone

Assigned Age: late Burdigalian

Equivalent Planktonic Foraminiferal Zone: upper part of M4a, M4b and lower part of M5a zones

Equivalent Nannoplankton Zone: NN4 Zone.

Samples: from ATD-146 to ATD-161 (Çukurköy Section); from TD-158 to TD-173 (Köpekli Section); from ATD-119 to ATD-120 (Sofular Section).

Definition: This interval is defined between the FO of *Labyrinthodinium truncatum* and the FO of *Cerebrocysta poulsenii* (Figure 24 and Figure 25). A significant acme of *Cleistrosphaeridium placacanthum* is recorded near the base of the zone and this acme is followed by a high abundance of *Lingulodinium machaerophorum*, *Melitasphaeridium choanophorum*, *Hystrichokolpoma rigaudiae* and *Spiniferites* spp.. FO of Compositae (liguliflorae-type) was also defined within this zone. Türkecan et al. (submitted) have defined M4a, M4b and M5b zones based on foraminifers in this interval. Two stratigraphically important planktonic foraminiferal events were defined within these zones. The first planktonic foraminiferal event is the LO of *Globigerinoides parawoodi*, which interpret the boundary between the M4a and M4b zones (Figure 24). The second one is the FO of *Praeorbulina sicana*, which marks the base of the M5a Zone. Türkecan *et al.* (submitted) have also identified NN4 Zone based on calcareous nannoplanktons within the same interval (Figure 24).

P-3. *Cerebrocysta poulsenii* Interval Zone

Assigned Age: Latest Burdigalian

Equivalent Planktonic Foraminiferal Zone: lower part of M5a Zone.

Equivalent Nannoplankton Zone: NN4 Zone.

Samples: from TD-173 to TD-174 (Köpekli Section); from ATD-120 to ATD-122 (Sofular Section).

Definition: The base of the zone is defined by the FO of *Cerebrocysta poulsenii* and the top is marked by the FO of *Unipontidinium aquaeductus* (Figure 24 and Figure 25). P-3 zone is composed of marine and terrestrial palynomorphs from rare to very rare. *Achomosphaera* cf. *andalousiensis, Cleistrosphaeridium placacanthum*, *Labyrinthodinium truncatum, Operclodinium centracarpum, Operclodinium piaseckii, Polysphaerdium zoharyi* and *Hystrichokolpoma rigaudiae* are some of the important Miocene dinoflagellates recognized
within this zone. The equivalent planktonic foraminiferal and nannoplankton zones of the P-3 Zone are M5a Zone and NN4 Zone, respectively (Türkecan *et al.*, submitted).

P-4. *Unipontidinium aquaeductus* Total Range Zone

Assigned Age: latest Burdigalian to earliest Langhian

Equivalent Planktonic Foraminiferal Zone: upper part of M5a Zone and lower part of M5b Zone.

Equivalent Nannoplankton Zone: NN4 and NN5 zones.

Samples: from ATD-122 to ATD-132 in the Sofular Section, from TD-175 to TD-184 in the Çorlu Section.

Definition: This interval is correspond to the total range of *Unipontidinium aquaeductus* (Figure 24 and Figure 25). The Sofular Section terminates within the limits of this zone, whereas the upper boundary of the zone is drawn by the last occurrence of the marker taxon at sample TD-184 in the Çorlu Section (Figure 24 and Figure 25). This zone contains diverse dinocyst assemblage and terrestrial taxa. A significant acme of *Operclodinium piaseckii* and a common occurrence of *Cerebrocysta poulsenii* are recorded within this zone. Türkecan et al. (submitted) identified M5a and M5b zones in this interval. The boundary between the M5a and M5b zones are defined by the FO of *Praeorbulina transitoria* and FO of *Praeorbulina glomerosa* (Figure 24). NN4-NN5 zones are also defined within this interval based on

calcareous nannoplanktons. The interval corresponding to these nannoplankton zones is characterized by the total range of *Sphenolithus heteromorphus* (Figure 24).

P-5. *Paleocystodinium ventricosum* Interval Zone

Assigned Age: Langhian

Equivalent Planktonic Foraminiferal Zone: upper part of M5b zone and lower part of M6 zone.

Equivalent Nannoplankton Zone: NN4 and NN5 zones.

Samples: from TD-184 to TD-236 in the Çorlu section.

Definition: The LO of *Unipontidinium aquaeductus* delimits the lower boundary of this zone, whereas the upper boundary is defined by the LO of *Paleocystodinium ventricosum*. This zone is characterized by a rich dinocyst assemblage including *Cleistosphaeridium ancyreum*, *Cleistosphaeridium placacanthum*, *Hystrichosphaeropsis obscura*, *Hystrichokolpoma rigaudiae, Labyrinthodinium truncatum*, *Lingulodinium machaerophorum*, *Operculodinium centrocarpum*, *Paleocystodinium ventricosum, Polysphaeridium zoharyi*, *Spiniferites mirabilis*, *Spiniferites pseudofurcatus*, *Spiniferites ramosus*, *Spiniferites* spp. and common long-ranging terrestrial taxa. In the Çorlu section, the upper part of the Köpekli Formation is not very suitable for the preservation of palynomorphs. Marine and terrestrial (non-bisaccate) palynomorphs are rare to very rare. Bisaccate pollen however are abundant throughout the section. upper part of M5b and lower part of M6 zones and NN4-NN5 zones are identifed in this interval based on foraminifers and nannofossils, respectively. The base of the M6 Zone is defined by the FO of *Orbulina suturalis* while the upper boundary of this zone cannot be detected properly due to unapropriate lithology. Based on biostratigraphical data derived from planktonic foraminifera and calcareous nannoplankton, a Langhian age is assigned for this interval.

P-6. *Cleistosphaeridium placacanthum* Interval Zone

Assigned Age: Langhian- Serravallian.

Equivalent Planktonic Foraminiferal Zone: M-6, M6-M7 and M7-M10 zones.

Equivalent Nannoplankton Zone: NN4-NN5 and NN5-NN7 zones

Samples: from TD-236 to TD-480 (Çorlu Section), from ATD-59 to ATD-79 (Koruklu Section).

Definition: This interval is defined between the LO of *Paleocystodinium ventricosum* and the LO of *Cleistosphaeridium placacanthum* (Figure 24 and Figure 25). Two different trends of species abundances were recorded within this zone. The first interval is caharacterized by a poor dinocysts assemblage whereas the second one is composed of a diverse dinocsyst taxa. There are also barren samples in some certain levels in this zone. M6, M6-M7 and M7-M10 zones and NN4-NN5 and NN5-NN7 zones are identifed in this interval based on foraminifers and nannofossils, respectively. Furthermore, the upper boundary of the interval corresponding to the M6-M7 zones were interpreted by the LO of *Globorotalia praescitula* (Figure 24). Additionally, the base of the interval corresponding to the M7-M10 zones are defined by the LO of *Globorotalia praescitula* and the top is marked by the FO of *Neogloboquadrina acostaensis*. The FO of *Triquetrorhabdulus rugosus* and *Discoaster exilis* and the LO of *Coccolithus miopelagicus*, *Cyclicargolithus floridanus, Discoaster aulokos* and *Discoaster deflandrei* differentiated the base and the top of the interval corresponding to the NN5-NN7 zones, respectively (Figure 24).

P-7. *Operculodinium centrocarpum* Partial Range Zone

Assigned Age: late Serrevalian

Equivalent Planktonic Foraminiferal Zone: M6-M10 zones and M10 Zone.

Equivalent Nannoplankton Zone: NN5-NN7 zones.

Samples: from ATD-79 to ATD-81 (Koruklu Section) and from ATD-1 to ATD-4 (Bekirli Section).

Definition: This interval is defined between the LO of *Cleistosphaeridium placacanthum* and the FO of *A* cf. *andalousiensis* and occurrence of *Operculodinium centrocarpum* (Figure 24 and Figure 25). This zone is characterized by a poor palynomorph assemblage. *Labyrinthodinium truncatum*, *Lingulodinium machaerophorum*, *Operclodinium centrocarpum* and *Spiniferites mirabilis* are some of the important Miocene dinoflagellates recognized within this zone. A common occurrence of Compositae (liguliflorae-type) is also detected in this zone. This interval contains a poor planktonic foraminifera and calcareous nannofossil assemblage in the Koruklu Section. Consequently, a detailed biozonation can not be achieved by

foraminifers and nannofossils in this section and the equivalent planktonic foraminiferal and calcareous nanoplakton zones are defined as M6-M10 and NN5-NN7 zones, respectively. Unlike in the Koruklu Section, the interval in the Bekirli Section is characterized by a relatively diverse planktonic foraminiferal assemblage. The base of the M10 Zone is differentiated by the FO of *Neogloboquadrina acostaensis* and the top is marked by the LO of *Sphaerodinellopsis disjuncta* (Figure 24).

P-8. *Achomosphaera* cf. *andalousiensis* Interval Zone

Assigned Age: latest Serravallian to earliest Tortonian

Equivalent Planktonic Foraminiferal Zone: M10 and M11 zones.

Equivalent Nannoplankton Zone: NN5-NN7 Zones.

Samples: from ATD-4 to ATD-58 (Bekirli Section) and from ATD-83 to ATD-99 (Güvenç Section).

Definition: This interval is defined between the FO of *A.* cf. *andalousiensis* and the FO of *Homotryblium tenuispinosum* (Figure 24 and Figure 25). This zone is composed of a diverse dinocysts assemblage including *Achomosphaera* cf. *andalousiensis*, *Cleistosphaeridium ancyreum, Hystrichokolpoma rigaudiae*, *Hystrichosphaeropsis obscura, Labyrinthodinium truncatum*, *Lingulodinium machaerophorum*, *Melitasphaeridium choanophorum, Nematosphaeropsis labyrinthus, Operclodinium centrocarpum*, *Polysphaeridium zoharyi*, *Spiniferites mirabilis, Spiniferites pseudofurcatus, Spiniferites ramosus* and *Spiniferites bentorii*. Although the terrestrial taxa forms the main constituents of this zone, they are all long-ranging terrestrial taxa and they are not stratigraphically important. M10 and M11 zones and NN5-NN7 zones are the equivalent biozones based on foraminifers and nannoplanktons, respectively (Figure 24).

P-9. *Homotryblium* Acme Zone

Assigned Age: earliest Tortonian

Equivalent Planktonic Foraminiferal Zone: M11 Zone

Equivalent Nannoplankton Zone: NN5-NN7 zones.

Samples: from ATD-99 to ATD-110 (Güvenç Section).

Definition: This zone is mainly characterized by the acme of *Homortyblium* dinoflagellate cysts including *Homotryblium floripes*, *Homotryblium pallidum*, *Homotryblium plectilum* and *Homotryblium tenuispinosum* (Figure 24 and Figure 25). This zone also includes a rich and diverse palynomorph assemblage. The equivalent planktonic foraminiferal zone is M11 Zone in this interval. The base of this zone is defined by the FO of *Globoturborotalita nepenthes* and this zone terminates in the limits of the Güvenç Section. NN5-NN7 zones are also interpreted in the same interval based on nannofossils (Figure 24).

3.2. BIOSTRATIGRAPHY OF THE MEASURED STRATIGRAPHIC SECTIONS

The distributions of biozones throughout the stratigraphic sections are explained in detail in the following sections.

3.2.1. Çukurköy Section

The Çukurköy Section consists of P-1 and P-2 zones indicating deposition during late Burdigalian (Figures 24, 25 and 26). P-1 Zone defined in this study corresponds to the lower part of M4a planktonic foraminifera zone, whereas P-2 Zone corresponds to the upper part of M4a, M4b and the lower part of M5a planktonic foraminifera zones (Türkecan et al., submitted) (Figure 27). Both P-1 and P-2 zones are equivalent to NN4 nannoplankton zone (Türkecan et al., submitted) (Figure 27).
P-1 Zone was defined in the lower part of the Çukurköy Section and corresponds to the lowermost part of the Köpekli Formation. This interval consists of marl layers intercalated with argillaceous limestone beds containing shell fragments from samples ATD-142 to ATD-146 (Figure 26). The base of P-1 Zone is interpreted by the LO of ?*Cordosphaeridium cantharellus* and the top of this zone is defined by the FO of *Labyrinthodinium truncatum* (Figure 24 and Figure 25). P-1 zone is mainly characterized by a poor dinocyst assemblage including *Achomosphaera* cf. *andalousiensis*, *Achomosphaera* sp., *Cleistosphaeridium placacanthum*, ?*Cordosphaeridium cantharellus*, *Cordosphaeridium* spp., *Cribroperidinium* sp., *Hystrichokolpoma rigaudiae*, *Impagidinium* sp., *Lingulodinium machaerophorum*,

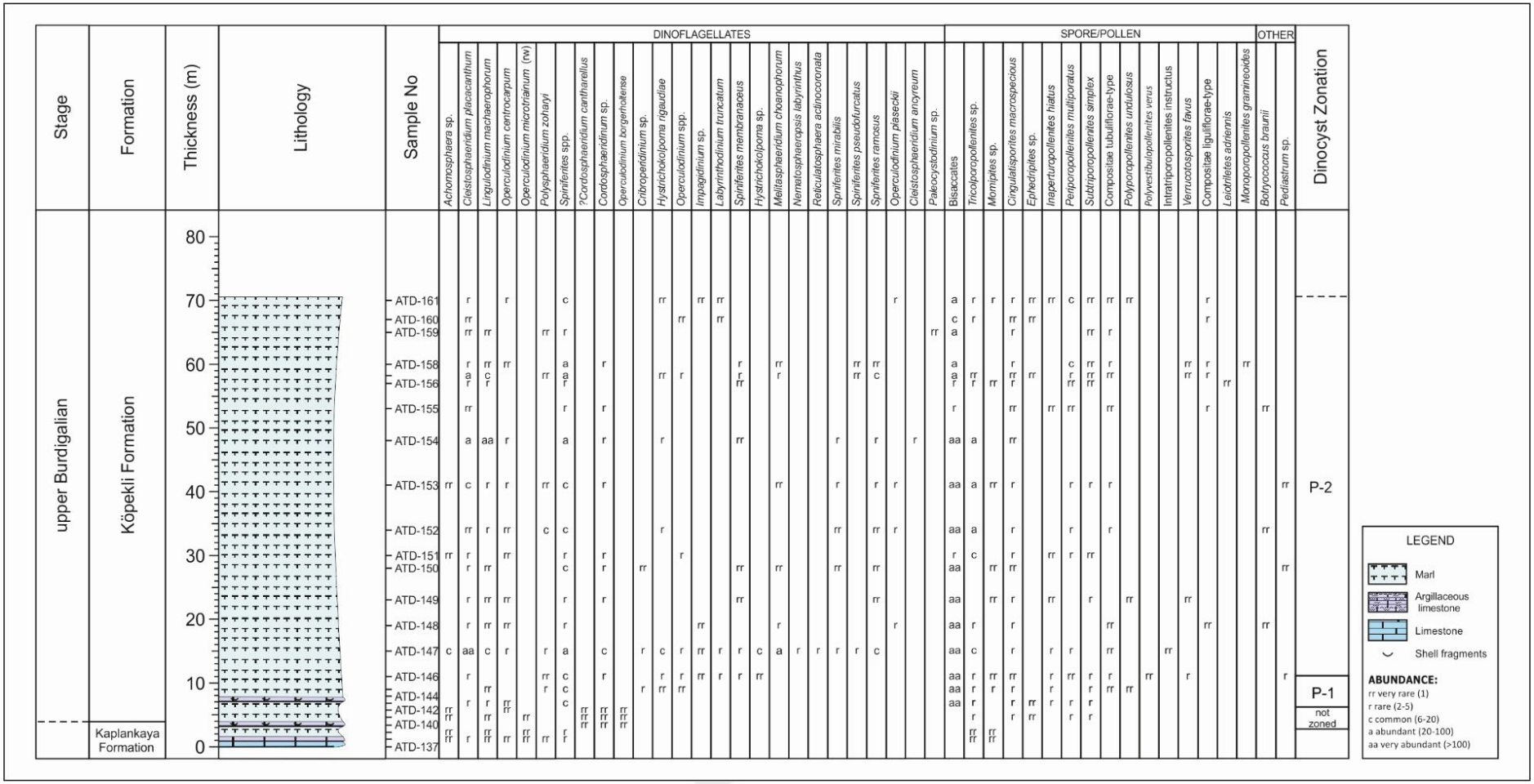

Figure 26. Stratigraphic range chart of palynomorphs and biostratigraphy in the Çukurköy Section.

Operculodinium borgerholtense, *Operclodinium centrocarpum*, *Operculodinium* spp., *Polysphaeridium zoharyi*, *Polysphaeridium* sp., *Spiniferites membranaceus* and *Spiniferites* spp. The terrestrial palynomorph assemblage is rich and diverse in the P-1 Zone and dominated by *Polyvestibulopollenites verus*, Bisaccates, *Cingulatisporites macrospecious,* Compositae (tubuliflorae-type), *Ephedripites* sp., *Inaperturopollenites hiatus, Intratriporopollenites instructus, Periporopollenites multiporatus, Polyporopollenites undulosus, Subtriporopollenites simplex, Tricolporopollenites* sp., *Triatriopollenites excelsus* and *Verrucatosporites favus.* P-1 Zone is also characterized by a common reworked taxa (e.g. *Operclodinium microtriainum*).

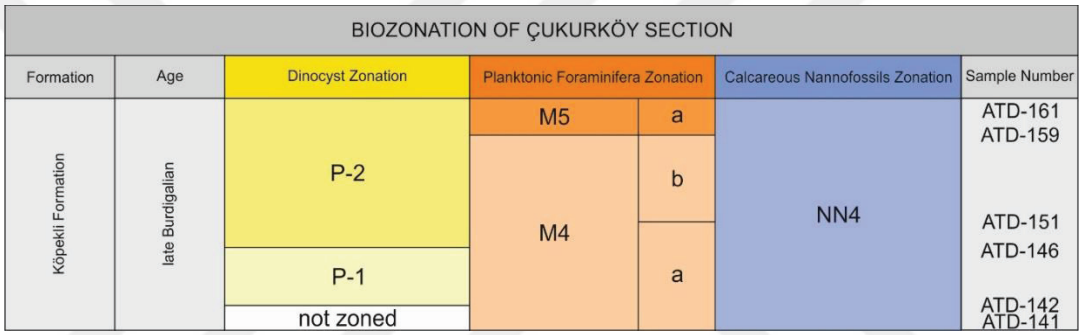

Figure 27. Correlation of the biozones based on palynomorphs, planktonic foraminifera and calcareous nannoplankton in the Çukurköy Section.

P-2 Zone overlies the P-1 Zone and comprises the interval from sample ATD-146 to ATD-161 (Figure 24, Figure 25 and Figure 26). This interval is characterized by a thick sequence of marn. The lower boundary of P-2 Zone is characterized by the entry of *Labyrinthodinium truncatum* (Figure 24). The taxa characterizing P-1 Zone are still present in the P-2 Zone, except the reworked taxon of *Operclodinium microtriainum*. P-2 Zone contains a very rich and diverse offshore dinocyst assemblage including; *Achomosphaera* cf. *andalousiensis*, *Achomosphaera* sp., *Cleistosphaeridium placacanthum*, *Cleistosphaeridium* sp., *Cordosphaeridium* spp., *Cribroperidinium* sp., *Hystrichokolpoma rigaudiae*, *Impagidinium* sp., *Impletosphaeridium* sp., *Labyrinthodinium truncatum*, *Lingulodinium machaerophorum*, *Melitasphaeridium choanophorum, Nematosphaeropsis labyrinthus, Operculodinium centrocarpum*, *Operculodinium piaseckii, Operculodinium* spp., *Palaeocystodinium* sp., *Polysphaeridium zoharyi*,

Polysphaeridium sp., *Reticulatosphaera actinocoronata, Spiniferites membranaceus*, *Spiniferites mirabilis, Spiniferites pseudofurcatus, Spiniferites ramosus, Spiniferites solidago* and *Spiniferites* spp. (Figure 26). The content of terrestrial palynomorph assemblage within the P-2 Zone is variable including *Polyvestibulopollenites verus*, *Cingulatisporites macrospecious,* Compositae (tubuliflorae-type), Compositae (liguliflorae-type), *Ephedripites* sp., *Monoporopollenites gramineoides*, *Inaperturopollenites hiatus, Intratriporopollenites instructus, Leiotriletes adriennis, Periporopollenites multiporatus, Polyporopollenites undulosus, Subtriporopollenites simplex, Tricolporopollenites* sp., *Triatriopollenites excelsus* and *Verrucatosporites favus* (Figure 26). These long-ranging terrestrial taxa recognized through the Çukurköy Section are not biostratigraphically significant.

Based on the biostratigraphical data, the Köpekli Formation in the measured Çukurköy Section started to deposit in the Adana Basin during the late Burdigalian (Figure 24, Figure 25 and Figure 26).

3.2.2. Köpekli Section

The Köpekli Section comprises P-2 and P-3 zones indicating deposition during the late Burdigalian (Figure 24, Figure 25 and Figure 28). The equivalent planktonic foraminifera zones and the nannoplankton zone of the P-2 Zone in this section are the upper part of M4a, M4b and the lowermost part of M5a zones and the NN4 Zone, respectively (Türkecan et al., submitted) (Figure 24 and Figure 29). P-3 Zone defined in this section corresponds to the lower part of M5a planktonic foraminifera zone and the NN4 nannoplankton zone (Türkecan et al., submitted) (Figure 24 and Figure 29).

P-2 Zone corresponds to the interval from sample TD-158 to TD-173 through the Köpekli Section (Figure 28). P-2 Zone is characterized by a rich and a diverse dinocyst assemblage including *Achomosphaera* sp, *Cribroperidinium tenuitabulatum*, *Cribroperidinium* sp., *Glaphyrocysta* sp., *Labyrinthodinium truncatum*, *Lingulodinium machaerophorum*, *Operclodinium centrocarpum*, *Operculodinium piaseckii*, *Palaeocystodinium* sp., *Pentadinium* sp., *Polysphaeridium zoharyi*, *Polysphaeridium* sp., *Spiniferites membranaceus*, *Spiniferites ramosus*, *Spiniferites* sp., *Homotryblium* sp., *Cleistosphaeridium placacanthum*, *Operculodinium*

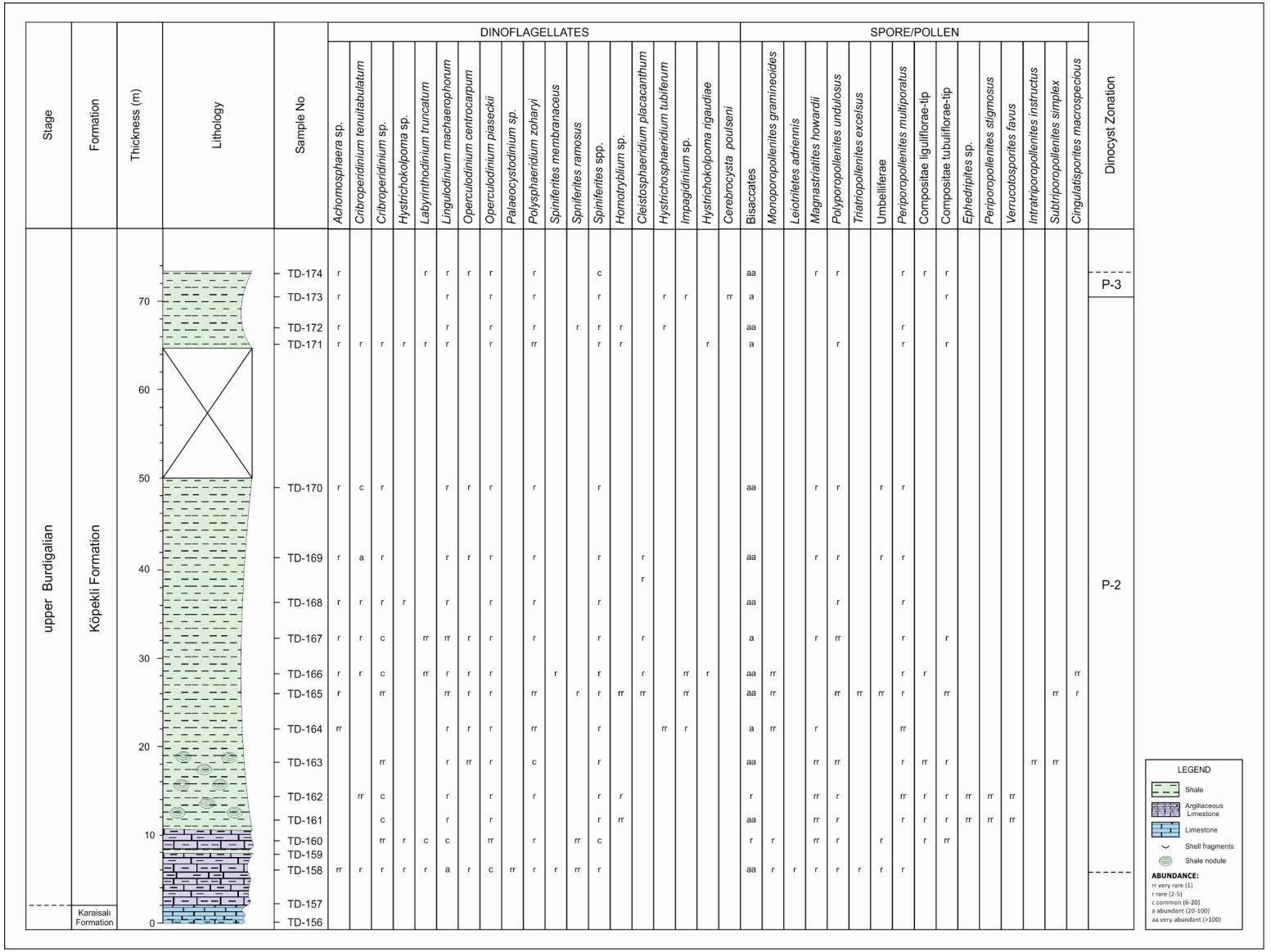

Figure 28. Stratigraphic range chart of palynomorphs and biostratigraphy in the Köpekli Section.

israelianum, *Hystrichosphaeridium tubiferum*, *Impagidinium* sp. and *Hystrichokolpoma rigaudiae* (Figure 28). *Distatodinium paradoxum* is the only species recognized as a reworked dinoflagellate cysts within this section. The terrestrial palynomorph assemblage within the P-2 Zone consists of Bisaccates, *Cingulatisporites macrospecious,* Compositae (tubuliflorae-type), Compositae (liguliflorae-type), *Ephedripites* sp., *Monoporopollenites gramineoides*, *Intratriporopollenites instructus*, *Leiotriletes adriennis, Magnastriatites howardii, Periporopollenites multiporatus, Periporopollenites stigmosus, Polyporopollenites undulosus, Subtriporopollenites simplex, Tricolporopollenites* sp., *Triatriopollenites excelsus*, Umbelliferae and *Verrucatosporites favus* (Figure 28). These long-ranging terrestrial taxa recognized through the Köpekli Section are not biostratigraphically significant.

Most of taxa present in the P-2 Zone also occur in the P-3 Zone, which is defined by the FO of *Cerebrocysta poulsenii and* the Köpekli Section terminates within the limits of the P-3 Zone (Figure 24, Figure 25 and Figure 28). Since P-3 Zone within the Köpekli Section is recognized only one sample (TD-174), the account of the taxa occurring in the P-3 Zone will be given in the following Sofular Section.

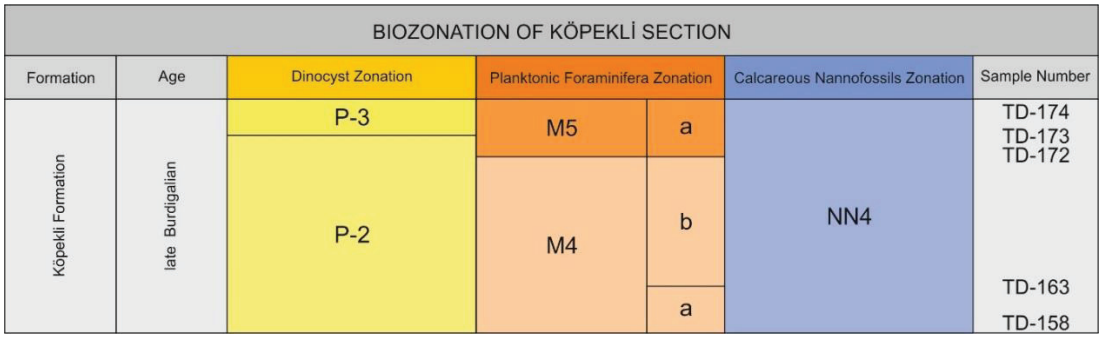

Figure 29. Correlation of the biozones based on palynomorphs, planktonic foraminifera and calcareous nannoplankton in the Köpekli Section.

The biostratigraphical data show that the deposition of the Köpekli Formation in the measured Köpekli Section has taken place during the late Burdigalian (Türkecan et al., submitted) (Figure 24, Figure 25 and Figure 28). The planktonic foraminiferal zones and nannoplankton zones defined in the Köpekli Section are similar to those recorded in the Çukurköy Section (Figure 27 and Figure 29). The Çukurköy Section

comprises the P-1 and P-2 zones, whereas the Köpekli Section starts with the P-2 Zone at the base and continues upward with the P-3 Zone (Figure 27 and Figure 29). Therefore, the Köpekli Section corresponds to the upper part of the Çukurköy Section and the Köpekli Section comes stratigraphically over the Çukurköy Section (Figure 25).

3.2.3. Sofular Section

The Sofular Section measured entirely in the Köpekli Formation comprises P-2, P-3 and P-4 zones indicating deposition during the latest Burdigalian-earliest Langhian (Figure 24, Figure 25 and Figure 30). P-2, P-3 and P-4 zones have been calibrated by the planktonic foraminifera and nannoplankton zones (Figure 31). According to the planktonic foraminifera scheme, the succession has been divided into two zones, namely M5a and M5b zones, corresponding to the latest Burdigalian to the earliest Langhian (Figure 24 and Figure 31). P-2 and P-3 zones corresponds to M5a planktonic foraminifera zone and NN4 nannoplankton zone (Türkecan et al., submitted) (Figure 31). The equivalent planktonic foraminifera and nannoplankton zones of the P-4 Zone are the upper part of M5a Zone and the lower part of M5b Zone and NN4 Zone, respectively (Türkecan et al., submitted) (Figure 31).

P-2 Zone is bounded by the base of the section at the bottom and the FO of *Cerebrocysta poulsenii* at the top (from sample ATD-119 to ATD-120 (Figure 24, Figure 25 and Figure 30)). This zone is characterized by a poor dinocyst assemblage including *Achomosphaera* cf. *andalousiensis*, *Cordosphaeridium* sp., *Labyrinthodinium truncatum*, *Operclodinium centrocarpum*, *Operculodinium* sp., *Polysphaeridium zoharyi*, *Polysphaeridium* sp., *Spiniferites membranaceus* and *Spiniferites* spp (Figure 30). The terrestrial palynomorph assemblage within the P-2 Zone consists of Bisaccates, *Cingulatisporites macrospecious*, Compositae (tubuliflorae-type), Compositae (liguliflorae-type), *Monoporopollenites gramineoides*, *Inaperturopollenites hiatus, Intratriporopollenites instructus, Periporopollenites multiporatus*, *Subtriporopollenites simplex*, *Tricolporopollenites* sp., *Triatriopollenites excelsus* and *Verrucatosporites favus* (Figure 30). These long ranging terrestrial taxa recognized through the Sofular Section are not biostratigraphically significant, like in Çorlu and Çukurköy sections.

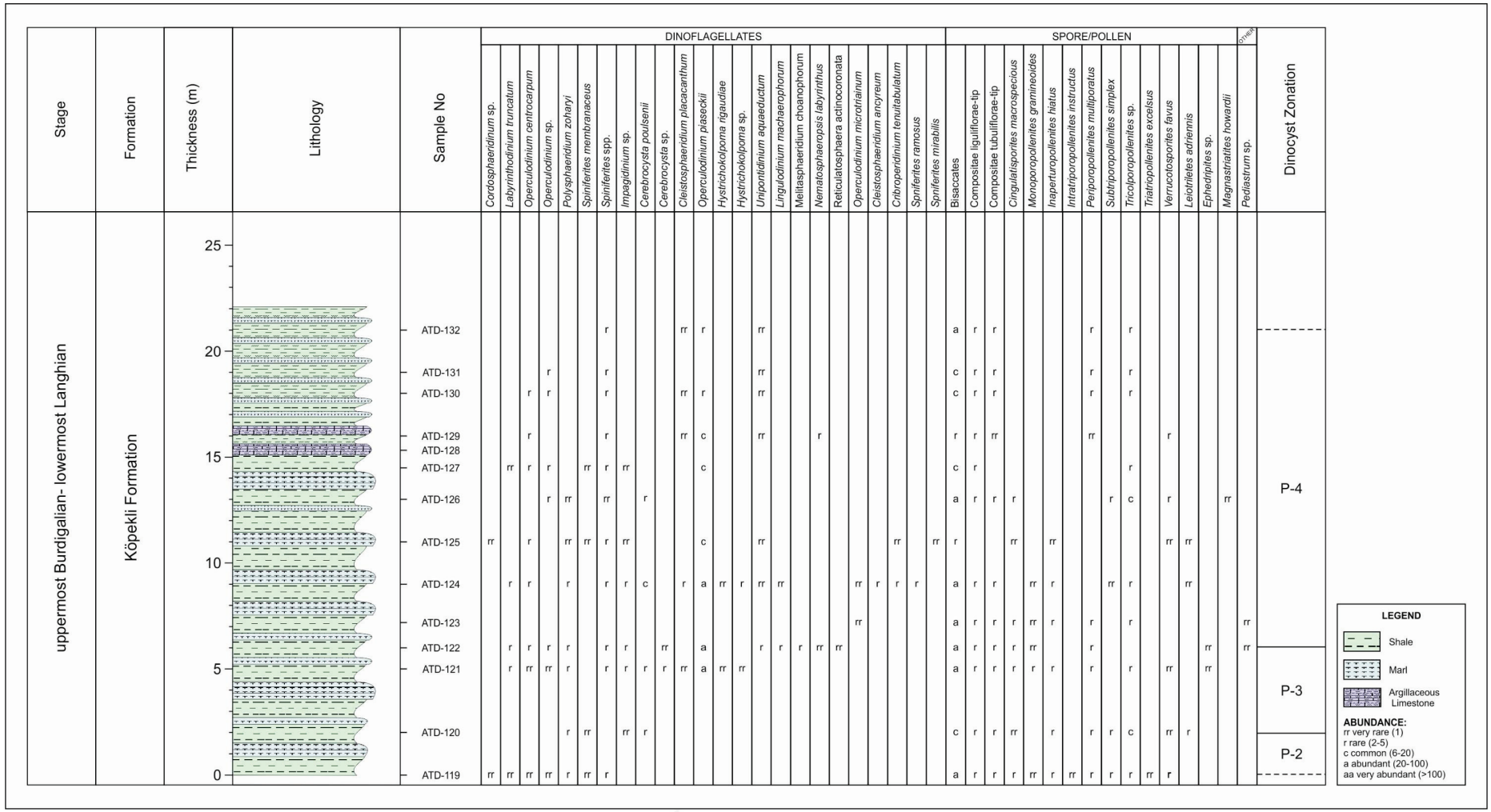

Figure 30. Stratigraphic range chart of palynomorphs and biostratigraphy in the Sofular Section.

P-3 Zone overlies the P-2 Zone and comprises the interval from sample TD-120 to TD-122 (Figure 30). P-3 Zone is characterized by a dinocyst assemblage consisting of *Cerebrocysta poulsenii*, *Cerebrocysta* sp., *Cleistosphaeridium placacanthum, Cordosphaeridium* sp., *Hystrichokolpoma rigaudiae, Impagidinium* sp., *Labyrinthodinium truncatum*, *Operclodinium centrocarpum*, *Operculodinium piaseckii, Operculodinium* sp., *Polysphaeridium zoharyi*, *Polysphaeridium* sp., *Spiniferites membranaceus* and *Spiniferites* spp (Figure 30). The base of the P-3 Zone is defined by the FO of *Cerebrocysta poulsenii* (Figure 24 and Figure 30). The terrestrial palynomorph assemblage of the P-3 Zone recognized in this section is composed of Bisaccates, *Cingulatisporites macrospecious*, Compositae (tubuliflorae-type), Compositae (liguliflorae-type), *Ephedripites* sp., *Monoporopollenites gramineoides*, *Inaperturopollenites hiatus, Intratriporopollenites instructus, Leiotriletes adriennis, Periporopollenites multiporatus*, *Subtriporopollenites simplex*, *Tricolporopollenites* sp., *Triatriopollenites excelsus* and *Verrucatosporites favus* (Figure 30). Especially, bisaccates have a common abundance in this zone.

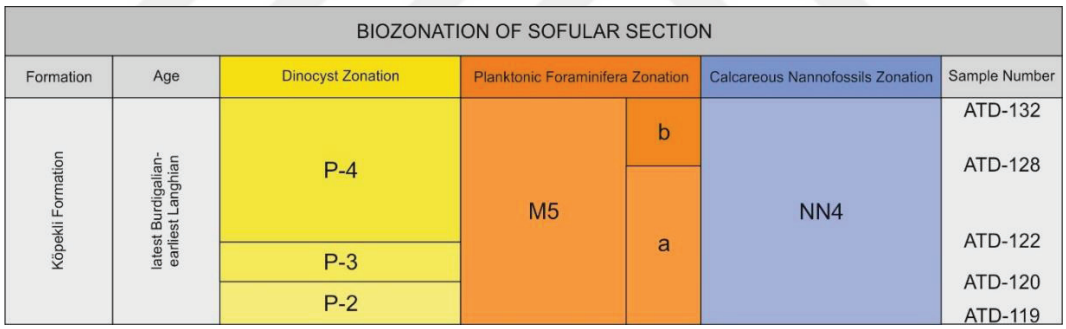

Figure 31. Correlation of the biozones based on palynomorphs, planktonic foraminifera and calcareous nannoplankton in the Sofular Section.

P-4 Zone comprises the interval from sample TD- 122 to TD-132 (Figure 30). It is characterized by a diverse dinocyst assemblage consisting of *Achomosphaera* cf. *andalousiensis*, *Cerebrocysta poulsenii*, *Cerebrocysta* sp., *Cleistosphaeridium placacanthum, Cleistosphaeridium* sp., *Cordosphaeridium* sp., *Cribroperidinium tenuitabulatum, Hystrichokolpoma rigaudiae, Hystrichokolpoma* sp., *Impagidinium* sp., *Labyrinthodinium truncatum*, *Lingulodinium machaerophorum*, *Melitasphaeridium choanophorum, Nematosphaeropsis labyrinthus, Nematosphaeropsis* sp., *Operclodinium centrocarpum*, *Operclodinium microtriainum*

(rw), *Operculodinium piaseckii, Operculodinium* sp., *Polysphaeridium zoharyi*, *Polysphaeridium* sp., *Reticulatosphaera actinocoronata, Spiniferites membranaceus*, *Spiniferites mirabilis, Spiniferites ramosus, Spiniferites* spp. and *Unipontidinium aquaeductus* (Figure 30). The base of this zone is defined by the FO of *Unipontidinium aquaeductus* which is one of the characteristic species for the Middle Miocene (Figure 24 and Figure 30). The terrestrial palynomorph assemblage characterizing the P-3 Zone are still present in this interval including *Magnastriatites howardii.* The fresh water algae *Pediastrum* sp. is also recorded in this zone.

Köpekli Formation in the measured Sofular Section deposited during the latest Burdigalian-earliest Langian based on the biostratigraphical data (Türkecan et al., submitted) (Figure 24 and Figure 30). According to the dinocyst and the planktonic foraminiferal zones, the Sofular Section corresponds to the upper part of the Köpekli Section and comes stratigraphically over the Köpekli Section (Figure 25).

3.2.4. Çorlu Section

The Çorlu Section covers the upper part of the P-4 Zone (*Unipontidinium aquaeductus* Range Zone), P-5 Zone and a considerable part of the P-6 Zone from bottom to top (Figure 24, Figure 25 and Figure 32).

P-4 Zone was defined in the lowermost part of the Çorlu Section and corresponds to the Köpekli Formation (Figure 32). The base of the P-4 Zone is limited with the base of the Çorlu Section, while the top is marked by the LO of *Unipontidinium aquaeductus* (Figure 24, Figure 25 and Figure 32). This interval consists of shale layers intercalated with thin sandstone beds from sample TD-175 to TD-184. P-4 zone is characterized by a rich dinocyst assemblage including *Cleistosphaeridium placacanthum, Cordosphaeridium* sp., *Cribroperidinium* sp., *Impagidinium* sp., *Labyrinthodinium truncatum*, *Lingulodinium machaerophorum*, *Nematosphaeropsis labyrinthus, Operclodinium centrocarpum*, *Operculodinium piaseckii, Operculodinium* sp., *Polysphaeridium zoharyi*, *Polysphaeridium* sp., *Spiniferites membranaceus*, *Spiniferites mirabilis, Spiniferites ramosus, Spiniferites* spp. and *Unipontidinium aquaeductus* (Figure 32). Moreover, P-4 Zone consists of a diverse terrestrial palynomorph assemblage including *Polyvestibulopollenites verus*,

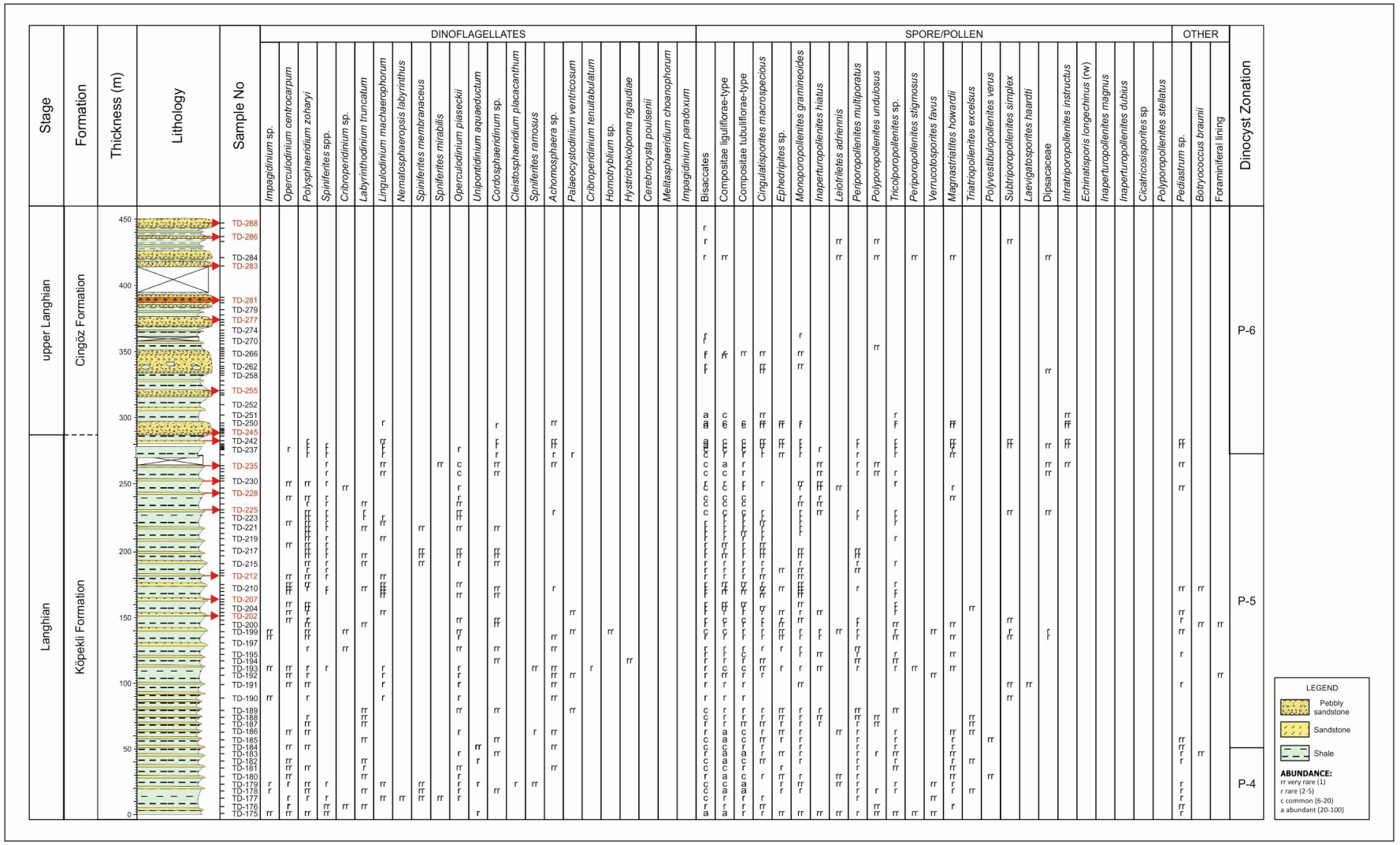

Figure 32. Stratigraphic range chart of palynomorphs and biostratigraphy in the Çorlu Section (red arrows show the collected sandstone samples).

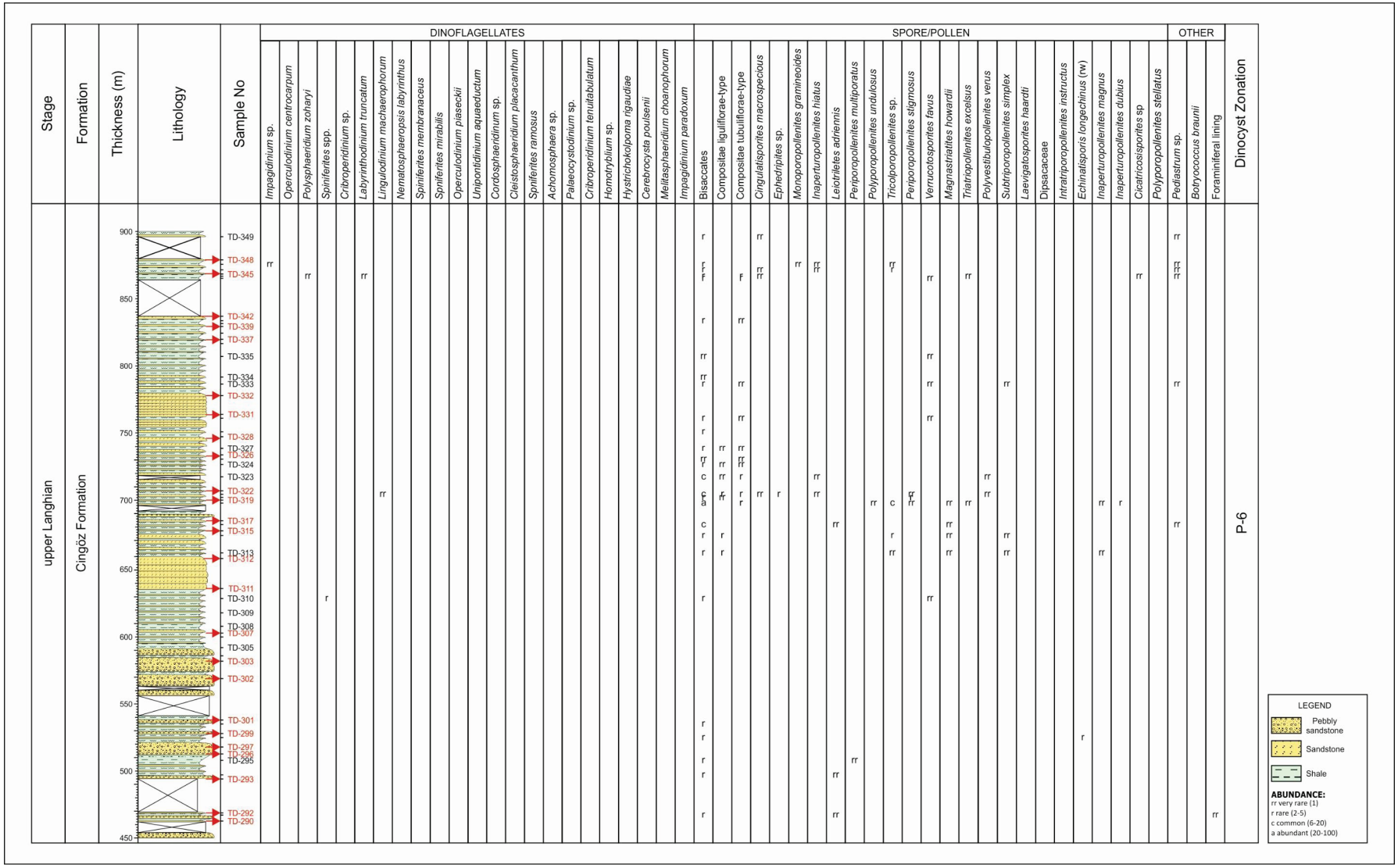

Figure 32. (Cont.)

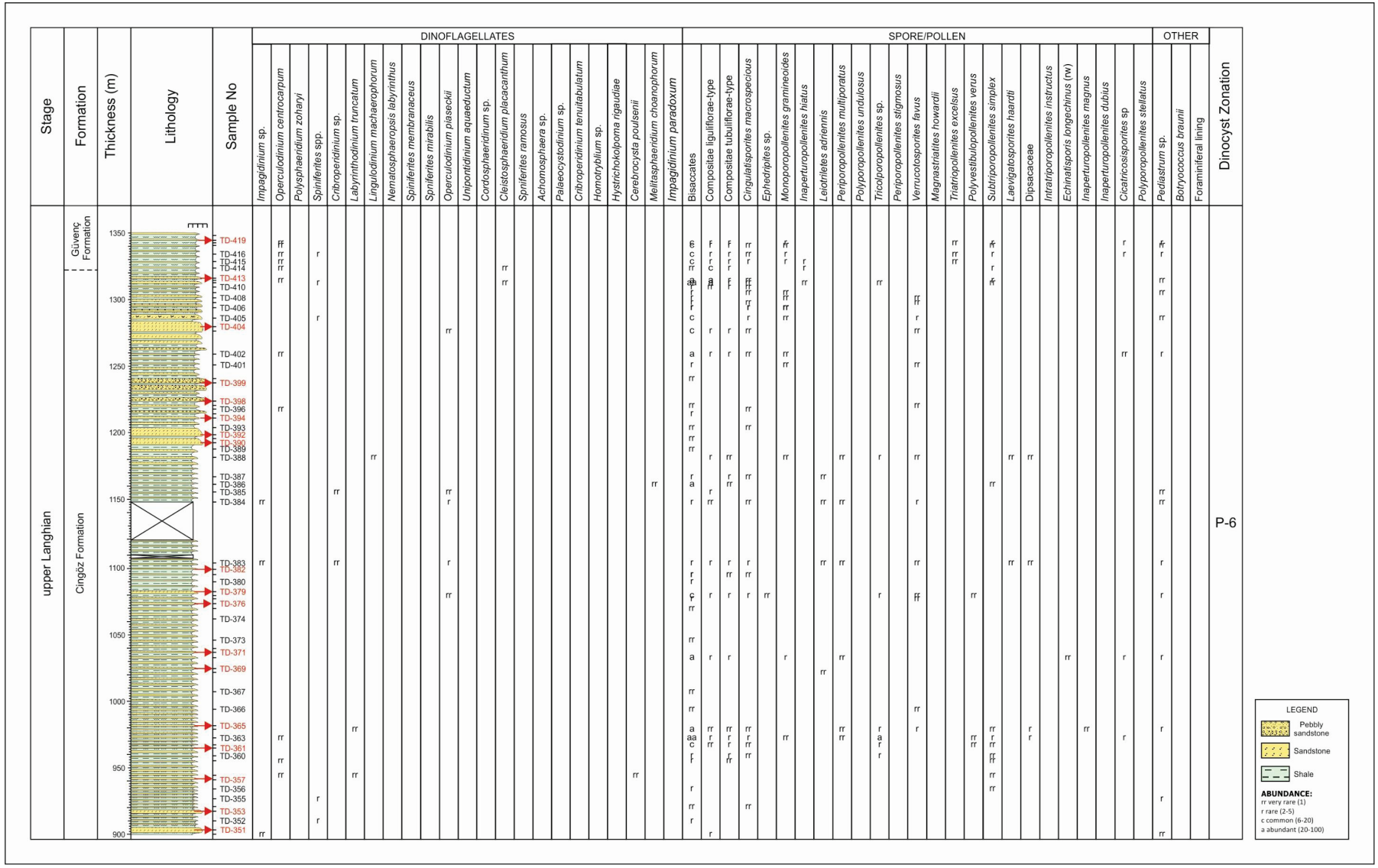

Figure 32. (Cont.)

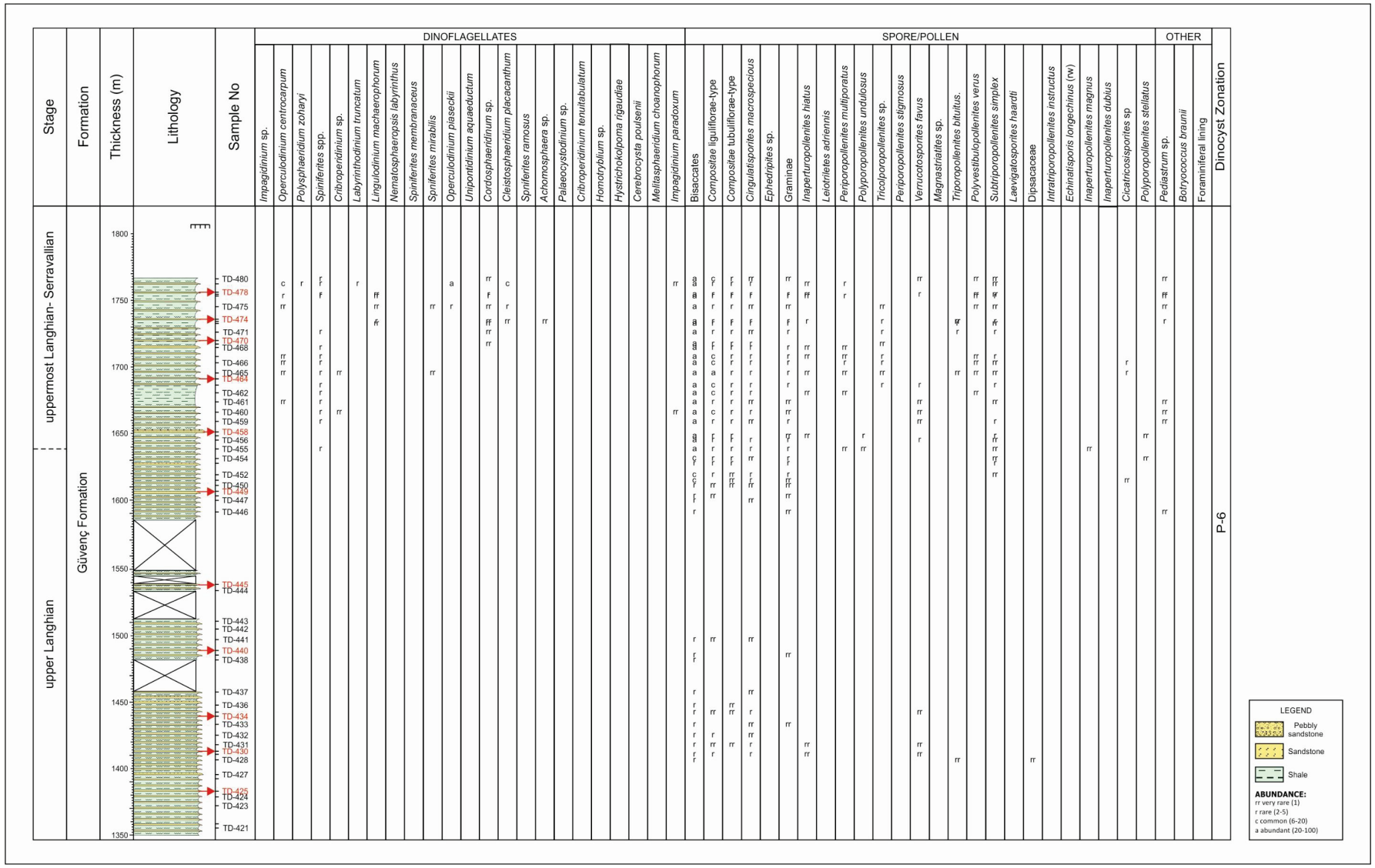

Figure 32. (Cont.)

Bisaccates, *Cingulatisporites macrospecious,* Compositae (tubuliflorae-type), Compositae (liguliflorae-type), *Ephedripites* sp., *Monoporopollenites gramineoides*, *Inaperturopollenites hiatus, Leiotriletes adriennis, Magnastriatites howardii*, *Periporopollenites multiporatus, Periporopollenites stigmosus*, *Polyporopollenites undulosus, Triatriopollenites excelsus, Tricolporopollenites* sp., *Triatriopollenites excelsus, Verrucatosporites favus, Pediastrum* sp. and *Botryococcus braunii* (Figure 32). This zone corresponds to the M5b and NN4-NN5 zones based on planktonic foraminifera and calcareous nannofossils, respectively (Figure 33).

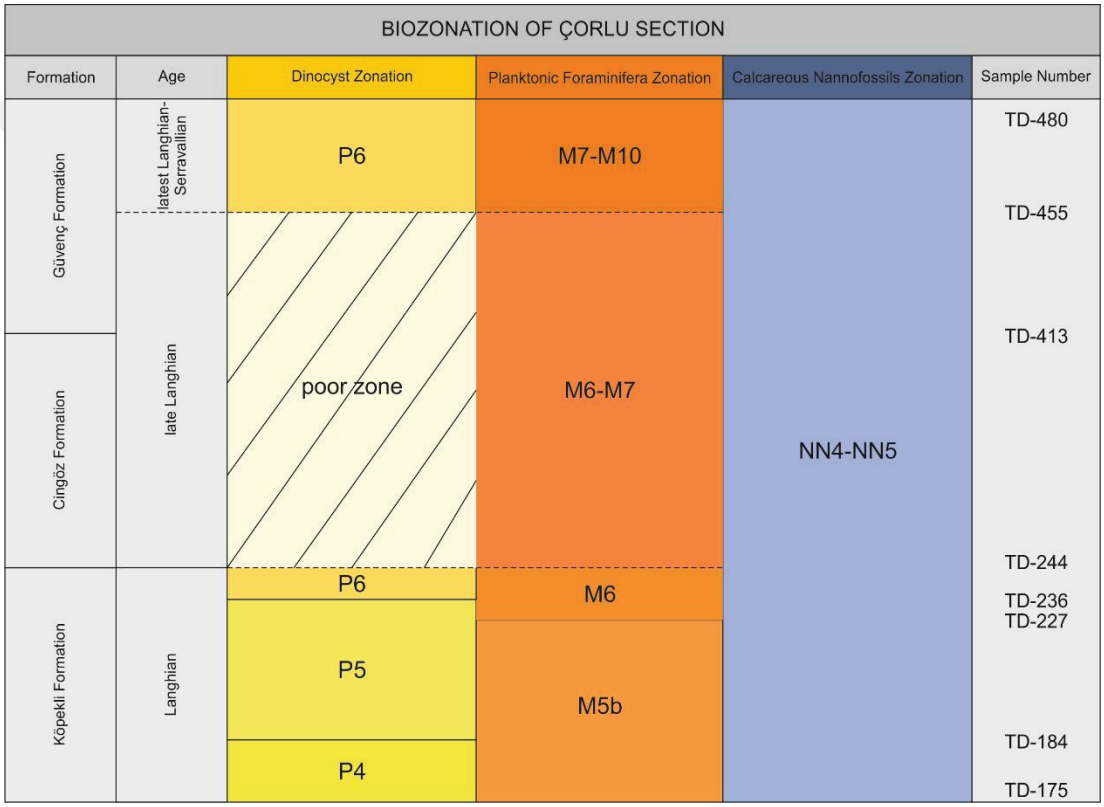

Figure 33. Correlation of the biozones based on palynomorphs, planktonic foraminifera and calcareous nannoplankton in the Çorlu Section.

P-5 Zone is defined only in the Çorlu Section and corresponds to the Köpekli Formation (Figure 32) and comprises the interval from sample TD- 184 to TD-236. This interval consists of shale layers intercalated with thin sandstone beds. The LO of *Unipontidinium aquaeductus* delimits the lower boundary of this zone, whereas the upper boundary is defined by the LO of *Paleocystodinium ventricosum* (Figure 24, Figure 25 and Figure 32). P-5 Zone is characterized by a rich dinocyst assemblage

including *Cleistosphaeridium ancyreum*, *Cleistosphaeridium placacanthum*, *Hystrichosphaeropsis obscura*, *Hystrichokolpoma rigaudiae, Labyrinthodinium truncatum*, *Lingulodinium machaerophorum*, *Operculodinium centrocarpum*, *Paleocystodinium ventricosum, Polysphaeridium zoharyi*, *Spiniferites mirabilis*, *Spiniferites pseudofurcatus*, *Spiniferites ramosus*, *Spiniferites* spp. and common long-ranging terrestrial taxa including Bisaccates, *Cingulatisporites macrospecious,* Compositae (tubuliflorae-type), Compositae (liguliflorae-type), Dipsacaceae, *Ephedripites* sp., *Monoporopollenites gramineoides*, *Inaperturopollenites hiatus, Intratriporopollenites instructus, Laevigatosporites haardti, Leiotriletes adriennis, Magnastriatites howardii, Periporopollenites multiporatus, Periporopollenites stigmosus*, *Polyporopollenites undulosus, Polyvestibulopollenites verus, Subtriporopollenites simplex, Triatriopollenites excelsus, Tricolporopollenites* sp., *Triatriopollenites excelsus, Verrucatosporites favus, Pediastrum* sp., and *Botryococcus braunii.* This zone corresponds to the upper part of M5b and lower part of M6 zones and NN4-NN5 zones based on planktonic foraminifera and calcareous nannofossils, respectively (Figure 33).

The overlying P-6 Zone comprises the interval from sample TD- 236 to TD-480 (Figure 32). This zone corresponds to the uppermost part of the Köpekli Formation, the Cingöz Formation from bottom to top and lower part of the Güvenç Formation (Figure 32). Two different intervals of palynomorph associations were recorded through this zone. The first interval consisting of shale layers intercalated with thin sandstone beds from sample TD-236 to TD-455 is mainly characterized by a poor palynomorph assemblage. However, the lower part of this interval consists of a relatively more diverse dinocysts and terrestrial taxa. This part is composed of several dinocysts taxa including *Cleistosphaeridium placacanthum, Cribroperidinium* sp., *Impagidinium* sp., *Labyrinthodinium truncatum*, *Lingulodinium machaerophorum*, *Operclodinium centrocarpum*, *Operculodinium piaseckii, Polysphaeridium* sp. and *Spiniferites* spp. and a common long-ranging terrestrial taxa consisting of *Polyvestibulopollenites verus*, Bisaccates, Compositae (tubuliflorae-type), Compositae (liguliflorae-type), *Cicatricosisporites* sp., Dipsacaceae, *Echinatisporis longechinus* (rw), *Ephedripites* sp., *Monoporopollenites gramineoides*, *Inaperturopollenites hiatus, Inaperturopollenites magnus, Intratriporopollenites instructus, Laevigatosporites haardti, Leiotriletes adriennis, Magnastriatites*

howardii, Periporopollenites multiporatus, *Periporopollenites stigmosus, Polyporopollenites undulosus, Subtriporopollenites simplex*, *Tricolporopollenites* sp., *Triatriopollenites excelsus* and *Verrucatosporites favus* (Figure 32). In addition to this palynomorph assemblage, *Botryococcus braunii*, *Pediastrum* sp. and some foraminiferal linings are detected in some certain levels in this interval. Moreover, there are several samples which are barren of palynomorphs in this interval. The submarine fan deposits of Cingöz Formation are composed of quite a diverse terrestrial taxa transported by river systems, whereas it consists of a poor dinocyst assemblage. Williams and Sarjeant (1967) suggested that sedimentation might be controlled by water turbulence in such depositional environments and spores, pollen, acritarchs and dinocysts, all being very light, may therefore never be deposited in regions of high turbulence. Thus, there are very limited amounts of palynomorphs within the turbidite deposits of the Cingöz Formation. Such a poor dinocyst assemblage is also detected in the lower part of the Güvenç Formation, since the Güvenç Formation shows a similar sedimentation pattern close to the boundary between the Cingöz Formation and the Güvenç Formation and at its certain levels (from sample TD-414 and TD-455; Figure 32). The diverse terrestrial taxa and the fresh water algeas (e.g. *Pediastrum* sp.) are also recorded in this zone. Dybkjaer (2004a) mentioned that fresh water carrying spores, pollen, fresh water algea and wood particles could probably be transported to the area by large river systems. In the same way, the terrestrial palynomorphs, woody and even coaly organic matters, fresh water algeas observed in this zone were most probably brought by rivers in this study. In addition, deposition of thick sandstone beds and conglomeratic sandstone also create unfavourable conditions for preservation of marine palynomorphs. Therefore, the poor occurrence in palynomorph association is controlled by sedimentation conditions and the lithology. This poor zone (from sample TD-236 to TD-455) also corresponds to the M6-M7 zones and the NN4-NN5 zones based on planktonic foraminifera and calcareous nannofossils, respectively (Figure 33).

The second interval within the P-6 Zone covers the upper part of the Güvenç Formation in the Çorlu Section (Figure 32). This part is composed of shale dominated sequences alternating with thin sandstone beds from sample TD-455 to TD-480 (Figure 32). This interval differs from the second interval of the P-5 Zone with its diversified dinoscyst assemblage. It mainly consists of the following dinoflagellates;

Cleistosphaeridium placacanthum, Cribroperidinium sp., *Impagidinium* sp., *Labyrinthodinium truncatum*, *Lingulodinium machaerophorum*, *Operclodinium centrocarpum*, *Operculodinium piaseckii, Polysphaeridium zoharyi*, *Spiniferites mirabilis* and *Spiniferites* spp.. On the other hand, terrestrial taxa including *Polyvestibulopollenites verus*, Bisaccates, *Cingulatisporites macrospecious,* Compositae (tubuliflorae-type), Compositae (liguliflorae-type), *Monoporopollenites gramineoides*, *Inaperturopollenites hiatus, Periporopollenites multiporatus, Subtriporopollenites simplex, Tricolporopollenites* sp., *Triatriopollenites excelsus* and *Verrucatosporites favus* are abundantly present in the upper part of the zone (Figure 32). The fresh water algeas (e.g. *Pediastrum* sp.) transported to the area by large river systems are also recorded in this interval. The equivalent planktonic foraminifera and calcareous nannoplankton zones of this interval (from sample TD-455 to TD-480) are the M7-M10 and NN4-NN5 zones, respectively (Figure 33).

The Köpekli Formation in the measured Çorlu Section deposited during the Langhian based on the biostratigraphical data (Türkecan et al., submitted) (Figure 32). The P-2, P-3 and P-4 zones were recorded in the Sofular Section and a part of the P-4, P-5 and the P-6 zones were defined in the Çorlu Section. Accordingly, the Çorlu Section comes stratigraphically over the Sofular Section (Figure 25). The submarine fan deposits of Cingöz Formation in the measured Çorlu Section is characterized by quite a diverse terrestrial taxa transported by river systems, whereas it consists of a poor dinocyst assemblage. According to the biostratigraphical data, the deposition of Çorlu Section occured during the late Langhian (Figure 32). Çorlu Section also comprises the lower part of the Güvenç Formation. Based on the biostratigraphical data, Güvenç Formation in the measured Çorlu Section deposited during the latest Langhian-Serravallian (Figure 32).

3.2.5. Koruklu Section

The Koruklu Section includes the upper part of the P-6 Zone and the lower part of the P-7 Zone indicating a deposition during the latest Langhian- Serravallian and comprises the interval from sample ATD- 60 to ATD-81 (Figure 24, Figure 25 and Figure 34). The P-6 and P-7 zones defined in this section corresponds to the M6-M10 planktonic foraminifera zones and NN5-NN7 nannoplankton zones (Figure 35).

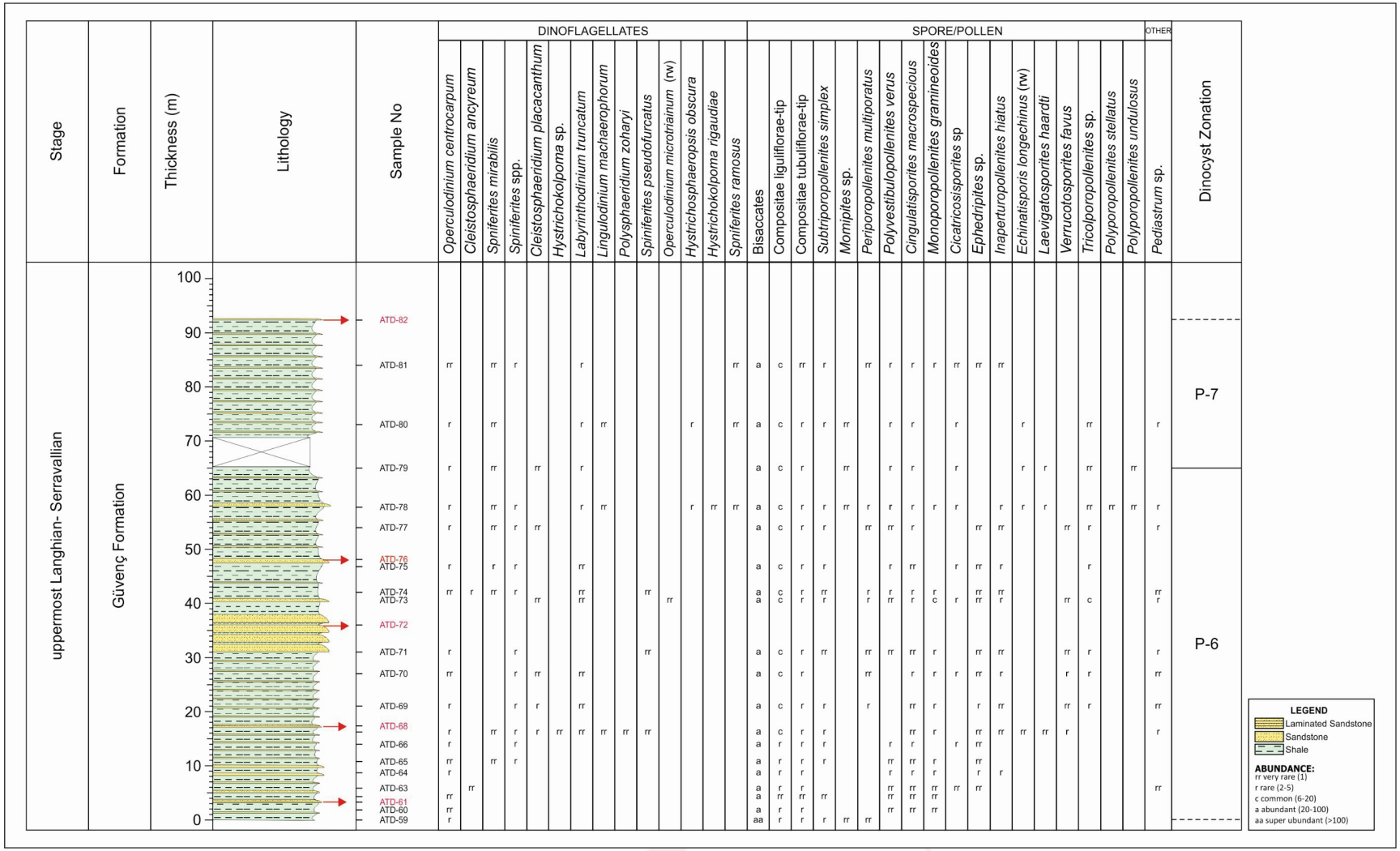

Figure 34. Stratigraphic range chart of palynomorphs and biostratigraphy in the Koruklu Section (red arrows show the collected sandstone samples).

P-6 Zone is bounded at the base by the base of the section, and the LO of *Cleistosphaeridium placacanthum* at its upper boundary (from sample ATD-60 to ATD-79; Figure 34). This interval consists of shale layers intercalated with thin sandstone beds. P-6 Zone is characterized by a rich dinocyst assemblage including *Cleistosphaeridium ancyreum*, *Cleistosphaeridium placacanthum*, *Hystrichosphaeropsis obscura*, *Hystrichokolpoma rigaudiae, Labyrinthodinium truncatum*, *Lingulodinium machaerophorum*, *Operclodinium centrocarpum*, *Polysphaeridium zoharyi*, *Spiniferites mirabilis*, *Spiniferites pseudofurcatus*, *Spiniferites ramosus*, *Spiniferites* spp. and a common long-ranging terrestrial taxa consisting of *Polyvestibulopollenites verus*, Bisaccates, *Cingulatisporites macrospecious,* Compositae (tubuliflorae-type), Compositae (liguliflorae-type), *Cicatricosisporites* sp., *Ephedripites* sp., *Monoporopollenites gramineoides*, *Inaperturopollenites hiatus, Laevigatosporites haardti, Periporopollenites multiporatus, Polyporopollenites stellatus*, *Polyporopollenites undulosus, Subtriporopollenites simplex, Tricolporopollenites* sp., *Triatriopollenites excelsus*, *Verrucatosporites favus* (Figure 34). Compositae (liguliflorae-type) appears towards the middle and uppermost parts of the measured section. Moreover, *Operculodinium microtrianium* and *Echinatisporis longechinus* are reworked palynomorphs from the Eocene.

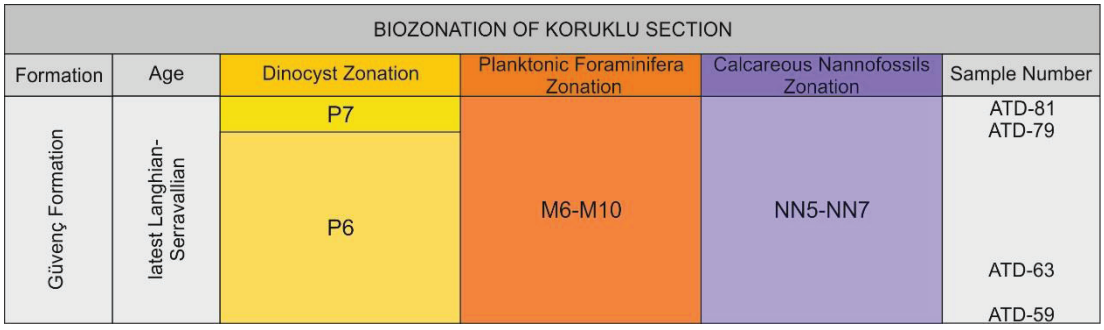

Figure 35. Correlation of the biozones based on palynomorphs, planktonic foraminifera and calcareous nannoplankton in the Koruklu Section.

P-7 Zone overlying the P-6 Zone comprises the interval from sample ATD-79 to ATD-81 (Figure 34). This zone consists of several dinocysts including *Cleistosphaeridium placacanthum*, *Hystrichosphaeropsis obscura*, *Labyrinthodinium truncatum*, *Lingulodinium machaerophorum*, *Operclodinium centrocarpum*,

Spiniferites mirabilis, *Spiniferites ramosus* and *Spiniferites* spp. and a common long-ranging terrestrial taxa consisting of *Polyvestibulopollenites verus*, Bisaccates, *Cingulatisporites macrospecious,* Compositae (tubuliflorae-type), Compositae (liguliflorae-type), *Cicatricosisporites* sp., *Ephedripites* sp., *Monoporopollenites gramineoides*, *Inaperturopollenites hiatus, Periporopollenites multiporatus, Subtriporopollenites simplex, Tricolporopollenites* sp. and *Momipites sp.* (Figure 34). In addition to this palynomorph assemblage, the fresh water algae *Pediastrum* sp. transported by river systems and *Echinatisporis longechinus* reworked from Eocene are also detected in this zone.

The biostratigraphical data shows that the deposition of the Güvenç Formation in the measured Koruklu Section has taken place during the latest Langhian-Serravallian (Figure 34). The planktonic foraminiferal zones defined at the upper part of the Çorlu Section (corresponding to the Güvenç Formation) are M6-M7 and M7-M10 zones, while M6-M10 zones are recorded in the Koruklu Section (Figure 33 and Figure 35). Moreover, the P-6 Zone, which starts in the Çorlu Section, is finalized in the Koruklu Section at the level corresponding to sample TD-79 (Figure 34 and Figure 35). In addition, P-7 Zone is defined above P-6 Zone in this section (Figure 34 and Figure 35). Therefore, the Koruklu Section corresponds to the upper part of the Çorlu Section and comes stratigraphically over the Çorlu Section (Figure 25).

3.2.6. Bekirli Section

The Bekirli Section comprises the upper part of the P-7 Zone and the lower part of the P-8 Zone indicating a deposition during the latest Serrevalian – earliest Tortonian (Figure 24, Figure 25 and Figure 36). P-7 and P-8 zones defined in this section have been calibrated by the planktonic foraminifera and nannoplankton zones (Figure 24 and Figure 37). According to the planktonic foraminifera scheme, the succession has been divided into two zones, namely M10 and M10-M11 zones (Figure 24 and Figure 37). This interval also corresponds to the NN5-NN7 nannoplankton zones (Figure 24 and Figure 37).

P-7 Zone covers the lower part of the measured section corresponding to the Güvenç Formation (Figure 36). This interval consists of shale dominated sequences intercalated with sandstone beds from sample ATD-1 to ATD-4 (Figure 36). P-7 Zone

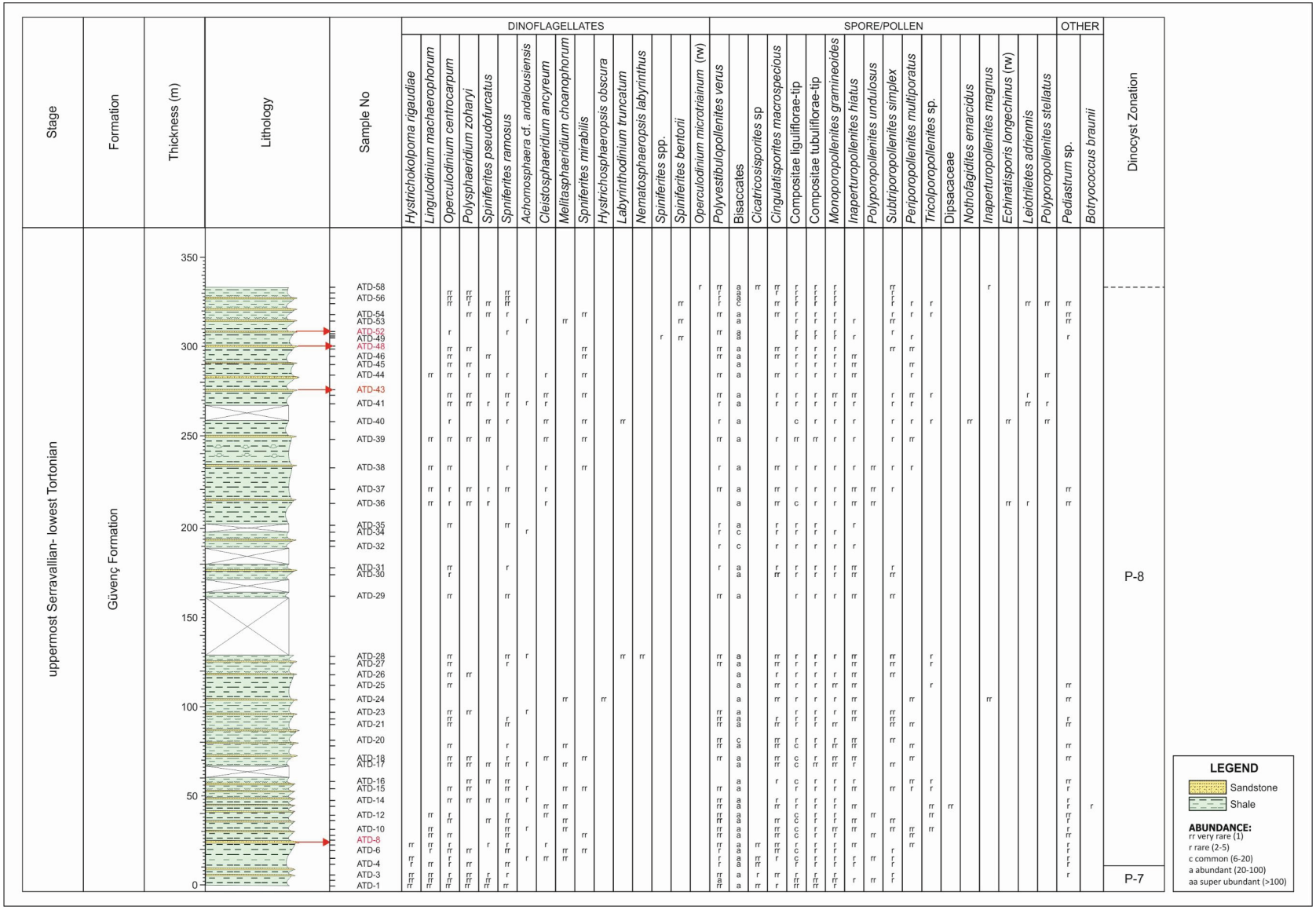

Figure 36. Stratigraphic range chart of palynomorphs and biostratigraphy in the Bekirli Section (red arrows show the collected sandstone samples).

is composed of several dinocysts including *Cleistosphaeridium ancyreum, Hystrichokolpoma rigaudiae*, *Lingulodinium machaerophorum*, *Melitasphaeridium choanophorum, Operclodinium centrocarpum*, *Polysphaeridium zoharyi*, *Spiniferites mirabilis, Spiniferites pseudofurcatus*, *Spiniferites ramosus* and the terrestrial taxa consisting of Bisaccates, *Cingulatisporites macrospecious,* Compositae (tubuliflorae-type), Compositae (liguliflorae-type), *Cicatricosisporites* sp., *Monoporopollenites gramineoides*, *Inaperturopollenites hiatus, Polyporopollenites undulosus* and *Subtriporopollenites simplex* (Figure 36). *Pediastrum* sp. is also identified as a fresh water algae in this level.

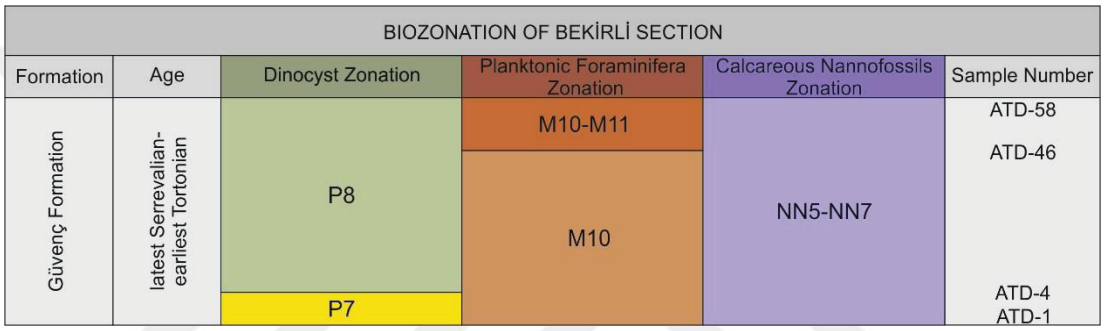

Figure 37. Correlation of the biozones based on palynomorphs, planktonic foraminifera and calcareous nannoplankton in the Bekirli Section.

P-8 Zone overlying the P-7 Zone comprises the interval from sample ATD-4 to ATD-58 (Figure 36). The base of the P-8 Zone is defined by the FO of the *Achomosphaera* cf. *andalousiensis* (Figure 24 and Figure 25). This zone consists of a diverse dinocysts assemblage including *Achomosphaera* cf. *andalousiensis*, *Cleistosphaeridium ancyreum, Hystrichokolpoma rigaudiae*, *Hystrichosphaeropsis obscura, Labyrinthodinium truncatum*, *Lingulodinium machaerophorum*, *Melitasphaeridium choanophorum, Nematosphaeropsis labyrinthus, Operclodinium centrocarpum*, *Polysphaeridium zoharyi*, *Spiniferites mirabilis, Spiniferites pseudofurcatus, Spiniferites ramosus, Spiniferites bentorii* and *Spiniferites* spp. In addition to this marine taxa, a long-ranging terrestrial taxa consisting of Bisaccates, *Cingulatisporites macrospecious,* Compositae (tubuliflorae-type), Compositae (liguliflorae-type), *Cicatricosisporites* sp., Dipsacaceae, *Monoporopollenites gramineoides*, *Inaperturopollenites hiatus, Inaperturopollenites magnus, Leiotriletes adriennis, Nothofagidites emarcidus, Periporopollenites multiporatus,*

Polyporopollenites stellatus, *Polyporopollenites undulosus*, *Subtriporopollenites simplex* and *Tricolporopollenites* sp. are defined in this zone (Figure 36). Furthermore, the fresh water algae *Botryococcus braunii* and *Pediastrum* sp., and *Echinatisporis longechinus* reworked from the Eocene were also detected in this zone.

According to the biostratigraphical data, the Güvenç Formation in the measured Bekirli Section deposited during the latest Serrevalian – earliest Tortonian (Figure 36). P-6 and P-7 zones were recorded in the Koruklu Section and P-7 and the P-8 zones were defined in the Bekirli Section (Figure 24, Figure 34 and Figure 35). Accordingly, Bekirli Section comes stratigraphically over the Koruklu Section with or without a time gap (Figure 25).

3.2.7. Güvenç Section

The Güvenç Section covers the upper part of the P-8 Zone, P-9 Zone and an undifferentiated interval indicating deposition during earliest Tortonian (Figure 24, Figure 25 and Figure 38). P-8 and P-9 Zones defined in this section corresponds to the M11 planktonic foraminiferal zone and the NN5-NN7 nannoplankton zones (Figure 24 and Figure 39).

P-8 zone comprises the interval from sample ATD-83 to ATD-93 (Figure 38). This zone is composed of several dinocysts including *Cleistosphaeridium ancyreum, Diphyes pseudoficusoides, Operculodinium borgerholtense*, *Operclodinium centrocarpum*, *Operculodinium piaseckii, Operculodinium* sp., *Polysphaeridium zoharyi*, *Spiniferites pseudofurcatus* and *Spiniferites* spp. and a diverse terrestrial taxa consisting of *Polyvestibulopollenites verus*, Bisaccates, *Cingulatisporites macrospecious,* Compositae (tubuliflorae-type), Compositae (liguliflorae-type), *Cicatricosisporites* sp., *Monoporopollenites gramineoides*, *Inaperturopollenites hiatus, Inaperturopollenites magnus, Laevigatosporites haardti, Periporopollenites multiporatus, Polyporopollenites stellatus*, *Subtriporopollenites simplex, Tricolporopollenites* sp., *Triatriopollenites excelsus* and *Verrucatosporites favus* (Figure 38). Moreover, a fresh water algae *Pediastrum* sp. is recorded within this zone. The P-8 zone is also characterized by a poor palynomorph assemblage and common reworked taxon (*Diphyes pseudoficusoides*) from the Eocene.

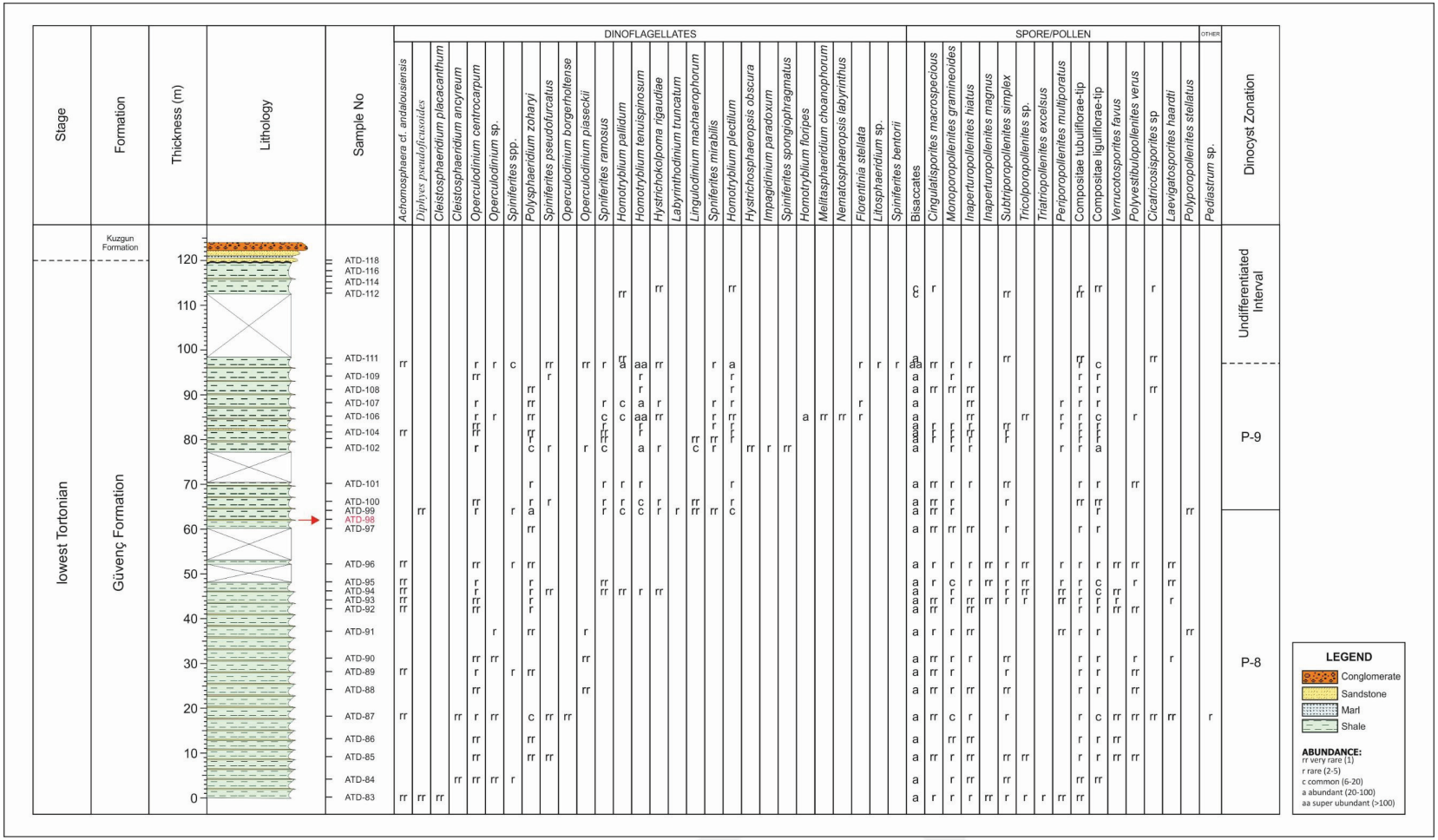

Figure 38. Stratigraphic range chart of palynomorphs and biostratigraphy in the Güvenç Section (red arrow shows the collected sanstone sample).

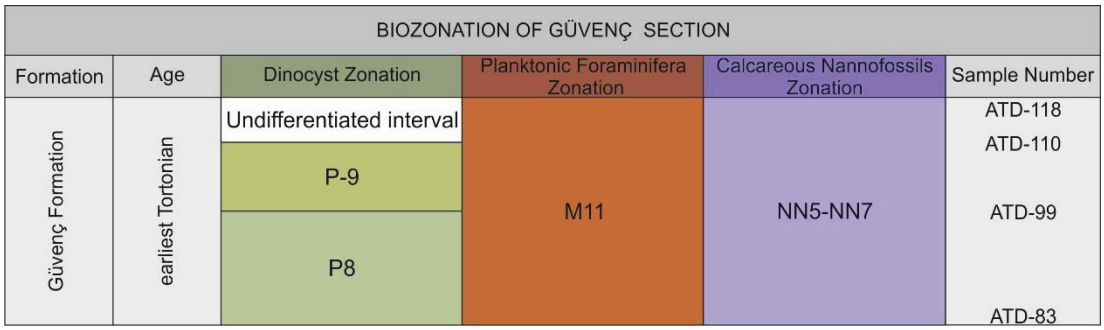

Figure 39. Correlation of the biozones based on palynomorphs, planktonic foraminifera and calcareous nannoplankton in the Güvenç Section.

P-9 Zone overlies the P-8 Zone and comprises the interval from sample ATD-93 to ATD-110 (Figure 38). This zone is mainly characterized by the acme of *Homotryblium* dinoflagellate cysts (e.g. *Homotryblium floripes*, *Homotryblium pallidum*, *Homotryblium plectilum*, *Homotryblium tenuispinosum*) (Figure 24, Figure 25 and Figure 38)). It also includes a rich and diverse dinocyst assemblage consisting of *Cleistosphaeridium ancyreum, Cordosphaeridium cantharellus, Diphyes pseudoficusoides, Florentinia stellata*, *Hystrichokolpoma rigaudiae, Hystrichosphaeropsis obscura*, *Impagidinium paradoxum*, *Labyrinthodinium truncatum*, *Lingulodinium machaerophorum*, *Litosphaeridium* sp., *Melitasphaeridium choanophorum, Nematosphaeropsis labyrinthus, Operclodinium borgerholtense*, *Operclodinium centrocarpum*, *Operculodinium piaseckii, Operculodinium* sp., *Polysphaeridium zoharyi*, *Spiniferites bentoii, Spiniferites pseudofurcatus, Spiniferites mirabilis, Spiniferites ramosus, Spiniferites spongiophragmatus*, *Spiniferites* spp. and a diverse terrestrial taxa including *Polyvestibulopollenites verus*, Bisaccates, *Cingulatisporites macrospecious,* Compositae (tubuliflorae-type), Compositae (liguliflorae-type), *Cicatricosisporites* sp., *Monoporopollenites gramineoides*, *Inaperturopollenites hiatus, Inaperturopollenites magnus, Laevigatosporites haardti, Periporopollenites multiporatus, Polyporopollenites stellatus*, *Subtriporopollenites simplex, Tricolporopollenites* sp. and *Verrucatosporites favus* (Figure 38). Fensome et al. (1993) and de Verteuil and Norris (1996) suggested that *Polysphaeridium zoharyi* has strong morphological similarities with *Homotyblium.* In this zone, a significant acme of *Polysphaeridium zoharyi* is also recorded at some certain levels (e.g. samples ATD-99 and ATD-102, Figure 38). According to Herdenbol et al. (1998), *Homotryblium* cyst-producing dinoflagellates

became extinct in the Late Miocene. When this zone is compared with the planktonic foraminifera and calcareous nannoplanktons, it coincides with them. Therefore, the deposition of the Güvenç Formation terminated within the earliest Tortonian.

Finally, an undifferentiated interval is detected at the uppermost part of the measured section (from sample ATD-111 to 118) (Figure 38). A few samples have been recovered from this partly covered interval. A poor palynomorph assemblage consisting of *Homotryblium pallidum*, *Homotryblium plectilum*, *Hystrichokolpoma rigaudiae,* Bisaccates, *Cingulatisporites macrospecious, Subtriporopollenites simplex,* Compositae (tubuliflorae-type), Compositae (liguliflorae-type), and *Cicatricosisporites* sp. have been identified in this interval (from sample ATD-111 to 118) (Figure 38).

According to the biostratigraphical data, the deposition of the Güvenç Formation in the measured Güvenç Section occured during latest Tortonian (Figure 38). The P-8 zone was defined at the upper part of the Bekirli Section and the same zone and the P-9 Zone were also recognized in the Güvenç Section (Figure 25, Figure 36 and Figure 38). This shows that the Güvenç Section comes stratigraphically over the Bekirli Section (Figure 25). Additionally, Schmidt (1961) documented that the Güvenç Formation was deposited in deeper parts of the basin in the Early-Middle Miocene. After Schmidt (1961), various researchers (e.g. Özçelik, 1993; Özçelik and Yetiş; 1993) reported that the Güvenç Formation was deposited during the Burdigalian-Serravallian interval based on planktonic foraminifera and nannofossils. According to this study, the deposition of the Güvenç Formation started in the latest Langhian and terminated within the earliest Tortonian (Figure 24, Figure 25, Figure 38 and Figure 39).

3.3. BIOSTRATIGRAPHIC CORRELATION WITH WELL-KNOWN DINOCYST EVENTS

In order to apply a worldwide biostratigraphic correlation based on dinoflagellates, the Miocene (late Burdigalian-earliest Tortonian) biozones defined in this study have been compared with previously published dinocyst zonations from Denmark, Germany, Netherlands, NW Europe and USA Eastcoast (Figure 40).

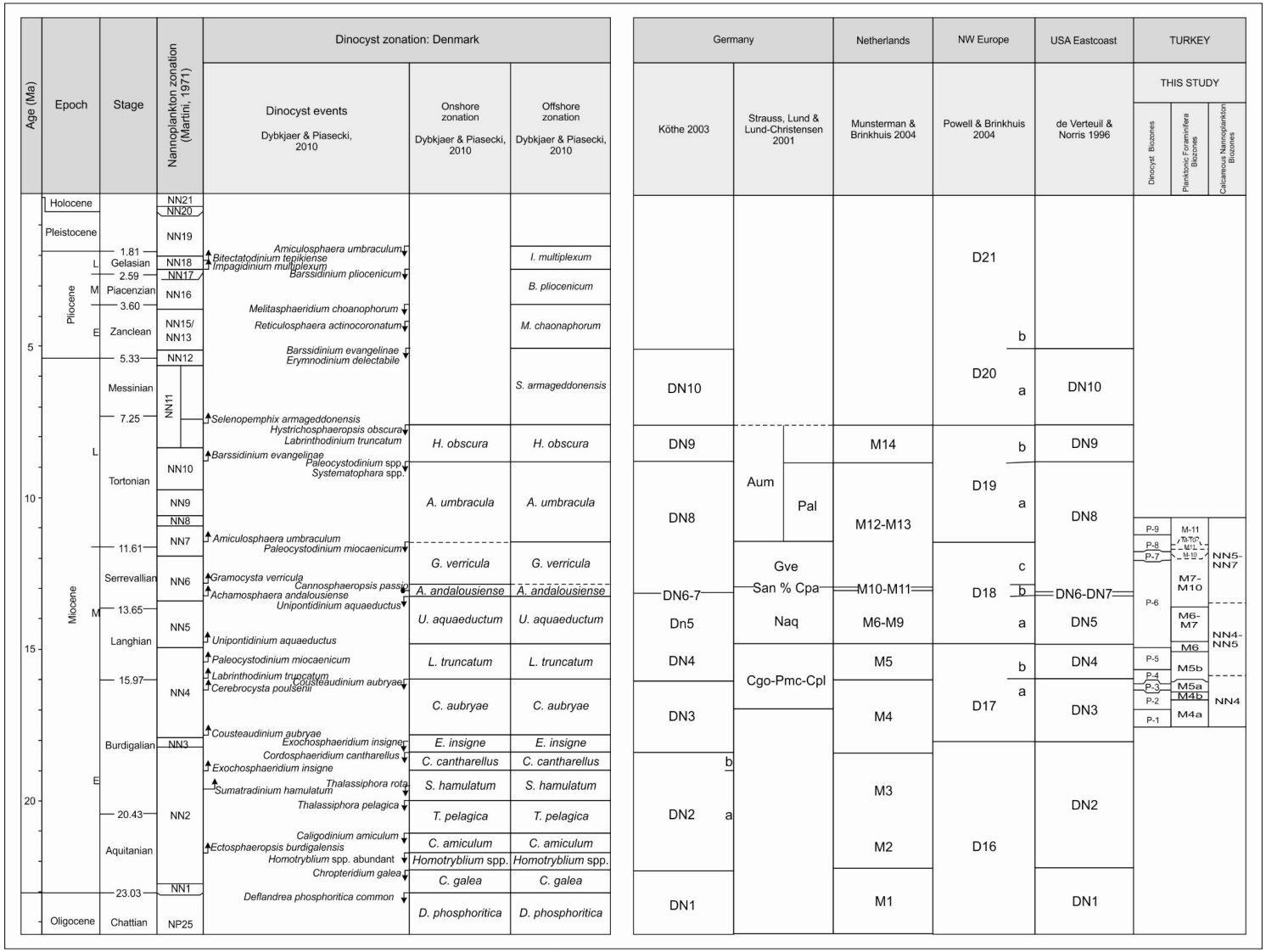

Figure 40. The biozonation defined in this study have been compared with previously published dinocyst zonations from Denmark, Germany, Netherlands, NW Europe and USA Eastcoast (modified from Dybkjaer & Piasecki).

Especially, the diagnostic species have been selected to construct the dinocyst zones through the Köpekli, Cingöz and Güvenç formations in the Adana Basin. The index dinocyst events recognized in this study are follows: The FO of *Labyrinthodinium truncatum, Cerebrocysta poulsenii, Unipontidinium aquaeductus* and *Achomosphaera* cf. *andalousiensis*; *Unipontidinium aquaeductus, Paleocystodinium ventricosum* and *Cleistosphaeridium placacanthum*; the acme of *Homotryblium* dinoflagellate cysts (e.g. *Homotryblium floripes*, *Homotryblium pallidum*, *Homotryblium plectilum*, *Homotryblium tenuispinosum*) (Figure 24 and Figure 25).

The first and significant study of Neogene dinocysts in Denmark was performed by Piasecki (1980) on the Middle and Upper Miocene deposits in western Jylland. Piasecki (1980) distinctly identified four biozones namely, the *L. truncatum* Zone, the *Nematosphaeropsis aquducta* (now *Unipontidinium aquaeductus*) Zone, the *Achomosphaera andalousiensis* Zone and the *Dinopterygium verriculum* (now *Gramocysta verricula*) Zone. This primitive zonation was widely used in later stratigraphic studies (e.g. Herngreen, 1987; Daniels et. al., 1990; Powell (1992); Rusbült and Straus, 1992; Straus and Lund, 1992; Straus et al., 2001; Krathus, 2000; Dybkjaer and Piasecki, 2010). Among these studies, Dybkjaer and Piasecki (2010), carried out a very detailed study on the Neogene deposits of the eastern North Sea Basin (Denmark). A Neogene dinocyst zonation, including a total number of dinocyst zones, was reconstructed by Dybkjaer and Piasecki (2010), four dinocyst zones of Dybkjaer and Piasecki (2010), are correlative with the biozones defined in this study. The first important dinocyst event recorded in this study is the FO *Labyrinthodinium truncatum* which marks the base of the P-2 Zone, whereas the top of this zone is defined by the FO of *Cerebrocysta poulsenii* (Figure 24 and Figure 25). The FO *Labyrinthodinium truncatum* was also recorded in the *Labyrinthodinium truncatum* Zone of Dybkjaer and Piasecki (2010) which was defined in the interval between the FO of *Labyrinthodinium truncatum* and the FO of *Unipontidinium aquaeductus* (Figure 40). The assigned age to the *Labyrinthodinium truncatum* Zone of Dybkjaer and Piasecki (2010) is Langhian. However P-2 Zone in this study is defined in the late Burdigalian. According to De Verteuil and Norris (1996) and Williams et al. (2004), the FO of *Labyrinthodinium truncatum* coincides with the Burdigalian-Langhian boundary. In this study, we have also recorded the FO of *Labyrinthodinium truncatum*

in late Burdigalian based on the correlation of P-2 Zone with the equivalent nannoplankton zone (middle and upper part of NN4) and the equivalent planktonic foraminiferal zone (upper part of M4a and lower part of M5a zones) (Figure 24 and Figure 25). Moreover, P-2 zone in this study is the equivalent to the middle part of the DN3 Zone of Köthe (2003), middle part of Pmc Zone of Strauss et al. (2001), middle part of M4 Zone of Munsterman and Brinkhuis (2004), lower part of D17a Zone of Powell and Brinkhuis (2004) and middle part of DN3 zone of De Verteuil and Norris (1996) (Figure 40). The LO of *Labyrinthodinium truncatum* in Denmark (Dybkjaer and Piasecki, 2010) and Netherlands (Munsterman and Brinkhuis, 2004) was recognized in the late Tortonian whereas the LO of *Labyrinthodinium truncatum* in Italy (Zevenboom, 1995) was marked in the middle Tortonian. Since *Labyrinthodinium truncatum* is recognized through all of our studied sections, the LO of *Labyrinthodinium truncatum* can not be detected in this study.

The second dinocyst event is the FO of *Cerebrocysta poulsenii* which defines the boundary between the P-2 Zone and the P-3 Zone (Figure 24 and Figure 25). Munsterman and Brinkhuis (2004) mentioned that *Labyrinthodinium truncatum* appears before *Cerebrocysta poulsenii* in Nieder Octenhausen (Strauss et al., 2001 in Munsterman and Brinkhuis, 2004) unlike the succession of events in Italy (Zevenboom, 1995) and Netherlands (Munsterman and Brinkhuis, 2004) where *Cerebrocysta poulsenii* has an earlier occurrence than *Labyrinthodinium truncatum.* In this study, the FO of *Cerebrocysta poulsenii* is also recognized after the FO of *Labyrinthodinium truncatum* (Figure 24 and Figure 25). P-3 Zone in this study comprises the interval between the FO of *Cerebrocysta poulsenii* and the FO of *Unipontidinium aquaeductus* (Figure 24 and Figure 25). The *Cerebrocysta poulsenii* Interval Zone (Cpl Zone) in Germany of Straus et al. (2001) is also defined by the strata between the FO of *Cerebrocysta poulsenii* and the FO of *Unipontidinium aquaeductus*. Cpl Zone of Straus et al. (2001) was defined in the early Langhian, whereas the assigned age to P-3 Zone of this study is the latest Burdigalian. Finally, P-3 Zone is equivalent to the upper part of the Dn3 Zone of Köthe (2003), middle part of Cpl Zone of Strauss et al. (2001), upper part of M4 Zone of Munsterman and Brinkhuis (2004), upper part of D17a Zone of Powell and Brinkhuis (2004) and upper part of DN3 zone of De Verteuil and Norris (1996) (Figure 40).

P-4 Zone in this study is defined as the total range zone of *Unipontidinium aquaeductus* (Figure 24 and Figure 25). According to Powell and Brinkhuis (2004), the FO of *Unipontidinium aquaeductus* is dated as 14.8 Ma and the LO is dated as 13.2 Ma indicating a total duration of 1.4 Ma. The P-4 Zone in this study covers the interval from the upper part of the M5a Zone to the middle part of the M5b Zone based on planktonic foraminifera (Figure 24). So, the total duration of *Unipontidinium aquaeductus* of this study approximately correlates with the interval defined by Powell and Brinkhuis (2004). However, the FO of *Unipontidinium aquaeductus* is recorded in early Langhian and the LO is defined in early Serrevallian, whereas the FO and LO of *Unipontidinium aquaeductus* is defined in latest Burdigalian and Langhian, respectively. Moreover, Zevenboom (1995) and Munsterman and Brinkhuis (2004) also defined the FO of *Unipontidinium aquaeductus* in the Langhian. All these utilized data indicate that the FO of and the LO of *Unipontidinium aquaeductus* are recorded earlier in the Adana Basin (Turkey) than Denmark, Germany, Netherlands, NW Europe and USA Eastcoast. To conclude, the P-4 Zone in this study is correlative with the middle part of the lower part of the Dn4 Zone of Köthe (2003), Cpl Zone of Strauss et al. (2001), lower part of M5 Zone of Munsterman and Brinkhuis (2004), lower part of D17b Zone of Powell and Brinkhuis (2004) and lower part of DN4 zone of De Verteuil and Norris (1996) (Figure 40).

The forth dinocyst event is recorded as the LO of *Paleocystodinium ventricosum*. The upper boundary of the P-5 Zone is marked with this important dinocyst event. The equivalent planktonic foraminiferal and nannoplankton zones of the P-5 Zone are M5b, M6 zones and NN4-NN5 zones, respectively. The base of the M6 Zone is defined by the FO of *Orbulina suturalis* while the upper boundary of this zone cannot be detected properly due to inappropriate lithology (Figure 18). The interval corresponding to these nannoplankton zones is characterized by the total range of *Sphenolithus heteromorphus* (Figure 18). According to Strauss *et al*. (2001), *Paleocystodinium ventricosum* is a marker species with a good range as Langhian-early Serravallian. In this study, we have recorded the LO of *Paleocystodinium ventricosum* in the Langhian based on the data derived from planktonic foraminifera and calcareous nannoplankton. Therefore, the obtained data indicates that the LO of *Paleocystodinium ventricosum* is recorded earlier in the Adana Basin (Turkey) than in Germany. To conclude, the P-5 zone in this study is equivalent to the upper part of the

DN4 Zone of Köthe (2003), upper part of Cpl Zone of Strauss *et al*. (2001), M5 Zone of Munsterman and Brinkhuis (2004), D17b Zone of Powell and Brinkhuis (2004) and middle part of DN4 zone of De Verteuil and Norris (1996) (Figure 19).

The fifth important dinoevent is *Cleistosphaeridium placacanthum,* which marks the upper boundary of P6 Zone, corresponds to the Serrevallian (Figure 24 and Figure 25). This level is correlative with those of defined in eastern USA, Europe and Egypt. The LO of *Cleistosphaeridium placacanthum* was well documented in the eastern USA by De Verteuil and Norris (1996), in Europe by Zevenboom (1995) and Jiménez -Moreno et al. (2006), in Egypt by Soliman et al. (2012). Strauss et al. (2001) emphasized that the last occurrence of *Cleistosphaeridium placacanthum* recorded at the middle part of the Naq Zone of Strauss et al. (2001) was defined in the early Serrevallian. On the other hand, the LO of *Cleistosphaeridium placacanthum* was reported from the top of the DN5 Zone by De Verteuil and Norris (1996) in the middle Serrevallian. Additionally, Soliman et al. (2012) emphasized that the most biostratigraphically significant datum in the *Cleistrosphaeridium placacanthum* Interval Zone was the LO of *Cleistrosphaeridium placacanthum* which was defined in the late Langhian-early Serrevallian. Soliman et al. (2012) mentioned that this datum was influenced strongly by environmental controls. Moreover, *Cleistosphaeridium placacanthum* was lastly recorded in the middle-late Serrevallian M9 zone of Munsterman and Brinkhuis (2004). In this study, P-6 Zone is defined in the interval between the LO of *Paleocystodinium ventricosum* and the LO of *Cleistosphaeridium placacanthum* and corresponds to the M6-M7 planktonic foraminifera zone and the NN4-NN5 and NN5-NN7 nannoplankton zones (Figure 24 and Figure 25). To conclude, the P-6 Zone in this study is equivalent to the upper part of the DN5 Zone of Köthe (2003), the Naq Zone of Strauss et al. (2001), the M6-M9, M10-M11 and lower part of the M12-M13 zones of Munsterman and Brinkhuis (2004), the D18 Zone of Powell and Brinkhuis (2004) and the DN5 Zone of De Verteuil and Norris (1996) (Figure 40).

The P-7 Zone is defined by the LO of *Cleistosphaeridium placacanthum* and the FO of *Achomosphaera* cf. *andalousiensis* (Figure 24 and Figure 25). No dinoevent is recorded in this zone. The P7 Zone in this study is correlative with upper part of the *Achomosphaera andalousiensis* Zone and the *Gramocysta verricula* Zone of Dybkjaer and Piasecki (2010), the lower part of DN8 Zone of Köthe (2003), the San and Cpa

Zone and the Gve Zone of Strauss et al. (2001), the M10-M1 Zone and the lower part of the M12-M13 Zone of Munsterman and Brinkhuis (2004), the D18b Zone and the D18C Zone of Powell and Brinkhuis (2004) and lower part of the DN6-DN7 Zone and the lower part of the DN8 Zone of De Verteuil and Norris (1996) (Figure 40).

The seventh dinocyst event is recognized as the FO of *Achomosphaera* cf. *andalousiensis* (Figure 24 and Figure 25). The lower boundary of P-8 Zone in this study is characterized by the first appearance of *Achomosphaera* cf. *andalousiensis* (Figure 24 and Figure 25). The equivalent planktonic foraminiferal zone of this level is defined as the M10 Zone (Figure 24). This level is correlative with those of defined in NW Europe and the Mediterranean. For instance, Manum et al. (1989) also defined the Middle-Late Miocene boundary with the FO of *Achomosphaera andalousiensis*, whereas the same boundary was defined by the LO of *Palaeocystodinium* by Herngreen (1987) and von Daniels et. al. (1990). *Palaeocystodinim* was not recognized in the P-8 Zone and further in this study. However, Zevenboom (1995) supported that neither of these dinocysts events occurred at this discussed boundary. According to Zevenboom (1995), the FO of *Achomosphaera andalousiensis* in Italy was interpreted within the Serrevallian, while the LO of *Palaeocystodinium* was recognized in the Tortonian. The P-8 Zone in this study is correlative with the uppermost part of the *Gramocysta verricula* Zone and the lower part of the *Amiculosphaera umbraculum* Zone of Dybkjaer and Piasecki (2010), the middle part of DN8 Zone of Köthe (2003), upper part of the Gve Zone and the lower parts of the Aum and Pal zones of Strauss et al. (2001), middle part of the M12-M13 Zone of Munsterman and Brinkhuis (2004), upper part of the D18C Zone and lower part of the D19a Zone of Powell and Brinkhuis (2004) and the middle part of the DN8 Zone of De Verteuil and Norris (1996) (Figure 40).

P-9 Zone is mainly characterized by an acme of *Homotryblium* dinoflagellate cysts including *Homotryblium floripes*, *Homotryblium pallidum*, *Homotryblium plectilum* and *Homotryblium tenuispinosum* (Figure 24 and Figure 25). The most dominating *Homotryblium* species is *Homotryblium tenuispinosum* in this zone. The equivalent planktonic foraminiferal zone and the equivalent nannoplanton zone of this zone is defined as M11 and NN5-NN7, respectively (Figure 24). According to the equivalent planktonic foraminiferal zone, the assigned age was decided as latest Serrevallian- early Tortonian (Figure 24). Dybkjaer and Piasecki (2010) also recorded

the last occcurrance of abundant *Homotryblium tenuispinosum* in the Hystrichosphaeropsis obscura Zone assigned to early Tortonian. In addition, Dybkjaer (2004b) mentioned that the stratigraphic range of *Homotryblium tenuispinosum* should be extended to the late Miocene for northwestern Europe, in accordance with the range known from the Mediterranean and the North Atlantic. Furthermore, the P-9 Zone in this study is correlative with the lower and middle part of the *Amiculosphaera umbraculum* Zone of Dybkjaer and Piasecki (2010), the middle part of DN8 Zone of Köthe (2003), lower parts of the Aum and the Pal zones of Strauss et al. (2001), middle part of the M12-M13 Zone of Munsterman and Brinkhuis (2004), upper part of the D19a Zone of Powell and Brinkhuis (2004) and the middle part of the DN8 Zone of De Verteuil and Norris (1996) (Figure 40).

In summary, the palynological analysis performed in the studied sections show that the FO of *Labyrinthodinium truncatum* was recognized in latest Burdigalian apparently before *Cerebrocysta poulsenii,* like recorded in Nieder Octenhausen (Strauss et al., 2001 in Munsterman and Brinkhuis, 2004) but unlike the succession of events in Italy (Zevenboom, 1995) and Netherlands (Munsterman and Brinkhuis, 2004). According to the Williams et al. (2004), the FO of *Labyrinthodinium truncatum* correlates with the Burdigalian-Langhian boundary. However, the FO of *Labyrinthodinium truncatum* was recognized earlier than the Burdigalian-Langhian boundary in this study. In addition, the FO of *Unipontidinium aquaeductus* corresponding to the upper part of M5a, M5b and M6 planktonic foraminiferal zones (latest Burdigalian-Langhian) and NN4 and NN5 nannoplankton zones (latest Burdigalian-Langhian) is apparently earlier in the Eastern Mediterranean than in Denmark (Dybkjaer and Piasecki (2010), in Germany (Köthe, 2003; Strauss et al., 2001), Netherlands (Munsterman and Brinkhuis, 2004), NW Europe (Powell and Brinkhuis, 2004) and in USA Eastcoast (De Verteuil and Norris, 1996) (Figure 40). On the basis of this evaluated data, it can be stated that these important dinocyst events (e.g. *Labyrinthodinium truncatum, Cerebrocysta poulsenii, Unipontidinium aquaeductus*) in the Adana Basin occurred apparently earlier than those recognized in Denmark, Germany, Netherlands, NW Europe and USA Eastcoast. Like the FO of *Unipontidinium aquaeductus*, the LO of *Unipontidinium aquaeductus* is also determined earlier in the Adana Basin (Turkey). On the other hand, the LO of the *Cleistrosphaeridium placacanthum* and the FO of *Achomosphaera* cf. *andalousiensis*

are correlative with those of defined in NW Europe and the Mediterranean. Finally, the acme of *Homotryblium* dinoflagellate cysts (e.g. *Homotryblium floripes*, *Homotryblium pallidum*, *Homotryblium plectilum* and *Homotryblium tenuispinosum*) has been recorded in the latest Tortonian clastic deposits of the Adana Basin (Turkey) which is also well correlated with NW Europe and the Mediterranean.

CHAPTER 4

TAXONOMY

In this study, the taxonomical work has been carried out for both marine and terrestrial palynomorphs. A total of 73 palynomorphs, including 43 dinoflagellates, 25 spores and pollen and 2 organic-walled green algae, have been identified.

4.1. POLLEN

Pollen are classified into two main groups, namely gymnospermous pollen (gymnospermous saccate pollen and gymnospermous non-saccate pollen) and angiospermous pollen, as discussed below.

Gymnospermous saccate pollen:

Gymnospermous saccate pollen differ from each other with their number of sulcus. Traverse (2008) mentioned that monosaccate, trisaccate, pseudosaccate and cavate or camerate fossil grains are mainly recognized in Mesozoic and Paleozoic sediments, wheras the bisaccate pollens are generally all extant saccates (such as; *Pinus*). Rudolph (1935) divided *Pinus* into two groups as "hypoxylon-group" and "diploxylon-group" in 1935. After Rudolph (1935), Potoniè (1958a) defined "hypoxylon-group" as "*Abietineaepollenites microalatus"* and "diploxylon-group" as "*Pollonites labdacus*". Then, these two groups were put in the same group and named as form-genus "*Pityosporites*" by Thomson and Pflug (1953). In this study, most of the bisaccate pollen, representing no stratigraphical importance, were not defined in species order. They were assigned as 'Bisaccates' in this study.

Bisaccates

(App. A, Pl. 14 (Figs. 1-12))

Description: The bisaccate pollen grain consists of a body with two laterally placed bladders (e.g. sacca, vesicles).
Dimension: 80-100 microns.

Gymnospermous non-saccate pollen:

Genus: ***Inaperturopollenites*** Pflug and Thomson in Thomson and Pflug, 1953
Type species: ***Inaperturopollenites dubius*** (Potoniè and Venitz, 1934) Pflug and Thomson *in* Thomson and Pflug, 1953

Inaperturopollenites hiatus (Potoniè, 1931a)
Pflug and Thomsan in Thomsan and Pflug, 1953.
(App. A, Pl. 19 (Figs. 6-9))

Description: This inaperturate pollen grain is spherical to ovoid in shape. A ligula is observed in this species. Our specimens have also psilate and commonly folded exines.
Dimension: 30-40 microns.

Inaperturopollenites magnus (Potoniè, 1934) Pflug and Thomson in Thomson and Pflug, 1953
(App. A, Pl. 19 (Figs. 10, 11))

Description: This inaperturate pollen grain is spherical to ovoid in shape. It is characterized by its large size. Our specimens have commonly folded exines.
Dimension: 80-90 microns.

Genus: ***Ephedripites*** (Bolkhovitina, 1953) Potoniè, 1958a
Type species: ***Ephedripites mediplobatus*** (Bolkhovitina, 1953) Potoniè, 1958a

Ephedripites sp.

(App. A, Pl. 16 (Figs. 1-4))

Description: The shape is recognized as elongate-oval to broadly elliptical. There are several longitudinal ribs running from one pole to another. This species is characterized by these longitudinal ribs and has thin and two-layered wall. In our specimens, the polar axis/equatorial axis ratio is larger than 1.

Dimension: 45-55 microns.

Angiospermous pollen:

Genus: ***Monoporopollenites*** Meyer, 1956

Type species: ***Monoporopollenites gramineoides*** Meyer, 1956

Monoporopollenites gramineoides Meyer, 1956

(App. A, Pl. 16 (Figs. 5-10))

Description: This monoporate pollen grain is elliptical in shape. A simple pore is recognized with an annulus that is sharply differentiated from the remainder of the exine. Furthermore, the nexine is continuous and much thickened around the pore region. Secondary folds were observed in most of our specimens due to fossilization.

Dimension: 30-40 microns.

Family: Umbelliferae

(App. A, Pl. 18 (Fig. 16); Pl.19 (1, 2)

Description: Pollen grains belonging to this family are small and dicolporate. They seem constricted in the middle with distinct colpa. The pores located at the constricted sides and beside these colpas.

Dimension: 25-40 microns.

Genus: ***Momipites*** Wodehouse, 1933

Type species: ***Momipites coryloides*** Wodehouse, 1933

***Momipites* sp.**

(App. A, Pl. 18 (Figs. 11-15))

Description: The shape is triangular to subtriangular. There are three simple pores oriented equatorially on the corners without any annulus. It has smooth surface.

Dimension: 30-40 microns.

Genus: ***Subtriporopollenites*** Pflug and Thomson *in* Thomson and Pflug, 1953

Type species: ***Subtriporopollenites anulatus*** Pflug and Thomsan *in* Thomsan and Pflug, 1953

Subtriporopollenites simplex (Potoniè and Venitz, 1934) Thomson and Pflug, 1953

(App. A, Pl. 17 (Figs. 13-16))

Description: This pollen grain is triangular to sub-spheroidal in shape. It is precisely characterized by having three pores located at the corners with 120^0 angle. The nexine is continuous and much thickened around the pore region.

Dimension: 40-50 microns.

Genus: ***Tricolporopollenites*** Pflug and Thomson *in* Thomson and Pflug, 1953

Type species: ***Tricolpopollenites dollium*** (Potoniè, 1931a) Thomson and Pflug, 1953.

***Tricolporopollenites* spp.**

(App. A, Pl. 19 (Fig. 12))

Description: This pollen grain is sub-elongated to elongated in shape. It is a tricolporate pollen grain which has three colpa extended from one pole to another pole and three pores located on the center of each colpa.

Remark: In this study, the pollen grains belonging to *Tricolporopollenites*, representing no stratigraphical importance, were evaluated as *Tricolporopollenites* spp..

Dimension: 35-45 microns.

Family: **Compositae**

Compositae (liguliflorae -type)

(App. A, Pl. 15 (Figs. 1-5))

Description: This pollen grain is spherical, fenestrate and clearly lophate in shape. It has spines on the ridges. Raised ridges forming polygonal pattern with small spicules are recognized on the surface of the pollen grain. Exine is substantially thin.

Dimension: 20-35 microns.

Compositae (tubuliflorae -type)

(App. A, Pl. 15 (Figs. 6-9))

Description: The shape of this tricolporate echinate pollen grain is spherical to subprolate. Colpi are long extending about 3/4 of diameter. Moreover, it has a thick and clearly identified tectal layer with a slightly undulate and rugosa surface. The exine is thick in the middle but gets thinner towards the edges.Tectum is thick and regularly distributed with low spines (less than 1 μm high).

Remarks: Compositae (tubuliflorae-type) belongs to Compositae Family. This tricolporate pollen is comparable with *Echitricolporites spinosus* (Van der Hammen, 1956) Germeraad et al., 1968, *Echitricolporites mcneillyi* Germeraad et al., 1968 and *Echitricolporites minutus* Regali et al., 1974. Compositae (tubuliflorae -type) is obviously differentiated from these species with its smaller size and much thinner exine in this study.

Dimension: 30-45 microns.

Family: **Dipsacaceae**

(App. A, Pl. 15 (Figs. 12, 13))

Description: Pollen grains belonging to this family is triangular to subtriangular in shape. It has three pores situated on each corner. This species is characterized by two-layered wall. Columellae is recognized within this species.

Dimension: 70-80 microns.

Genus: **Nothofagaceae** Potoniè, 1960

Type species: ***Nothofagidites flemingii*** (Couper, 1953) Potoniè, 1960

Nothofagidites emarcidus (Cookson 1959) Harris 1965

(App. A, Pl. 16 (Figs. 11-14))

Description: This pollen grain is peroblate in shape. It has seven pores located at the corners. The sexine appears to be slightly thicker than nexine and surface is finely granulate.

Remarks: This pollen grain is differentiated from other species of *Nothofagidites* by the number of pores.

Dimension: 25-35 microns.

Genus: ***Intratriporopollenites*** Pflug and Thomsan *in* Thomson and Pflug, 1953

Type species: ***Intratriporopollenites instructus*** Pflug and Thomsan *in* Thomson and Pflug, 1953

Intratriporopollenites instructus Pflug and Thomson *in* Thomson and Pflug, 1953

(App. A, Pl. 18 (Figs. 1-4))

Description: This triporate pollen grain is broadly rounded to triangular in shape. Pores located at the middle of the sides are circular and equatorial. They always have a postvestibulum. This species has distinctive annulus.

Dimension: 30-40 microns.

Genus: ***Periporopollenites*** Pflug and Thomson *in* Thomson and Pflug, 1953

Type species: ***Periporopollenites multiporatus*** Pflug and Thomson *in* Thomson and Pflug, 1953

Periporopollenites multiporatus Pflug and Thomson *in* Thomson and Pflug, 1953

(App. A, Pl. 16 (Figs. 15, 16); Pl. 17 (1, 2)

Description: This pollen characterized by its small circular outline with various number of pores regularly distributed over the whole surface. The surface is irregularly granular.

Dimension: 25-30 microns.

Periporopollenites stigmosus (Potoniè, 1931b) Thomson and Pflug, 1953

(App. A, Pl. 17 (Figs. 3, 4))

Description: This pollen grain is spherical in shape. It has various rounded to elongated pores without atrium. These pores are regularly distributed over the whole surface. The outer layer is minutely reticulate.

Dimension: 25-35 microns.

Genus: ***Polyporopollenites*** Pflug *in* Thomson and Pflug, 1953

Type species: ***Polyporopollenites undulosus*** (Wolf, 1934) Thomson and Pflug, 1953

Polyporopollenites undulosus (Wolf, 1934) Thomson and Pflug, 1953

(App. A, Pl. 17 (Figs. 9, 10))

Description: This polyporate pollen grain is characterized by its rounded outline with widely and irregularly distributed pores on the whole surface. The wall surface is densely and finely undulated.

Dimension: 30-45 microns.

Polyporopollenites stellatus (Potoniè and Venitz, 1934) Thomson and Pflug, 1953

(App. A, Pl. 17 (Figs. 5, 8))

Description: This polyporate pollen grain is characterized by its polygonal outline with pores located on the equator and in the corners. In our specimens, we recognized seven pores in this species.

Dimension: 40-45 microns.

Genus: ***Polyvestibulopollenites*** Pflug *in* Thomson and Pflug, 1953

Type species: ***Polyvestibulopollenites verus*** (Potoniè, 1931b) Thomson and Pflug, 1953

Polyvestibulopollenites verus (Potoniè, 1931b) Thomson and Pflug, 1953

(App. A, Pl. 17 (Figs. 11, 12))

Description: This pollen grain is rectangular-polygonal in shape. Our specimens has four to five distinct pores with labrum and vestibulum. The adjacent vestibula pairs are connected with tubes between sexine and nexine. They symmetrically placed with regard to equator and they run like garlands.

Dimension: 30-40 microns.

4.2. SPORES

Spores are classified into two main groups, namely monolete spores and trilete spores, as discussed below.

Monolete Spores:

Genus: ***Laevigatosporites*** İbrahim, 1933

Type species: ***Laevigatosporites vulgaris*** (İbrahim, 1933) İbrahim, 1933

Laevigatosporites haardti (Potoniè and Venitz, 1934) Thomson and Pflug, 1953

(App. A, Pl. 18 (Figs. 5, 6))

Description: This monolete spore is elliptical in shape and a bean-shaped contour is recognized in the lateral view. The exospore is thin and laevigate. Furthermore, secondary folds were recognized in some of our specimens due to fossilization.

Dimension: 35-45 microns.

Genus: ***Verrucatosporites*** Pflug and Thomson *in* Thomson and Pflug, 1953

Type species: ***Verrucatosporites alienus*** (Potoniè, 1931c) Thomson and Pflug, 1953

Verrucatosporites favus (Potoniè, 1931c) Thomson and Pflug, 1953

(App. A, Pl. 19 (Figs. 3-5))

Description: This monolete spore is characterized by its verrucate ornamentation. A bean-shaped contour is recognized in the lateral view.

Dimension: 55-70 microns.

Trilete Spores:

Genus: ***Cingulatisporites*** Thomson *in* Thomson and Pflug, 1953

Type species: ***Cingulatisporites levispeciosus*** Pflug *in* Thomson and Pflug, 1953

Cingulatisporites macrospeciosus (Potoniè and Gelletich, 1933) Nakoman, 1966

(App. A, Pl. 14 (Figs. 13-16))

Description: This trilete spore is broadly triangular in shape. Its sides are straight and apices are rounded. The exine is thin and smooth. It is characterized by having a cingulum and verrucate ornamentation.

Dimension: 50-60 microns.

Genus: ***Echinatisporis*** Krutzsch, 1959

Type species: ***Echinatisporis longenhinatus*** Krutzsch, 1959

Echinatisporis longechinatus Krutzsch, 1959

(App. A, Pl. 15 (Figs. 14-16))

Description: This trilete spore is formed by rounded to triangular convex sides. It has echinate ornamentation. This species is differentiated from the other species of *Echinatisporis* by having relatively longer spines.

Remarks: *Echinatisporis longechinatus* was evaluated as a reworked spore in our specimens.

Dimension: 55-60 microns.

Genus: ***Leiotriletes*** (Naumova, 1937) Potoniè and Kremp, 1954

Type species: ***Leiotriletes sphaerotriangulus*** (Loose, 1932) Potoniè and Kremp, 1954

Leiotriletes adriennis (Potoniè and Gelletich, 1933) Krutzsch, 1959

(App. A, Pl. 18 (Figs. 7-10))

Description: This trilete spore is broadly triangular in shape. Its sides are straight and apices are rounded. The trilete marker is straight and sharply cut. Furthermore, it does not reach to the corners. The exine is thin and smooth.

Dimension: 55-60 microns.

Genus: ***Magnastriatites*** Germeraad et al., 1968

Type species: ***Magnastriatites howardii*** Germeraad et al., 1968

Magnastriatites howardii Germeraad et al., 1968

(App. B, Pl. 15 (Figs. 10-11))

Description: This trilete spore is subcircular to subtriangular in shape. It is coarsely striate except on the proximal contact area which is surrounded by circular ridge.

Dimension: 40-45 microns.

4.3. ORGANIC-WALLED GREEN ALGAE

Division **Chlorophyta** Pascher, 1914

Class **Chlorophyceae** Kützing, 1843

Order **Chlorococcales** Marchand, 1895 orth. mut. Pascher, 1915

Family **Hydrodictyaceae** (Gray) Dumortier, 1829

Genus: ***Pediastrum*** Meyen, 1829

Type species: ***Pediastrum duplex*** Meyen, 1829

***Pediastrum* sp.**

(App. A, Pl. 19 (Figs. 15)

Description: This freshwater algae is characterized by having flat and plate-like feature. They are mainly formed by circular to disc-shaped colonies occurred by irregularly triangular cells. These individual cells in our specimens are almost the same in size and shape. They are generally seen as 2 or 3 rings or rows in arrangement. They are recognized from fresh to brackish water environment.

Dimension: 70-100 microns

Family **Botryococcaceae** Wille, 1909

Genus: ***Botryococcus*** Kützing, 1849

Type species: ***Botryococcus braunii*** Kützing, 1849

***Botryococcus braunii*.**

(App. A, Pl. 19 (Figs. 16)

Description: This species is recognized as small colony of cells forming conspicuous masses of colonies in our specimens. We observed each colony appearing as a mass of cup-shaped cells. In some specimens, colonies were seen small and round to concave in shape. Since some of the small colonies were connected to each other, we defined these compound colonies in varios shapes and sizes. Furthermore, an elaborately branching system was discernible in some of our well-preserved specimens.

Dimensions: 30-120 microns

4.4. DINOFLAGELLATES

Division **DINOFLAGELLATA** (Bütschli, 1885) Fensome et al., 1993

Subdivision **DINOKARYOTA** Fensome et al., 1993

Class **DINOPHYCEAE** Pascher, 1914

Subclass **PERIDINIPHYCIDAE** Fensome et al., 1993

Order **GONYAULACALES** Taylor, 1980

Suborder **GONYAULACINEAE** (Autonym)

Family **GONYAULACACEAE** Lindemann, 1928

Subfamily **GONYAULACOIDEAE** (Autonym)

Genus: ***Achomosphaera*** Evitt, 1963a

Type species: ***Achomosphaera ramulifera*** (Deflandre, 1937) Evitt, 1963a

Achomosphaera* cf. *andalousiensis Jan du Chêne, 1977

(App. A, Pl. 1 (Figs. 1, 2))

1977 *Achomosphaera andalousiensis,* Jan du Chêne, pl.1, figs. 1-4

1977 Spiniferites septentrionalis, Harland, pl. 1, figs. 12-15, 17, 18

1988 Spiniferites aquilonius, Matsuoka and Bujak, pl. 11, fig. 6, pl. 12, fig.1

1992 *Spiniferites andalousiensis,* Strauss and Lund, pl. 4, figs. 4-5

1992 *Achomosphaera andalousiensis,* Powell, pl. 1, fig. 2

2004 *Achomosphaera andalousiensis*, Munsterman and Brinkhuis, fig. 17

2001 *Spiniferites* cf. *andalousiensis,* Strauss et al., pl. 6, figs. 11

Description: *Achomosphaera andalousiensis* was firstly defined by Jan du Chêne (1977). According to him, the cyst of *Achomosphaera andalousiensis* has an ovoidal central body, with a precingular opening. The processes are long, slender, formed by the extension of the outer cyst layer and sutural ridges are not observed. Distally the processes are complex, first trifurcate, then in the form of closed, large-mesh reticules. Every external corner of the reticule bears a slender spine (Jan du Chêne, 1977). Each of the final furcations were connected to the nearest ones by narrow trabeculae. These trabeculae form a polygonal reticulum with a spine at each angle.

Remarks: Although most of the morphological characters were recognized in *Achomosphaera* cf. *andalousiensis* defined in this study, the polygonal reticulum could not be detected obviously. We still have doubts if the polygonal reticulum exists or not. It was very difficult to figure out the distal ends of the process under microscope since the preservation of the dinocyst is not very good. Therefore, we defined this dinocyst as *Achomosphaera* cf. *andalousiensis.* Strauss et al. (2001) mentioned that the use of *Spiniferites andalousiensis* sensu stricto (now *Achomosphaera andalousiensis*) as a zonal marker species might be considered problematic due to some uncertainty in taxonomic differentiation from the precursor types. Variation of distal process termination could be recognized in *Spiniferites* cf. *andalousiensis* (Strauss et al., 2001), as in our samples (Figure 41). This taxon is important since it has an excellent first occurrence in the Miocene.

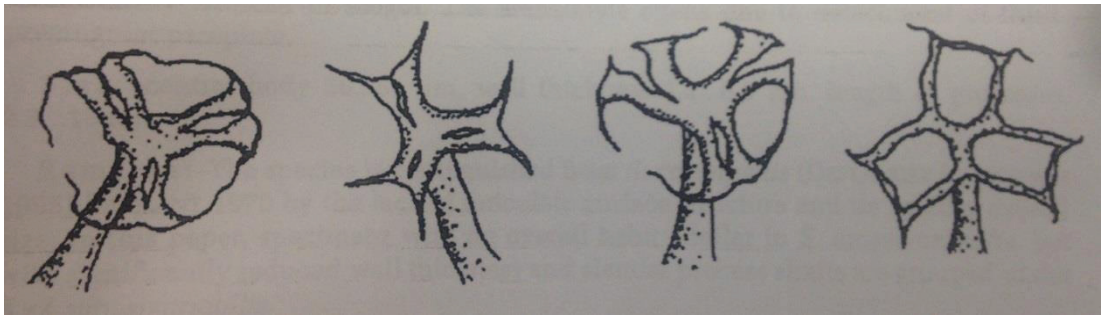

Figure 41. Variation of distal process termination in Spiniferites cf. andalousiensis (Strauss et al., 2001).

One of the taxonomic junior synonym is *Spiniferites septentrionalis* (according to Harland, 1983). Although the distal parts of the processes seem to be less complex and less extensively subdivided in *S. septentrionalis*, and because the holotype of latter species could not be studied, this synonymy is maintained. *Spiniferites speetonensis* has processes similar to those of *A. andalousiensis*, but differs from it in the possession of low septa and intragonal processes (Jan du Chene and Londeix, 1988). *Spiniferites perforatus* is another taxonomic synonym which has parasutural septa that may be relatively high, locally, and sutural processes (Bujak et al. 1980).

Dimensions: 40-50 microns

***Achomosphaera* sp.**

(App. A, Pl. 12 (Figs. 12-14))

Description: The test contains a spherical to ellipsoidal central body with precingular archaeopyle. It has spine-like processes. Although it was difficult to figure out the distal process termination in our specimens, tips of processes are observed as interconnected. Furthermore, specimens assigned to this species have been recognized with relatively small dimensions.

Remarks: *Achomosphaera* differs from *Spiniferites* either in lacking parasutural features all together or in having only faint linear markings between bases of processes. It is known that transitional forms with parasutural features intermediate between those on typical species of each genus make consistent identification difficult. Therefore, we defined this species as *Achomosphaera* sp. in this study.

Dimensions: 30-40 microns

Genus: ***Cerebrocysta*** Bujak, 1980

Type species: ***Cerebrocysta poulsenii*** de Verteuil and Norris, 1996

Cerebrocysta poulsenii de Verteuil and Norris, 1996

(App. A, Pl. 1 (Figs. 5-14)

1980 Gen. et sp. indet., Piasecki, pl. 3, fig. 3, pl. 6. figs. 5-6

1984 Gen. et sp. indet., Edwards, pl. 5, fig. 7

1989c Gen. et sp. indet., Head et al., pl. 12,figs.10-14

1989 Gen. et sp. indet., Manum et al., pl.10,figs.1-3

1992 Gen. et sp. indet., Straus and Lund, pl.1, figs. 13, 14, 16

1996 *Cerebrocysta poulsenii,* de Verteuil and Norris, pl. 12, figs. 9-21; pl. 13, figs. 1-12

Description: It was first defined as 'Gen. et. sp. indet. PIASECKI' and then classified by Zevenboom (1995, unpubl) as the new genus *Imperfectodinium* nom. nud. as *I. bulbosum* and *I. septatum*. According to de Verteuil and Norris (1996), this is a small ovoidal cyst characterized by a thin, evenly granulate autoblast with discontinuous, even septa that suggest but do not delimit tabulation. The septa recognized within our specimens are quite variable in length and density with respect to spacing. Some specimens have essentially non-tabular, short septa representing a little connectivity. The other specimens have longer septa with several bends and greater connectivity forming fence-like patterns. The septa have straight tops and terminate abruptly but their height among specimens is variable. The archaeopyle is precingular. There are no depressions on the cyst to indicate cingulum or sulcus and no apical pore structure observed.

Remarks: *Cerebrocysta poulsenii* is a very distinctive species with its discontinuous, nontabular septa. If the septa of *Cerebrocysta poulsenii* sometimes were poorly developed and recognized as isolated blade structures, it could be confused with *Operculodinium piaseckii* and *Operculodinim janduchenei*. This morphological character helps us to define this species as *Cerebrocysta poulsenii* in this study. Additionally, it is important to note that *Cerebrocysta poulsenii* is never common in the shallow to marginal marine deposits whereas it seems to have an outer neritic environmental preference. Moreover, the lowest and highest occurrances of *Cerebrocysta poulsenii* are useful biostratigraphic horizons.

Dimensions: 30-40 microns.

***Cerebrocysta* sp.**

(App. A, Pl. 1 (Figs. 15, 16); Pl. 2 (Figs. 1-4)

Description: The cyst is spherical to ovoidal with a mid-dorsal precingular archaeopyle. Since the septa were poorly developed, it is difficult to distinguish this species. Because of the preservation problems, it was difficult to exactly define them as *Cerebrocysta poulsenii*. However, the short septa representing a little connectivity helps to define it as *Cerebrocysta* sp. in this study.

Dimensions: 30-40 microns.

Genus: ***Cleistosphaeridium*** Davey et al., 1966

Type species: ***Cleistosphaeridium diversispinosum*** Davey et al., 1966

Cleistosphaeridium ancyreum (Cookson and Eisenack, 1965a) Eaton et al., 2001

(App. A, Pl. 2 (Figs. 5-7))

Description: The cyst is slightly oval with a rather thick, densely granular wall. It has numerous slender, flexuous, occasionally forked appendages with capitate and slightly bifurcate apices. An apical archaeopyle is recognized. The preservation is quite well in some of our specimens and the appendages delimit circular or polygonal areas. These polygonal areas are recognized as variable in size and are separate from one another.

Remarks: *Cleistosphaeridium ancyreum* is very similar to *Systematophora areolate*. However, *Cleistosphaeridium ancyreum* differs from *Systematophora areolate* in that the boundaries of the fields from which the processes arise are not always complete, nor always separate from one another. The same morphological feature also separate *Cleistosphaeridium ancyreum* from *Cleistosphaeridium placacanthum*. Accordingly, these characteristics help us to define this species as *Cleistosphaeridium ancyreum.*

Dimensions: 80-90 microns.

Cleistosphaeridium placacanthum (Deflandre and Cookson, 1955)

(App. A, Pl. 2 (Figs. 8-14), Pl. 3 (Figs. 3, 4))

1955 *Hystrichosphaeridium placacantha,* Deflandre and Cookson, pl. 9, figs. 1-2

1996 *Systematophora placacantha*, Gedl, pl. 7, figs. k, m

2004 *Systematophora placacantha,* Fauconnier and Masure, pl.76, figs.14-16

2004 *Systematophora placacantha*, Munsterman and Brinkhuis, fig. 7

Description: The cyst is spherical to slightly ovoidal in shape with a large number of solid processes. Processes are branched with pointed or hammer-shaped extremities, widening at the base. The most important characteristic feature of the dinocyst is its process distribution. Davey et al. (1969) mentioned that processes are aligned to divide the whole surface into more or less polygonal fields. Similarly, we easily detected these polygonal fields in our specimens. Each field is separated from its neighbors by an area devoid of appendages. Sometimes the bases of two or more processes are connected by bridge-like strands. The surface of the shell is finely reticulate. Archaeopyle is apical (Type A) and operculum is free.

Dimensions: 80-90 microns.

Genus: ***Cordosphaeridium*** Eisenack, 1963a emend. He Chengquan, 1991

Type species: ***Cordosphaeridium inodes*** (Klump, 1953) Eisenack, 1963a emend. Morgenroth, 1968 emend. Sarjeant, 1981

?Cordosphaeridium cantharellus (Brosius, 1963) Gocht, 1969

(App. A, Pl. 6 (Fig. 11)

Description: The cyst is spherical to ovoidal in shape. It has 15-20 hollow tree-like processes. The processes are of variable thickness They are mostly broad and cylindrical, narrow slightly in the middle and broaden weakly distally. They consists of thin, parallel fibre strings. Archaeopyle is precingular and operculum is free.

Remarks: Because of preservation problems in our specimens, a questionmark is kept with *Cordosphaeridium cantharellus.*

***Cordosphaeridium* sp.**

(App. A, Pl. 12 (Fig. 3)

Description: The cyst has a spherical to ellipsoidal body, which is covered with approximately homogenous and rather regularly distributed radial appendages, which

appear cord-like. The process walls are fibrous, the fibres with or without root-like proximal extensions. Archaeopyle is precingular and operculum is free. Because of preservation problems in our specimens, the species of *Cordosphaeridium* could not be assigned and it kept as *Cordosphaeridium* sp.

Remarks: Stover and Evitt (1978) mentioned that *Cordosphaeridium* differs from *Kleithriasphaeridium* in having fibrous rather than smooth or faintly striate processes. *Cordosphaeridium* sp. can be compared with the other genera having fibrous processes and precingular archaeopyle; such as, *Amphorosphaeridium*, *Fibrocysta* and *Turbiosphaera*. *Amphorosphaeridium* has mainly nontabular processes with only occasionally intratabular processes; *Fibrocysta* has a more elongate body than *Cordosphaeridium* and generally a larger number of paracingular processes; *Turbiosphaera* is more elongate, its processes are typically wide and flat, and the paracingulum is represented by a shelf-like projection. By the help of these morphological features, we defined this species as *Cordosphaeridium* sp. in this study.

Dimensions: 60-80 microns.

Genus: ***Cribroperidinium*** Neale and Sarjeant, 1962 emend. Helenes, 1984

Type species: ***Cribroperidinium sepimantum*** Neale and Sarjeant, 1962

Cribroperidinium tenuitabulatum (Gerlach, 1961) Helenes, 1984

(App. A, Pl. 13 (Figs 9, 10))

1961 *Gonyaulax tenuitabulatum,* Gerlach, pl.25, figs.10-11

1969 *Gonyaulacysta tenuitabulata*, De Coninck

1978 *Millioudinium tenuitabulatum*, Stover and Evitt

1984 *Cribroperidinium tenuitabulatum*, Helenes, pl.2, fig.3

1996 *Cribroperidinium tenuitabulatum*, Gedl, pl. 4, figs. d-i; pl. 10, figs. I, J

Description: The cyst is spheroidal to broadly rounded-subpolygonal and usually recognized with a short, tapering and blunt apical horn. The most important and distinctive morphological feature is tabulation. Low narrow crests delimit tabulation. Although there are preservation problems in our samples, the tabulation could be

recognized in our specimens. Additionally, cingulum could be easily detected and its two ends differing in anteroposterior position by 1/2 times its width. The archaeopyle is single-plate precingular (type P) and operculum is free.

Dimensions: 80-85 microns.

***Cribroperidinium* sp.**

(App. A, Pl. 11 (Figs. 1-4))

Description: The cyst is subspherical to ellipsoidal and usually recognized with a prominent apical horn. Crests are numerous and well developed in our specimens. Archaeopyle is precingular and operculum is free.

Remarks: Stover and Evitt (1978) stated that *Cribroperidinium* differs from *Millioudodinium* in having accessory ridges in the areas between parasutural ridges; *in Millioudodinium*, these areas lack accessory ridges. According to Stover and Evitt (1978) *Cribroperidinium* differs from *Corrudinium* in being considerably larger and in usually having an apical horn, which *Corrudinium* lacks. Sarjeant (1982) discussed that *Cribroperidinium* differs from *Millioudodinium*, and resembles *Corrudinium*, in its intensive development of secondary crests; it differs from the latter genus in size and the development of an apical horn. In this study, this genus could be distinguished from other genus by the height and shape of the parasutural and intratabular ridges; geometry, size and abundance of the intratabular elements of ornamentation (commonly short spines or granules, or ridges); size and shape of the body and apical horn; thickness of the wall, and relative sizes of the epicyst and hypocyst. Therefore, this species was assigned as *Cribroperidinium* sp.

Dimensions: 85-90 micron.

Genus: ***Diphyes*** Cookson, 1965 emend. Goodman and Witmer, 1985

Type species: ***Diphyes colligerum*** Deflandre and Cookson, 1955 emend. Cookson, 1965 emend. Goodman and Witmer, 1985

Diphyes pseudoficusoides Bujak, 1994

(App. A, Pl. 3 (Figs. 1, 2))

1994 *Diphyes pseudoficusoides,* Bujak, pl. 2, figs. 2-3

Description: Posterior portion of the shell is usually smaller and thinner-walled than the anterior portion, roughly bell-shaped with straight or convex sides. The most distinctive feature of this species is its large antapical process which enable easy orientation of our specimens. This antapical process is hollow, conical, occasionally closed, and bears small tubules towards the distal extremity. The smaller processes are commonly simple, occasionally united proximally, and may be open or closed distally. The preservation is quite well in some of our specimens and a centrally-placed, cone-like projection with a small circular opening could be recognized in these well preserved cysts. It has numerous broadly-based, stiff or flexuous processes. These unbranched tubular appendages show variations in lengths and widths. Additionally, they get narrower towards the ends and show funnel-shaped apices. Both types of processes are slightly fibrous and do not communicate with the interior of the central body. Archaeopyle is apical.

Remarks: The most distinctive morphological features of *Diphyes pseudoficusoides*, which differ it from most other fossil cysts, are its large antapical process and the numerous other small processes. For instance, *D. pseudoficusoides* is distinguished from other species of *Diphyes* by its antapical process, which is intermediate in morphology between that on *D. colligerum* and *D. ficusoides.*

Dimensions: 60-70 microns.

Genus: ***Florentinia*** Davey and Verdier, 1973; emend. Duxbury, 1980

Type species: ***Florentinia laciniata*** Davey and Verdier, 1973

Florentinia stellata (Maier, 1959) Below, 1982

(App. A, Pl. 3 (Figs. 5, 6))

Description: The cyst is spherical with a fibrous membrane. Processes are narrow and symmetrically arranged. They are differentiated into two categories as narrower and

broader diameters. In our specimens, the broad processes arranged in a plane. They are connected and isosceles triangle arises. It has distally serrate processes, which widen in a funnel-like fashion. This morphological character is very distinctive for this species.

Remarks: *Florentinia stellate* is similar to *Hystrichokolpoma bulbosum. Hystrichokolpoma bulbosum* has bottle-shaped processes that taper more strongly and are distally serrate, while *Florentinia stellate* has distally serrate processes which widen in a funnel-like fashion. Furthermore, *Florentinia stellate* differs from *Achilleodinium biformoides* in having distally opened wide processes. In our specimens, this species could be easily differentiated from those by these diagnostic features and defined as *Florentinia stellate*.

Dimensions: 80-90 microns.

Genus: ***Homotryblium*** Davey and Williams, 1966b

Type species: ***Homotryblium tenuispinosum*** Davey and Williams, 1966b

Homotryblium pallidum Davey and Williams, 1966

(App. A, Pl. 3 (Figs. 9-12))

Description: The cyst is subspherical to ovoidal with a thin inner endophragm and granular periphragm. The processes in our specimens are variable in size. Furthermore, they are simple and tubiform, forming a circle where they arise from central body. Besides the tubiform processes, they are often present 1 to 5 slender small acuminate processes. They reflects generic tabulation. The archaeopyle is epitractal.

Remarks: *Homotryblium pallidum* differs from *Homotryblium tenuispinosum* in having a thinner wall, generally broader processes with more variable distal margins, and a well-marked proximal circle where they arise from the central body.

Dimensions: 70-80 microns.

Homotryblium plectilum Drug and Loeblich, 1967

(App. A, Pl. 3 (Figs. 13, 14))

Description: The cyst is spherical with thin endophragm and periphragm, the latter giving rise to the processes. The wall is smooth to faintly and delicately granulate. The processes are intratabular, buccinate, and open distally but not opening into the central cavity. The most distinctive feature of this species is that the walls of the processes are striate and may be faintly fibrous. The archaeopyle is epitractal.

Remarks: *Homotryblium plectilum* differs from *Homotryblium tenuispinosum* in having striate processes, more robust singular processes, and weakly granulate wall.

Dimensions: 80-90 microns.

Homotryblium tenuispinosum Davey and Williams, 1966 b

(App. B, Pl. 3 (Figs. 15, 16), Pl. 4 (Figs. 1-6))

Description: The cyst is spherical with smooth endophragm and strongly granular periphragm. Processes are curved, tubiform, rarely perforate, simple and open distally with serrate or aculeate margin. The length of the processes are variable in size and is about half the diameter of the central body. Furthermore, they restricted to one per plate area and indicate a reflected tabulation of 3', 6", 6c, 5"', 1p, 1"" and 1-5s. The archaeopyle is epitractal.

Remarks: *Homotryblium tenuispinosum* differs from other species of *Homotryblium* in having a coarsely granular wall and its tabulation.

Dimensions: 90-100 microns.

Homotryblium floripes (Deflandre and Cookson, 1955) emend. Stover, 1975

(App. A, Pl. 3 (Figs. 7, 8))

Description: The cyst is nearly spherical with 14-16 tubular processes not communicating with the interior. We recognized the processes generally consisting of from 2 to 6 tubes. They joined along the greater part of their length and the individual tubes widening and sometimes separating from one another distally.

Dimensions: 100-120 microns.

Genus: ***Hystrichokolpoma*** Klump, 1953 emend. Williams and Downie, 1966a

Type species: ***Hystrichokolpoma cinctum*** Klump, 1953

Hystrichokolpoma rigaudiae Deflandre and Cookson, 1955

(App. A, Pl. 1 (3, 4); Pl. 4 (Figs. 7, 8))

1955 *Hystrichokolpoma rigaudiae,* Deflandre and Cookson, pl. 6, fig. 6

1992 *Hystrichokolpoma rigaudiae,* Powell, pl. 3, fig. 5

1992 *Hystrichokolpoma rigaudiae,* Brinkhuis, Powell and Zevenboom, pl. 8, fig. 5

1996 *Hystrichokolpoma rigaudiae*, Gedl, pl. 5, figs. a-c, f

Description: The cyst is globular and ellipsoidal with approximately axial symmetry. There are two types of processes as large and narrow. Bases of the large processes marked by lines forming quadrangular area that give the impression of plates and they are always closed at their distal extremities, generally widened and provided with more or less numerous and sometimes relatively long horns. The large process situated at the apical pole is often longer than the others and is sometimes prolonged into a hollow horn, while the narrow tubular processes are slightly widened or divided at their extremities, which are either open or closed. The narrow processes orientated at the equatorial part of the cyst. Below the equator there is a circle of 6 large processes. The orientation of these narrow and large processes are the distinctive features of this species.

Remarks: *Hystrichokolpoma rigaudiae* differs from *Hystrichokolpoma cinctum* by the general form of the large processes. The processes of *H. rigaudiae* are rarely cylindrical but usually slightly narrowed and then widened at their extremities, which are always closed. Furthermore, *H. rigaudiae* has smaller number of narrow despite apparently more robust equatorial processes.

Dimensions: 75-85 microns.

***Hystrichokolpoma* sp.**

(App. A, Pl. 4 (Figs. 9, 10))

Description: The cyst is globular and ellipsoidal with large penitabular processes, except those reflecting paraplates 6" and 1'''. The large processes are hollow, slightly fibrous and distally closed, denticulate and perforate.

Dimensions: 70-90 microns.

Genus: ***Hystrichosphaeropsis*** Deflandre, 1935 emend. Sarjeant, 1982

Type species: ***Hystrichosphaeropsis ovum*** Deflandre, 1935

Hystrichosphaeropsis obscura Habib, 1972

(App.A, Pl. 4 (Figs. 11-14))

Description: This species is bicavate. Outline of our specimens are essentially rectangular in shape. It has a short rounded horn appearing arched at the apex. There is an internal capsule which is oval in shape and closely appressed to outer membrane in the area of the cingulum. Antapical pericoel and apical pericoel are well-developed in our specimens. We also noticed that the former was usually larger than the latter. The archeopyle is precingular (3"). Although the preservation was not very well, we could observe the surface of internal capsule as densely granular and the scabrate outer membrane.

Remarks: We distinguished *Hystrichosphaeropsis obscura* from *Rottnestia borussica* and *Hystrichosphaeropsis ovum* by its lack of furcate processes arising from the cingulum and elsewhere on the periphragm.

Dimensions: 60-65 microns.

Genus: ***Impagidinium*** Stover and Evitt, 1978

Type species: ***Impagidinium dispertitum*** (Cookson and Eisenack, 1965) Stover and Evitt, 1978

Impagidinium paradoxum (Wall, 1967) Stover and Evitt, 1978

(App.A, Pl. 4 (Figs. 15, 16); Pl. 5 (Figs. 1-4))

Description: The cyst is very small and ovoid to polyhedral in shape. We defined this species by its low sutural septa which are sometimes reduced in the ventral area. The test is smooth and the archeopyle is precingular.

Dimensions: 25-40 microns.

Impagidinium aculeatum (Wall, 1967) Lentin and Williams, 1981

(App. A, Pl. 5 (Figs. 5-8))

Description: The cyst is small and ovoid with a relatively wide girdle zone and extensive ventral area. The sutural septa of this species most strongly developed in the posterior intercalary area. A single, small and subquadrangular antapical area is recognized in our specimens. A trapezoidal archeopyle is also detected in this species.

Dimensions: 25-35 microns.

***Impagidinium* sp.**

(App. A, Pl. 13 (Figs. 1-8))

Description: The cyst is small and subspherical to ellipsoidal in shape typically without apical projection or horn. Archaeopyle is precingular. Surface of the cyst seems microreticulate. It has low level sutural septa forming a tabulation that is characteristically reduced on the ventral surface. The test appears weakly ovoid in lateral view and circular in polar view. Since only the characteristic outer shape of the cyst with a precingular archeopyle and the septa forming tabulation are observed, the species of the genus can not be assigned and it is kept as *Impagidinium* sp.

Remarks: Stover and Evitt (1978) compared *Impagidinium* with *Leptodinium* (Klement, 1960). They mentioned that *Impagidinium* differs from *Leptodinium* in having the first and fourth apical paraplates of similar shape, of about equal length, and often imperfectly separated. In general, species of *Impagidinium* tend to be subspherical to ellipsoidal, to lack an apical projection, and to have reduced paratabulation in some instances. Species of *Leptodinium*, in contrast, tend to be more elongate, even subpolygonal, to possess an apical horn, and rarely, if ever, to have reduced paratabulation. Additionally, epicystal intercalary paraplates occur on some

species of *Leptodinium*, whereas such paraplates are observed on species of *Impagidinium*.

Dimensions: 100-120 microns.

Genus: ***Labyrinthodinium truncatum*** Piasecki, 1980

Type species: ***Labyrinthodinium truncatum*** Piasecki, 1980

Labyrinthodinium truncatum

(App. A, Pl. 5 (Figs. 9-11); Pl. 12 (Figs. 4-11))

1980 *Labyrinthodinium truncatum,* Piasecki, pl. 2, figs. 9-11

Description: The cyst is small, proximate to proximochorate and spherical in shape. This species consists of two wall layers. However, the two wall layers can not be clearly separable when periphragma is thin and smooth. The processes variably developed from laevigate to scabrate tegillum were recognized. It has numerous low, blade-like and nontabular septa. Although the preservation is not very good, we can examine this features in our specimens. On some of our specimens, the tegillum forms discontinuous septa that partially join processes proximally, forming an open, incomplete reticulum over the spongy luxuriae. The archaeopyle is large and apical.

Remarks: As a species, *Labyrinthodinium truncatum* is very similar to *Cordosphaeridium minimum* sensu Benedek and Sarjeant 1981, which is also small and has an apical archeopyle and tubiform processes (de Verteuil and Norris, 1996). However, the latter species lacks the spongy luxuriae and septate reticulum characteristic of *Labyrinthodinium truncatum*.

Dimensions: 25-40 microns.

Genus: ***Lingulodinium*** Wall, 1967 emend. Dodge, 1989

Type species: ***Lingulodinium machaerophorum*** (Deflandre and Cookson, 1955) Wall, 1967

Lingulodinium machaerophorum (Defladre and Cookson, 1955) Wall, 1967

(App. A, Pl. 5 (Figs. 12-16))

1955 *Hystrichosphaeridium machaerophorum,* Defladre and Cookson, pl. 9, fig. 4

1961 *Baltisphaeridium machaerophorum*, Gerlach

1967 *Lingulodinium machaerophorum,* Wall

Description: The cyst subspherical to ellipsoidal. It has numerous long, stiff, conical and pointed processes of variable length. Their bases are circular and minutely striated and there is a tendency towards flattening of the spines. The surface of the body is punctate. The archeopyle is precingular.

Dimensions: 70-80 microns.

Genus: ***Melitasphaeridium*** Harland and Hill, 1979

Type species: ***Melitasphaeridium choanophorum*** (Deflandre and Cookson, 1955) Harland and Hill, 1979

Melitasphaeridium choanophorum (Deflandre and Cookson, 1955) Harland and Hill, 1979

(App. A, Pl. 6 (Figs. 1-6))

1955 *Hystrichosphaeridium choanophorum*, Deflandre and Cookson, figs. 23-26

1979 *Melitasphaeridium choanophorum*, Harland and Hill, p.39, 41

Description: The cyst is spherical to subspherical in shape. Processes are tubular, cylindro-conical, abruptly widened into a small funnel with a rough margin and terminated by two recurved spine-like outgrowths. They do not connect to the interior of the cyst and are approximately half the diameter of the central body in length. Furthermore, they are rigid to sligthly flexuous. The distal ends of the process which open to the anterior are flared and basically star-shaped. In some of our specimens, the tips are infundibular with an array of short spines along the margin, whereas in others the star-shape is much more pronounced with a fewer number of long spines. Wall layers are smooth to microreticulate. The archeopyle is precingular.

Remarks: Both *Melitasphaeridium choanophorum* and *Hystrichosphaeridium tubiferum* contain funnel-like processes; however, the bases of these processes in

Hystrichosphaeridium tubiferum are open, in contrast to *Melitasphaeridium choanophorum*.

Dimensions: 54-63 microns.

Genus: ***Nematosphaeropsis*** Deflandre and Cookson, 1955; emend. Williams and Downie, 1966; emend. Wrenn, 1988

Type species: ***Nematosphaeropsis balcombiana*** Deflandre and Cookson, 1955

Nematosphaeropsis labyrinthus

(App. A, Pl. 6 (Figs. 7-10))

Description: The cyst is spherical and slightly elongate in equatorial view. The surface and processes are smooth. We recognized the processes as bifurcate and trifurcate. The tips of the bifurcate and trifurcate processes arise from the outer layer of a thin two layered wall and are usually connected to adjacent processes by parallel trabeculae. These trabeculae replicate the sutures joining the processes at their bases.

Dimensions: 45-65 microns.

Genus: ***Operculodinium*** Wall, 1967

Type species: ***Operculodinium centrocarpum*** Deflandre and Cookson, 1955

Operculodinium borgerholtense Louwye 2001 emend.

(App. A, Pl. 6 (Fig. 12))

Description: The cyst is spherical to ovoid in shape. The cyst is ornamented with low luxuriate and numerous long virgae. The processes are acuminate and capitate. They are fairly distributed over cyst, except in antapical area. The archeopyle is recognized as precingular with well-defined angles. Operculum is free.

Dimensions: 45-55 microns.

Operculodinium centrocarpum (Deflandre and Cookson, 1955) Wall 1967

(App. A, Pl. 6 (Figs. 13-16))

1955 *Hystrichosphaeridium centrocarpum*, Deflandre and Cookson, pl. 8, figs. 3-4

1961 *Baltisphaeridium centrocarpum*, Gerlach

1965 *Cordosphaeridium centrocarpum*, De Coninck

1966 *Cordosphaeridium tiara* ssp. *centrocarpum*, Morgenroth

1967 *Cordosphaeridium centracarpum,* Wall, p. 111

1969 *Cordosphaeridium microtriainum* ssp. *centrocarpum*, De Coninck

1978 Cleistosphaeridium centrocarpum, Jiabo

Description: The cyst is globular in shape. It has numerous straight, solid, slender processes placed irregularly. The slightly widened apices of the processes are fringed with curved spines. The spine tips bear small hooklets which are visible only at high magnifications. The archaeopyle is precingular.

Remarks: We recognized this species in different sizes, even in the same slide.

Dimensions: 55-80 microns.

Operculodinium microtriainum (Klump, 1953) İslam, 1983

(App. A, Pl. 7 (Figs. 1-4))

Description: The cyst is spherical in shape. It has numerous processes that are formed by the outer layer and terminate in three small hooks. The outer layer is irregularly sculptured and the netlike ridges rising along the hollow processes. The archaeopyle is precingular.

Dimensions: 60-90 microns.

Operculodinium piaseckii (Strauss and Lund, 1992)

(App. A, Pl. 7 (Figs. 5-12); Pl. 12 (15-16)

1992 *Operculodinium piaseckii*, Strauss and Lund, pl.3, figs. 2-3

Description: The cyst is small and ovoidal in shape. It has numerous nontabularly arranged, short and subconical processes. The processes can vary from small granulae or baculae. The archaeopyle is precingular.

Remarks: The process morphology of *Operculodinium piaseckii* exhibits a great range of variation in Lower-Middle Miocene assemblages, whereas the size, shape, and wall structure of the central body are usually identical (Strauss and Lund, 1992). We differentiated this species from others by its small size, ellipsoidal shape and short solid processes.

Dimensions: 30-55 microns.

***Operculodinium* sp.**

(App. A, Pl. 7 (Figs. 13-16))

Description: The cysts have a subspherical to ovoidal central body with numerous, small and subconical, nontabularly arranged processes. The processes are all similar in size. Archaeopyle is precingular and operculum is free.

Remarks: According to Stover and Evitt (1978), *Operculodinium* is differentiated from *Exochosphaeridium* and *Amphorosphaeridium* in lacking fibrous processes and apical and/or antapical processes. Moreover, it is very similar to *Cleistosphaeridium* if the archaeopyle cannot be seen due to its orientation. *Cleistosphaeridium* has an apical archaeopyle, while *Operculodinium* has a precingular archeopyle.

Dimensions: 50-60 microns.

Genus: ***Paleocystodinium*** Alberti, 1961

Type species: ***Palaeocystodinium golzowense*** Alberti, 1961

Palaeocystodinium striatogranulosum Zevenboom and Santarelli in Zevenboom, 1995

(App. A, Pl. 8 (Figs. 3, 4; Pl. 11 (Figs. 13, 14), Pl. 13 (Figs. 13-16))

Description: The cyst is elongate and subspherical with long apical and antapical periphragmal horns. The most distinctive feature of this species is its striate and granulate periphragmal horns. The archaeophyle is intercalary.

Dimensions: 110-130 microns.

Palaeocystodinium ventricosum, Zevenboom and Santarelli in Zevenboom, 1995

(App. A, Pl. 11 (Figs. 15, 16); Pl. 13 (Figs. 11, 12))

Description: The cyst is subspherical to spherical in shape. It is characterized by long apical and antapical periphragmal horns with spines. Horns are nearly equal in size with spiny ornaments getting denser at the tips. The archaeophyle is intercalary.Since our specimens are not well-preserved, apical and antapical paraplates cannot be properly observed.

Remarks: This species is differentiated from other species of *Paleocystodinium* in its account of size, broad ellipsoidal central body and surface ornament. In addition, *P. ventricosum* differs from all other *Paleocystodinium* spp., except *P. striatogranulosum* in having granules on the apical and antapical horns and in having a round subsphaerical central body.

Dimensions: 110-120 microns.

***Paleocystodinium* sp.**

(App. A, Pl. 8 (Figs. 5, 6))

Description: The cyst is elongate, ellipsoidal with a single slender pointed apical and antapical horn at both ends. The orientation of cingulum is obvious. Archaeopyle is intercalary and operculum is free.

Remarks: This species differs from the other species of *Paleocystodinium* with its larger size. Although it is not well-preserved, presence of apical and antapical horns at both pole and absence of paratabulation help us to assign this species as *Paleocystodinium* sp.

Dimensions: 110-130 microns.

Genus: ***Polysphaeridium*** Davey and Williams, 1966b emend. Bujak et al., 1980

Type species: ***Polysphaeridium subtile*** Davey and Williams, 1966b emend. Bujak et al., 1980

Polysphaeridium zoharyi (Rossignol, 1962) Bujak et al., 1980

(App. A, Pl. 8 (Figs. 7-12))

1962 *Hystrichosphaeridium zoharyi,* Rossignol, pl. 2, fig. 10

1967 *Hemicystodinium zoharyi*, Wall

1980 *Polysphaeridium zoharyi,* Bujak et al.

Description: The cyst is hemispherical in shape. The test is smooth to microreticulate. Spine bases are weakly striate. It has numerous, simple, capitate and bifurcate processes in variable sizes. The archeopyle is apical.

Dimensions: 55-85 microns.

Genus: ***Reticulatosphaera*** Matsuoka, 1983 emend. Bujak and Matsuoka, 1986

Type species: ***Reticulatosphaera actinocoronata*** (Benedek, 1972) Bujak and Matsuoka, 1986 emend. Bujak and Matsuoka, 1986

Reticulatosphaera actinocoronata (Benedek, 1972) Bujal and Matsuoka, 1986 emend. Bujak and Matsuoka, 1986

(App. A, Pl. 8 (Figs. 13-16))

Description: The cyst is chorate and subspherical in shape. It has solid, irregular, tubiform to cylindrical, intratabular processes with ramifying distal extremities. An irregular network is formed by distal trabeculae connecting adjacent processes. The archaeopyle is precingular and operculum is free.

Dimensions: 35-50 microns.

Genus: ***Spiniferites*** Mantel, 1850 emend. Sarjeant, 1970

Type species: ***Spiniferites ramosus*** (Ehrenberg, 1838) Mantell, 1854

Spiniferites bentorii (Rossignol, 1964) Wall and Dale, 1970

(App. A, Pl. 9 (Figs. 1, 2))

Description: The cyst is ovoidal in shape. The processes are recognized at the plate corners. They are trifurcate and each branch finely bifurcate. The two antapical dorsals are very well developed. Archeopyle is precingular.

Dimensions: 45-70 microns.

Spiniferites membranaceus (Rossignol, 1964) Sarjeant, 1970

(App. A, Pl. 9 (Figs. 3-6))

1964 *Hystrichosphaera furcata* var. *membranacea*, Rossignol, pl. 1, figs. 4, 9-10

1966a Hystrichosphaera ramosa var. membranacea, Davey and Williams

1967 Hystrichosphaera membranacea, Wall, p. 102-103

1970 *Spiniferites membranaceus,* Sarjeant

Description: The cyst is circular, ovoid and weakly-elongated. The surface of the cyst is scabrate to microgranular and ornamented by membranous sutural septa which are stronger where they fuse at the corners of plate-areas. Distal projections arising from the septa are trifurcate at plate corners. The archeopyle is dorsal and precingular (3") and the furrow is weakly inclined and broader posteriorly.

Remarks: *Spiniferites membranaceus* differs from *Spiniferites mirabilis* by lacking strong rows of spines over its test; instead its processes are weak and membranous.

Dimensions: 75-105 microns.

Spiniferites mirabilis (Rossignol, 1964) Sarjeant, 1970

(App. A, Pl. 9 (Figs. 7-13))

1964 *Hystrichosphaera mirabilis*, Rossignol, pl. 2, figs. 1-2

1970 *Spiniferites mirabilis,* Sarjeant

Description: The cyst is ovoid in shape. The processes are recognized as trifurcate at the junctions of three plates. The intercalary processes are also detected as bifurcate along the sutures and each branch finely bifurcate. It has a thin double layered wall. It has also parasutural processes, sometimes two per suture. There is a conspicuous sutural flange bordering the margins of the antapical area. The plate sutures are weakly visible in our specimens due to a large number of processes. Archeopyle is precingular.

Dimensions: 80-100 microns.

Spiniferites pseudofurcatus (Klump, 1953) Sarjeant, 1970 emend. Sarjeant, 1981

(App. A, Pl. 9 (Figs. 14-16))

Description: The cyst is broadly ovoidal to subpolygonal. It has long, hollow, distally open trifurcate and tetrafurcate processes. They are linked together by low sutural crests. The wall is laevigate. The archaeopyle is precingular and operculum is free.

Dimensions: 90-115microns.

Spiniferites ramosus (Ehrenberg, 1838) Mantell, 1854

(App. A, Pl. 10 (Fig. 1, 2))

1838 *Xanthidium ramosus,* Ehrenberg, pl. 1, figs. 1-2, 5

1966a *Hystrichosphaera ramosa*, Davey and Williams, p. 32

1970 *Spiniferites ramosus*, Sarjeant, p.75

Description: The cyst is ovoidal to subpolygonal in shape. It has a granulated and thin-walled central body. The intergonal processes always extend beyond confines of sutural crests, the latter closed distally. The gonal processes are trifurcate and the sutural processes are bifurcate. The archeopyle is precingular.

Dimensions: 70-80 microns.

Spiniferites spongiophragmatus Strauss et. al., 2001

(App. B, Pl. 10 (Figs. 3, 4))

Description: The cysts is subspherical to ovoidal in shape with a thick wall characterized by a spongeous appearance. It has delicate and granulate periphragm forming gonal and sutural processes. The processes are bifurcate to trifurcate with acute tips. Thin parasutural membraneous crests are recognized around the paracingular paraplates. The archeopyle is precingular.

Remarks: *Spiniferites spongiophragmatus* is differentiated from *Spiniferites antistatus* in having no distinct sutural ledges.

Dimensions: 90-100 microns.

***Spiniferites* spp.**

(App. A, Pl. 11 (Figs. 5-12), Pl. 12 (Figs. 1, 2))

Description: The cysts have a subspherical to ovoidal central body with numerous diversely developed processes. The cyst is generally divided into polygonal fields by projecting suture lines. *Spiniferites* is generally characterized by its processes arising from the points of junctions of these sutural lines. Processes are solid and branching. Length of processes are variable. Archaeopyle is precingular and operculum is free. Moreover, paratabulation is distinctly differentiated. According to preservation problems, only the characteristic processes arising from the points of junctions of these sutural lines were observed. Additionally, dinoflagellate species belonging to this genera is widely distributed in the palynological slides but most of them have no or little stratigraphic importance. The species of the genus cannot be assigned and it is kept as *Spiniferites* spp. Therefore, all the undetermined species belonging to *Spiniferites* are documented as *Spiniferites* spp. in this study.

Remarks: *Spiniferites* is differentiated from *Achomosphaera* in having parasutural ridges or septa which connect the bases of processes. There are transitional forms between them and they can be easily confused. In that case, assignment to either *Spiniferites* or *Achomosphaera* is suspicious.

Dimensions: 60-100 microns.

Genus: ***Unipontidinium*** Wrenn, 1988

Type species: ***Unipontidinium aquaeductum*** (Piasecki, 1980) Wrenn, 1988

Unipontidinium aquaeductus (Piasecki, 1980) Wrenn, 1988

(App. A, Pl. 10 (Figs. 5-16))

1980 *Nematosphaeropsis aquaeducta,* Piasecki, 1980, pl.1, figs.1-3; pl.5, figs.1-2

1988 *Impagidinium aquaeductum,* Wrenn, 1988, p.148

1992 *Nematosphaeropsis aquaeducta,* Strauss and Lund, 1992

1996 *Unipontidinium aquaeductum*, Gedl, pl. 5, figs. d, e, g, h, j, k

2004 *Unipontidinium aquaeductum*, Munsterman and Brinkhuis, fig. 11

Description: The cyst is characterized by its spherical to slightly ovoidal central body and sutural processes and trabeculae forming an outer sphere. The most important distinctive features of this species are its small sized spherical cyst body and its short processes distally branched and connected, reflecting the paratabulation. Cyst wall is finely granulated. It has a precingular archeopyle which is rarely observable.

Remarks: *Unipontidinium aquaeductus* differs from other species of the genus *Unipontidinium* by its short, simple and stout processes and trabeculae. Baltes (1969) figures a specimen identified as *Nematosphaeropsis balcombiana* Deflandre and Cookson, 1955. However, it appears from the figures that this specimen has the short and stout processes and trabeculae here used to define *U. aquaeductus* instead of the long and thin processes and trabeculae typical of *N. balcombiana*.

This species is rarely observed within our specimens. Since it is a very important species recognized within the Miocene deposits, it is essentially evaluated within this study.

Dimensions: 35-40 microns.

4.5. CHITINOUS FORAMINIFERAL LININGS

(App. A, Pl. 19 (Figs. 13, 14))

Description: Chitinous foraminiferal linings are the preserved inner layers of foraminifera while preparing the palynological samples by standard palynological technique.

Remarks: Although they cannot be used biostratigraphically, they are very essential in paleoenviromental evaluations. They represent a marine depositional environment, even in shallow water conditions.

Dimensions: 100-160 microns in length, 60-85 microns in breadth.

CHAPTER 5

PALEOCLIMATE AND PALEOENVIRONMENT

Fensome et al. (1996), described the dinoflagellates as single-celled, predominantly marine, eukaryotic plankton that typically occur as motile cells in surface water. Most of the dinoflagellates are known as autotrophic. However, many dinoflagellates have heterotrophic life styles and may rank among the zooplankton (Sluijs et al., 2005). Dinoflagellates are one of the most essential marine primary producers in the oceans today (Sluijs et al., 2005). Brasier (1985) also emphasized that dinoflagellates play a prominent role in the global carbon cycle. Sluijs et al. (2005) discussed the strong interest in dinocysts in terms of its economic gainings. Especially, the importance of dinocyst analysis has been increasingly recognized in hydrocarbon exploration. Sluijs et al. (2005) yielded a higher stratigraphic resolution with dinocyst than with calcareous microfossils in many oil and gas provinces (e.g. the Paleogene of the North Sea Basin). According to Ayres et al. (1982), remains of dinocysts are very important constituents of petroleum source rocks because of their ability to stock up lipids (Bold, 1973; Horner, 1985; Sluijs et al., 2005).

In addition to these prominent features, dinoflagellates are very useful and sensitive (paleo-) environmental indicators (Downie et al., 1971; Wall et al., 1977; Mudie and Harland, 1996; Dale 1996, Pross et al., 2004; Sluijs et al., 2005). Unlike planktonic foraminifers and calcareous nannoplanktons, dinoflagellates are not affected by post-depositional decalcification processes. Dinoflagellates have very high tolerance to chemical dissolution and can reach high abundances in both coastal and oceanic settings. They may live or survive in all aquatic environments from fresh water to hypersaline conditions. Therefore, dinoflagellates are very useful indicators of paleoecological variations and they yield important information about the surface water temperature, salinity, paleobathymetry, and productivity (Wall et al., 1977; Köthe, 1990; Brinkhuis, 1994; Stover and Hardenbol, 1994; Dale, 1996; Powell et al., 1996; Marret and Zonnoveld, 2003; Van Simaeys, 2004; Van Simaeys et al., 2004).

5.1. PRODUCTIVITY TRENDS

Berger et al., (1989), Bertrand et al. (1996), and Sluijs et al. (2005) mentioned that reconstruction of eukaryotic productivity patterns in marine environments are very important since they are directly linked to essential climate characteristics such as surface current patterns, upwelling systems, water mass mixing, surface winds, and the global carbon cycle. Sluijs et al. (2005) discussed that the micropaleontological data have traditionally been attained from benthic and planktic foraminifera, coccolithophorids, diatoms, and radiolarian while reconstructing a marine eukaryotic productivity. They mentioned that the obtained marine productivity by these groups is limited by the fact that their representatives are recognized in open marine environments. Dale and Fjellsa (1994) defined that an important part of modern marine primary productivity originates on neritic environments. Furthermore, de Vernal and Mudie (1992) stated that unlike dinoflagellates, all the remains of those groups are affected by post-depositional decalcification processes and have very low tolerance to chemical dissolution which limits their utility in paleoceanographic reconstructions, especially at high latitudes, Therefore, dinoflagellates represents a major part of the eukaryotic primary productivity with benthic and planktic foraminifera, coccolithophorids, diatoms, and radiolarian (Parsons et al., 1984).

Harland (1973) described a concept in that gonyaulacoid (G) versus peridinioid (P) cysts of dinocysts assemblages gives clues about the productivity variations. This approach, which has its bases in observations on Quaternary dinocyst assemblages, is founded on the different life style and feeding strategies in dinoflagellates forming peridinioid and gonyaulacoid cysts (Sluijs et al., 2005). For instance, low G/P ratio represents a significant freshwater input (Harland, 1973).While using this concept, there is an important and critical point that Harland (1973) calculated this G/P ratio by using the number of species. Hultberg (1987) has also criticized that some authors used G/P ratio with the number of specimens instead of the number of species.

The dinocysts recorded in this study were also evaluated in terms of the G/P ratios. Since all the identified dinocysts in this study are gonyaulacoid cysts, the G/P ratios can not be used to detect the productivity variations. Gedl and Peryt (2011) discussed that the absence of peridinioids might be related to primary conditions which are not suitable for this group of dinocysts. According to them, that might happen

because of low nutrient conditions of the surface water. Zonneveld et al. (1997) also suggested that the absence of peridinioids might be due to unfavorable syn- and post-depositional conditions related to aerobic conditions at the bottom and in the sediment. Therefore, one of these theories might be connected to the depositional environment of the Köpekli, Cingöz and Güvenç Formations.

5.2. TEMPERATURE TRENDS

Wefer et al. (1999) defined that sea surface temperature is one of the most important parameters for describing environmental conditions of past oceans and is an essential factor in paleoclimate modelling. Since dinoflagellates are resistant to chemical dissolution and reach high abundances in proximal and distal settings, they provide an interesting point of view for sea surface temperature reconstructions (Sluijs et al., 2005). Moreover, temperature has an effective control on the growth rate of dinoflagellates and any other group of microorganisms, by giving important clues about the distribution of them (Vernal et al., 1994). According to de Vernal et. al. (1993, 1994, 1998, 2000, 2001), Versteegh (1994), Versteegh and Zonneveld (1994), Rochon et al. (1998), Grøsfjeld et al. (1999), Devillers and de Vernal (2000), Boessenkool et al. (2001), Sangiorgi et al. (2002, 2003), and Sluijs et al. (2005), combined evidence may also represent that dinoflagellates are particularly sensitive to temperature changes compared to other microfossil groups, making them an excellent tool for sea surface temperature reconstructions. In this study, distribution of dinoflagellates and the qualitative cyst information are used to infer sea surface temperature trends in each measured section. The distribution of dinoflagellates are evaluated for each formation (e.g. Köpekli Formation, Cingöz Formation and Güvenç Formation).

The Köpekli Formation is composed of a diverse dinocyst assemblage. According to Harland et al. (1980), such a relatively diverse dinocyst assemblage is rather typical of warm environments, contrary to cold water assemblages, which are characterized usually by much lower diversity (three to four specimens) (Gedl, 1996). One of the most important and the abundant species *Spiniferites ramosus* is presumed to have a broad temperature range (Wall et. al., 1977). As *Spiniferites ramosus, Operculodinium*

centrocarpum, abundant species found in the Köpekli Formation, has a wide thermal tolerance (Harland, 1983; Dale, 1983). Based on Wall et. al. (1977), *Operculodinium centrocarpum* was observed at temperate and subtropical latitudes and its abundance tended to decrease tropicwards. *Lingulodinium machaerophorum* is another crucial dinoflagellate seen in the Köpekli Section. Especially, this species was very abundant at the level corresponding to sample ATD-154 in the Çukurköy Section (Figure 26). Furthermore, abundance of *Polysphaeridium zoharyi* and *Spiniferites* spp. indicate warm seasurface water (Edwards, 1986). Zonneveld et al. (2009) defined that one of their dinocyst associations including *Spiniferites mirabilis*, *Spiniferites pachydermus*, *Spiniferites ramosus* and *Spiniferites* spp. have their highest relative abundances in the sites at the plume margin and are characterized by relatively warm upper waters. Based on the dinocyst assemblages recorded in this formation, the sea surface should be warm at the time of the deposition of the Köpekli Formation during late Burdigalian to Langhian in the Adana Basin (Eastern Mediterranean) (Figure 42).

The Cingöz Formation is characterized by much lower diversity. Especially, the occurrence of *Lingulodinium machaerophorum*, *Operculodinium centrocarpum*, *Polysphaeridium zoharyi,* and *Spiniferites* spp. dominating the Cingöz Formation reflect warm sea-surface water (Wall et. al., 1977; Bradford and Wall, 1984; Bakkenand Dale, 1986; Edwards, 1986) as discussed above. Thus, the temperature of the sea surface was most probably warm during deposition of the Cingöz Formation in the late Langhian.

The Güvenç Formation consists of a relatively diverse dinocyst assemblage. Diverse dinocyst assemblage was promoted as a typical of warm environment by Gedl (1996). Especially, an abundant occurrence of *Homotryblium* dinoflagellate cysts have been interpreted in the Güvenç Formation. According to Williams (1977) and Williams and Bujak (1977), elevated abundance of *Homotryblium* spp. was most probably associated with warm conditions. To conclude, the temperature of the sea surface should be warm while the deposition of the Güvenç Formation was taking place in the Adana Basin (Eastern Mediterranean) during the latest Langhian-earliest Tortonian.

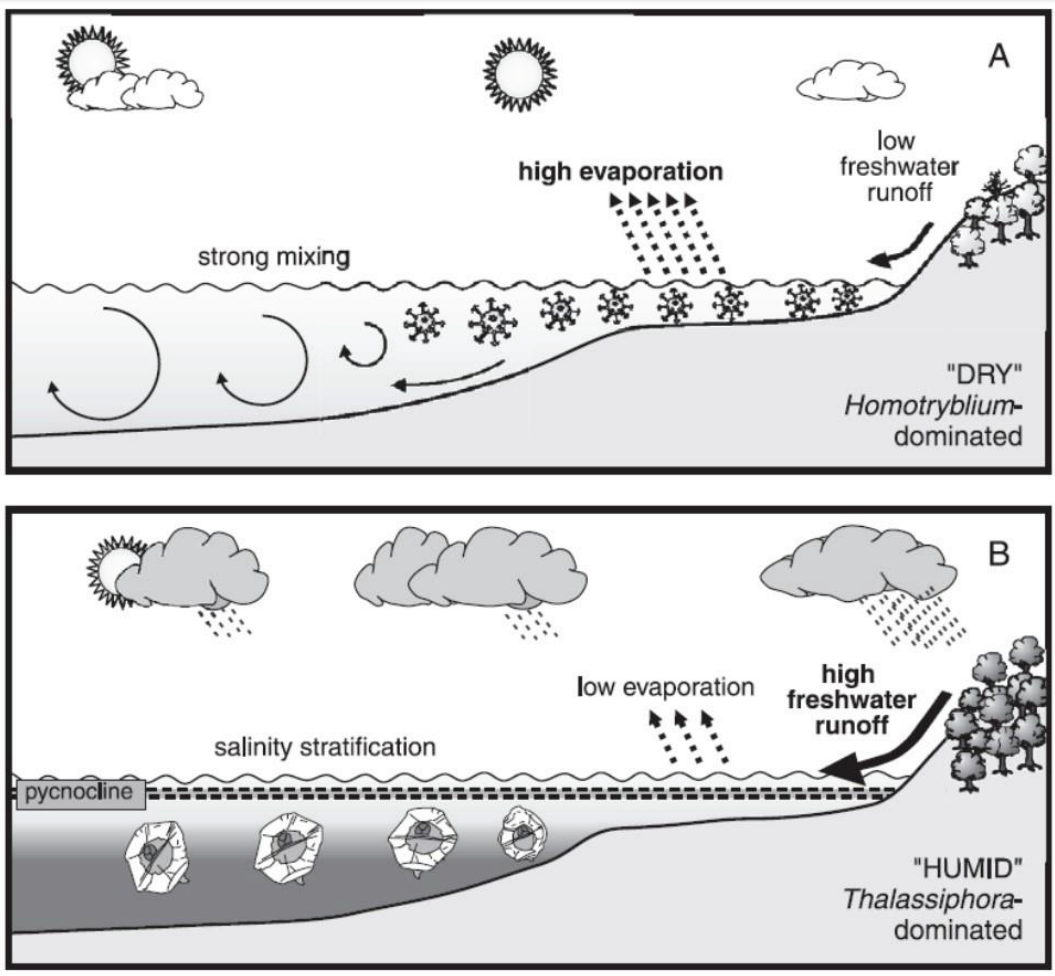

Figure 42. Model for the response of cyst-forming dinoflagellate populations to climate-induced oceanographic changes in the lower Oligocene of southern Germany. (A) High sea-surface salinity is caused by reduced runoff and strong evaporation during relatively dry periods (dominance of *Homotryblium tenuispinosum*). (B) Increased nutrient input, salinity stratification and a decrease in bottom water oxygenation is caused by high freshwater discharge during relatively humid periods (dominance of *Thalassiphora pelagica*) (Pross and Schmiedl (2002) *in* Sluijs et al., 2005).

5.3. SALINITY TRENDS

Sluijs et al. (2005) mentioned that salinity determines density of water masses and represents an important component controlling thermohaline circulation when compared with temperature. Vernal et al. (1994) discussed that salinity plays an important role in the distribution of dinocysts since salinity is a prime factor controlling osmotic exchanges in microorganisms.

The morphological diversity of cysts is generally used as a paleoenvironmental indicator (Batten, 1982; MacLennan and Trewin 1989; Smelror and Leereveld, 1989; Leckie and Singh, 1991; Riding et al., 1991; Habib et al., 1994). Wall et al. (1973) and

Wall and Dale (1974) described how the morphological variations in dinocyst are affected by the salinity. They performed some important paleoenvironmental analyses on Holocene material from the Black Sea. They also went in detail with other environmental stresses had influence upon dinocysts. They reported that an increased number of dinocysts with reduced processes, variations in septal development, and a cruciform rather than a rounded endocyst were generated in low-salinity environments. Within the morphologically diversified cysts, changes in archeopyle formation were identified as a result of salinity fluctuations by Wall et al. (1977). The hypothesis, in which salinity was a controlling factor for variations in cyst morphology (such as, process length in various chorate dinocysts), were predominantly utilized by certain studies (e.g. de Vernal et al., 1989; Nehring, 1994a,b; Matthiessen and Brenner, 1996; Dale, 1996; Ellegaard, 2000; Lewis et al., 1999, 2003).

Kokinos and Anderson (1995) also suggested that the morphological diversity of cysts is most probably related to an early rupture of the outer membrane surrounding the dinoflagellate theca and cyst. Sluijs et al. (2005) mentioned that based on laboratory studies there should be a more complex relationship between cyst morphology and salinity. Sluijs et al. (2005) emphasized the reduction in process length in *Lingulodinium machaerophorum* due to low salinity conditions (e.g. Nehring, 1994a, b; Lewis and Hallet, 1997); however, Kokinos and Anderson (1995) supported development of different process lengths under stable salinity conditions in monoclonal cultures of this taxon. *Spiniferites membranaceus* and *S. ramosus,* which show different cyst morphologies under stable salinity (Lewis et al., 1999), can also be given as examples of this argument. Among these studies, Mudie et al. (2001) performed a very detailed paleoenvironmental and paleoecological studies on late Quaternary dinocysts from the Black, Marmara and Aegean Seas. Based on their studies, the relationship between process length of *Lingulodinium machaerophorum* and salinity was predominantly utilized and no clear statistical relationship was inferred. Therefore, salinity is probably not the only factor controlling these morphological changes and other parameters of environmental stress may also be involved (Sluijs et al., 2005).

The Köpekli Formation is associated with a rich and diverse dinocyst assemblage based on palynological analysis performed in this study. Addition to this diverse dinocyst assemblages, the fresh water algae (such as *Botryoccus braunii*, *Pediastrum*

sp.) were recorded within the Köpekli Formation. Dybkjaer (2004a) supported that the dominance of terrestrial palynomorphs, the sparse, low diversity dinocyst assemblage, and the consistent fresh water algae indicate a possibly low-salinity depositional environment. However, the Köpekli Formation is dominated with diverse dinocyst assemblage and limited amount of terrestrial palynomorph (except bisaccate pollen which can be transported through long distances by wind and wave activity) and fresh water algae (from very rare to rare). Mudie et al. (2004) performed very detailed statistical analysis based on late glacial, Holocene, and modern dinocysts assemblages in the Aegean-Marmara-Black Sea corridor. Mudie et al. (2004) suggested that an assemblage dominated by cysts of autotrophic gonyaulacoids distinguishes the hypersaline Aegean-Mediterranean water, whereas heterotrophic protoperidinioids characterize the low-salinity Marmara-Black Sea water according to the Principle component analysis of 16 core-top samples in the study area. Similarly, all of the dinocysts recorded in this study are autotrophic gonyaulacoids. Furthermore, *Cleistosphaeridium placacathum, Lingulodinium machaerophorum*, *Operculodinium centrocarpum, Polysphaeridium zoharyi,* and *Spiniferites* spp. are some of the dominating dinocysts recorded in the Köpekli Formation. The process length of *Lingulodinium machaerophorum* and *Operculodinium centrocarpum* may have shorter processes in lower saline conditions (Wall and Dale, 1973; Dale, 1996; Ellegaard, 2000, Gedl and Peryt, 2011). In our samples, they have rather long processes suggesting normal salinity. The dinocyst assemblage suggests a saline to hypersaline condition during deposition of the Köpekli Formation.

The Cingöz Formation is mainly characterized by a poor and low diversity dinocyst assemblage, and the dominance of terrestrial palynomorphs with fresh water algae. The Cingöz Formation is known as the submarine fan deposits of the Adana Basin and is composed of transported sediments by river systems. The scarcity of dinocysts recorded in this formation is due to high turbulence (Williams and Sarjeant, 1967). Furthermore, fresh water transporting spores, pollen, fresh water algae, and wood particles were probably introduced to the area in large river systems (discussed in Biostratigraphy Chapter). Since the existing dinocysts defined in the Cingöz Formation gave very limited information about salinity, making any comment might not be possible.

The Güvenç Formation is mainly characterized by a diverse and rich dinocyst assemblage as discussed in detail within the previous sections. The most dominating species are *Homotryblium* dinoflagellate cysts (including *Homotryblium floripes*, *Homotryblium pallidum*, *Homotryblium plectilum* and *Homotryblium tenuispinosum*) within the P-8 Zone in the uppermost part of the Güvenç Formation (the interval from sample ATD-93 to ATD-110 (Figure 38)). Dybkjaer (2004b) performed a very detailed and significant study on variations in morphology and abundance in *Homotryblium*-cyst assemblages related to depositional environments through uppermost Oligocene-Lower Miocene deposits of Jylland (Denmark). According to Dybkjaer (2004b), the abundant occurrences of *Homotryblium* cysts were interpreted as reflecting deposition in hyper salinity or low salinity environments based on the species of the genus *Homotryblium.* Dybkjaer (2004b) emphasized that the distribution of *Homotryblium tenuispinosum*, which is the most dominating *Homotryblium*-cyst recognized within the Güvenç Formation in the measured Güvenç Section, is associated with higher salinity environments (Figure 38). Moreover, Pross and Schmiedl (2002) also performed a very detailed study based on paleoenvironmental and paleoclimatic implications and construct a model for the response of cyst-forming dinoflagellate populations to climate-induced oceanographic changes (Figure 42). Pross and Schmiedl (2002) defined alternating intervals characterized by richness of *Homotryblium tenuispinosum*/ *Homotryblium floripes* and *Thalassiphora pelagica* indicating high salinity and low salinity conditions, respectively. According to the model of Pross and Schmiedl (2002), abundant *Homotryblium tenuispinosum* and *Homotryblium floripes* indicated drier periods and reduced runoff resulting in strong evaporation and increased salinity in nearshore settings. Pross and Schmiedl (2002) also emphasized that *Polysphaeridium zoharyi*, *Homotryblium tenuispinosum,* and *Homotryblium floripes* are considered to indicate inner neritic, possibly lagoonal environments with increased salinity based on the morphological similarities with the extant high-salinity indicator. Furthermore, Köthe (1990) recorded abundant *Homotryblium* in northwest of Germany through Oligocene-Miocene indicating a high salinity condition. Sluijs et al. (2005) also noticed that *Homotryblium* provides an essential tool in dinocyst-based salinity reconstructions for most of the Paleogene since it first occurs in the early Paleocene and continues to the Miocene. *Polysphaeridium zoharyi, Lingulodinium machaerophorum*, *Operculodinium centrocarpum,* and

Spiniferites spp. are the other common and abundant species recorded in the Güvenç Formation. According to the morphological variations of these essential taxa discussed above, deposition of the Güvenç Formation was most probably taking place in a high salinity environment during latest Langhian to earliest Tortonian.

5.4. PROXIMAL-DISTAL TRENDS

In order to support a model for paleo-depositional environments and to improve the geological models in the Miocene deposits of the Adana Basin, proximal-distal trends of dinocysts were studied in detail. Sluijs et al. (2005) emphasized that marine dinocysts show strong proximal-distal signals due to the general life strategy of dinocysts and the adaptation of many species to specific surface water conditions. Moreover, dinoflagellates also provide promising information for stratigraphic correlation because they can be found in neritic and deeper marine depositional conditions (Stover and Hardenbol, 1994). Brinkhuis (1994) performed a very significant study about paleoenvironment interpretations in the Mediterranean that are based on dinocysts. Brinkhuis (1994) proposed a schematic conceptual model of quantitative dinocyst distribution along a proximal-distal transect based on the ecological and/or sedimentary variations, distribution patterns of dinocysts and other palynomorph categories, and using previous environmental interpretations of the measured sections in his study. The schematic model has been applied and modified by various authors (Crouch, 2001; Pross and Schmiedl, 2002; Sluijs et al., 2005).

Brinkhuis (1994) mentioned that only a few taxa or complexes of morphologically related taxa are quantitatively important, while evaluating the existing dinocyst assemblage. Brinkhuis (1994) differentiated four dinocyst groups as follows:

(1) the "*Spiniferites*" –group including *Achomosphaera* and *Spiniferites* (mainly *Spiniferites ramosus* types);

(2) the "*Operculodinium*" –group including representatives of *Operculodinium,* and *Impletosphaeridium* (mainly *Operculodinium centrocarpum*, *Operculodinium microtriainum* and tiara-types);

(3) the "*Homotryblium* spp." –group including *Homotryblium plectilum* and *Homotryblium aculeatum*);

(4) the "*Deflandrea* spp." –group including *Deflandrea phosphoritica, Deflandrea granulata* and *Deflandrea arcuate).*

Among these dinocyst groups, Brinkhuis (1994) differentiated a fifth group as "other taxa". Brinkhuis (1994) mentioned that certain other taxa also play an important role in the quantitative composition in some samples.

Similarly, five groups are identified while reconstructing proximal-distal trends of the dinocysts recorded in this study. The quantitatively important dinocysts are as follows:

(1) the *Spiniferites* group including *Spiniferites membranaceus*, *Spiniferites mirabilis*, *Spiniferites pseudofurcatus*, *Spiniferites ramosus*, *Spiniferites* spp.;
(2) the *Operculodinium* group including *Operculodinium borgerholtense*, *Operculodinium centrocarpum*, *Operculodinium piaseckii*;
(3) the *Cleistosphaeridium* group including *Cleistosphaeridium ancyreum*, *Cleistosphaeridium placacanthum*;
(4) the *Homotryblium* spp. group including *Homotryblium floripes*, *Homotryblium pallidum*, *Homotryblium plectilum*, *Homotryblium tenuispinosum*;
(5) the *Impagidinium* spp. group including *Impagidinium paradoxum*, *Impagidinium* sp. and *Nematosphaeropsis labyrinthus.*

According to the quantitatively important dinocyst groups recorded in the studied sections measuring the Köpekli, Cingöz and Güvenç formations, a summary of available information is given hereafter.

5.4.1. The *Spiniferites* group

The *Spiniferites* group mainly consists of *Spiniferites membranaceus*, *Spiniferites mirabilis*, *Spiniferites pseudofurcatus*, *Spiniferites ramosus* and *Spiniferites* spp. (can not be identified as a species due to preservation problems, so evaluated as *Spiniferites* spp.). *Spiniferites ramosus* is considered to be an inner to outer neritic form by Harland (1983). Gedl (1996) mentioned that its frequent appearance in open marine environments is probably due to current transportation.

According to Brinkhuis (1994), extant representatives of *Spiniferites ramosus* have a rather cosmopolitan distribution and occur in both oceans and marginal seas today. *Spiniferites pseudofurcatus* is recorded as more common in the marginal settings in the studied sections of Brinkhuis (1994) than in more offshore depositional settings in the pelagic sections (central Italy) of Brinkhuis and Biffi (1993). *Spiniferites mirabilis* and *Spiniferites mambranaceus* were geographically and environmentally widespread and the only definitive aspect of their distribution were their cosmopolitanism (Wall et. all., 1977). Wall et. all. (1977) interpreted *Spiniferites mirabilis* as neritic and cosmopolitan since its distribution seemed to be parallel that of *Operculodinium centrocarpum*.

Therefore, the group herein is considered to have a similar paleoecological significance as of *Spiniferites* group of Brinkhuis (1994) and represents open marine neritic watermasses or influence of the latter (Figure 43, Table 2).

5.4.2. The *Operculodinium* group

The *Operculodinium* group recognized in this study is composed of *Operculodinium borgerholtense*, *Operculodinium centrocarpum,* and *Operculodinium* piaseckii.

Operculodinium centrocarpum is characterized as a neritic species (Wall et. al., 1977; Morzadec-Kerfourn, 1983). Brinkhuis (1994) defined that extant representatives of the *Operculodinium* group occur in a wide variety of sedimentary settings, from oceanic to restricted marine. According to Brinkhuis (1994), the distribution of *Operculodinium centrocarpum* is in any sense cosmopolitan, although it is often mentioned that high frequencies of it in more offshore settings are primarily due to transportation (Wall et. al., 1977; Harland, 1983; Edwards and Andrle, 1992). Wall et. al. (1977) described the reasons why *Operculodinium centrocarpum* is interpreted as a neritic species in their classification; that are: the parentel species (*Protoceratium reticulatum*) is generally considered to be a neritic dinocyst and the cysts correspondingly were defined most abundantly only in sediments beneath surface waters with a major coastal water component (Wall et al., 1977). Wall et al. (1977) noticed that observations on cysts within modern plankton confirm this affinity for coastal waters in nearshore and outer neritic hydrographic zones. Wall et al. (1977)

also mentioned that it can not be classified either neritic or oceanic, in spite of its strong presence in many continental slope and rise zone sediments since they believe that these occurrences are related to the coastal and not the oceanic component of slope or transitional waters and to the penecontemporaneous displacement of specimens from nearby shelf sediments plus submarine erosion of others from Pleistocene and relict sediments. *Operculodinium borgerholtense* is also defined as neritic species by Soliman et al. (2009) and he emphasized that it is promising as a stratigraphic marker particularly in those neritic settings in which adverse paleoenvironmental factors have excluded other species. The *Operculodinium* group considered herein is regarded as to represent from inner to outer neritic watermasses or the influence of the latter similar to the *Operculodinium* group of Brinkhuis (1994) (Figure 43, Table 2).

5.4.3. The *Cleistosphaeridium* group

Cleistosphaeridium group includes *Cleistosphaeridium ancyreum* and *Cleistosphaeridium placacanthum*. Brinkhuis (1994) mentioned that a little information was also available about the habitat characteristics of *Cleistosphaeridium;* however, some common data suggested that it is a neritic genus. The *Cleistosphaeridium* group of taxa indicate deposition from inner to outer neritic depositional conditions.

5.4.4. The *Homotryblium* spp. group

The *Homotryblium* spp. group defined in this study is mainly characterized by *Homotryblium floripes*, *Homotryblium pallidum*, *Homotryblium plectilum,* and *Homotryblium tenuispinosum*. Dybkjaer (2004) performed a very detailed and significant study based on variations in morphology and abundance in *Homotryblium*-cyst assemblage related to depositional environments through uppermost Oligocene-Lower Miocene deposits in Jylland (Denmark). Dybkjaer (2004) suggested that abundant occurrence of *Homotryblium* dinoflagellate cysts have been interpreted as reflecting deposition in near-shore, marginal marine areas. According to Dybkjaer (2004), the process length of *Homotryblium* cysts is related to proximity to coast. Moreover, Islam (1984) also discussed that *Homotryblium* with long processes indicates more open marine environments while those with shorter processes reflect

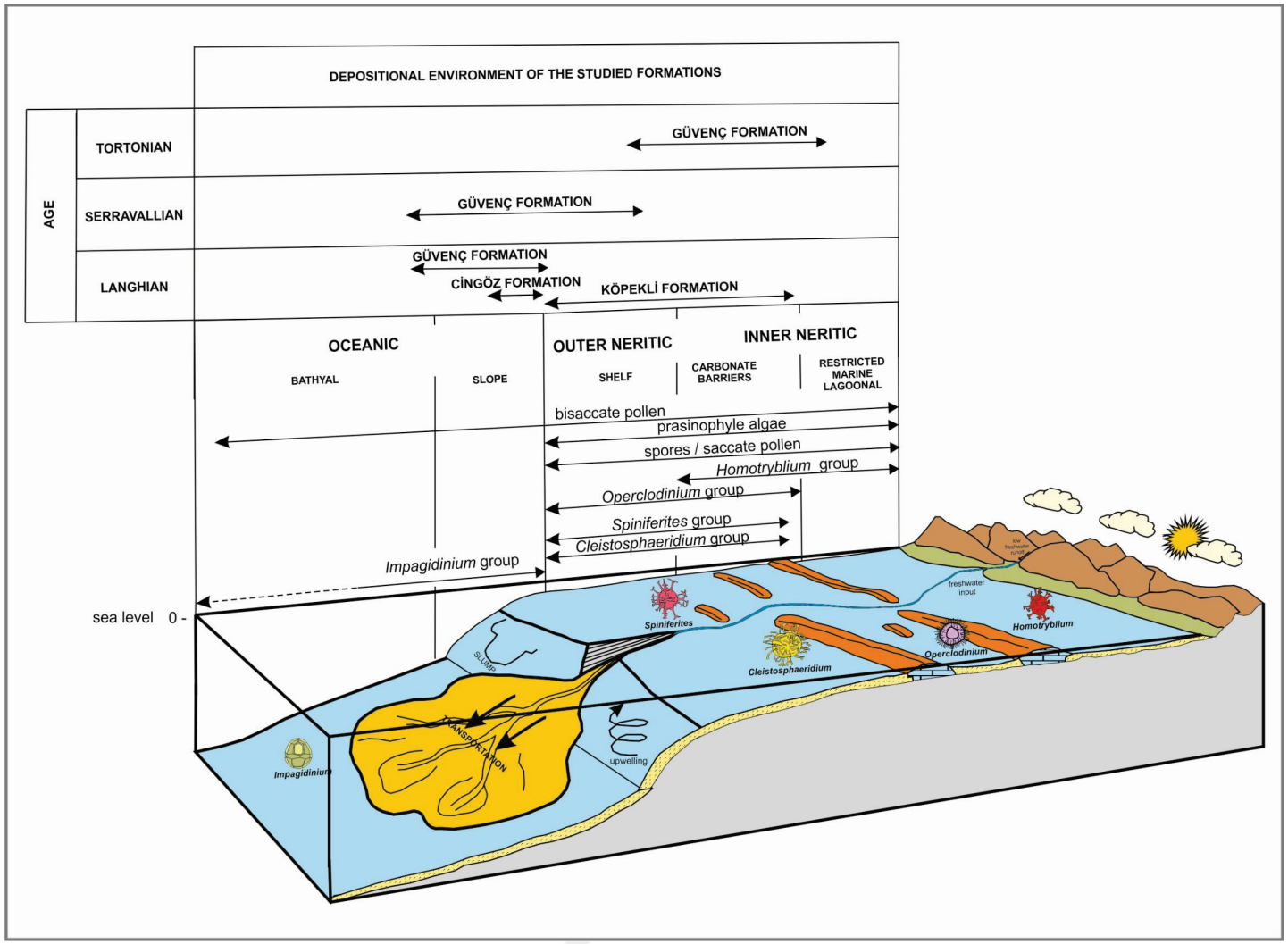

Figure 43. Schematic model for the distribution of dinocyst associations along a proximal –distal transect during the Langhian to Tortonian in the Adana Basin.

Table 2. Distribution of palynomorph associations along proximal-distal transect during the latest Burdigalian to earliest Tortonian within the Köpekli, Cingöz and Güvenç formations in the Adana Basin.

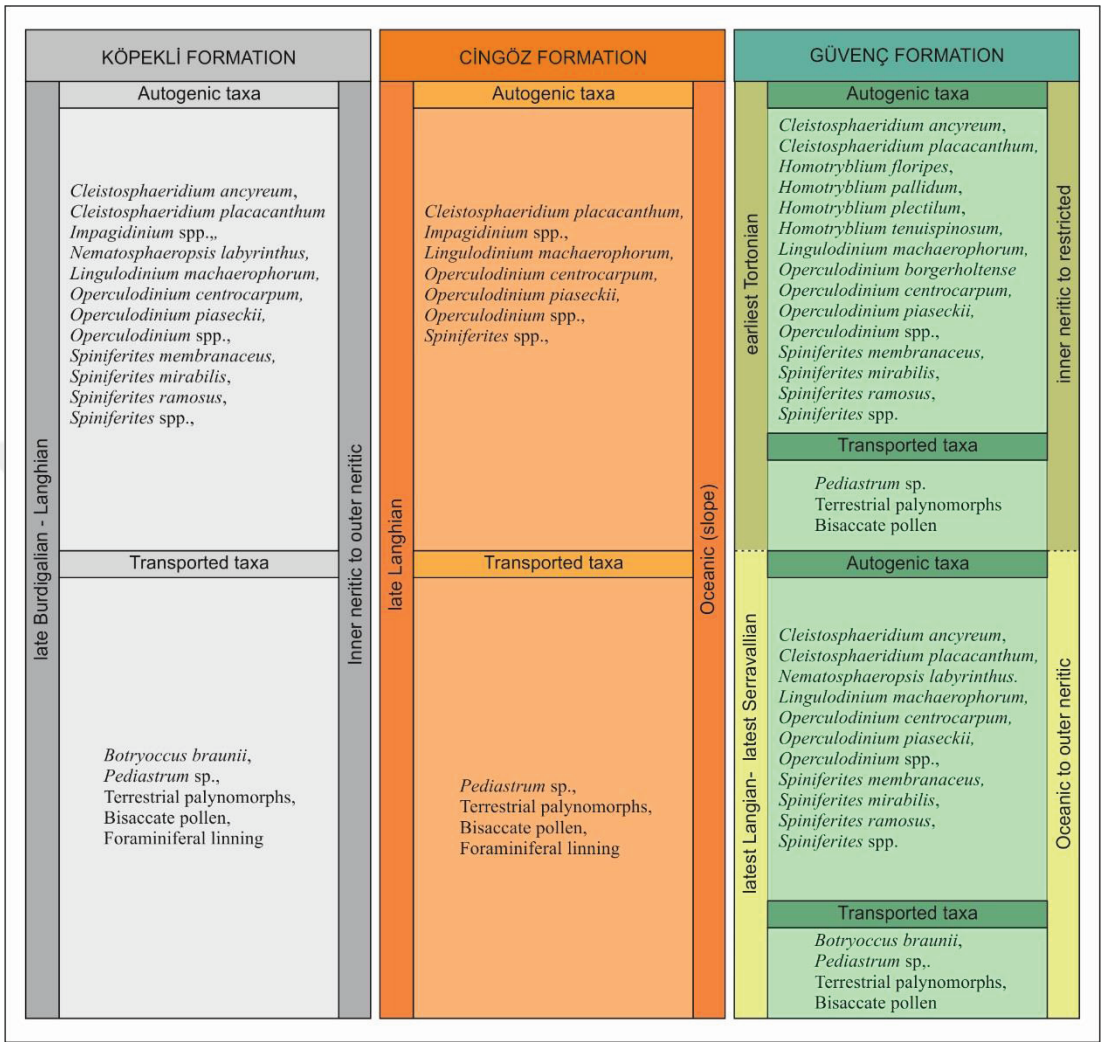

brackish water, inner shelf, and estuarine deposits (Dybkjaer, 2004). Dybkjaer (2004) mentioned that *Homotryblium plectilum* dominates the proximal areas, whereas *Homotryblium tenuispinosum* dominates more distal areas. To conclude, *Homotryblium* spp. implies low- to mid-latitude, restricted marine to open marine, and inner neritic settings (Williams and Bujak, 1977; Stover, 1977; Liengjarern et. al. 1980; Sarkar and Singh, 1988; Köthe, 1990; Brinkhuis, 1994). Therefore, representatives of *Homotryblium* spp. are herein regarded as to represent restricted

marine to inner neritic watermasses or the influence of the latter, similar to the *Homotryblium* spp. group of Brinkhuis (1994) (Figure 43, Table 2).

5.4.5. The *Impagidinium* spp. group

The *Impagidinium* spp. group defined in this study includes *Impagidinium paradoxum*, *Impagidinium* sp. and *Nematosphaeropsis labyrinthus.* Mudie (1992), Brinkhuis et. al. (1992), Edwards (1992), and Dale (1996) suggested that *Impagidinium* and *Nematosphaeropsis* were oceanic taxa. On the other hand, Dale (1996) supported that not all the species of *Impagidinium* and *Nematosphaeropsis* reflect open marine conditions (Figure 43, Table 2).

5.4.6. Other taxa

Other certain taxa also play an important role in quantitative composition in the studied samples. *Lingulodinium machaerophorum, Polysphaeridium zoharyi,* and *Hystrichokolpoma* are the other dominating species recorded in this study. Brinkhuis (1994) suggested that *Hystrichokolpoma* may occur virtually in every marine environment and have a global distribution. *Lingulodinium machaerophorum* was reported as an estuarine species by Wall et. al. (1977). Moreover, Bakrac et al. (2012) mentioned that *Lingulodinium machaerophorum* could be found in the open environment since facies migrations were common due to fluctuations in sea level. According to Williams and Bujak (1977), Stover (1977), Liengjarern et al. (1980), Sarkar and Singh (1988) and Köthe (1990), *Homotryblium* spp. has a possible relationship with *Polysphaeridium zoharyi,* which shows a similar latitudinal distribution (Brinkhuis, 1994).

Bisaccate pollen are also the dominating terrestrial taxa in the studied sections. Due to their high buoyancy, the bisaccates can be transported in large numbers to offshore, even oceanic sites (Traverse and Ginsburg, 1966; Brinkhuis, 1994). Brinkhuis (1994) also mentioned that other pollen types and spores are considered to be transported less far into the marine environment. According to Brinkhuis bisaccate pollen can be recognized from inner neritic to oceanic environments (Figure 43).

Similarly, bisaccate pollen, for which river input is the main transportation mechanism, dominate most of the samples in the measured sections including the Köpekli, Cingöz and Güvenç formations. Praus and Riegel (1989) discussed that fresh water algae (e.g. *Botryococcus braunii*, *Pediastrum* sp.) generally indicate depositionary settings from marginal marine to fresh water environments. However, they can be transported further offshore similar to other palynomorphs (Brinkhuis, 1994). *Botryococcus braunii* and *Pediastrum* sp. are also defined in our samples in a similar way. However, their relative abundances correlated with other palynomorph groups may indicate sea level fluctuations during the deposition (will be discussed in the "Recognition of sea-level fluctuations based on palynological data"). Brinkhuis (1994) also mentioned that the highest relative abundances occur almost exclusively in relatively nearshore and inner neritic settings.

Based on the ecologically determined distribution patterns of dinocysts and other palynomorph groups, the studied sections were evaluated and the depositional settings of the Köpekli, Cingöz and Güvenç Formations were reconstructed (Figure 43).

In the Köpekli Formation (measured in Çukurköy, Köpekli, Sofular and Çukurköy sections), the *Spiniferites* group, *Operculodinium* group, and *Cleistosphaeridium* group (very abundant) are the most common elements, suggesting inner neritic water to outer neritic (Figure 43, Table 2). Moreover, bisaccate pollen, which are well known by their floating capacity, are also an essential constituent of the palynological association through the Köpekli Formation. To sum up, the Köpekli Formation was deposited from inner neritic to outer neritic waters during late Burdigalian to Langhian (Figure 43, Table 2).

The Cingöz Formation measured in Çukurköy Section from bottom to top is characterized by the *Spiniferites* group, *Operculodinium* group and *Impagidinium* spp. group (Figure 43, Table 2). Dale (1996) discussed that the occurrence of a few specimens of *Impagidinium* might reflect an oceanic environment. Furthermore, Sluijs et al. (2005) mentioned that occurrence of *Impagidinium* could provide a tool to differentiate distal, oligotrophic settings from other, more proximal environments. Terrestrial taxa mainly dominated by bisaccate pollen and fresh water algae, which are

probably introduced to the area by large river systems, are recorded through the Cingöz Formation. Furthermore, the Cingöz Formation, mainly characterized by a poor and low diversity dinocyst assemblage, is known as the turbidite deposits of the Adana Basin. Williams and Sarjeant (1967) discussed that the scarcity of dinocysts defined in such depositional settings was due to high turbulence. *Lingulodinium machaerophorum* and *Operculodinium centrocarpum* are other quantitatively important species, which are characterized as cosmopolitan in estuarine and neritic environments, respectively (Wall et. al., 1977). According to Dybkjaer and Rasmussen (2000), the co-occurrence of outer neritic to oceanic taxa and the inner neritic taxa together is interpreted as to reflect that material from inner neritic settings was transported out and deposited in the deeper parts of the basin. Bakrac et al. (2012) also mentioned that *Lingulodinium machaerophorum* could be found in the open marine environments since facies migrations are common due to fluctuations in sea level. On the basis of utilized information, Cingöz Formation was deposited in the slope part of the oceanic environment during late Langhian (Figure 43, Table 2).

The Güvenç Formation (measured in Çukurköy, Koruklu, and Bekirli sections) is mainly dominated by the *Spiniferites* group, the *Operculodinium* group, the *Cleistosphaeridium* group, and the *Homotryblium* spp. group (Figure 43, Table 2). Moreover, only two specimens of *Impagidinium paradoxum* are recorded (e.g. samples TD-460 and TD-479, Figure 32) at the lower parts of the Güvenç Formation (the Güvenç Formation has a transitional contact with the Cingöz Formation at this level). In addition to this valuable data, an acme of *Homotryblium* spp. group, reflecting restricted marine to inner neritic water, is recorded at the upper part of the Güvenç Formation (measured in Güvenç Section). Furthermore, the terrestrial assemblage and fresh water algae are defined in the Güvenç Formation, as in the Köpekli and Cingöz Formations. Additionally, not only the bisaccate pollen but also the angiosperm pollen and spores were identified in the terrestrial palynomorph assemblage, especially at the middle and upper parts of the Güvenç Formation. Based on the observed distribution patterns of the ecologically important dinocysts, it can be suggested that the deposition of the Güvenç Formation was started at oceanic to outer neritic environment during

the latest Langhian-latest Serrevallian and followed by inner neritic to restricted marine water during the earliest Tortonian (Figure 43, Table 2).

5.5. RECOGNITION OF SEA-LEVEL FLUCTUATIONS BASED ON PALYNOLOGICAL DATA

The content of dinocyst assemblages and dinocyst diversity can give important clues about water masses which are related with shoreline proximity (Sluijs *et al.,* 2005). Therefore, variations within the composition and diversity of palynomorphs can be used to predict sea level fluctuations indicating transgressive and regressive phases. Similarly, Brinkhuis and Biffi (1993) and Brinkhuis (1994) differentiated the sea-level changes across the Eocene/Oligocene transition in Italy on the basis of oceanic versus neritic taxa. They interpreted transgressive trends by the increase in the number of outer neritic versus oceanic taxa (e.g. *Nematasphoropsis*, *Impagidinium*), while regressive trends indicated by the ascending trend of neritic to coastal taxa. Moreover, Peeters *et al.* (1998) documented sea level fluctuations across the Eocene-Oligocene transition in Greece based on dinocyst diversity. Powell *et al.* (1996) also reconstructed a sequence stratigraphic framework based on dinocysts for late Paleocene-early Eocene deposits in southeast England. Likely, Stover and Hardenbol (1994), Zeevenbook *et al.* (1994), Zevenboom (1996), Wilpshaar et al. (1996), Iokovleva *et al.* (2001), Van den berghe *et al.* (2003) and Sluiijs *et al.* (2005) used similar approaches while establishing sea level fluctuations based on dinocyst diversity. Stover and Hardenbol (1994) emphasized that the number of dinocysts represents an increasing trend in transgressive trends, whereas the number of dinocysts decreases during regressive trends. Additionally, Sluiijs *et al.* (2005) mentioned that the first occurrences of dinocyst events were recorded during transgressive trends and also defined that transgression fosters the evolution of new dinoflagellate species due to widening of shelfal dinoflagellate habitats. Furthermore, intensive reworked palynomorphs can be recognized during regressive trends (Sluiijs *et al.,* 2005). Moshkoviz and Habib (1993) performed a study for the upper Cretaceous and lowermost Paleogene deposits in the southern U.S. based on a similar approach. They

mentioned that a minimum number of dinocysts were recorded during regressive trends, whereas the maximum number of dinocysts was found at the maximum flooding surfaces.

Therefore, not only the quality but also the quantity of dinocysts give important clues about proximal/distal differentiation and sea level fluctuations. The variation in dinocyst association, assemblage diversity and cyst abundances are strongly related to the paleoenvironmental conditions. Thus, dinoflagellates can be used to determine sea level fluctuations successfully due to the strong expression of the proximal/distal signal in dinocyst assemblages (Sluiijs *et al.,* 2005). According to the changes in palynomorph association, diversity charts were plotted on the basis of quantitative distribution patterns of palynomorph groups based on dinocysts (counted with terrestrial palynomorphs to reach 100 %). According to the quantitative distribution patterns of dinocysts, sea level fluctuation patterns were defined in the Köpekli Formation within the Çukurköy, Köpekli, Sofular, and Çorlu sections. A transgressive trend was recognized at the upper part of the P-1 Zone within the Çukurköy Section. The FO of *Labyrinthodinium truncatum* is recorded during this transgressive phase (at the level corresponding to ATD-146 (Figure 44)). A regressive trend is identified at the lower part of the P-2 Zone (interval between samples ATD-147 and ATD-151 (Figure 44)), while a transgressive trend is recognized at the middle part of this zone (interval between samples ATD-151 and ATD-157 (Figure 44)). Finally, a relative sea level fall is detected at the upper part of this zone based on the descending trend in the quantitative distribution patterns of dinocysts (interval between samples ATD-157 and ATD-161 (Figure 44)). Moreover, Brenec and Rishards (2001) stated that high numbers of fresh water algae and low numbers of marine dinocysyts were found in low relative sea levels indicating early stages of regressive trends. Accordingly, quite reduced fresh water algae (e. g. *Botryococcus braunii* and *Pediastrum* sp.) were identified during the early periods of regressive phase in this section (level corresponding to samples ATD-148 and ATD-152, Figure 26). Moreover, Jaramillo and Oboh-Ikuenobe (2001) mentioned that amorphous type organic matter and outer neritic to oceanic dinoflagellate taxa were recognized at high percentages within the time of maximum trasgression. In the same way, the highest percentage of amorphous

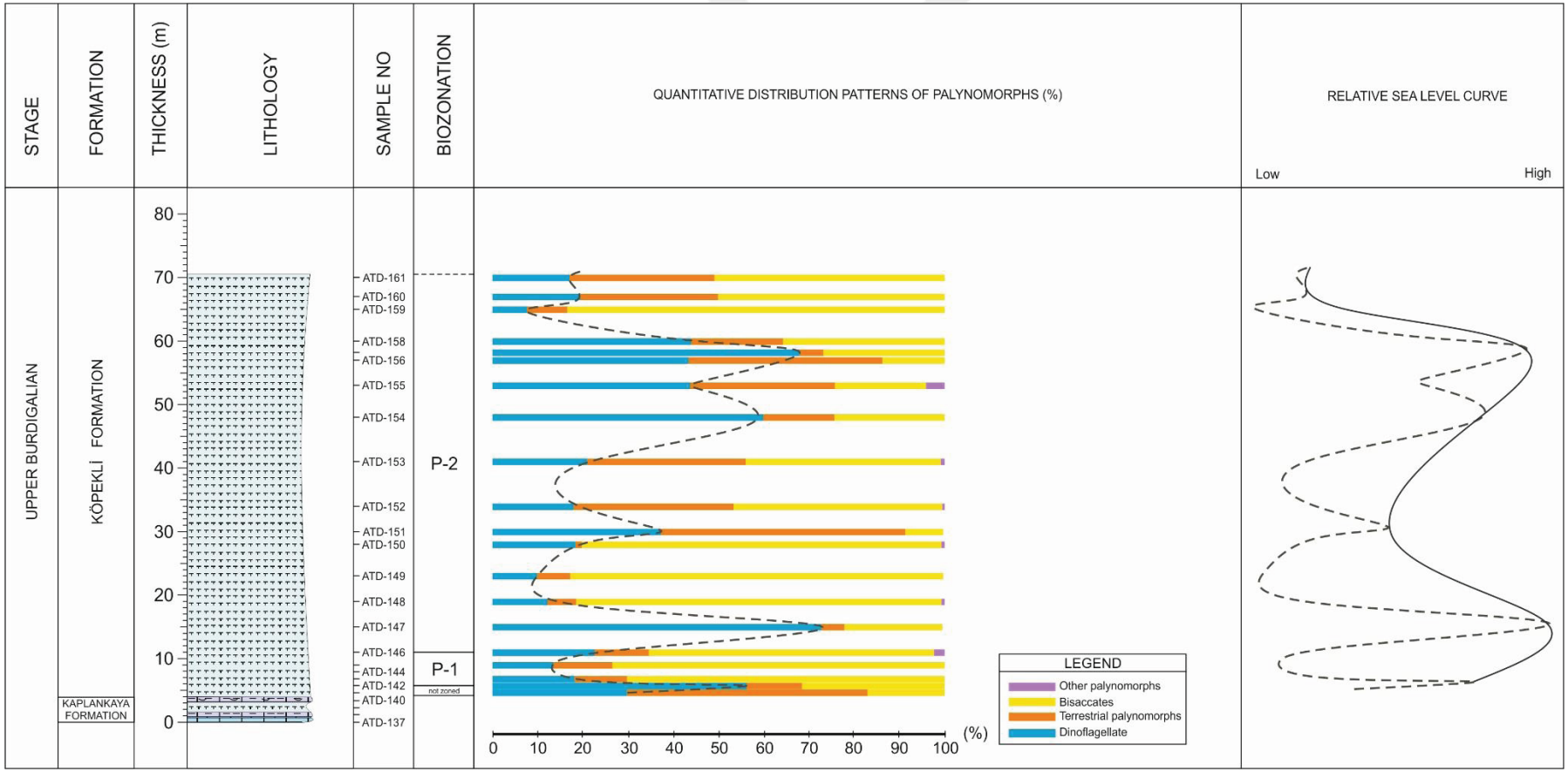

Figure 44. Diversity chart of Çukurköy Section plotted on the basis of quantitative distribution patterns of palynomorph groups.

type organic matter and outer neritic to oceanic dinoflagellate taxa (e.g. *Impagidinium* sp., *Nematosphaeropsis labyrinthus*) were recognized in the interval corresponding from ATD-145 to ATD-147 (Figure 26). On the base of this evaluated data, transgression occurred during the deposition of Çukurköy Section covering the lowermost part of the Köpekli Formation through late Burdigalian (Figure 44). Based on biostratigraphical interpretation, Köpekli Section is correlative to Çukurköy Section. Especially, the quantitative distribution pattern of dinocysts in P-2 Zone is very similar within these two sections. Similarly, a relative sea level fall is recorded at the lower part of the Köpekli Section (interval between samples ATD-158 and ATD-163 (Figure 45)) and a relative sea level rise is detected at the middle part of the section corresponding to the P-2 Zone (interval between samples ATD-163 and ATD-169 (Figure 45)) based on the decreasing and increasing trends of the quantitative distribution pattern of dinocysts, respectively. Finally, the section continues with a regressive phase through the upper part of the section corresponding to the upper part of the P-2 Zone and the lower part of the P-3 Zone (interval between samples ATD-169 and ATD-174 (Figure 45)). Sofular Section starts with a transgressive trend (interval between samples ATD-119 and ATD-125 (Figure 46)) and continues upward with a regressive trend (interval between samples ATD-125 and ATD-132 (Figure 46)). The transgressive phase covers the upper part of the P-2 Zone, P-3 Zone and the lower part of the P-4 Zone within this section. The FO of *Cerebrocysta poulsenii* and *Unipontidinium aquaeductum* were defined again during the relative sea level rise. In addition, the highest percentage of amorphous type organic matter and outer neritic to oceanic dinoflagellate taxa (e.g. *Impagidinium* sp.) were recognized at the level corresponding to sample ATD-125 indicating a maximum flooding surface (Figure 30). Through the Köpekli Formation within Çorlu Section, five regressive phases (e.g. intervals as follows: TD-175 – TD-184, TD-192 – TD-198, TD-213 – TD-219, TD-223 – TD-230 and TD-234 – TD-244) and four transgressive phase (e.g. intervals as follows: TD-184 – TD-192, TD-198 – TD-213, TD-219 – TD-223 and TD-230 – TD-234) were interpreted during the Langhian (Figure 47). The first regressive trend was recognized at the lower part of the section corresponding to the P-4 Zone, whereas the following transgressive and regressive trends were recorded through the P-5 Zone. The

last regressive trend is terminated within the P-6 Zone (TD-236 – TD-244) in this section. The quantitative distribution patterns of dinocysts in the Cingöz Formation do not give good response to the relative sea level fluctuations, since the diversity of dinocysts are low due to turbidity currents as discussed before. Therefore, sea level fluctuations could not be performed for the Cingöz Formation.

According to the same hypothesis, sea level fluctuation patterns were defined for the Güvenç Formation in Çorlu, Koruklu, Bekirli, and Güvenç formations. Since the lower part of the Güvenç Formation in Çorlu section was characterized by a poor zone, only the upper part of the section could be considered based on dinocyst diversity. In this section, a relative sea level fall (interval between samples TD-460 and TD-469) and a relative sea level rise (interval between samples TD-469 and TD-480) were detected at the upper part of the Çorlu Section corresponding to the P-6 Zone (Figure 48) based on the descending and ascending trends of the quantitative distribution pattern of dinocysts.

On the other hand, the Koruklu Section was characterized by a relatively diverse dinocyst assemblage. Two transgressive phase (intervals ATD-59 – ATD-67 and ATD-71 – ATD-78) and two regressive phase (intervals ATD-67 – ATD-71 and ATD-78 – ATD-81) were interpreted during the deposition of the Güvenç Formation within the Koruklu Section during the latest Langhian-Serravallian (Figure 49). The quantitative distribution of the marine dinocyst taxa in the Koruklu Section varies from 1-13 % representing a lower diversity than those in other sections discussed above. A transgressive trend was recognized at the lower part of the section, whereas the following regressive and transgressive trends were recorded in the middle and upper part of the section corresponding to the P-6 Zone. This section terminates within the last regressive phase corresponding to the P-7 Zone.

Bekirli Section contains three regressive trends (e.g. intervals as follows: ATD-1 – ATD-9, ATD-24 – ATD-29 and ATD-41 – ATD-58) and two transgressive trends (e.g. intervals as follows: ATD-9 – ATD-24 and ATD-29 – ATD-41) from bottom to top during the latest Serravallian-earliest Tortonian (Figure 50). The FO of *Achomosphaera* cf. *andalousiensis* was also defined in the transgressive phase (at the level corresponding to ATD-4; Figure 34). The quantitative distribution of the marine

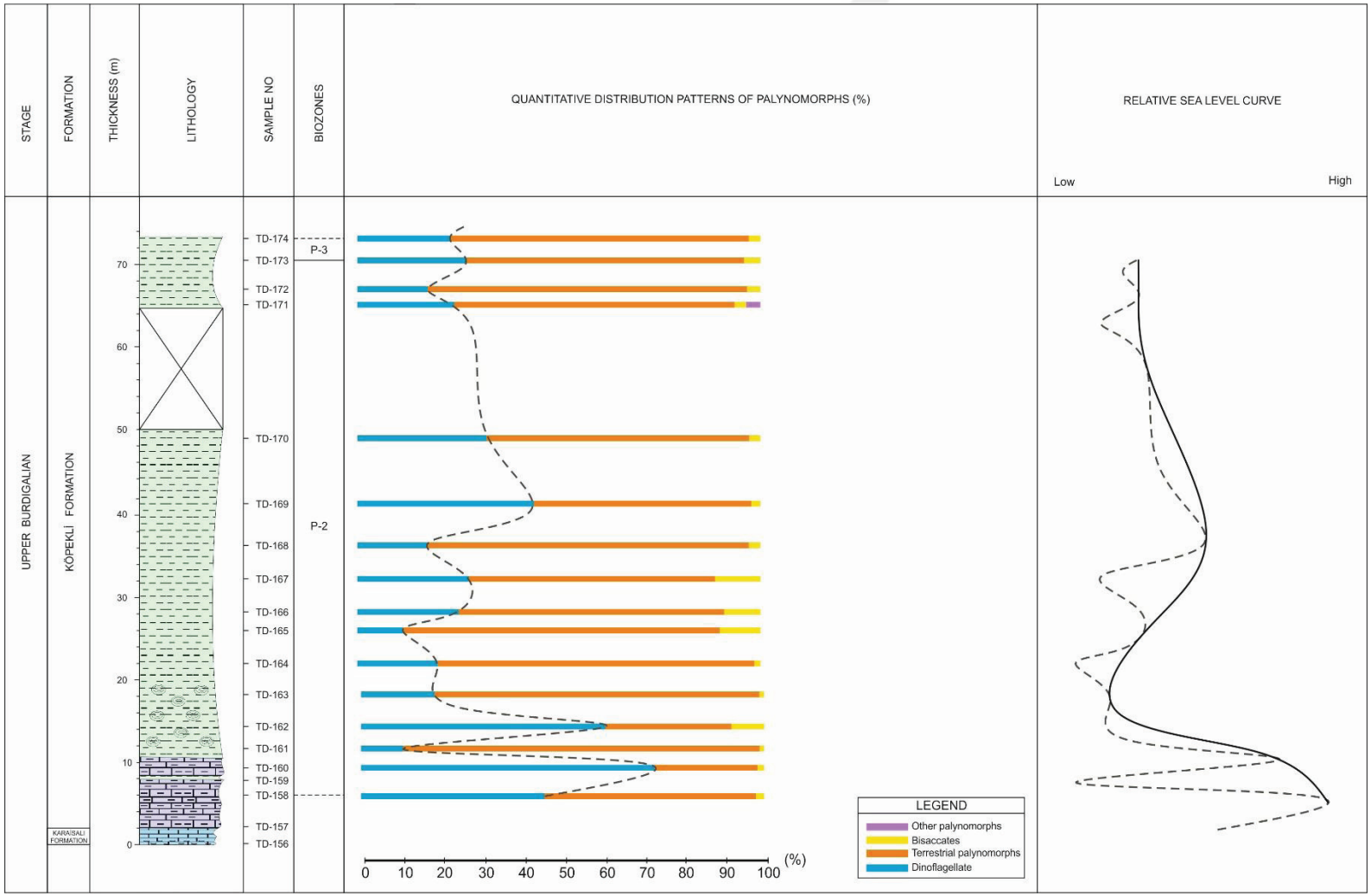

Figure 45. Diversity chart of Köpekli Section plotted on the basis of quantitative distribution patterns of palynomorph groups.

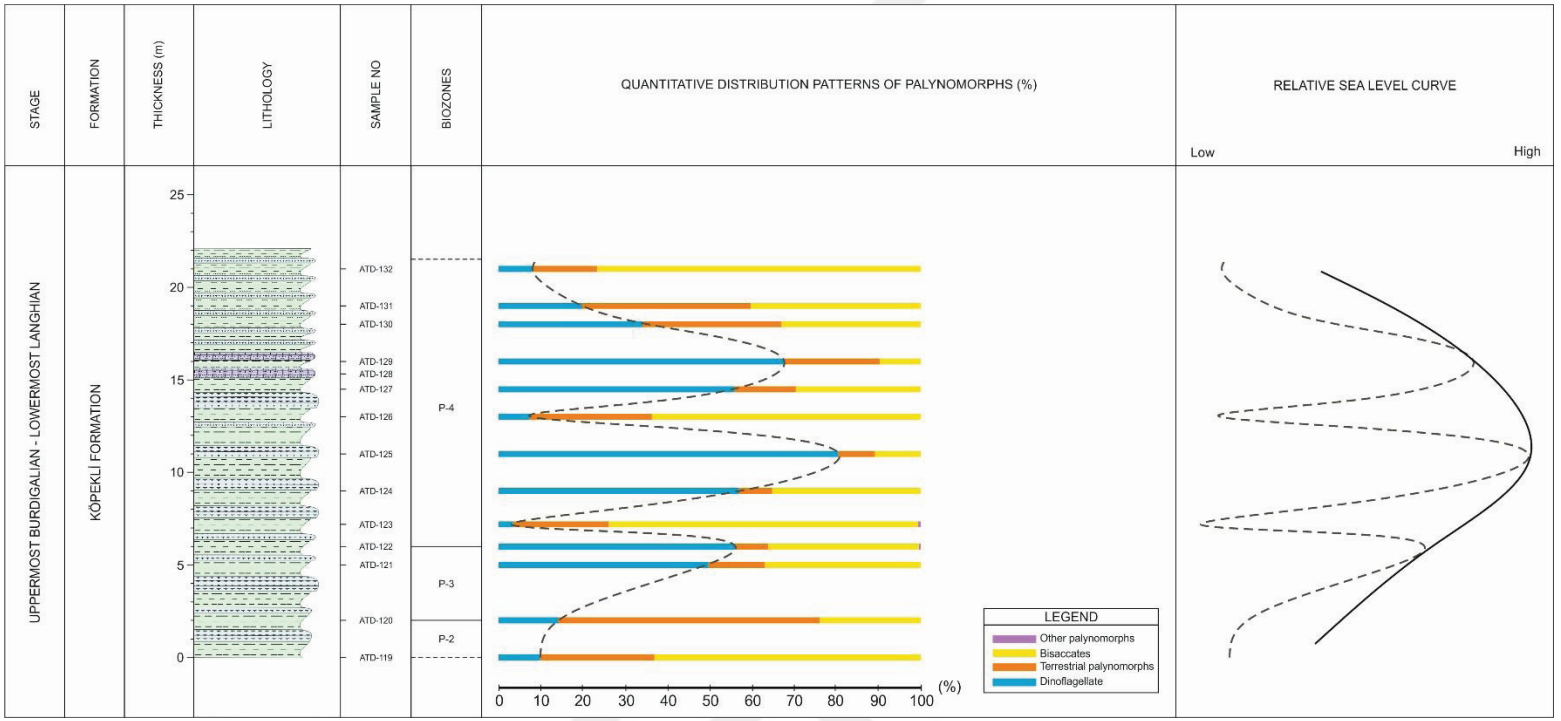

Figure 46. Diversity chart of Sofular Section plotted on the basis of quantitative distribution patterns of palynomorph groups.

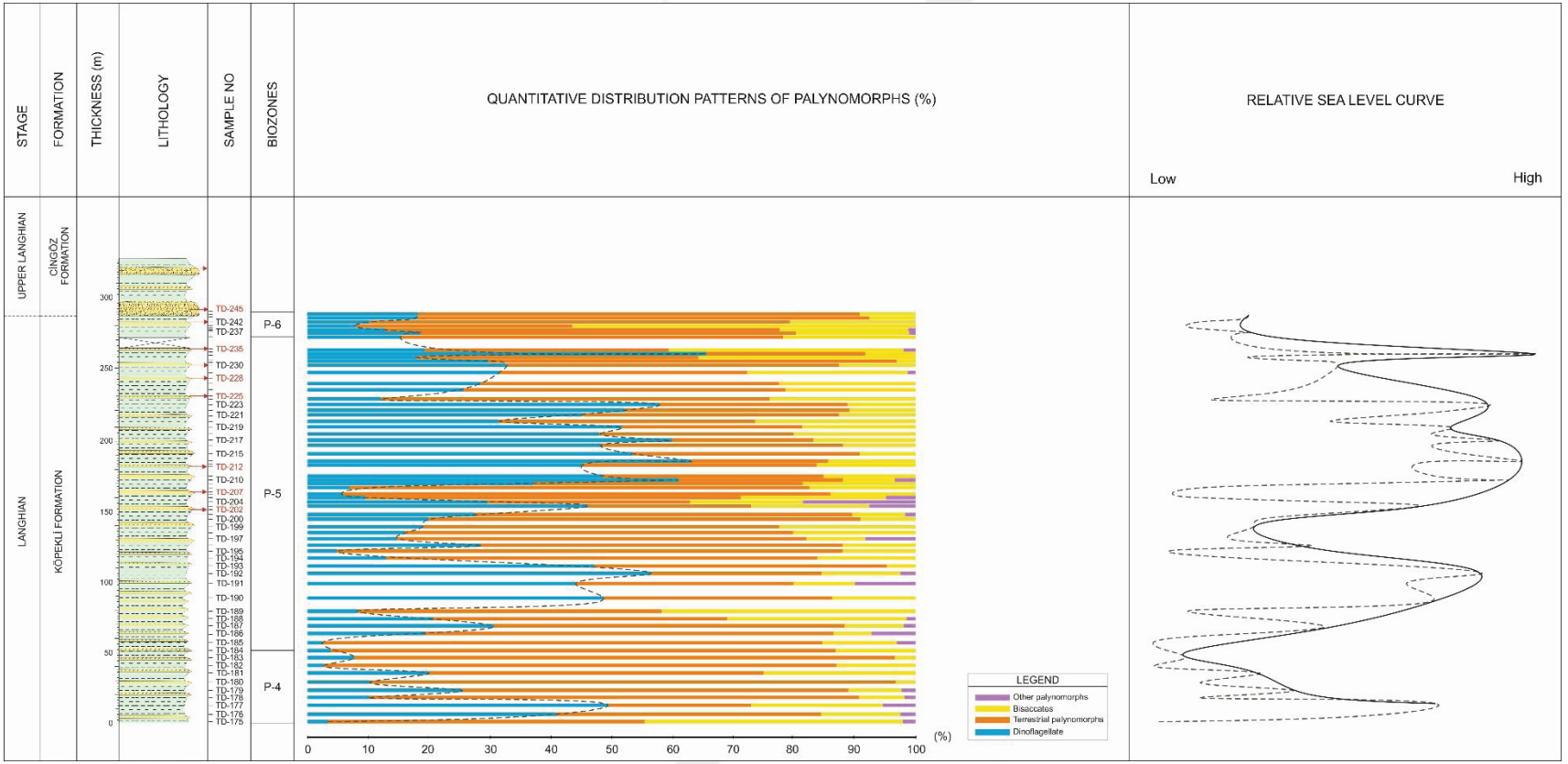

Figure 47. Diversity chart of Çorlu Section including Köpekli Formation plotted on the basis of quantitative distribution patterns of palynomorph groups.

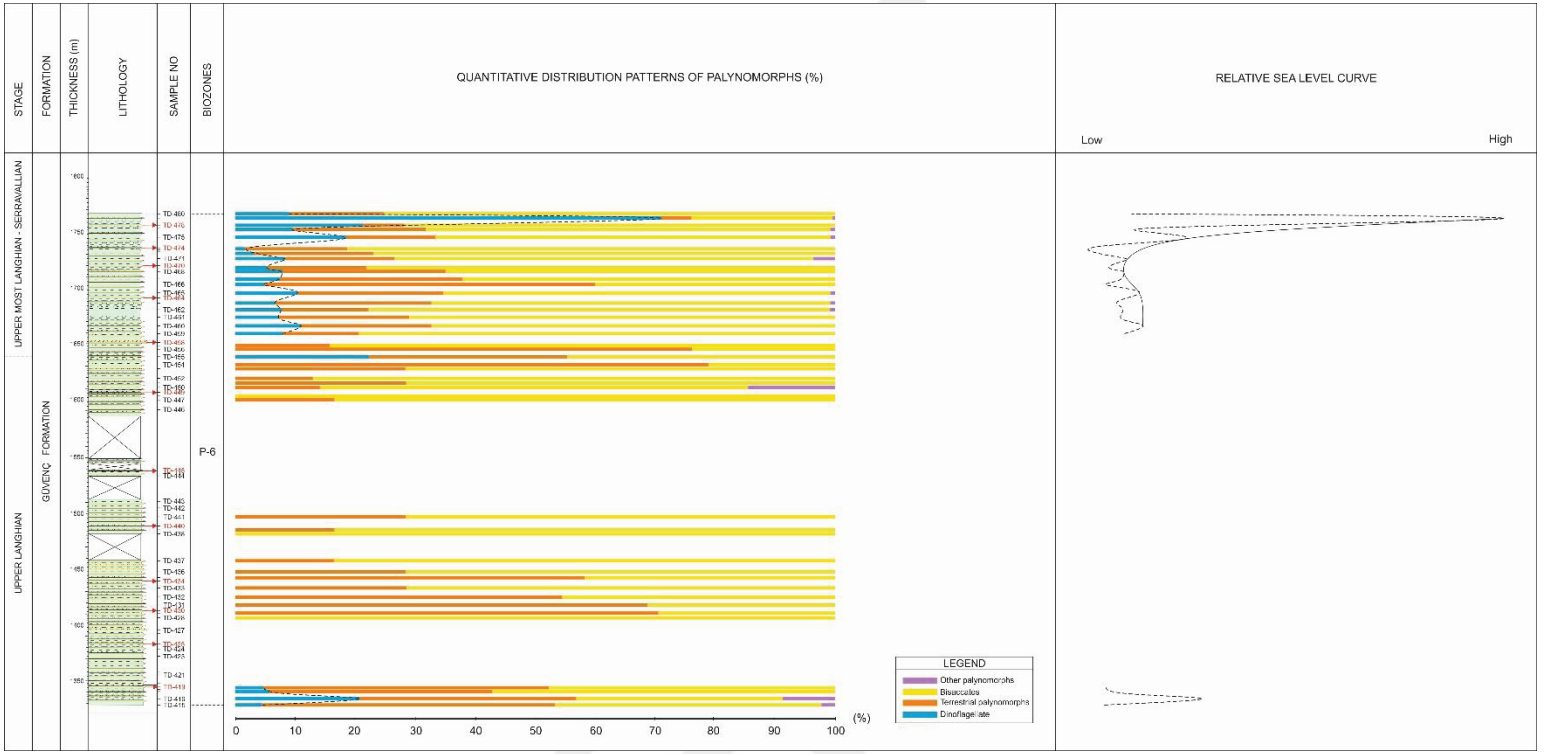

Figure 48. Diversity chart of the Güvenç Formation within Çorlu Section plotted on the basis of quantitative distribution patterns of palynomorph groups.

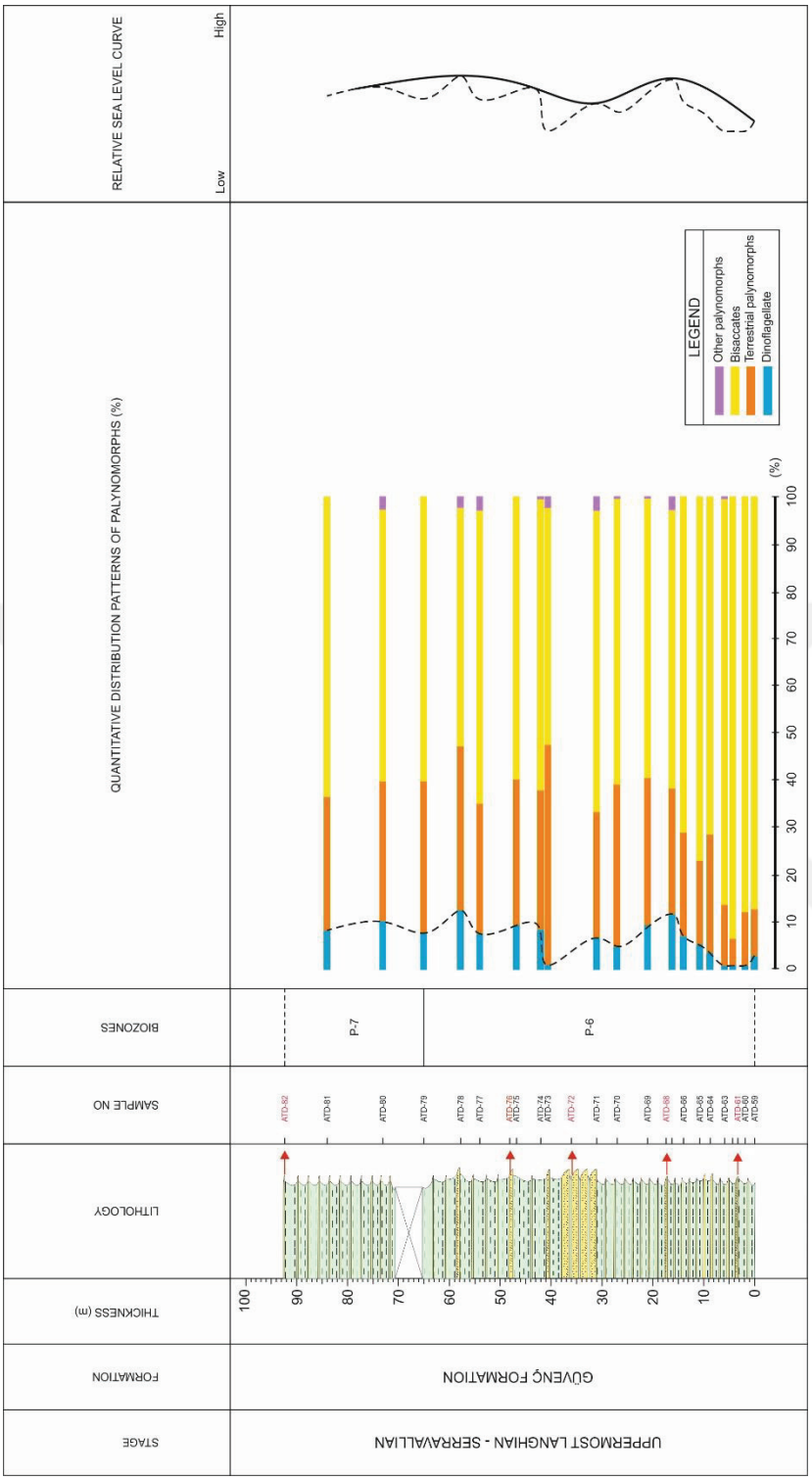

Figure 49. Diversity chart of Koruklu Section plotted on the basis of quantitative distribution patterns of palynomorph groups.

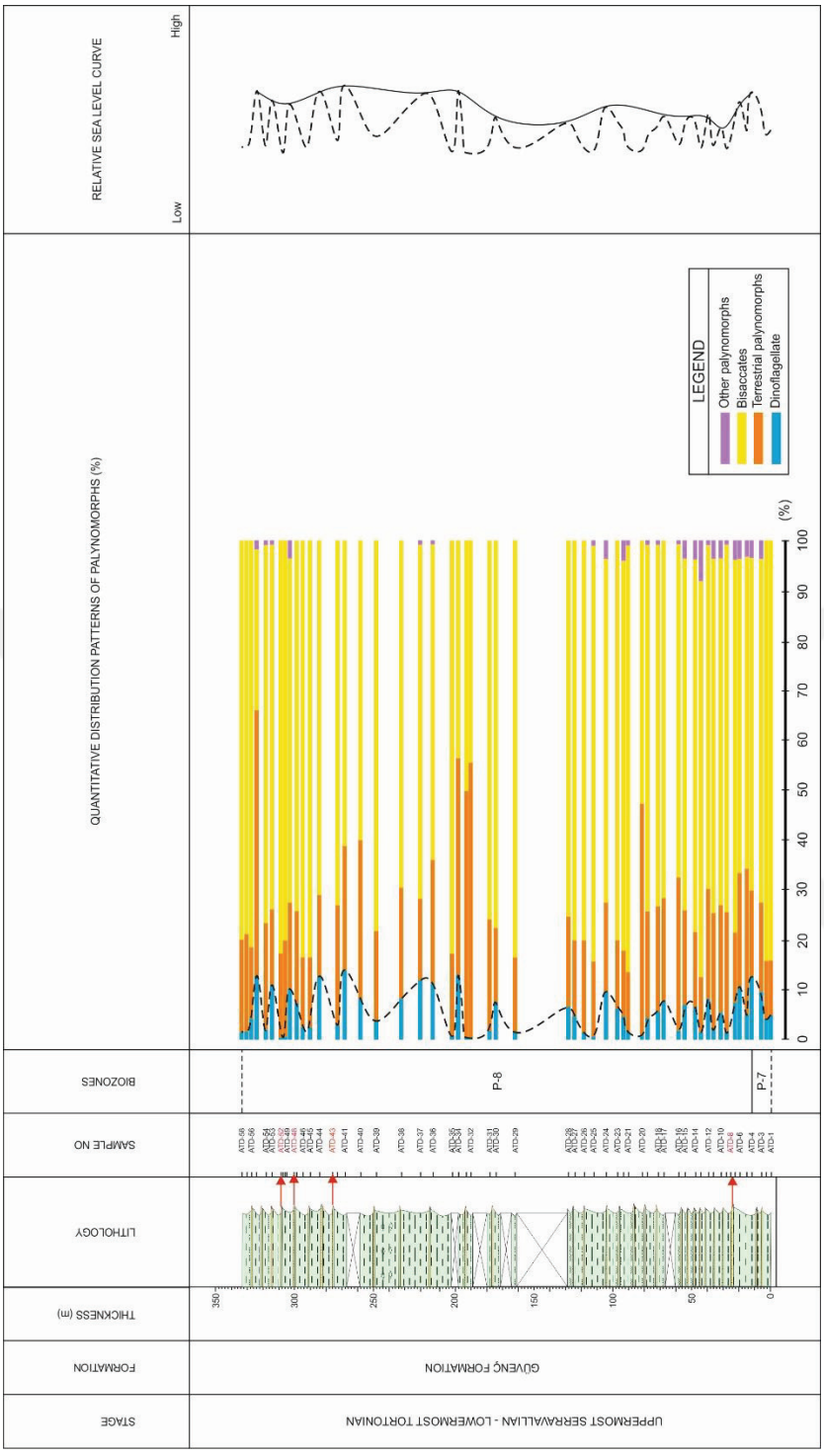

Figure 50. Diversity chart of Bekirli Section plotted on the basis of quantitative distribution patterns of palynomorph groups.

dinocyst taxa in the Bekirli Section reaches upto 16 % representing a relatively higher diversity rather than Koruklu Section. Through Güvenç Section including the upper part of the Güvenç Formation, a relative sea level rise (ATD-83 – ATD-87) and a relative sea level fall (ATD-87 – ATD-89) were recognized at the lower part of the section corresponding to the P-8 Zone (Figure 50). Then, a still-stand to relative sea-level rise was realized at the middle part of the section (ATD-89 – ATD-99). Towards the upper part of the section, a regressive trend (ATD-89 – ATD-102) and a transgressive trend (ATD-102 – ATD-111) were detected based on the quantitative distribution pattern of dinocysts. Since a considerable covered area exists at the uppermost part of the section, any sea level fluctuation pattern cannot be identified. The most dominating species within the *Homotyrblium* group was *Homotryblium tenuispinosum* in this section. Dybkjaer (2004) suggested that a stepwise increase in relative abundance of *Homotryblium tenuispinosum* were related to the marine flooding surfaces. Such a pattern was recorded at the level corresponding to ATD-99, ATD-102, ATD-106 and ATD-110 indicating times of maximum transgression (Figure 51).

A relative sea level curve was constructed based on dinocyst diversity (Figure 52). The plotted curve based on the quantitative distribution patterns of dinocysts in this study was correlated with the eustatic sea level curve of the Haq *et al.* (1987) (Figure 52). A relative sea level fall is detected in the lower part of the P-2 Zone based on the quantitative distribution pattern of dinocysts in the late Burdigalian. A regressive trend is also detected in the eustatic sea level curves of Haq et al. (1987). This regression is followed by a transgressive trend from the upper part of the P-2 Zone to the lower part of the P-4 Zone during the late Burdigalian to the earliest Langhian. Similar transgressive trend is recognized within the eustatic sea level curves of Haq et al. (1987) during the same time interval. Then a descending of relative sea level is detected at the upper part of the P-4 Zone based on the decreasing trend in the quantitative distribution pattern of dinocysts during the early Langhian as recorded in the eustatic sea level curves of Haq. et. al. (1987). Based on the evaluation of the data, a possible relative sea level fall is proposed within the P-5 Zone during the early Langhian- early Serravallian. Since the P-6 Zone is mainly characterized by a poor and

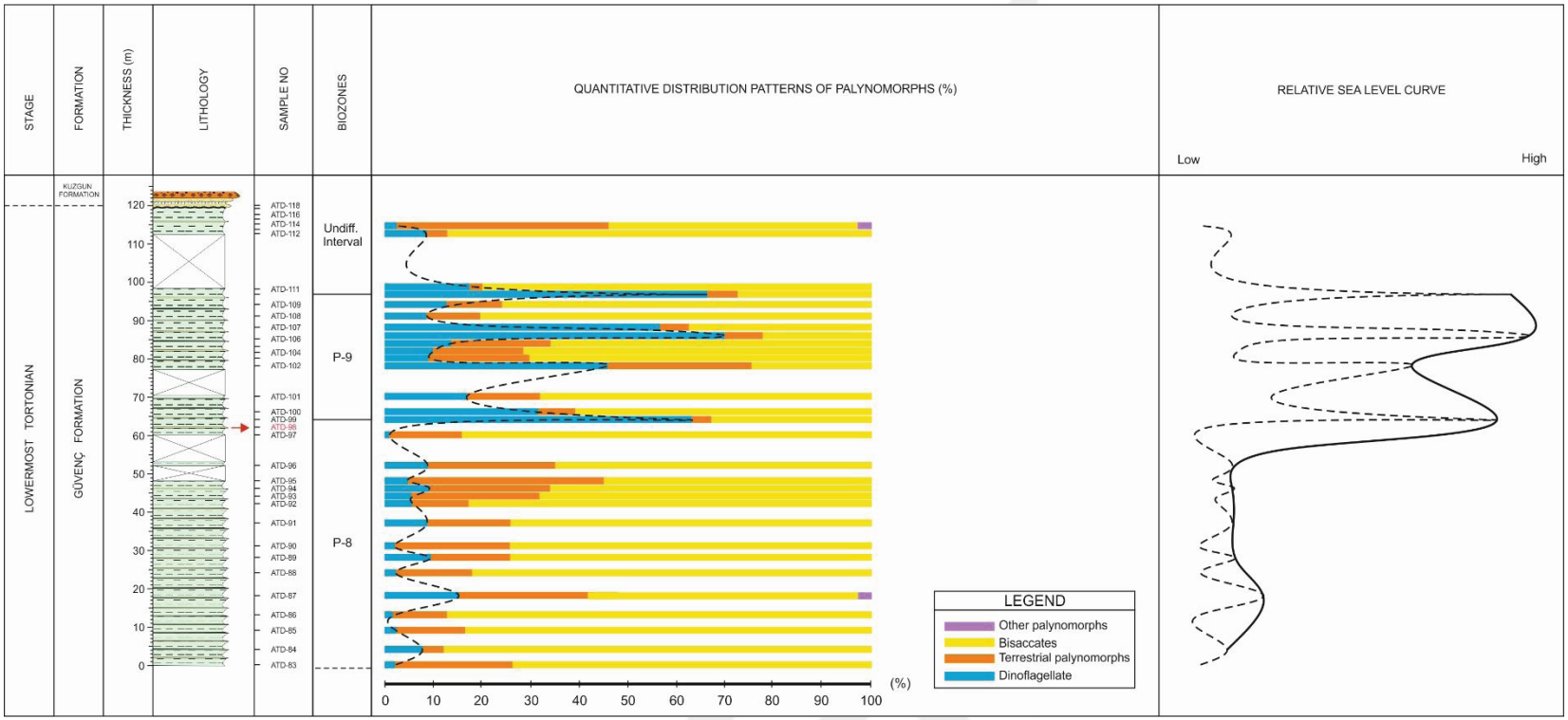

Figure 51. Diversity chart of Güvenç Section plotted on the basis of quantitative distribution patterns of palynomorph groups.

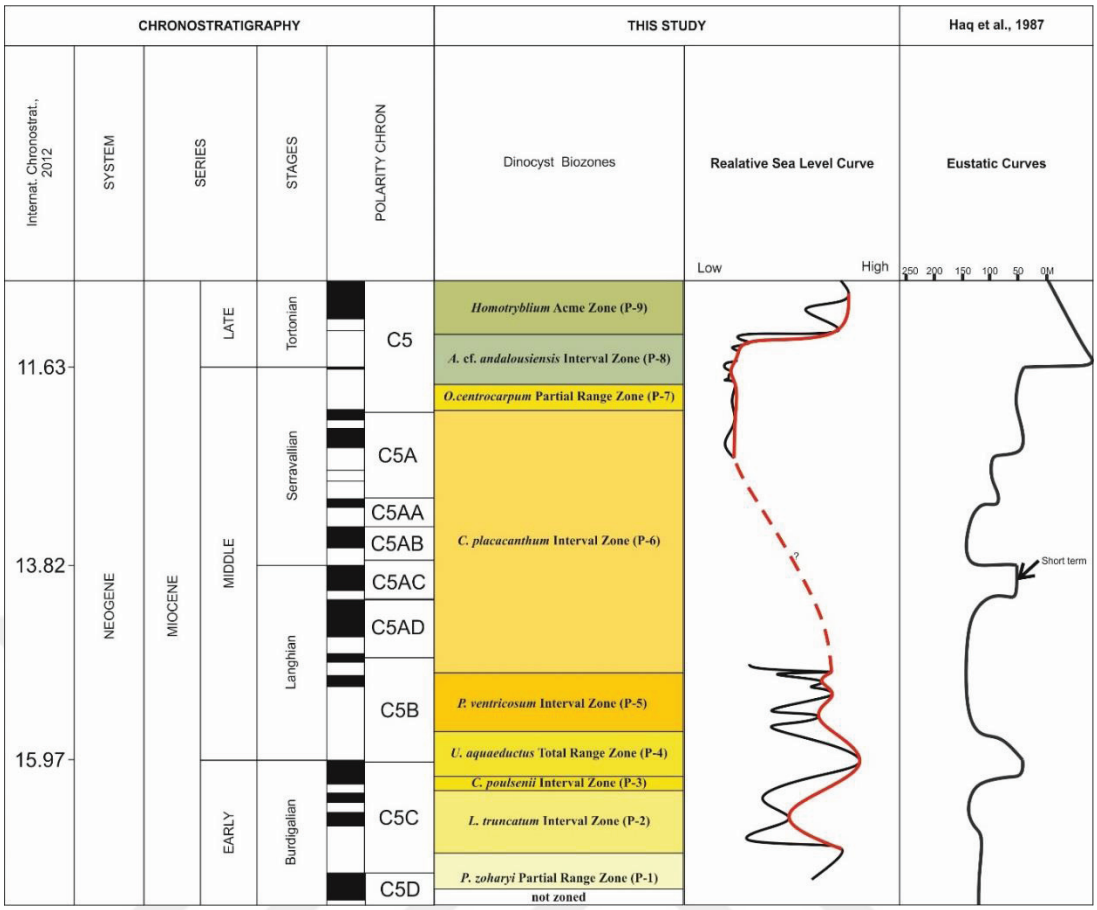

Figure 52. Relative changes in sea level were plotted s based on the quantitative distribution patterns of dinocysts in this study and these curves were correlated with the eustatic sea level curves of the Haq et al., 1987 (red line shows the finilized relative sea level curve pollted in this study).

a less diverse dinoflagellate assemblage, the existing data cannot be used to plot the relative sea level curve in this interval. Only an assumption is made in this interval (as shown by red dash line in the Figure 52), since the quantitative distribution pattern of dinocysts only in the uppermost part of the P-6 Zone is known. At this point, the plotted relative sea level curve in this study and the euastatic sea level curve of Haq et al. (1987) do not represent similar trends in this interval. The quantitative distribution pattern of dinocysts within the upper part of the P-6 Zone, characterized by a rich and diverse dinocyst assemblage, represents a transgressive trend in the latest Serravallian-earliest Tortonian. Similarly, a transgression is recorded in the eustatic sea level curves of Haq et al. (1987). A following relative sea level fall is realized in the P-9 Zone in the earliest Tortonian. Likely, the eustatic sea level curve of Haq et al. (1987)

represents a regressive trend. Therefore, the curve plotted for Miocene dinocysts in this study reflect striking similarities to the general trend of the eustatic sea level curves of the Haq *et al.* (1987).

CHAPTER 6

PALYNOFACIES ANALYSIS

There is an upsurge in interest in palynofacies analysis, since the composition of sedimentary organic matter gives clues about the depositional environments. Comboz (1964) defined the term 'palynofacies' as all the acid-resistant organic matter, which is obtained from the sedimentary rocks by palynological processing techniques using HCL and HF. After Comboz (1964), Batten (1996) emphasized that the occurrence and composition of organic matter in sediments and sedimentary rocks reflect an enormous number of variation that influence the terrestrial or aquatic environments, in which it is generated, it is transported to the depositional site, and its alteration once deposited. Moreover, the factors affecting the character of sedimentary organic matter are important, since these factors control the type of organic matters and the variations of their percentages in a sedimentary succession. Batten (1996) stated that on a global scale, time, climate, tectonics, and changes in sea level affect the character and geographic occurrence of sedimentary organic matter. Batten (1996) also mentioned that the availability of sediments in the general depositional regime, the rate of accumulation, the proximity and composition of the terrestrial vegetation if any, and the chemical composition of the water and the biological activity within it as well as on and in the accumulating sediment are regionally important. Furthermore, types and compositions of sedimentary organic matters are affected by the sea level fluctuations. Batten (1996) defined that if there has been a rise in sea level and/or subsidence of a sedimentary basin and a reduction in sediment supply, it may result in reworking and an increase in chemically and biologically formed deposits. According to Hart (1986), Habib and Miller (1989) and Jaramillo (1995), the variations in the percentages of the sedimentary organic matter constituents give important clues about the paleoenvironment. For example, palynofacies dominated by amorphous organic matter mostly represent deep marine environments, while palynofacies dominated by

terrestrial organic matter (woody and coaly) indicate much shallower and more near-shore conditions. However, amorphous organic matter can also be seen in nonmarine environments caused by the biodegradation of cellular remains and products of that process under similar anoxic conditions (Batten, 1983). Batten (1996) mentioned that the obtained data from palynofacies investigations should always be integrated with information derived from the palynomorphs. In general, composition of the sedimentary organic matter can successfully be used in studies regarding depositional environments (Batten, 1996).

The suggested classifications of sedimentary organic matters based on visual examination under microscope by Burges (1974), Tissot and Welte (1978), Masran and Pocock (1981), Teichmüller (1985), Boulter (1994), Hart et. al. (1994) and Tyson (1995) are represented in Figure 53. Among these studies, Burges (1974) carried out a detailed study about microscopic examination of kerogens and suggested four groups of organic matter components that are algal, amorphous, herbaceous, and woody and coaly. After Burges (1974), Tissot and Welte (1978) named these four groups of organic matter as I, II, III, and IV. Then, Masrah and Pocock (1981) carried out a more detailed classification of sedimentary organic matter and distinguished six groups including amorphous, resin, structured aqueous material, spore and pollen, structured terrestrial material, and charcoal. Moreover, Teichmüller (1985) preferred to use a standard terminology of coal petrology while reconstructing the classification of sedimentary organic matter. He defined five different categories as variable, alginate, liptinite, huminite, and inertinite. After Teichmüller (1985), Boulter (1994) differentiated four groups of the organic matter constituents as amorphous matter, algal, palynomorph and palynowafers. Additionally, Hart et. al. (1994) suggested a new classification based on biological origin and preservation stages of organic matter. They classified organic matter into five groups consisting of amorphous, protistoclast, phytoclast, sclerotoclast, and black debris. Finally, Tyson (1995) reconstructed the most extensive classification and he differentiated three major groups including amorphous, palynomorphs (e.g. phytoplanktons, aporomorph, and zoomorph), and phytoclasts. The comparison of these organic matter classifications in different studies was represented in Figure 53.

In this study, palynofacies analysis was carried out based on the classification of Burges (1974). The amorphous (the structureless, disseminated and shapeless

Amorphous (+ Resin)	Amorphous		Amorphous	Amorphous (as secondary product)	Amorphous Resin	? Resin	Amorphous	Variable	I-II
Acritarch	Phytoplankt. tons.	Palynomorphs	Algal	Protistoclast	Stuructured Aqueous	Marine Palynomorp	Algal	Alginite	I
Algae (prasinophyta-tasman. cholorococcale-pedias., botryc.)						(Freswater) Algal			
Dinoflagellata			Palynomorph			Marine Palynomorph.			
Spore & pollen	Sporomorph			Phytoclast	Spore & Pollen	Terrestrial Palynomorph.	Herbaceous	Liptinite	II
Chitinozoa	Zoomorph		?	?	?	?	?	?	?
Scelocodont			?	?	?	?	?	?	?
Microforaminifera			?	?	?	Foraminiferal linings	?	?	?
Fungal Remains (mostly F.spores)	Sporomorph		?	Sclerotoclast	Fungi	?	?	Inertinite	IV
Woody tissue of land plants	Phytoclasts		Palynowafers	Phytoclast	Structured Terrestrial	Brown wood	Woody	Vitrinite / Huminite	III
Epidermal tissue of land plants(cuticles)						Cuticle	Herbaceous	Liptinite	II
Non-woody, non-epidermal tissue of land plants						?	?	?	?
Opaque & semi-opaque particles					Charcoal	Black wood.	Coaly	Inertinite	IV
Om types / Author	Tyson, 1995		Boulter, 1994	Hart, etal 1994	Masran & Pocock, 1981	Parry, etal 1981	Burges, 1974	Teichmüller, 1985 COAL MACERALS	Tissot, welte 1978 CHEMICAL OM TYPES

Figure 53. Organic matter classifications in different studies (Tekin, 2002).

particles recognized under the microscope), herbaceous (spores and pollen), woody (woody remains of land plants and plant tissue), and coaly (the opaque particles defined within the palynological slides) type organic matters are evaluated for the palynofacies analysis. Therefore, all of the kerogen slides have been examined based on their percentages of the organic matter constituents (e.g. amorphous, herbaceous, woody, and coaly). The organic matter distribution of all samples was documented in detail for each measured section. Moreover, charts representing the organic matter contents and their distribution were constructed.

In order to evaluate the palynofacies of the Köpekli Formation, samples coming from the Çukurköy Section, Köpekli Section, Sofular Section, and the lower part of the Çorlu Section were analyzed. Marine-derived amorphous organic matter content within the Çukurköy Section varies from 15 % to 60 %, whereas the terrestrial type organic matter (e.g. herbaceous, woody and coaly) is in the range of 40-75 % (Figure 54 and App. C, Table 1). As mentioned above, while analyzing the palynofacies, the obtained data should always be integrated with the information derived from palynomorphs. Percentages of marine dinoflagellates vary from 8-72 % depending on the sea level fluctuations, whereas the terrestrial palynomorphs are in the range of 28-92 %. Especially, the intervals; from ATD-142 to ATD-147, from ATD-151 to ATD-155, and from ATD-158 to ATD-161 are characterized by increases in the percentages of amorphous organic matter. Similarly, the dinocyst assemblages represent an ascending trend at these levels indicating a rise in sea level (Figure 44). On the other hand, terrestrial palynomorphs constitute the majority in certain levels of the section. However, it is important to note that most of the terrestrial palynomorphs in this study are of bisaccate group gymnosperms, which can travel long distances by wind and wave activity. The organic matter association in the Köpekli Section is composed of 30-45 % amorphous organic matter and 55-70 % terrestrial organic matter (Figure 55 and App. C, Table 2). Moreover, percentages of dinocyst assemblage and the terrestrial palynomorphs vary between 11-74 % and between 26-89%, respectively (Figure 45). The same ascending trends are recorded in the intervals TD-158- TD-161 and TD-167- TD-170 in terms of the distribution of amorphous organic matter and the dinocyst assemblage (Figure 45 and Figure 55). Percentages of amorphous organic matter from Sofular Section is 20-45 % while the terrestrial organic matter dominates the assemblage about 55-80 % (Figure 56 and App. C, Table 3).

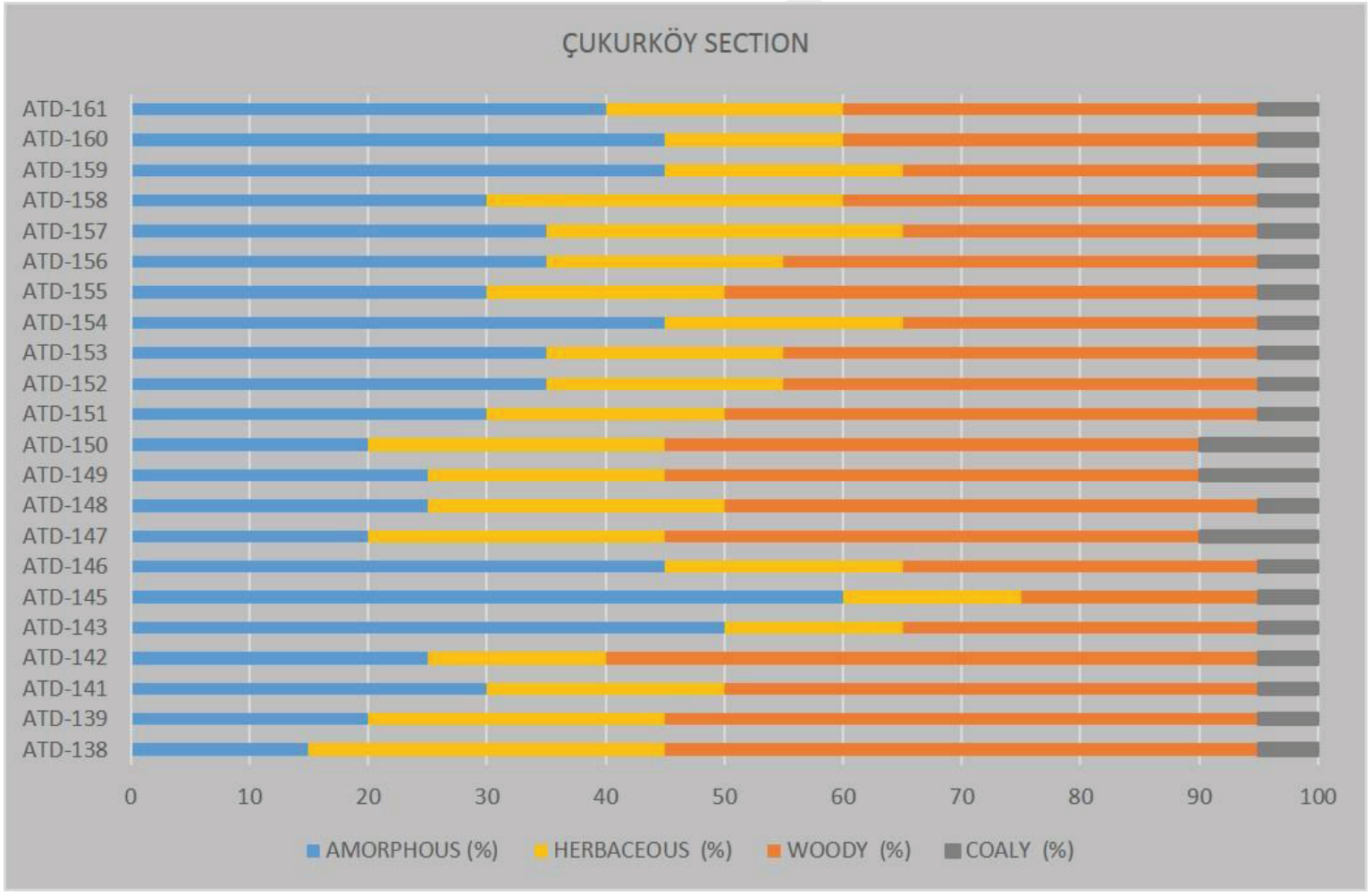

Figure 54. The organic matter distribution chart for the Köpekli Formation in the Çukurköy Section.

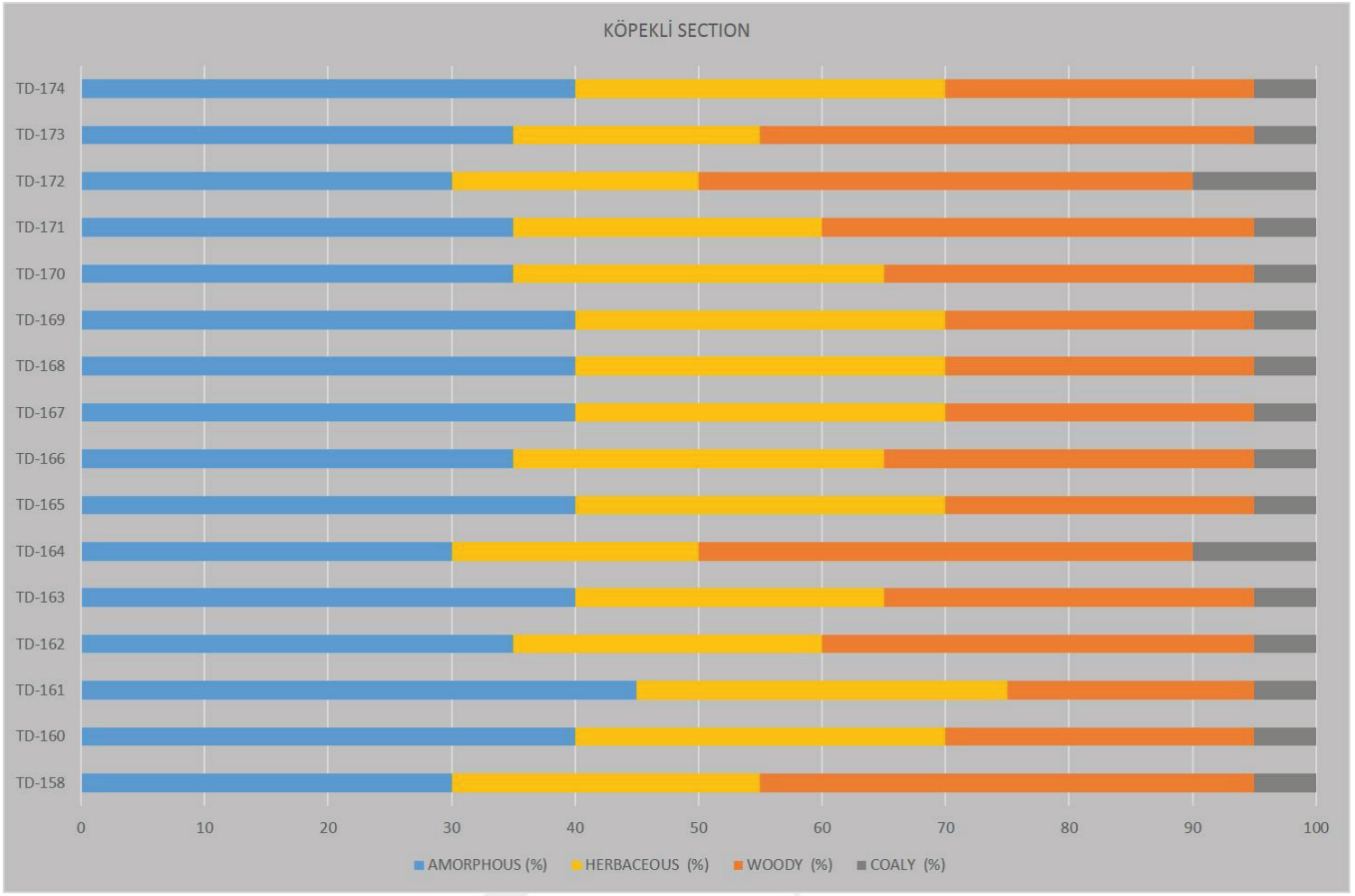

Figure 55. The organic matter distribution chart for the Köpekli Formation in the Köpekli Section.

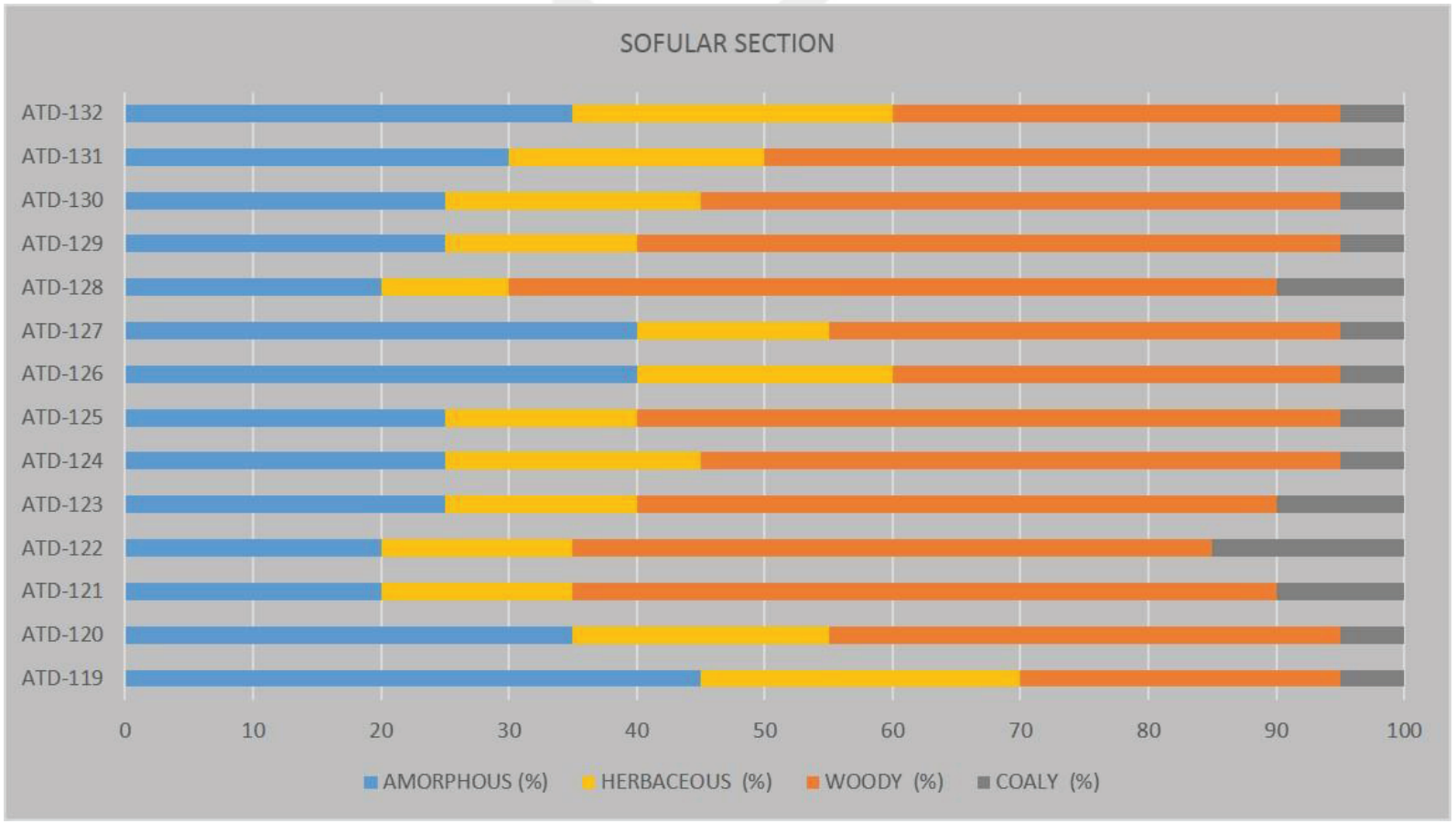

Figure 56. The organic matter distribution chart for the Köpekli Formation in the Sofular Section.

Furthermore, dinocyst assemblages vary between 4-80 % (Figure 46). Especially, the number of dinocysts represents an ascending trend in the middle part of the section (from ATD-124 to ATD-129), as the amorphous organic matter increases in the same interval. Additionally, the bisaccate pollen mainly dominate the section from bottom to top. The organic matter assemblage in the Köpekli Formation measured within the Çorlu Section consists of 5-40 % amorphous organic matter while the terrestrial organic matter dominates the section in the range of 60-95 % (Figure 57 and App. C, Table 4). Percentages of marine dinoflagellates vary between 2-66 %, whereas the terrestrial palynomorphs are in the range of 34-98 % (Figure 47 and Figure 57). Several peak points were recognized at levels corresponding to the samples TD-175, TD-177, TD-187, TD-213, TD-229, TD-239, and TD-243 in terms of organic matter distributions based on amorphous organic matter (Figure 57). Similarly, ascending trends were recorded in the dinocyst distribution patterns at these certain levels. Finally, it can be concluded that the organic matter distributions are consistent with the palynomorph assemblages within the Köpekli Formation.

The Cingöz Formation, characterized generally by turbidite deposits, was measured in the Çorlu Section. Marine-derived amorphous organic matter content varies between 5-35%, whereas the terrestrial organic matter is in the range of 65-95 % (Figure 58 and App. C, Table 5). The amount of organic matter varies from very low to very high indicating a wide range. In addition, some barren samples (i.e. lack of any organic matter) were encountered through this formation. Williams and Sarjeant (1967) discussed that spores, pollen, acritarchs, and dinocysts, all being very light may never be deposited in regions of high turbulence. This is probably the reason why the organic matter was not deposited within the turbidite deposits of the Cingöz Formation. The Cingöz Formation is mainly characterized by a poor and low diversity dinocyst assemblage and a common terrestrial taxa dominated by bisaccate pollen and fresh water algae probably introduced to the area by large river systems. Accordingly, the palynomorph assemblage did not give good response to the distribution pattern of organic matter in the Cingöz Formation. Therefore, palynofacies investigations could not be done with the information obtained from the palynomorphs.

The Güvenç Formation was studied in the Çorlu Section, Koruklu Section, Bekirli Section, and Güvenç Section. Marine-derived amorphous organic matter content in the Çorlu Section varies between 2-71% while the terrestrial organic matter

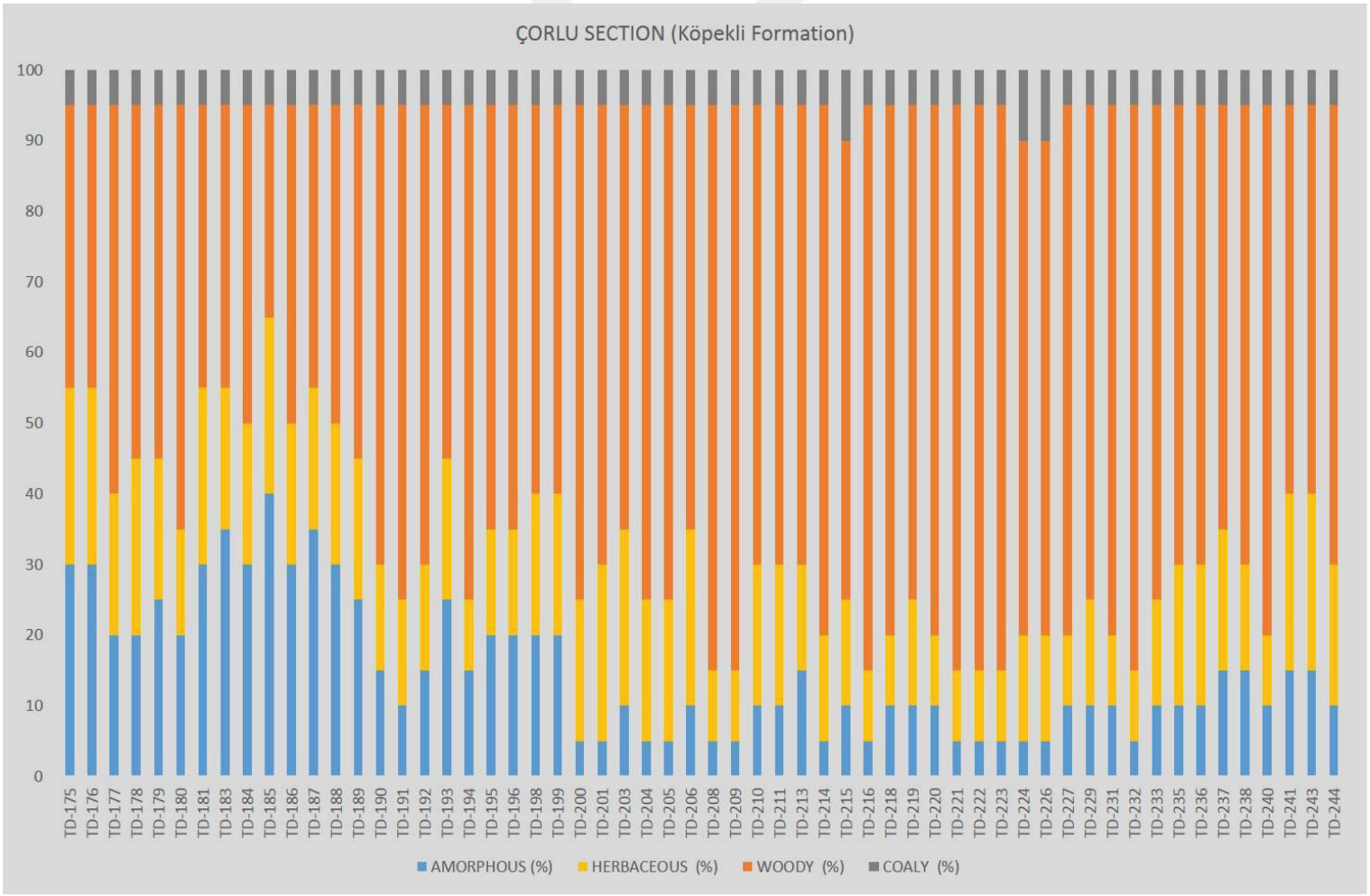

Figure 57. The organic matter distribution chart for the Köpekli Formation in the Çorlu Section.

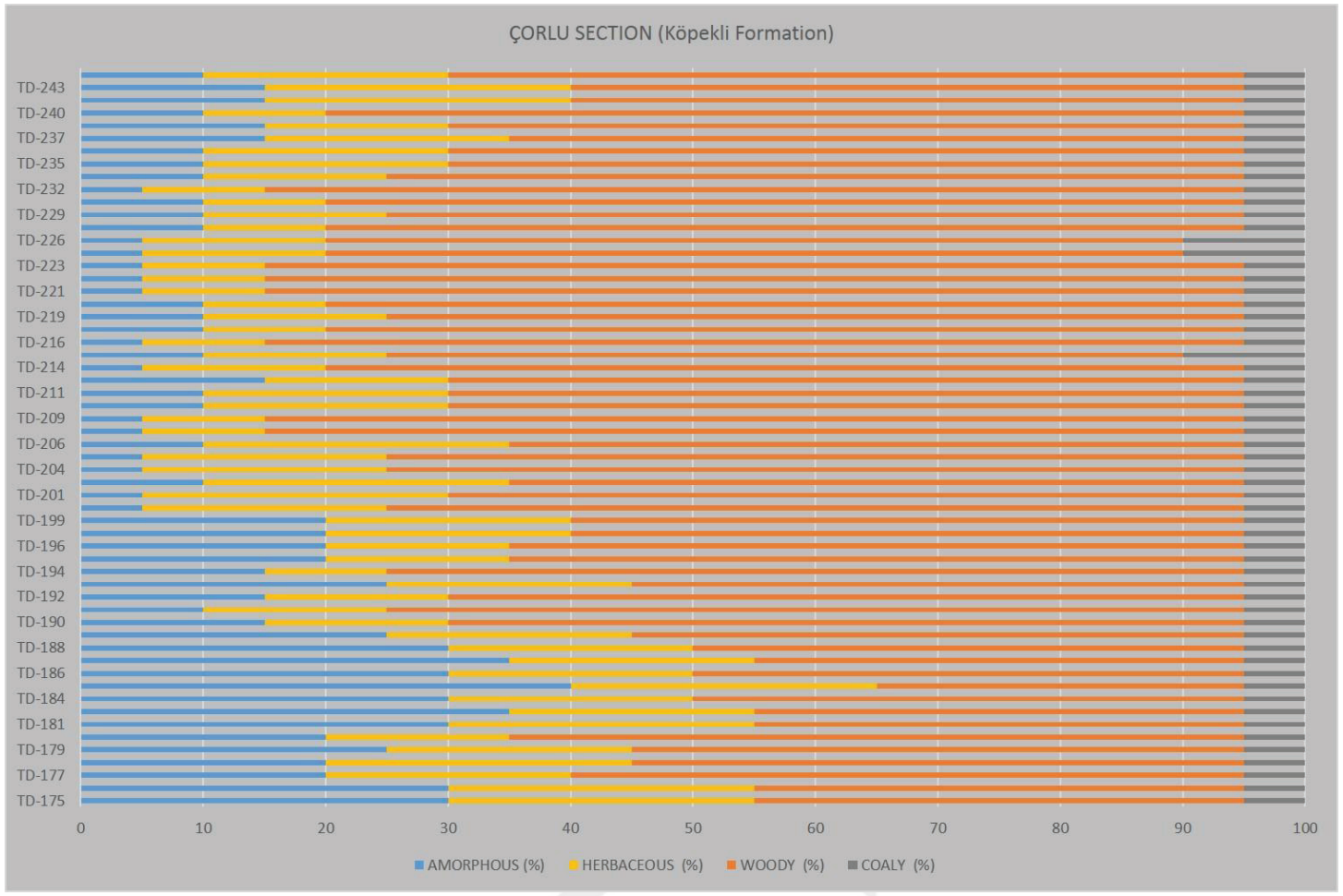

Figure 58. The organic matter distribution chart for the Cingöz Formation in the Çorlu Section.

is in the range of 29-98 % (Figure 59 and App. C, Table 6). As it is discussed in the "Biostratigraphy" section, a poor zone was defined in the P-6 Zone, which includes both the Cingöz Formation and lower part of the Güvenç Formation (Figure 32). Since the Cingöz Formation changes into the Güvenç Formation transitionally, the lower part of the Güvenç Formation reflects similar characteristics in terms of palynomorph assemblage. On the other hand, the organic matter distribution of the upper part of the Güvenç Formation (in the Çorlu Section) correlates well with the distribution of the palynomorph assemblage. The stratigraphic levels corresponding to the samples TD-459-460, TD-465, TD-475, and TD-479 display an increase in the number of the amorphous organic material (Figure 59). Similarly, the marine dinocyst assemblages show peaks at these certain stratigraphic levels (Figure 48). The organic matter assemblages from the Güvenç Formation measured in the Koruklu Section consist of 10-35 % amorphous organic matter while the terrestrial organic matter dominates the section in the range of 65-90 % (Figure 60 and App. C, Table 7). Percentages of marine dinoflagellates vary between 1-13 %, whereas the terrestrial palynomorphs are in the range of 87-99 % (Figure 49). The amorphous organic matter reflects two distinct peak points at stratigraphic levels corresponding to the samples ATD-67 and ATD- 79. Likewise, the marine dinocysts represent similar increasing trends at these levels. Bekirli Section, comprising the Güvenç Formation, is composed of 15-45 % amorphous organic matter while the terrestrial organic matters dominates the section in the range of 55-85 % (Figure 61 and App. C, Table 8). Distributions of amorphous organic matter and the dinocysts assemblages show similar ascending trend at several intervals (e.g. from ATD-4 to ATD-5, from ATD-10 to ATD-11, from ATD-21 to ATD-23, from ATD-36 to ATD-38, from ATD-46 to ATD-49, and from ATD-53 to ATD-55) (Figure 50 and Figure 61). Percentages of amorphous organic matter from the Güvenç Section vary between 20-45% while the terrestrial organic matter dominates the assemblage in the range of 55-80 % (Figure 62 and App. C, Table 9). Moreover, dinocyst assemblages alternate between 1-66% (Figure 51). The distribution of amorphous organic matter show a few ascending trends in the following intervals: Samples from ATD-87 to ATD-90, ATD-97 to ATD-99, and ATD-109 to ATD-110 (Figure 62). Marine dinocyst assemblage also represents an increasing pattern at these intervals (Figure 51).

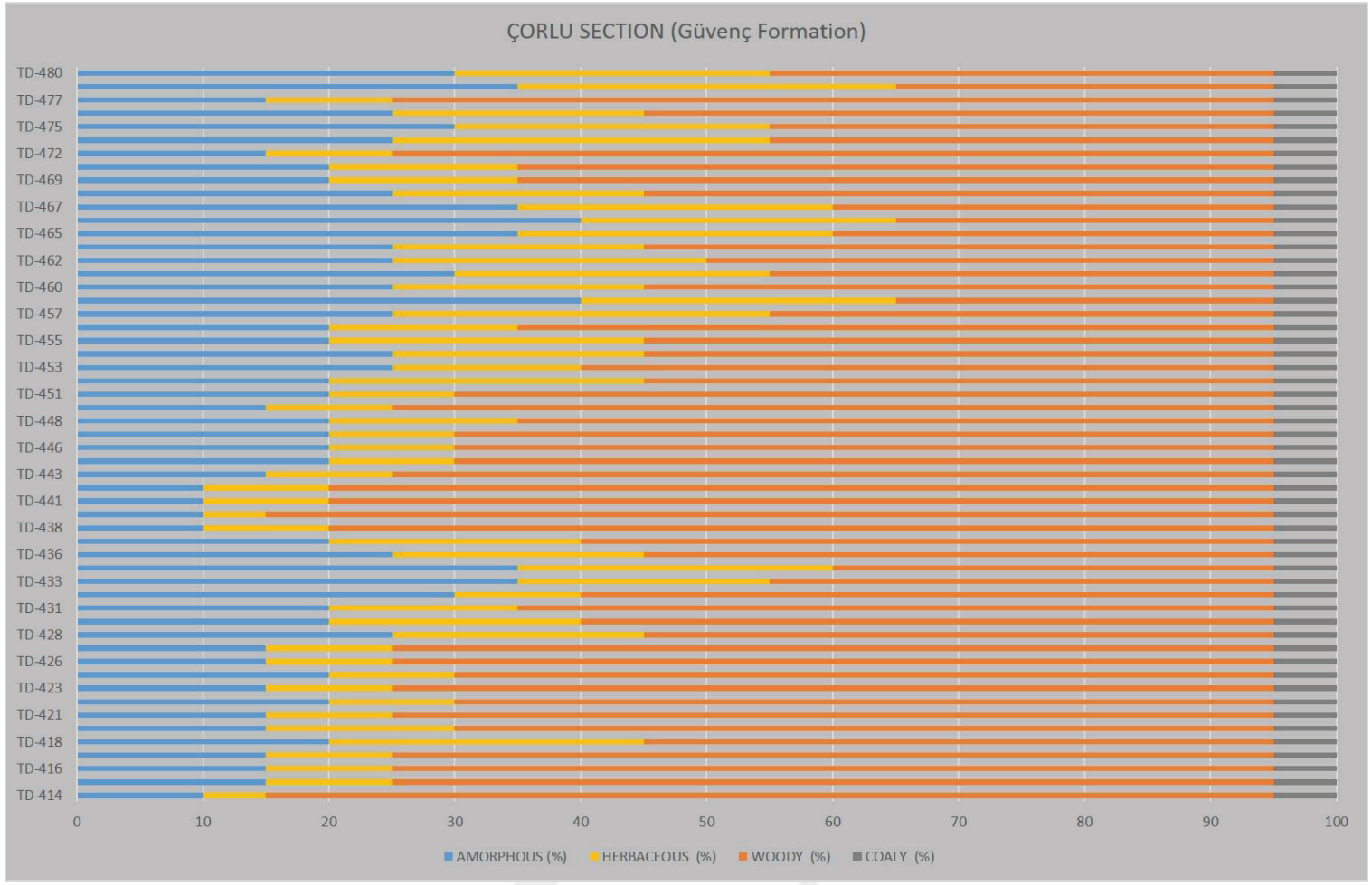

Figure 59. The organic matter distribution chart for the Güvenç Formation in the Çorlu Section.

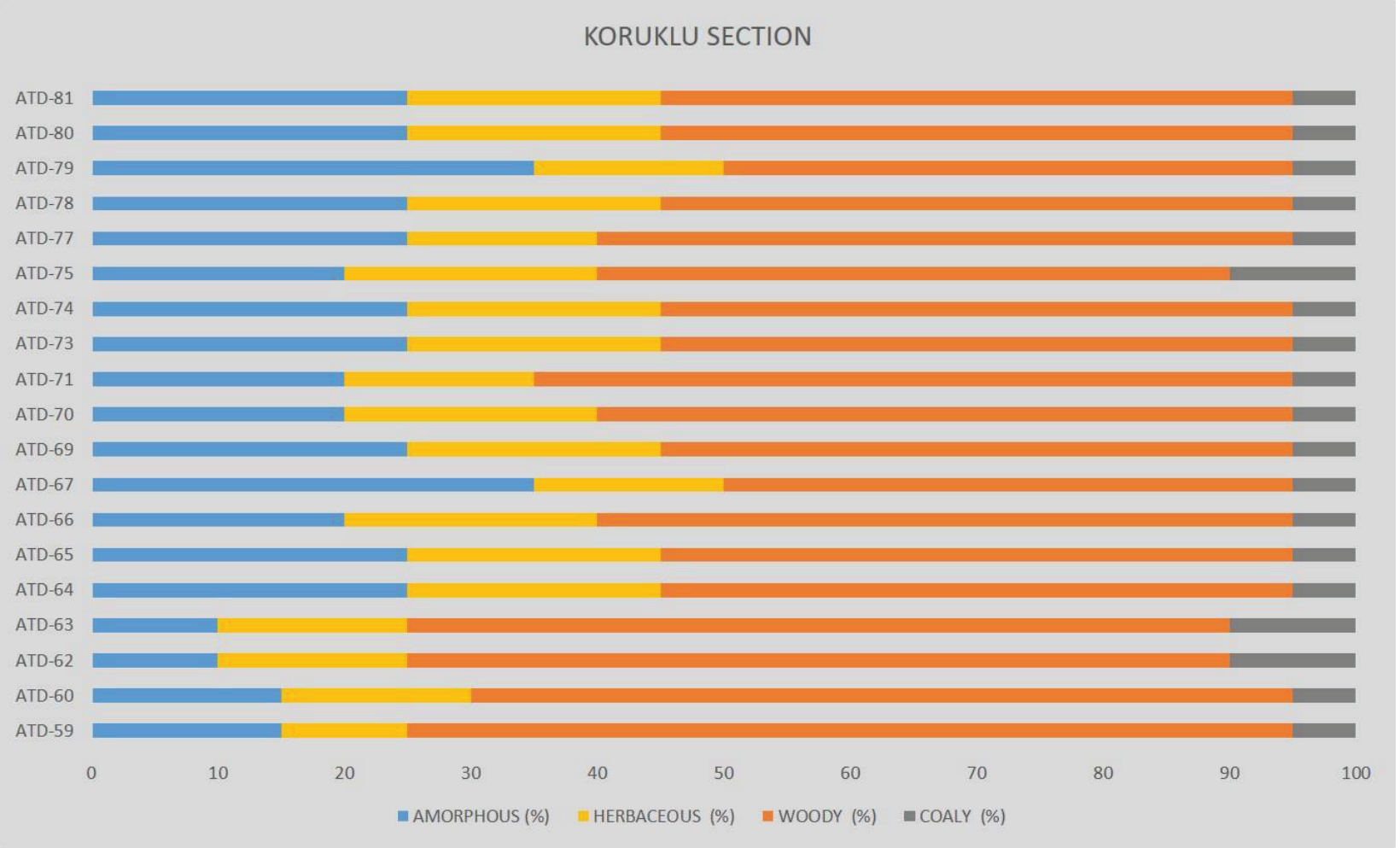

Figure 60. The organic matter distribution chart for the Güvenç Formation in the Koruklu Section.



Figure 61. The organic matter distribution chart for the Güvenç Formation in the Bekirli Section.

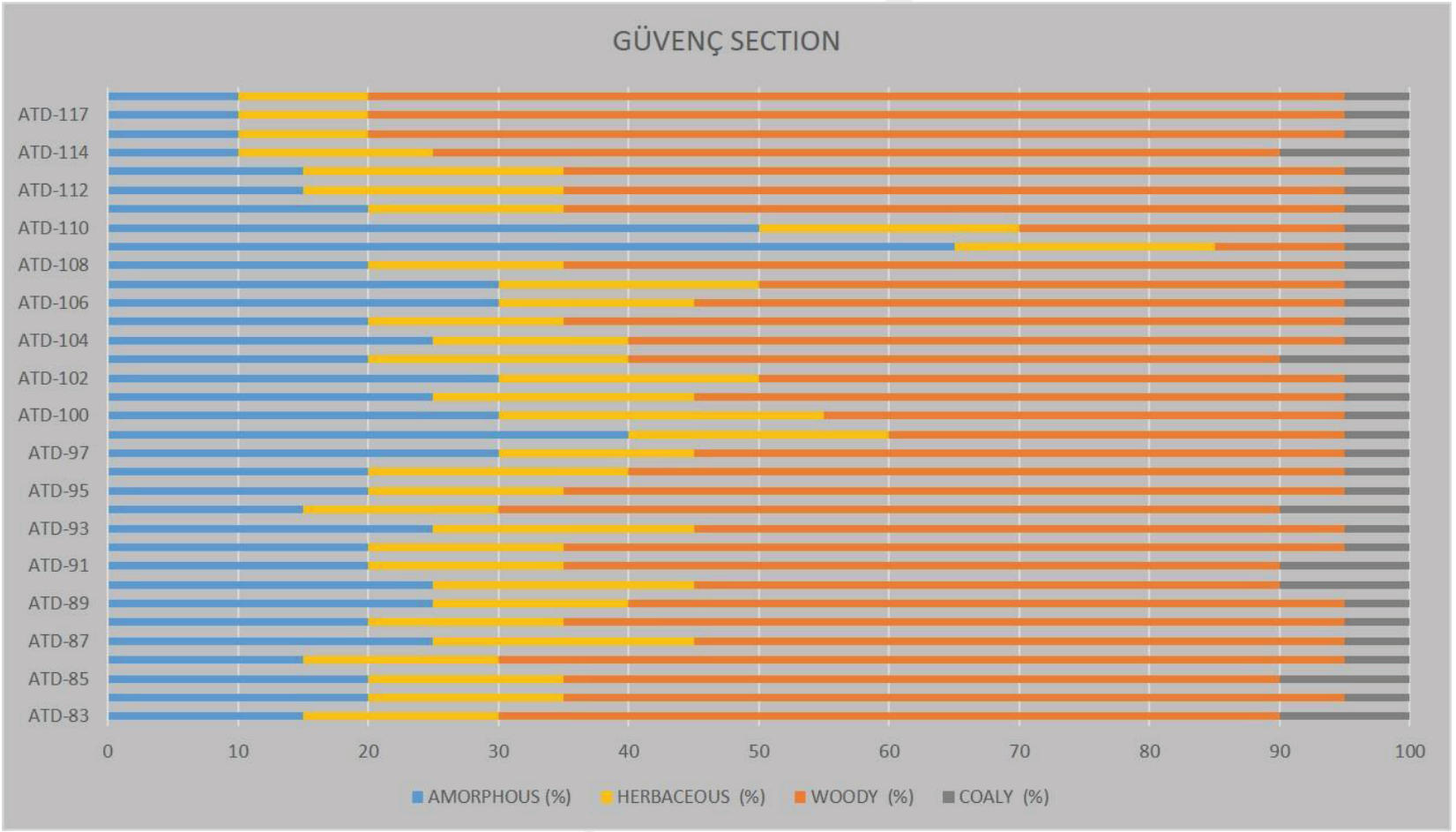

Figure 62. The organic matter distribution chart for the Güvenç Formation in the Bekirli Section.

According to Jaramillo (1995), the variation in the percentages of the sedimentary organic matter constituents gives important clues about the paleoenvironment (e.g. amorphous dominated palynofacies mostly represents deep marine environments while terrestrial organic matter dominated palynofacies indicates much shallower and near-shore conditions). The distribution of organic matter represents a correlative manner with the palynomorph assemblages from the Köpekli and Güvenç formations. All the obtained data based on the proximal-distal trends and the quantitative distribution pattern of dinocysts and types of organic matter represent that Köpekli Formation was deposited from neritic to inner neritic environment during the late Burdigalian-Langhian, whereas the Güvenç Formation was started to deposit at oceanic to outer neritic environment during the latest Langhian-latest Serrevallian and followed by inner neritic to restricted marine water during the earliest Tortonian (Figure 43, Table 2). Since the depositional environment of the Cingöz Formation was not suitable for the sedimentation and/or preservation of the organic matter, this concept could not be considered for this formation.

CHAPTER 7

DISCUSSION AND CONCLUSION

7.1. DISCUSSION

In order to investigate a detailed biozonation in Miocene deposits of the Adana Basin (Eastern Mediterranean), seven stratigraphic sections were measured across the well-exposed clastic deposits of the Köpekli, Cingöz and Güvenç formations and a total number of 482 samples have been studied in terms of their palynomorph content. Based on the first and last occurrences and also the acme of some selected taxa, a total of nine biozones were desorbed through the Köpekli, Cingöz and Güvenç formations.

In this study, the Köpekli shale member of Schmidt (1961) has been raised to a formation rank and four stratigraphical sections, namely Çukurköy, Köpekli, Sofular, and Çorlu sections, were measured in order to understand the age span of the formation. Recognition of consistent dinocyst events in the measured sections allow to tie the measured sections with each other (Figure 25). According to this detailed biostratigraphical framework, it can be concluded that the Köpekli Formation was deposited in the late Burdigalian-Langhian time interval. The Cingöz Formation, consisting of submarine fan deposits, was measured from bottom to top in the Çorlu Section. In contrast to its poor dinocyst assemblage, the Cingöz Formation is very rich in diverse terrestrial taxa. Williams and Sarjeant (1967) suggested that sedimentation might have been controlled by water turbulence and spores, pollen, acritarchs, and dinocysts, all of which are very light, may never be deposited in regions of high turbulence. Since limited amount of palynomorph has been found within the turbidite deposits of the Cingöz Formation, a detailed biozonation scheme could not be constructed. Apart from data coming from planktonic foraminifera and nannofossils, the age span of the Cingöz Formation was determined as late Langhian with the help of well-dated underlying and overlying formations. Additionally, the Güvenç Formation was studied in four different stratigraphical sections, namely Çorlu, Koruklu, Bekirli and Güvenç sections. According to Schmidt (1961), the Güvenç Formation was deposited in deeper parts of the basin in the Early-Middle Miocene.

After Schmidt (1961), various researchers (e.g. Özçelik, 1993; Özçelik and Yetiş; 1993) reported that the Güvenç Formation was deposited during the Burdigalian-Serravallian interval based on planktonic foraminifera and nannofossils. According to this study, the deposition of the Güvenç Formation started in the latest Langhian and terminated within the earliest Tortonian.

In order to correlate the biostratigraphy of the studied region worldwide, the dinocyst zonation constructed in this study was compared with the previously published dinocyst zonations from Denmark, Germany, Netherlands, NW Europe, and USA Eastcoast. Diagnostic species (e.g. *Labyrinthodinium truncatum*, *Cerebrocysta poulsenii*, *Unipontidinium aquaeductum*, *Paleocystodinium ventricosum, Cleistosphaeridium placacanthum*, and *Achomosphaera* cf. *andalousiensis*) have been selected to construct the dinocysts zonation, these dinocyst events were essential to produce such a worldwide correlation. Based on the palynological analyses conducted in the studied sections, the FO of *Labyrinthodinium truncatum* was recognized in the late Burdigalian, apparently before the FO of *Cerebrocysta poulsenii*, as recorded in Nieder Octenhausen (Strauss et al., 2001 in Munsterman and Brinkhuis, 2004), which is not consistent with the succession of events in Italy (Zevenboom, 1995) and Netherlands (Munsterman and Brinkhuis, 2004). According to the Williams et al. (2004), the FO of *Labyrinthodinium truncatum* corresponds to the Burdigalian-Langhian boundary. However, the FO of *Labyrinthodinium truncatum* was recognized earlier than the Burdigalian-Langhian boundary in this study. In addition, the FO of *Unipontidinium aquaeductum* corresponding to the upper part of M5a, M5b, and M6 planktonic foraminiferal zones (latest Burdigalian-Langhian) and NN4 and NN5 nannoplankton zones (latest Burdigalian-Langhian) is appearing earlier in the Eastern Mediterranean than those recorded in Denmark (Dybkjaer and Piasecki (2010), in Germany (Köthe, 2003; Strauss et al., 2001), in Netherlands (Munsterman and Brinkhuis, 2004), in NW Europe (Powell and Brinkhuis, 2004), and in the eastern U. S. (De Verteuil and Norris, 1996). On the other hand, the LO of the *Cleistosphaeridium placacanthum* and the FO of *Achomosphaera* cf. *andalousiensis* in this study are correlative with those defined in NW Europe and in the Mediterranean. Finally, the acme of *Homotryblium* dinoflagellate cysts (e.g. *Homotryblium floripes*, *Homotryblium pallidum*, *Homotryblium plectilum,* and *Homotryblium tenuispinosum*) was recorded in the lowest Tortonian clastic deposits of the Adana Basin (Turkey),

which is also well correlated with NW Europe and the Mediterranean. Therefore, it can be stated that these important dinocyst events (e.g., *Labyrinthodinium truncatum*, *Cerebrocysta poulsenii*, *Unipontidinium aquaeductum*) occured apparently earlier in the Adana Basin than those recorded in Denmark, Germany, Netherlands, NW Europe, and the eastern U.S.

Stover and Hardenbol (1994) mentioned that dinoflagellates provide promising information for stratigraphic correlation because they can be found in both neritic and deeper marine depositional conditions. In contrast to planktonic foraminifers and calcareous nannoplanktons, dinoflagellates are not affected by post-depositional decalcification processes. Dinoflagellates have very high tolerance to chemical dissolution and can be highly abundant in both coastal and oceanic settings. In other words, they may be present in all aquatic environments from fresh water to hypersaline conditions. Thus, dinoflagellates are very useful indicators of paleoecological conditions and they yield important information about the surface water temperature, salinity, paleobathymetry and productivity depending on morphological variations (Wall et al., 1977; Köthe, 1990; Brinkhuis, 1994; Stover, and Hardenbol, 1994; Dale, 1996; Powell et al., 1996; Marret and Zonnoveld, 2003; Van Simaeys, 2004; Van Simaeys et al., 2004). Harland (1973) described a concept on peridinioid (P) versus gonyaulacoid (G) cysts of dinoflagellate assemblages, which gives clues about the productivity variations. The G/P ratios cannot be used to detect the productivity variations, since all of the species are gonyaulacoid in this study. Gedl and Peryt (2011) discussed that the absence of peridinioids might be related to primary conditions that are not suitable for this group of dinocysts. Moreover, dinoflagellates are particularly sensitive to temperature changes compared to other microfossils, making them an excellent tool for sea surface temperature reconstructions (Vernal et. al., 1993), 1994, 1998, 2000, 2001; Versteegh, 1994; Versteegh and Zonneveld, 1994; Rochon et al., 1998; Grøsfjeld et al., 1999; Devillers and de Vernal, 2000; Boessenkool et al., 2001; Sangiorgi et al., 2002, 2003; Sluijs et al., 2005). In this study, distribution of dinoflagellates and the qualitative cyst information were used to infer sea surface temperature trends in each measured section. Based on the distribution of dinoflagellates, it can be stated that the sea surface should be warm during the deposition of the Köpekli, Cingöz and Güvenç Formations from the late Burdigalian to earliest Tortonian in the Adana Basin (Eastern Mediterranean). As salinity is an

important controlling factor for osmotic exchange in microorganisms, it plays an essential role in the distribution of dinocysts (Vernal et al., 1994). Furthermore, the morphological diversity of cysts is generally used as a paleoenvironmental indicator (Batten, 1982; MacLennan and Trewin 1989; Smelror and Leereveld, 1989; Leckie and Singh, 1991; Riding et al., 1991; Habib et al., 1994). Based on these hypotheses, the dinocyst assemblage suggests a saline to hypersaline condition during the deposition of the Köpekli Formation, whereas the Güvenç Formation was most probably deposited in a high salinity environment during the latest Langhian-earliest Tortonian. Making any comment on salinity could not be possible, since the dinocysts found in the Cingöz Formation provided very limited information about salinity.

Based on the distribution patterns of ecologically important dinocysts and other palynomorph groups, the studied sections were evaluated and the depositional settings of the Köpekli, Cingöz and Güvenç Formations were reconstructed. The Köpekli Formation is mainly composed of the *Spiniferites* group, *Operculodinium* group, and *Cleistosphaeridium* group (very abundant) suggesting an inner neritic water to outer neritic depositional environment during the late Burdigalian-Langhian time interval. On the other hand, the Cingöz Formation consists of the *Spiniferites* group, *Operculodinium* group and *Impagidinium* spp. group. According to Dale (1996) and Sluijs et al. (2005), the occurrence of a few specimens of *Impagidinium* might reflect an oceanic environment. *Operculodinium centrocarpum* belonging to *Operculodinium* group is characterized as cosmopolitan in neritic environments (Wall et. al., 1977). Dybkjaer and Rasmussen (2000) discussed that the co-occurrence of outer neritic to oceanic taxa and the inner neritic taxa together is interpreted as to reflect that material from inner neritic settings was transported out and deposited in the deeper parts of the basin. The Cingöz Formation, is also characterized by a poor and low diversity dinocyst assemblage, is known as the turbidite deposits of the Adana Basin. According to Williams and Sarjeant (1967), the scarcity of dinocysts defined in such depositional settings was due to high turbulence. In addition, bisaccate pollen, which are well known by their floating capacity, are also an essential constituent of the palynological association through the Cingöz Formation. Based on these utilized data, Cingöz Formation was deposited in an oceanic environment during late Langhian. The Güvenç Formation is mainly composed of the *Spiniferites* group, the *Operculodinium* group, the *Cleistosphaeridium* group, and the *Homotryblium* spp. group. In addition to this

ecologically important dinocyst groups, only two specimens of *Impagidinium paradoxum* are recorded at the lower parts of the Güvenç Formation which has a transitional contact with the Cingöz Formation at this certain level. On the other hand, an acme of *Homotryblium* spp. group, reflecting a restricted marine to inner neritic water, is recorded at the upper part of the Güvenç Formation. Based on these evaluated data, it can be suggested that the deposition of the Güvenç Formation was started at oceanic to outer neritic environment during the latest Langhian-latest Serrevallian and followed by inner neritic to restricted marine water during the earliest Tortonian.

In order to interpret sea-level fluctuations, dinocyst diversity was studied within the measured sections. According to the quantitative distribution patterns of dinocysts, diversity charts were plotted and sea level fluctuation patterns were defined in the Köpekli Formation (within the Çukurköy, Köpekli, Sofular, and Çorlu sections) and Güvenç Formation (within the Çorlu, Koruklu, Bekirli and Güvenç sections). On the other hand, diversity charts for the Cingöz Formation could not be constructed based on the quantitative distribution patterns of dinocysts due to low diversity of dinocysts in this formation. On the basis of the utilized diversity charts, a relative sea level curve was constructed (Figure 52). Then, the plotted curve based on the quantitative distribution patterns of dinocysts in this study was correlated with the eustatic sea level curve of the Haq *et al.* (1987) (Figure 52). Based on the dinocyt diversity, two regressive and one transgressive phases were interpreted during the deposition of the Köpekli Formation from the late Burdigalian to the early Langhian. The similar regressive and transgressive trends were also recognized in the eustatic sea level curves of Haq et al. (1987). A relative sea level rise was recognized during the deposition of the Güvenç Formation from the latest Serravallian to earliest Tortonian, whereas a relative sea level fall is detected in the earliest Tortonian. The eustatic sea level curve of Haq et al. (1987) also represents similar transgressive and regressive trends in the same time intervals. Consequently, the curve plotted for Miocene dinocysts in this study reflect striking similarities to the general trend of the eustatic sea level curves of the Haq *et al.* (1987).

Since the composition of sedimentary organic matter gives clues about the depositional environments, the amorphous (the structureless, disseminated, and shapeless particles recognized under the microscope), herbaceous (spores and pollen), woody (woody remains of land plants and plant tissue), and coaly (the opaque particles

defined within the palynological slides) type organic matters are evaluated in all of the kerogen slides for the palynofacies analysis. The obtained data should always be integrated with the information derived from palynomorphs, while analyzing the palynofacies (Batten, 1996). Based on palynofacies data, the distribution of organic matter represents a correlative manner with the palynomorph associations in the Köpekli and Güvenç formations. Since the depositional environment of the Cingöz Formation was not suitable for the sedimentation and/or preservation of the organic matter due to high turbidity currents, this concept could not be applied to this formation.

7.2. CONCLUSION

In this study, seven stratigraphic sections were measured across the well-exposed clastic deposits of the Köpekli, Cingöz and Güvenç formations, which are the fundamental Miocene units of the Adana Basin. Based on palynological analyses, a detailed biochronostratigraphic framework was properly established in this study for the Lower-Middle Miocene sediments of the Adana Basin, Eastern Mediterranean. Based on palynomorph data, a systematic palynology was given in detail. A total of 73 palynomorphs, including 43 dinoflagellates, 25 spores and pollen and 2 organic-walled green algae, have been identified. Based on the first and last occurrences and also the acme of some selected taxa, a total of nine biozones were desorbed through the Köpekli, Cingöz and Güvenç formations (Figure 24). In addition, constructed dinocyst biozones were calibrated with those of planktonic foraminifera and calcareous nannofossils (Figure 24). This multidisciplinary study is the first in the Adana Basin and allows the correlation of the measured sections based on the standard subdivisions of the Miocene.

In this study, the Köpekli shale member of Schmidt (1961) has been raised to a formation rank and the age span of the Köpekli Formation has been determined as the late Burdigalian-Langhian time interval based on biostratigraphical data. According to the detailed biostratigraphical framework performed in this study, it can be concluded that the Cingöz Formation was deposited during late Langhian, while the

deposition of the Güvenç Formation started in the latest Langhian and terminated within the earliest Tortonian.

In order to correlate the biostratigraphy of the studied region worldwide, the dinocyst zonation constructed in this study was compared with the previously published dinocyst zonations from Denmark, Germany, Netherlands, NW Europe, and USA Eastcoast. Therefore, it can be stated that these important dinocyst events (e.g., FO of *Labyrinthodinium truncatum*, FO of *Cerebrocysta poulsenii*, FO and LO of *Unipontidinium aquaeductum*) occured apparently earlier in the Adana Basin than those recorded in Denmark, Germany, Netherlands, NW Europe, and the eastern U.S. The palynological analysis reveals that the recorded dinocyst events (e.g. *Labyrinthodinium truncatum, Cerebrocysta poulsenii, Unipontidinium aquaeductus*) occurred chronostratigraphically older in Turkey than those in Denmark, Germany, Netherlands, NW Europe and the eastcoast U.S.

In this study, distribution of dinoflagellates and the qualitative cyst information were used to infer the productivity, surface temperature and salinity trends in each measured section. Because all the identified dinocysts in this study are gonyaulacoid cysts, the G/P ratios can not be used to detect the productivity variations. Based on the distribution patterns of ecologically important dinoflagellates, it can be stated that the sea surface should be warm during the deposition of the Köpekli, Cingöz and Güvenç Formations from the late Burdigalian to earliest Tortonian in the Adana Basin (Eastern Mediterranean). In addition, the recorded dinocyst assemblage suggests a saline to hypersaline condition during the deposition of the Köpekli Formation, whereas the Güvenç Formation was most probably deposited in a high salinity environment during the latest Langhian-earliest Tortonian. Making any comment on salinity could not be possible, since the dinocysts found in the Cingöz Formation provided very limited information about salinity.

In order to develop a model for depositional environments of the studied formations and to improve the geological models for the Miocene deposits of the Adana Basin, proximity trends of dinocysts were studied in detail. Based on the observed distribution patterns of the ecologically important dinocysts, a schematic model is constructed for the distribution of dinocyst associations along a proximal - distal transect during the Langhian to Tortonian in the Adana Basin. According to this model derived from the biostratigraphical data, the Köpekli Formation was deposited

from inner neritic to outer neritic water during the late Burdigalian-Langhian, whereas the Cingöz Formation was deposited in oceanic environment during the late Langhian. On the other hand, deposition of the Güvenç Formation was started at oceanic to outer neritic environments during the latest Langhian-Serravallian and followed by an inner neritic to restricted marine water during the earliest Tortonian.

In order to interpret sea-level fluctuations, dinocyst diversity was studied within the measured sections and diversity charts were plotted for the Köpekli Formation and Güvenç Formation. On the other hand, diversity charts for the Cingöz Formation could not be constructed due to low diversity of dinocysts in this formation. Based on the quantitative distribution patterns of dinocysts in this stuy, a relative sea level curve is constructed and correlated with the eustatic sea level curve of Haq et al. (1987). The curve plotted for Miocene dinocysts in this study reflects striking similarities to the general trend of the eustatic sea level curve of Haq et al. (1987).

In this study, palynofacies analysis was carried out based on the classification of Burges (1974). On the basis of the palynofacies data, the distribution of organic matter represents a correlative manner with the palynomorph associations in the Köpekli and Güvenç formations. However, the depositional environment of the Cingöz Formation was not suitable for the sedimentation and/or preservation of the organic matter due to high turbidity currents and this concept could not be applied to this formation.

Investigation of palynostratigraphic and palynofacies studies of the Miocene Units in the Adana Basin (Eastern Mediterranean) were performed by the palynological analysis in the measured sections within the Köpekli, Cingöz and Güvenç formations. By means of this study, a biozonation based on important dinocyst events was documented in the study area for the first time and the established biozones are correlated with those of planktonic foraminifera and calcareous nannofossils. As a pioneering study, the evaluation of the data for this study enables the construction of a more accurate stratigraphical framework in the Mediterranean Sea Region for future observations.

REFERENCES

Abacı, Ş, 1986. Çukurova Baseni Karsanti Yöresi Genç Tersiyer İstifinin Kil Minerolojisi. M. S. Thesis, Çukurova University. 59 p.

Aksu, A. E., Calon, T. J., Hall, J., Mansfield, S. and Yaşar, D., 2005. The Cilica-Adana Basin complex, Eastern Mediterranean: Neogene evolution of an active fore-arc basin in an obliquely convergent margin. Marine Geology, 221: 121-159.

Alberti, G., 1961. Zur Kenntnis mesozoischer und alttertiärer Dinoflagellaten und Hystrichosphaerideen von Nord und Mitteldeutschland sowie einigen anderen europäischen Gebieten. Palaeontographica, Abteilung A, 116: 1-58.

Ayres, M. G., Bilal, M., Jones, R. W., Slentz, L. W., Tartir, M. and Wilson, A. O., 1982. Hydrocarbon habitat in main producing areas, Saudi Arabia. American Association of Petroleum Geologists Bulletin, 66: 1-9.

Bakken, K. and Dale, B., 1986. Dinoflagellate cysts in Upper Quaternary sediments from southwestern Norway and potential correlations with the oceanic record. Boreas, 15: 185-190.

Bakrac, K., Koch, G. and Sremac, J., 2012. Middle and Late Miocene palynological biozonation of the south-western part of Central Paratethys (Croatia). Geologia Croatica, 65 (2): 207-222.

Baltes, N., 1969. Distribution stratigraphique des Dinoflagelles et des acritarches Tertiaires en Roumanie. In: Brönnimann, P. and Renz, H. H. (eds.), Proceedings of the First International Conference on Planktonic Microfossils, Geneva, 1967. E. J. Brill, Leiden, 1: 26-45.

Batı, Z., 1996. Palynostratigraphy and coal petrography of the Upper Oligocene lignites of the Northern Thrace Basin, NW Turkey. PhD. Thesis, Middle East Technical University, 341 p.

Batten, D. J., 1982. Palynofacies and salinity in the Purbeck and Wealden of southern England. In Aspects of micropalaeontology, Banner, F. T. and Lord, A. R. (eds.), 278-308.

Batten, D. J., 1983. Identification of amorphous sedimentary organic matter by transmitted light microscopy. In: Brooks, J. (ed.); Petroleum geochemistry and exploration of Europe, Geological Society, London. Special Publication, 11:275-287.

Batten, D. J., 1996. Palynofacies and paleoenvironmental interpretation. In: Jansonius, J. and McGregor, D. C. (eds.); Palynology: principles and applications, American Association of Stratigraphic Palynologists Foundation, 3: 1011-1064.

Below, R., 1982. Scolochorate Zysten der Gonyaulacaceae (Dinophyceae) aus der Unterkreide Marokkos. Palaeontographica Abteilung B: 1-51.

Benedek, P. N., 1972. Phytoplankton aus dem Mittel und Oberoligozan von Tonisberg (Niederrheingebiet). Palaeontographica, B, 137: 1-71.

Benedek, P. N. and Sarjeant, W. A. S., 1981. Dinoflagellate cysts from the Middle and Upper Oligocene of Toenisberg (Niederrheingebiet): a morphological and taxonomical restudy. Nova Hedwigia, 35: 313-356.

Berger, W. H., Smetacek, V. S. and Wefer, G., 1989. Ocean productivity and paleoproductivity an overview. In: Berger, W. H., Smetacek, V. S., Wefer, G. (eds.). Productivity of the Ocean: Present and Past. Life Sciences Research Report, 44: 1-34.

Bertrand, P., Shimmield, G., Martinez, P., Grousset, F., Jorissen, F., Paterne, M., Pujol, C., Bouloubassi, I., Buat Menard, P., Peypuquet, J. P., Beaufort, L., Sicre, M. A., Lallier-Verges, E., Foster, J. M. and Ternois, Y., 1996. The glacial ocean productivity hypothesis: the importance of regional temporal and spatial studies. Marine Geology, 130: 1-9.

Biffi, U. and Manum, S. B., 1988. Late Eocene-Early Miocene dinoflagellate cyst stratigraphy from the Marche Region (central Italy). Boll. Soc. Paleontol. Ital., 27: 163-212.

Blumenthal, M. M., 1941. Niğde ve Adana vilayetleri dahilindeki Torosların jeolojisine umumi bir bakış. Ankara MTA Enstitüsü Derleme Rapor, B. 6.

Blumenthal, M. M., 1944. Bozkır Güneyinde Toros Sıradağlarının Serisi ve Yapısı. İstanbul Üniversitesi Fen Fakültesi Mec., B, 9: 95-125.

Blumenthal, M. M., 1947. Beyşehir-Seydişehir Hinterlandındaki Toros Dağlarının Jeolojisi. Maden Tetkik Arama Enst. Derg. D, 2: 242 p.
Blumenthal, M. M., 1951. Batı Toroslarda Alanya Ard Ülkesinde Jeolojik Araştırmalar. Maden Tetkik Arama Enst. Derg. D, 5: 194 p.

Blumenthal, M. M., 1952. Toroslarda Yüksek Aladağ Silsilesinin Coğrafyası, Stratigrafisi ve Tektononigi Hakkında Yeni Etüdler. Maden Tetkik Arama Enst. Derg. D, 6: 1-109.

Blumenthal, M. M., 1955. Yüksek Bolkardağın Kuzeyindeki Kenar Bölgelerin ve Batı Uzantılarının Jeolojisi. Maden Tetkik Arama Enst. Derg. D, 7: 1-169.
Blumenthal, M. M., 1956. Karaman Konya Havzası Güneybatısında Toros Kenar Silsileleri ve Şist Radyolarit Formasyonu Stratigrafi Meselesi. Maden Tetkik Arama Enst. Derg. C, 48: 1-36.

Boessenkool, K. P., Van Gelder, M. J., Brinkhuis, H. and Troelstra, S. R., 2001. Distribution of organic-walled dinoflagellate cysts in surface sediments from transects across the Polar Front offshore southeast Greenland. Journal of Quaternary Science, 16 (7): 661-666.

Bold, H. C., 1973. Morphology of Plants. Harper, New York, 668 p.

Bolkhovitina, N. A., 1953. Spores and pollen characteristic of Cretaceous deposits of central regions of USSR. Trudy Geologièeskago Instituta Russkoj Akademii Nauk, 145 (61).

Boulter, M. C., 1994. Towards a review of Tertiary palaeobotany in the boreal realm. In Cenozoic plants and climates of the Arctic. Springer Berlin Heidelberg, 1-11.

Bradford, M. R. and Wall, D. A., 1984. The distribution of recent organic-walled dinoflagellate cysts in the Persian Gulf, Gulf of Oman, and northwestern Arabian Sea. Palaeontographica, 192: 16-84.

Brasier, M. D., 1985. Fossil indicators of nutrient levels. 1: eutrophication and climate change. In: Bosence, D. W. J., Allison, P. A. (eds.), Marine Palaenvironmental Analysis from Fossils. Special Publication. Geological Society, 83: 113-132.

Brenac, P. and Richards, K., 2001. *Pediastrum* as a guide fossil in sequence stratigraphy: In: Goodman, D. K. and Clarke, R. T. (eds.), Proceedings of the IX. International Palynological Congrees, Houston, Texas, U. S. A., 1996. American Association of Stratigraphic Palynologists Foundation, 239-241.

Brinkhuis, H. and Biffi, U., 1993. Dinoflagellate Cyst Stratigraphy of the Eocene/Oligocene Transition in Central Italy. Marine Micropaleontology, 22 (1-2): 131-183.

Brinkhuis, H., 1994. Late Eocene to Early Oligocene dinoflagellate cysts from the Priabonian type-area (northeast Italy); biostratigraphy and paleoenviromental implication. Palaeogeography, Palaeoclimatology, Palaeoecology, 107: 121-163.

Brinkhuis, H., Powell, A. J. and Zevenboom, D., 1992. High-resolution dinoflagellate cyst stratigraphy of the Oligocene/Miocene transition interval in northwest and central Italy. In: Head, M. J. and Wrenn, J. H. (eds.), Neogene and Quaternary dinoflagellate cysts and acritarchs. American Association of Stratigraphic Palynologists Foundation, Salt Lake City, 219-258.

Bujak, J. P. (ed.), 1980. Dinoflagellate cysts and acritarchs from the Eocene of southern England. Palaeontological Association, 24-29.

Bujak, J. P. and Matsuoka, K., 1986. Taxonomic re-allocation of Cenozoic dinoflagellate cysts from Japan and Bering Sea. Palynology, 10: 235-241.

Bujak, J. P., Downie, C., Eaton, G. L. and Williams, G. L., 1980. Taxonomoy of some Eocene dinoflagellate cyst species from southern England. In Bujak, J. P., Downie, C., Eaton, G. L. and Williams, G. L., Dinoflagellate cysts and 218 acritarchs from the Eocene of southern England. The Paleontological Association, Special Papers in Paleontology, 24: 1-100.

Burges, J. D., 1974. Microscopic examination of kerogens (Dispersed organic matter) in petroleum exploration. Geol. Soc. Am. Special Paper, 153: 19-30.

Burton, R., 2003. Structural and sedimentary evolution of the Adana Basin, eastern Mediterranean. Unpublished MSc thesis. Memorial University of Newfoundland, 209 p.

Burton-Ferguson, R., Aksu, A. E., Calon, T. J. and Hall, J., 2005. Seismic stratigraphy and structural evolution of the Adana Basin, eastern Mediterranean. Mar. Geol. 221 (1-4), 189 p.

Bütschli, O., 1885. Erster Band. Protozoa. In: Dr. H. G. Broonn's Klassen und Ordnungen des Their-Reichs, wissenschaftlich dargelstellt in Wort und Bild. Leipzig and Heidelberg, C. F. Winter'sche Verlagshandlung, 865-1088.

Büyükutku, A. G., 2009. Reservoir properties of Karaisalı formation in the Adana Basin, Southern Turkey. Journal of Petroleum Science and Engineering, 65: 33-44.

Büyütutku, A. G. and Bağcı, A. S., 2005. Clay controls on reservoir properties in sandstone of Kuzgun formation and its relevance to hydrocarbon exploration, Adana Basin, Southern Turkey. Journal of Petroleum Science and Engineering, 47: 123-135.

Combaz, A., 1964. Les Palinofacies, Rev. Micropaleon., 7: 205-218.

Cookson, I. C., 1959. Fossil pollen grains of Nothofagus from Australia. Proceedings of the Royal Society of Victoria, 71: 25-30.

Cookson, I. C., 1965. Cretaceous and Tertiary microplankton from southeastern Australis. Proceedings of the Royal Society of Victoria, 78: 183-191.

Cookson, I. C. and Eisenack, A., 1965, Microplankton from the Browns Creek Clays, SW. Proceedings of the Royal Society of Victoria, 79, 119-131.

Costa, L. I. and Downie, C., 1979. Cenozoic dinocyst stratigraphy of sites 403 to 406 (Rockall Plateau), IPOD, Leg 48. Initial reports of the Deep Sea Drilling project, 48: 513-529.

Couper, R. A., 1953. Upper Mesozoic and Cenozoic spores and pollen grains from New Zealand, Alexander Doweld, 22.

Covey, M., 1986. The evolution of foreland basins to study state: Evidence from the W Taiwan foreland basin. In: Allen, P. A. and Homewood, P. (eds.), Foreland Basins. International Association of Sedimentologists Special Publications, 77-90.

Cronin, B. T., Gürbüz, K., Hurst, A. and Satu, N., 2000. Vertical and lateral organization of a carbonate deep-water slope marginal to a submarine fan system, Miocene, southern Turkey. Sedimentology, 47: 801-824.

Crouch, E. M., 2001. Environmental change at the time of the Paleocene-Eocene biotic turnover. Laboratory of Palaeobotany and Palynology Contribution Series, 14: 216 p.

Dale, B., 1983. Dinoflagellate resting cysts: ‘‘benthic plankton’’. In: Fryxell, G.A. (ed.), Survival Strategies of the Algae. Cambridge Univ. Press, Cambridge, 69-136.

Dale, B., 1996. Dinoflagellate cyst ecology: modeling and geological applications, In: Jansonius, J. and McGregor, D. C., (eds.), Palynology: principles and applications. American Association of Stratigraphic Palynologists Foundation, 3: 1249-1275.

Dale, B. and Fjellsa, A., 1994. Dinoflagellate cysts as paleoproductivity indicators: state of the art, potential and limits. In: Zahn, R., Pedersen, T. F., Kaminski, M. A., Labeyrie, L. (eds.), Carbon Cycling in the Glacial Ocean: Constraints on the Ocean’s Role in Global Change. Springer, Berlin, 521-537.

Daniels, C. H. V., Lund, J. J., Lund-Christensen, J. and Uffenorde, H., 1990. The Langenfeldian (Miocene) of Gross Pampau, Schleswig-Holstein. Foraminifer, dinocyst, and ostracod stratigraphy and paleoecology (preliminary account). Veröffentlichungen aus dem Übersee-Museum, Bremen, A. 10: 11-38.

Darbaş, G. and Nazik, G., 2010. Micropaleontology and paleoecology of the Neogene sediments in the Adana Basin (South of Turkey). Journal of Asian Earth Sciences, 39: 136-147.

Davey, R. J. and Williams, G. L., 1966a. The genera *Hystrichosphaera* and *Achomosphaera*, In: R. J. Davey et al. (eds.), Studies on Mesozoic and Cenozoic dinoflagellate cysts, Bull. of the British Museum (Natural History) Geology, Supplement 3: 4-7.

Davey, R. J. and Williams, G. L., 1966b. The genus *Hystrichosphaeridium* and its allies. In Davey, R. J., Downie, C., Sarjeant, W. A. S., and Williams, G. L., Studies on Mesozoic and Cenozoic dinoflagellate cysts. Bulletin of the Museum (Natural History) Geology, Supplement 3: 28-52.

Davey, R. J. and Verdier, J. P., 1973. An investigation of microplankton assemblages from latest Albian (Vraconian) sediments. Revista Espanola de Micropaleontologia, 5 (2): 173-212.

Davey, R. J., Downie, C., Sarjeant, W. A. S., and, Williams, G. L., 1969. Appendix to "Studies on Mesozoic and Cenozoic dinoflagellate cysts". Bulletin of the Museum (Natural History) Geology, Appendix to Supplement 3: 15-17.

De Coninck, L. A. P., 1965. Systématique des nématodes. Traité de Zoologie: anatomie, systématique, biologie, 4 (2): 1-731.

De Vernal, A. and Mudie, P. J., 1992. Pliocene and Quaternary dinoflagellate cyst stratigraphy in the Labrador Sea: paleoenvironmental implications. Neogene and Quaternary dinoflagellate cysts and acritarchs. American Association of Stratigraphic Palynologists Fouondation, 329-346.

De Vernal, A., Goyette, C. and Rodrigues, C. G., 1989. Contribution palynostratigraphique (dinokystes, pollen et spores) a` la connaissance de la mer de Champlain: coupe de Saint Cezaire, Que´bec. Canadian Journal of Earth Sciences, 26: 2450-2464.

De Vernal, A., Hillaire-Marcel, C., Turon, J. L. and Matthiessen, J., 2000. Reconstruction of sea-surface temperature, salinity, and sea-ice cover in the northern North Atlantic during the last glacial maximum based on dinocyst assemblages. Canadian Journal of Earth Sciences, 37: 725-750.

De Vernal, A., Matthiessen, J., Mudie, P. J., Rochon, A., Boessenkool, K. P., Eynaud, F., Grøsfjeld, K., Guiot, J., Hamel, D., Harland, R., Head, M. J., Kunz-Pirrung, M., Loucheur, V., Peyron, O., Pospelova, V., Radi, T., Turon, J. L. and Voronina, E., 2001. Dinoflagellate cyst assemblages as tracers of sea-surface conditions in the northern North Atlantic, Arctic and sub-Arctic seas: the new ''n-677'' data base and its application for quantitative paleoceanographic reconstruction. Journal of Quaternary Science, 16: 681-698.

De Vernal, A., Rochon, A., Turon, J. L. and Matthiessen, J., 1998. Organic-walled dinoflagellate cysts: palynological tracers of sea-surface conditions in middle to high latitude marine environments. Geobios, 30: 905-920.

De Vernal, A., Turon, J. L. and Guiot, J., 1993. Dinoflagellate cyst distribution in high-latitude marine environments and quantitative reconstruction of sea-surface salinity, temperature, and seasonality. Canadian Journal of Earth Sciences, 31: 48-62.

De Vernal, A., Turon, L. and Guiot, J., 1994. Dinoflagellate distribution in high-lattitude marine environments and quantitative reconstruction of sea-surface salinity, temperature and seasonality. Canadian Journal of Earth Sciences, 31: 48-62.

Deflandre, G., 1935. Considérations biologiques sur les microorganisms d'origine planctonique conservés dans les silex de la craie. Bulletin biologique de la France et de la Belgique, 69: 213-244.

Deflandre, G., 1937a. *Phanerodinium*, genre nouveau de dinoflagellé fossile des silex. La Société française de microscopie, Bulletin, 6: 109-115.

Deflandrea, D. and Cookson, I. C., 1955. Fossil microplankton from Australian Late Mesozoic and Tertiary sediments. Australian Journal of Marine and Freshwater Research, 6: 242-313.

Derman, A. S. and Gürbüz, K., 2007. Nature, provenance and relationships of early Miocene palaeovalley fills, northern Adana Basin, Turkey: Their significance for sediment-bypassing on a carbonate shelf. Turkish Journal of Earth Sciences, 16: 181-209.

Dercourt, J., Ricou, L. E. and Vrielynck, B. (Eds.), 1993. Atlas Tethys Palaeoenvironmental Maps: Explanatory Notes. Liste Des Articles, Communications, Cartes Et Theses. Programme GS-Tethys. 1986-1993. Gauthier-Villars.

De Verteuil, L. and Norris, G., 1996. Miocene dinoflagellate stratigraphy and systematics of Maryland and Virginia. Micropaleontology, 42: 172 p.

Dewey, J. F., Hempton, M. R., Kidd, W. S. F., Şaroğlu, F. and Şengör, A. M. C., 1986. Shortening of continental lithosphere: the neotectonics of eastern Anatolia, a young collision zone. In: Coward, M. P., Ries, A. C. (eds.), Collision Tectonics. Geological Society Special Publication, 19: 3-36.

Devillers, R. and de Vernal, A., 2000. Distribution of dinoflagellate cysts in surface sediments of the northern North Atlantic in relation to nutrient content and productivity in surface waters. Marine Geology, 166: 103-124.

Dodge, J. D., 1989. Some revisions of the family Gonyaulacaceae (Dinophyceae) based on scanning electron microscope study. Botanica Marina, 32: 275-298.

Downie, C., Hussain, M. A., and Williams, G. L., 1971. Dinoflagellate Cyst and Acritarch Associations in the Paleogene of Southeast England. Geoscience and Man, 3 (1): 29-35.

Drugg, W. S. and Loeblich, A. R., Jr, 1967. Some Eocene and Oligocene phytoplankton from the Gulf Coast, U. S. A.. Tulane Studies in Geology, 5: 181-194.

Dybkjær, K., 2004a. Dinocyst stratigraphy and palynofacies studies used for refining a sequence stratigraphic model- uppermost Oligocene to lower Miocene, Jylland, Denmark. Review of Palaeobotany and Palynology, 131 (3-4): 201-249.

Dybkjær, K., 2004b. Morphological and abundance variations in Homotryblium-cyst assemblages related to depositional environments; uppermost Oligocene-Lower Miocene, Jylland, Denmark. Palaeogeography, Palaeoclimatology, Palaeoecology, 206 (1-2): 41-58.

Dybkjær, K. and Piasecki, S., 2008. A new Neogene biostratigraphy for Denmark. Geological Survey of Denmark and Greenland Bulletin, 15: 29-32.

Dybkjær, K. and Piasecki, 2010. Neogene dinocyst zonation for the eastern North Sea Basin, Denmark. Review of Palaeobotany and Palynology, 161 (1): 1-29.

Dybkjær, K. and Rasmussen, E. S., 2000. Palynological dating of the Oligocene-Miocene successions in the Lille Bælt area, Denmark. Bull. Geol. Soc. Den., 47: 87-103.

Dybkjær, K. and Rasmussen, E. S. 2007. Dinocyst stratigraphy in an expanded Oligocene-Miocene boundary section in the eastern North Sea Basin (the Frida-1 well, Denmark) and correlation from basinal to marginal areas. Journal of Micropalaeontology, 26: 1-17.

Eaton, G. L., Fensome, R. A., Riding, J. B. and Williams, G. L., 2001. Re-evaluation of the status of the dinoflagellate cyst genus Cleistosphaeridium. Neues Jahrbuch für Geologie und Paläontologie, Abhandlungen, 219 (1/2): 171-205.

Ediger, V. Ş., 1984. Some practical and theoretical consideration about palynological processing, Program and Abstracts. American Association of Stratigraphical Palynologists, 17th Annuan Meeting, (Abstract).

Ediger, V. Ş., 1986a. Paleopalynological biostratigraphy, organic matter deposition and basin analysis of the Triassic- (?) Jurassic Richmont rift basin, Virginia, U. S. A. The Pennsylvania State University, The Graduate School, Department of Geoscience, PhD., Thesis, 548 p. (unpublished)

Ediger, V. Ş., 1986b. Sieving techniques in palynological sample processing with special reference to the MRA system. Micropaleontology, 32 (2): 256-270.

Edwards, L. E., 1984. 14. Miocene dinocysts from Deep Sea Drilling Project Leg 81, Rockall Plateau, Eastern North Atlantic Ocean. Initial Reports of the Deep Sea Drilling Project, 81: 581-594.

Edwards, L. E., 1986. Late Cenozoic dinoflagellate cysts from South Carolina, USA. In: Wrenn, J. H., Duffield, S. C. and Stein, J. A. (Eds.), Papers from the first symposium on Neogene dinoflagellate cyst biostratigraphy. Am. Assoc. Stratigr. Palynol. Contrib. Ser., 17: 47-57.

Edwards, L. E., 1992. New semiquantitative (paleo) temperature estimates using dinoflagellate cysts, an example from the North Atlantic Ocean. Neogene and Quaternary Dinoflagellate Cysts and Acritarchs, 69-87.

Edwards, L. E. and Andrle, V. A. S., 1992. Distribution of selected dinoflagellate cysts in modern marine sediments. Neogene and Quaternary dinoflagellate cysts and acritarchs, 259-288.

Ehrenberg, C. G., 1838. Über das Massenverhältniss der jetzt lebenden Kiesel-Infusorien und über ein neues Infusorien-Conglomerat als Polirschiefer von Jastraba in Ungarn, Königliche Akademie der Wissenschaften zu Berlin, Abhandlungen, 1836: 109-135.

Eisenack, A., 1963a. *Cordosphaeridium* d.g. *ex Hystrichosphaeridium*, Hystrichosphaeridea, Neues Jahrbuch für geologie und Paläontologie, Abhandlungen, 118: 260-265.

Ellegaard, M., 2000. Variations in dinoflagellate cyst morphology under conditions of changing salinity during the last 2000 years. Review of Palaeobotany and Palynology, 109: 65-81.

Erünal-Erentöz, L., 1956. Stratigraphie des Bassins neogenes de Turquie, plus specialement d'Anatolie Meridionale et comparaisons avec le Domaine Mediterraneen dans son ensemble. M. T. A. Enst. Yayınl., C (3).

Evitt, W. R., 1963a. A discussion and proposals concerning fossil dinoflagellates, hystrichospheres, and acritarchs. I. National Academy of Sciences, Washington, Proceedings, 49: 158-164.

Fauconnier, D. and Masure, E., 2004. Les dinoflagellés fossiles: guide pratique de détermination. Groupe de travail Dinoflagellés.

Faranda, C., Gliozzi, E., Cipollari, P., Grossi, F., Darbaş, G., Gürbüz, K., Nazik, A., Gennari, R. and Cosentino, D., 2013. Messinian paleoenviromental changes in the easternmost Mediterranean Basin: Adana Basin, southern Turkey. Turkish Journal of Earth Sciences, 22: 839-863.

Fensome, R. A., Taylor, F. J. R., Norris, G., Sarjeant, W. A. S., Wharton, D. I., and Williams, G. L., 1993. A classification of living and fossil dinoflagellates. Micropaleontology Special Publication, 7: 351 p.

Fensome, R. A., MacRae, R. A., Moldowan, J. M., Taylor, F. J. R. and Williams, G. L., 1996. The early Mesozoic radiation of dinoflagellates. Paleobiology, 22 (03): 329-338.

Fidancı, M., 2006. Adana Baseni Miyosen istifinde *Globigerinoidespraeorblina* ve *Orbulina* cinslerinin evolüsyonu. M. S. Thesis, Çukurova University, Adana, Turkey, 43 p.

Foley, E. J., 1937. Report on the stratigraphy of the Seyhan region. Miner Res Explor Inst. Rep., 248 (unpublished).

Garfunkel, Z., 1998. Constraints on the origin and history of the eastern Mediterranean basin. Tectonophysics, 298: 5 –37.

Gedl, P., 1996. Middle Miocene dinoflagellate cysts from the Korytnica Clays (Gory Swietokrzyskie Mountains, Poland). Annales Societatis Geologorum Poloniae, 66: 191-218.

Gedl, P. and Peryt, D., 2011. Dinoflagellate cyst, palynofacies and foraminiferal records of environmental changes related to the late Badenian (Middle Miocene) transgression at Kudryntsi (Western Ukraine). Annales Societatis Geologorum Poloniae, 81: 1-19.

Gerlach, E., 1961. Mikrofossilien aus dem Oligozään und Miozän Nordwestdeutschlands, unter besonderer Berücksichtigung der Hystrichosphären und Dinoflagellaten. Neues Jahrbuch für geologie und Paläontologie, Abhandlungen, 112: 143-228.

Germeraad, J. J., Hopping, G. A. and Muller, J., 1968. Palynology of Tertiary sediments from tropical areas. Review of Paleobotany and Palynology, 6: 189-348.

Goodman, D. K. and Witmer, R. J., 1985. Archeopyle variation and paratabulation in the dinoflagellate Diphyes colligerum (Deflandre and Cookson, 1955) Cookson 1965. Palynology, 9 (1): 61-84.

Gökçen, S. L., Kelling, G., Gökçen, N. and Floyd, P. A., 1988. Sedimentology of Late Cenozoic collisional sequence: the Misis complex, Adana, southern Turkey. Sediment Geol., 59: 205-235.

Görür, N., 1977. Depositional history of Miocene sediments of NW flank of the Adana Basin. Sixth colloquim on Geology of the Agean Region, İzmir.

Görür, N., 1979. Karaisalı Kireçtaşının (Miyosen) sedimantolojisi. TJKB, 22 (2): 227-234.

Görür, N., 1985. Depositional history of Miocene sediments on the NW flank of the Adana Basin. Proc. Sixth Colloquium on Geology of the Aegean region, İzmir, 185-208.

Görür, N., 1992. A tectonically controlled alluvial fan which developed into a marine fan delta at a complex triple junction. Miocene Gildirli Formation of the Adana Basin, Turkey. Sediment. Geol., 81: 243-252.

Görür, N., 1994. Tectonic control in the development of a Lower Miocene reef at a complex triple junction: depositional history of the Karaisali Formation of the Adana Basin Turkey. Geol. Mediterr. XXI: 49-67.

Grøsfjeld, K., Larsen, E., Sejrup, H. P., de Vernal, A., Flatebf, T., Vestbf, M., Haflidason, H. and Aarseth, I., 1999. Dinoflagellate cysts reflecting surface-water conditions in Voldafjorden, western Norway during the last 11.300 years. Boreas, 28: 403– 415.

Gürbüz, K., 1993. Sedimentology of the Cingöz and Güvenç Formations of the Adana Basin, SE Turkey. PhD thesis, University of Keele.

Gürbüz, K., 1999. Regional implications of structural and eustatic controls in the evolution of submarine fans: an example from the Miocene Adana Basin, southern Turkey. Geol. Mag., 136.

Gürbüz, K. and Gökçen, S. L., 1985. Provenance and sedimentology of the Late Tertiary foreland deposits of the northen Adana Basin, Turkey. Int Symposium on Foreland Basins, abstracts, Freiburg, 66 p.

Gürbüz, K. and Kelling, G., 1992. Internal/external controls on submarine fan development: two examples from the Neogene of southern Turkey. 29th Int Geol Congres, Kyoto (abstracts), 2: 292 p.

Gürbüz, K., Kelling, G., 1993. Provenance of Miocene Submarine Fans in the northern Adana Basin: a test of discriminant function analysis. Geological Journal, 28: 277-295.

Gürbüz, K., Nazik, A. and Cronin, B. T., 1998. Eğner, Akören (Aladağ/Adana-Türkiye) civarında yüzeylenen basen kenarı ve kıta yokuşu çökellerinin

sedimantolojisi ve biyostratigrafisi. Fırat Üniversitesi Jeoloji Eğitiminin 20. Yılı Sempozyumu Bildirileri, 45-61.

Habib, D., 1972. Dinoflagellate biostratigraphy, Leg 11. Deep Sea Drilling Project, Initial Reports, D. S. D. P., 11: 367-425.

Habib, D. and Miller, J. A., 1989. Dinoflagellate species and organic facies evidence of marine transgression and regression in the Atlantic Coastal Plain. Palaeogeogr., Paleoclimatol., Palaeoecol., 74: 23-47.

Habib, D., Eshet, Y. and Van Pelt, R., 1994. Palynology of sedimentary cycles. Sedimentation of organic particles. Cambridge University Press, Cambridge, 311-335.

Haq, B. U., Premoli-Silva, I. and Lohmann, G. P., 1987. Calcareous plankton paleobiogeographic evidence for major climatic fluctuation in the Early Cenozoic Atlantic Ocean. J. Geophys. Res., 82 (27): 3861-3876.

Hardenbol, J., Thierry, J., Farley, T. J., de Graciansky, P. C. and Vail, P. R., 1998. Mesozoic and Cenozoic sequence chronostratigraphic framework of European basins. In: de Graciansky, P. C., Hardenbol, J., Jacquin, T., Vail, P. R. (eds.), Mesozoic and Cenozoic Sequence Stratigraphy of European Basins, 60 (SEPM Special Publication): 3–13.

Harland, R., 1973. Dinoflagellate Cysts and Acritarchs from the Bearpaw Formation (Upper Campanian) of Southern Alberta, Canada. Palaeontology, 16 (4): 665-706.

Harland, R., 1977. Recent and late Quaternary (Flandrian and Devensian) dinoflagellate cysts from marine continental shelf sediments around the British Isles. Palaeontographica, Abt. B. 164: 87-126. Norris, G., 1980. Systematic and stratigraphic palynology.

Harland, R., 1983. Distribution maps of recent dinoflagellate cysts in bottom sediments from the North-Atlantic Ocean and adjacent seas. Palaeontology, 26 (MAY): 321-387.

Harland, R. and Hill, J., 1979. A reappraisal of the Cenozoic dinoflagellate cyst, *Hystrichosphaeridium choanophorum* Deflandrea & Cookson. Rev. Palaeobot. Palynol., Amsterdam, 28: 37-45.

Harland, R., Reid, P. C., Dobell, P. and Norris, G., 1980. Recent and Sub-Recent Dinoflagellate Cysts from the Beaufort Sea. Canadian Arctic: Grana, 19 (3): 211-225.

Hart, G. F., 1986. Origin and classification of organic matter in clastic systems. Palynology, 10: 1-23.

Hart, G. F., Pasley, M. A. and Gregory, W. A., 1994. Particulate organic matter, maceral facies models and applications to sequence stratigraphy, In: Sedimentation of organic particals, Traverse, A., (ed.), Chambridge Univ. Press.: 337-390.

He Chengquan, 1991, Late Cretaceous-Early Tertiary microphytoplankton from the Western Tarim Basin in southern Xinjiang, China, Nanjing. Inst. of Geol. and Paleontology, Academia Sinica, 19: 143-192.

Head, M. J., 1998. Marine environmental change in the Pliocene and early Pleistocene of eastern England; the dinoflagellate evidence reviewed. In: van Kolfschoten, T., Gibbard, P.L. (Eds.), The Dawn of the Quaternary. Mededelingen Nederlands Instituut voor Toegepaste Geowettenschappen TNO, 60: 199–226.

Head, M. J., and Norris, G., 1989c. Palynology and dinocyst stratigraphy of the Eocene and Oligocene in ODP Leg 105, Hole 647A, Labrador Sea. Proceedings of the Ocean Drilling Program, Scientific Results, 105: 515-550.

Head, M. J., Norris, G. and Mudie, P. J., 1989b. Palynology and dinocyst stratigraphy of the Upper Miocene and lowermost Pliocene. Proceedings of the Ocean Drilling Program, Scientific Results, 105: 423-451.

Helenes, J., 1984. Morphological analysis of Mesozoic-Cenozoic *Cribroperidinium* (Dinophyceae), and taxonomic implications, Palynology, 8: 107-137.

Herngreen, G. F. W., 1987. Correlation between Miocene beds of the SE Netherlands and Italy based on dinoflagellate biozonation. Meded. Werkgr. Tert. Kwart. Geol., 24 (1-2): 31-40.

Horner, R. A., 1985. Sea Ice Biota. CRC Press. Boca Raton., 215 p.

Hultberg, S. U., 1987. Palynological evidence for a diachronous low-salinity event in the C-T boundary clay at Stevns Klint, Denmark. Journal of Micropalaeontology, 6 (2), 35-40.

İbrahim, A. C., 1933. Sporenformen des Aegirhorizontes des Ruhrreviers, Diss. TH, Berlin.

İlker, S., 1975. Adana Baseni Kuzey Batısının Jeolojisi ve Petrol olanakları. TPAO, Ankara, no. 973: 63 p.

Islam, M. A., 1983. Dinoflagellate cysts from the Eocene cliff sections of the Isle of Sheppey, southeast England. Revue de Micropal., 25: 231-250.

Islam, M. A., 1984. A study of Early Eocene palaeoenvironments in the Isle of Sheppey as determined from microplankton assemblage composition. Tertiary Research, 6 (1), 11-21.

Jan du Chêne, R., 1977. Étude palynologique du Miocène supérieur Andalou (Espagne). Revista española de micropaleontología, 9: 97-114.

Jan du Chêne, R. and Londeix, L., 1988. Données nouvelles sur Achomosphaera andalousiense Jan du Chêne, 1977, kyste de dinoflagellé fossile. Bulletin des Centres de recherches exploration-production Elf-Aquitaine, 12 (1), 237-250.

Jaramillo, C. A., 1995. Dinoflagellate cyst biostratigraphy and palynofacies of the Late Eocene-Early Oligocene in southern Mississippi and Alabama, U. S. Gulf Coast. M. S. Thesis, University of Missouri, Rolla, 97 p. (unpublished).

Jaramillo, C. A. and Oboh-Ikuenobe, F. E., 2001. Sequence stratigraphy of the Pachuta-Marianna Interval (Upper Eocene-Lower Oligocene) in the U.S. Gulf Coast. In: Goodman, D. K. and Clarke, R. T. (eds.), Proceedings of the IX. International Palynological Congrees, Houston, Texas, U. S. A., 1996. American Association of Stratigraphic Palynologists Foundation, 263-276.

Jiménez-Moreno, G., Head, M. J. and Harzhauser, M., 2006. Early and Middle Miocene dinoflagellate cyst stratigraphy of the Central Paratethys, Central Europe. J. Micropaleontol. 25: 113-139.

Harland, R., 1983. Distribution maps of recent dinoflagellate in bottom sediments from the North Atlantic Ocean and adjacent seas. Palaeontology, 26: 321-387.
Iakovleva, A. I., Brinkhuis, H. and Cavagnetto, C., 2001. Late Palaeocene-early Eocene dinoflagellate cysts from the Turgay Strait, Kazakhstan; correlations across ancient seaways. Palaeogeography, Palaeoclimatology, Palaeoecology, 172: 243-268.

Kelling, G., Gökçen, S. L., Floyd, P. A. and Gökçen, N., 1987. Neogene tectonics and plate convergence in the eastern Mediterranean: new data from southern Turkey. Geology, 15: 425-429.

Kerey, I. E., Yetiş, C. and Demirkol, C., 1985. Meandering plain deposits and marginal sea processes in the Upper Miocene Kuzgun Formation of the Adana Basin in Turkey. 6th European Regional Meeting of Sedimentology (abstracts), Lleida. Spain, 217-218.

Kirk, H. M., 1935. Initial geological report for Seyhan region. M.T.A. Report, 219 (unpublished).

Klement, K. W., 1960. Dinoflagellaten und Hystrichosphaerideen aus dem untern und mittleren Malm Sudwestdeutschlands. Palaeontographica, Abt. A, 114: 1-104.

Klump, B., 1953. Beitrag zur Kenntnis der Mikrofossilien des mittleren und oberen Eozän, Palaeontographica, Abt. A, 103: 377-406.

Kokinos, J. P., Anderson, D. M., 1995. Morphological development of resting cysts in cultures of the marine dinoflagellate Lingulodinium polyedrum (=L. machaerophorum). Palynology, 19: 143-166.

Kozlu, H., 1987. Structural development and stratigraphy of the Misis-Andirin region. Proceedings of the 7th Petroleum Congress of Turkey, 104-116.

Kozlu, H., 1991. AR/TPO/2646, 2647, 2648, 2649, 2650, 2651, Hak sıra no'lu ruhsatların terk raporu. Turkish Petroleum Corporation, Report No. 2100: 1-12 (unpublished).

Köthe, A., 1990. Paleogene dinoflagellates from Northwest Germany Biostratigraphy and Paleoenvironment. Geologishes Jahrbuch A, 118: 3-111.

Köthe A., 2003. Dinozysten-Zonierung im Tertiar Norddeutschlands. Revue de Pale´obiologie, 22 (2): 895-923.

Krathus, T., 2000. Biostratigrafisk undersøgelse af miocæne dinoflagellater I Sønderjylland. MSc. Thesis, Geological Institute, University of Århus, Denmark.

Krutzsch, W., 1959. Micropaläontologie (sporenpaläontologische) Unterschungen in der Braunkohle des Geiseltasles. I. Die Sporen und die Sporenartigen sowie die ehemals zu Sporites gestellten Formeinheiten der Sporae dispersae der mitteeozanen Braunkohle des mittleren Geiseltales (Tagebau Neumark-West i. W. S.), unter Berücksichtigung und Revision weiterer sporenformen aus der bisherigen Literatur, Geologie/Beih., 21/22, Berlin.

Kützing, F. T., 1843. Phycologia generalis: oder Anatomie, Physiologie und Systemkunde der Tange. Brockhaus.

Kützing, F. T., 1849. Species algarum. FA Brockhaus, Leipzig, 922 p.

Lagap, H., 1985. Kırılan-Karakılıç-Karaisalı (NW, Adana) Alanının Litostratigrafik Kronostratigrafik İncelemesi. MSc. Thesis, Çukurova University, Institute of Applied Science.

Laursen, G. V., Poulsen, N. E. and Rasmussen, L. B., 1998. Correlation of Northwest European Miocene stages with the international stages preliminary results. Newsl. Stratigr, 36: 55–61.

Leckie, D. A. and Singh, C., 1991. Estuarine deposits of the Albian Paddy Member (Peace River Formation) and lowermost Shaftesbury Formation, Alberta, Canada. Journal of Sedimentary Research, 61 (5).

Lentin, J. K. and Williams, G. L., 1981. Fossil dinoflagellates: index to genera and species, 1981 edition. Bedford Institute of Oceanography Report Series BI, 345 p.

Lewis, J. and Hallet, R., 1997. *Lingulodinium polyedrum* (Gonyaulax polyedra), a blooming dinoflagellate. Oceanography and Marine Biology Annual Review, 35: 97-161.

Lewis, J., Rochon, A. and Harding, I., 1999. Preliminary observations of cyst-theca relationships in *Spiniferites ramosus* and *Spiniferites membranaceus* (Dinophyceae). Grana, 38: 113-124.

Lewis, J., Ellegaard, M., Hallett, R., Harding, I. and Rochon, A., 2003. Environmental control of cyst morphology in Gonyaulacoid dinoflagellates. In: Matsuoka, K., Yoshida, M., Iwataki, M. (eds.), Dino7, Seventh International Conference on Modern and fossil Dinoflagellates, Abstract Volume. Additional Abstract.

Liengjarern, M., Costa, L. I. and Downie, C., 1980. Dinoflagellate cysts from the Upper Eocene-Lower Oligocene of the Isle of Wight. Palaeontology, 23: 475-499.

Lindemann, E., 1928. Abteilung Peridineae (Dinoflagellatae). Die Natürlichen Pflanzenfamilien nebst ihren Gattungen und wichtigeren Arten insbesondere den Nutzpflanzen. Zweite stark vermehrte und verbesserte Auflage herausgegeben von A. Engler, 2: 3-104.

Loose, F., 1932. Beschreibung von sporenformen aus Floz Bismarck. Potonie, R., Sporenformen aus den Flozen Agir und Bismarck des Ruhrgebietes: Neues Jahrb., Beilage, 67: 449-452.

Louwye, S., 2001. New species of dinoflagellate cysts from the Berchem Formation, Miocene, northern Belgium (southern North Sea Basin). Geobios, 34 (2): 121-130.

MacLennan, A. M. and Trewin, N. H., 1989. Palaeoenvironments of the late Bathonian to mid-Callovian in the Inner Moray Firth. Northwest European Micropalaeontology and Palynology. British Micropalaeontological Society Series, Ellis Horwood Limited, Chichester, 92-117.

Maier, D., 1959. Planktonuntersuchungen in tertiären und quartären marinen Sedimenten. Ein Beitrag zur Systematik, Stratigraphie und Ökologie der Coccolithophorideen, Dinoflagellaten und Hystrichosphaerideen vom Oligozän bis zum Pleistozän. Neues Jahrbuch für Geologie und Paläontologie, Abhandlungen, 107: 278-340.

Manum, S. B., Boulter, M. C., Gunnarsdottir, H., Ragnes, K. and Scholze, A., 1989. Eocene to Miocene palynology of the Norwegian Sea (ODP leg 104). In: Eldholm, O., Thiede, J., Taylor, E. (eds.), Proceedings of the Ocean Drilling Program. Scientific Results, 104: 611-661.

Mantell, G. A., 1850. A pictorial atlas of fossil remains, consisting of coloured illustrations selected from Parkinson's "Organic remains of a former world", and Artis's "Antediluvian phytology", Henry G. Bohn, London, xii, 207 p.

Mantelll, G. A., 1854. The medals of Creation; or, First Lessons in Geology and the study of organic remains. Second edition, Henry G. Bohn, London, 2, 930 p.

Marret, F. and Zonneveld, K. A. F., 2003. Atlas of organic-walled dinoflagellate cyst distribution. Review of Paleobotany and Palynology, 125: 1-200.

Masran, T. C. and Pocock, S. A. J., 1981. The classification of plant derived particulate organic matter in sedimentary rocks. In: Brooks, J. (ed.), 237. Organic Maturation Studies and Fossil Fuel Exploration. Academic Press, London, 145-147.

Matthiessen, J., Brenner, W., 1996. Chlorococcalalgen und Dinoflagellatenzysten in rezenten Sedimenten des Greifswalder Boddens (südliche Ostsee). Senckenbergiana Maritima, 27: 33-48.

Matsuoka, K., 1983. Late Cenozoic dinoflagellates and acritarchs in the Niigata District, central Japan. Palaentographica, Abt. B, 187: 89-154.

Matsuoka, K. and Bujak, J. P., 1988: Cenozoic dinoflagellate cysts from the Navarin Basin, Norton Sound and St. George Basin, Bering Sea. Nagasaki University, Faculty of Liberal Arts, Natural Science, Bulletin, 29 (1): 1-147.

McCay, G. A. and Robertson, A. H. F., 2012. Late Eocene-Neogene sedimentary geology of the Girne (Kyrenia) Range, northern Cyprus: A case history of sedimentation related to progressive and diachronous continental collision. Sedimentary Geology, 265: 30-55.

Meyen, F. J. F., 1829. Beobachtungen über einige niedere algenformen.

Meyer, B. L., 1956. Mikroflorishtische Untersuchungen an jungtertiären Braunkohlen im östlichen Bayern, Geol. Bavarica, 25: 100-128.

Mobil Exploration Mediterranean Inc., 1960. Bulgurdağ Oil Field-Turkey's First Light Oil. Petrol. Admin. Public. Bull., Ankara, No. 5.

Morgenroth, P., 1966. Mikrofossilien und Konkretionen des nordwesteuropäischen Untereozäns, Palaeontographica, Abt. B, 119: 1-53.

Morgenroth, P., 1968. Zur Kenntnis der Dinoflagellaten und Hystrichosphaeridien des Danien. Geologisches Jahrbuch, Hannover, 86: 533-578.

Morzadec-Kerfourn, M. T., 1983. Intérêt des kystes de dinoflagellés pour l'établissement de reconstitution paléogéographique: exemple du Golfe de Gabés (Tunisie). Cahiers de Micropaléontologie, 4: 15-22.

Moshkovitz, S. and Habib, D., 1993. Calcareous nannofossil and dinoflagellate stratigraphy of the Cretaceous-Tertiary boundary, Alabama, and Georgia. Micropaleontology, 39: 167–191.

Munsterman, D. K. and Brinkhuis, H., 2004. A southern North Sea Miocene dinoflagellate cyst zonation. Netherlands Journal of Geoscience/ Geologie en Mijnbouw, 83 (4): 267-285.

Mudie, P. J., 1992. Circum-Arctic Quaternary and Neogene marine palynofloras: paleoecology and statistical analysis. Neogene and Quaternary dinoflagellate cysts and acritarchs, 10: 347-390.

Mudie, P. J., Aksu, A. and Yaşar, D., 2001. Late Quaternary dinoflagellate cysts from the Black, Marmara and Aegean seas: variations in assemblages, morphology and paleosalinity. Marine Micropaleontology, 43 (1): 155-178.

Mudie, P. J. and Harland, R., 1996. Aquatic Quaternary. In: Jansonius, J. and McGregor, D. C. (eds.), Palynology: Principles and Applications. American Association of Stratigraphic Palynologists Foundation, Dallas, 843– 877.

Mudie, P. J., Rochon, A., Aksu, A. E. and Gillespie, H., 2004. Late glacial, Holocene and modern dinoflagellate cyst assemblages in the Aegean-Marmara-Black Sea corridor: statistical analysis and re-interpretation of the early Holocene Noah's Flood hypothesis. Review of Palaeobotany and Palynology, 128 (1): 143-167.

Mutti, E., 1985. Turbidite systems and their relations to depositional sequences. In: Zuffa GG (ed.) Provenance of Arenites. Reidel, Dordrecht, 65-93.

Nakoman, E., 1966. Contribution a l'étude palynologique des formations tertiares du Bassin de Thrace. 1. -Etude qualitative. Ann. Soc. Geol. du Nord. T., LXXXVI: 65-107.

Naumova, S. N., 1937. Spores and Pollen from the USSR, Tr. Sessii meshdunar geol., 17 (1): 353-364.

Nazik, A**.** and Gürbüz, K., 1991. *Globigerinanus* cinsinin yeni türü ve stratigrafik konumu, Suat Erk Semp*.,* 2-5 Eylül 1991, Ankara. Bildiri Özleri, 58-59.

Nazik, A. and Gürbüz, K., 1992. Karaisalı-Çatalan-Eğner yöresi (KB Adana) Alt-Orta Miyosen yaşlı denizaltı yelpazelerinin planktonic foraminifer biyostratigrafisi. T. J. K. Bült. C, 35 (1), 67-80.

Nazik, A. and Toker, V., 1986. Karaisalı yöresi Orta Miyosen istifinin foraminifer biyostratigrafisi. M. T. A Dergisi, 103/104: 139-153.

Nazik, A., Toker, V. Şenol, M. ve Öğrünç, G., 1997. Tarsus yöresi (Adana havzası) Üst Tersiyer-Kuavaterner istifinin mikropaleontolojik (planktik foraminifer, ostrakod, nannoplankton) incelemesi. Çukurova Üniversitesi'nde jeoloji mühendisliği eğitiminin 20. Yılı sempozyumu, Geosaund. Yerbilimleri, 371-383.

Neale, J. W. and Sarjeant, W. A. S., 1962. Microplankton from the Speeton Clay of Yorkshire. Geological Magazine, 99: 439-458.

Nehring, S., 1994a. Dinoflagellaten-Dauercysten in deutschen Küstengewassern: Vorkommen, Verbreitung und Bedeutung als Rekrutierungspotential. Berichte des Instituts für Meereskunde der Christian-Albrechts-Universitat Kiel, 259: 1-231.

Nehring, S., 1994b. Spatial distribution of dinoflagellate resting cysts in Recent sediments of Kiel Bight, Germany (Baltic Sea). Ophelia, 39: 137-158.

Okay, A. I. and Tüysüz, O., 1999. Tethyan sutures of northern Turkey. Geological Society, London, Special Publications, 156 (1): 475-515.

Öğrünç, G., Gürbüz, K. and Nazik, A., 2000. Adana Baseni Üst Miyosen-Pliyosen istifinde "Messiniyen tuzluluk krizine ait bulgular". Yerbilimleri, 22: 183-192.

Öğrünç, G. and Nazik, A., 1998. Yenice (Tarsus) kuzeyi (Adana Havzası) Üst Miyosen-Pliyosen istifinin ostrakod faunası. Türkiye Jeoloji Bülteni, 41(1): 63-84.

Özçelik, N., 1993. Facies and enviromental aspects of the Güvenç Formation in the Adana Basin. MSc. Thesis, Çukurova University.

Özçelik, N. and Yetiş, C., 1993. Facies and enviromental aspects of the Güvenç Formation in the Adana Basin. Geol. Bull Turk, 36: 58-69.
Özçelik, N. and Yetiş, C., 1994. Adana baseni Tersiyer istifi Güvenç formasyonunun planktik foraminifer biyostratigrafisi. Yerbilimleri, 25: 21-30.

Özer, B., Duval, B., Courrier, P. and Letouzey, J., 1974. Antalya-Mut-Adana Neojen Havzaları Jeolojisi. Türkiye II. Petrol Kongresi, Türkiye Petrol Jeologları Derneği, Ankara, 57-58.

Özgül, N., 1976. Toroslar'm bazı temel jeoloji özellikleri. Bulletin of the Geological Society of Turkey, 19: 65-78.

Öztümer, E., Bizon, G., Bizon, J. J. and Feinberg, H., 1974. Mut ve Adana havzaları Tersiyer biyostratigrafisi ve mikropaleontoloji yenilikleri. Türkiye II-Petrol Kong. Tebliğleri, 217-228.

Parsons, T. R., Takahashi, M. and Hargrave, B., 1984. Biological Oceanographic Processes. Pergamon Press, Oxford. 330 p.

Pascher, A., 1914. Über Flagellaten und Algen. Deutsche Botanische Gesellschaft, Berichte, 32: 136-160.

Peeters, F.J.C., Hoek, R.P., Brinkhuis, H., Wilpshaar, M., de Boer, P.L., Krijgsman, W. and Meulenkamp, J.E., 1998. Differentiating glacio-eustasy and tectonics; a case study involving dinoflagellate cysts from the Eocene– Oligocene of the Pindos Foreland Basin (NW Greece). Terra Nova, 10: 245– 249.

Piasecki, S., 1980. Dinoflagellate cyst stratigraphy of the Miocene Hodde and Gram Formations, Denmark. Bull. Geol. Soc., Denmark, 29: 53-76.

Piasecki, S., 2005. Dinoflagellate cysts of the Middle-Upper Miocene Gram Formation, Denmark. In: Roth, F., Hoedemarkers, K. (Eds.), The Gram Book. Palaeontos, 7: 29-45.

Potonié, R., 1931a. Pollenformen der miocänen Braunkohle (2 Mitteilung), Sits.-Ber. Ges. Naturf. Fr. Berlin, 1-3: 24-29.

Potonié, R., 1931c. Pollenformen aus tertiäres Braunkohlen, Jb. Preuß. Geol. L. Amt, 52: 1-7.

Potonié, R., 1934. Zur Morphologie der fossilen Pollen und Sporen. Arb. Inst. Pälaobotanik Petrographie Brennsteine, 4: 5-24.

Potonié, R., 1958a. Synopsisder Gattungen der Sporae dispersae. II. Teil: Sporites (Nachträge), Saccites, Aletes, Praecolpates, Polyplicates, Monocolpates, Beihefte zum Geologischen Jahrbuch, 31, Hannover.

Potonié, R., 1960a. Sporologie der eozänen Kohle von Kalewa in Burma. Senckenbergiana Lethaea, 41: 451-481.

Potonié, R. and Gelletich, J., 1933. Über die Pteridophytensporeneiner aozänen Braunkohle aus Dorog, Ungarn, Sitz. Ber. Ges. Naturforsch. Freunde, 33: 517-528.

Potonié, R. and Kremp, G., 1954. Die Gattungen der paläzoichen Sporae dispersae und ihre Stratigraphie, Geol. Jb., 69: 111-194.

Potonié, R. and Venitz, H., 1934. Zur Mikrobotanik des miozänen Humodils der niederrheinischen Bucht, Arb. Inst. Paläobot. Petrogr. Brennsteine, 5: 5-58.

Powell, A. J., 1986a. A dinoflagellate cyst biozonation for the Late Oligocene to Middle Miocene succession of the Langhe Region, Northwest Italy. American Association Stratigraphic Palynologists Contribution Series, 17: 105-127.

Powell, A. J., 1986b. The stratigraphic distribution of Late Miocene dinoflagellate cysts from the Castellanian superstage stratotype, northwest Italy. In: Wrenn, J.H., Duffield, S.L., Stein, J.A. (eds.), American Association Stratigraphic Palynologists Contribution Series, 17: 129-149

Powell, A. J., 1988. A modified dinoflagellate cyst biozonation for latest Palaeocene and earliest Eocene sediments from the central North Sea. Review of palaeobotany and palynology, 56 (3-4): 327-344.

Powell, A. J., 1992. Dinoflagellate cysts of the Tertiary system In Powell, A. J., ed., A stratigraphic index of dinoflagellate cysts: British Micropaleontological Society series, London, Chapman and Hall, P., 155-251.

Powell, A. and Brinkhuis, H., 2004. Paleogene time scale-dinoflagellate stratigraphy: A Geological Time Scale. Cambridge University Press, Cambridge, 397.

Powell, A. J., Brinkhuis, H. and Bujak, J. P., 1996. Upper Paleocene-Lower Eocene dinoflagellate cyst sequence biostratigraphy of southeast England. In: Knox, R. W. O. B., Corfield, R. M., Dunay, R. E. (Eds.), Correlation of the Early Paleogene in Northwest Europe. Geological Society Special Publication, 101: 145-183.

Prauss, M. and Riegel, W., 1989. Evidence from phytoplankton associations for causes of black shale formation in epicontinental seas. Neues. Jahrb. Geol. Pfilaontol. Monatsh. 11: 671 681.

Pross, J., Kotthoff, U. and Zonneveld, K. A. F., 2004. Die Anwendung organischwandiger Dinoflagellatenzysten zur Rekonstruktion von Palaoumwelt, Palaoklima und Palaozeanographie: Möglichkeiten und Grenzen. Palaontologische Zeitschrift, 78: 5-39.

Pross, J. and Schmiedl, G., 2002. Early Oligocene Dinoflagellate Cysts from the Upper Rhine Graben (SW Germany): Paleoenvironmental and Paleoclimatic Implications. Marine Micropaleontology, 45 (1): 1-24.

Rasmussen, E. S., 2004a. The interplay between true eustatic sea-level changes, tectonics and climatic changes: what is the dominating factor in sequence formation of the Upper Oligocene–Miocene succession in the eastern North Sea Basin, Denmark Glob. Planet. Change, 41: 15-30.

Rasmussen, E. S., 2004b. Stratigraphy and depositional evolution of the uppermost Oligocene–Miocene succession in western Denmark. Bull. Geol. Soc. Den., 51: 89–109.

Rasmussen, E. S., 2005. The geology of the upper Middle-Upper Miocene Gram Formation in the Danish area. Palaeontos, 7: 5-18.

Rasmussen, E. S., Dybkjær, K. and Piasecki, S., 2004. The Billund delta: a possible new giant aquifer in central and western Jutland. Geological Survey of Denmark and Greenland Bulletin, 4: 21-24.

Rasmussen, E. S. and Dybkjær, K., 2005. Sequence stratigraphy of the Upper Oligocene-Lower Miocene of eastern Jylland, Denmark: role of structural relief and variable sediment supply in controlling sequence development. Sedimentology, 52: 25–63.

Rasmussen, E. S., Dybkjær, K. and Piasecki, S., 2006. Neogene fluvial and nearshore marine deposits of the Salten section, central Jylland, Denmark. Bulletin of the Geological Society of Denmark, 53: 23–37

Regali, M. D. S., Uesugui, N. and Santos, A. D. S., 1974. Palinologia dos sedimentos meso-cenozoicas do Brasil (I). Boletim Técnico da Petrobrás, 17.

Riding, J. B., Walton, W. and Shaw, D., 1991. Toarcian to Bathonian (Jurassic) palynology of the Inner Hebrides, northwest Scotland. Palynology, 15 (1): 115-179.

Robertson, A. H. F., 1998. Mesozoic-Tertiary tectonic evolution of the easternmost Mediterranean area: Integration of Marine and land evidence. In: Robertson, A.H.F., Emeis, K. C., Richter, C. and Camerlenghi, A. (eds.), Proceedings of the Ocean Drilling Program, Scientific Results, 160: 723-782.

Robertson, A. H. F., 2002. Overview of the genesis and emplacement of Mesozoic ophiolites in the Eastern Mediterranean Tethyan region. Lithos, 65: 1-67.

Robertson, A. H. F. and Dixon, J. E., 1984. Introduction: aspects of the geological evolution of the Eastern Mediterranean. In: Dixon, J. E. and Robertson, A. H. F. (eds.), The Geological Evolution of the Eastern Mediterranean. Geological Society London, Special Publications, 17: 1-74.

Robertson, A. H. F., Poisson, A. and Akıncı, Ö., 2003. Developments in research concerning Mesozoic-Tertiary Tethys and neotectonics in the Isparta Angle. Geol. J, 38: 195-235.

Rochon, A., de Vernal, A., Sejrup, H. P. and Haflidason, H., 1998. Palynological evidence of climatic and oceanographic changes in the North Sea during the last deglaciation. Quaternary Research, 49: 197-207.

Rossignol, M., 1962. Analyse pollinique de sédiments marins Quaternaires en Israël. I: Sédiments Récents. Pollen et Spores, 3: 303-324.

Rossignol, M., 1964. Hystrichosphères du Quaternaire en Méditerranée orientale, dans les sédiments Plistocènes et les boues marines actuelles. Rev. de Micropal., 7: 83-99.

Rudolph, K., 1935. Mikrofloristische Untersuchungen Tertiarer Ablagerungen im nördlichen Böhmen, Beih. Bot. Zbl. Paris, 54: 244-328.

Rusbült, J. and Strauss, C., 1992. Mikrofossilien des Unter- und Mittelmiozäns in der Braunkohlenbohrung Lübtheen 46/84 (Südwest-Mecklenburg). N. Jahrb. Geol. Paläontol. Monatsh., 3: 150-170.

Sancay, R. H., 2000. Palynology and Paleoecology of Late Eocene Manning Formation (Jackson Group) of the Lake Somerville Spillway of east-central, MSc Thesis, Texas A&M University, 189 p.

Sancay, R. H., 2005. Palynostratigraphic and palynofacies investigation of the Oligocene-Miocene units in the Kars-Erzurum-Muş sub-basins (Eastern Anatolia). PhD Thesis, Middle East Technical University, Ankara, Turkey, 364 p.

Sangiorgi, F., Capotondi, L. and Brinkhuis, H., 2002. A centennial scale organic-walled dinoflagellate cyst record of the last deglaciation in the South Adriatic Sea (central Mediterranean). Palaeogeography, Palaeoclimatology, Palaeoecology, 186 (3-4): 199-216.

Sangiorgi, F., Capotondi, L., Combourieu Nebout, N., Vigliotti, L., Brinkhuis, H., Giunta, S., Lotter, A. F., Morigi, C., Negri, A. and Reichart, G. J., 2003. Holocene seasonal sea surface temperature variations in the South Adriatic Sea inferred from a multi-proxy approach. Journal of Quaternary Science, 18 (8): 723-732.

Sarjeant, W. A. S., 1970. The genus *Spiniferites* Mantell, 1850 (Dinophyceae). Grana, 10: 74-78.

Sarjeant, W. A. S., 1981. A Restudy of Some Dinoflagellate Cyst Holotypes in the University of Kiel Collections: VI. Late Cretaceous Dinoflagellate Cysts and Other Palynomorphs in the Otto Wetzel Collection. Meyniana, 37: 129-185.

Sarjeant, W. A. S., 1982. The dinoflagellate cysts of the Gonyaulacysta group: a morphological and taxonomic study, A. A. S. P., Contribution Series, 9, 80 p.

Sarkar, S. and Singh, H. P., 1988. Palynological investigation of the Subathu Formation (Eocene) in the Banethi-Bagthan area of Himachal Pradesh, India. Palaeontographica Abt. B, 209: 29-109.

Satur, N., Hurst, A., Cronin, B., Kelling, G. and Gürbüz, K., 2000. Sand body geometry in a sand-rich, deep-water clastic system, Miocene Cingöz Formation of southern Turkey. Marine and Petroleum Geology, 17 (2): 239-252.

Schmidt, G. C., 1961. Stratigraphic nomenclature for the Adana region petroleum district. VII. Petroleum Administration Bulletin, Ankara, 6: 47-63.

Sluijs, A., Pross, J. and Brinkhuis, H., 2005. From greenhouse to icehouse; organic-walled dinoflagellate cysts as paleoenvironmental indicators in the Paleogene. Earth-Science Reviews, 68 (3-4): 281-315.

Smelror, M. and Leereveld, H., 1989. Dinoflagellate and acritarch assemblages from the late Bathonian to early Oxfordian of Montagne Crussol, Rhône Valley, southern France. Palynology, 13 (1): 121-141.

Soliman, A., Head M. J. and Louwye, S., 2009. Morphology and distribution of the Miocene dinoflagellate cyst Operculodinium? borgerholtense Louwye 2001, emend. Palynology, 33 (2): 73-84.

Soliman, A., Ćorić, S., Head, M. J., Piller, W. E. and El Beialy, S. Y., 2012. Lower and Middle Miocene biostratigraphy, Gulf of Suez, Egypt based on dinoflagellate cysts and calcareous nannofossils. Palynology, 36 (1): 38-79.

Stover, L. E., 1975. Observations on some Australian Eocene dinoflagellates. Geoscience and Man, 11 (1): 35-44.

Stover, L. E., 1977. Oligocene and early Miocene dinoflagellates from Atlantic corehole 5/5b, Blake Plateau. In: Elsik, W. C. (ed.), Contributions of Stratigraphic Palynology. 1: Cenozoic Palynology. Contributions Series-American Association of Stratigraphic Palynologists, 5A: 66-89.

Stover, L. E. and Evitt, W. R., 1978, Analyses of pre-Pleistocene organicwalled dinoflagellates. Stanford Univ. Publications, Geological Sciences, 15: 300 p.

Stover, L. E. and Hardenbol, J., 1994. Dinoflagellates and depositional sequences in the lower Oligocene (Rupelian) Boom Clay Formation, Belgium. Bulletin de la Societe belge de Geologie, 102 (1-2): 5-77.

Strauss, C., 1991. Dinozysten-biostratigrafie im Unter und Mittel Miozän von Ostdeutschland. Tagungsmaterial. Jahrestg, GGW, Berlin, 38: 67-68.

Strauss, C. and Lund, J. J., 1992. A Middle Miocene dinoflagellate cyst microflora from Papendorf near Hamburg, Germany. Mitteilungen Geologisch-Paläontologischen Institut der Universität Hamburg, 73: 159-189.
Strauss, C., Lund, J. J. and Lund-Christensen, J., 2001. Miocene dinoflagellate cyst biostratigraphy of the Nieder Ochtenhausen research borehole (NW Germany). Geologisches Jahrbuch, Serie A, 152: 395-447.

Şafak, Ü., 1993a. Işıktepe-Dalakdere (KB Mersin) civarının Miyosen biyostratigrafisi. Yerbilimleri, 22: 127-49.

Şafak, Ü., 1993b. Antakya Havzası planktonik foraminifer biyostratigrafisi. Suat Erk Jeoloji Sempozyumu Bildirileri, 143-56.

Şafak, Ü. and Ünlügenç, U., 1992. Kozoluk, Solaklı ve Kevizli (Adana K'i) civarında yüzeylenen Oligosen-Orta Miyosen yaşlı istiflerin Ostracod faunası ve biyostratigrafisi. Yerbilimleri, 21: 117-139.

Şafak, Ü., Nazik, A., 1994. Eshab-I Kehf (Tarsus-Mersin) dolayı Neojen istifinin ortamsal yorumu. Yerbilimleri Geosaund, 15. Yıl sempozyumu, 22: 291-300.

Şengör, A. M. C., 1980. Türkiye'nin neotektoniğinin esasları. Türk. Jeol. Kürüm. Konferans Series, 2, 40.

Şengör, A. M. C., Görür, N. and Saroğlu, F., 1985. Strike-slip faulting and related basin formation in zones of tectonic escape: Turkey as a case study. In Biddle K. S. and Christie-Blick, N. (eds.) Strike-slip Deformation, Basin Formatin and Deformation. Society Economic Paleontologists and Mineralogists Special Publication, 37: 227-264.

Şengör, A. M. C. and Yılmaz, Y., 1981. Tethyan evolution of Turkey: a plate tectonic approach. Tectonophysics, 75: 181-241.

Sınacı, M., Toker, V., 2010. Neogene Nannoplankton biostratigraphy in the Adana Basin. Journal of the Earth Sciences Application and Research Centre of Hacettepe University, 21 (2), 83-98. Yerbilimleri, 31 (2): 83-98.

Tanar, O., 1985. Molluscan fauna of Karaisalı, Kuzgun and Memişli formations in Körlü (Tarsus-Mersin) area. Bull. Geol. Eng., 24: 17-31.

Taylor, F. J. R., 1980. On dinoflagellate evolution. BioSystems, 13: 65-108.

Teichmüller, M., 1985. Organic petrology of source rocks, History and State of Art, Adv. in Org. Geochem., 10: 581-589.

Tekin, T., 2002. Source rock potential and organic facies properties od the Oligo-Miocene deposits in the Pasinler-Horasan, Tercan-Aşkale basins (East Anatolia), PhD. Thesis, Middle East Technical University, 212 p.

Ternek, Z., 1957. Adana Havzasının Alt Miyosen (Burdigaliyen) Formasyonları; Bunların Diğer Formasyonlarla Olan Münasebetleri ve Petrol imkanları. M. T. A. Der., 49: 48-66.

Thomson, P. W. and Pflug, H., 1953. Pollen und sporen des Mitteleuropaischen Tertiars. Palaeontographica Abt. B, 91 (1-4): 1-138.

Tissot, B. and Welte, D. H., 1978. Petroleum Formation and Occurrence, Springer-Verlag, New York, 538 p.

Traverse, A., 1988. Paleopalynology. Allen and Unwin Ltd., U. S. A., 600 p.

Traverse, A., 2008. Founding the AASP: Critical mass reached in Tulsa in 1967. In Palynology, 32: 271-271.

Traverse, A. and Ginsburg, R. N., 1966. Palynology of the surface sediments of Great Bahama Bank as related to water movements and sedimentation. Mar. Geol., 4 (6): 417-459.

Türkecan, A. T., Munsterman, D. K., Işık, U., Altıner, D., Pınar, M., Çevik, T. and Alay, Z., (submitted). Miocene microfossil biostratigraphy of the Adana Basin, Eastern Mediterranean, Turkey. Palynology.

Tyson, R. V., 1995. Sedimentary Organic Matter: Organic Facies and Palynofacies. Chapman & Hall, London, 253 p.

Uffenorde, H., Lund, J.J. and Georgi, K.H., 1990. Biostratigraphy of the Neogene in the Iskenderun Basin. Turkish Association of Petroleum Geologists. Proceedings of the 8th Petroleum Congress of Turkey, 363–370.

Ünlügenç, U. C., 1993. Structural and stratigraphic evolution of the Adana Basin, SE Turkey. PhD. thesis, University of Keele.

Ünlügenç, U. C. and Demirkol, C., 1988. Kızıldağ Yayla (Adana) dolayının stratigrafisi. Jeoloji Mühendisliği, 32-33: 17-25.

Ünlügenç, U. C. and Demirkol, C., 1991. Karsanti-Akdam-Egner (K-KD Adana) Dolaylarının stratigrafik incelenmesi. In Yetiş, C. (ed.), Ahmet Acar Jeoloji Sempozyumu, Adana, 239-254.

Ünlügenç, U. C., Kelling, G. and Demirkol, C., 1990. Aspect of basin evolution in the Neogene Adana Basin, SE Turkey. Int. Earth Sci. Cong. Aegean Reg., 353-369.

Van der Hammen, T., 1956. A palynological systematic nomenclature. Bol. Geol., Bogota, 4 (2-3): 63-101.

Vandenberghe, N., Brinkhuis, H. and Steurbaut, E., 2003. The Eocene/ Oligocene boundary in the North Sea area: a sequence stratigraphic approach. In: Prothero, D. R., Ivany, L.C., Nesbitt, E.A. (eds.), From Greenhouse to Icehouse: the Marine Eocene Oligocene Transition. Columbia Univ. Press, New York, 419-437.

Van Simaeys, S., 2004. Stratigraphic and paleoenviromental analysis of the Rupelian and Chattian in their type regions: Implications for Global Oligocene Chronostratigraphy, PhD. Thesis, Katholieke Universiteit Leuven-Belgium.

Van Simaeys, S., De Man, E., Vandenberghe, N., Brinkhuis, H. and Steubaut, E., 2004. Stratigraphic and paleoenviromental analysis of the Rupelian-Chattian transition in the type region: evidence from dinoflagellate cysts, foraminifera and calcareous nannofossils, Palaeogeography, Palaeoclimatology, Palaeoecology, 208: 31-58.

Versteegh, G. J. M., 1994. Recognition of cyclic and non-cyclic environmental changes in the Mediterranean Pliocene: a palynological approach. Marine Micropaleontology, 23: 147-183.

Versteegh, G. J. M. and Zonneveld, K. A. F., 1994. Determination of (palaeo-)ecological preferences of dinoflagellates by applying Detrended and Canonical Correspondence analysis to late Pliocene dinoflagellate cyst assemblages of the south Italian Singha secion. Review of Palaeobotany and Palynology, 84: 181-199.

Wall, D., 1967, Fossil microplankton in deep-sea cores from the Caribbean Sea, Paleontology, 10: 95-123.

Wall, D. and Dale, B., 1970. Living hystrichosphaerid dinoflagellate spores from Bermuda and Puerto Rico. Micropaleontology, 47-58.

Wall, D. and Dale, B., 1973. Paleosalinity relationships of dinoflagellates in the Late Quaternary of the Black Sea- a summary. Geoscience and Man. 7 (1): 95-102.

Wall, D. and Dale, B., 1974. Dinoflagellates in late Quaternary deep-water sediments of Black Sea. In: Degens, E. T. and Ross, D. A. (eds.), The Black Sea—Geology, Chemistry and Biology. Memoir-American Association of Petroleum Geologists, 364-380.

Wall D., Dale, B. and Harada, K., 1973. Descriptions of new fossil dinoflagellates from the late Quaternary of the Black Sea. Micropaleontology, 19: 18-31.

Wall, D., Dale, B., Lohmann, G. P. and Smith, W. K., 1977. The environmental and climatic distribution in modern marine sediments from regions in the North and South Atlantic oceans and adjacent seas, Marine Micropaleontology, 2: 121-200.

Wefer, G., Berger, W. H., Bijma, J. and Fischer, G., 1999. Clues to ocean history: a brief overview of proxies. In: Fischer, G., Wefer, G. (eds.), Use of Proxies in Paleoceanography, Examples from the South Atlantic. Springer, Berlin, 1-68.

Wille, N., 1909. Conjugatae, Chlorophyceae in Engler und Prantl, Die natürlichen Pflanzen-familien. Nachträge zu Teil, i, Abt, 2.

Williams, G. L., 1977. Dinoflagellate cysts, their classification, biostratigraphy and palaeoecology. In: Ramsay, A.T.S. (ed.), Oceanic Micropalaeontology. Academic Press, London, 1231-1325.

Williams, D. B. and Sarjeant, W. A. S., 1967. Organic-walled microfossils as depth and shoreline indicators: Marine Geology, 5 (5-6), 389-412.

Williams, G., Brinkhuis, H., Pearce, M., Fensome, R. and Weegink, J., 2004. Southern Ocean and global dinoflagellate cyst events compared: index events for the Late Cretaceous-Neogene. Proceedings Proceedings of the Ocean Drilling Program, Scientific Results, 189: 1-98.

Williams, G. L. and Bujak, J. P., 1977. Cenozoic palynostratigraphy of offshore eastern Canada. American Association of Stratigraphic Palynologists Contributions Series A, 5: 14-47.

Williams, G. D., Ünlügenç, U. C., Kelling, G. and Demirkol, C., 1995. Tectonic control on stratigraphic evolution of the Adana Basin. Turkey J. Geol. Soc., 152: 873-882.

Williams, G. L. and Downie, C., 1966a. The genus *Hystrichokolpoma*. In Davey, R. J., Downie, C., Sarjeant, W. A. S., and Williams, G. L., Studies in 258 Mesozoic and Caniozoic dinoflagellate cysts. Bull. of the British Museum (Natural History) Geology, Supplement 3: 176-181.

Wilpshaar, M., Santarelli, A., Brinkhuis, H. and Visscher, H., 1996. Dinoflagellate cysts and mid-Oligocene chronostratigraphy in the central Mediterranean region. Journal of the Geological Society (London), 153: 553-561.

Wodehouse, R. P., 1933. Tertiary pollen-II The oil shales of the Eocene Green River formation. Bulletin of the Torrey Botanical Club, 60 (7): 479-524.

Wolff, H., 1934. Microfossilien des pliozänen Humodils der Grube Freigericht bei Dettingen a. M. Und Vergleich mit älteren Schichten des Tertiars sowie posttertiären Ablagerungen, Arb. Inst. Paläobot. U. Petrogr. Brennsteine, 5: 55-88.

Wrenn, J. H., 1988. Paleogene dinoflagellate cyst biostratigraphy of Seymour Island, Antarctica, 321-447 in Geological Society of America, Memoir, 169.

Yalçın, N. M. and Görür, N., 1984. Sedimentological evolution of the Adana Basin. In: Tekeli, O. and Göncüoğlu, M. C. (eds.) Proceedings of the International Symposium on the Heology of Taurus Belt, Ankara, 165-172.

Yetiş, C., 1988. Reorganisation of the Tertiary stratigraphy in the Adana Basin, southern Turkey. Newsl Stratigr, 20 (1): 43-58.

Yetiş, C. and Demirkol, C., 1986. Adana Baseni Batı Kesiminin Detay Jeolojik Etüdü. M.T.A., Rapor no: 8037.

Yetiş, C., Kelling, G., Gökçen, S. I. and Baroz, F., 1995. A revised stratigraphic framework for Late Cenozoic sequences in the northeastern Mediterranean region. Geol. Rudsch, 84: 794-812.

Yetiş, C., Demirkol, C. and Kerey, E., 1986. Adana havzası Kuzgun formasyonunun (Üst Miyosen) fasiyes ve ortamsal nitelikleri. Türkiye Jeoloji Kurumu Bülteni, C 29: 81-96.

Yılmaz, Y., Gürpınar, O. and Yiğitbaş, E., 1988. Tectonic evolution of the Miocene basins at the Amanos Mountains and the Maraş region. Bull. Turk. Assoc. Petrol. Geol. 1(1): 52– 72.

Yurtmen, S., 1986. Çukurova Baseni Karsanti Yöresi Kırıntılı Kayaçlarının Petrografik ve Petrolojik Özellikleri. M. S. Thesis, Çukurova University. 80 p.

Zevenboom, D., 1995. Dinoflagellate cysts from the Mediterranean Late Oligocene and Miocene (published PhD. Thesis). (Utrecht (The Netherlands)): State University of Utrecht, CIP Gegevens Koninklijke Bibliotheek, Den Haag. 221 p.

Zevenboom, D., 1996. Late Oligocene-early Miocene dinoflagellate cysts from the Lemme-Carrosio section (NW Italy); biostratigraphy and palaeoenvironmental interpretation. In: Steininger, F. F., Iaccarino, S., Cati, F. (eds.), In search of the Paleogene-Neogene boundary; Part 3, The global stratotype.

Zevenboom, D., Brinkhuis, H. and Visscher, H., 1994. Dinoflagellate cysts palaeoenvironmental analysis of the Oligocene/Miocene transition in northwest and central Italy. In: Coccioni, R., Montanari, A., Odin, G. S. (eds.), Miocene Stratigraphy of Italy and Adjacent Regions. Giornale di Geologia, 56 (1): 155-169.

Zonneveld, K. A. F., Versteegh, G. J. M. and de Lange, G. J., 1997. Preservation of organic-walled dinoflagellate cysts in different oxygen regimes: a 10,000 year natural experiment. Marine Micropaleontology, 29 (3-4): 393-405.

Zonneveld, K. A. F., Chen, L., Möbius, J. and Mahmoud, M. S., 2009. Enviromental significance of dinoflagellate cysts from the proximal part of the Po-river discharge plume (off southern Italy, Eastern Mediterranean. Journal of Sea Research, 62: 189-213.

APPENDICES

A. 1-19. DIGITAL IMAGES OF THE PALYNOMORPHS AND EXPLANATIONS.

PLATE-1

1. *Achomosphaera* cf. *andalousiensis,* ATD-5, 60.2 µm, Bekirli Sectiın.

2. *Achomosphaera* cf. *andalousiensis,* ATD-5, 60.2 µm, (fluorescent light), Bekirli Sectiın.

3. *Hystrichokolpoma rigaudiae*, TD-194, 78.2 µm, Çorlu Section.

4. *Hystrichokolpoma rigaudiae*, TD-194, 78.2 µm, (fluorescent light), Çorlu Section.

5. *Cerebrocysta poulsenii,* ATD-121, 43.8 µm, Sofular Section.

6. *Cerebrocysta poulsenii,* ATD-121, 43.8 µm, (fluorescent light), Sofular Section.

7. *Cerebrocysta poulsenii,* ATD-124, 39.1 µm, Sofular Section.

8. *Cerebrocysta poulsenii,* ATD-124, 39.1 µm, (fluorescent light), Sofular Section.

9. *Cerebrocysta poulsenii,* ATD-122, 43.2 µm, Sofular Section.

10. *Cerebrocysta poulsenii,* ATD-122, 43.2 µm, (fluorescent light), Sofular Section.

11. *Cerebrocysta poulsenii,* ATD-121, 40.1 µm, Sofular Section.

12. *Cerebrocysta poulsenii,* ATD-121, 40.1 µm, (fluorescent light), Sofular Section.

13. *Cerebrocysta poulsenii,* ATD-124, 46.1 µm, Sofular Section.

14. *Cerebrocysta poulsenii,* ATD-124, 46.1 µm, (fluorescent light), Sofular Section.

15. *Cerebrocysta* sp., ATD-124, 35.7 µm, Sofular Section.

16. *Cerebrocysta* sp., ATD-124, 35.7 µm, (fluorescent light), Sofular Section.

PLATE-1

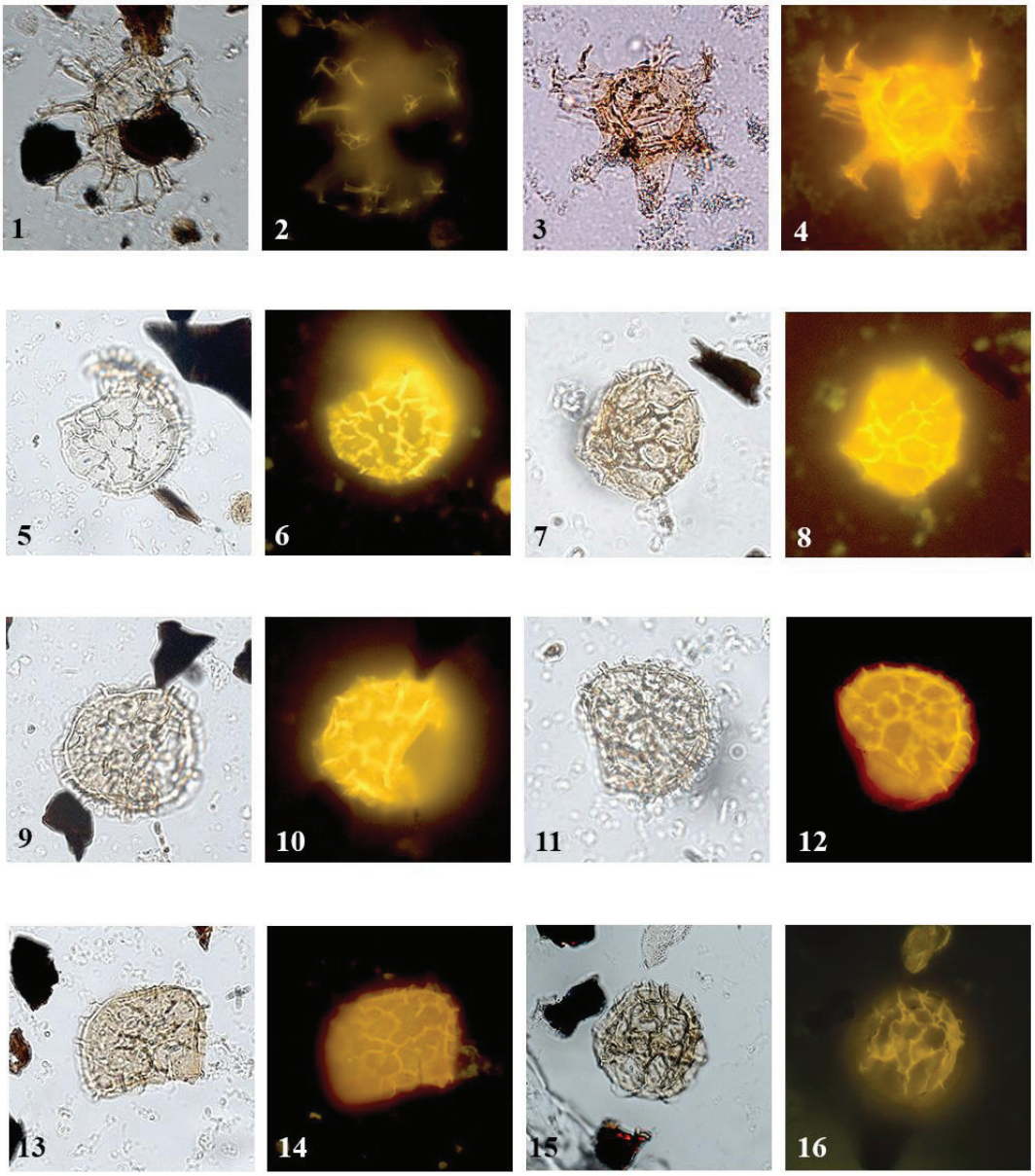

PLATE-2

1. *Cerebrocysta* sp., ATD-124, 46.3 µm, Sofular Section.

2. *Cerebrocysta* sp., ATD-124, 46.3 µm, (fluorescent light), Sofular Section.

3. *Cerebrocysta* sp., ATD-124, 46.3 µm, (fluorescent light), Sofular Section.

4. *Cerebrocysta* sp., ATD-124, 46.3 µm, (fluorescent light), Sofular Section.

5. *Cleistosphaeridium ancyrea*, ATD-36, 81.5 µm, Bekirli Section.

6. *Cleistosphaeridium ancyrea*, ATD-36, 81.5 µm, (fluorescent light), Bekirli Section.

7. *Cleistosphaeridium ancyrea*, ATD-36, 81.5 µm, (fluorescent light), Bekirli Section.

8. *Cleistosphaeridium placacantha*, ATD-124, 87.7 µm, Sofular Section.

9. *Cleistosphaeridium placacantha*, ATD-124, 87.7 µm, (fluorescent light), Sofular Section.

10. *Cleistosphaeridium placacantha*, ATD-124, 76.3 µm, Sofular Section.

11. *Cleistosphaeridium placacantha*, ATD-124, 76.3 µm, (fluorescent light), Sofular Section.

12. *Cleistosphaeridium placacantha*, ATD-124, 82.2 µm, Sofular Section.

13. *Cleistosphaeridium placacantha*, ATD-124, 82.2 µm, (fluorescent light), Sofular Section.

14. *Cleistosphaeridium placacantha*, ATD-124, 82.2 µm, (fluorescent light), Sofular Section.

15. *Nematosphaeropsis labyrinthus*, ATD-122, 56.8 µm, Sofular Section.

16. *Nematosphaeropsis labyrinthus*, ATD-122, 56.8 µm, (fluorescent light), Sofular Section.

PLATE-2

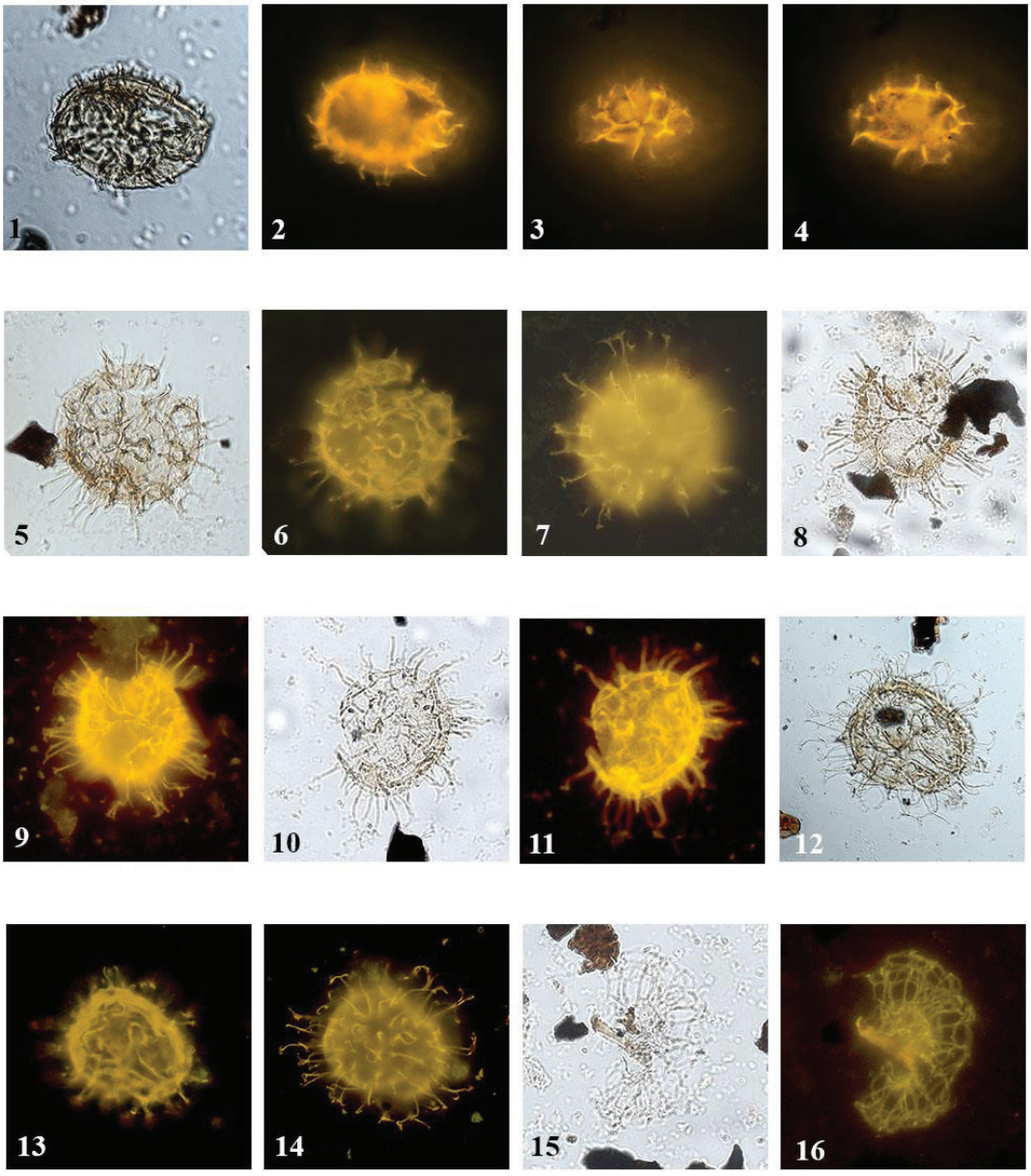

PLATE-3

1. *Diphyes pseudoficusoides*, ATD-99, 68.2 µm, Güvenç Section.

2. *Diphyes pseudoficusoides*, ATD-99, 68.2 µm, (fluorescent light), Güvenç Section.

3. *Cleistosphaeridium placacantha*, ATD-179, 86.2 µm, Çukurköy Section.

4. *Cleistosphaeridium placacantha*, ATD-179, 86.2 µm, (fluorescent light), Çukurköy Section.

5. *Florentinia stellata*, ATD-106, 80.2 µm, Güvenç Section.

6. *Florentinia stellata*, ATD-106, 80.2 µm, (fluorescent light), Güvenç Section.

7. *Homotryblium floripes*, ATD-106, 74.3 µm, Güvenç Section.

8. *Homotryblium floripes*, ATD-106, 74.3 µm, (fluorescent light), Güvenç Section.

9. *Homotryblium pallidum*, ATD-113, 51.3 µm, Güvenç Section.

10. *Homotryblium pallidum*, ATD-113, 51.3 µm, (fluorescent light), Güvenç Section.

11. *Homotryblium pallidum*, ATD-95, 52.7 µm, Güvenç Section.

12. *Homotryblium pallidum*, ATD-95, 52.7 µm, (fluorescent light), Güvenç Section.

13. *Homotryblium plectilum*, ATD-106, 75.8 µm, Güvenç Section.

14. *Homotryblium plectilum*, ATD-106, 75.8 µm, (fluorescent light), Güvenç Section.

15. *Homotryblium tenuispinosum*, ATD-102, 75.8 µm, Güvenç Section.

16. *Homotryblium tenuispinosum*, ATD-102, 75.8 µm, (fluorescent light), Güvenç Section.

PLATE-3

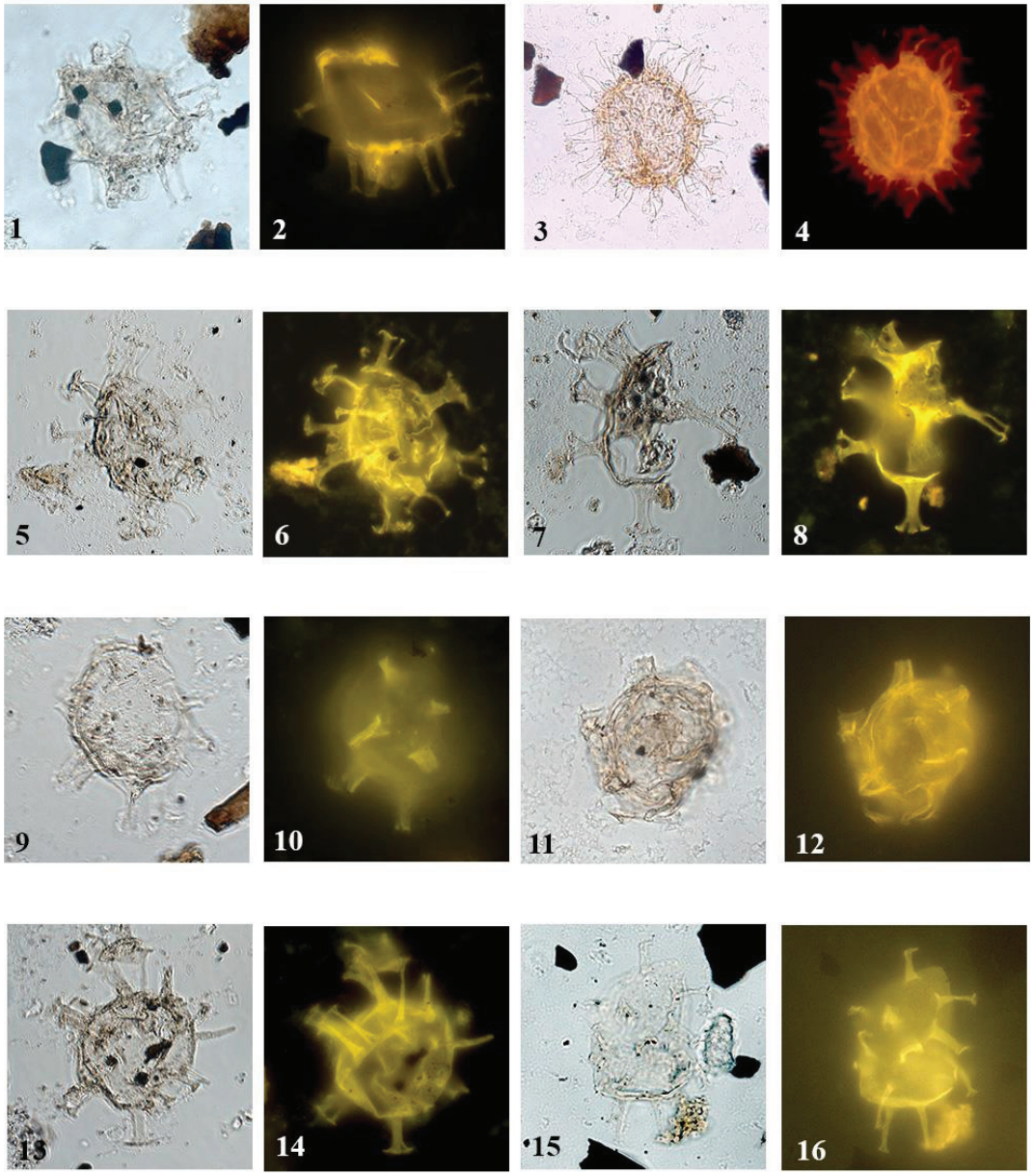

PLATE-4

1. *Homotryblium tenuispinosum*, ATD-102, 71.7 µm, Güvenç Section.

2. *Homotryblium tenuispinosum*, ATD-102, 71.7 µm, (fluorescent light), Güvenç Section.

3. *Homotryblium tenuispinosum*, ATD-99, 57.2 µm, Güvenç Section.

4. *Homotryblium tenuispinosum*, ATD-99, 57.2 µm, (fluorescent light), Güvenç Section.

5. *Homotryblium tenuispinosum*, ATD-99, 57.2 µm, (fluorescent light), Güvenç Section.

6. *Homotryblium tenuispinosum*, ATD-99, 57.2 µm, (fluorescent light), Güvenç Section.

7. *Hystrichokolpoma rigaudiae*, ATD-147, 87.9 µm, Çukuköy Section.

8. *Hystrichokolpoma rigaudiae*, ATD-147, 87.9 µm, (fluorescent light), Çukuköy Section.

9. *Hystrichokolpoma* sp., ATD-124, 78.6 µm, Sofular Section.

10. *Hystrichokolpoma* sp., ATD-124, 78.6 µm, (fluorescent light), Sofular Section.

11. *Hystrichosphaeropsis obscura*, ATD-102, 95.3 µm, Güvenç Section.

12. *Hystrichosphaeropsis obscura*, ATD-102, 95.3 µm, (fluorescent light), Güvenç Section.

13. *Hystrichosphaeropsis obscura*, ATD-24, 78.5 µm, Bekirli Section.

14. *Hystrichosphaeropsis obscura*, ATD-24, 78.5 µm, (fluorescent light), Bekirli Section.

15. *Impagidinium paradoxum*, TD-460, 28.7 µm, Çorlu Section.

16. *Impagidinium paradoxum*, TD-460, 28.7 µm, (fluorescent light), Çorlu Section.

PLATE-4

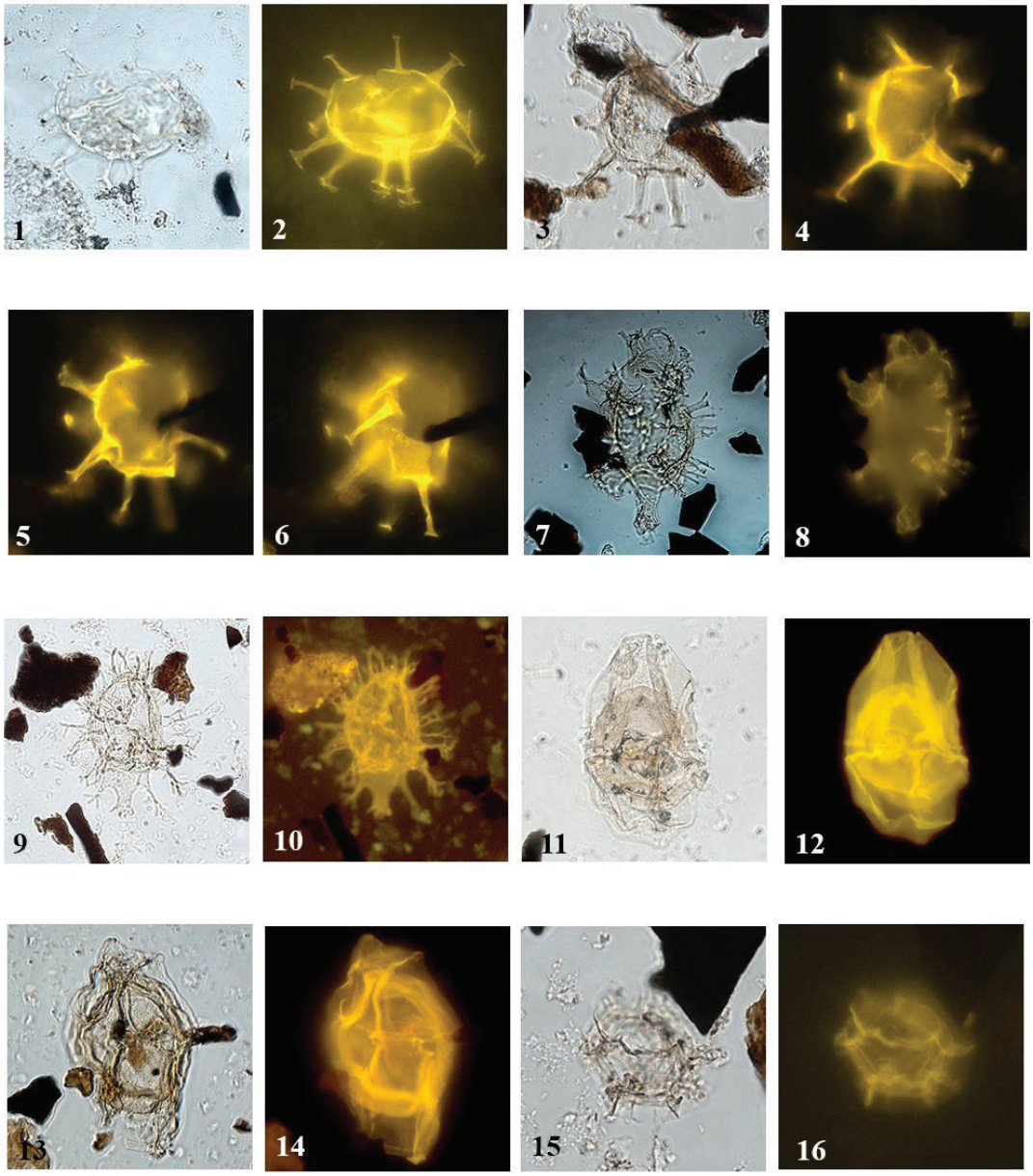

PLATE-5

1. *Impagidinium paradoxum*, ATD-73, 32.2 µm, Koruklu Section.

2. *Impagidinium paradoxum*, ATD-73, 32.2 µm, (fluorescent light), Koruklu Section.

3. *Impagidinium paradoxum*, ATD-73, 32.2 µm, (fluorescent light), Koruklu Section.

4. *Impagidinium paradoxum*, ATD-73, 32.2 µm, (fluorescent light), Koruklu Section.

5. *Impagidinium aculeatum*, ATD-120, 28.4 µm, Sofular Section.

6. *Impagidinium aculeatum*, ATD-120, 28.4 µm, (fluorescent light), Sofular Section.

7. *Impagidinium aculeatum*, ATD-121, 30.1 µm, Sofular Section.

8. *Impagidinium aculeatum*, ATD-121, 30.1 µm, (fluorescent light), Sofular Section.

9. *Labyrinthodinium truncatum*, TD-181, 28.7 µm, Çorlu Setion.

10. *Labyrinthodinium truncatum*, TD-181, 28.7 µm, (fluorescent light), Çorlu Setion.

11. *Labyrinthodinium truncatum*, TD-181, 28.7 µm, (fluorescent light), Çorlu Setion.

12. *Lingulodinium machaerophorum*, ATD-99, 64.8 µm, Güvenç Formation.

13. *Lingulodinium machaerophorum*, ATD-99, 64.8 µm, (fluorescent light), Güvenç Formation.

14. *Lingulodinium machaerophorum*, ATD-102, 64.1 µm, Güvenç Formation.

15. *Lingulodinium machaerophorum*, ATD-102, 64.1 µm, (fluorescent light), Güvenç Formation.

16. *Lingulodinium machaerophorum*, ATD-102, 64.1 µm, (fluorescent light), Güvenç Formation.

PLATE-5

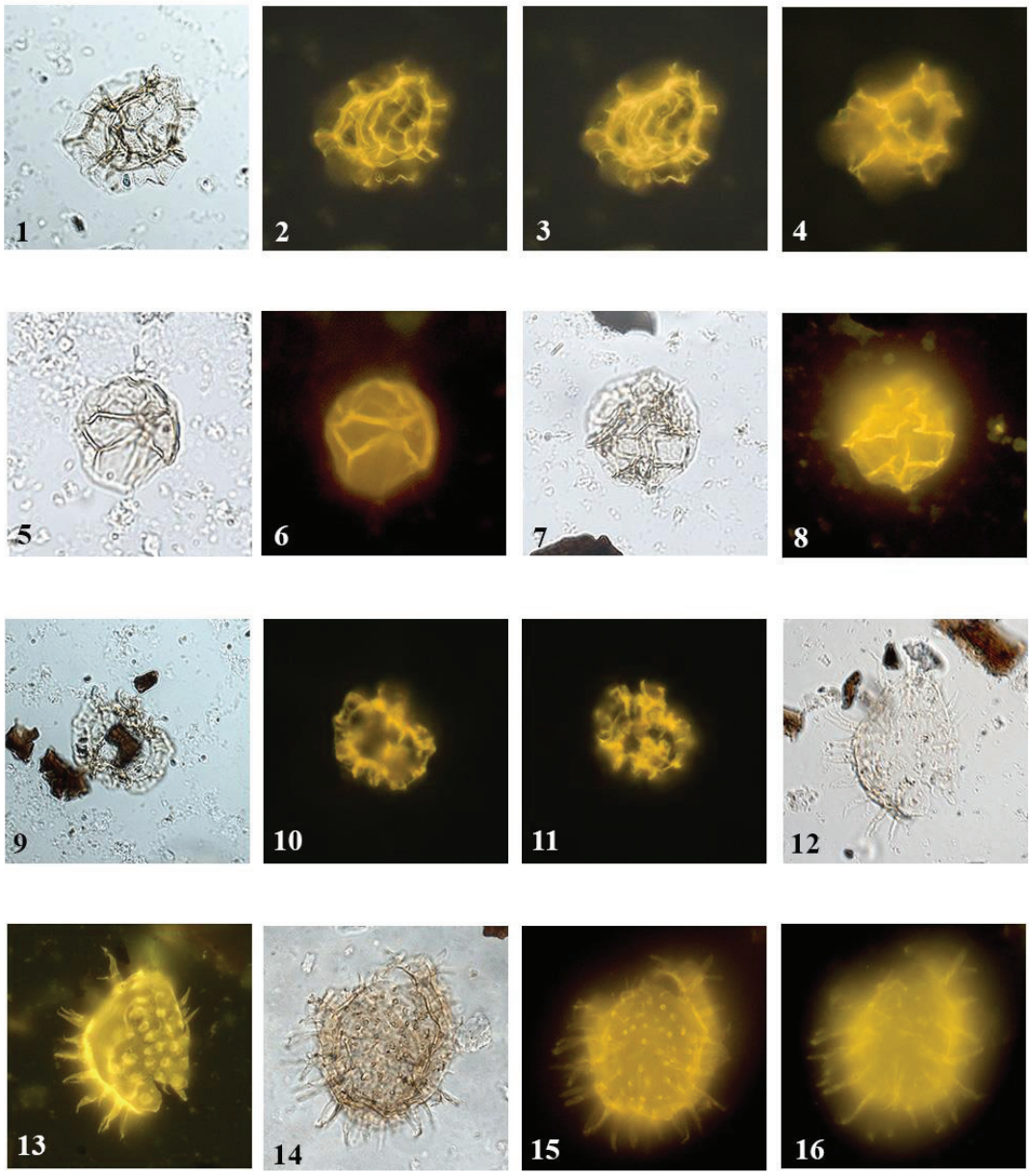

PLATE-6

1. *Melitasphaeridium choanophorum*, ATD-124, 57.4 µm, Sofular Section.

2. *Melitasphaeridium choanophorum*, ATD-124, 57.4 µm, (fluorescent light), Sofular Section.

3. *Melitasphaeridium choanophorum*, ATD-124, 53.7 µm, Sofular Section.

4. *Melitasphaeridium choanophorum*, ATD-124, 53.7 µm, (fluorescent light), Sofular Section.

5. *Melitasphaeridium choanophorum*, ATD-122, 52.8 µm, Sofular Section.

6. *Melitasphaeridium choanophorum*, ATD-122, 52.8 µm, (fluorescent light), Sofular Section.

7. *Nematosphaeropsis labyrinthus*, ATD-147, 48.1 µm, Çukurköy Section.

8. *Nematosphaeropsis labyrinthus*, ATD-147, 48.1 µm, (fluorescent light), Çukurköy Section.

9. *Nematosphaeropsis labyrinthus*, ATD-129, 68.6 µm, Sofular Section.

10. *Nematosphaeropsis labyrinthus*, ATD-129, 68.6 µm, (fluorescent light), Sofular Section.

11. *Cordosphaeridium cantharellus*, ATD-142, 77.1 µm, Çukurköy Section.

12. *Operculodinium borgerholtense*, ATD-87, 68.7 µm, (fluorescent light), Güvenç Section.

13. *Operculodinium centrocarpum*, ATD-87, 56.9 µm, Güvenç Section.

14. *Operculodinium centrocarpum*, ATD-87, 56.9 µm, (fluorescent light), Güvenç Section.

15. *Operculodinium centrocarpum*, ATD-110, 79.8 µm, Güvenç Section.

16. *Operculodinium centrocarpum*, ATD-110, 79.8 µm, (fluorescent light), Güvenç Section.

PLATE-6

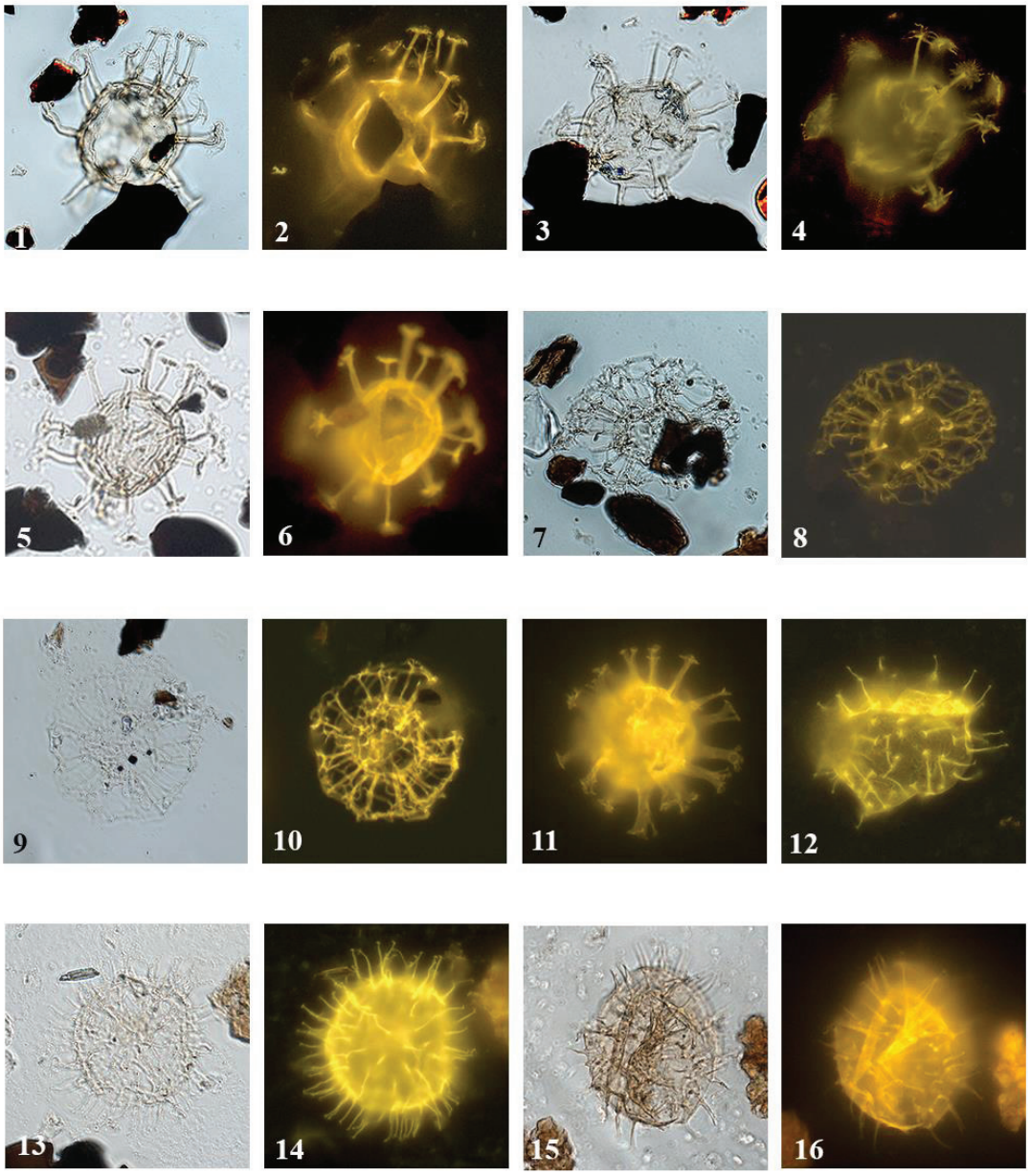

PLATE-7

1. *Operculodinium microtriainum*, ATD-123, 71.9 µm, Sofular Section.

2. *Operculodinium microtriainum*, ATD-123, 71.9 µm, (fluorescent light), Sofular Section.

3. *Operculodinium microtriainum*, ATD-124, 61.4 µm, Sofular Section.

4. *Operculodinium microtriainum*, ATD-124, 61.4 µm, (fluorescent light), Sofular Section.

5. *Operculodinium piaseckii*, ATD-102, 40.2 µm, Güvenç Section.

6. *Operculodinium piaseckii*, ATD-102, 40.2 µm, (fluorescent light), Güvenç Section.

7. *Operculodinium piaseckii*, ATD-78, 43.9 µm, Koruklu Section.

8. *Operculodinium piaseckii*, ATD-78, 43.9 µm, (fluorescent light), Koruklu Section.

9. *Operculodinium piaseckii*, ATD-125, 30.4 µm, Sofular Section.

10. *Operculodinium piaseckii*, ATD-125, 30.4 µm, (fluorescent light), Sofular Section.

11. *Operculodinium piaseckii*, ATD-124, 68.5 µm, Sofular Section.

12. *Operculodinium piaseckii*, ATD-124, 68.5 µm, (fluorescent light), Sofular Section.

13. *Operculodinium* sp., ATD-106, 68.4 µm, Güvenç Section.

14. *Operculodinium* sp., ATD-106, 68.4 µm, (fluorescent light), Güvenç Section.

15. *Operculodinium* sp., ATD-106, 66.6 µm, Güvenç Section.

16. *Operculodinium* sp., ATD-106, 66.6 µm, (fluorescent light), Güvenç Section.

PLATE-7

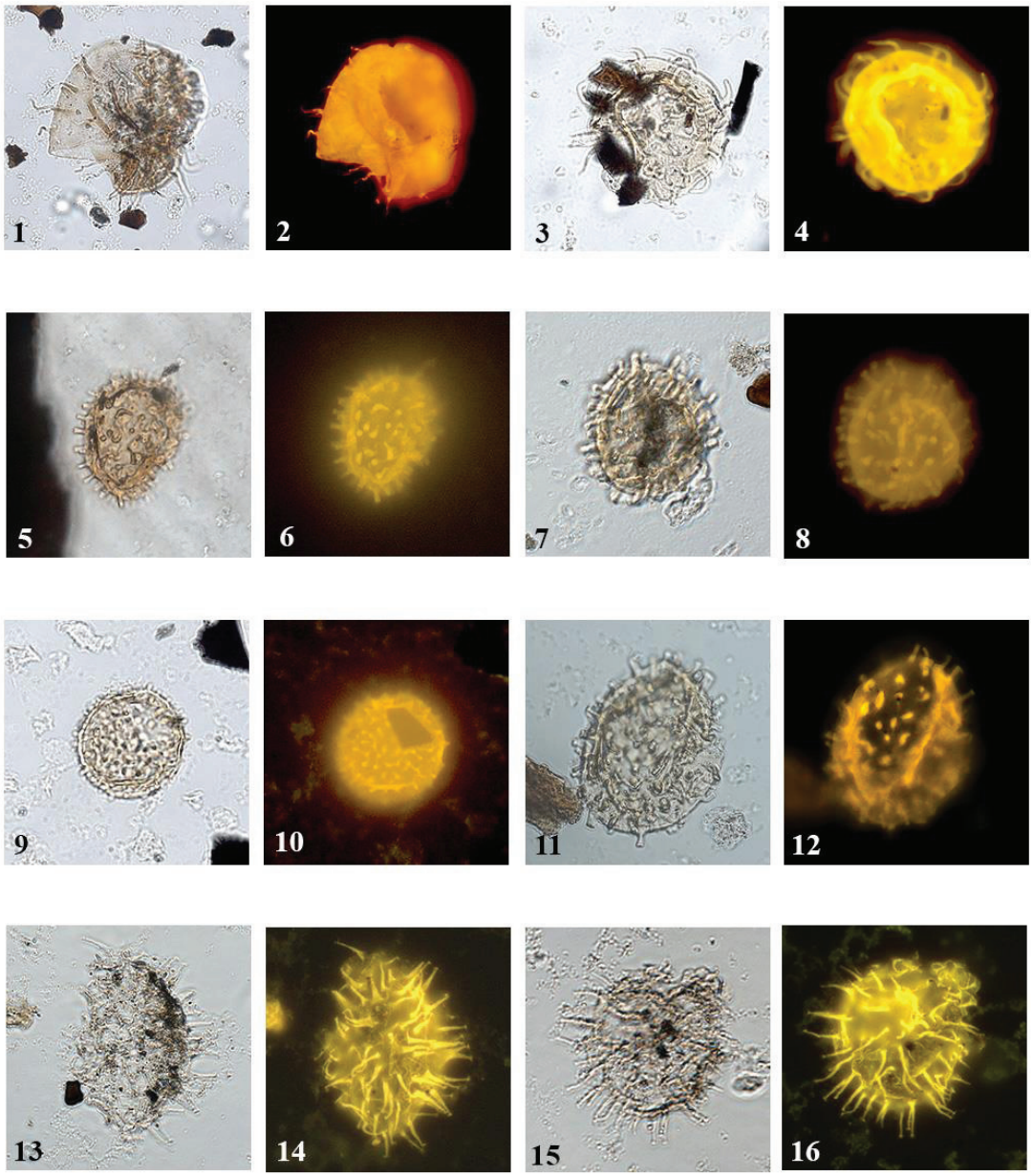

PLATE-8

1. *Palaeocystodinium striatogranulosum*, TD-192, 116.4 µm, Çorlu Section.

2. *Palaeocystodinium striatogranulosum*, TD-192, 116.4 µm, (fluorescent light), Çorlu Section.

3. *Palaeocystodinium striatogranulosum*, TD-192, 110.4 µm, Çorlu Section.

4. *Palaeocystodinium striatogranulosum*, TD-192, 110.4 µm, (fluorescent light), Çorlu Section.

5. *Palaeocystodinium* sp., TD-158, 125.5 µm, Köpekli Section.

6. *Palaeocystodinium* sp., TD-158, 125.5 µm, (fluorescent light), Köpekli Section.

7. *Polysphaeridium zoharyi*, ATD-16, 81.3 µm, Bekirli Section.

8. *Polysphaeridium zoharyi*, ATD-16, 81.3 µm, (fluorescent light), Bekirli Section.

9. *Polysphaeridium zoharyi*, ATD-55, 57.8 µm, Bekirli Section.

10. *Polysphaeridium zoharyi*, ATD-55, 57.8 µm, (fluorescent light), Bekirli Section.

11. *Polysphaeridium zoharyi*, ATD-87, 77.2 µm, Güvenç Section.

12. *Polysphaeridium zoharyi*, ATD-87, 77.2 µm, (fluorescent light), Güvenç Section.

13. *Reticulatosphaera actinocoronata*, ATD-122, 39.5 µm, Sofular Section.

14. *Reticulatosphaera actinocoronata*, ATD-122, 39.5 µm, (fluorescent light), Sofular Section.

15. *Reticulatosphaera actinocoronata*, ATD-124, 45.1 µm, Sofular Section.

16. *Reticulatosphaera actinocoronata*, ATD-124, 45.1 µm, (fluorescent light), Sofular Section.

PLATE-8

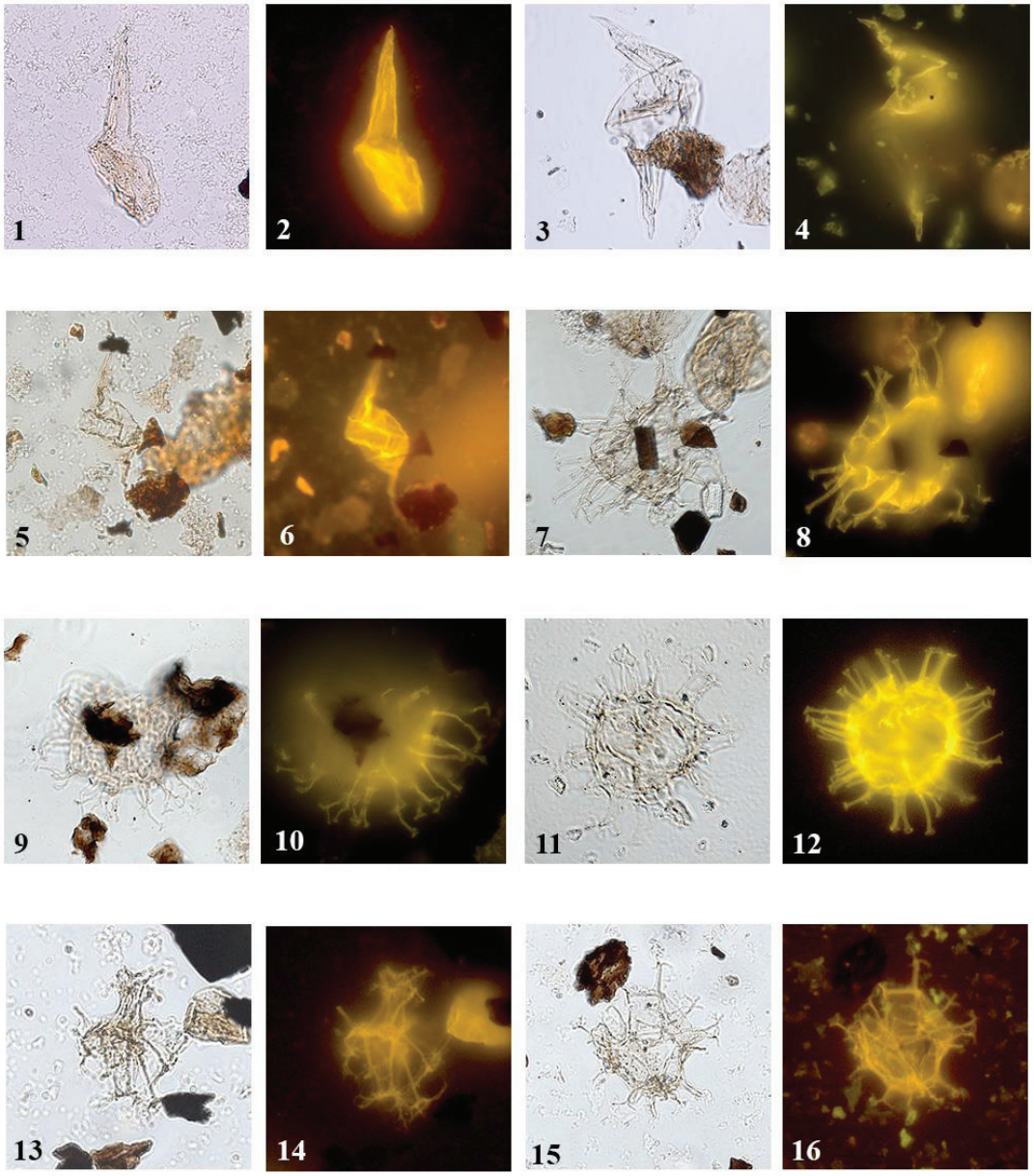

PLATE-9

1. *Spiniferites bentorii*, ATD-64, 46.9 µm, Bekirli Section.

2. *Spiniferites bentorii*, ATD-64, 46.9 µm, (fluorescent light), Bekirli Section.

3. *Spiniferites membranaceus*, ATD-102, 75.5 µm, Güvenç Section.

4. *Spiniferites membranaceus*, ATD-102, 75.5 µm, (fluorescent light), Güvenç Section.

5. *Spiniferites membranaceus*, ATD-127, 100.2 µm, Sofular Section.

6. *Spiniferites membranaceus*, ATD-127, 100.2 µm, (fluorescent light), Sofular Section.

7. *Spiniferites mirabilis*, ATD-102, 93.5 µm, Güvenç Section.

8. *Spiniferites mirabilis*, ATD-102, 93.5 µm, (fluorescent light), Güvenç Section.

9. *Spiniferites mirabilis*, ATD-102, 93.5 µm, (fluorescent light), Güvenç Section.

10. *Spiniferites mirabilis*, ATD-110, 99.6 µm, Güvenç Section.

11. *Spiniferites mirabilis*, ATD-110, 99.6 µm, (fluorescent light), Güvenç Section.

12. *Spiniferites mirabilis*, ATD-110, 99.6 µm, (fluorescent light), Güvenç Section.

13. *Spiniferites mirabilis*, ATD-110, 99.6 µm, (fluorescent light), Güvenç Section.

14. Spiniferites pseudofurcatus, ATD-110, 112.7 µm, Güvenç Section.

15. Spiniferites pseudofurcatus, ATD-110, 112.7 µm, (fluorescent light), Güvenç Section.

16. Spiniferites pseudofurcatus, ATD-110, 112.7 µm, (fluorescent light), Güvenç Section.

PLATE-9

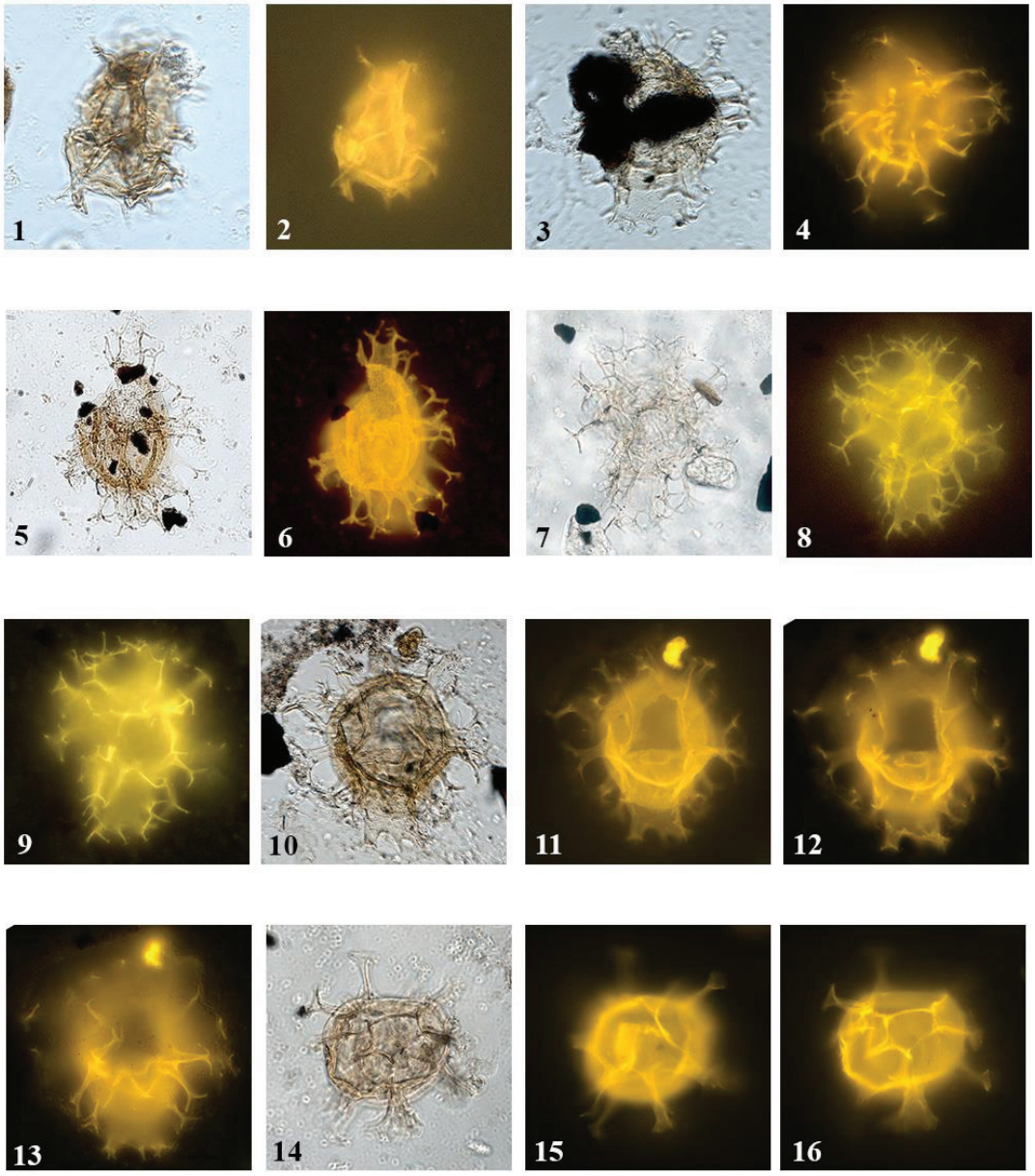

PLATE-10

1. *Spniferites ramosus*, ATD-124, 67.3 µm, Sofular Section.

2. *Spniferites ramosus*, ATD-124, 67.3 µm, (fluorescent light), Sofular Section.

3. *Spiniferites spongiophragmatus*, ATD-102, 97.9 µm, Güvenç Section.

4. *Spiniferites spongiophragmatus*, ATD-102, 97.9 µm, (fluorescent light), Güvenç Section.

5. *Unipontidinium aquaeductum*, ATD-122, 33.1 µm, Sofular Section.

6. *Unipontidinium aquaeductum*, ATD-122, 33.1 µm, (fluorescent light), Sofular Section.

7. *Unipontidinium aquaeductum*, ATD-122, 32.7 µm, Sofular Section.

8. *Unipontidinium aquaeductum*, ATD-122, 32.7 µm, (fluorescent light), Sofular Section.

9. *Unipontidinium aquaeductum*, ATD-124, 30.5 µm, Sofular Section.

10. *Unipontidinium aquaeductum*, ATD-124, 30.5 µm, (fluorescent light), Sofular Section.

11. *Unipontidinium aquaeductum*, ATD-124, 31.4 µm, Sofular Section.

12. *Unipontidinium aquaeductum*, ATD-124, 31.4 µm, (fluorescent light), Sofular Section.

13. *Unipontidinium aquaeductum*, ATD-127, 37.9 µm, Sofular Section.

14. *Unipontidinium aquaeductum*, ATD-127, 37.9 µm, (fluorescent light), Sofular Section.

15. *Unipontidinium aquaeductum*, ATD-124, 36.2 µm, Sofular Section.

16. *Unipontidinium aquaeductum*, ATD-124, 36.2 µm, (fluorescent light), Sofular Section.

PLATE-10

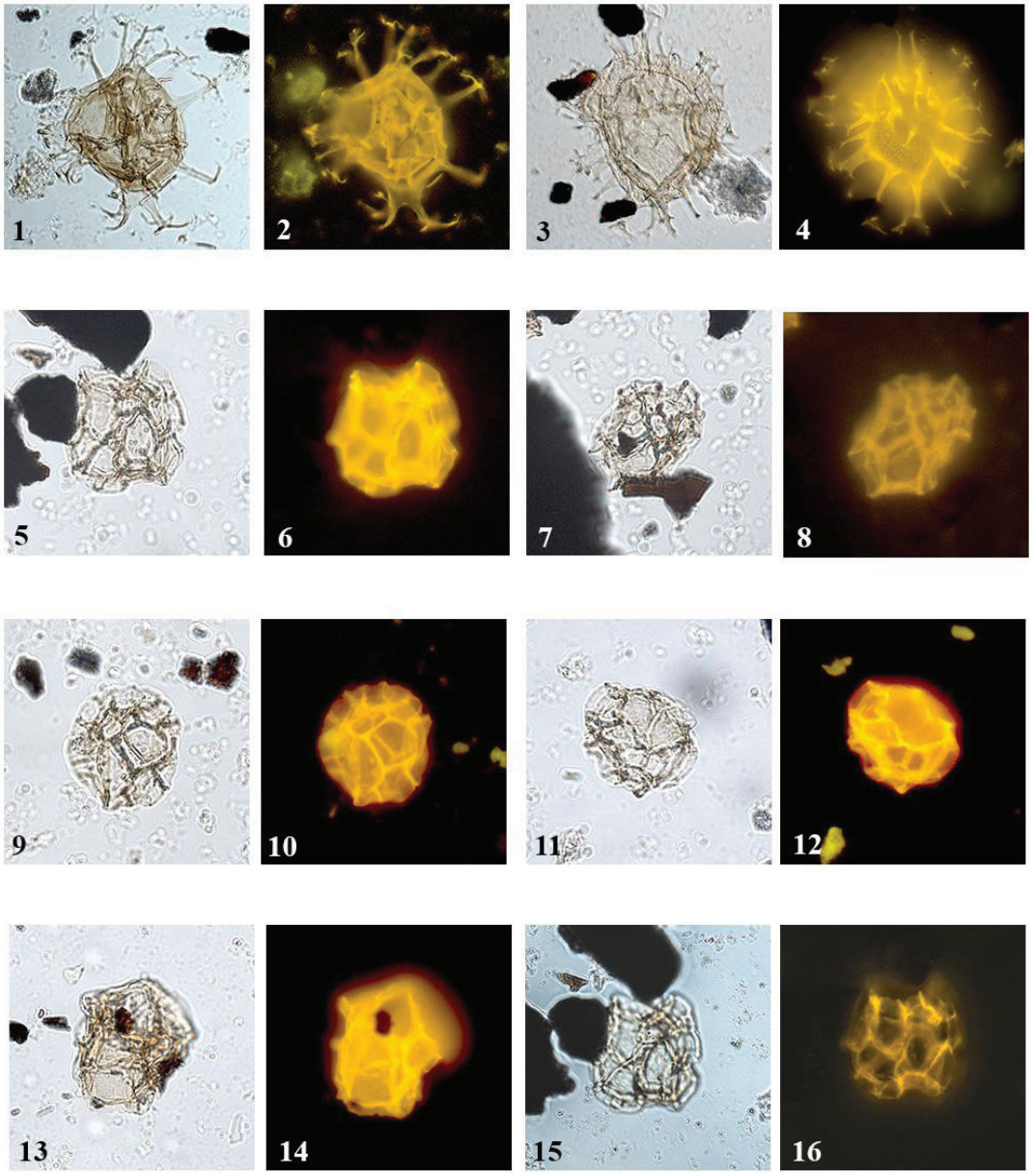

PLATE-11

1. *Cribroperidinium* sp., TD-163, 85.8 µm, Köpekli Section.

2. *Cribroperidinium* sp., TD-163, 85.8 µm, (fluorescent light), Köpekli Section.

3. *Cribroperidinium* sp., TD-161, 89.2 µm, Köpekli Section.

4. *Cribroperidinium* sp., TD-161, 89.2 µm, (fluorescent light), Köpekli Section.

5. *Spiniferites* sp., TD-158, 85.3 µm, Köpekli Section.

6. *Spiniferites* sp., TD-158, 85.3 µm, (fluorescent light), Köpekli Section.

7. *Spiniferites* sp., TD-158, 71.3 µm, Köpekli Section.

8. *Spiniferites* sp., TD-158, 71.3 µm, (fluorescent light), Köpekli Section.

9. *Spiniferites* sp., TD-158, 75.2 µm, Köpekli Section.

10. *Spiniferites* sp., TD-158, 75.2 µm, (fluorescent light), Köpekli Section.

11. *Spiniferites* sp., TD-158, 91.2 µm, Köpekli Section.

12. *Spiniferites* sp., TD-158, 91.2 µm, (fluorescent light), Köpekli Section.

13. *Spiniferites* sp., ATD-110, 75.2 µm, Güvenç Section.

14. *Spiniferites* sp., ATD-110, 75.2 µm, (fluorescent light), Güvenç Section.

15. *Paleocystodinium ventricosum*, TD-199, 112.7 µm, Çorlu Section.

16. *Paleocystodinium ventricosum*, TD-199, 112.7 µm, (fluorescent light), Çorlu Section.

PLATE-11

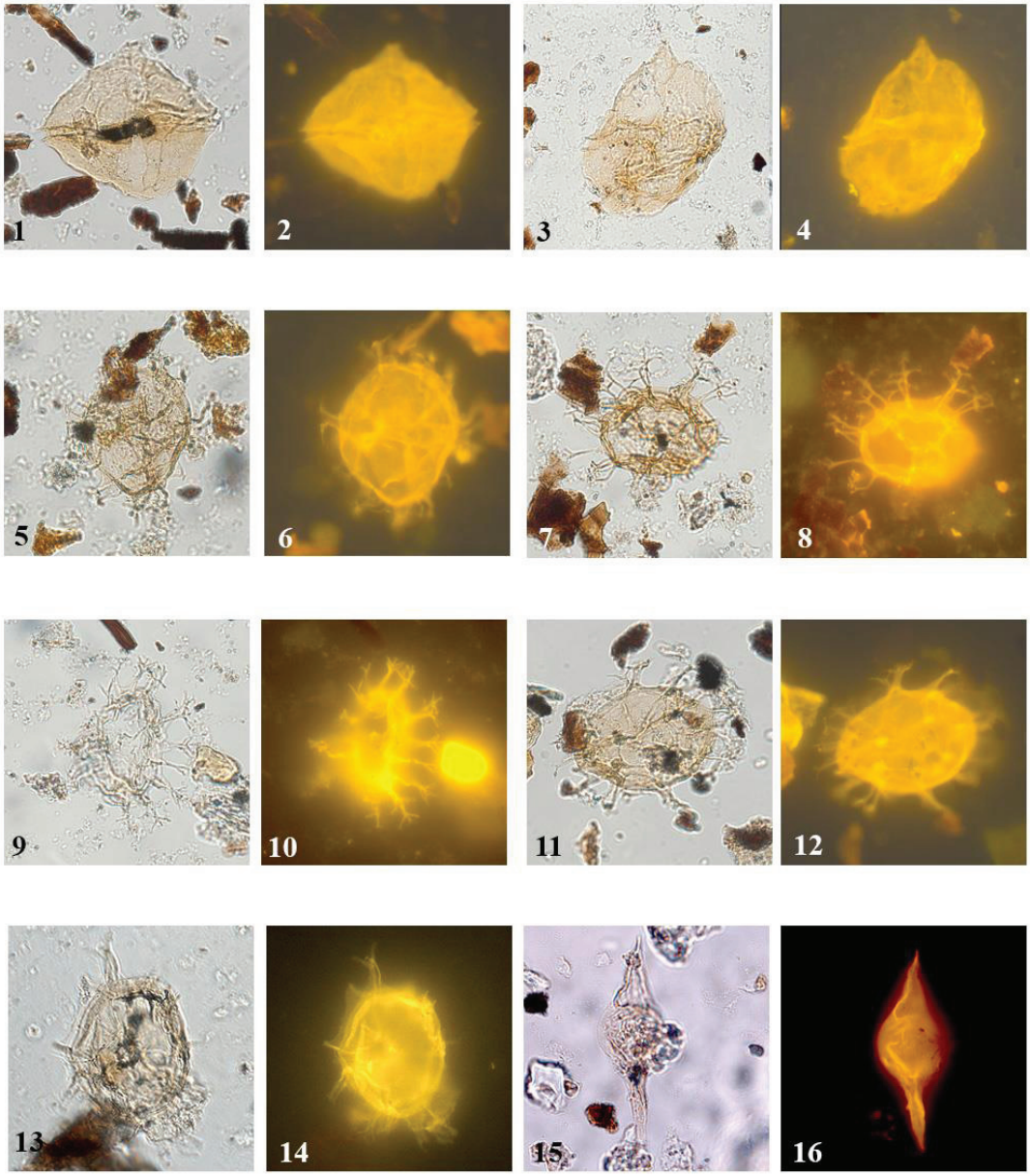

PLATE-12

1. *Spiniferites* sp., ATD-127, 82.7 µm, Sofular Section.

2. *Spiniferites* sp., ATD-127, 82.7 µm, (fluorescent light), Sofular Section.

3. *Cordosphaeridium* sp., TD-178, 62.6 µm, (fluorescent light), Çorlu Section.

4. *Labyrinthodinium truncatum*, TD-180, 30.1 µm, Çorlu Section.

5. *Labyrinthodinium truncatum*, TD-180, 30.1 µm, (fluorescent light), Çorlu Section.

6. *Labyrinthodinium truncatum*, TD-180, 28.9 µm, Çorlu Section.

7. *Labyrinthodinium truncatum*, TD-180, 28.9 µm, (fluorescent light), Çorlu Section.

8. *Labyrinthodinium truncatum*, TD-181, 30.4 µm, Çorlu Section.

9. *Labyrinthodinium truncatum*, TD-181, 30.4 µm, (fluorescent light), Çorlu Section.

10. *Labyrinthodinium truncatum*, TD-181, 29.6 µm, Çorlu Section.

11. *Labyrinthodinium truncatum*, TD-181, 29.6 µm, (fluorescent light), Çorlu Section.

12. *Achamosphaera* sp., TD-158, 53.3 µm, Köpekli Section.

13. *Achamosphaera* sp., TD-158, 53.3 µm, (fluorescent light), Köpekli Section.

14. *Achamosphaera* sp., TD-158, 53.3 µm, (fluorescent light), Köpekli Section.

15. *Operculodinium piaseckii*, TD-178, 42.8 µm, Çorlu Section.

16. *Operculodinium piaseckii*, TD-178, 42.8 µm, (fluorescent light), Çorlu Section.

PLATE-12

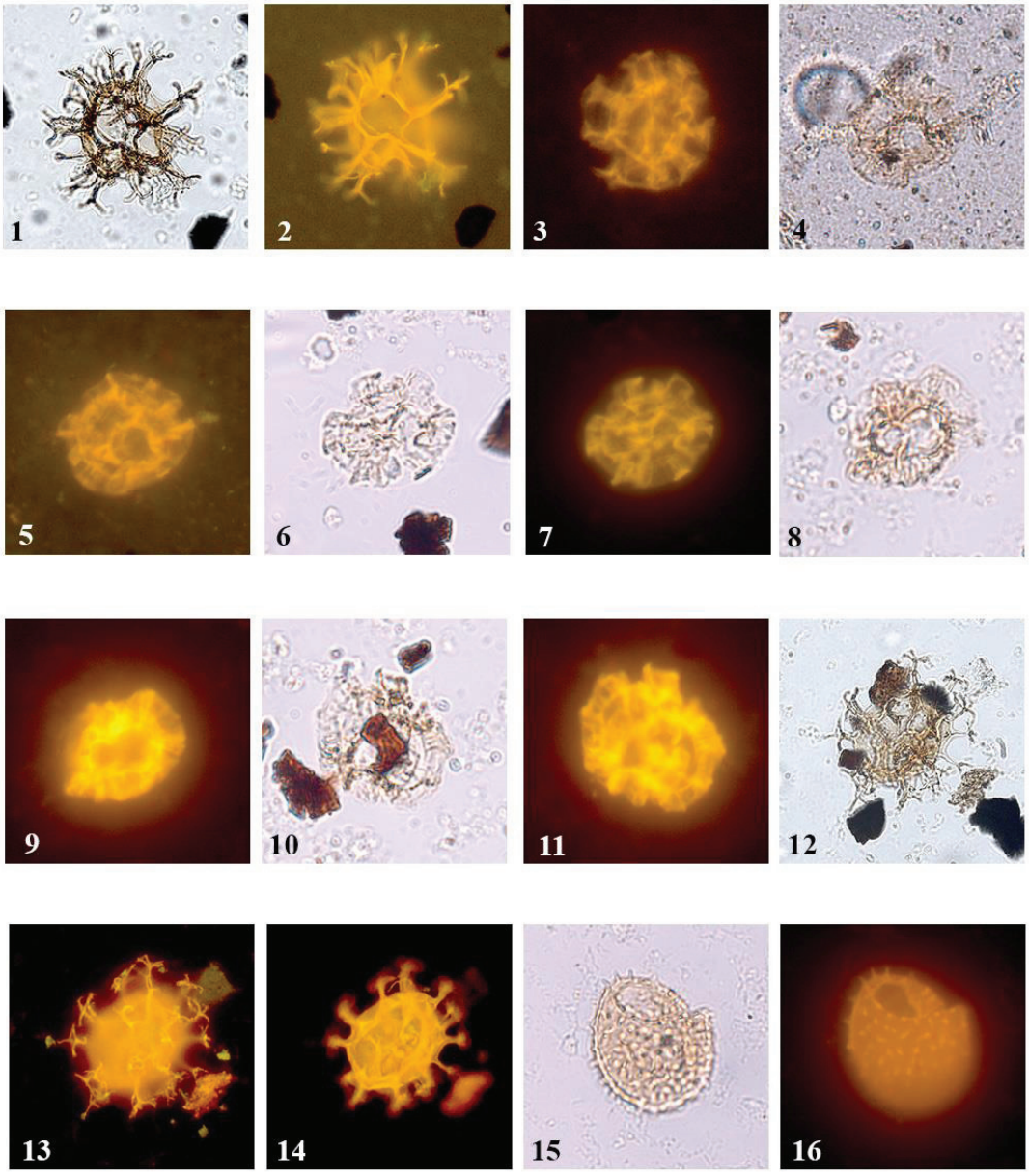

PLATE-13

1. *Impagidinum* sp. ATD-124, 94.8 µm, Sofular Section.

2. *Impagidinum* sp. ATD-124, 94.8 µm, (fluorescent light), Sofular Section.

3. *Impagidinum* sp. ATD-124, 97.1 µm, Sofular Section.

4. *Impagidinum* sp. ATD-124, 97.1 µm, (fluorescent light), Sofular Section.

5. *Impagidinum* sp. ATD-124, 94.9 µm, Sofular Section.

6. *Impagidinum* sp. ATD-124, 94.9 µm, (fluorescent light), Sofular Section.

7. *Impagidinum* sp. ATD-124, 78.9 µm, Sofular Section.

8. *Impagidinum* sp. ATD-124, 78.9 µm, (fluorescent light), Sofular Section.

9. *Cribroperidinium tenuitabulatum*, TD-193, 90.8 µm, Çorlu Section.

10. *Cribroperidinium tenuitabulatum*, TD-193, 90.8 µm, (fluorescent light), Çorlu Section.

11. *Paleocystodinium ventricosum*, TD-189, 118.2 µm, Çorlu Section.

12. *Paleocystodinium ventricosum*, TD-189, 118.2 µm, (fluorescent light), Çorlu Section.

13. *Palaeocystodinium striatogranulosum*, TD-193, 128.3 µm, Çorlu Section.

14. *Palaeocystodinium striatogranulosum*, TD-193, 128.3 µm, (fluorescent light), Çorlu Section.

15. *Palaeocystodinium striatogranulosum*, TD-193, 127.8 µm, Çorlu Section.

16. *Palaeocystodinium striatogranulosum*, TD-193, 127.8 µm, (fluorescent light), Çorlu Section.

PLATE-13

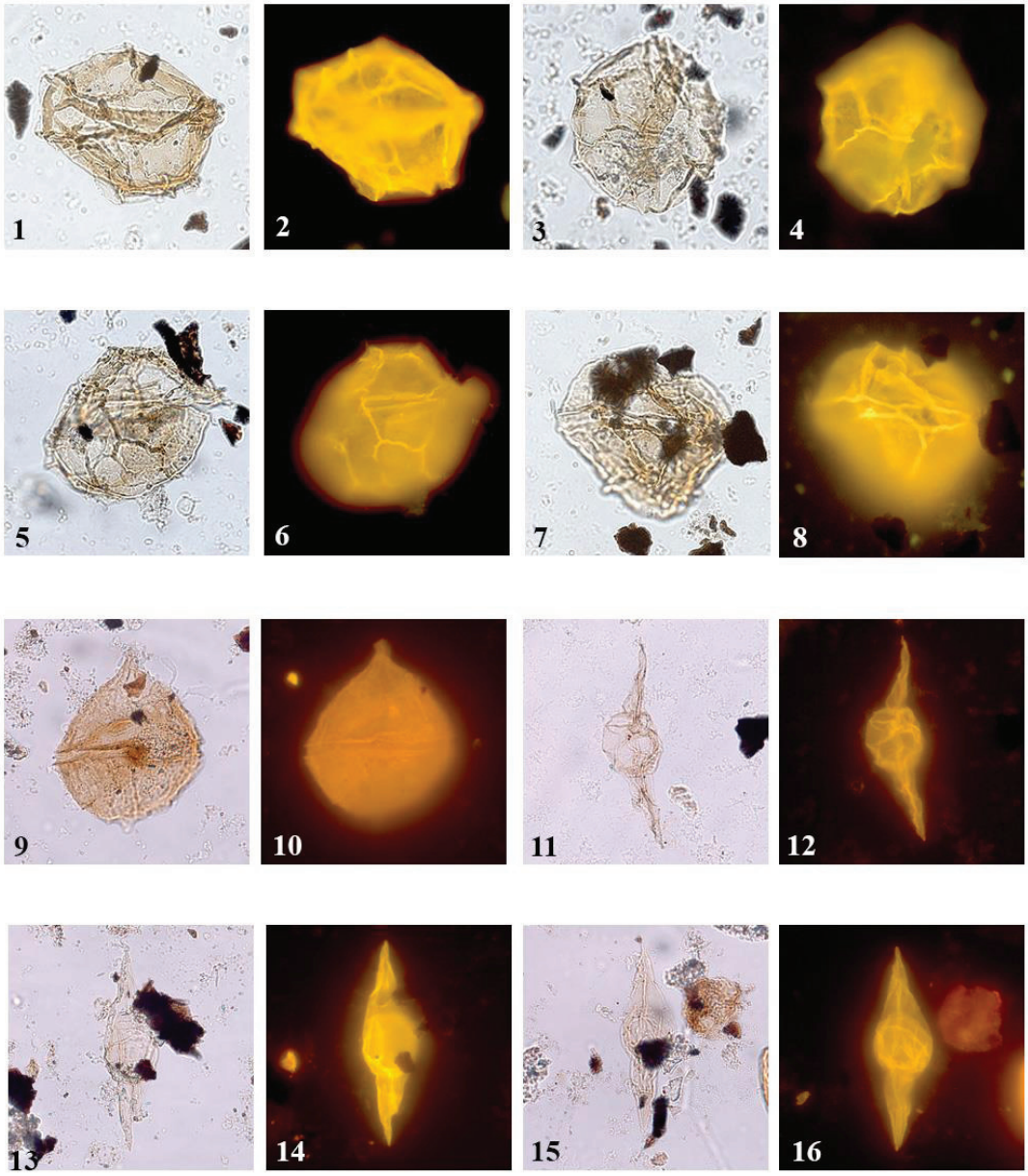

PLATE-14

1. Bisaccate pollen, ATD-176, 86.2 µm, Çorlu Section.

2. Bisaccate pollen, ATD-176, 86.2 µm, (fluorescent light), Çorlu Section.

3. Bisaccate pollen, ATD-189, 94.7 µm, Çorlu Section.

4. Bisaccate pollen, ATD-189, 94.7 µm, (fluorescent light), Çorlu Section.

5. Bisaccate pollen, ATD-216, 95.6 µm, Çorlu Section.

6. Bisaccate pollen, ATD-216, 95.6 µm, (fluorescent light), Çorlu Section.

7. Bisaccate pollen, ATD-320, 88.7 µm, Çorlu Section.

8. Bisaccate pollen, ATD-320, 88.7 µm, (fluorescent light), Çorlu Section.

9. Bisaccate pollen, ATD-380, 94.2 µm, Çorlu Section.

10. Bisaccate pollen, ATD-380, 94.2 µm, (fluorescent light), Çorlu Section.

11. Bisaccate pollen, ATD-410, 91.6 µm, Çorlu Section.

12. Bisaccate pollen, ATD-410, 91.6 µm, (fluorescent light), Çorlu Section.

13. *Cingulatisporites macrospecious,* ATD-122, µm, Sofular Section.

14. *Cingulatisporites macrospecious,* ATD-122, µm, (fluorescent light), Sofular Section.

15. *Cingulatisporites macrospecious,* ATD-89, 56.4 µm, Güvenç Section.

16. *Cingulatisporites macrospecious,* ATD-89, 56.4 µm, (fluorescent light), Güvenç Section.

PLATE-14

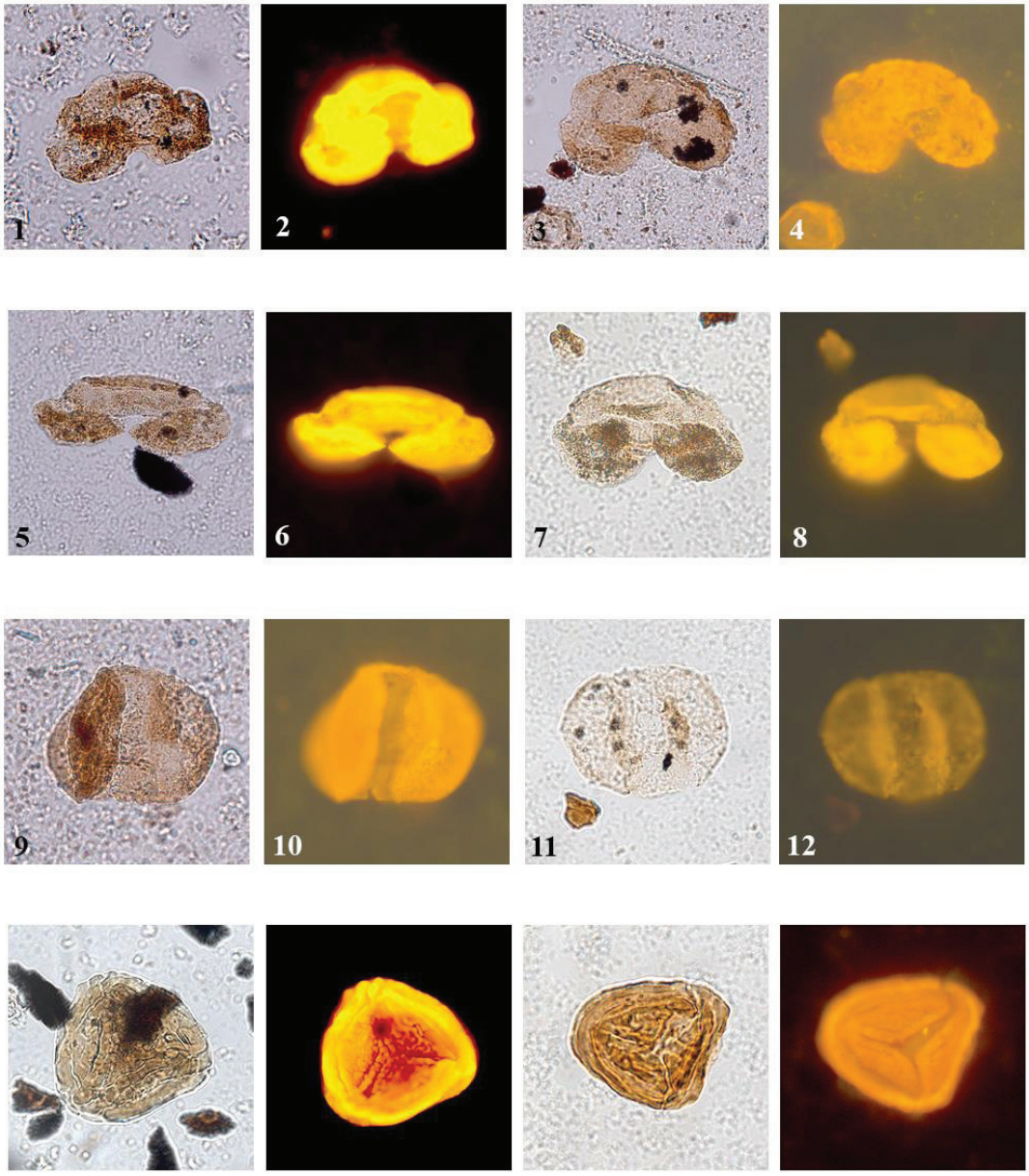

PLATE-15

1. Compositae (liguliflorae-type), TD-160, 28.4 µm, Köpekli Section.

2. Compositae (liguliflorae-type), TD-160, 28.4 µm, (fluorescent light), Köpekli Section.

3. Compositae (liguliflorae-type), TD-175, 27.6 µm, (fluorescent light), Çorlu Section.

4. Compositae (liguliflorae-type), ATD-78, 25.7 µm, Koruklu Section.

5. Compositae (liguliflorae-type), ATD-78, 25.7 µm, (fluorescent light), Koruklu Section.

6. Compositae (tubuliflorae-type), ATD-77, 32.6 µm, Koruklu Section.

7. Compositae (tubuliflorae-type), ATD-77, 32.6 µm, (fluorescent light), Koruklu Section.

8. Compositae (tubuliflorae-type), TD-178, 31.7 µm, Çorlu Section.

9. Compositae (tubuliflorae-type), TD-178, 31.7 µm, (fluorescent light), Çorlu Section.

10. *Magnastriatites howardii*, TD-158, 42.6 µm, Çorlu Section.

11. *Magnastriatites howardii*, TD-158, 42.6 µm, (fluorescent light), Çorlu Section.

12. Dipsacaceae, TD-231, 72.2 µm, Çorlu Section.

13. Dipsacaceae, TD-231, 72.2 µm, (fluorescent light), Çorlu Section.

14. *Echinatisporis longechinus* (rw), ATD-24, 56.2 µm, Bekirli Section.

15. *Echinatisporis longechinus* (rw), ATD-36, 58.6 µm, Bekirli Section.

16. *Echinatisporis longechinus* (rw), ATD-36, 58.6 µm, (fluorescent light), Bekirli Section.

PLATE-15

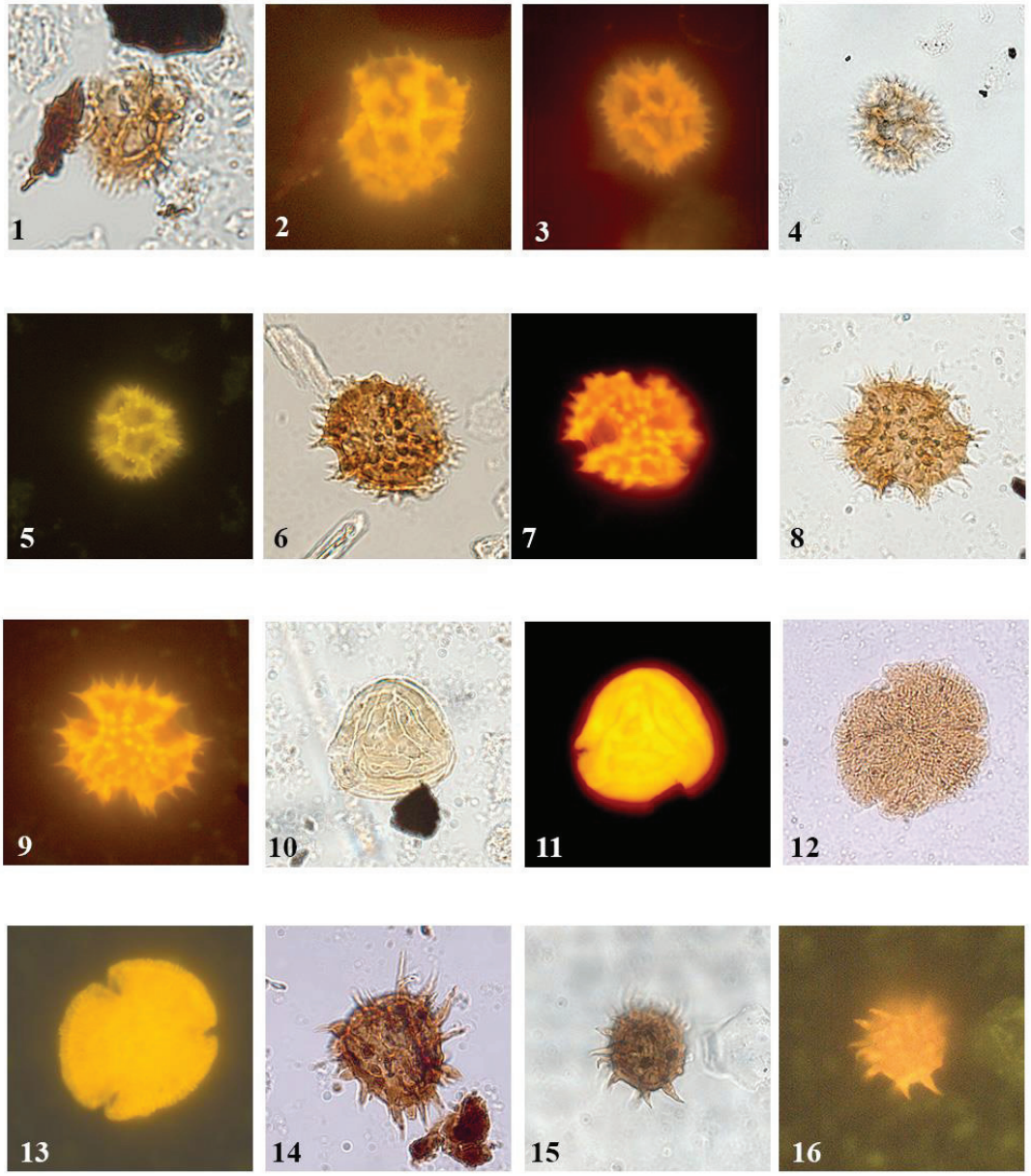

PLATE-16

1. *Ephedripites* sp., TD-175, 51.2 µm, Çorlu Section.

2. *Ephedripites* sp., TD-175, 51.2 µm, (fluorescent light), Çorlu Section.

3. *Ephedripites* sp., TD-178, 56.7 µm, Çorlu Section.

4. *Ephedripites* sp., TD-178, 56.7 µm, (fluorescent light), Çorlu Section.

5. *Monoporopollenites gramineoides*, TD-184, 38.2 µm, Çorlu Section.

6. *Monoporopollenites gramineoides*, TD-184, 38.2 µm, (fluorescent light), Çorlu Section.

7. *Monoporopollenites gramineoides*, ATD-63, 37.6 µm, Koruklu Section.

8. *Monoporopollenites gramineoides*, ATD-63, 37.6 µm, (fluorescent light), Koruklu Section.

9. *Monoporopollenites gramineoides*, ATD-121, 38.4 µm, Sofular Section.

10. *Monoporopollenites gramineoides*, ATD-121, 38.4 µm, (fluorescent light), Sofular Section.

11. *Nothofagidites emarcidus*, ATD-40, 34.2 µm, Bekirli Section.

12. *Nothofagidites emarcidus*, ATD-40, 34.2 µm, (fluorescent light), Bekirli Section.

13. *Nothofagidites emarcidus*, ATD-16, 32.6 µm, Bekirli Section.

14. *Nothofagidites emarcidus*, ATD-16, 32.6 µm, (fluorescent light), Bekirli Section.

15. *Periporopollenites multiporatus*, ATD-119, 28.4 µm, Sofular Section.

16. *Periporopollenites multiporatus*, ATD-119, 28.4 µm, (fluorescent light), Sofular Section.

PLATE-16

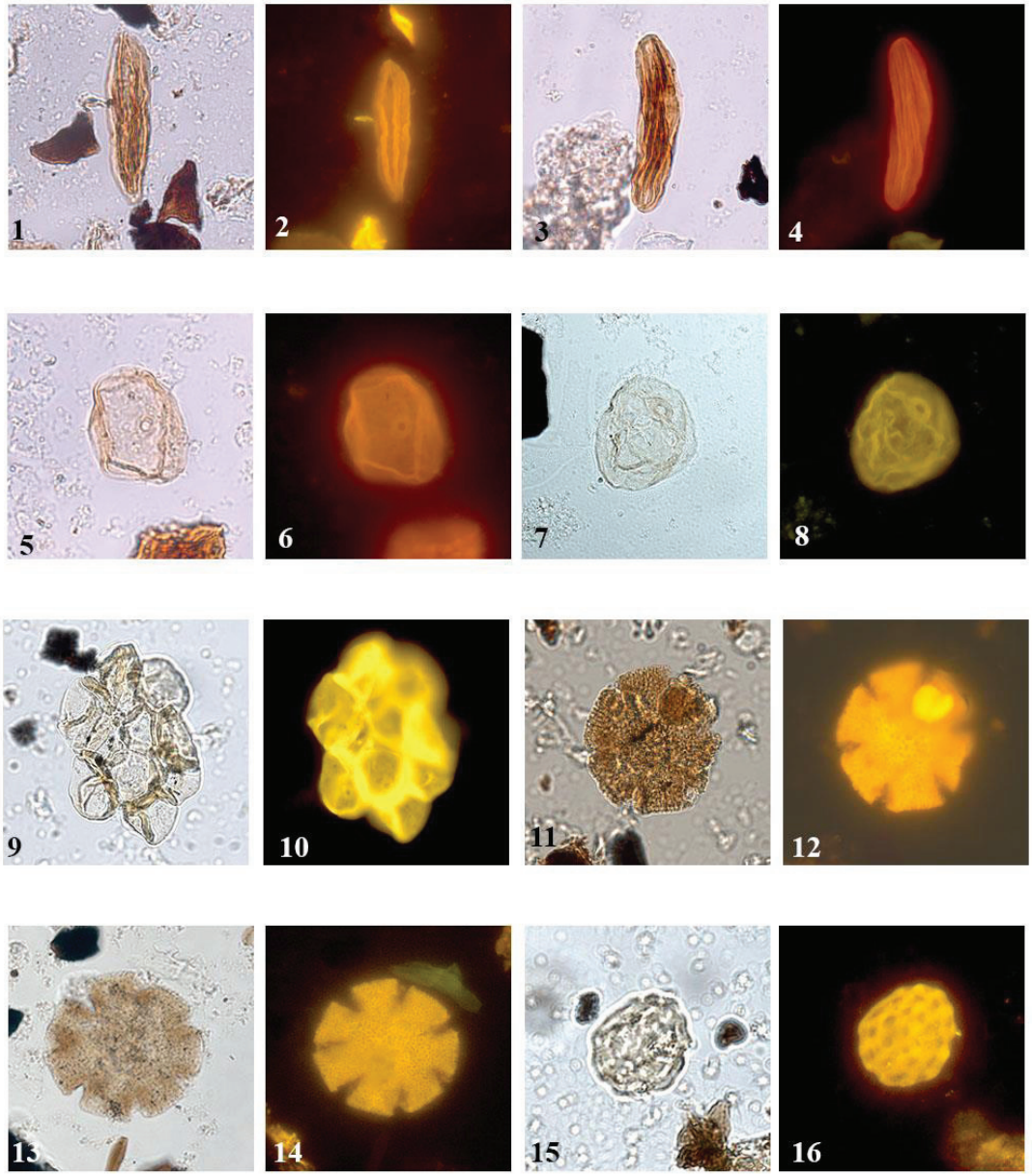

PLATE-17

1. *Periporopollenites multiporatus*, ATD-146, 24.2 µm, Çukurköy Section.

2. *Periporopollenites multiporatus*, ATD-146, 24.2 µm, (fluorescent light), Çukurköy Section.

3. *Periporopollenites stigmosus*, TD-175, 25.6 µm, Çorlu Section.

4. *Periporopollenites stigmosus*, TD-175, 25.6 µm, (fluorescent light), Çorlu Section.

5. *Polyporopollenites stellatus*, ATD-73, 42.2 µm, Koruklu Section.

6. *Polyporopollenites stellatus*, ATD-73, 42.2 µm, (fluorescent light), Koruklu Section.

7. *Polyporopollenites stellatus*, TD-158, 43.6 µm, Köpekli Section.

8. *Polyporopollenites stellatus*, TD-158, 43.6 µm, (fluorescent light), Köpekli Section.

9. *Polyporopollenites undulosus,* TD-175, 32.5 µm, Çorlu Section.

10. *Polyporopollenites undulosus,* TD-175, 32.5 µm, (fluorescent light), Çorlu Section.

11. *Polyvestibulopollenites verus,* ATD-95, 37.1 µm, Güvenç Section.

12. *Polyvestibulopollenites verus,* ATD-95, 37.1 µm, (fluorescent light), Güvenç Section.

13. *Subtriporopollenites* simplex, ATD-126, 45.2 µm, Sofular Section.

14. *Subtriporopollenites* simplex, ATD-126, 45.2 µm, (fluorescent light), Sofular Section.

15. *Subtriporopollenites* simplex, ATD-83, 42.6 µm, Sofular Section.

16. *Subtriporopollenites* simplex, ATD-83, 42.6 µm, (fluorescent light), Sofular Section.

PLATE-17

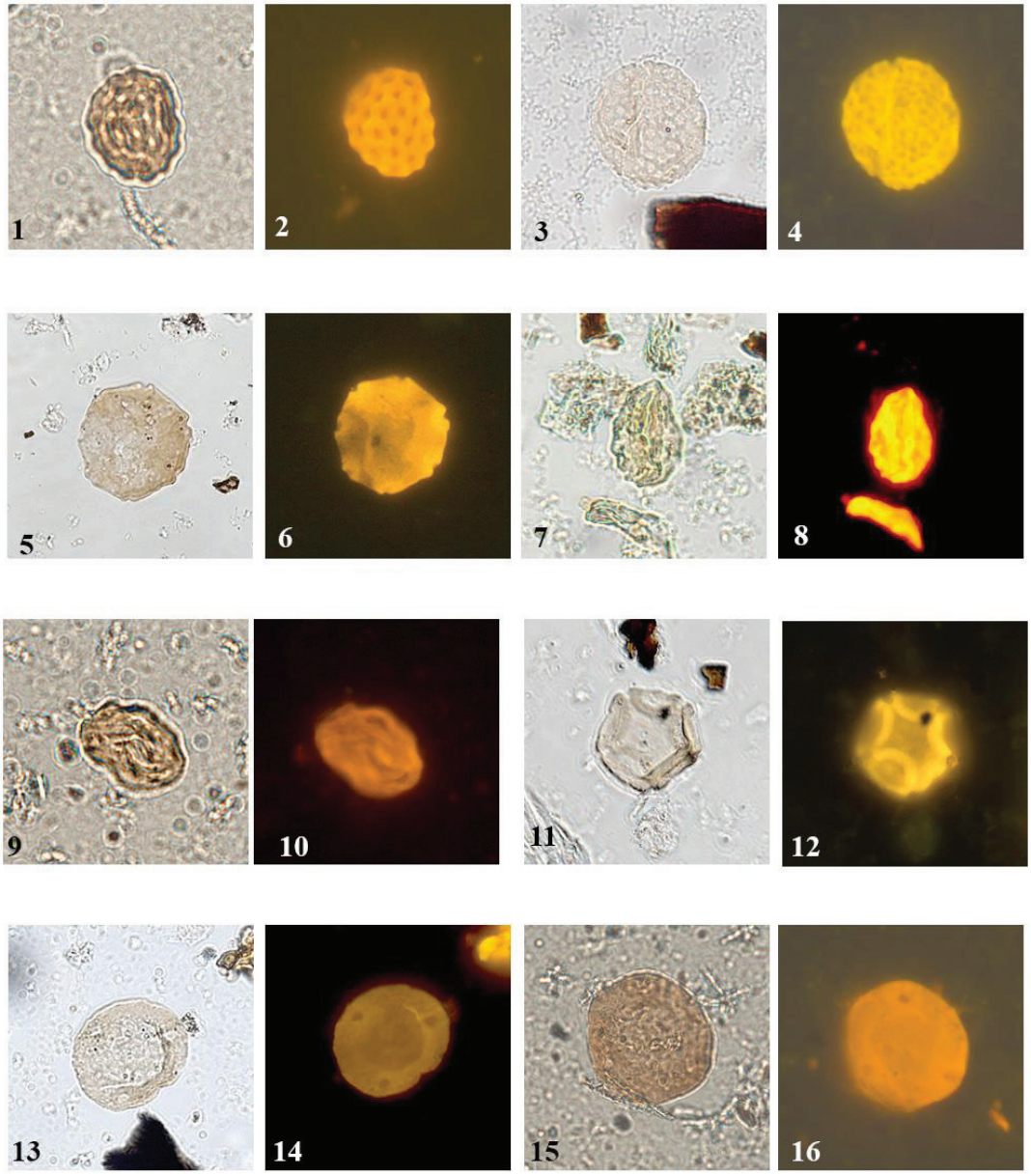

PLATE-18

1. *Intratriporopollenites instructus*, TD-178, 32.7 µm, Çorlu Section.

2. *Intratriporopollenites instructus*, TD-178, 32.7 µm, (fluorescent light), Çorlu Section.

3. *Intratriporopollenites instructus*, ATD-120, 36.2 µm, Sofular Section.

4. *Intratriporopollenites instructus*, ATD-120, 36.2 µm, (fluorescent light), Sofular Section.

5. *Laevigatosporites haardti*, ATD-87, 42.3 µm, Güvenç Section.

6. *Laevigatosporites haardti*, ATD-87, 42.3 µm, (fluorescent light), Güvenç Section.

7. *Leiotriletes adriennis,* TD-180, 44.6 µm, Çorlu Section.

8. *Leiotriletes adriennis,* TD-180, 44.6 µm, (fluorescent light), Çorlu Section.

9. *Leiotriletes adriennis,* ATD-102, 58.6 µm, Güvenç Section.

10. *Leiotriletes adriennis,* ATD-102, 58.6 µm, (fluorescent light), Güvenç Section.

11. *Momipites* sp.*,* ATD-153, 32.7 µm, Çukurköy Section.

12. *Momipites* sp.*,* ATD-161, 31.4 µm, Çukurköy Section.

13. *Momipites* sp.*,* ATD-161, 31.4 µm, (fluorescent light), Çukurköy Section.

14. *Momipites* sp.*,* TD-415, 36.2 µm, Çorlu Section.

15. *Momipites* sp.*,* TD-415, 36.2 µm, (fluorescent light), Çorlu Section.

16. Umbelliferae, ATD-146, 32.4 µm, Çukurköy Section.

PLATE-18

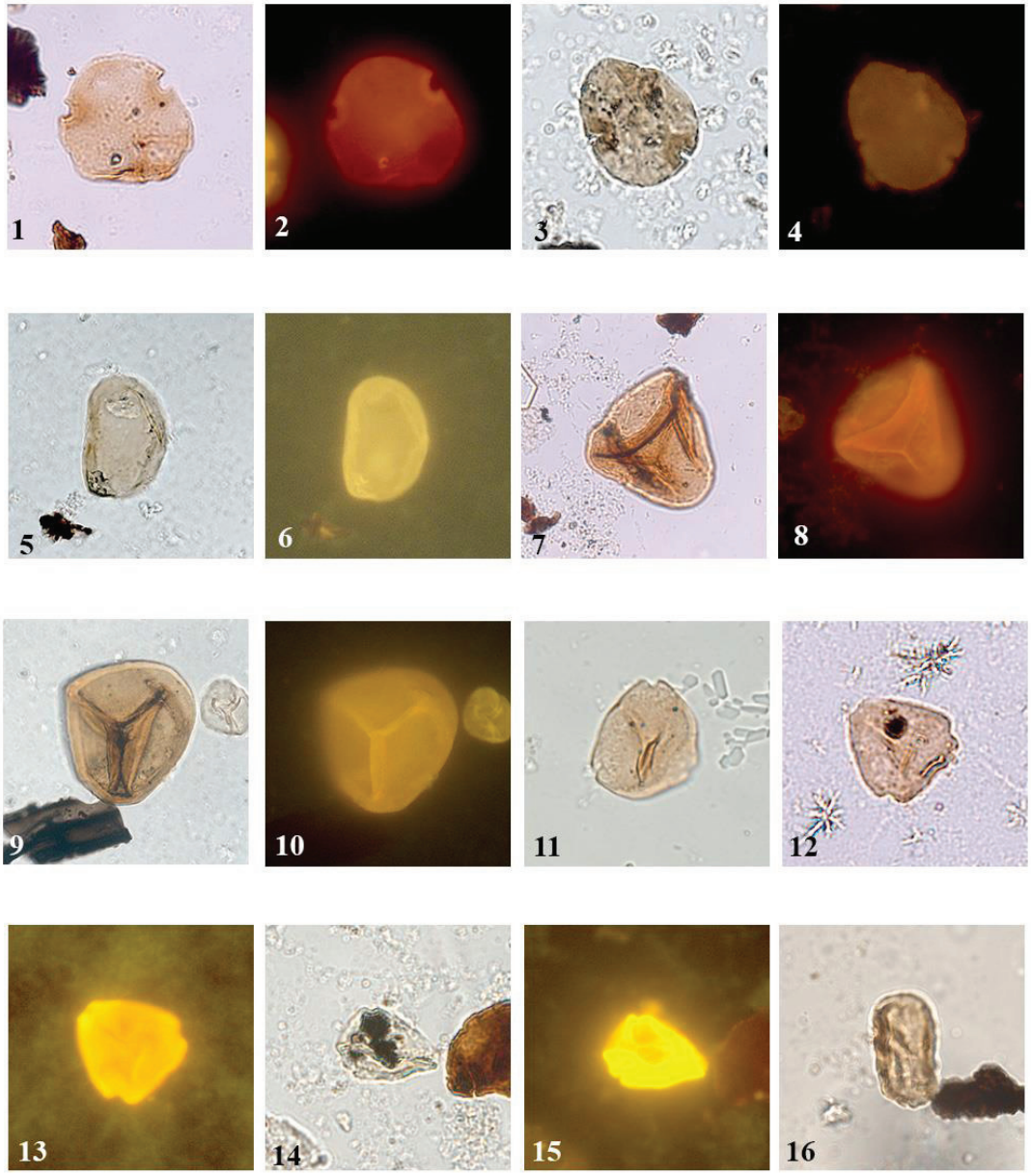

PLATE-19

1. Umbelliferae, ATD-120, 38.4 µm, Sofular Section.

2. Umbelliferae, ATD-120, 38.4 µm, (fluorescent light), Sofular Section.

3. *Verrucatosporites favus*, ATD-119, 58.3 µm, Sofular Section.

4. *Verrucatosporites favus*, ATD-147, 55.2 µm, Çukurköy Section.

5. *Verrucatosporites favus*, ATD-147, 55.2 µm, (fluorescent light), Çukurköy Section.

6. *Inaperturopollenites hiatus,* TD-175, 36.2 µm, Çorlu Section.

7. *Inaperturopollenites hiatus,* TD-175, 36.2 µm, (fluorescent light), Çorlu Section.

8. *Inaperturopollenites hiatus,* ATD-121, 32.7 µm, Sofular Section.

9. *Inaperturopollenites hiatus,* ATD-121, 32.7 µm, (fluorescent light), Sofular Section.

10. *Inaperturopollenites magnus,* ATD-64, 87.4 µm, Bekirli Section.

11. *Inaperturopollenites magnus,* ATD-64, 87.4 µm, (fluorescent light), Bekirli Section.

12. *Tricolporopollenites* sp., ATD-126, 36.2 µm, Sofular Section.

13. Chitinious foraminiferal linings, TD-158, 126.8 µm, Çukurköy Section.

14. Chitinious foraminiferal linings, TD-158, 126.8 µm, (fluorescent light), Çukurköy Section.

15. *Pediastrum* sp., ATD-73, 86.3 µm, (fluorescent light), Koruklu Section.

16. *Botryococcus braunii*, TD-183, 56.2 µm, Çorlu Section.

PLATE-19

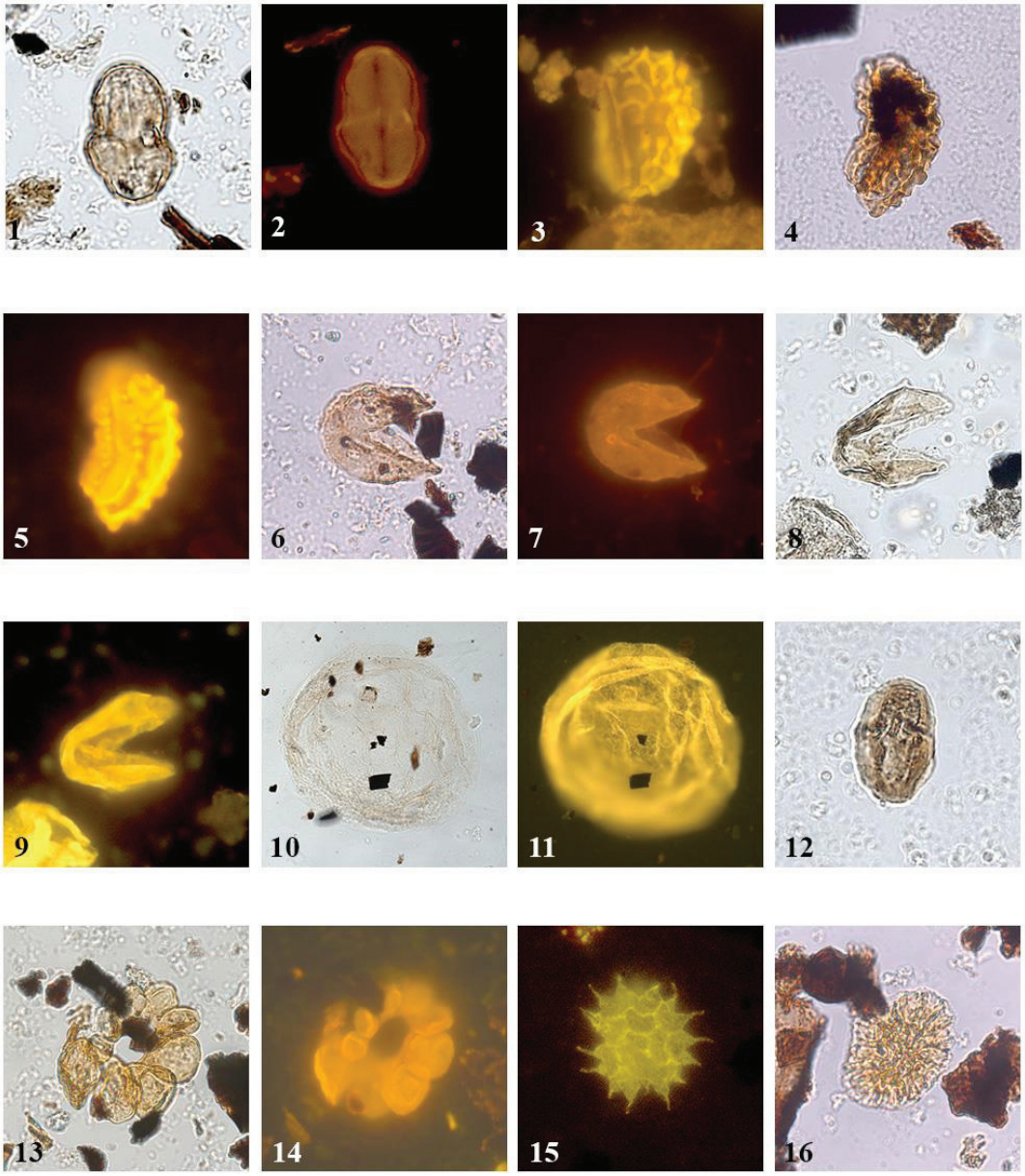

B. MEASURED SECTIONS IN THE ADANA BASIN

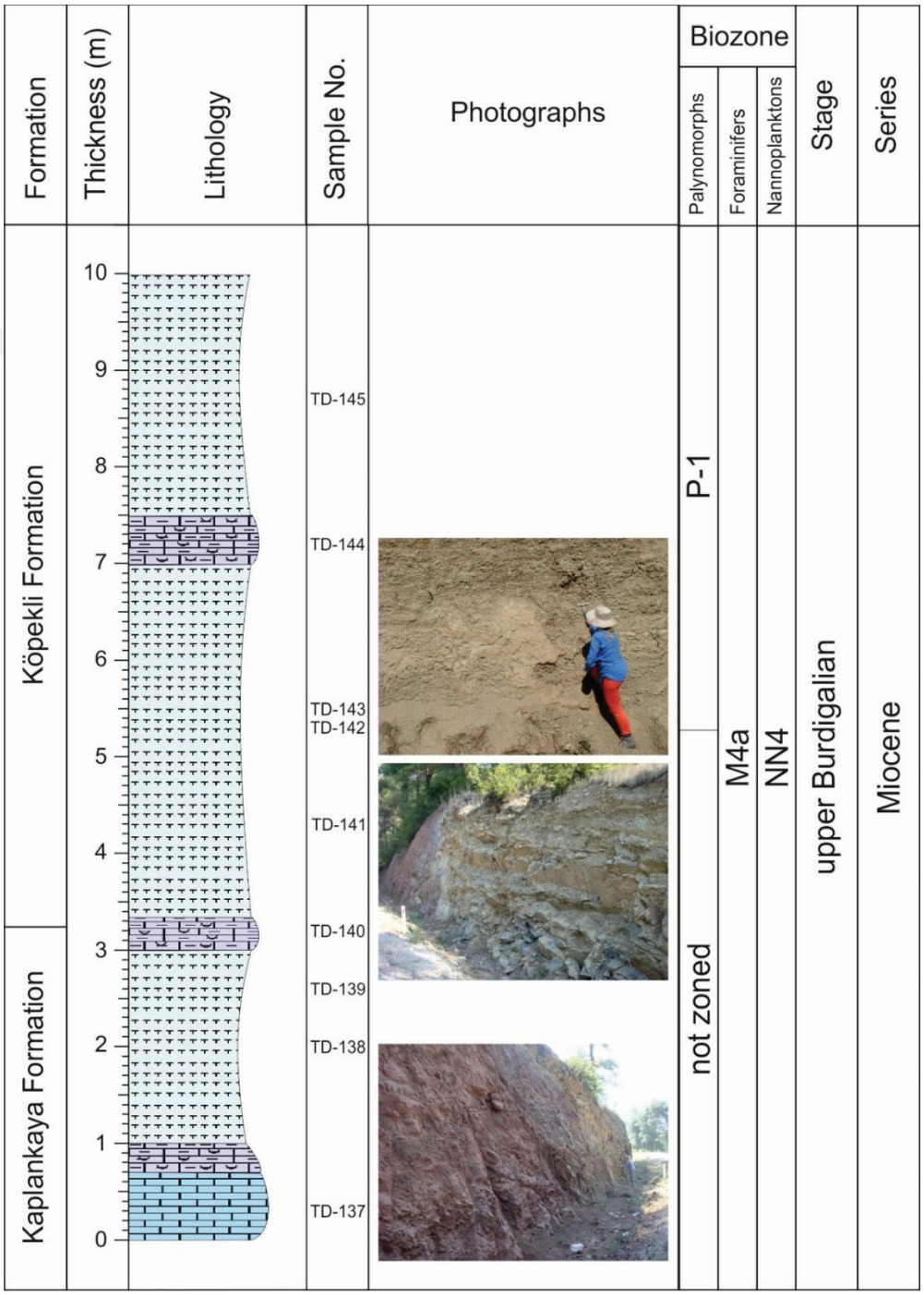

Figure 63. Çukurköy Measured Stratigraphic Section.

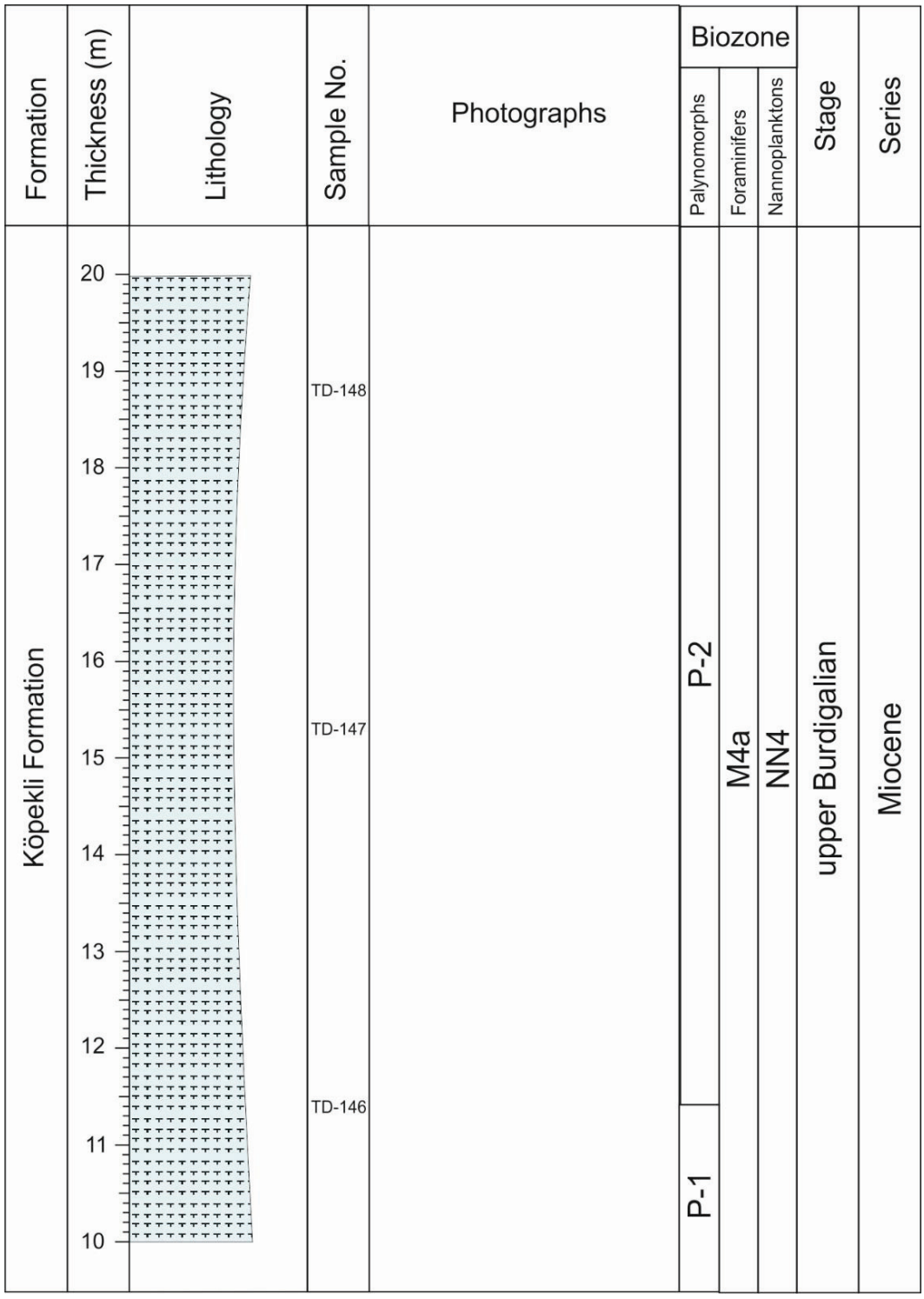

Figure 63. (cont'd)

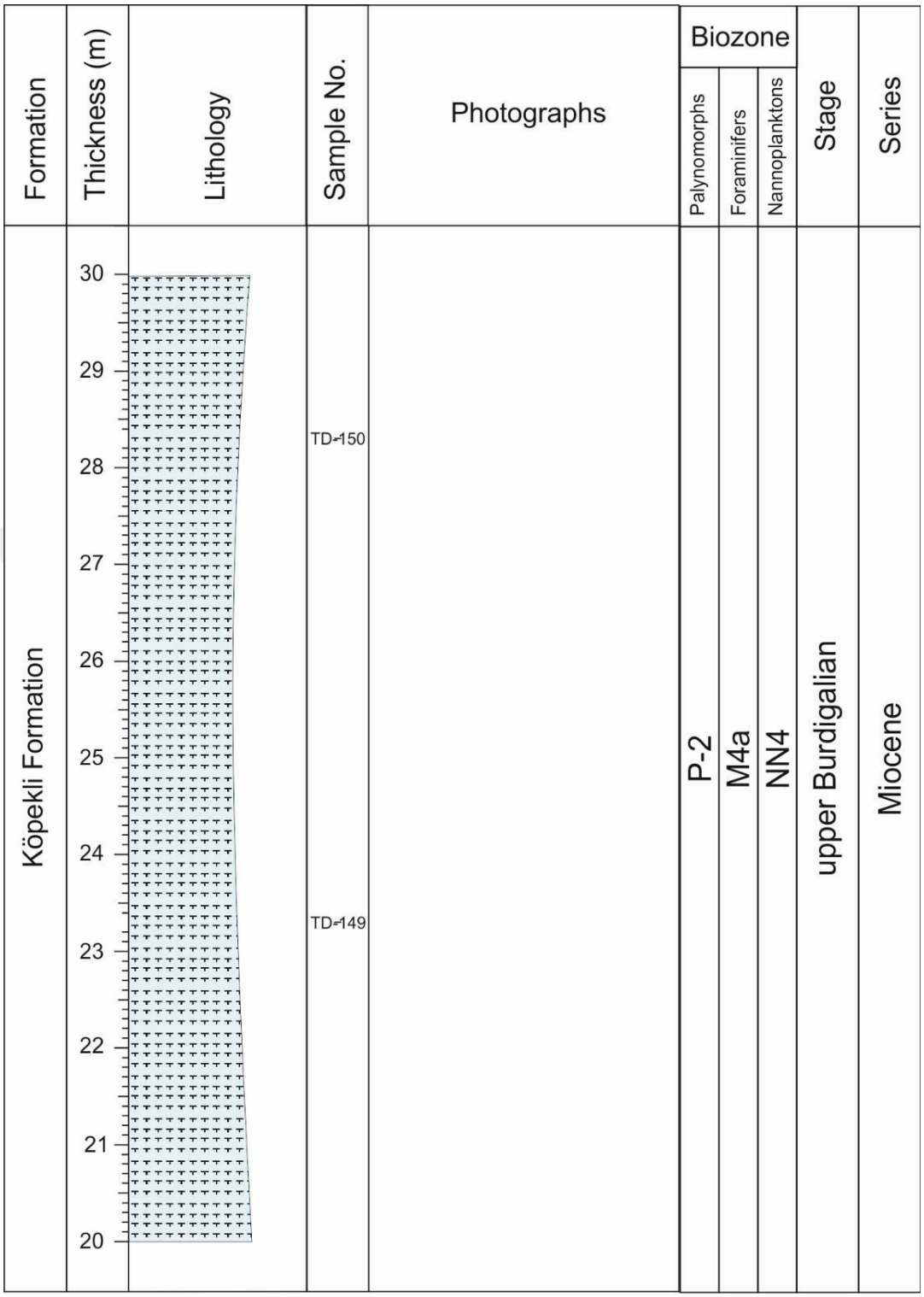

Figure 63. (cont'd)

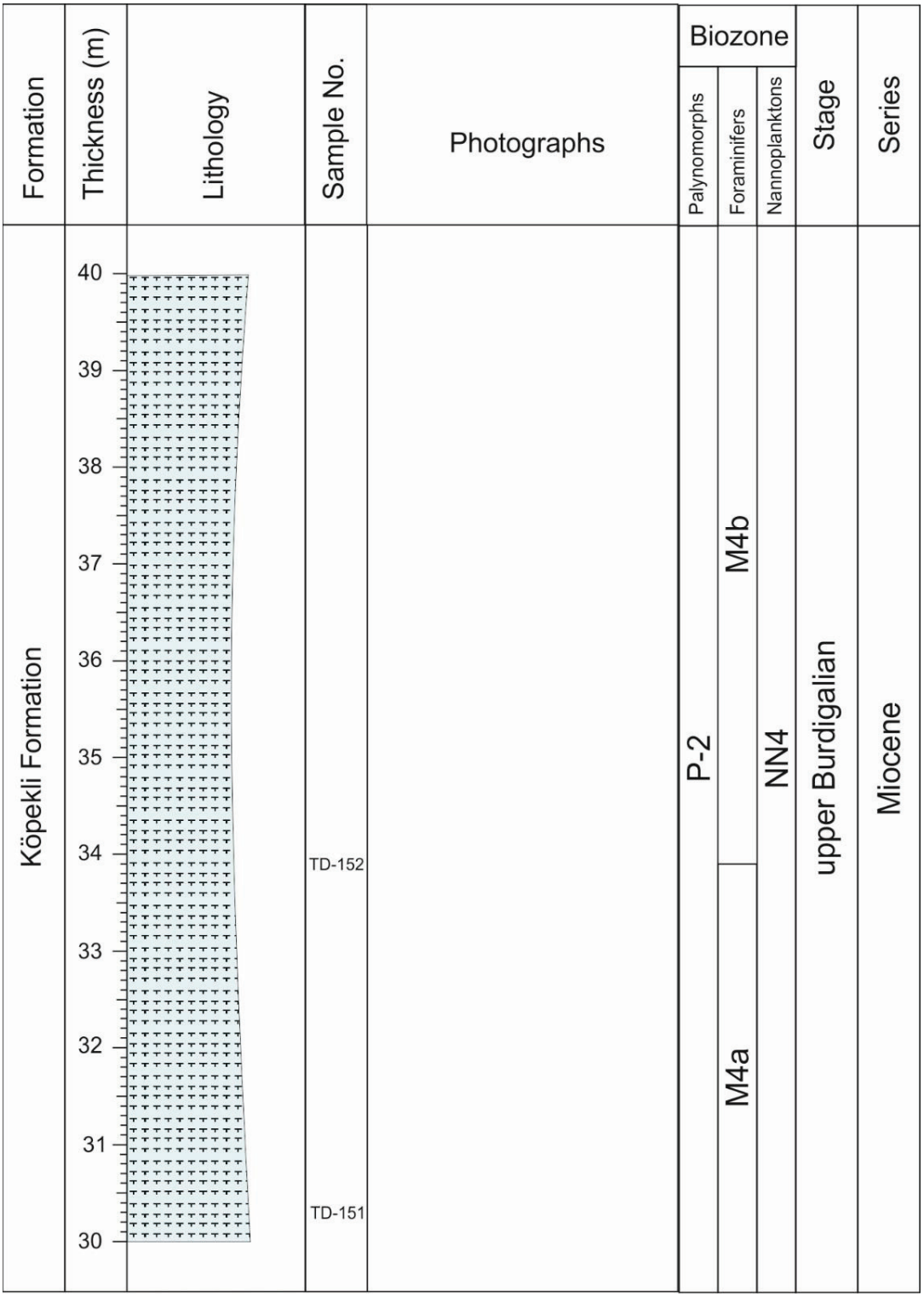

Figure 63. (cont'd)

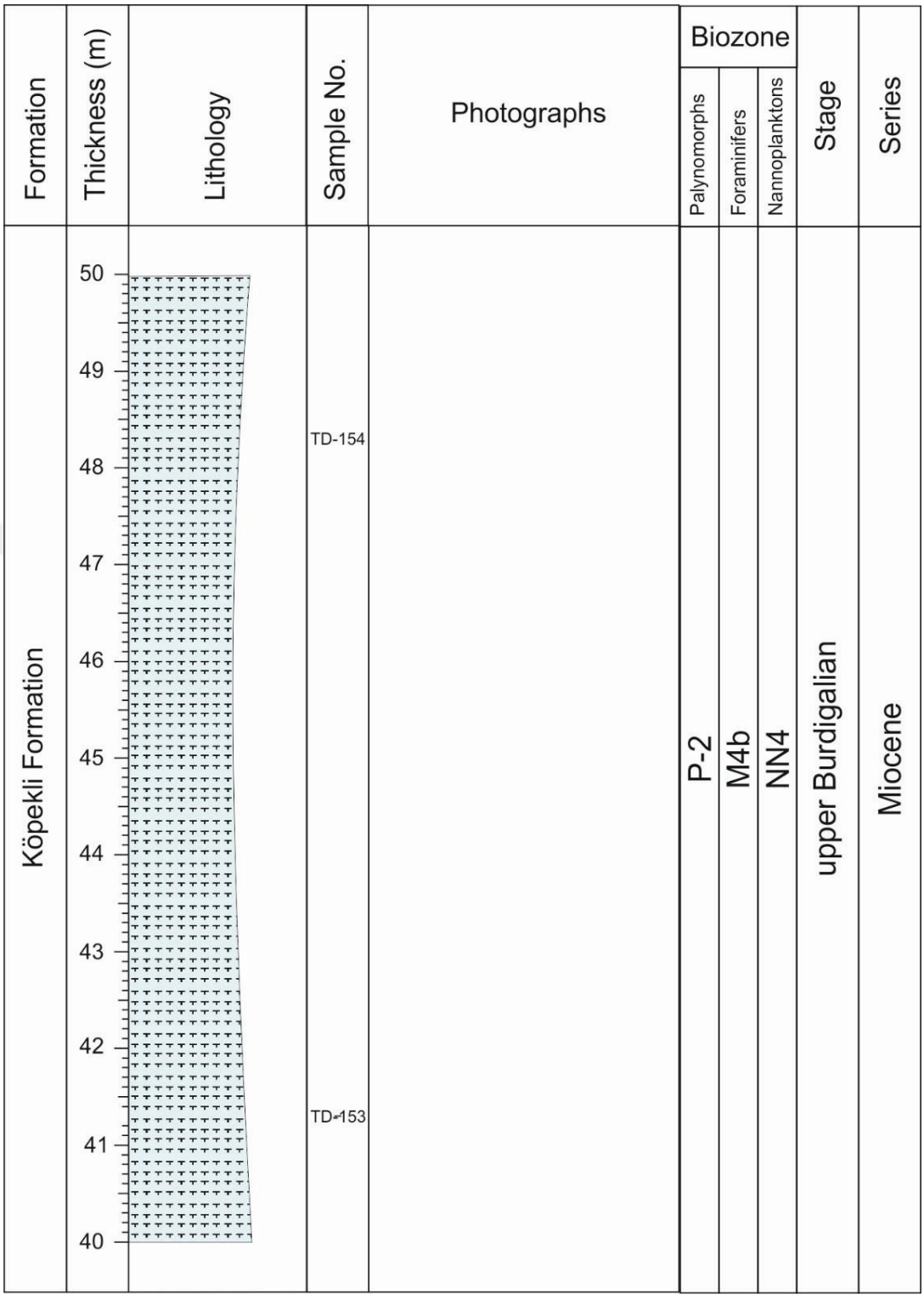

Figure 63. (cont'd)

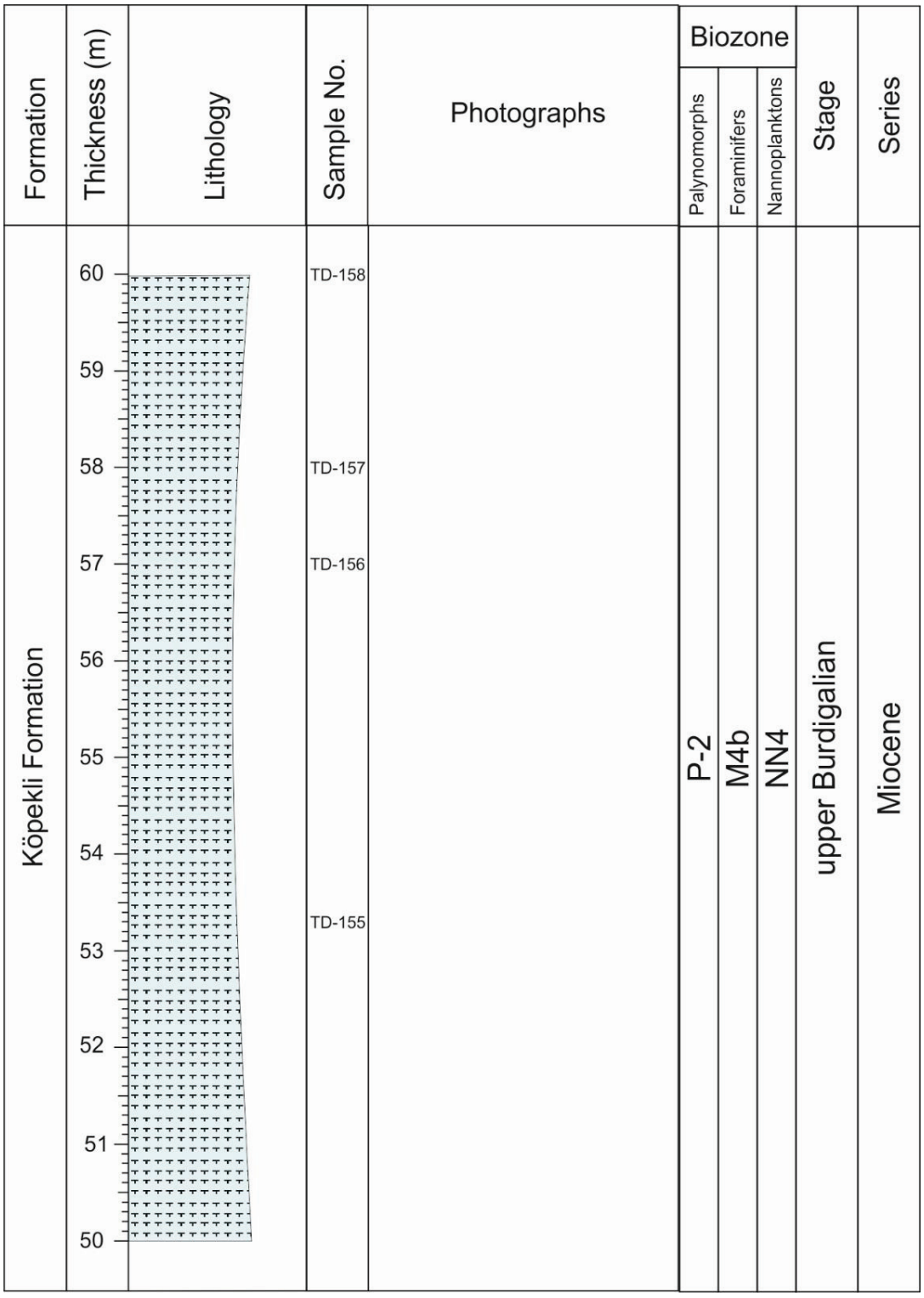

Figure 63. (cont'd)

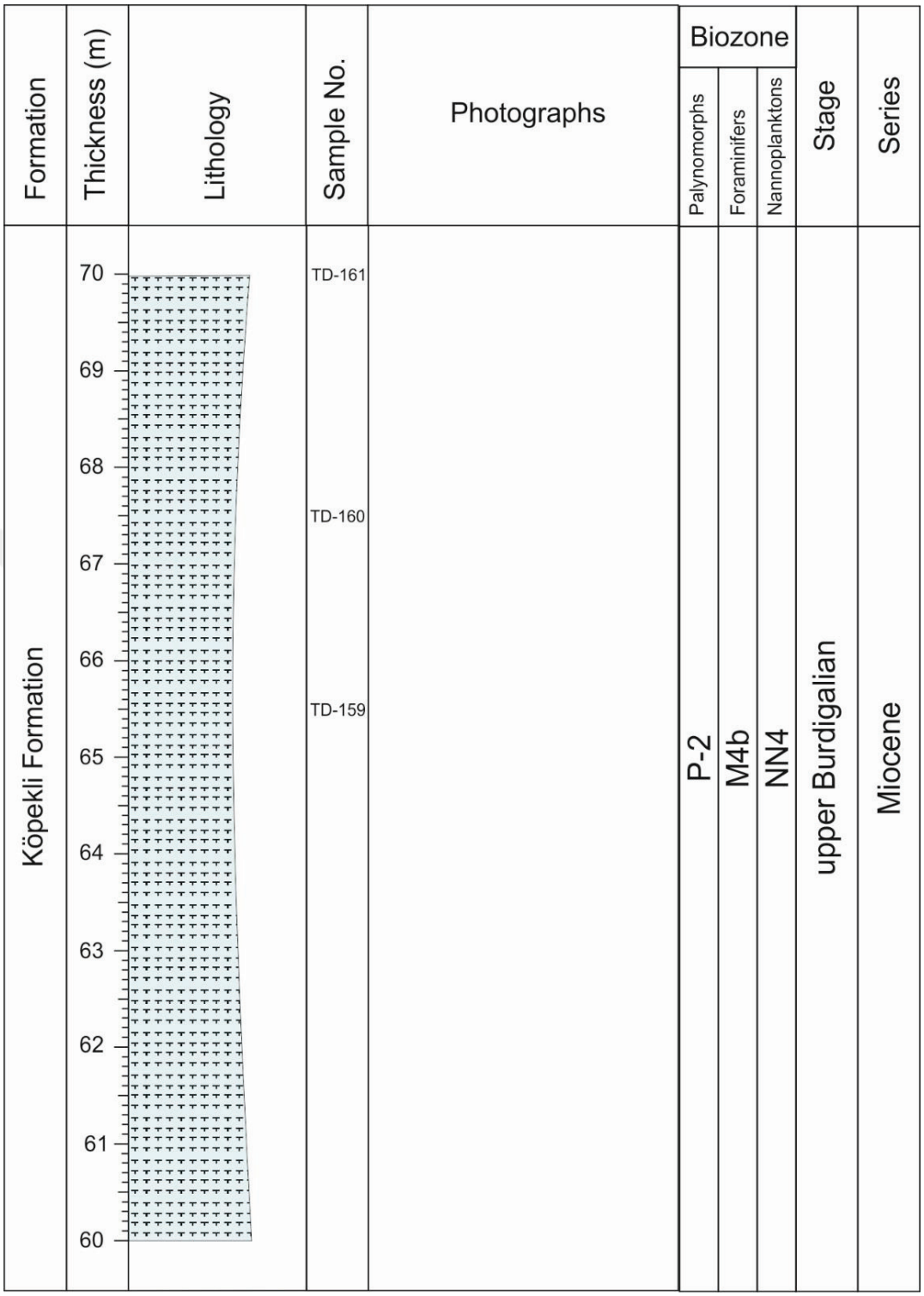

Figure 63. (cont'd)

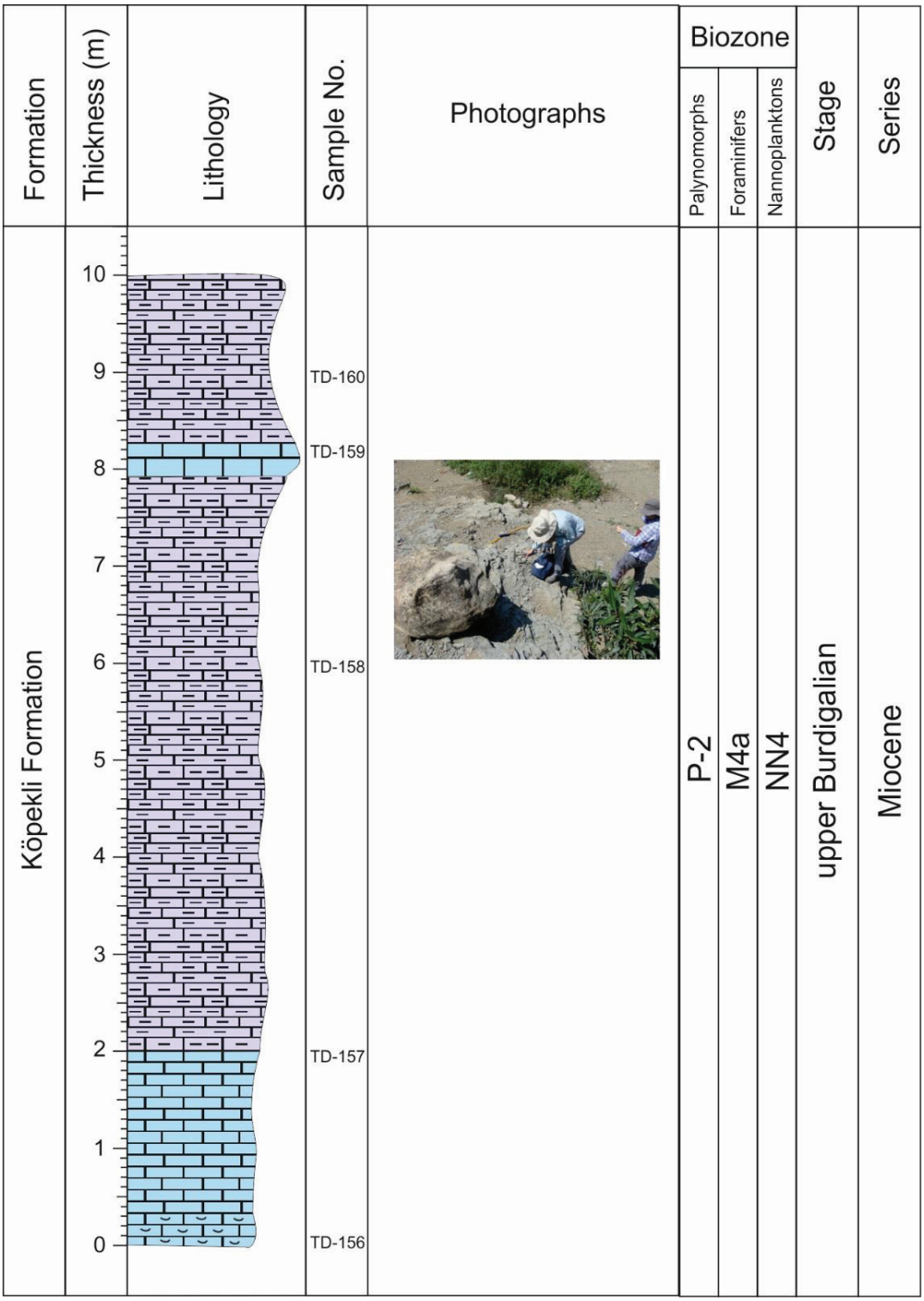

Figure 64. Köpekli Measured Stratigraphic Section.

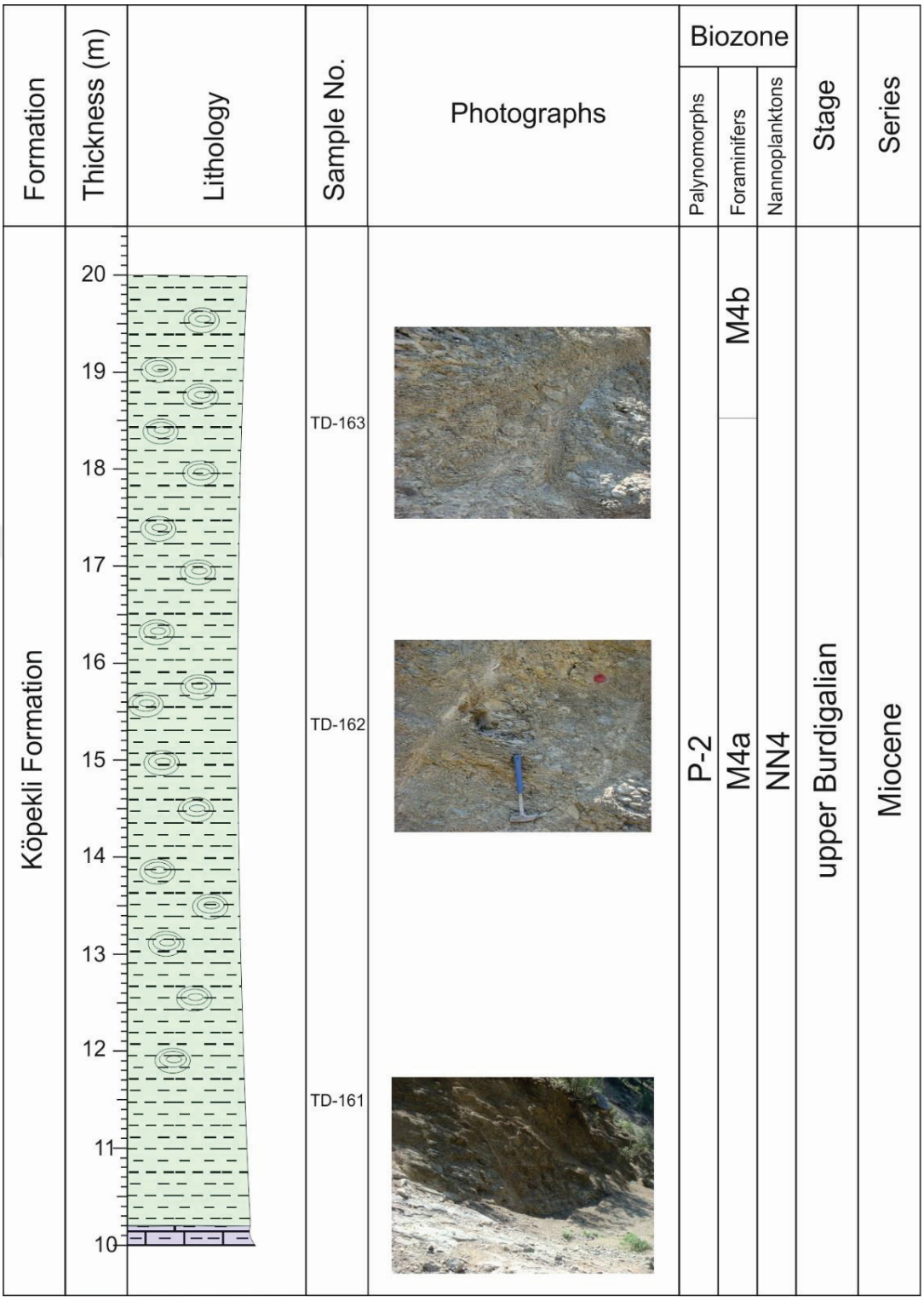

Figure 64. (cont'd)

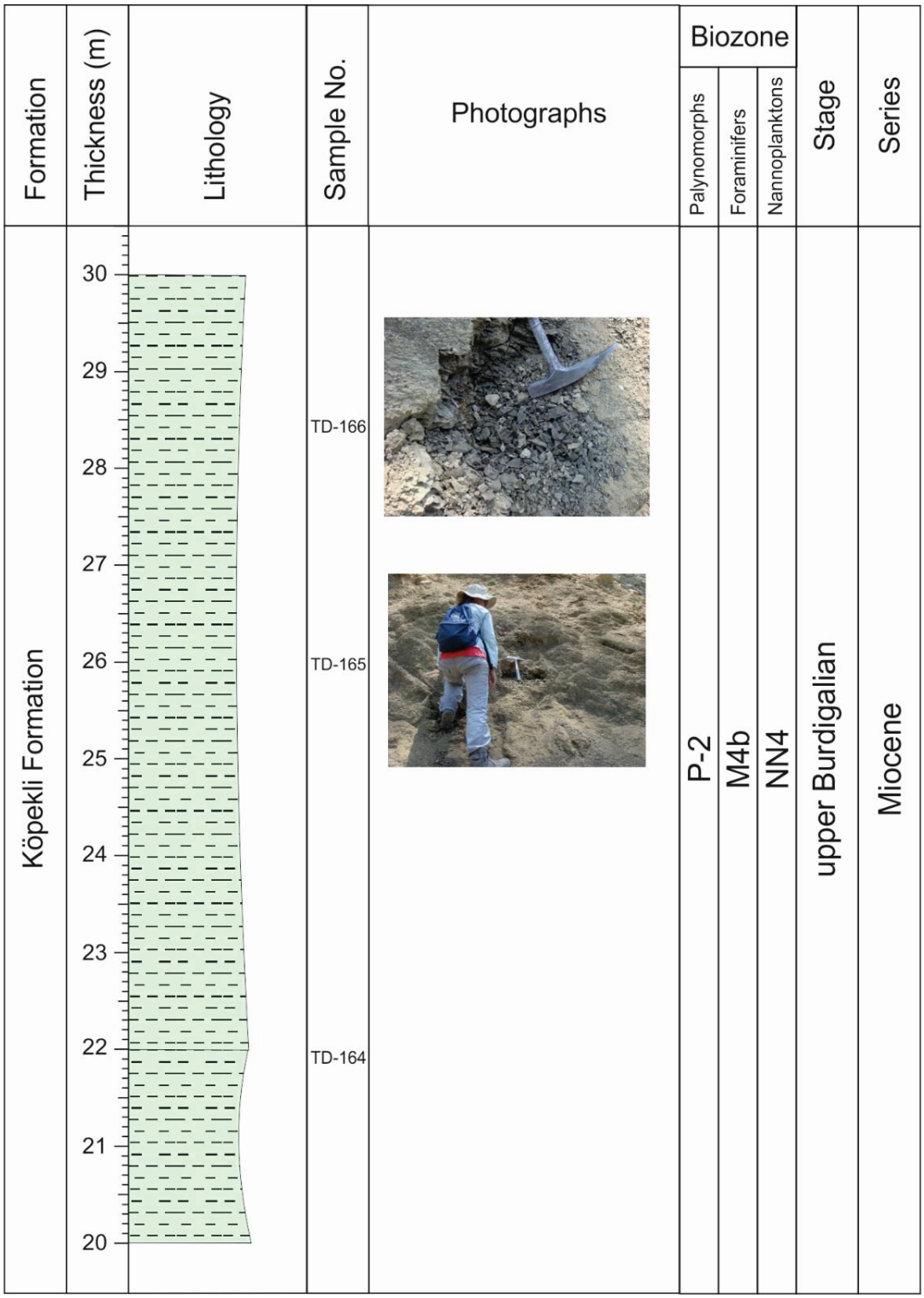

Figure 64. (cont'd)

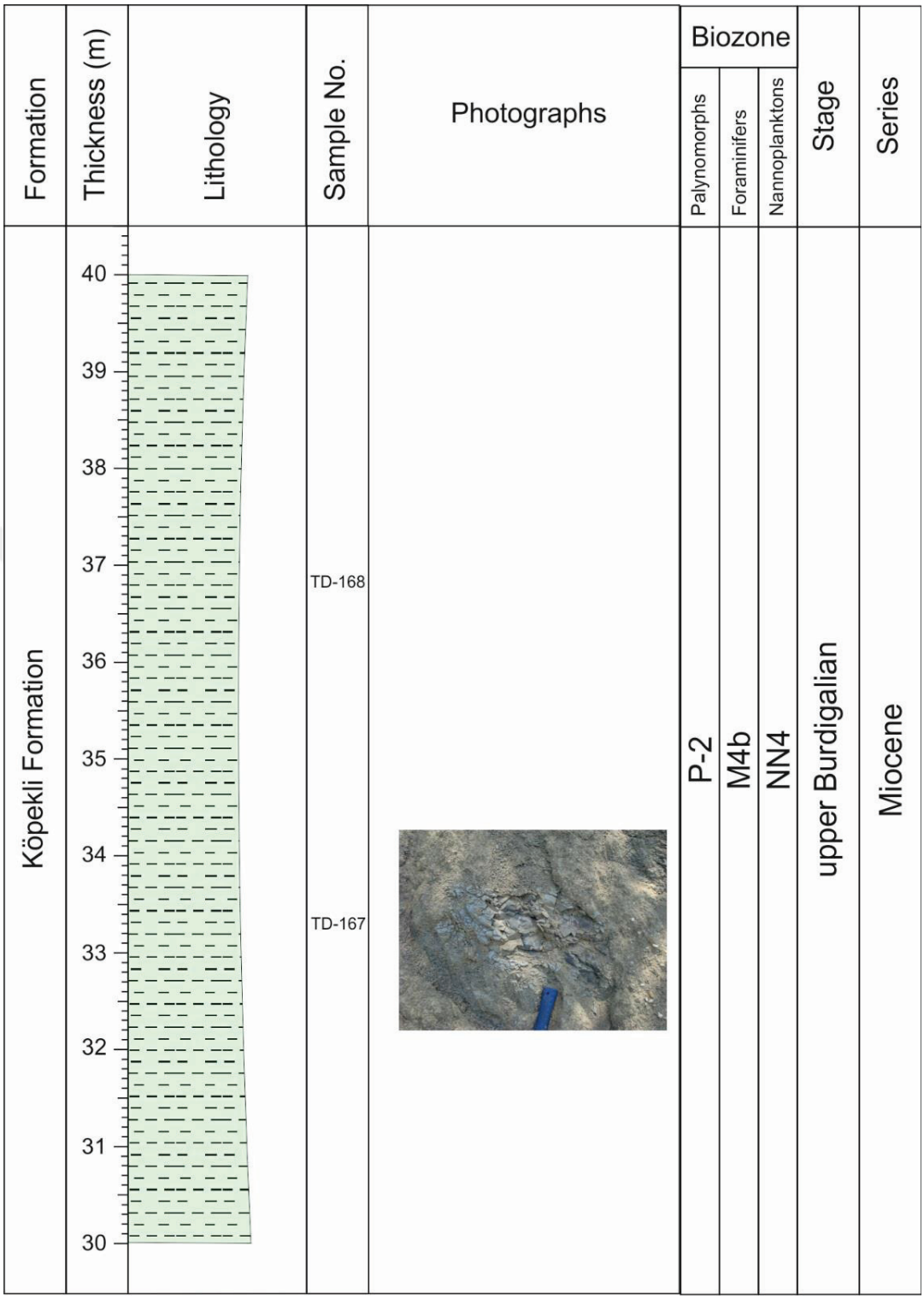

Figure 64. (cont'd)

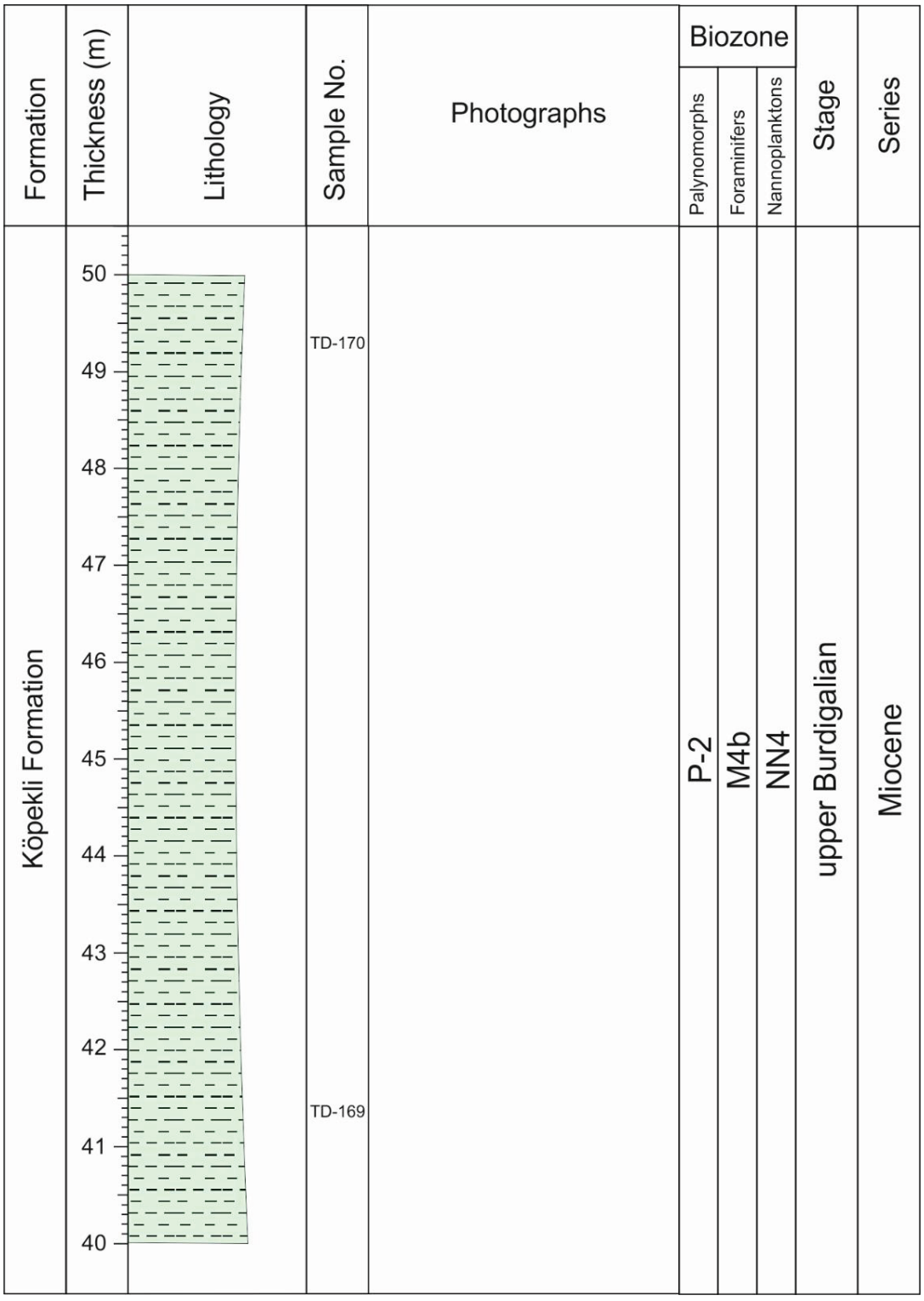

Figure 64. (cont'd)

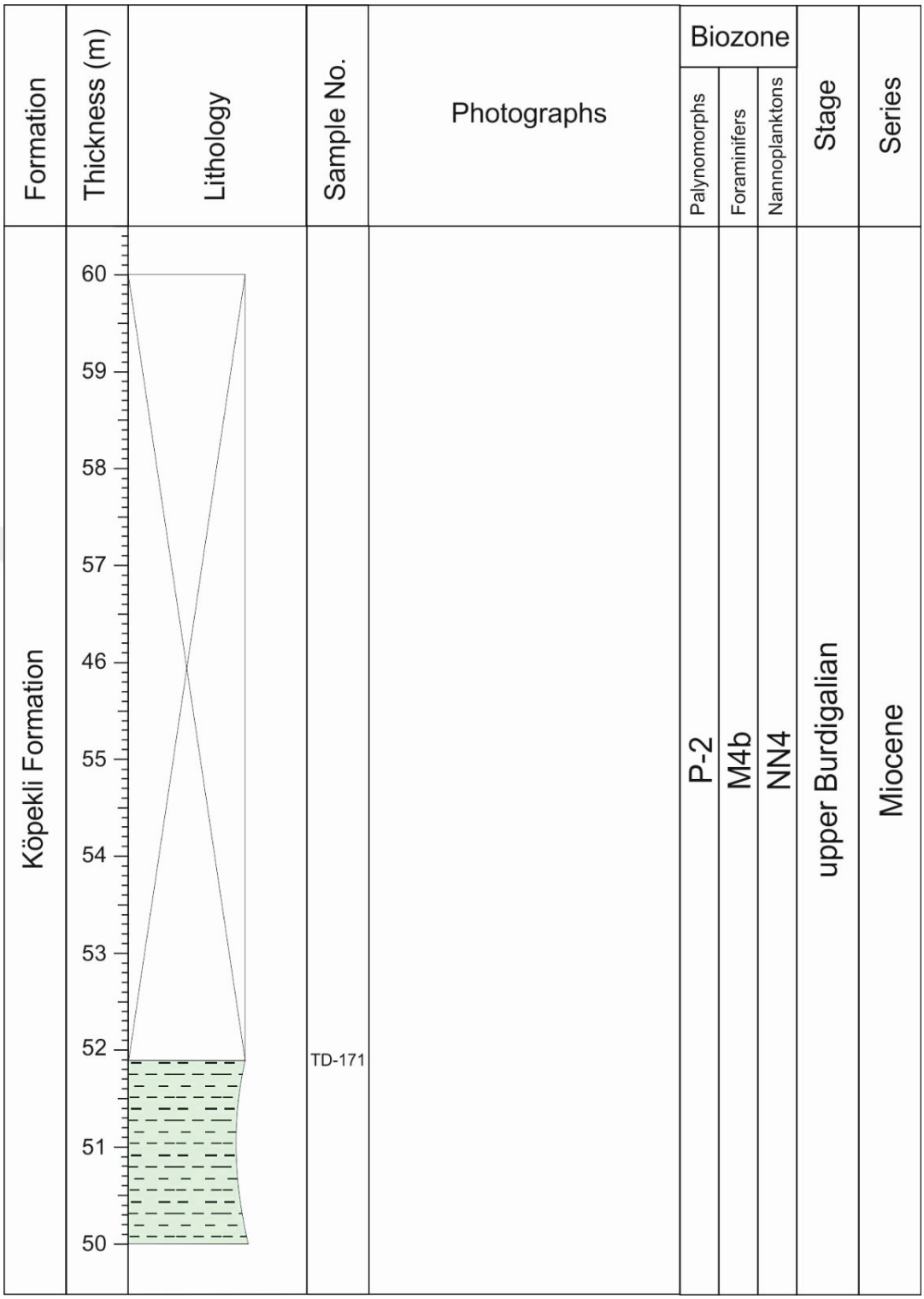

Figure 64. (cont'd)

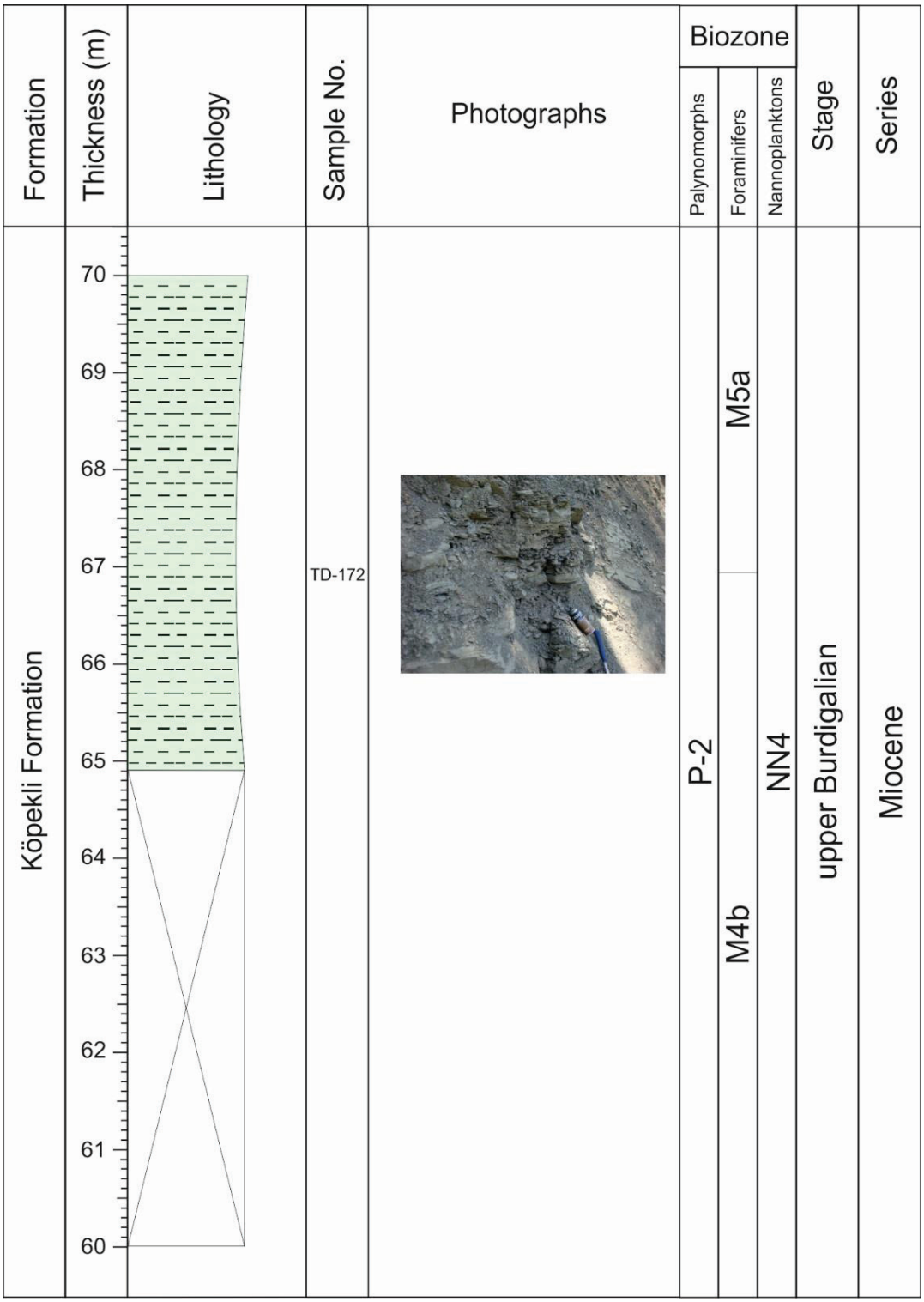

Figure 64. (cont'd)

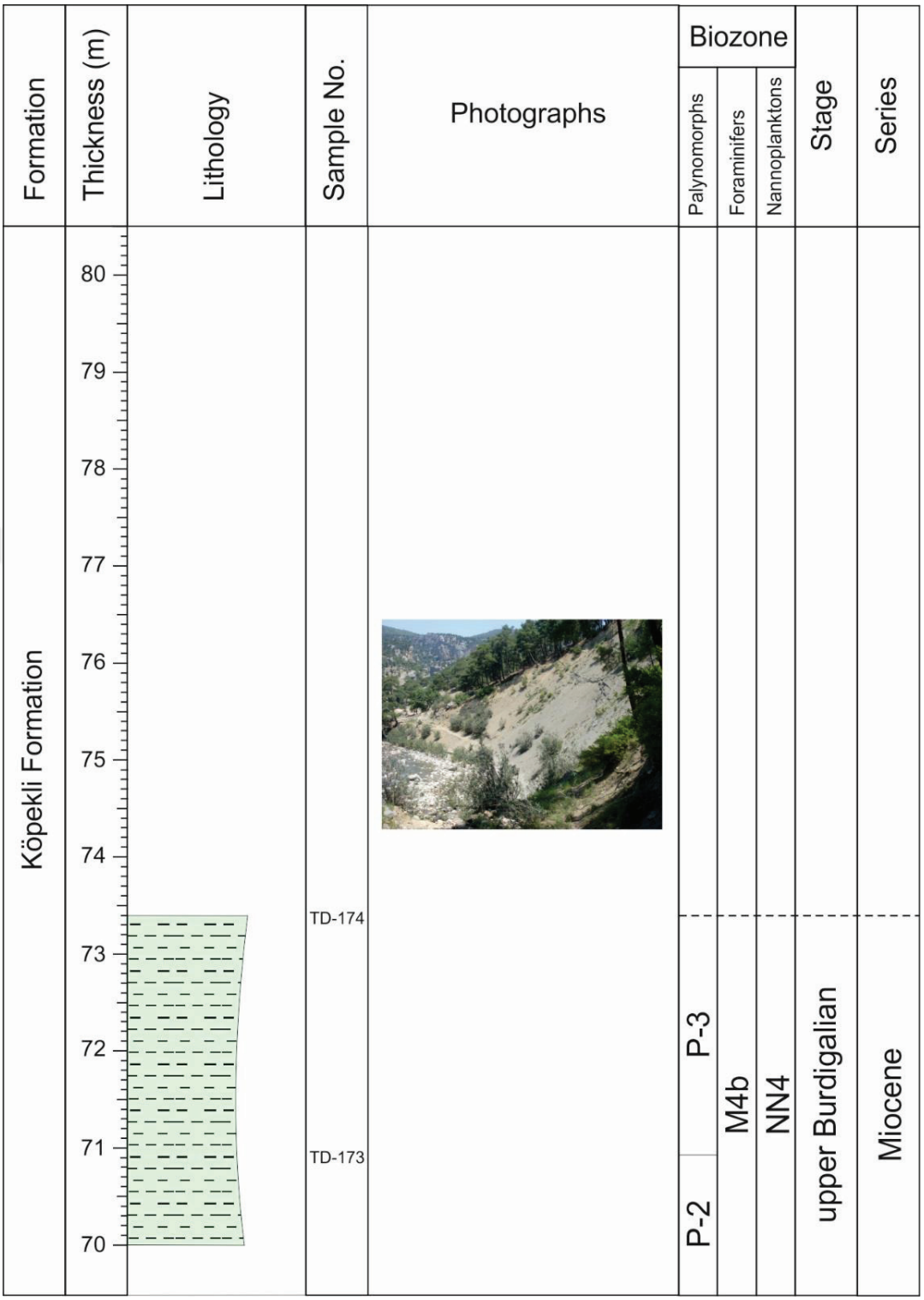

Figure 64. (cont'd)

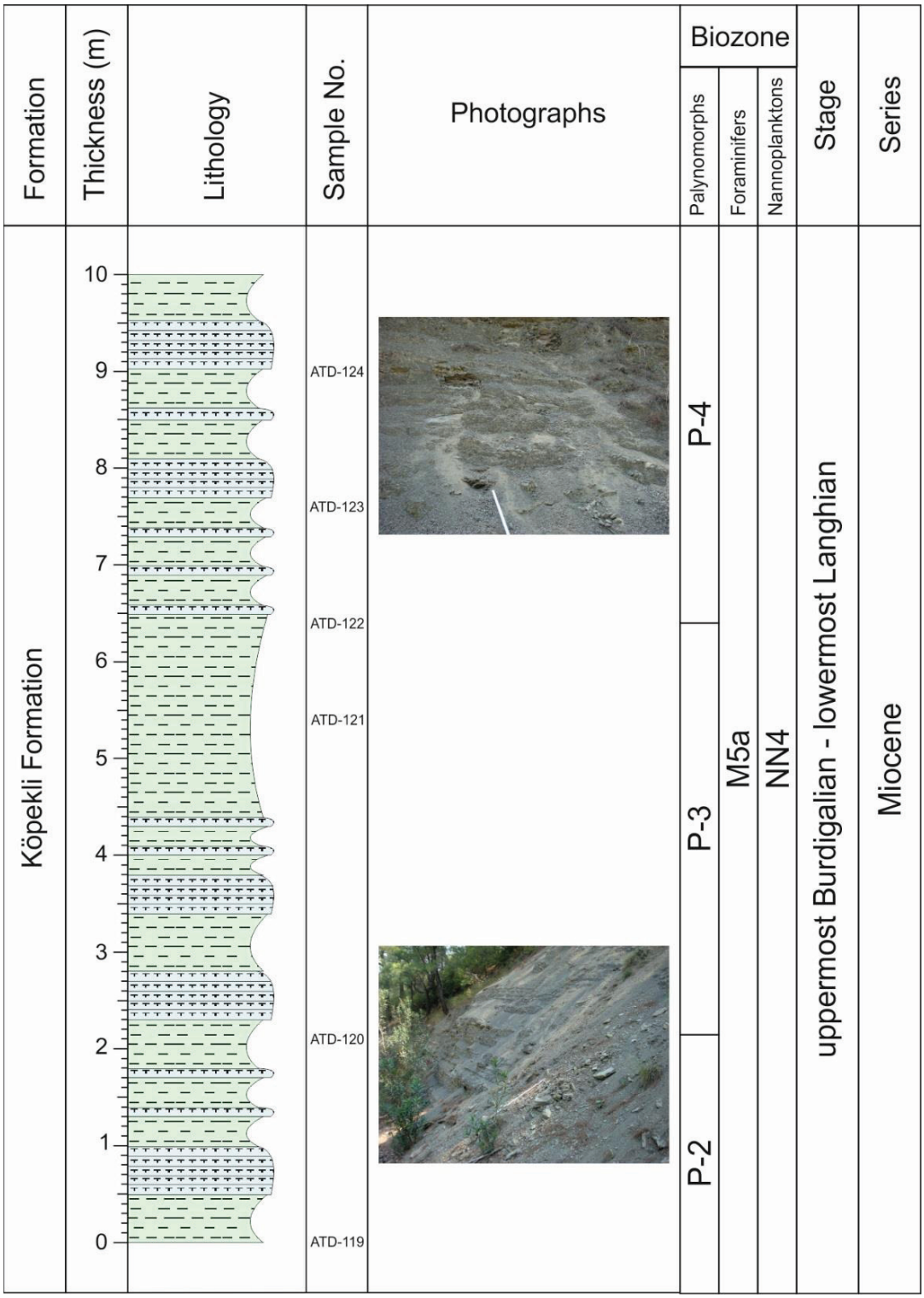

Figure 65. Sofular Measured Stratigraphic Section.

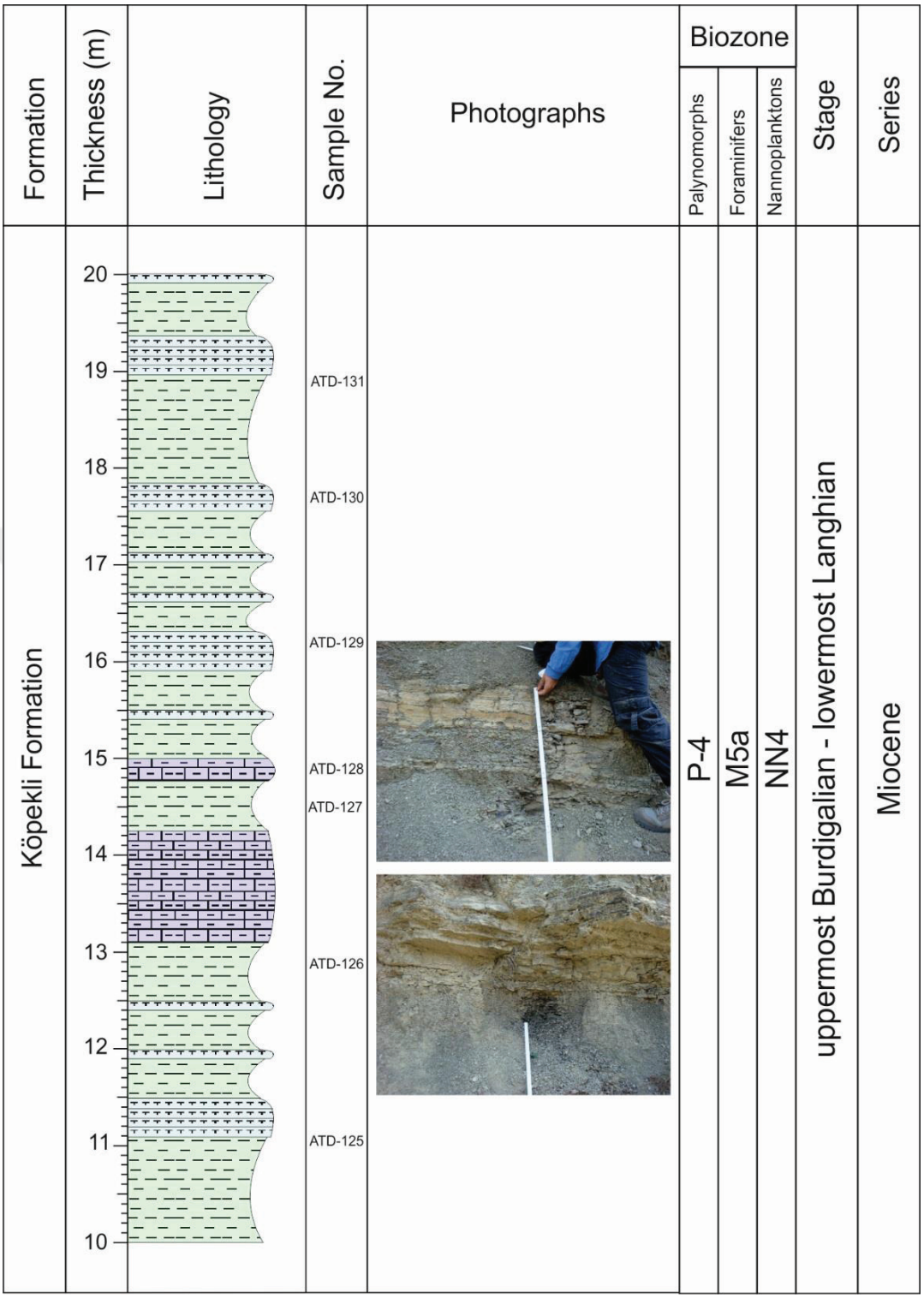

Figure 65. (cont'd)

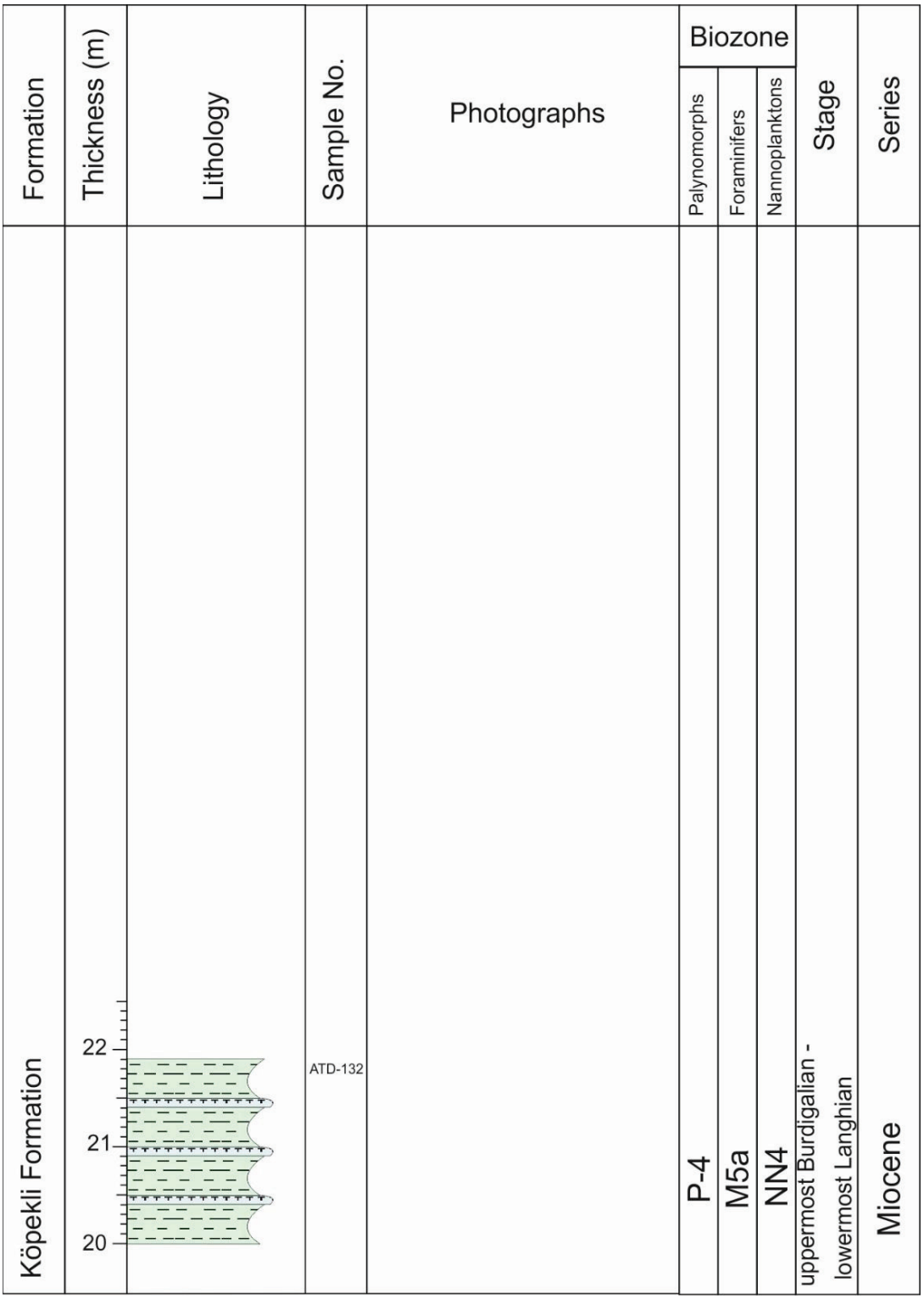

Figure 65. (cont'd)

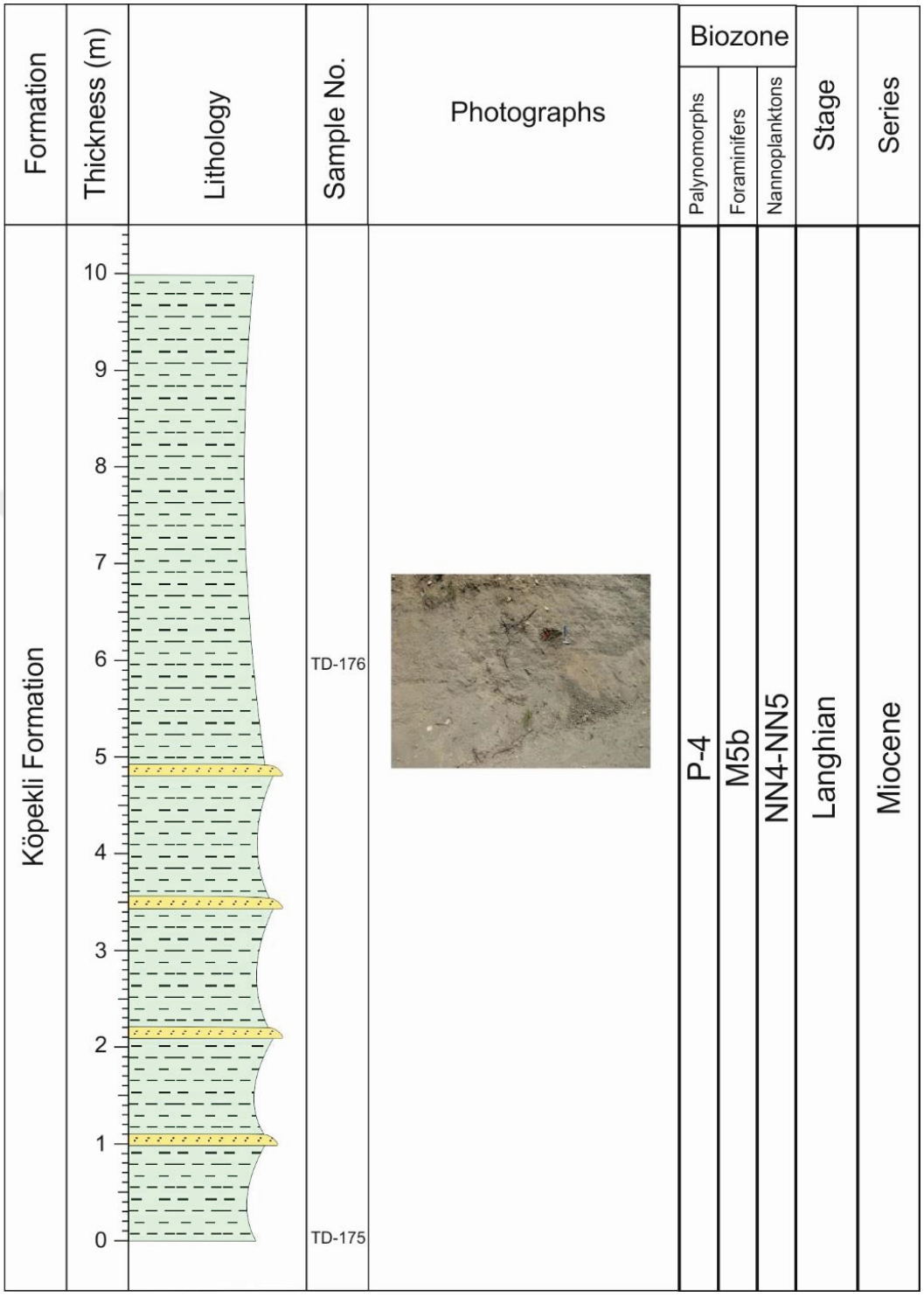

Figure 66. Çorlu Measured Stratigraphic Section.

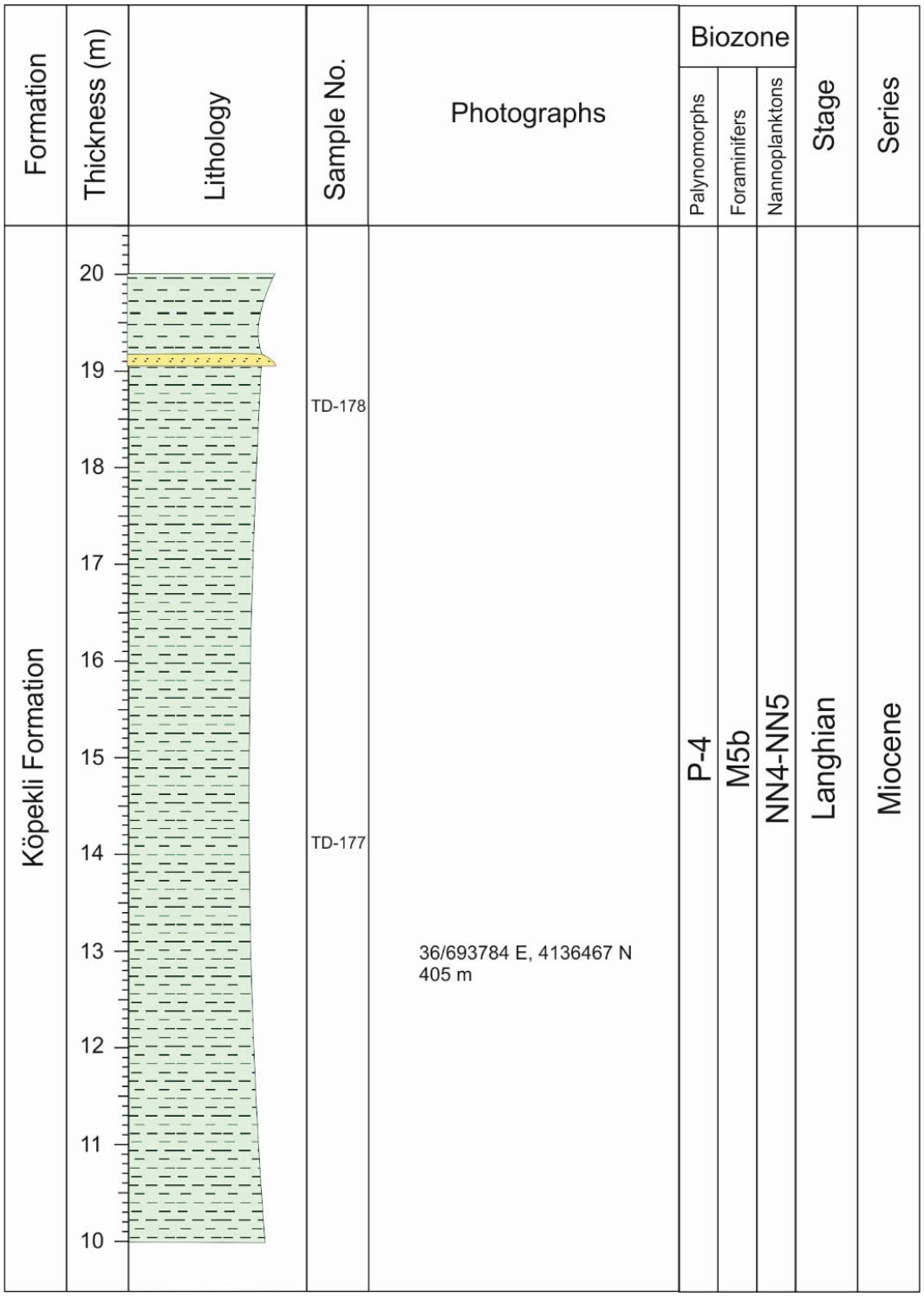

Figure 66. (cont'd)

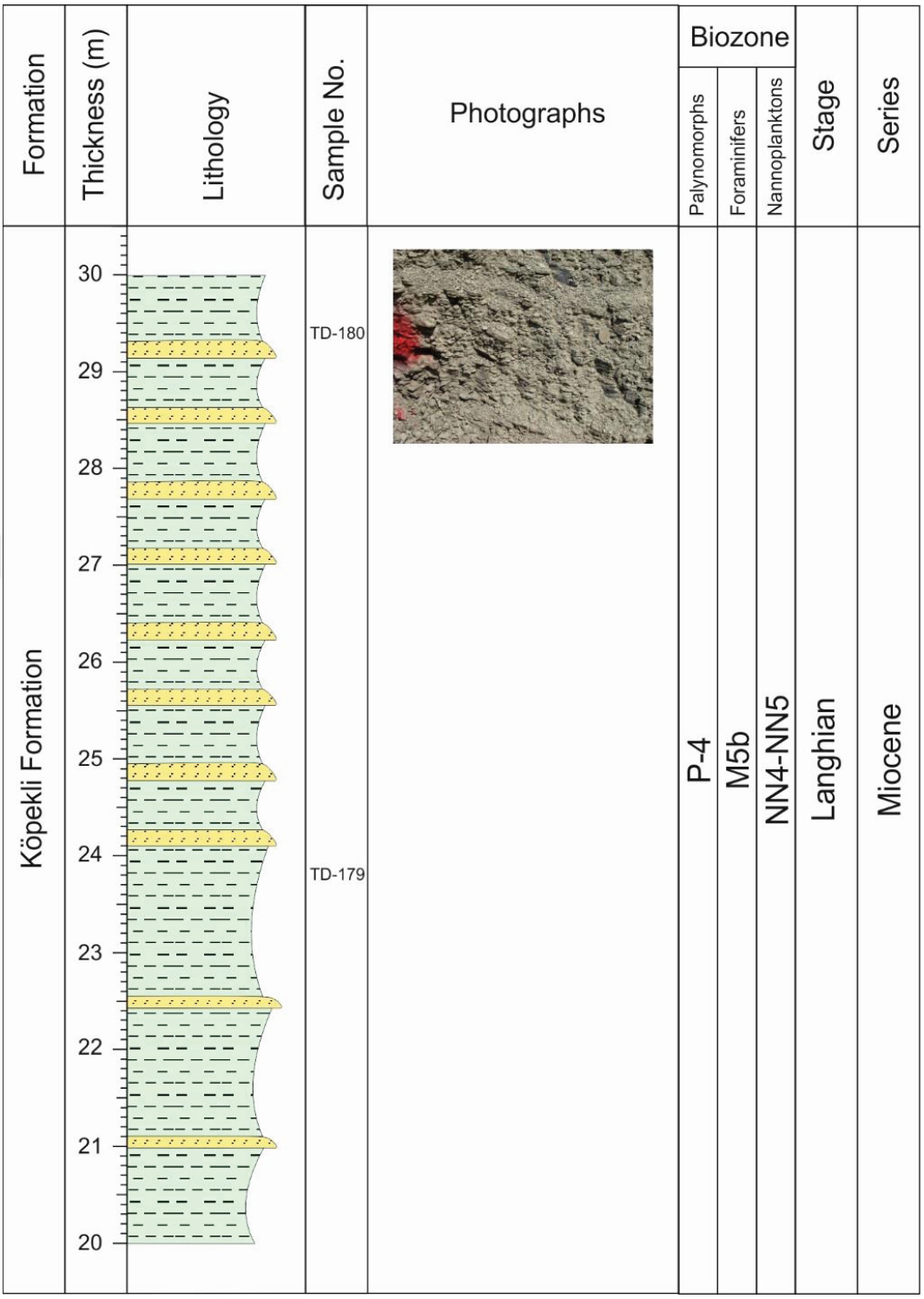

Figure 66. (cont'd)

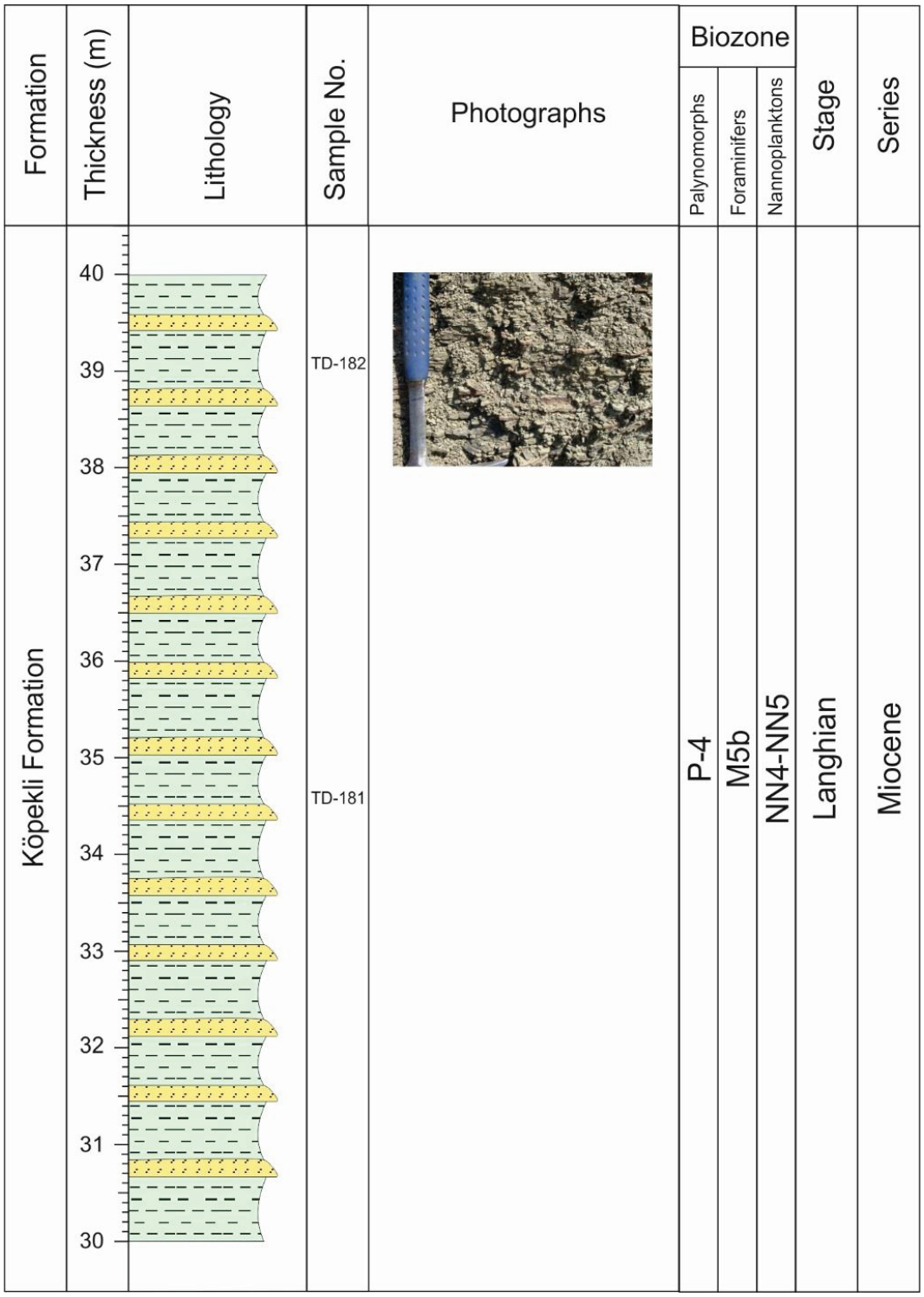

Figure 66. (cont'd)

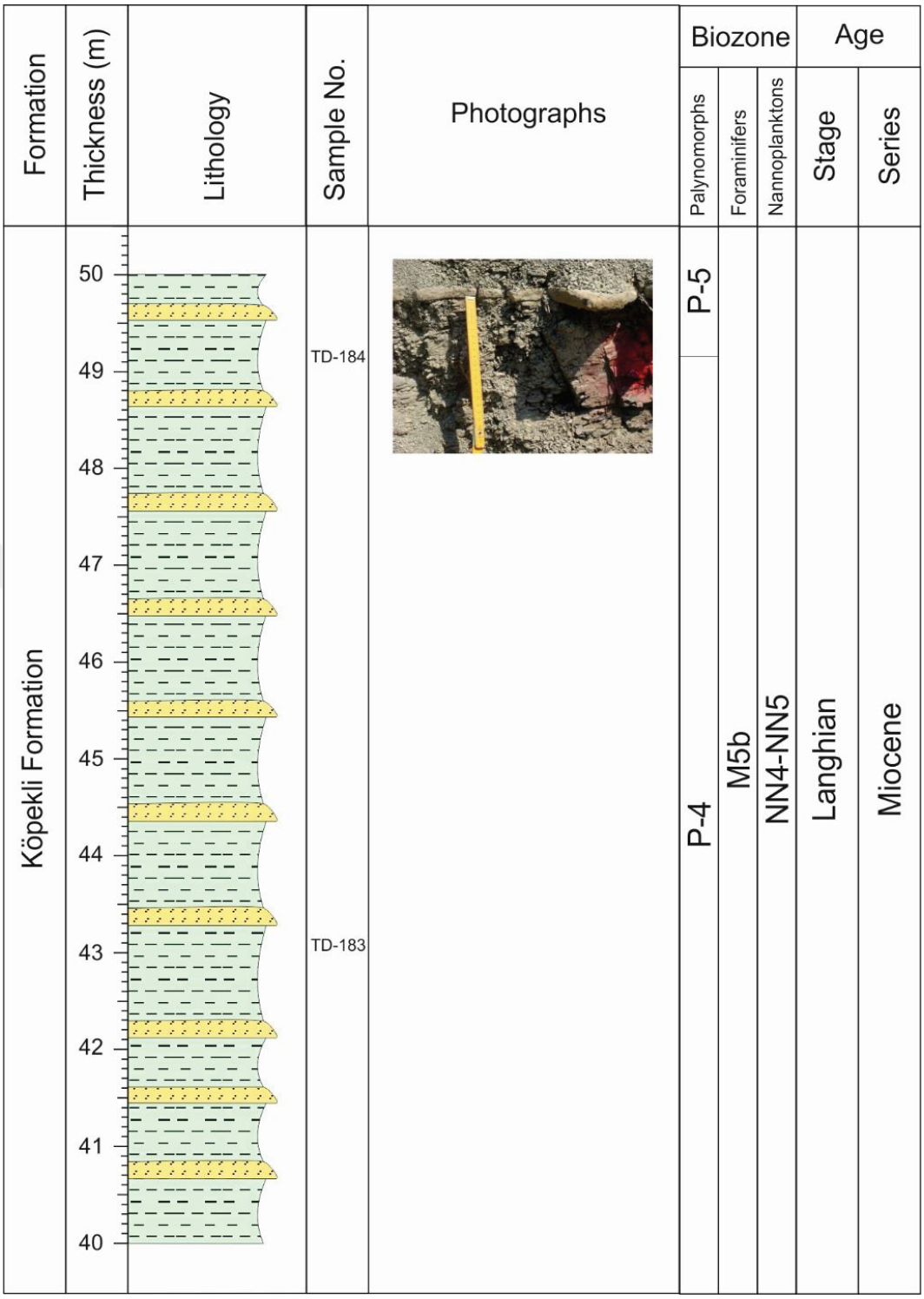

Figure 66. (cont'd)

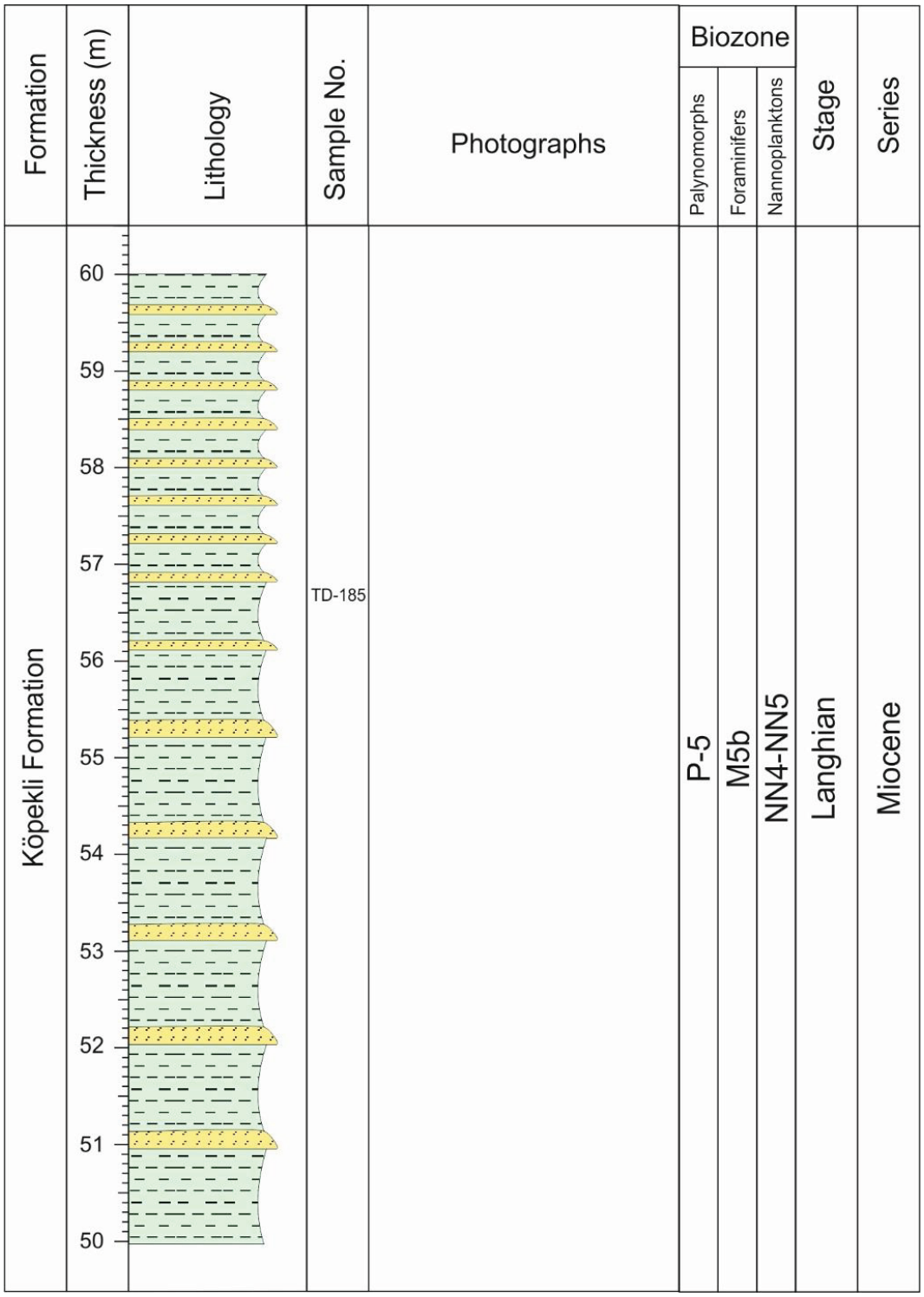

Figure 66. (cont'd)

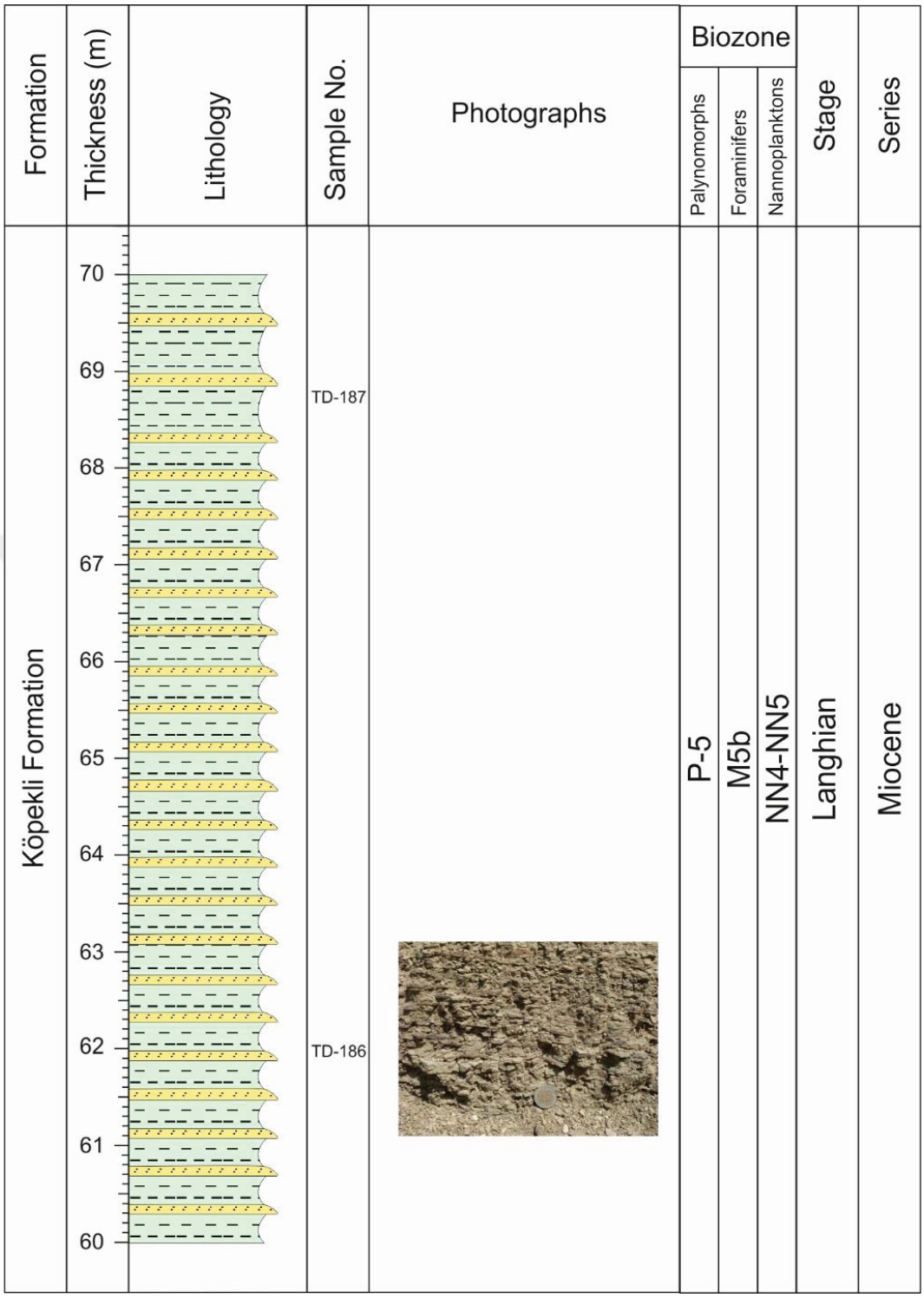

Figure 66. (cont'd)

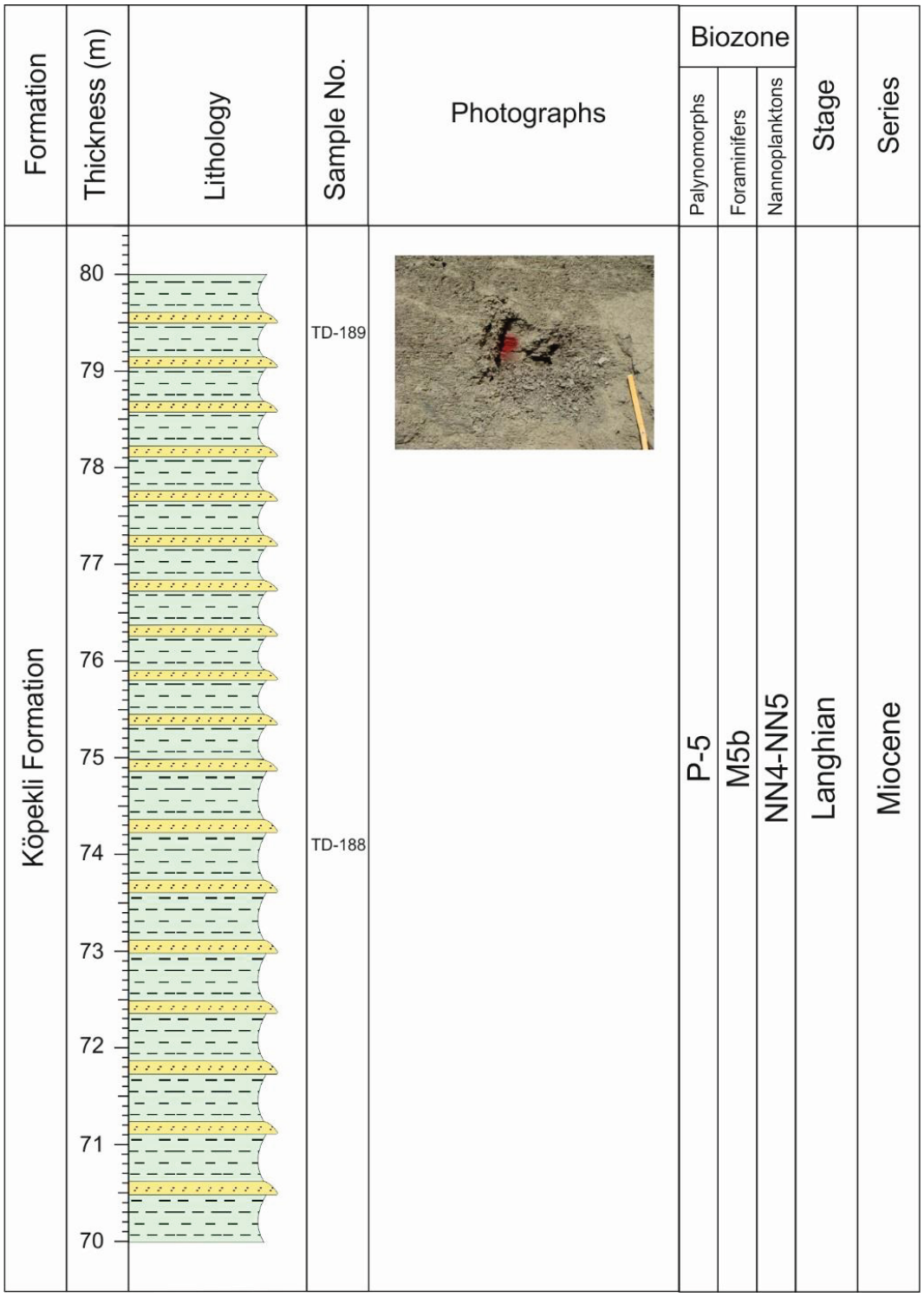

Figure 66. (cont'd)

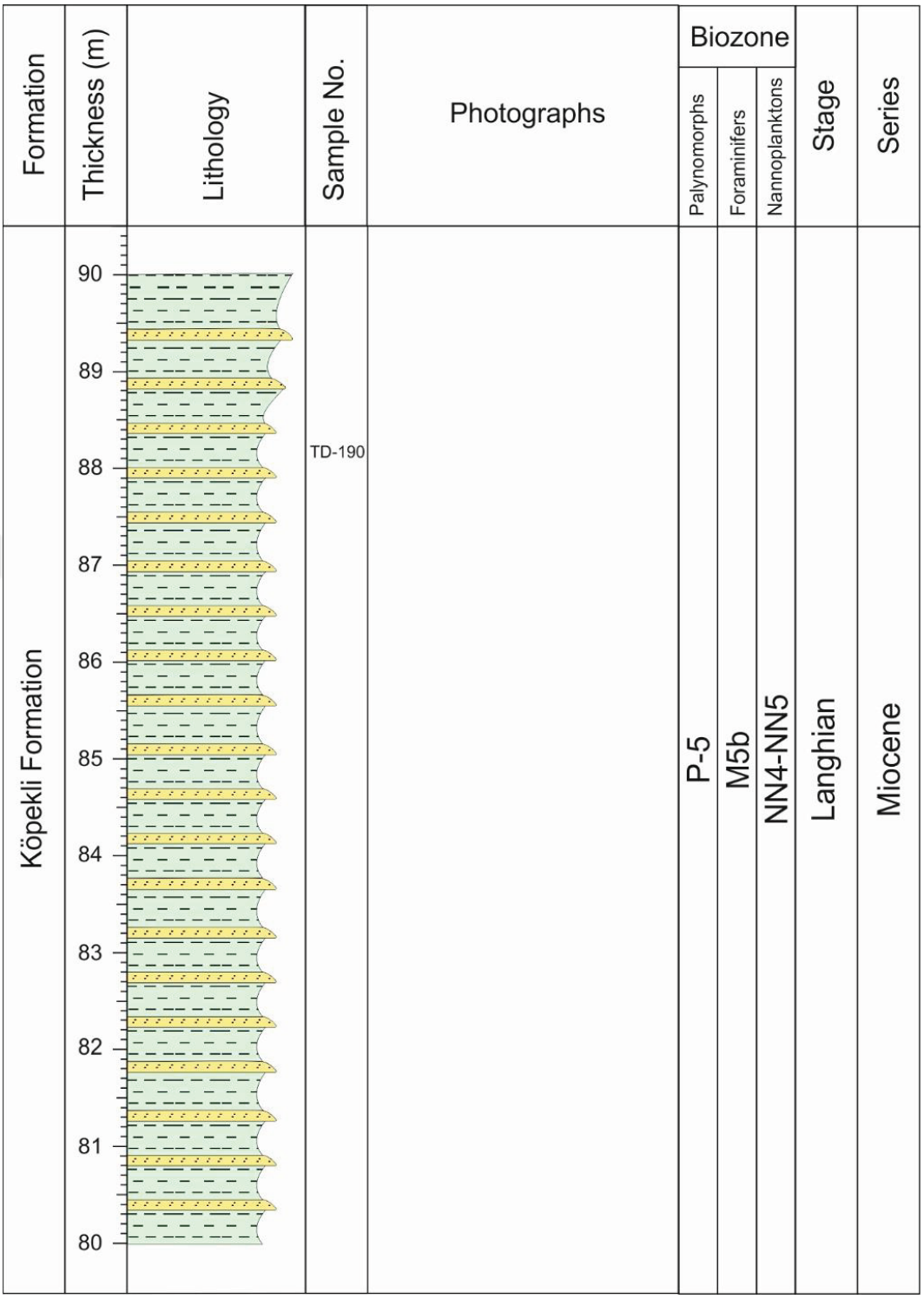

Figure 66. (cont'd)

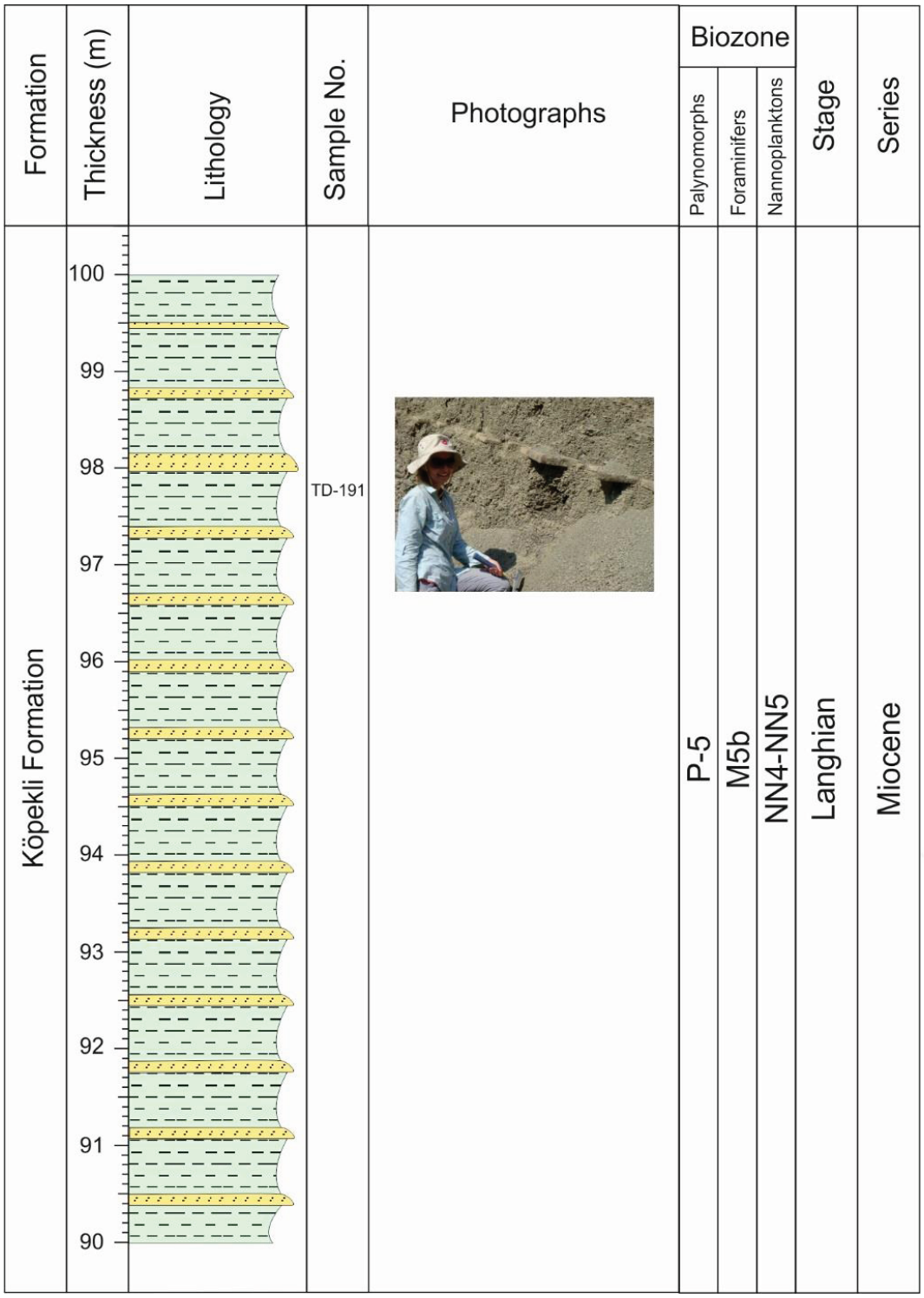

Figure 66. (cont'd)

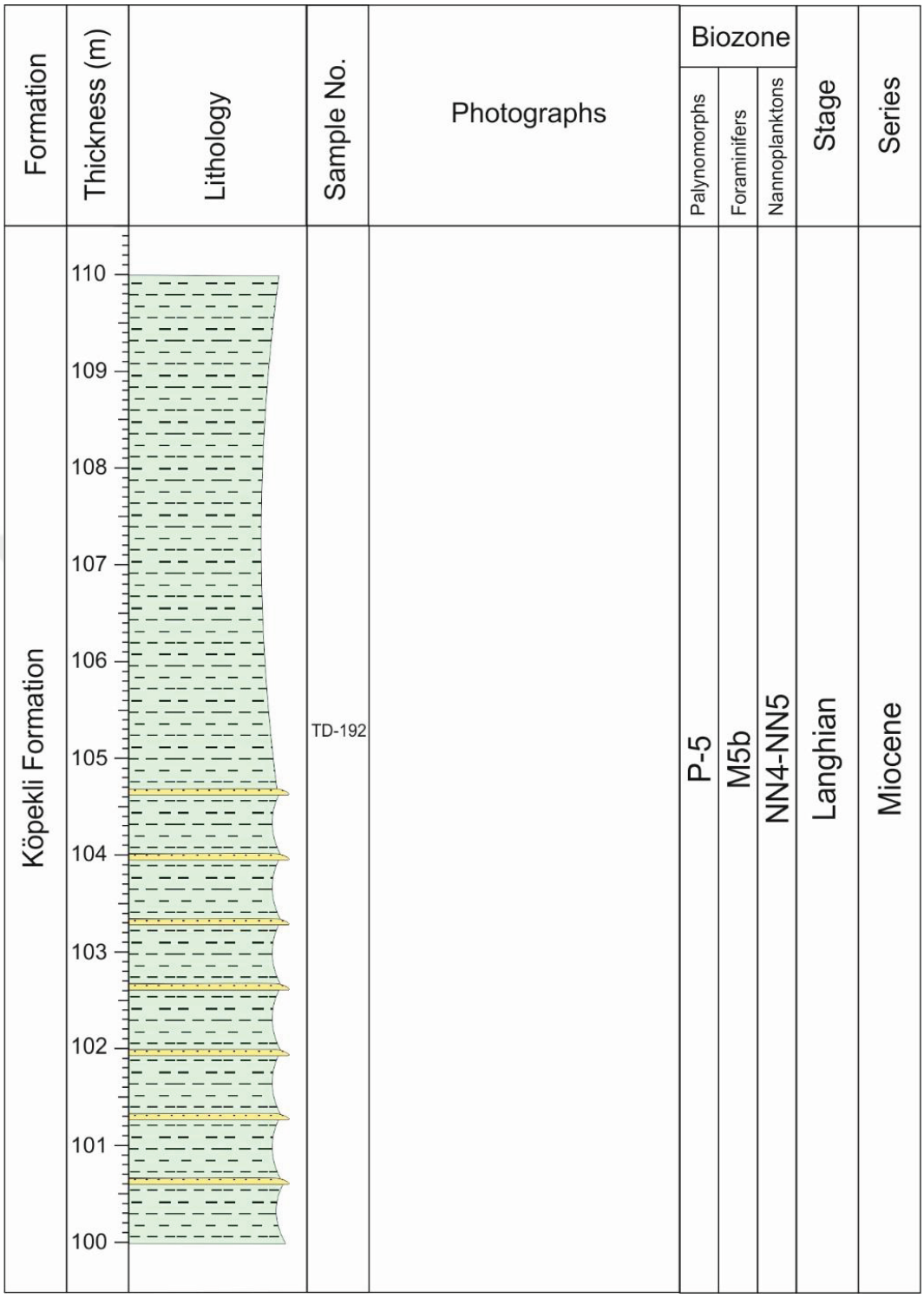

Figure 66. (cont'd)

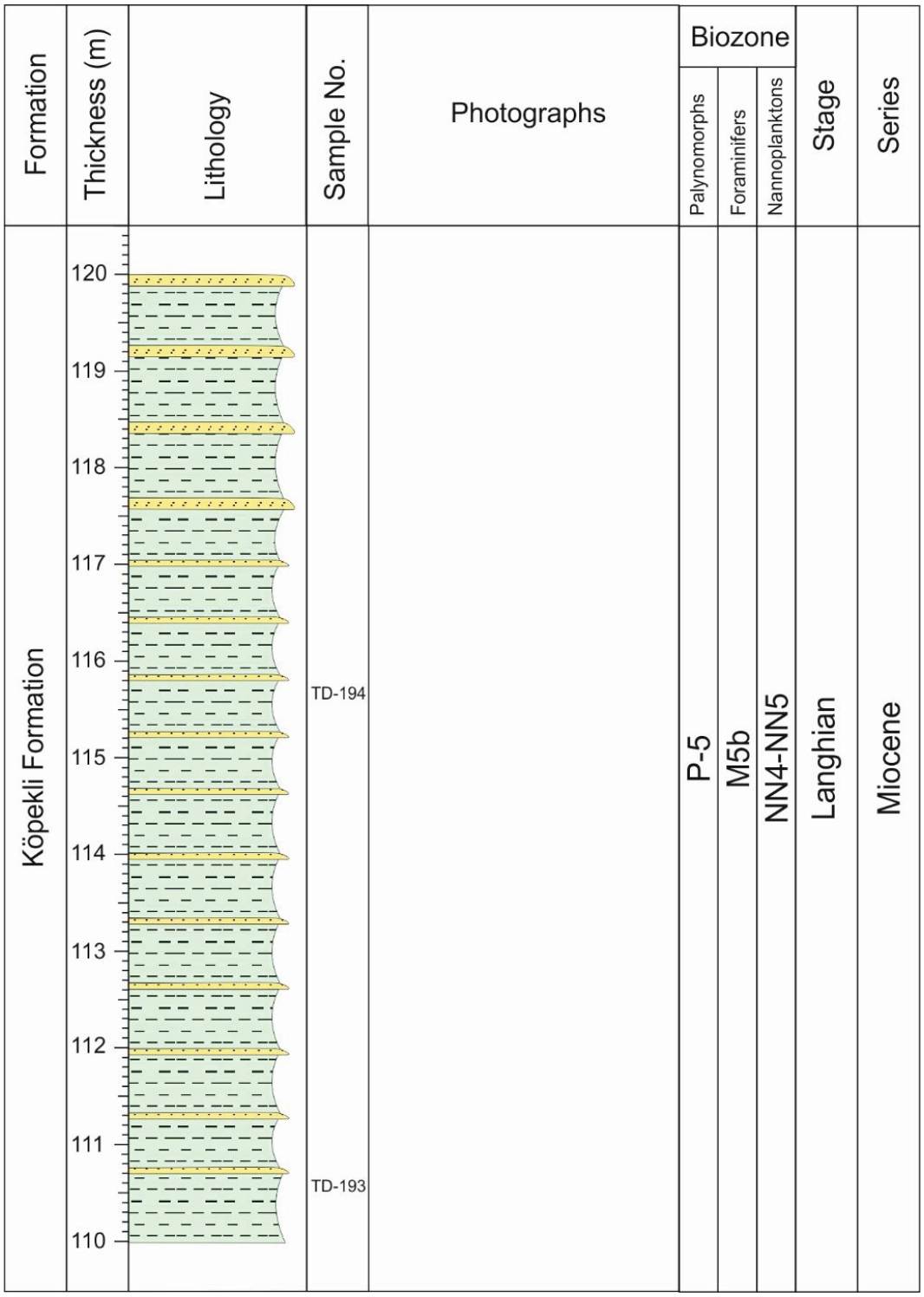

Figure 66. (cont'd)

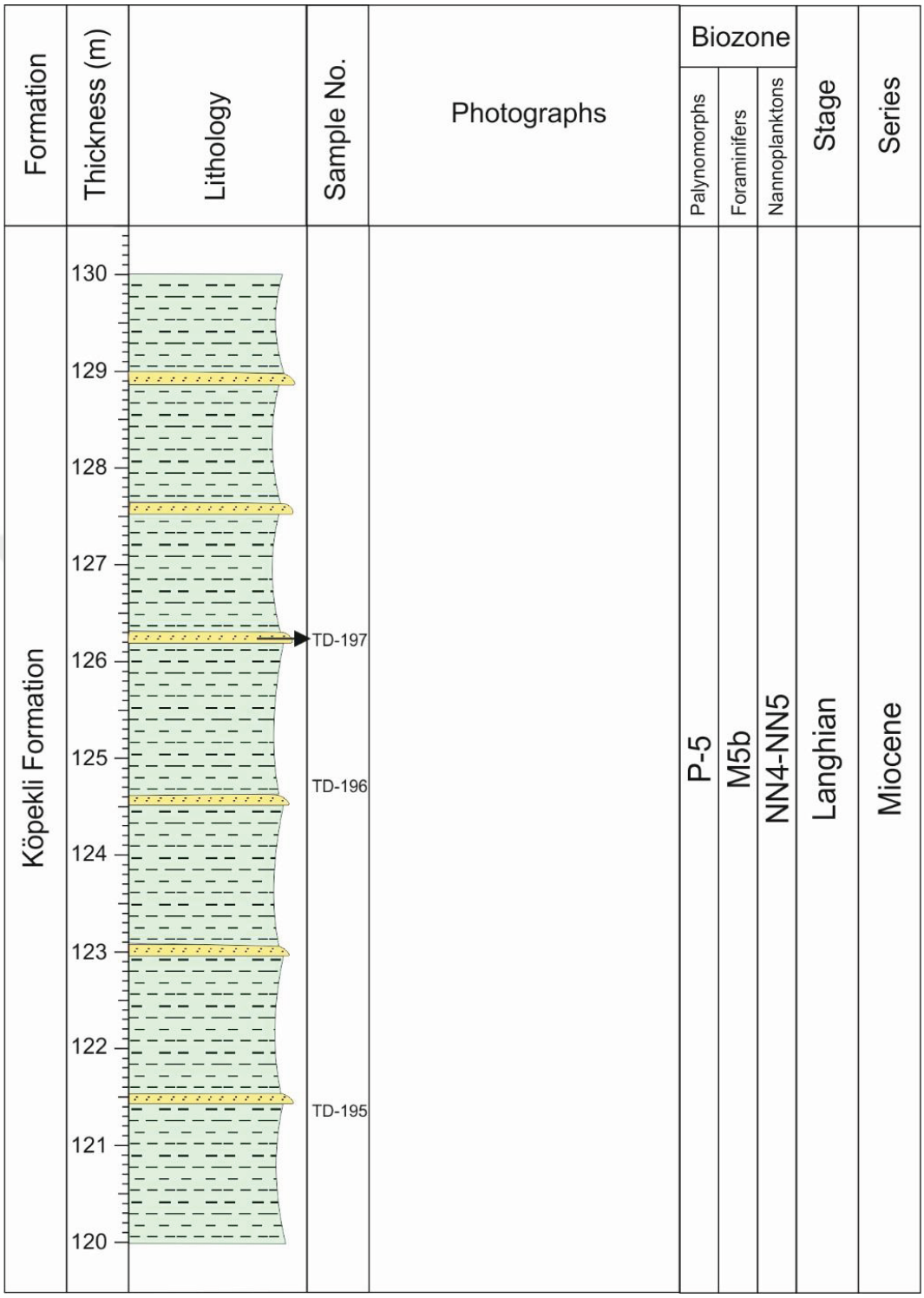

Figure 66. (cont'd)

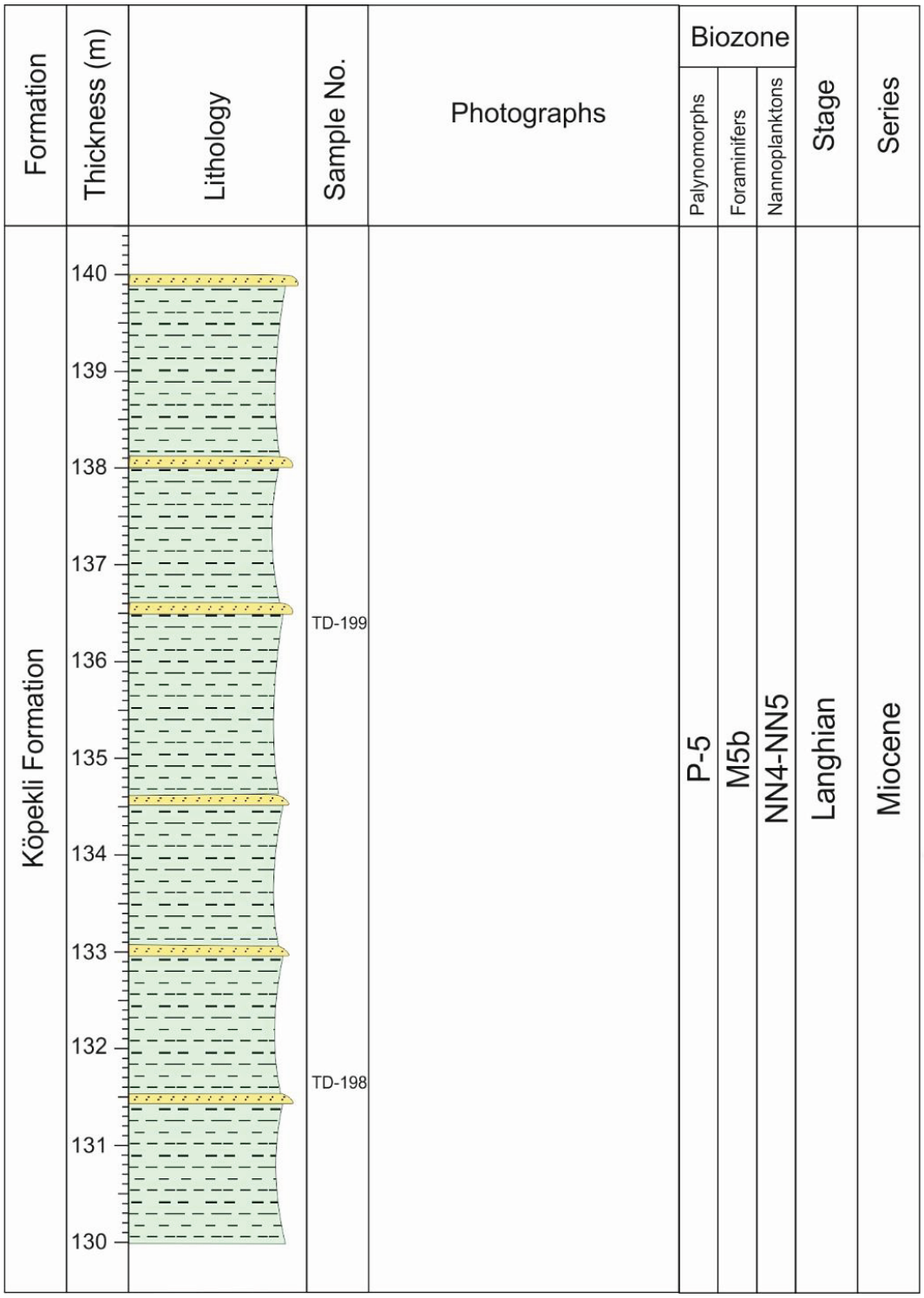

Figure 66. (cont'd)

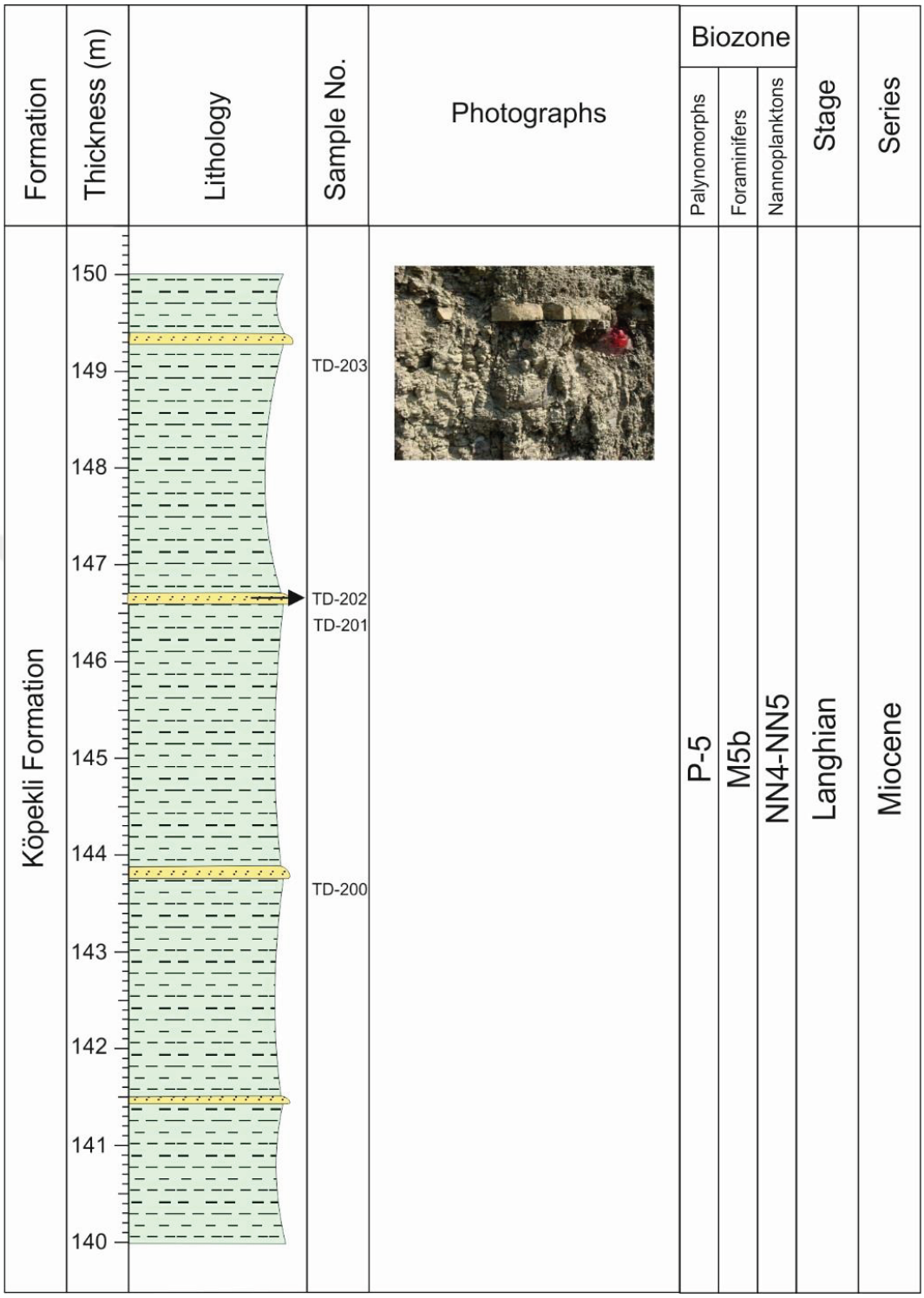

Figure 66. (cont'd)

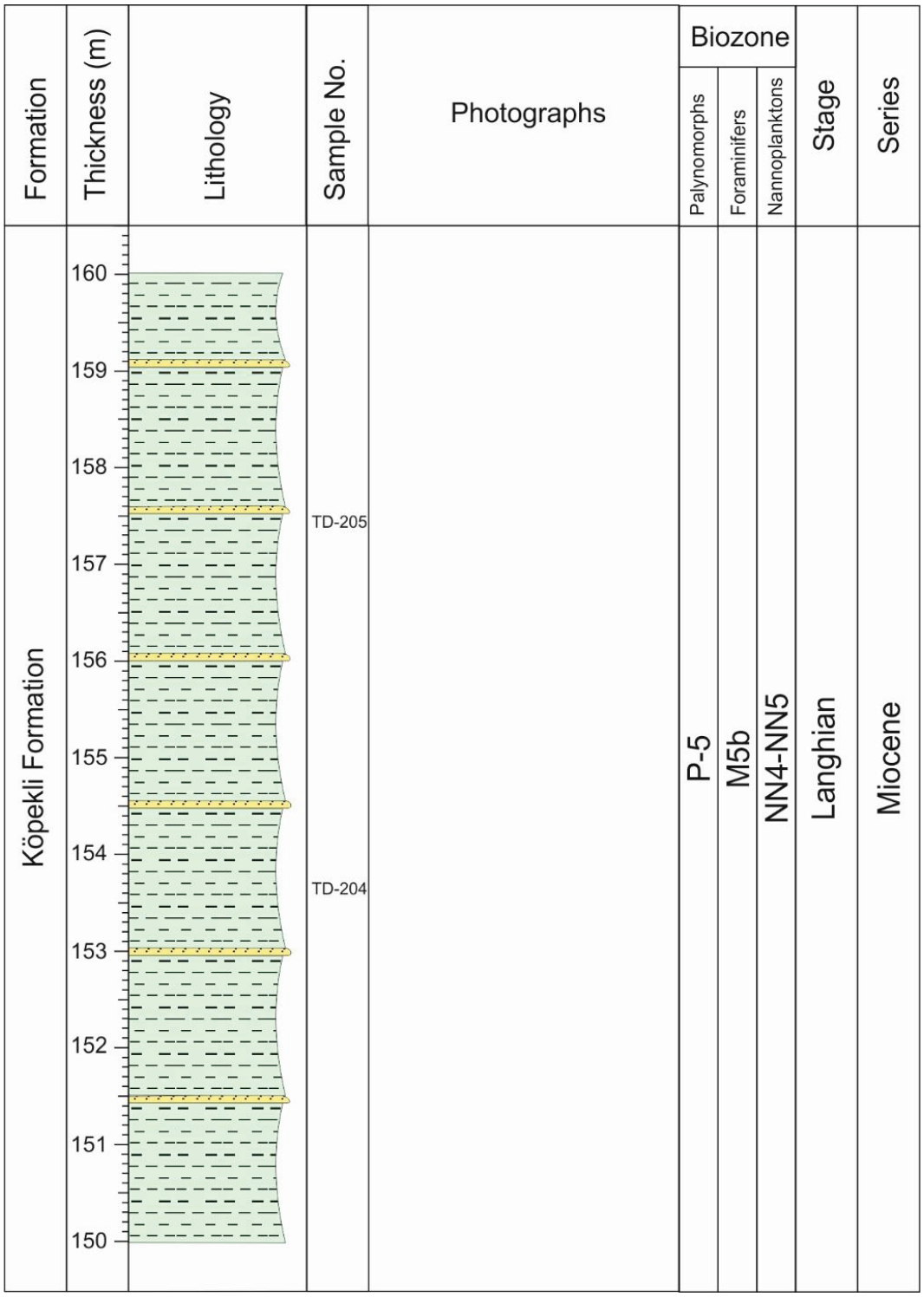

Figure 66. (cont'd)

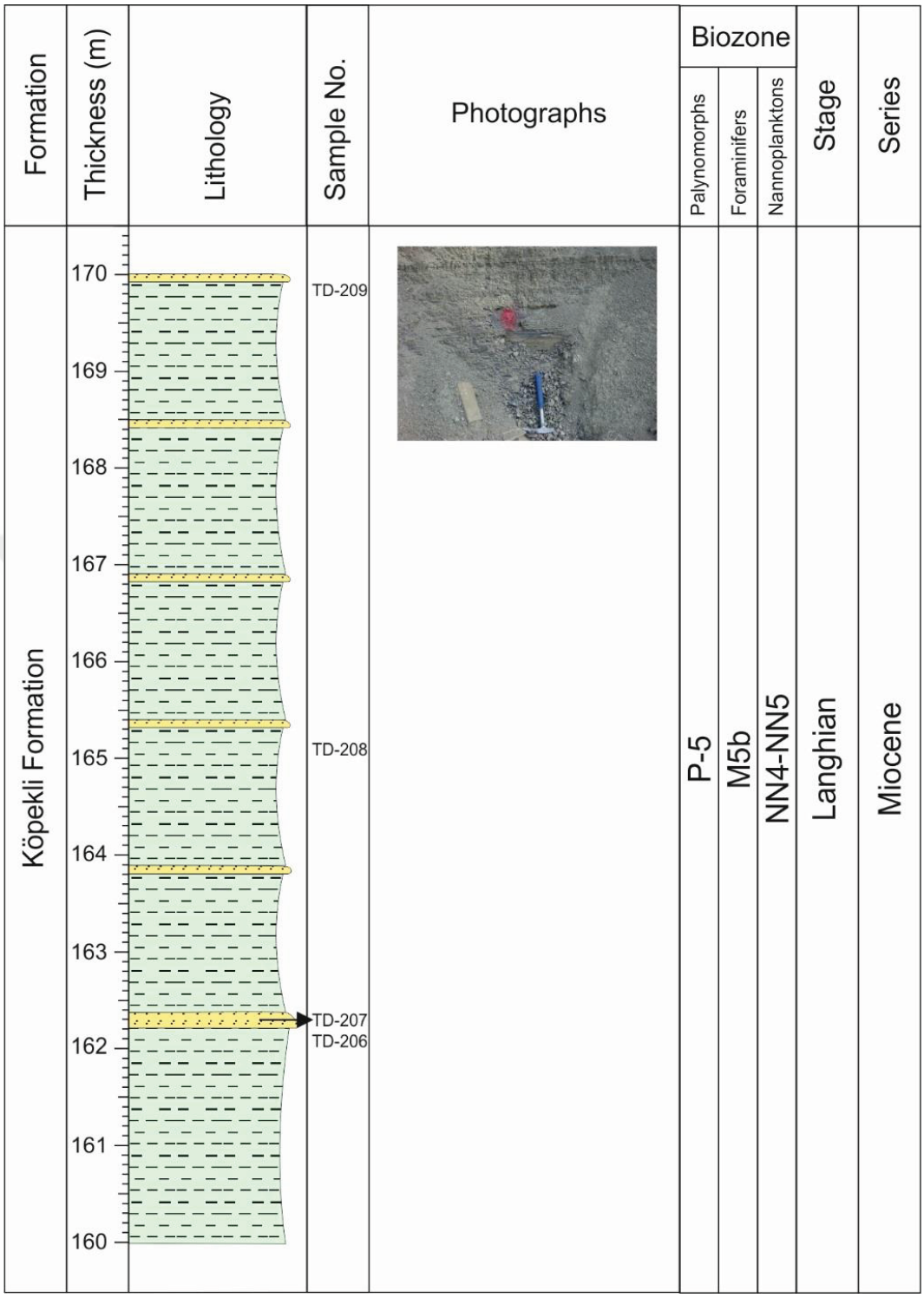

Figure 66. (cont'd)

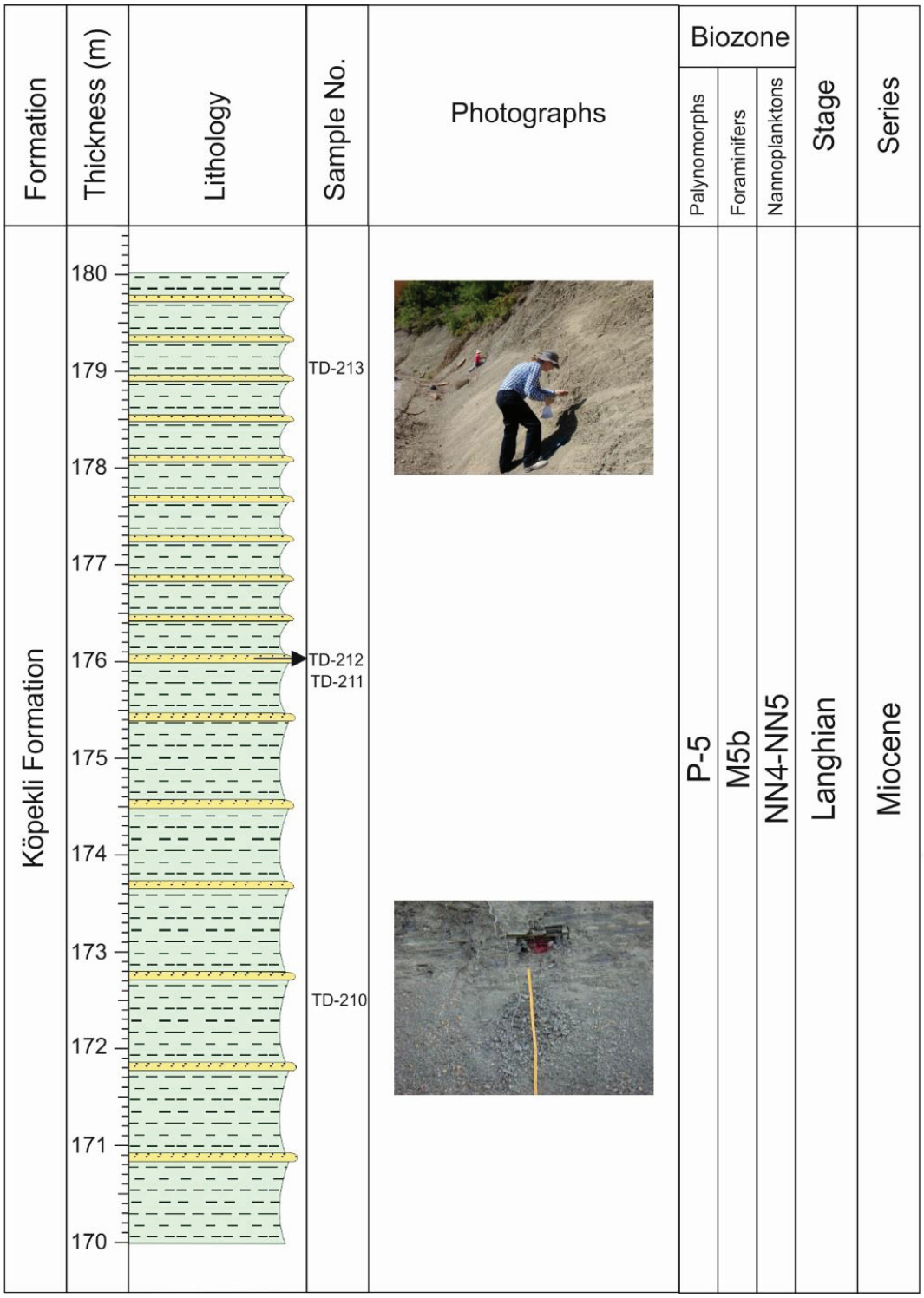

Figure 66. (cont'd)



Figure 66. (cont'd)

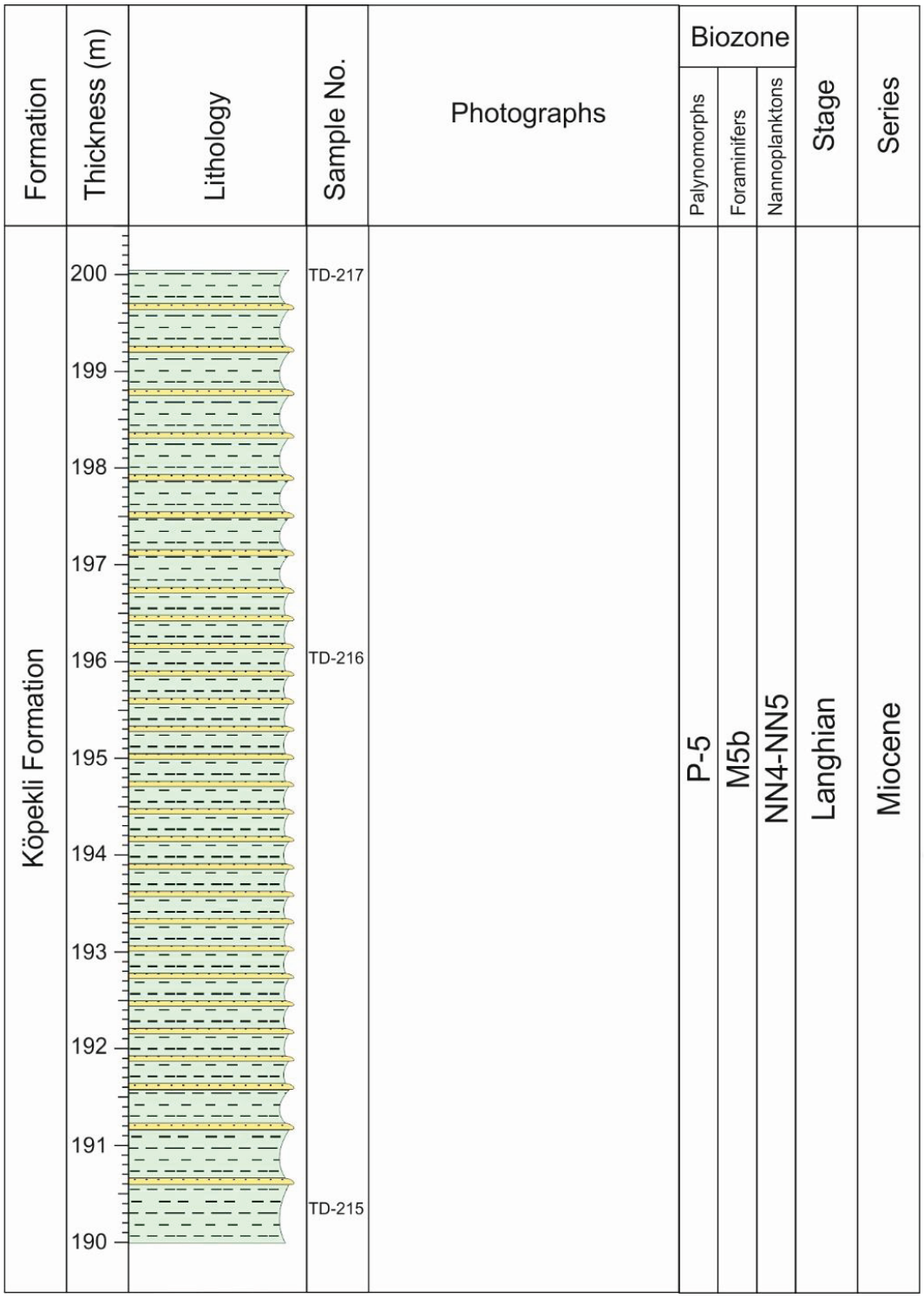

Figure 66. (cont'd)

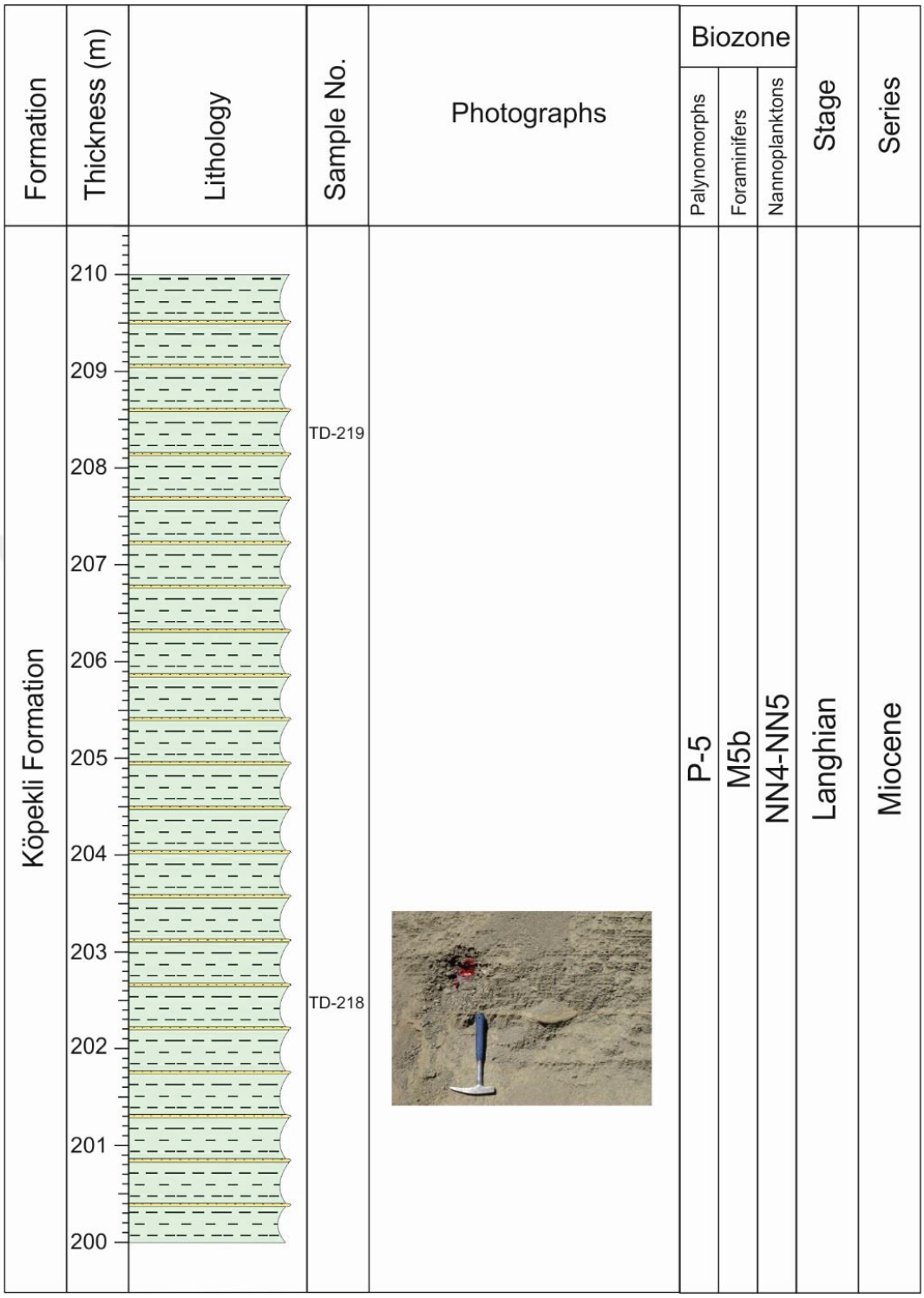

Figure 66. (cont'd)

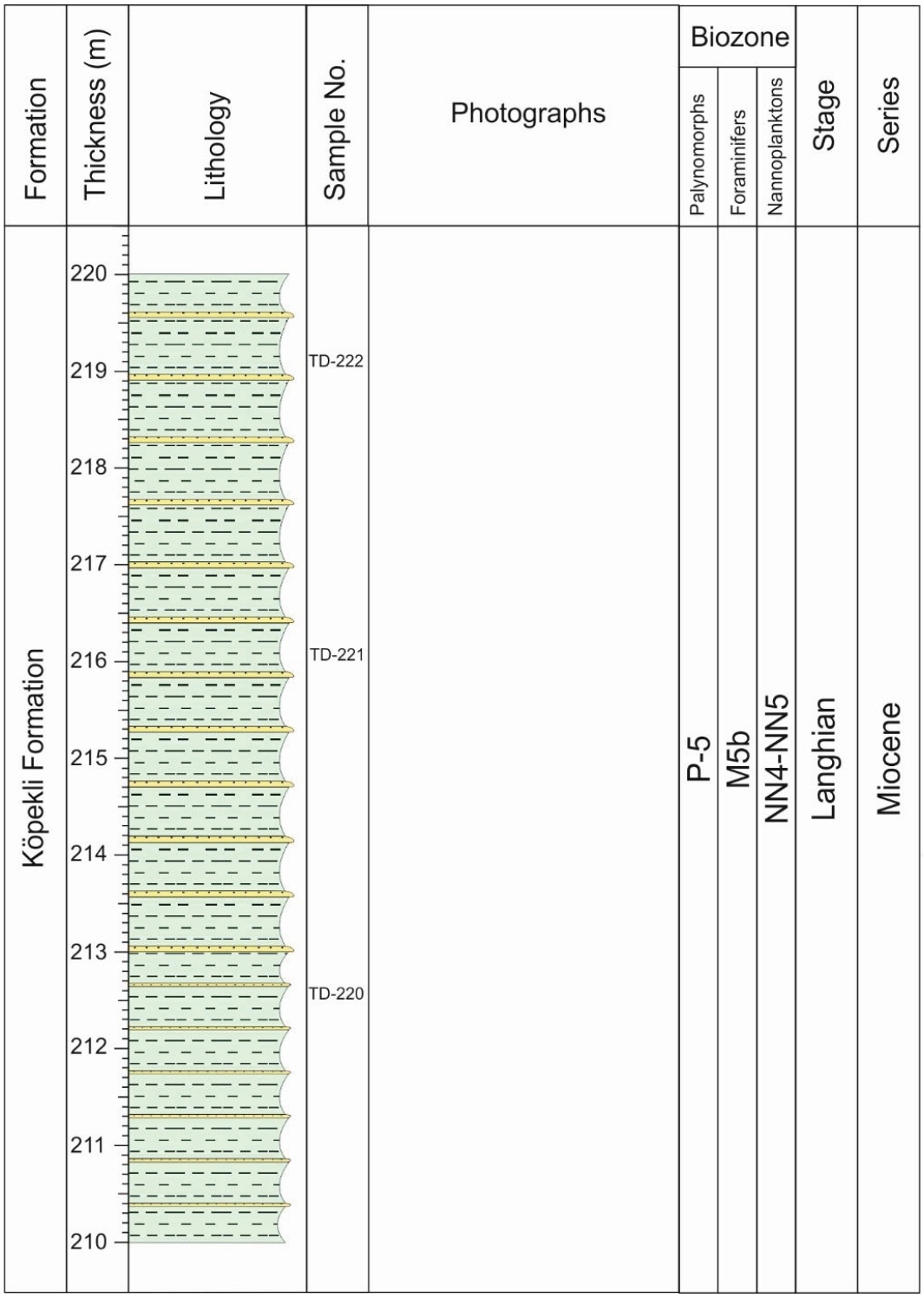

Figure 66. (cont'd)

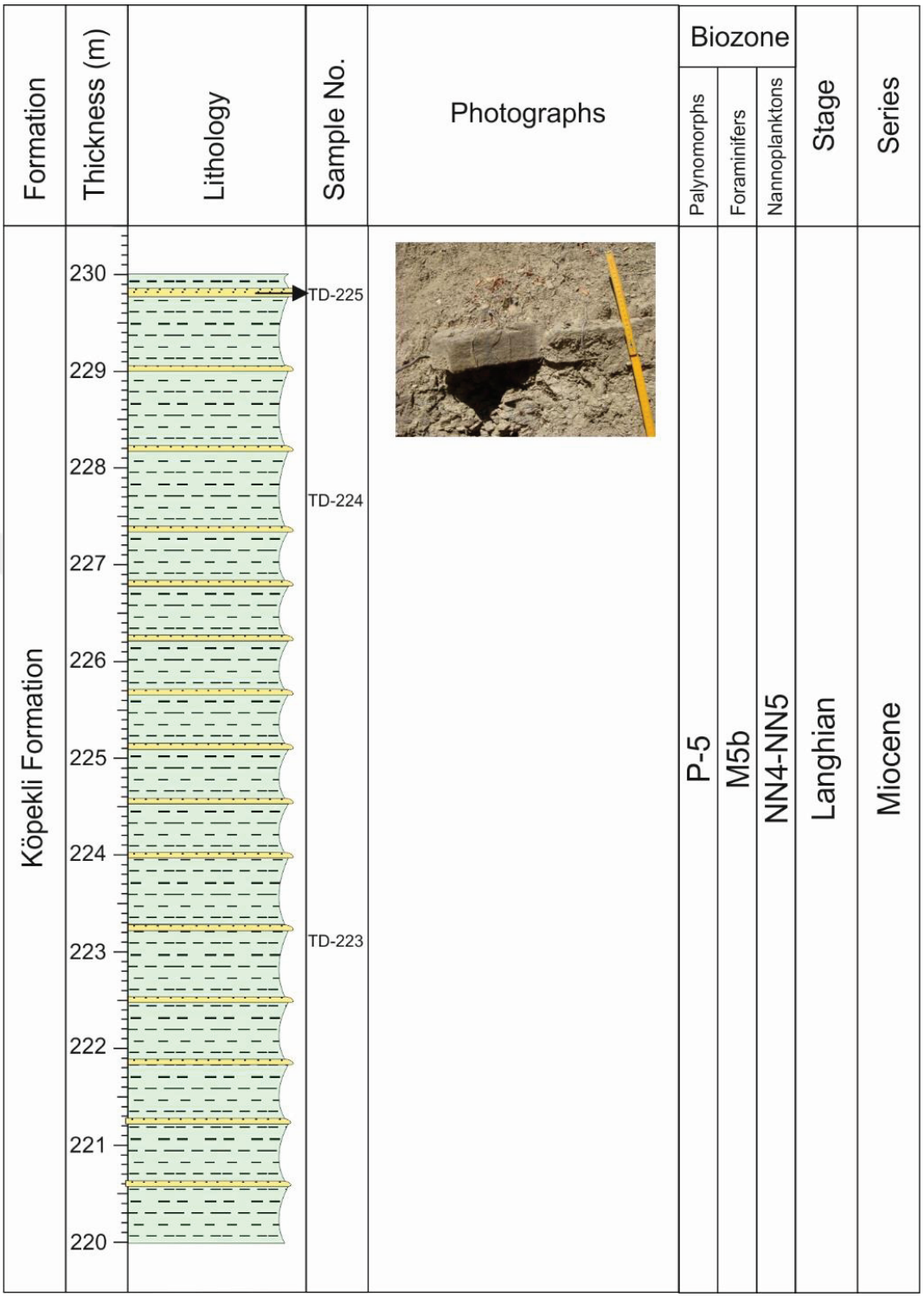

Figure 66. (cont'd)

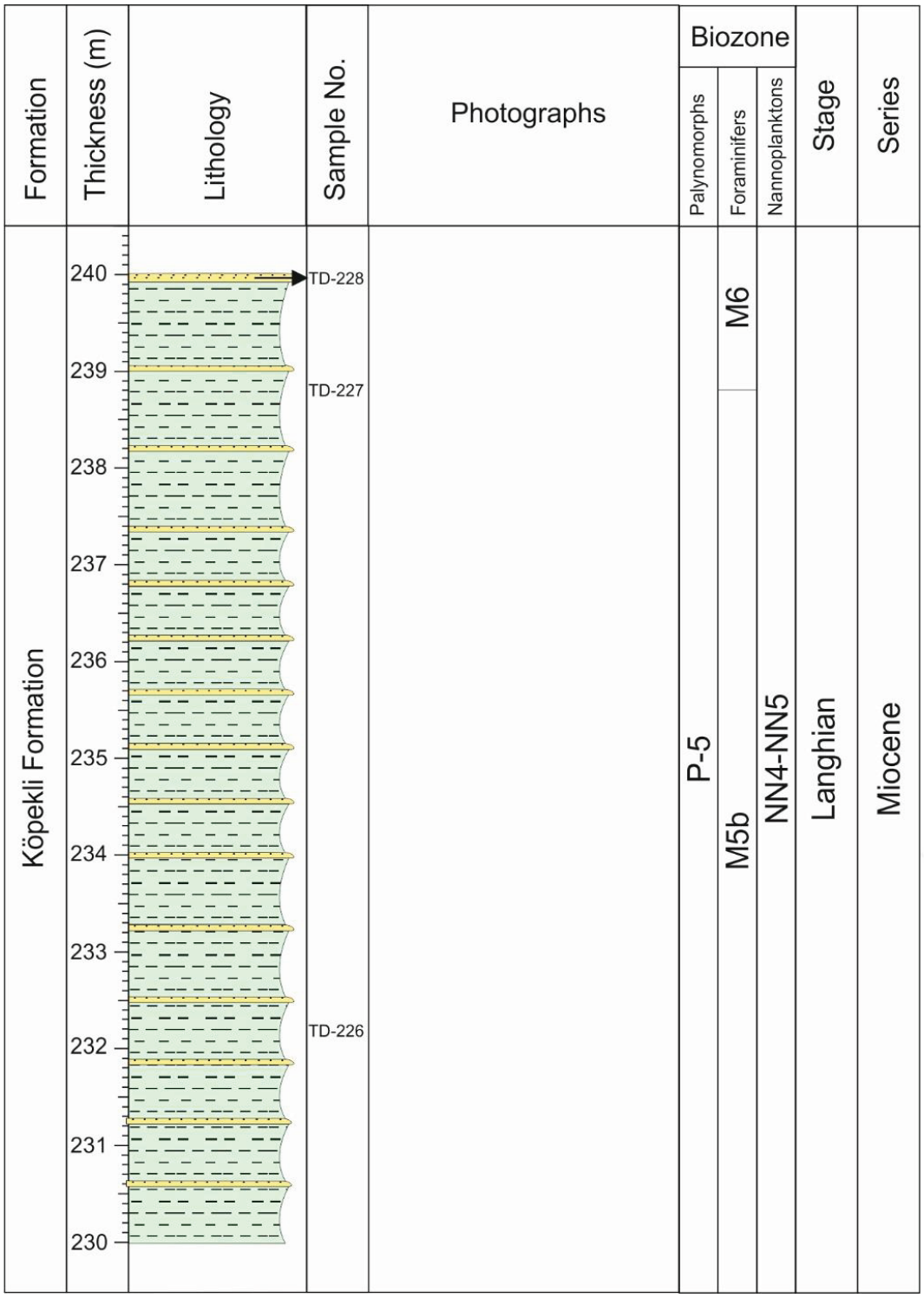

Figure 66. (cont'd)

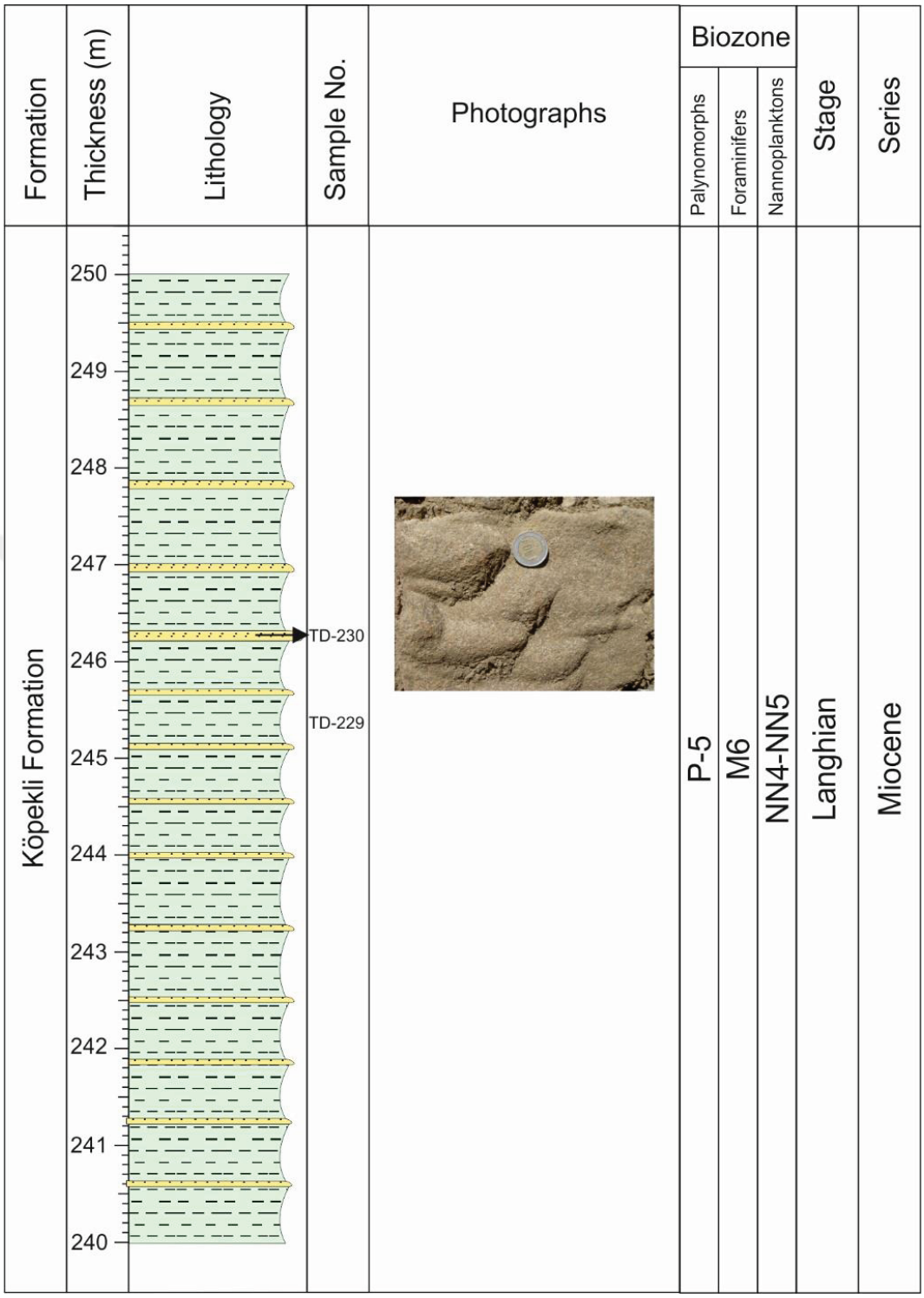

Figure 66. (cont'd)

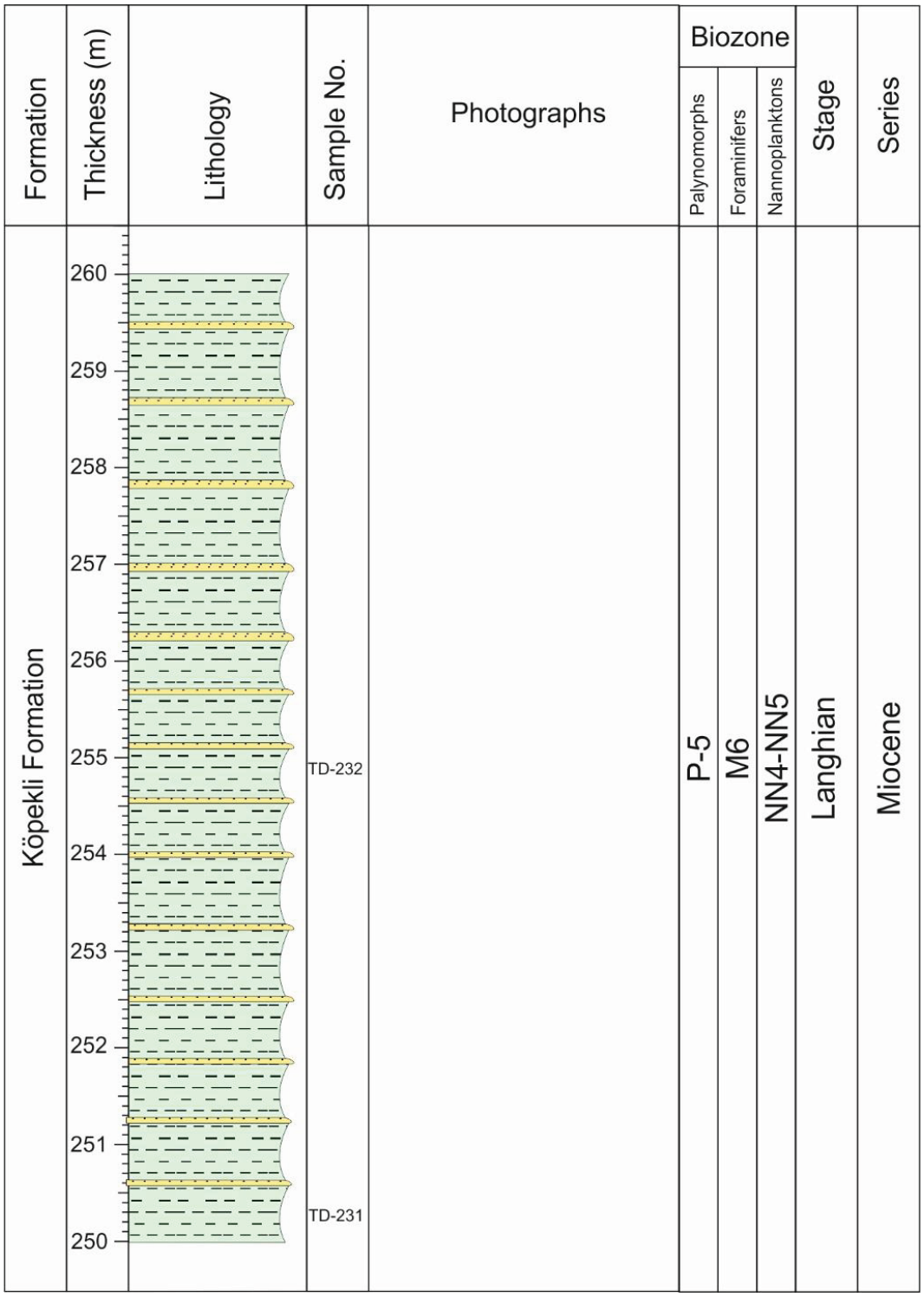

Figure 66. (cont'd)

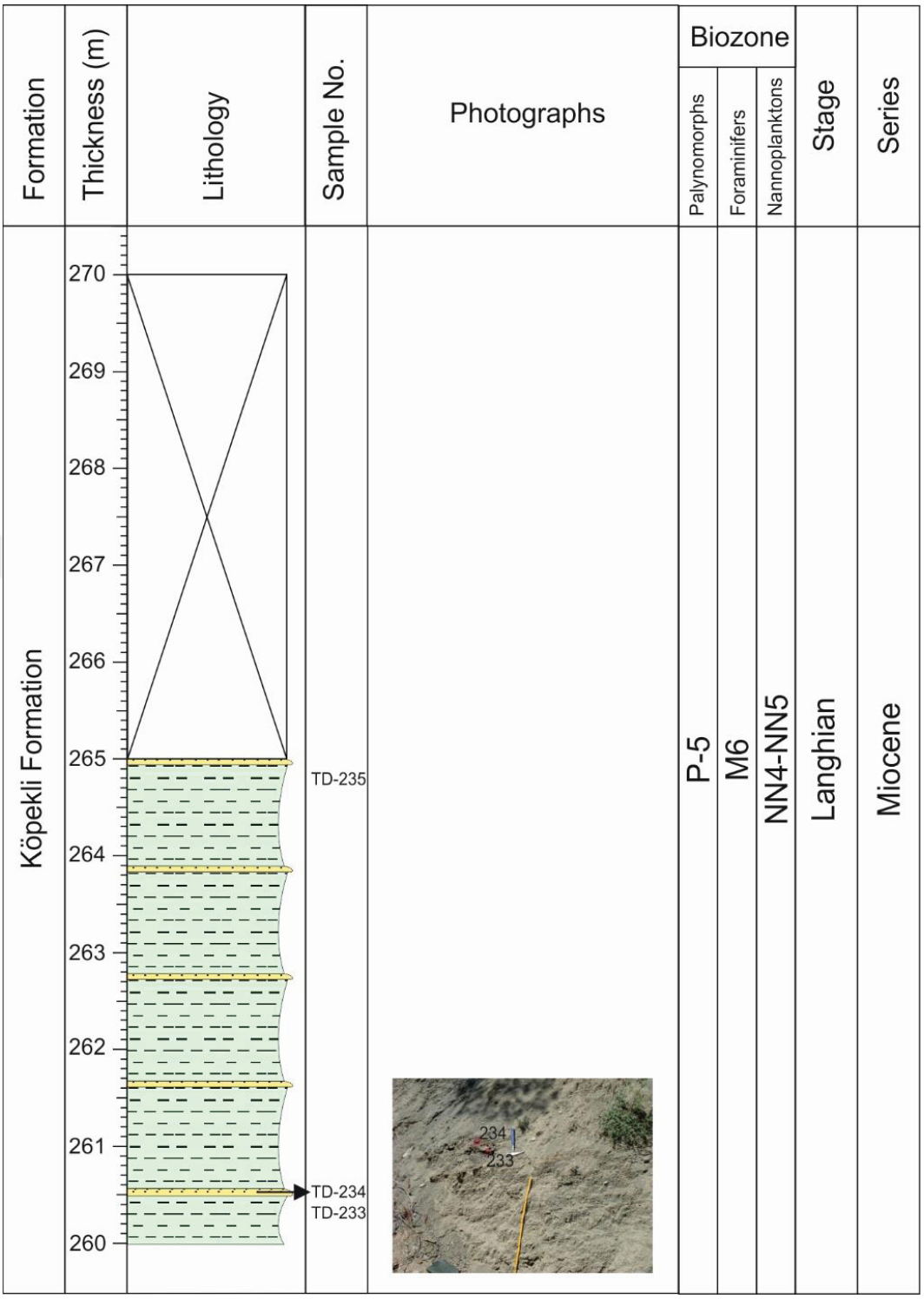

Figure 66. (cont'd)

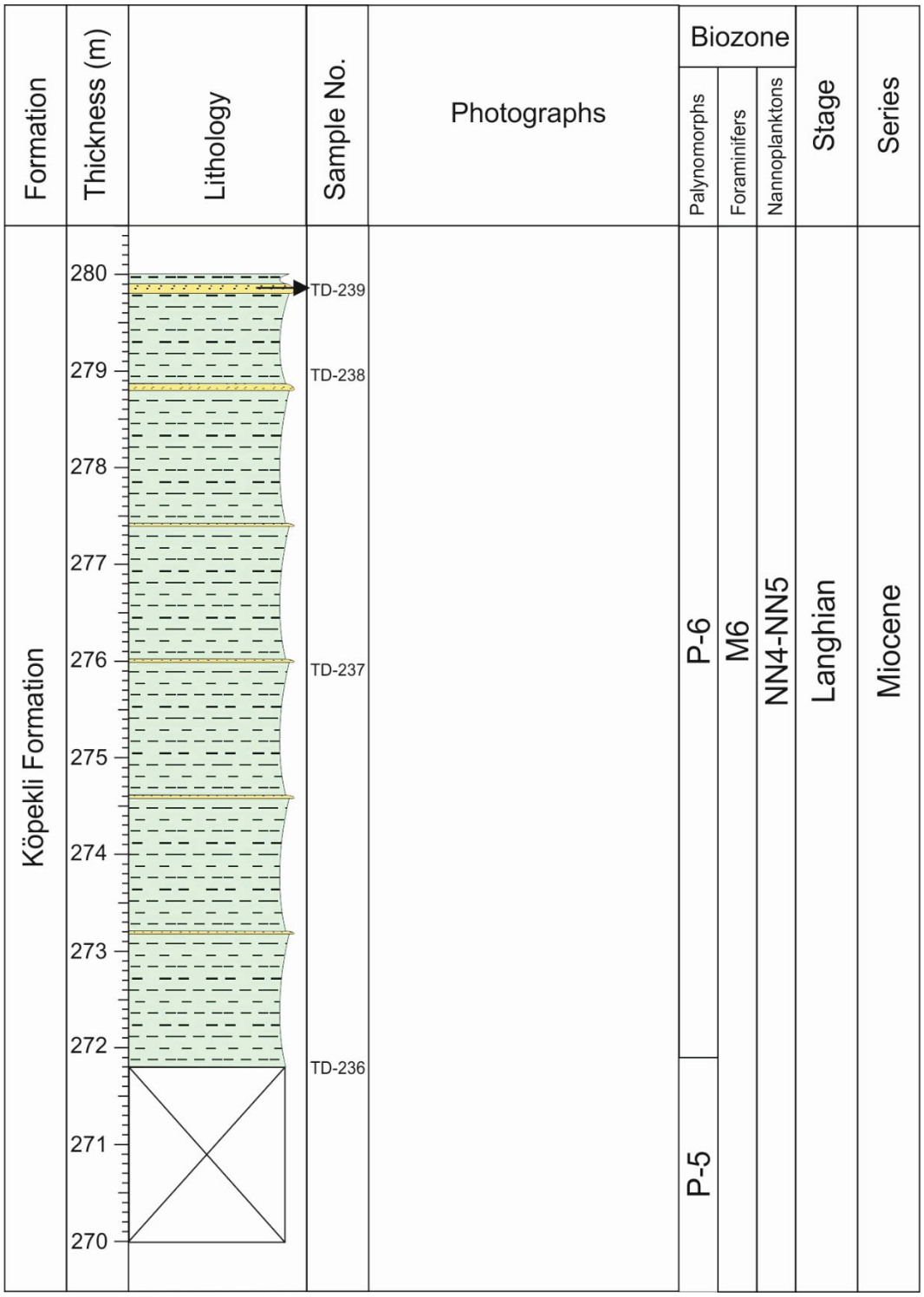

Figure 66. (cont'd)

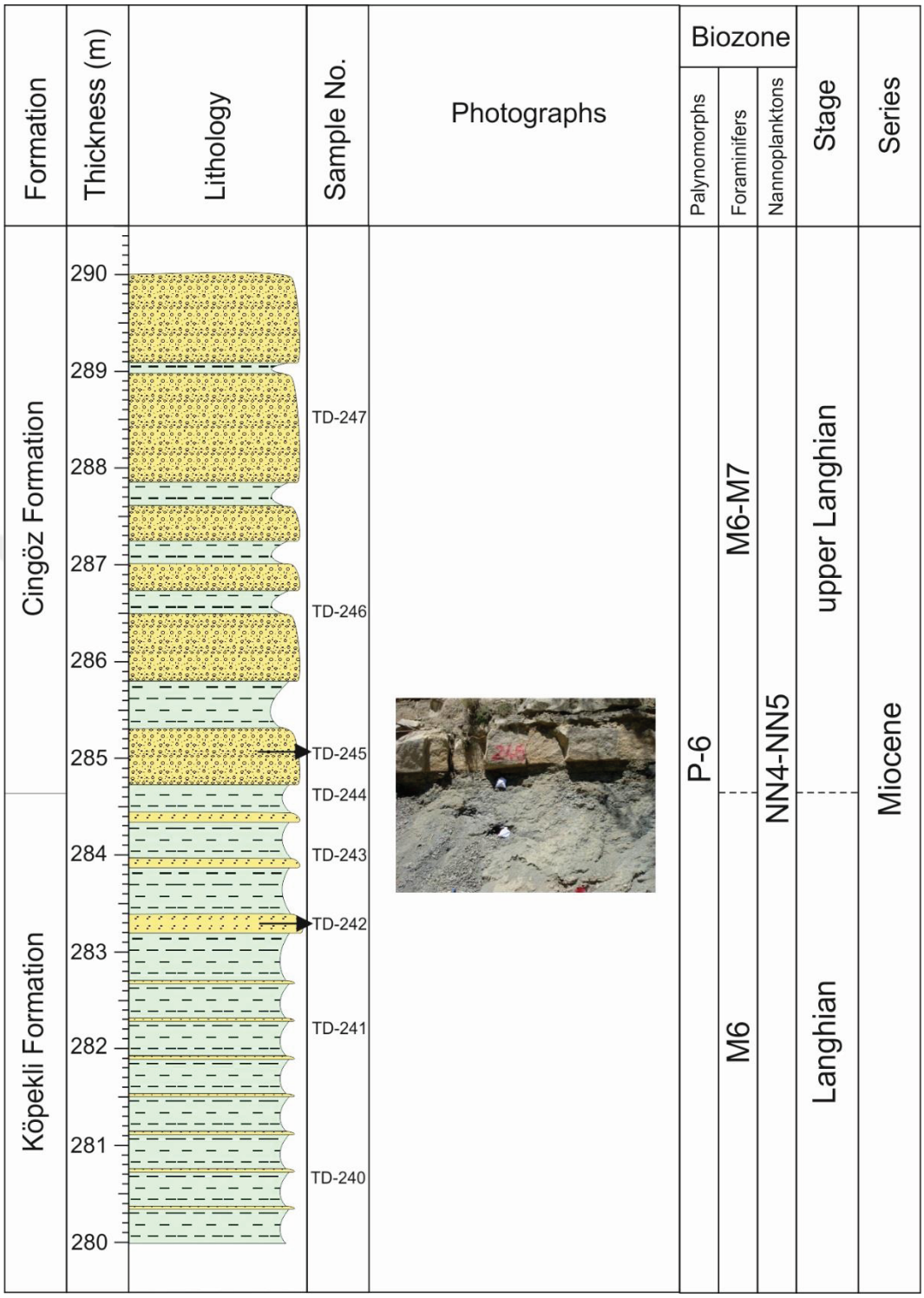

Figure 66. (cont'd)

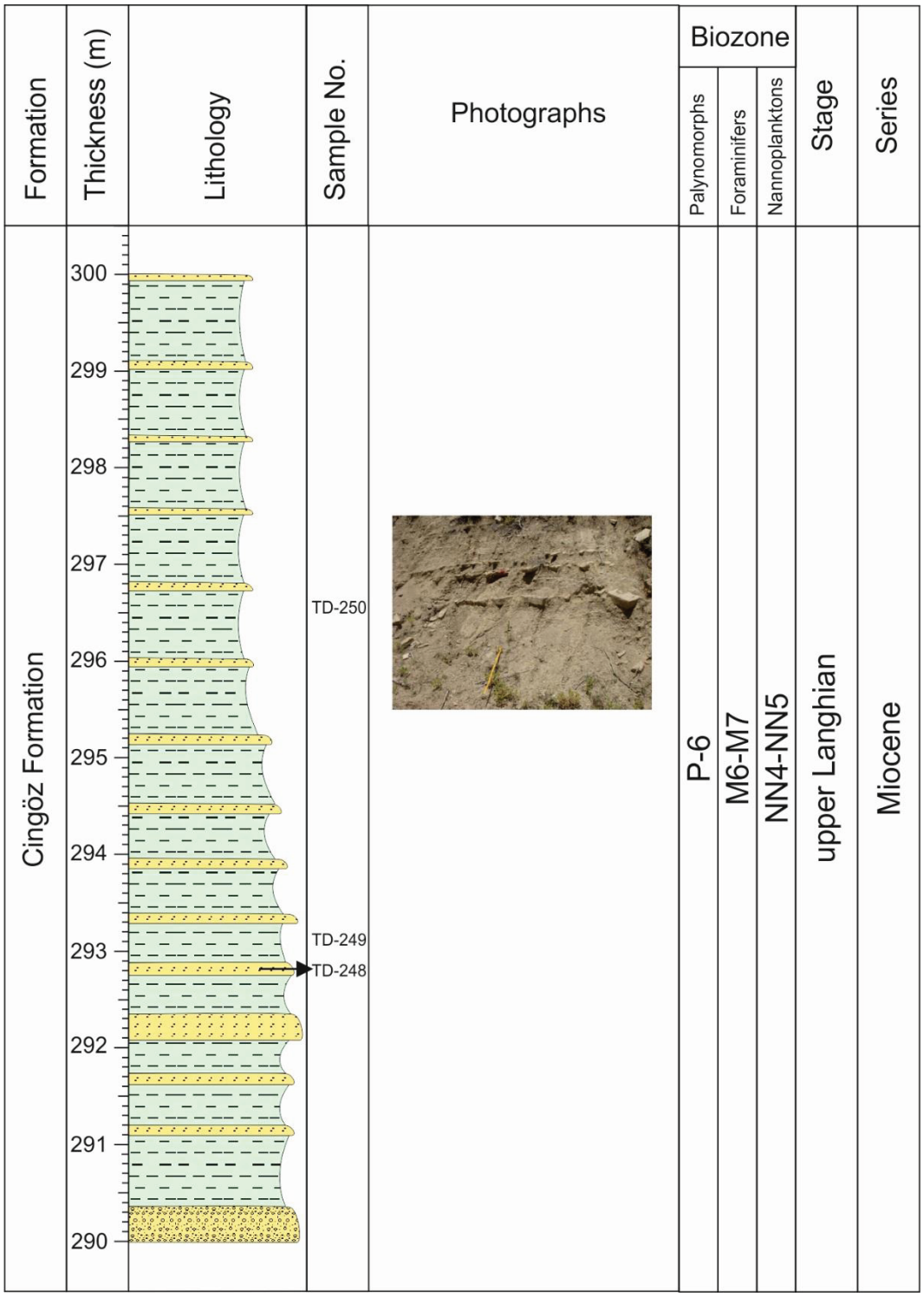

Figure 66. (cont'd)

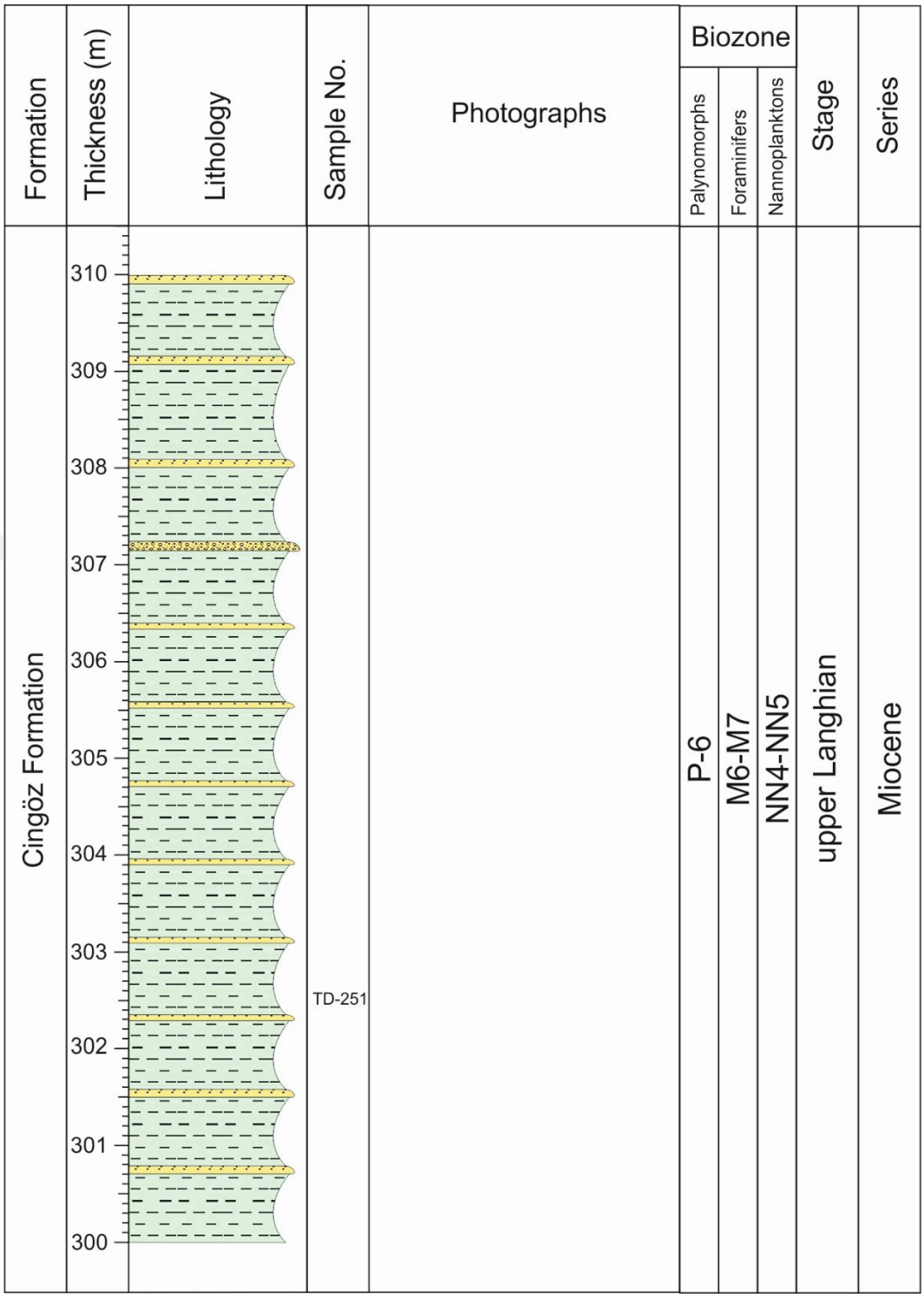

Figure 66. (cont'd)

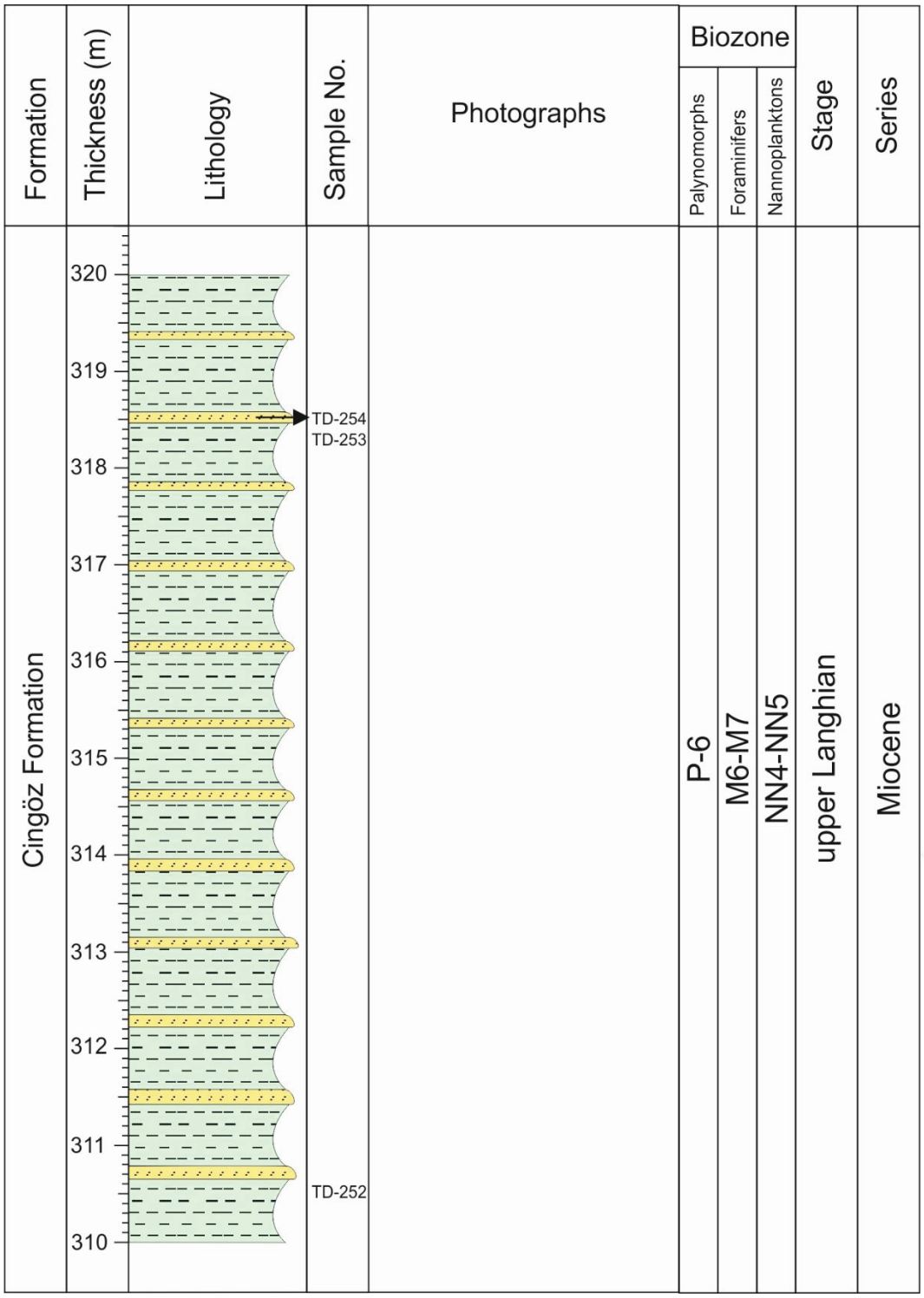

Figure 66. (cont'd)

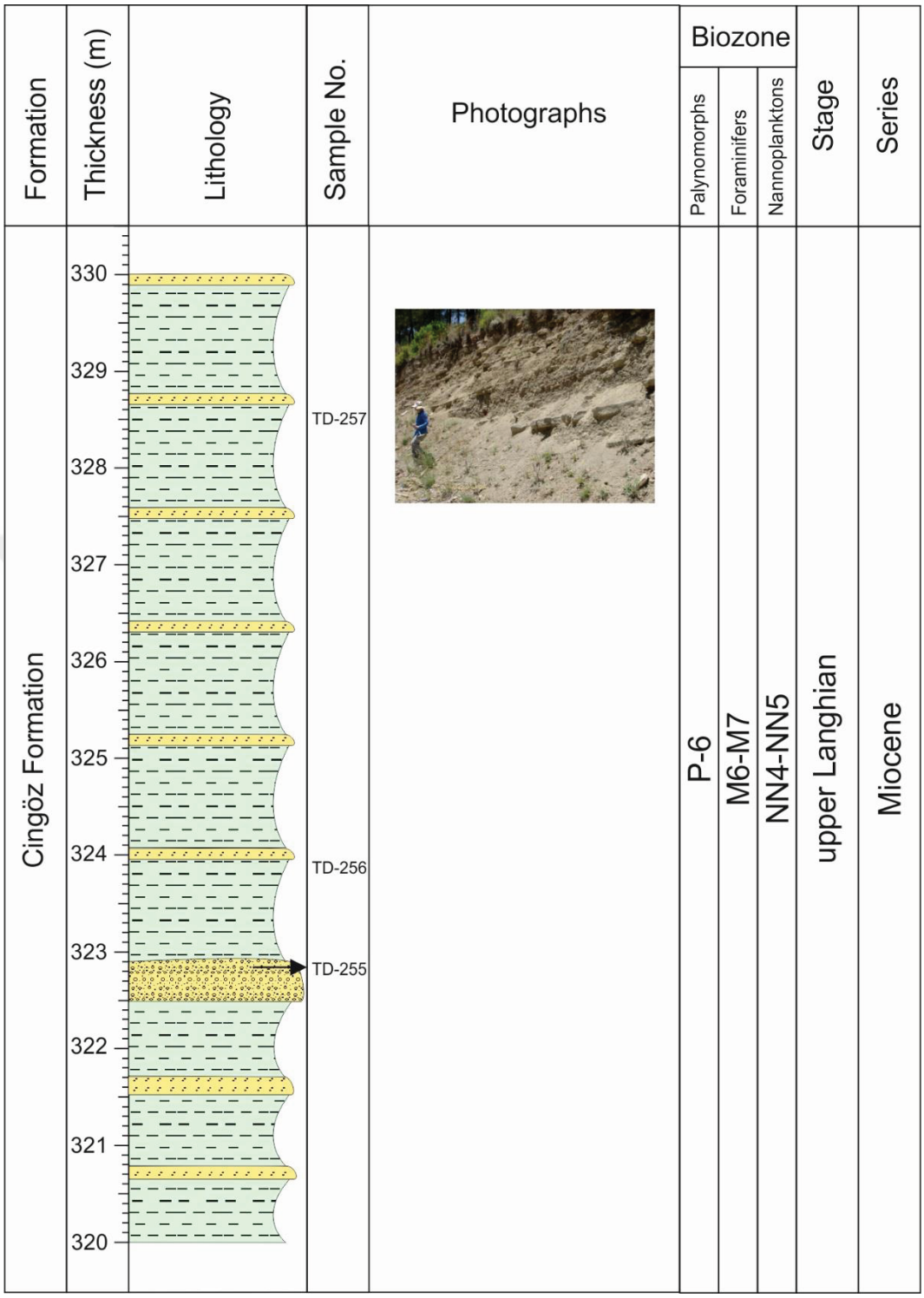

Figure 66. (cont'd)

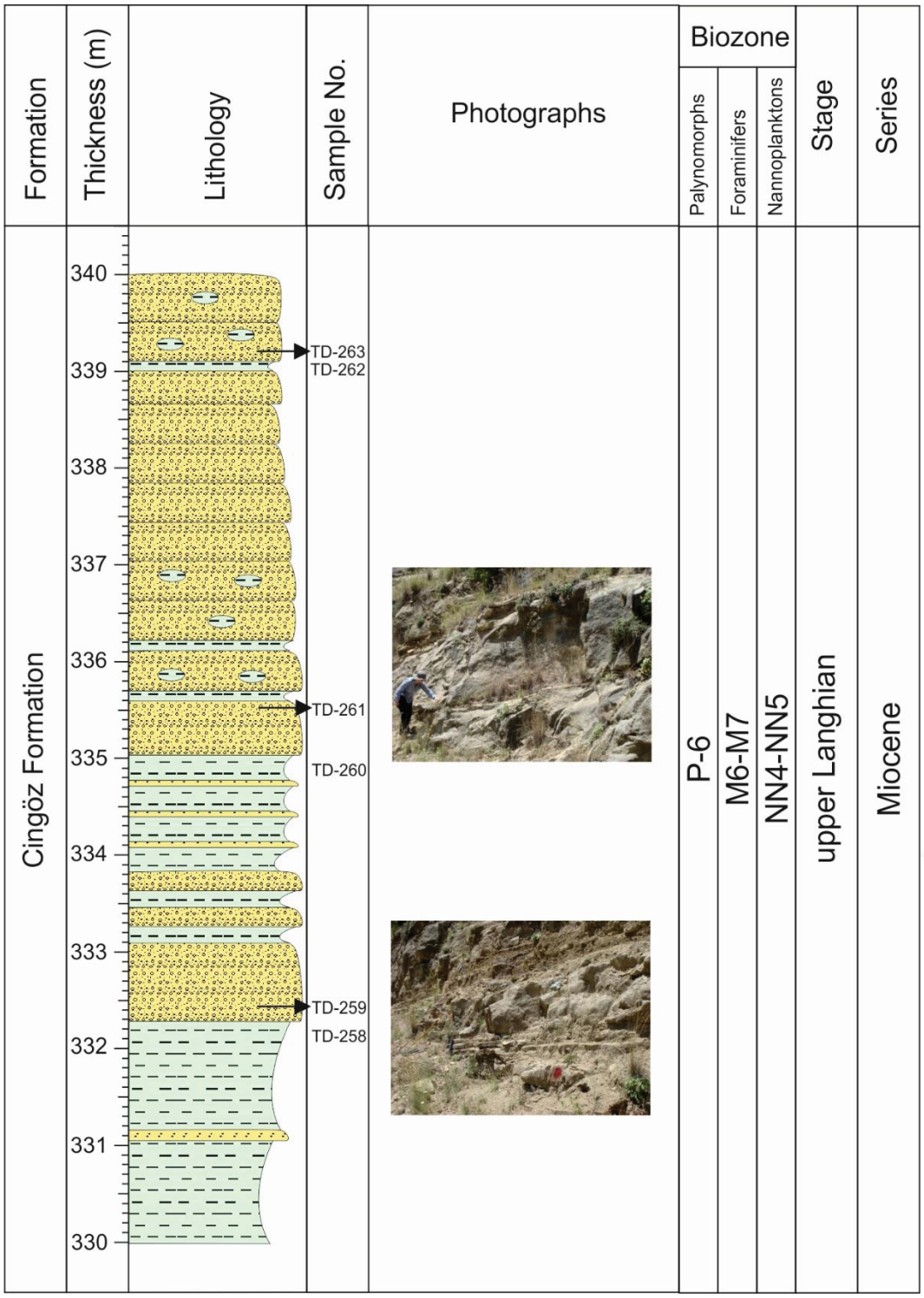

Figure 66. (cont'd)

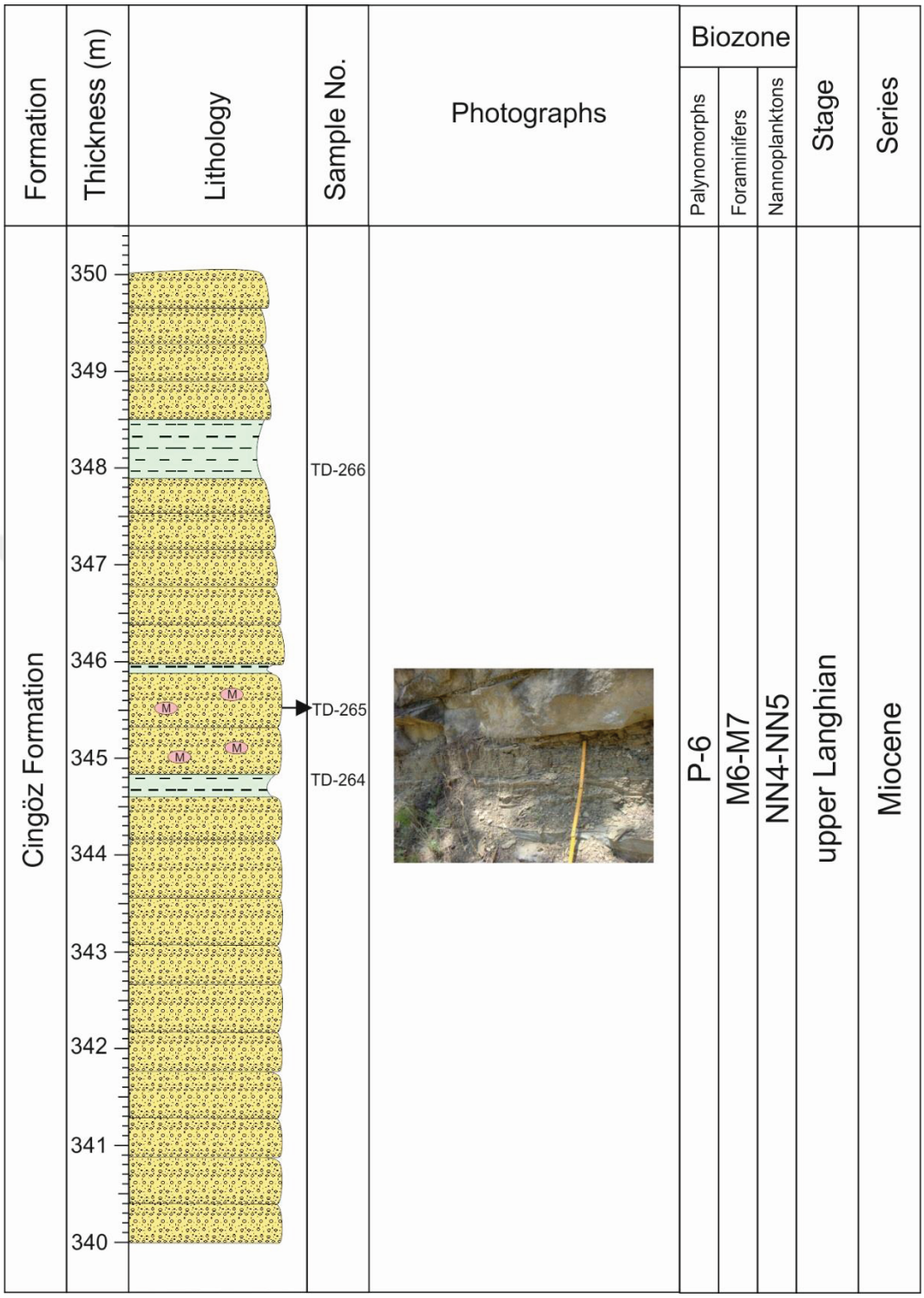

Figure 66. (cont'd)

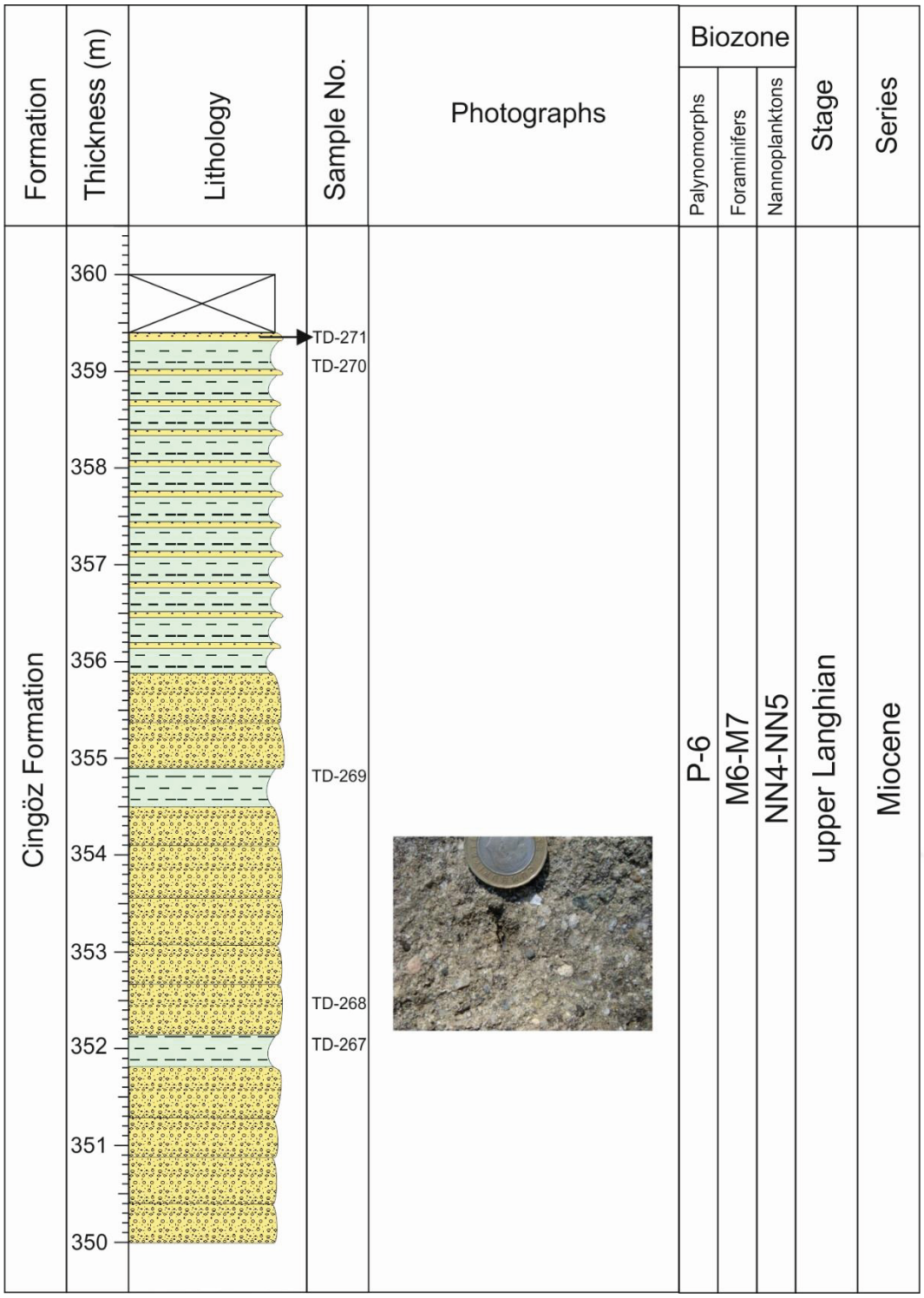

Figure 66. (cont'd)

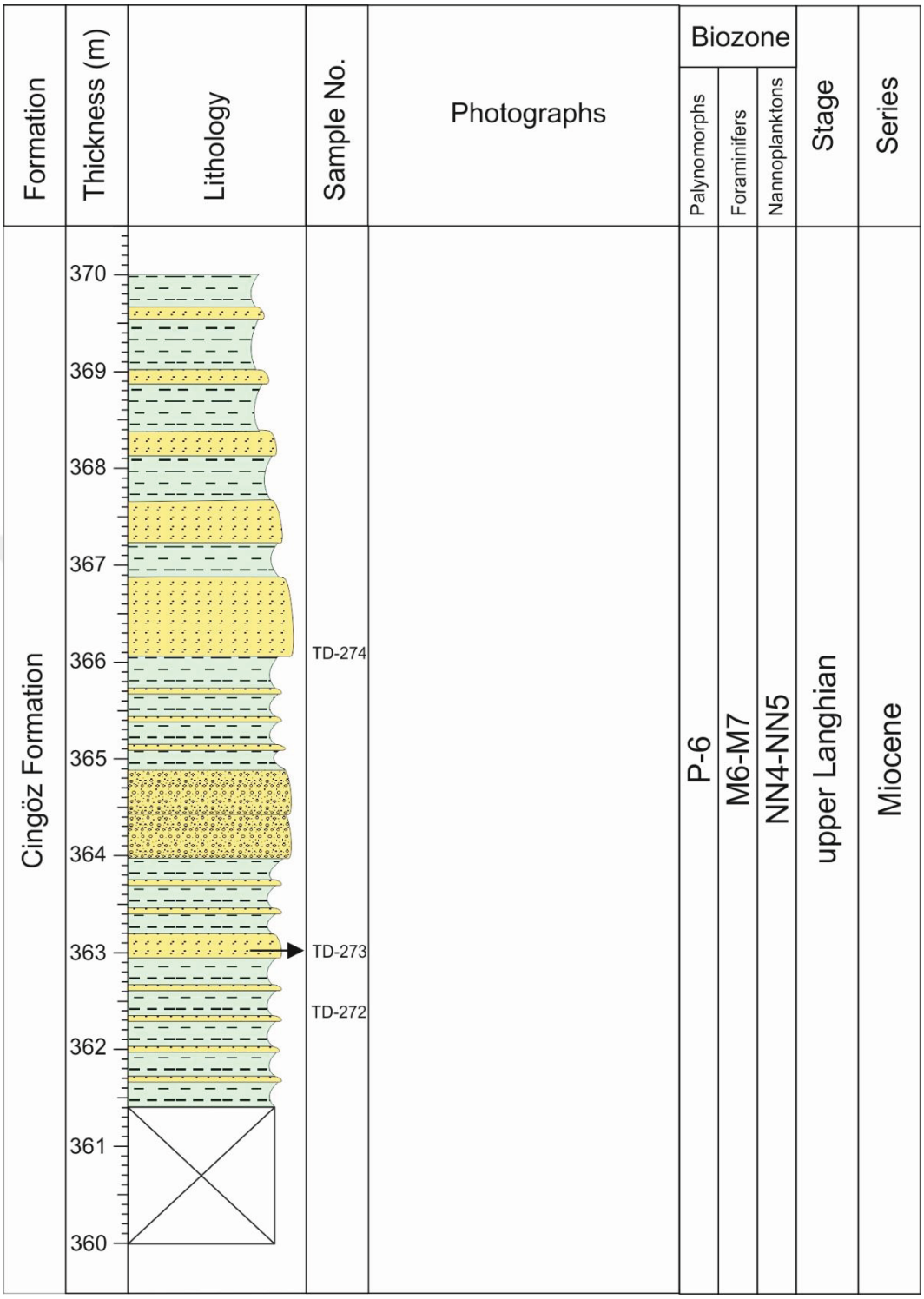

Figure 66. (cont'd)

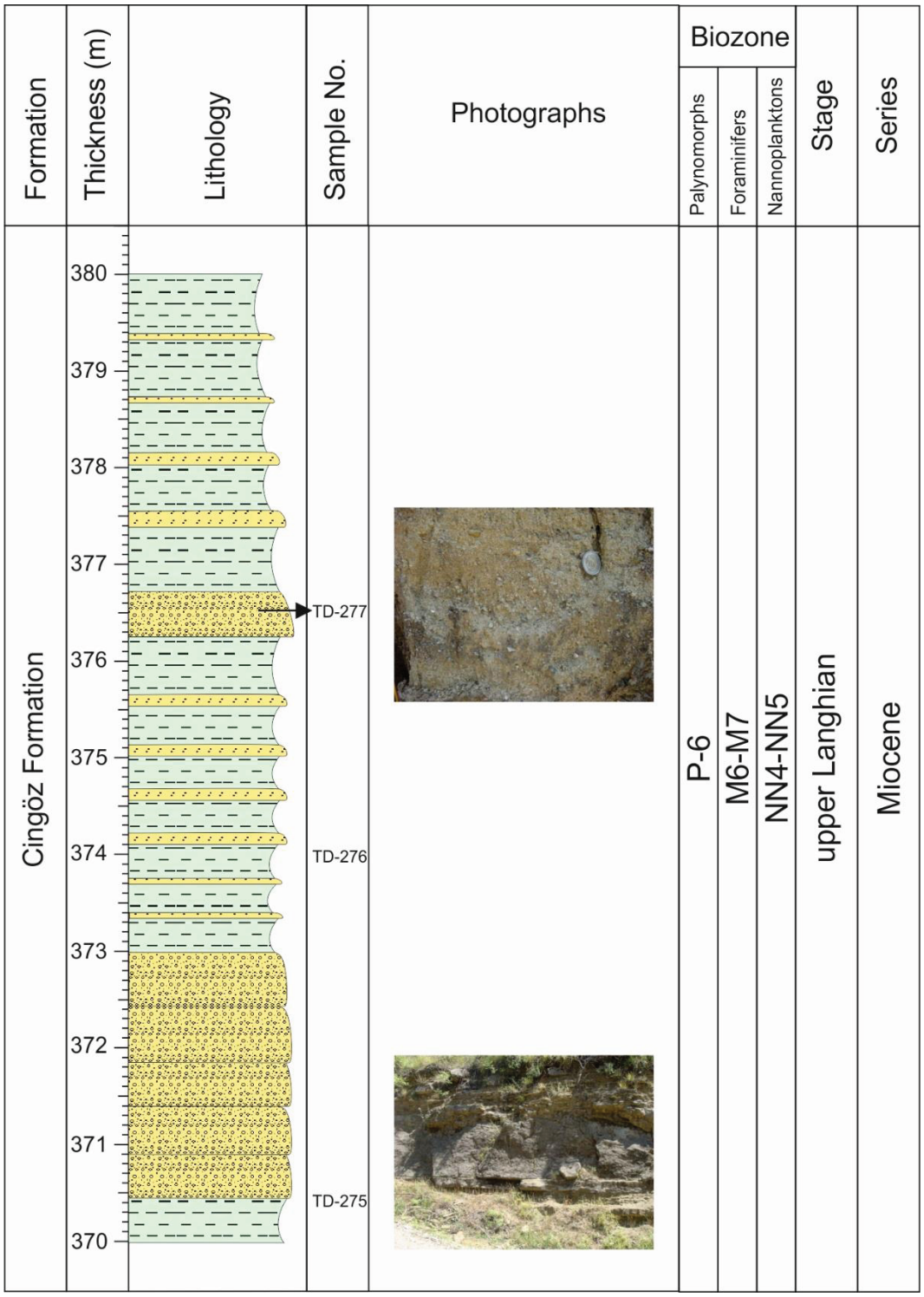

Figure 66. (cont'd)

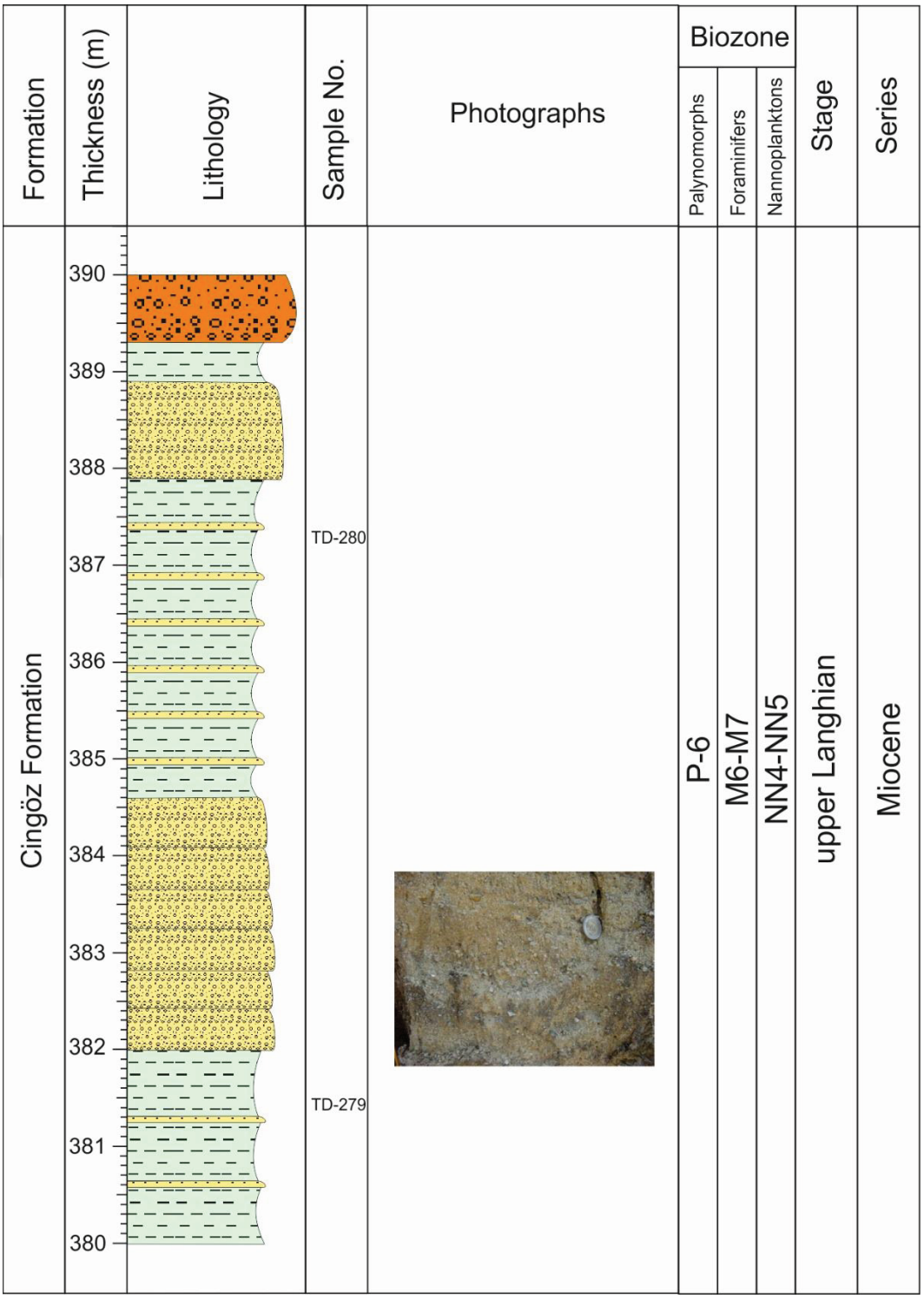

Figure 66. (cont'd)

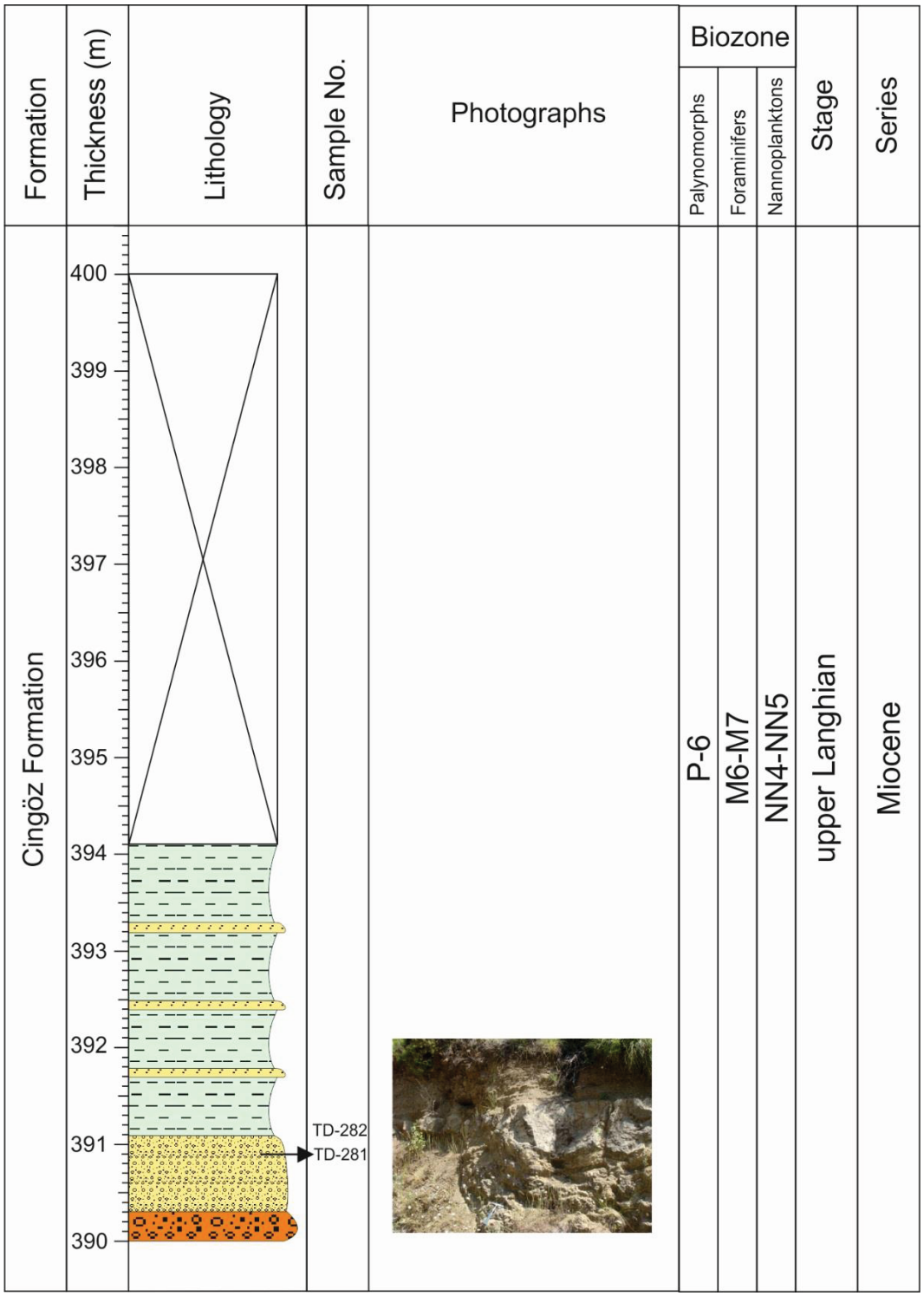

Figure 66. (cont'd)

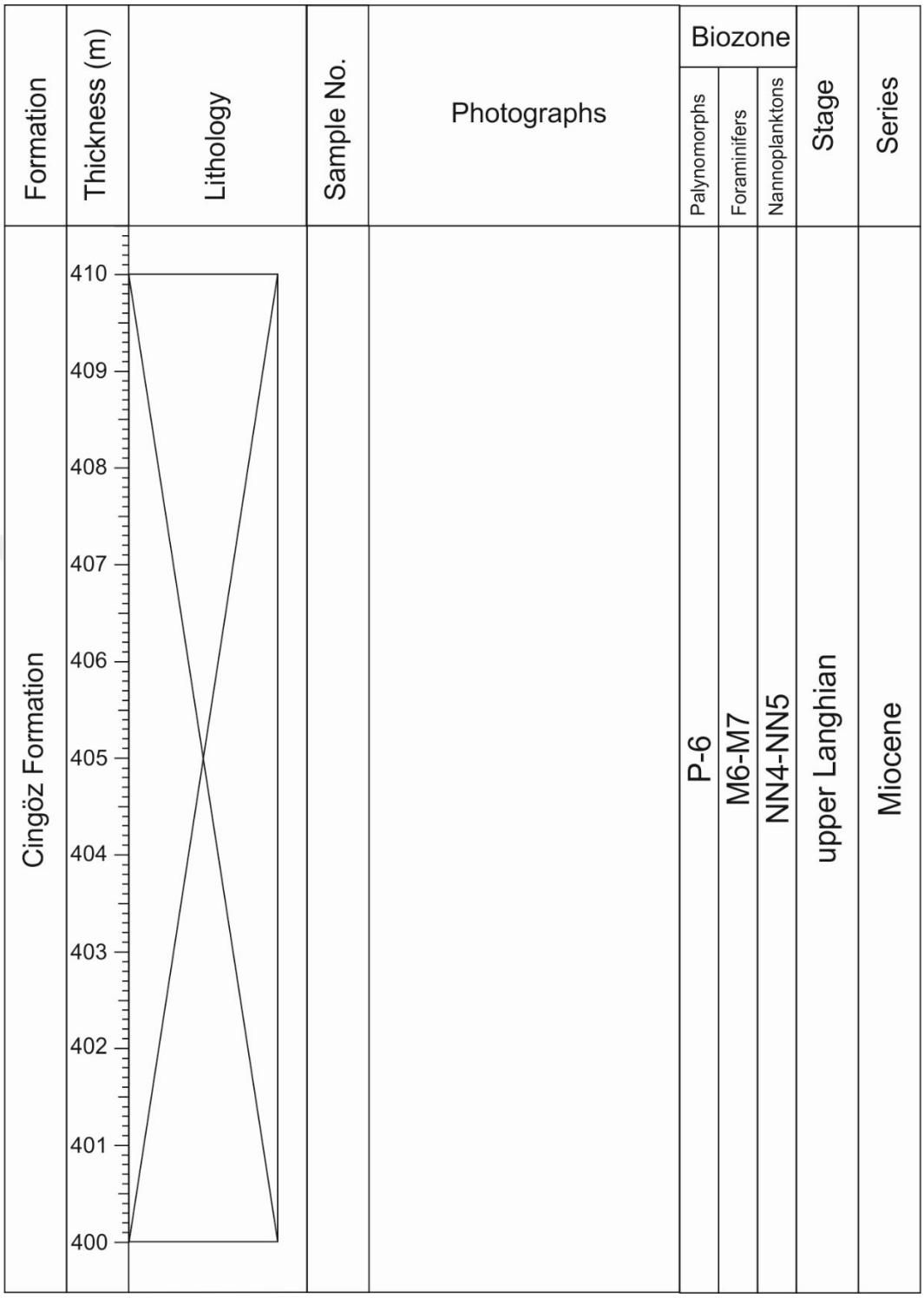

Figure 66. (cont'd)

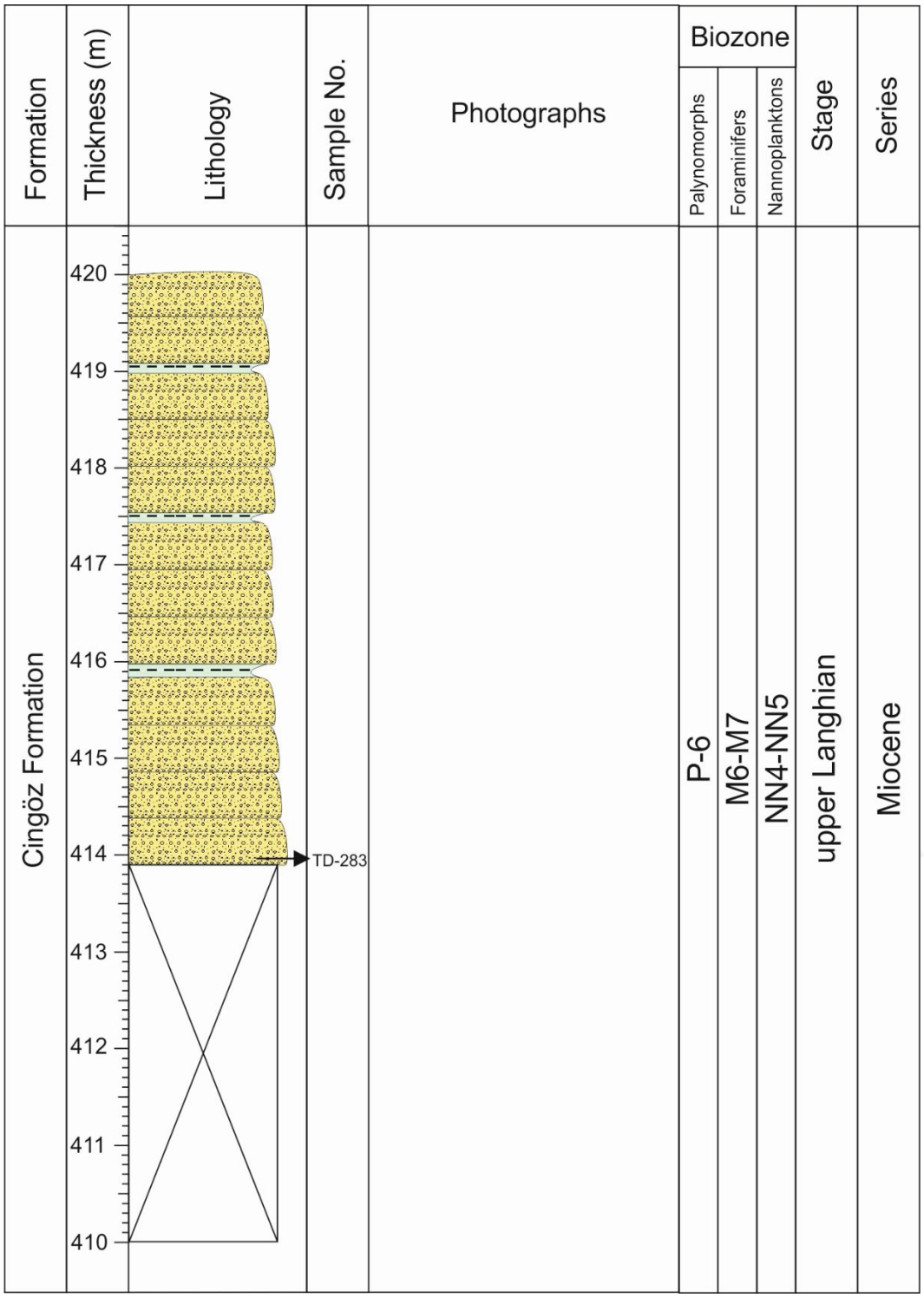

Figure 66. (cont'd)

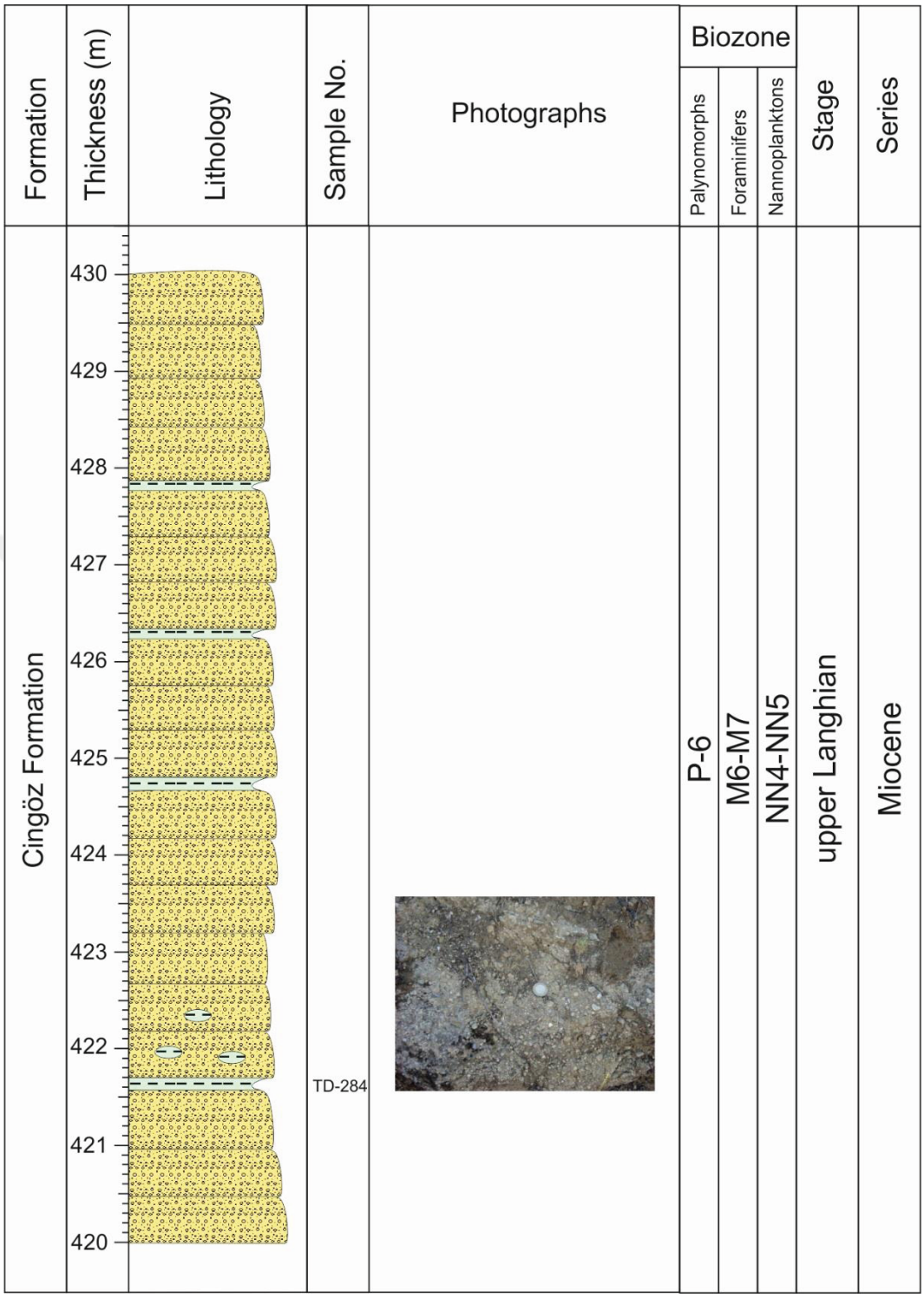

Figure 66. (cont'd)

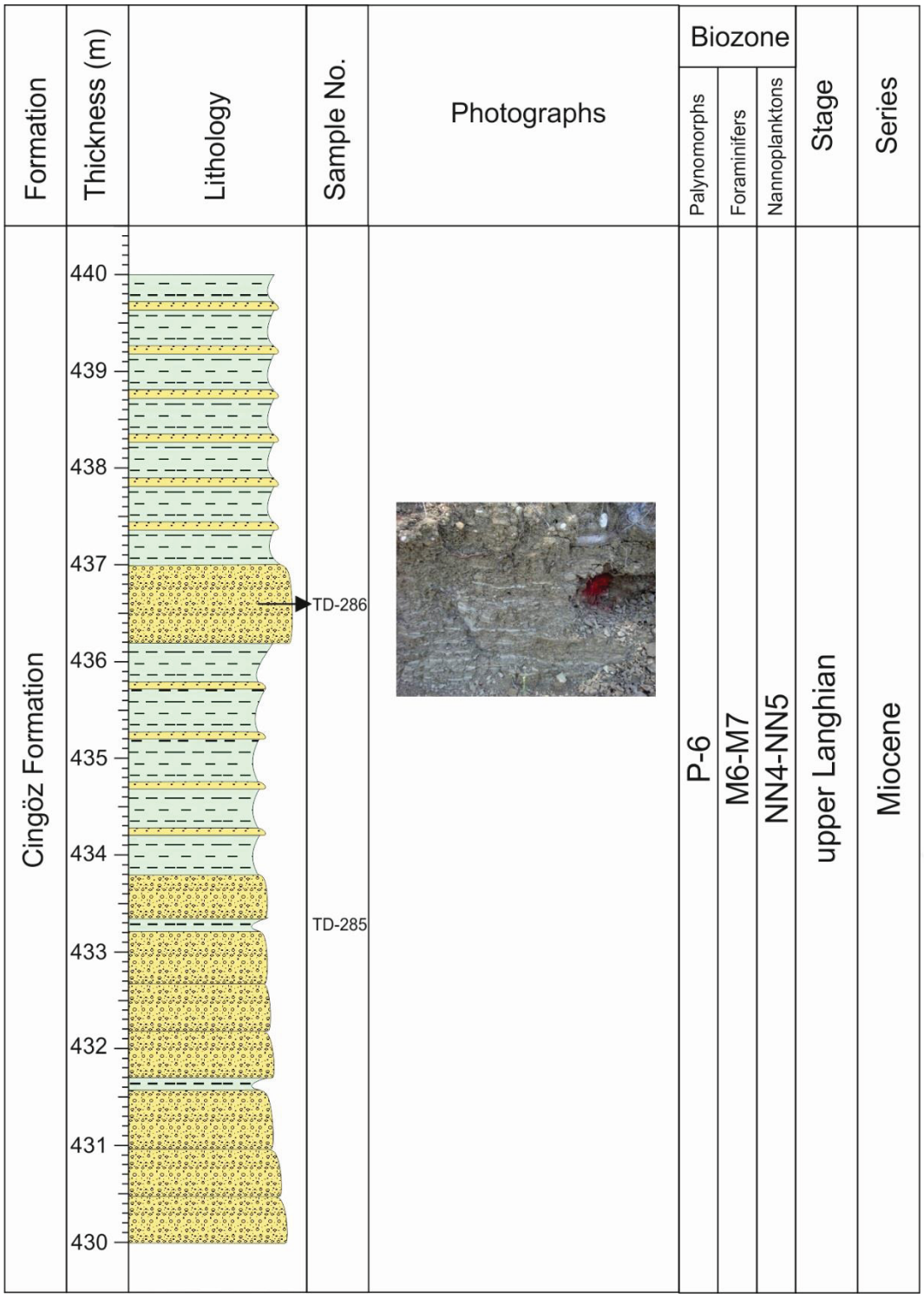

Figure 66. (cont'd)

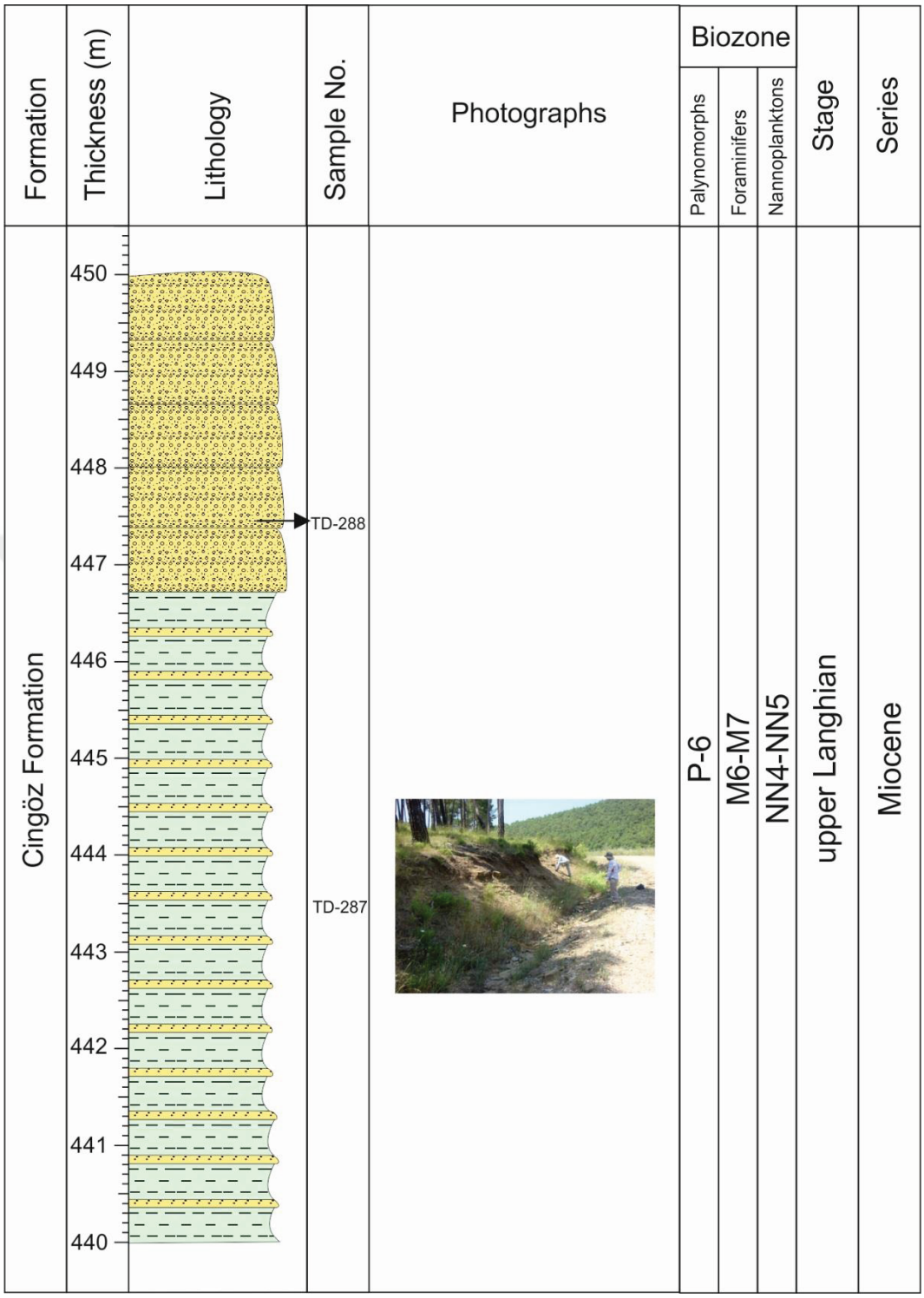

Figure 66. (cont'd)

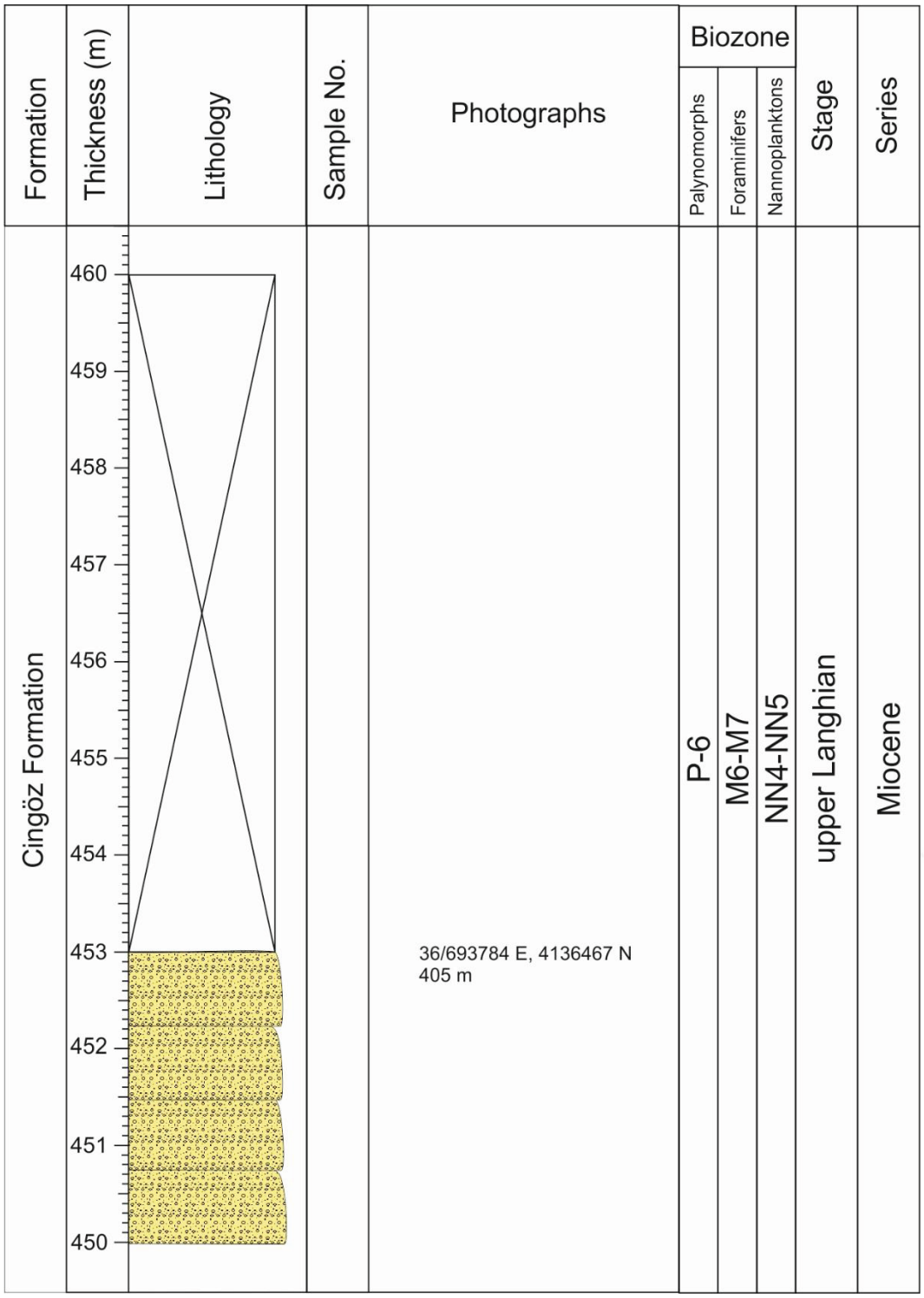

Figure 66. (cont'd)

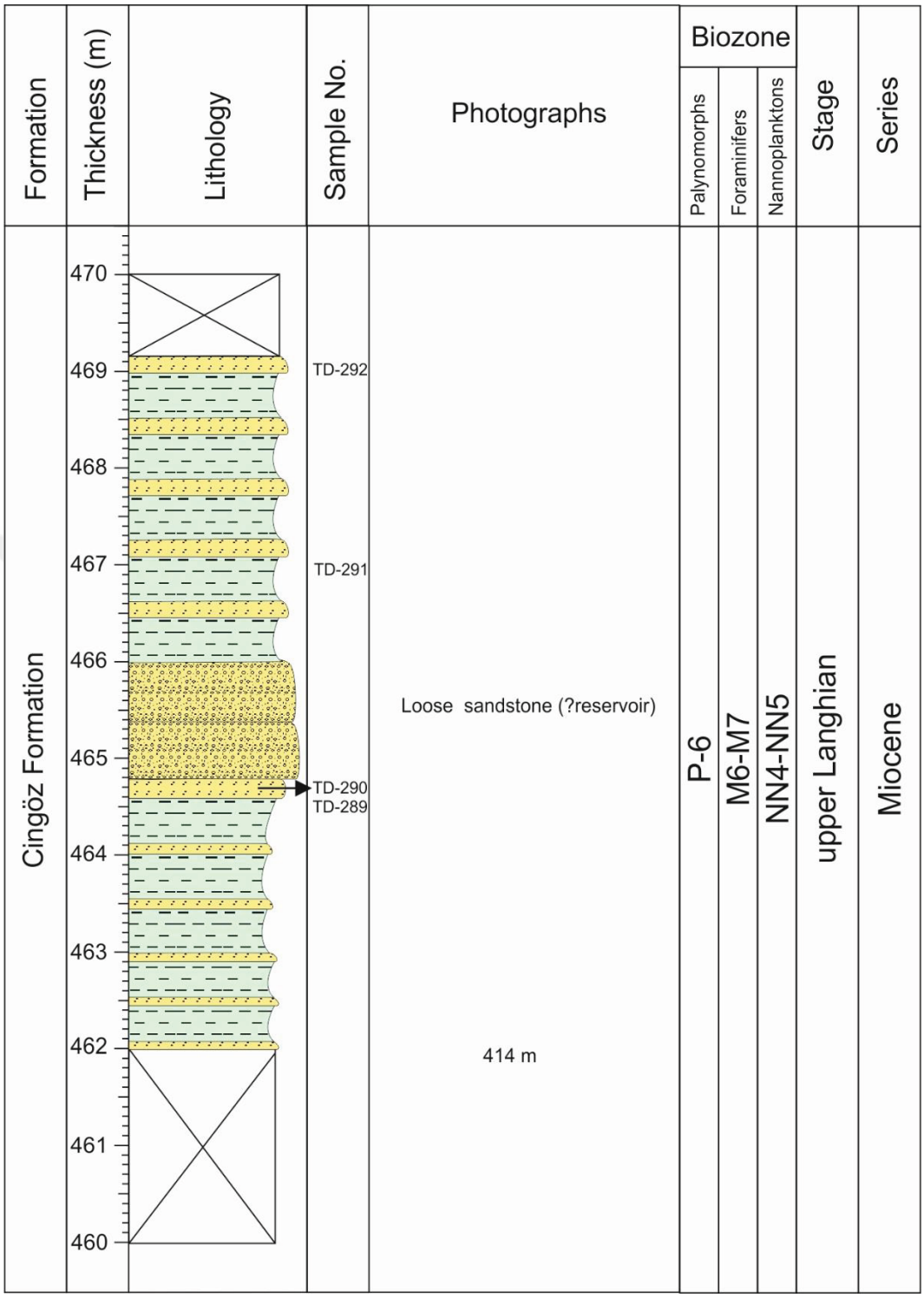

Figure 66. (cont'd)

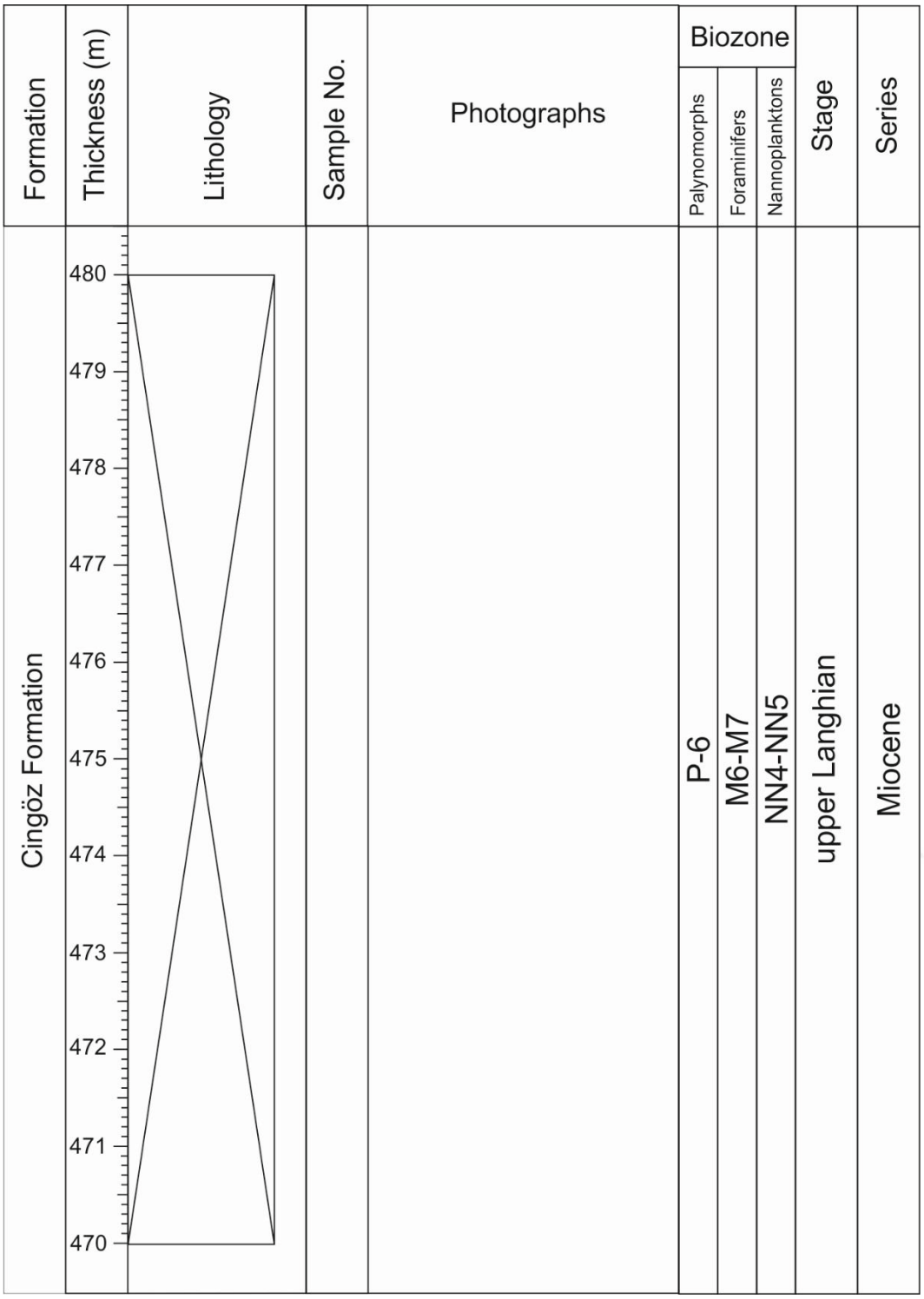

Figure 66. (cont'd)

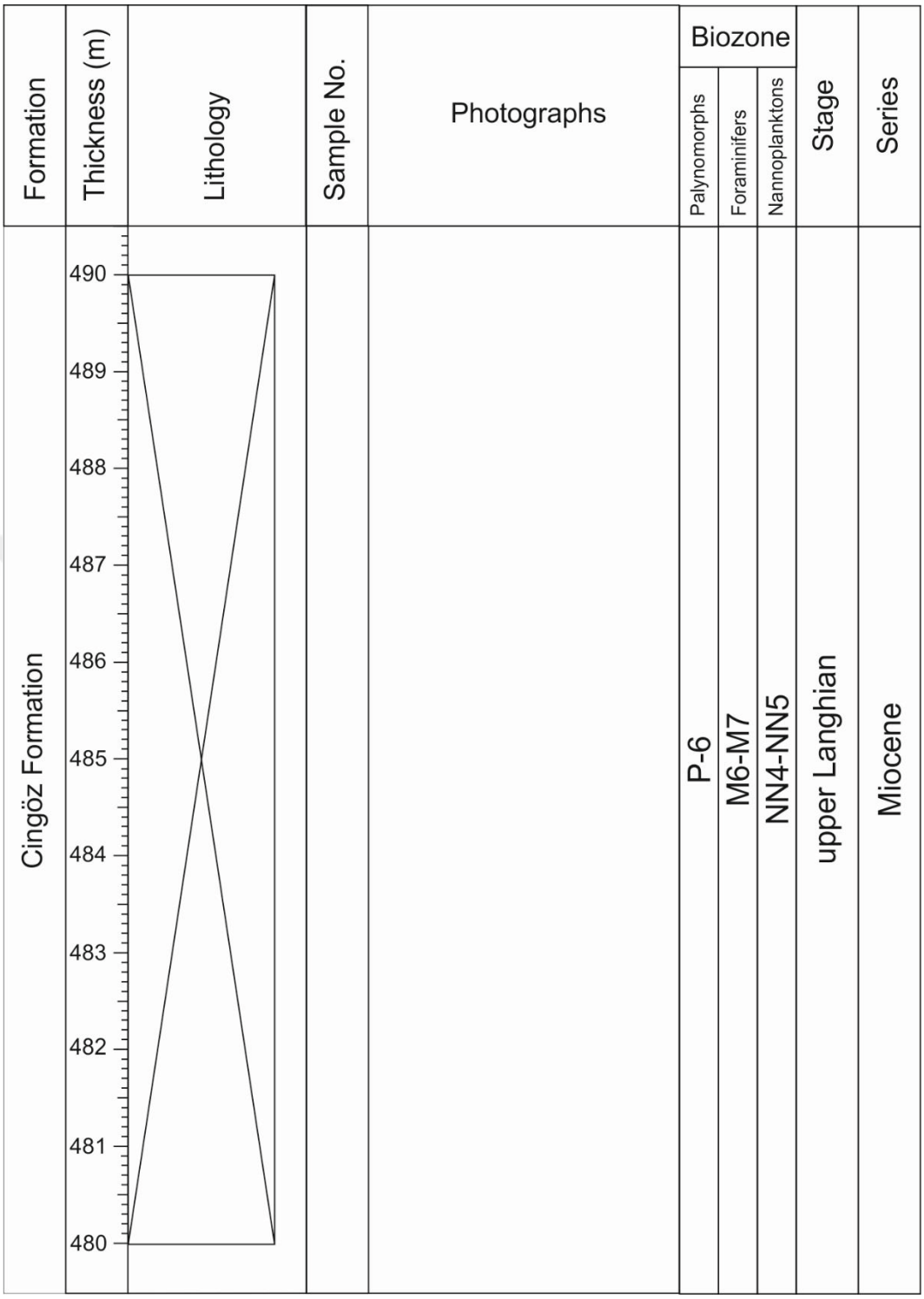

Figure 66. (cont'd)

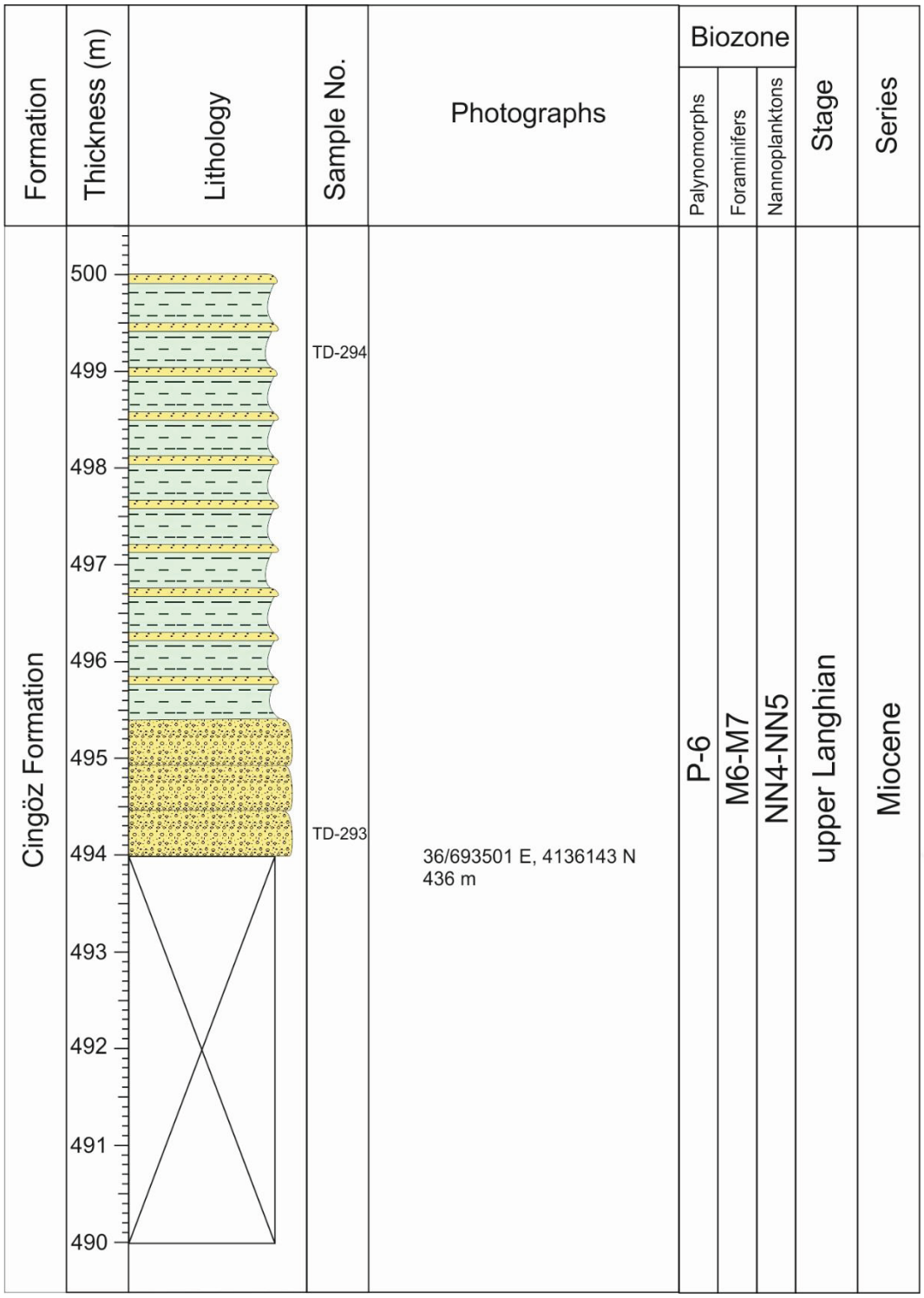

Figure 66. (cont'd)

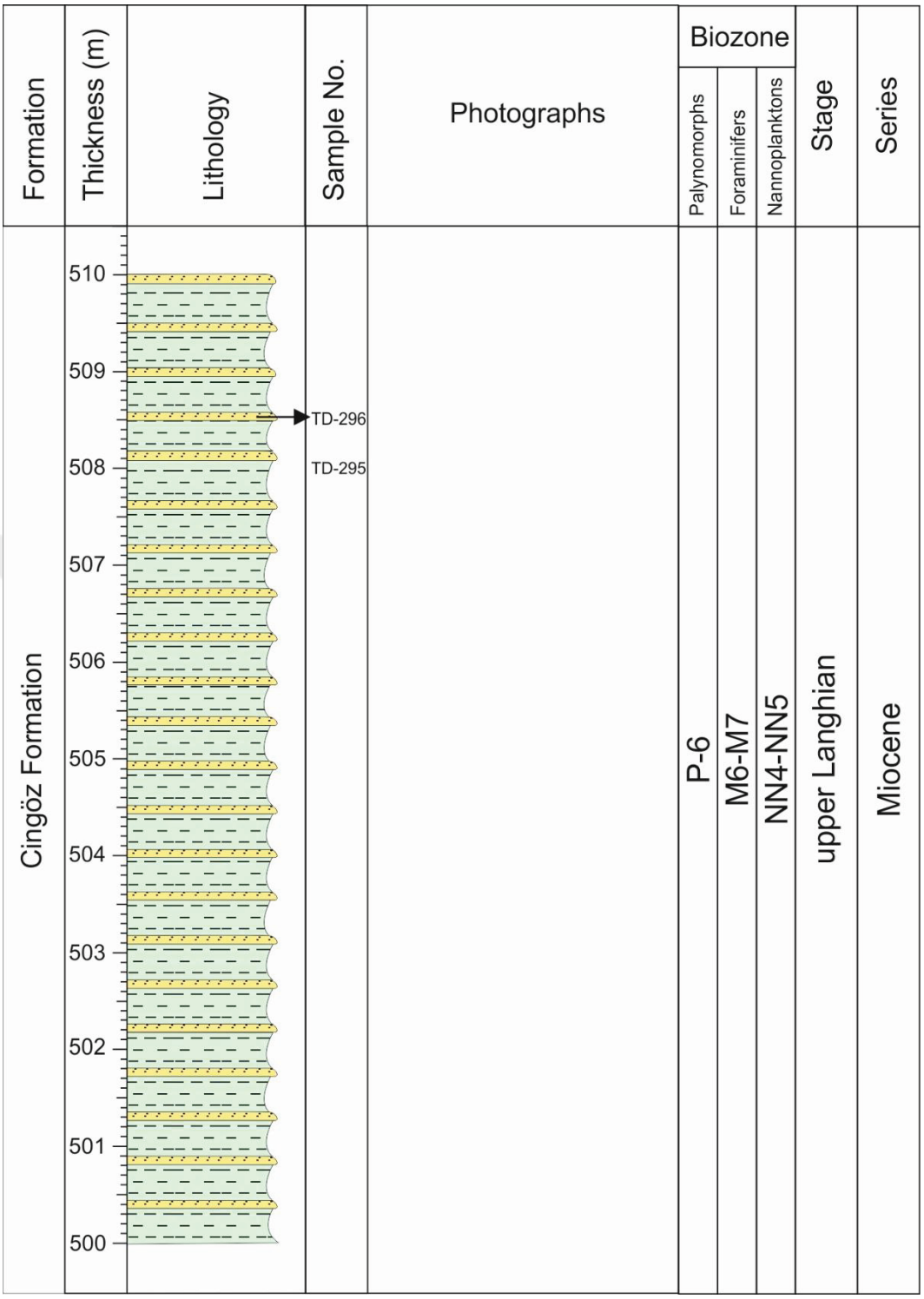

Figure 66. (cont'd)

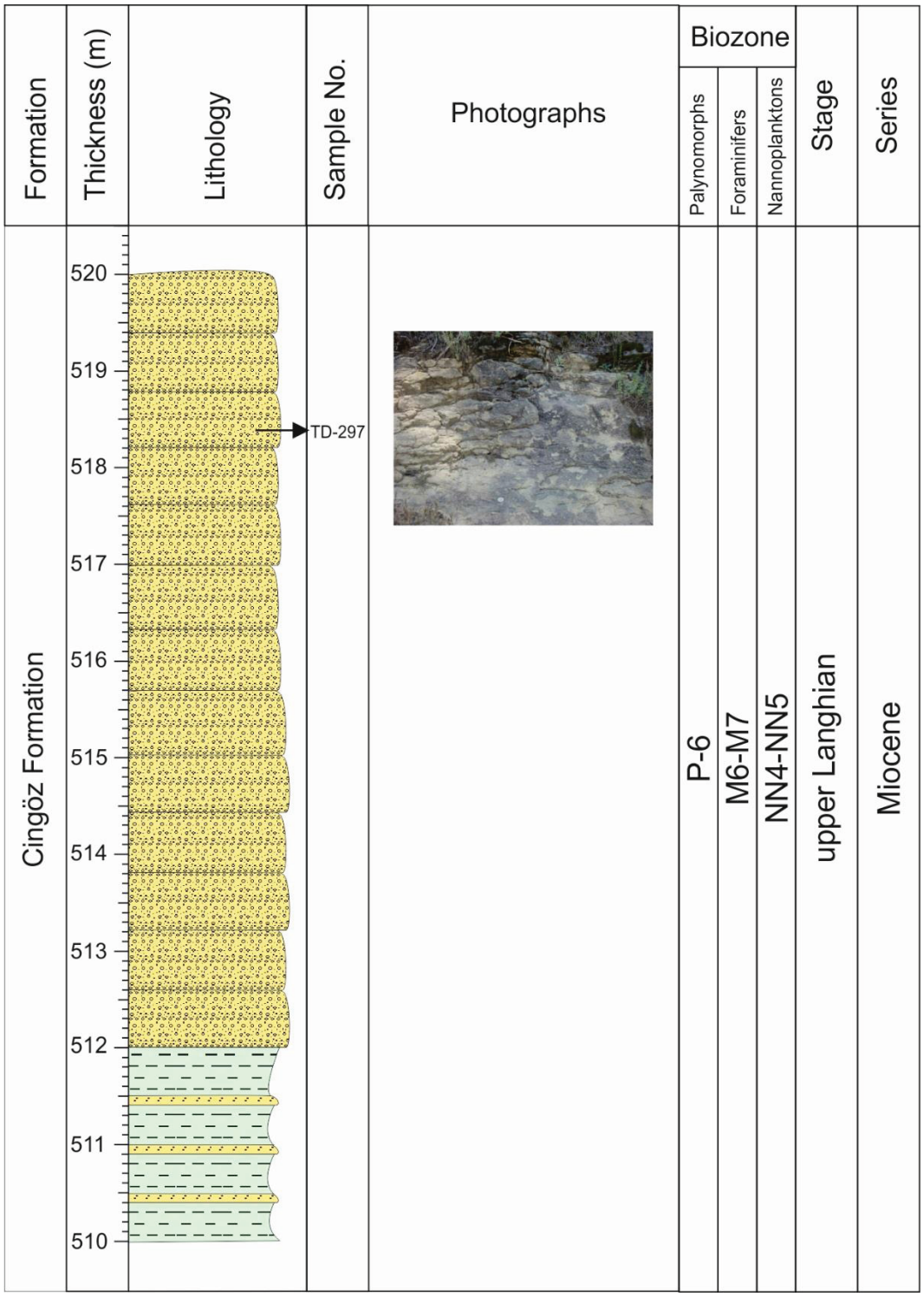

Figure 66. (cont'd)

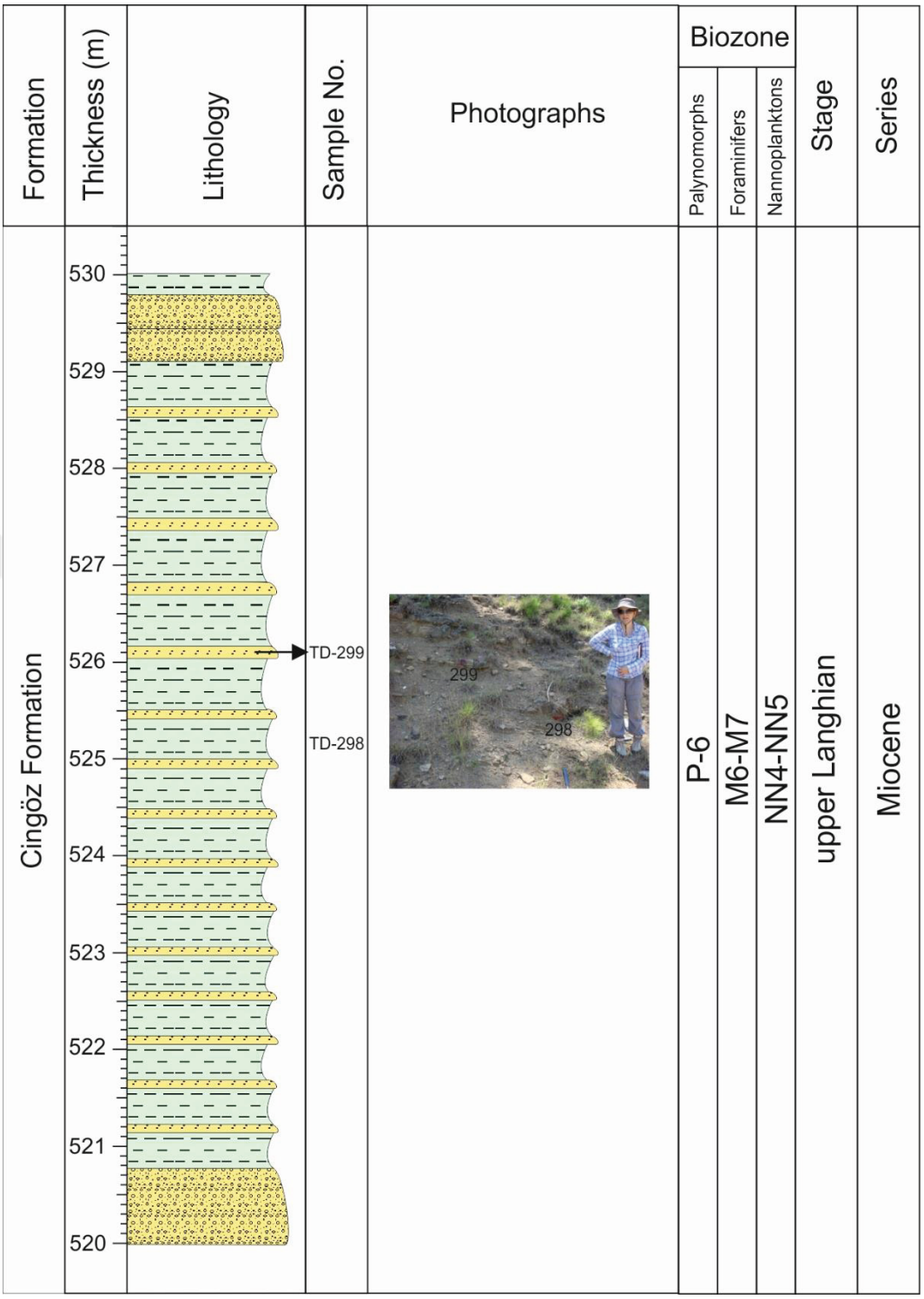

Figure 66. (cont'd)

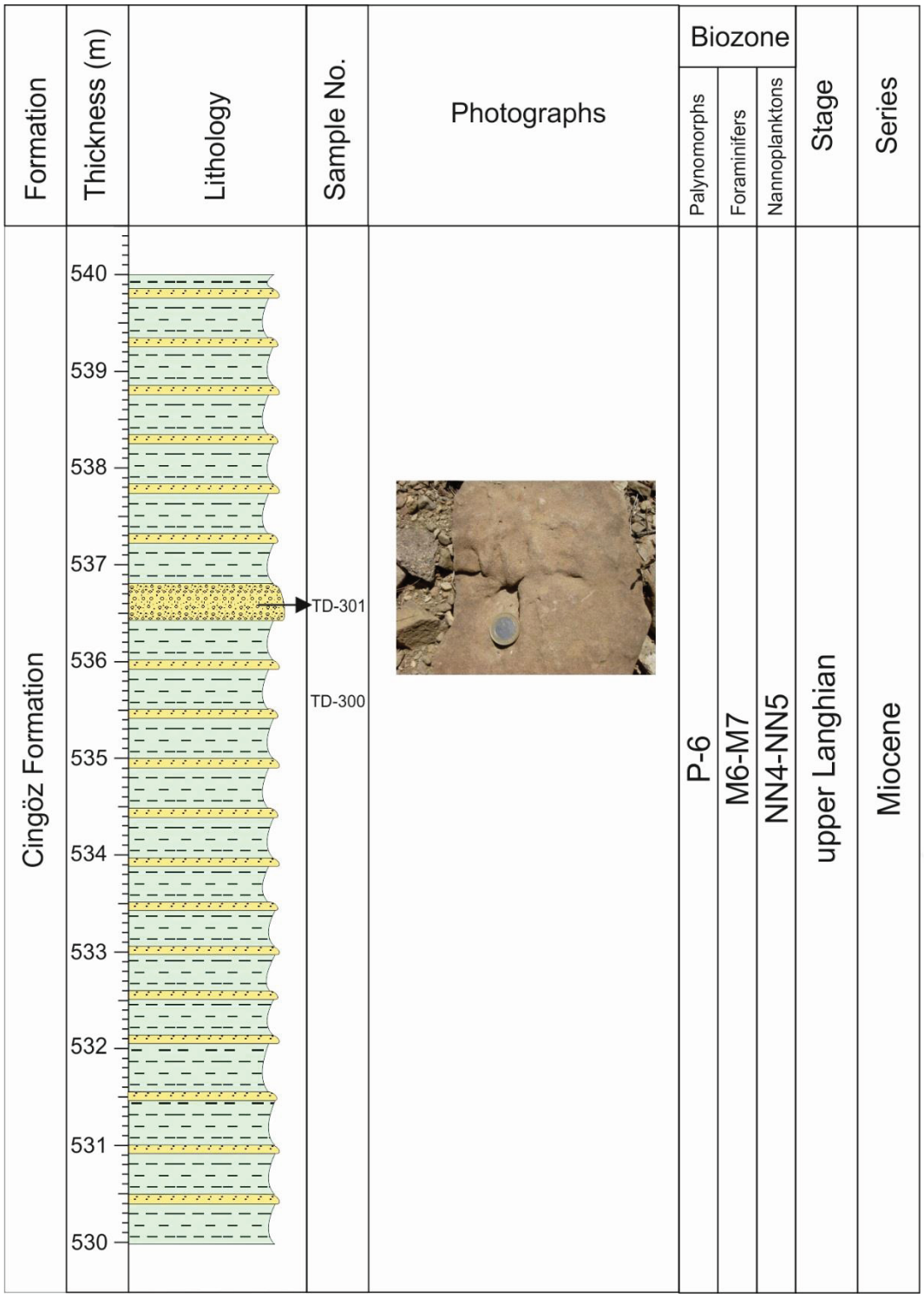

Figure 66. (cont'd)

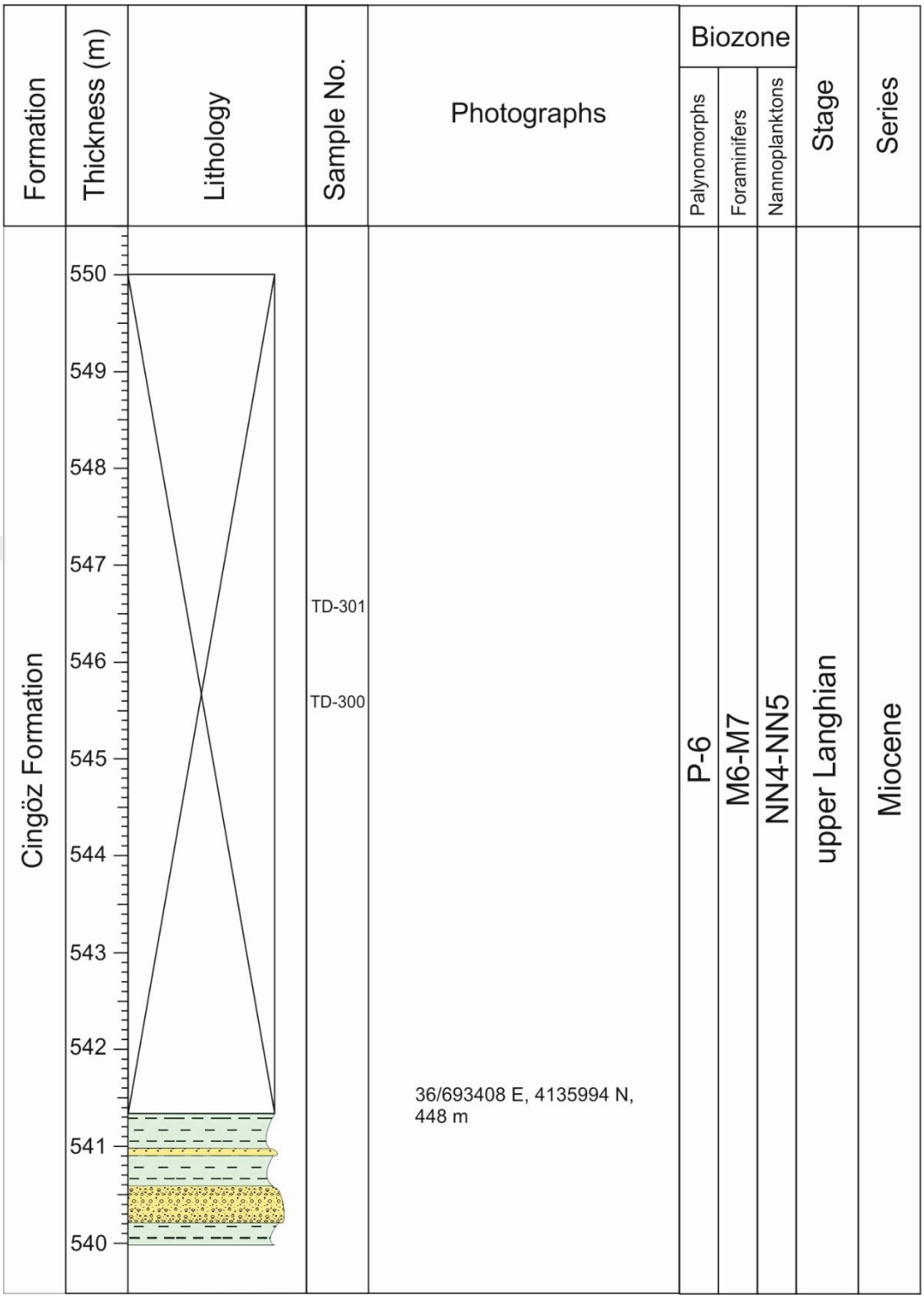

Figure 66. (cont'd)

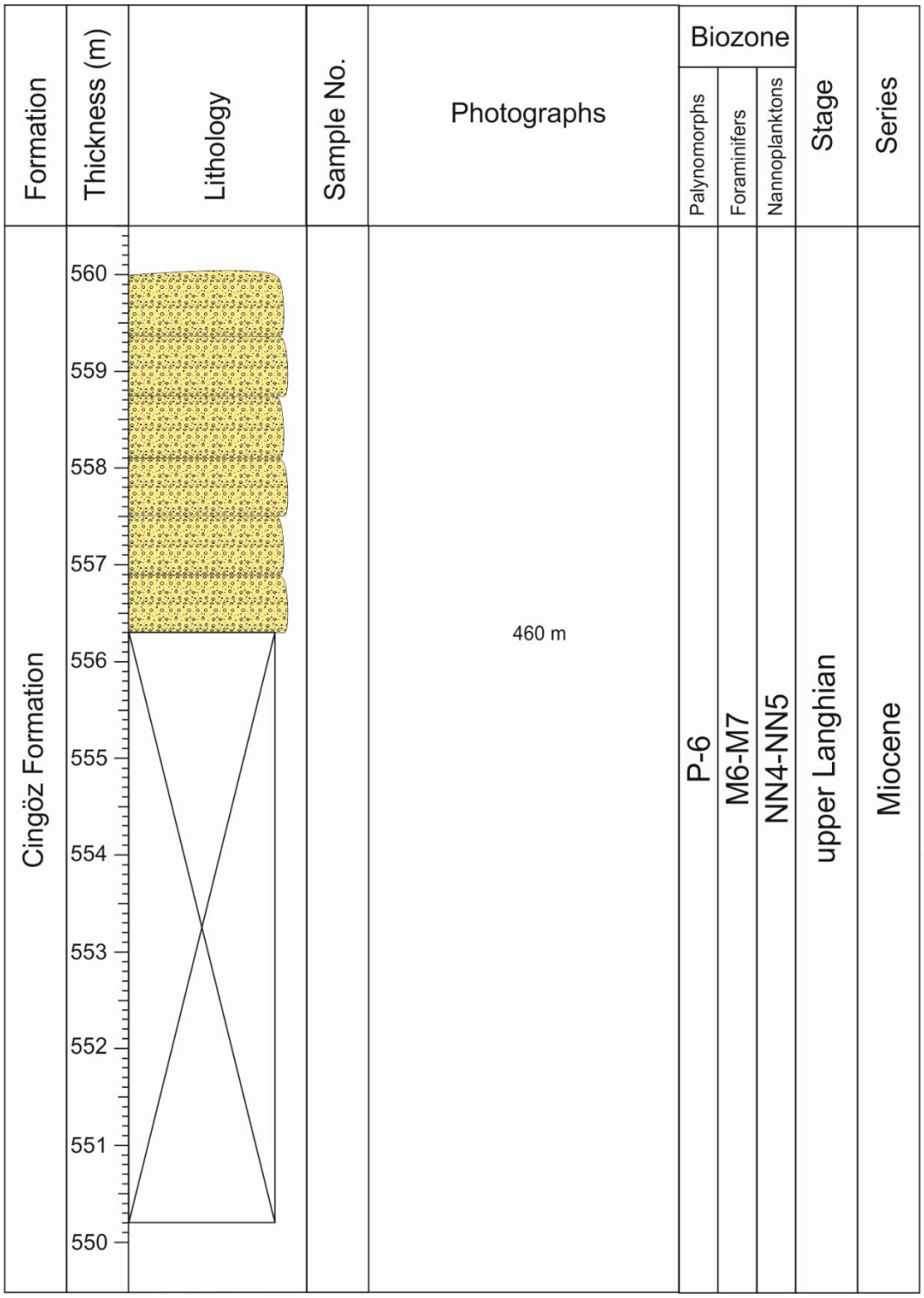

Figure 66. (cont'd)

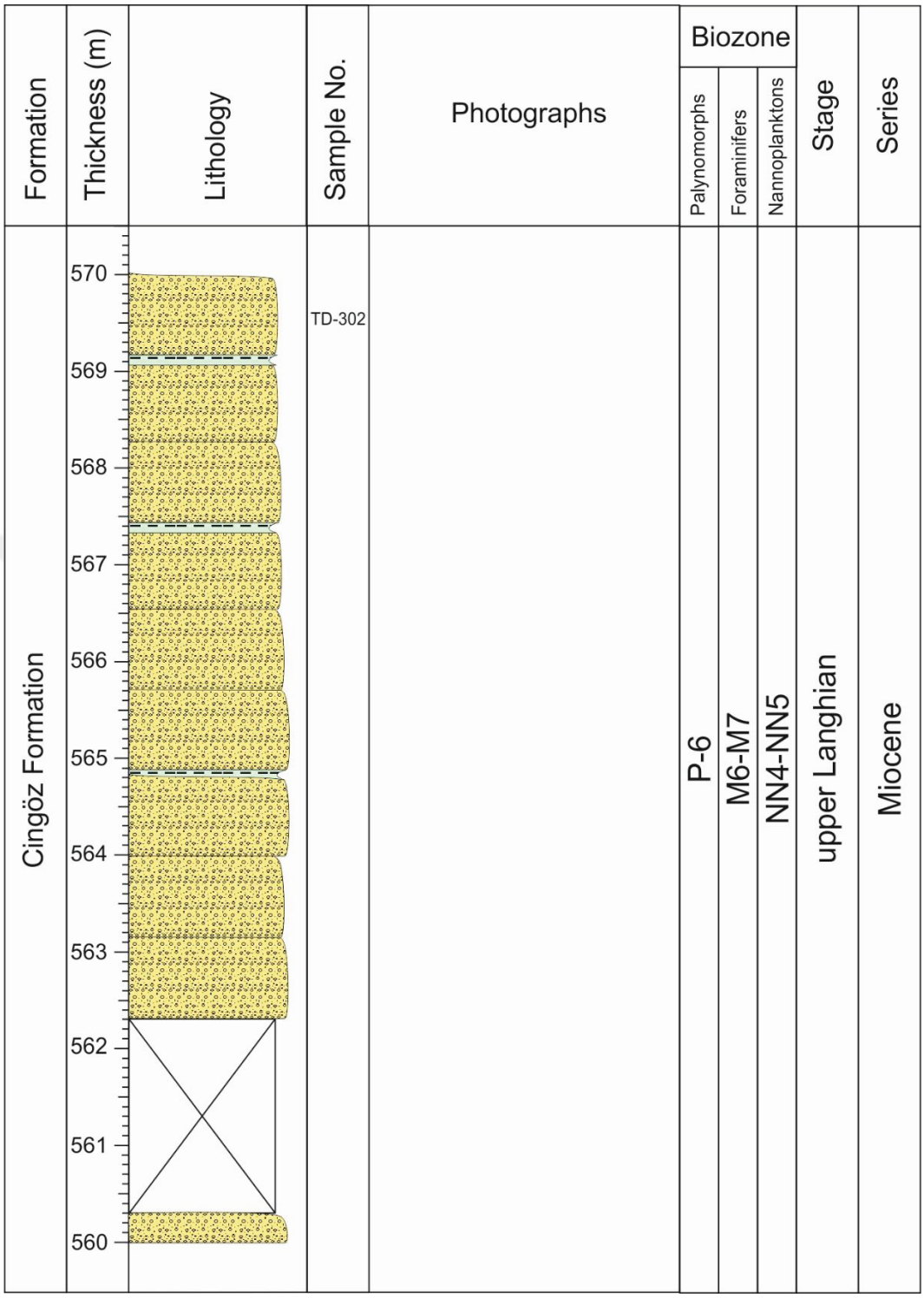

Figure 66. (cont'd)

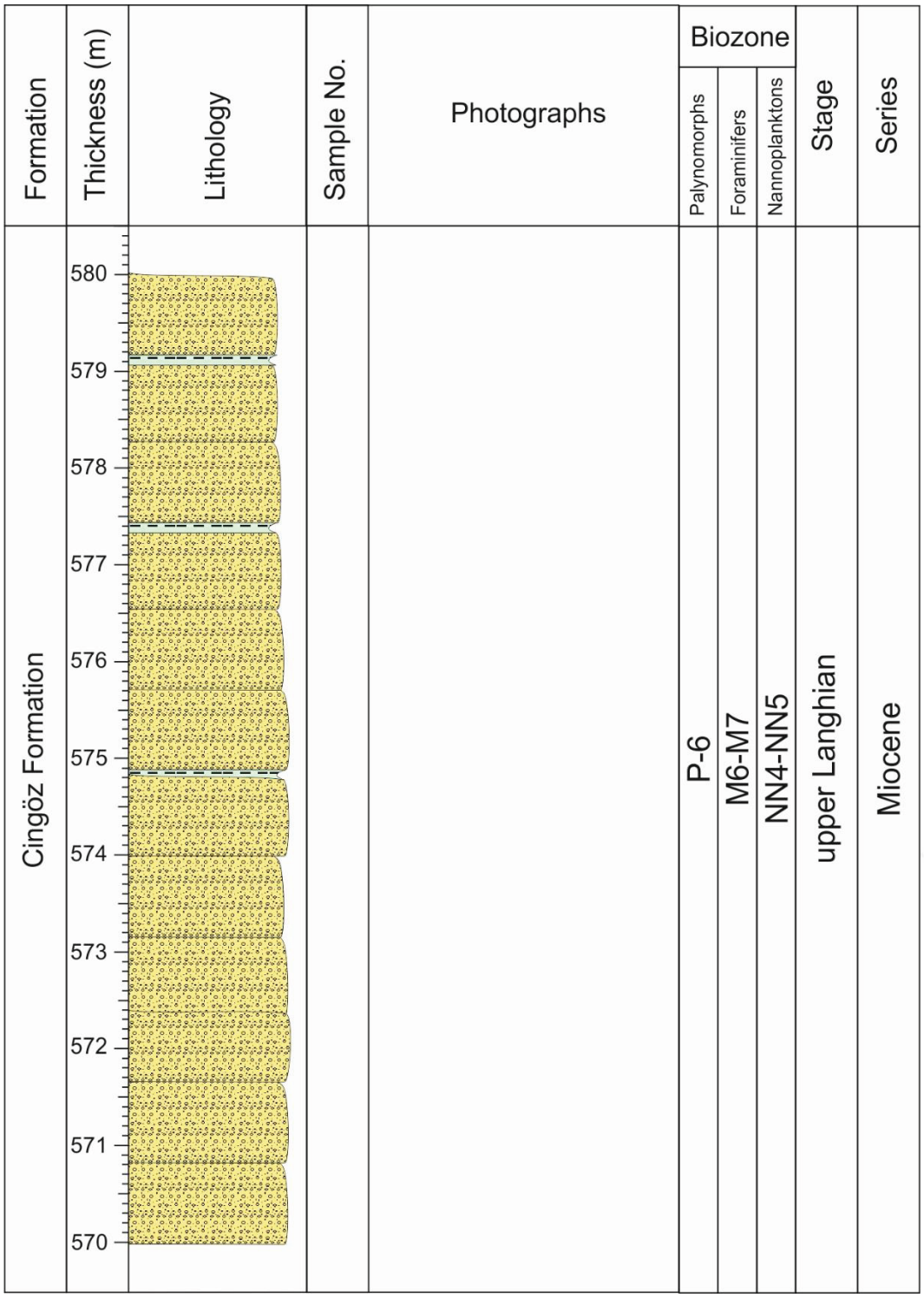

Figure 66. (cont'd)

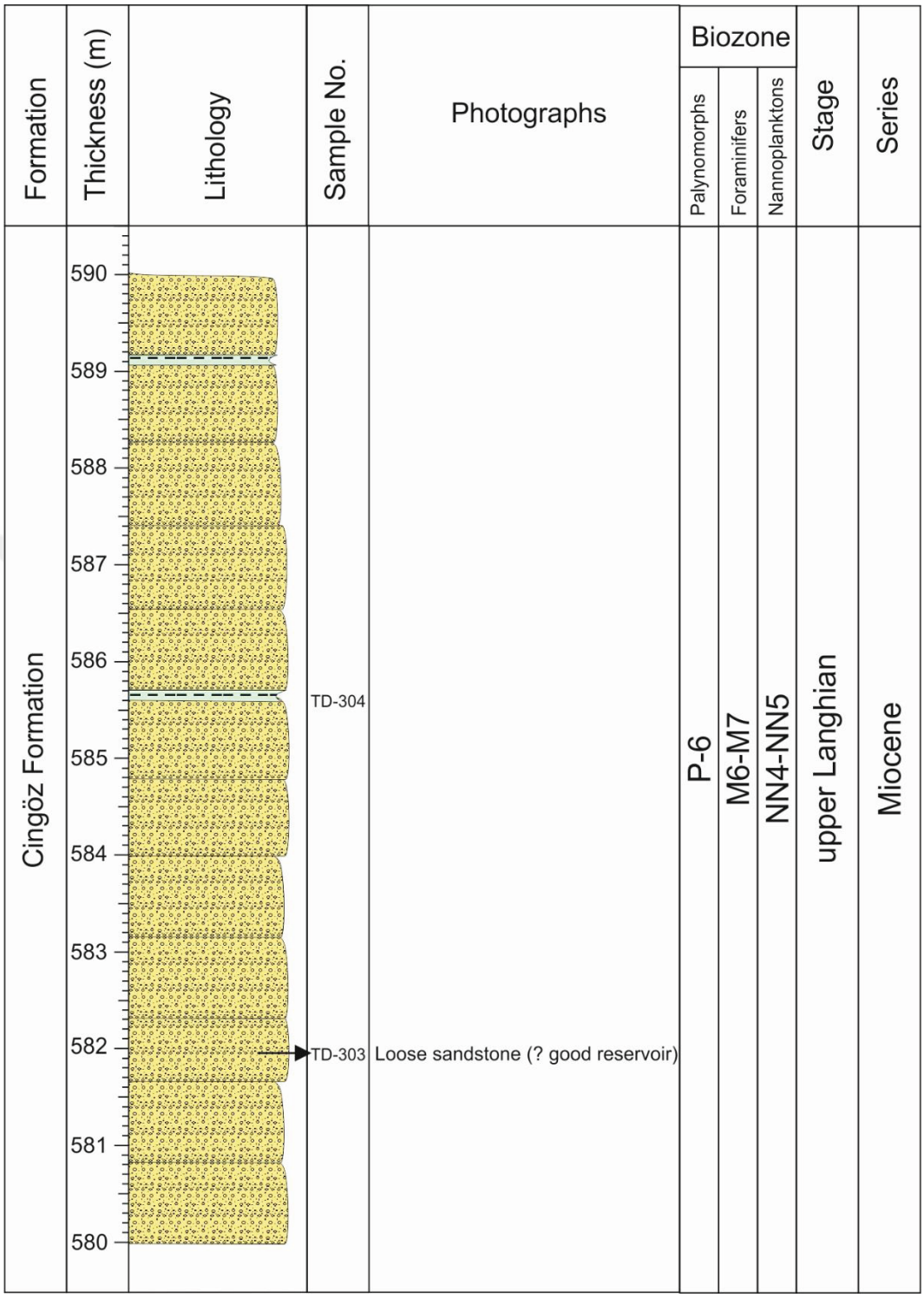

Figure 66. (cont'd)

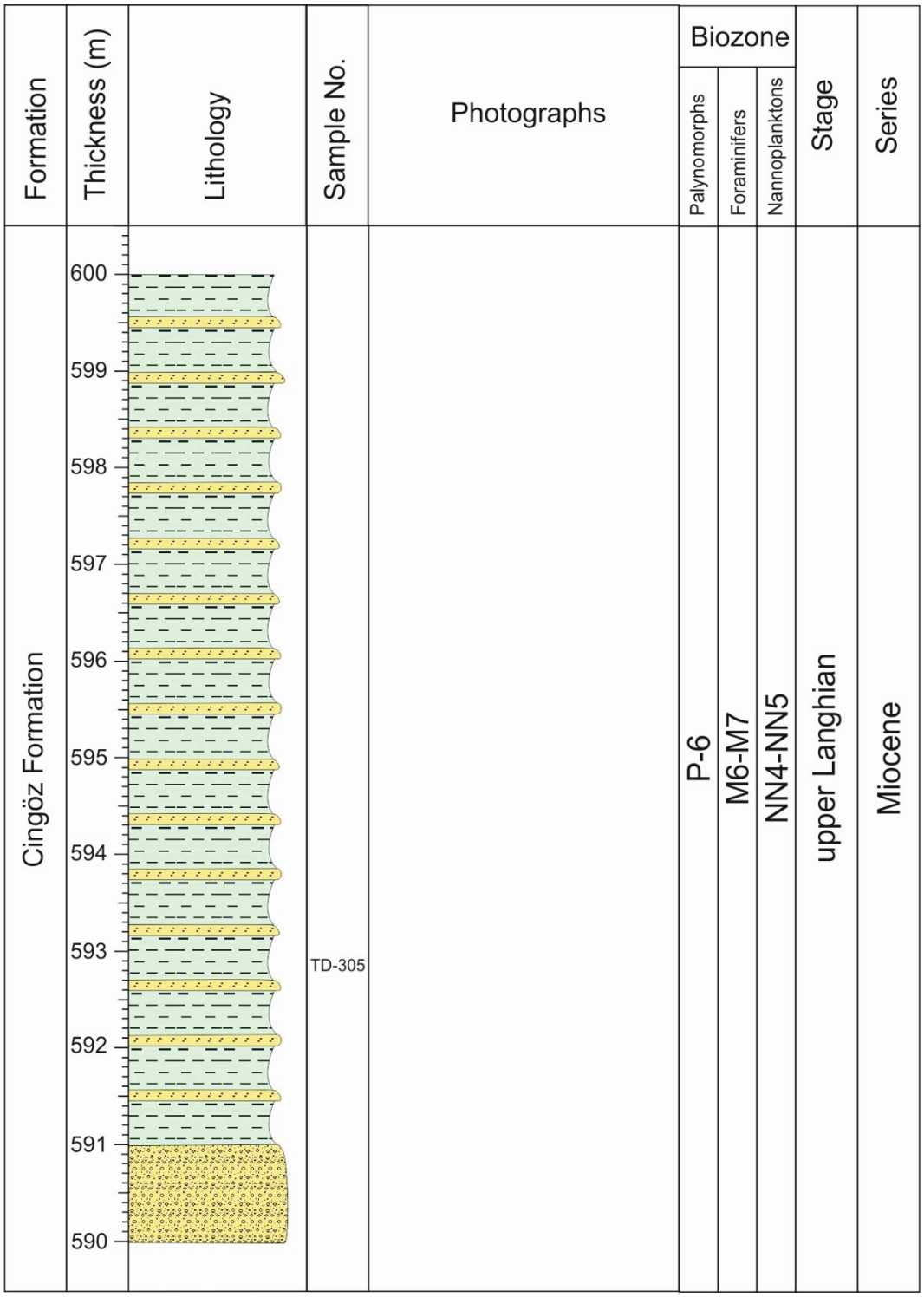

Figure 66. (cont'd)

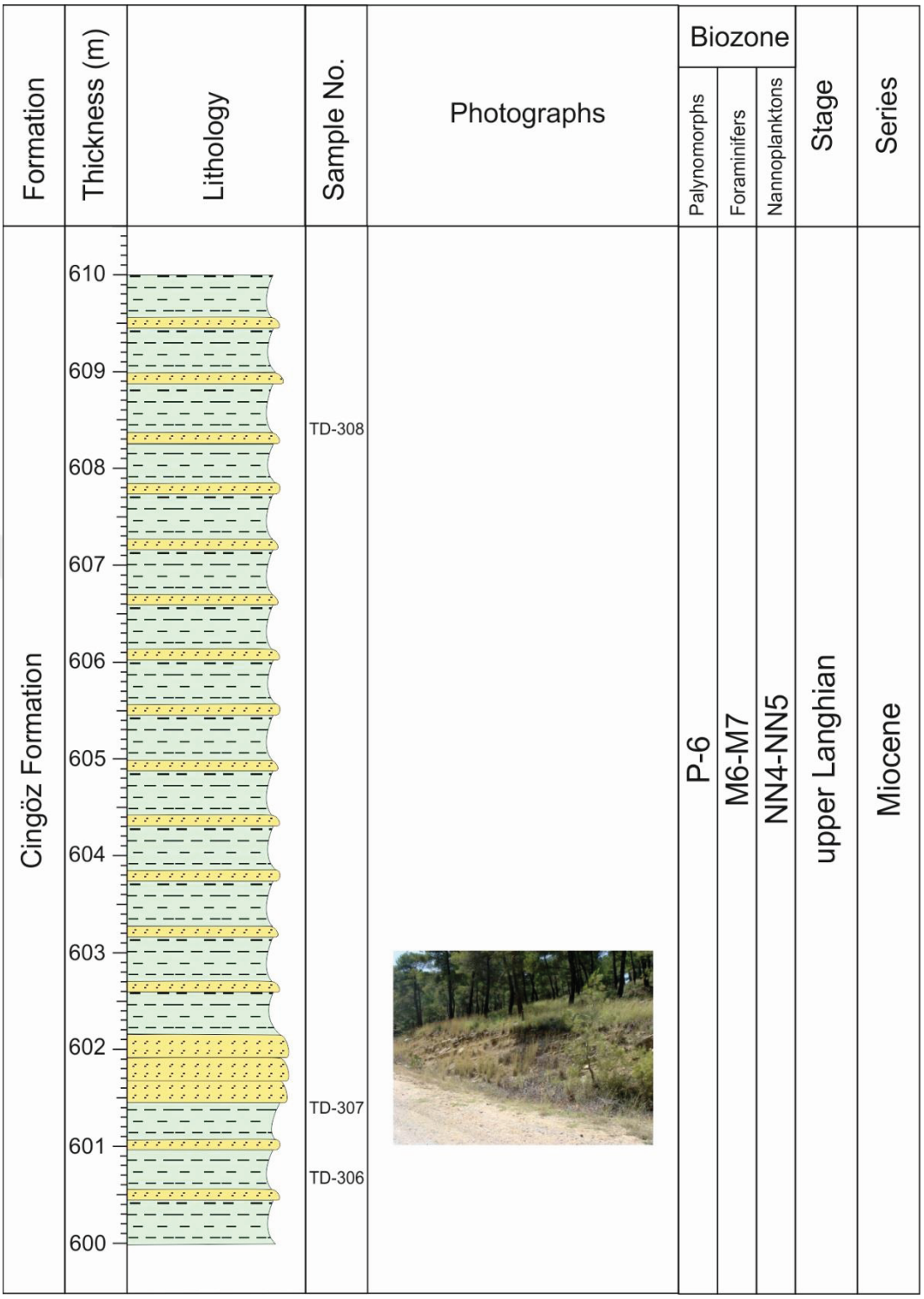

Figure 66. (cont'd)

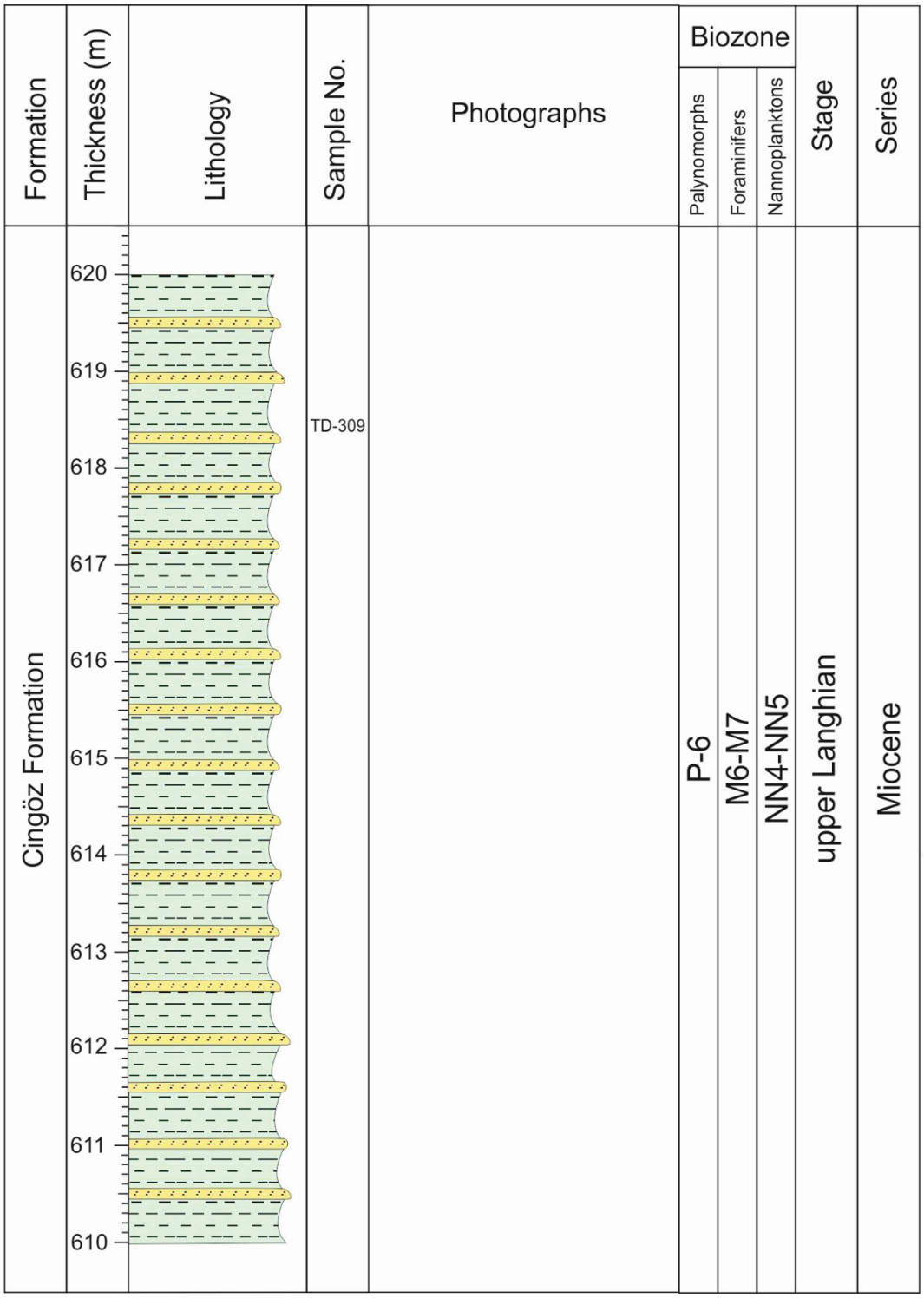

Figure 66. (cont'd)

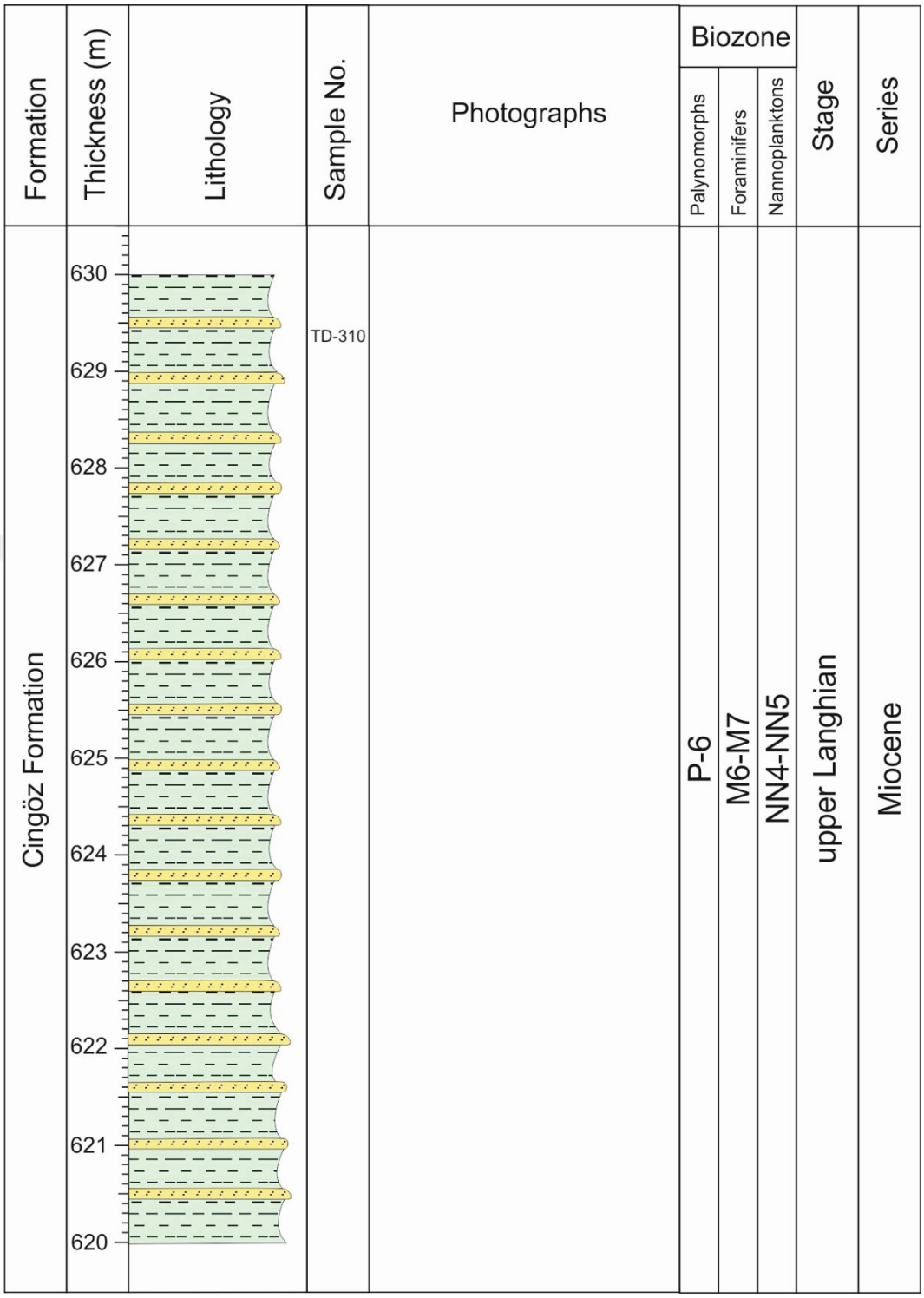

Figure 66. (cont'd)

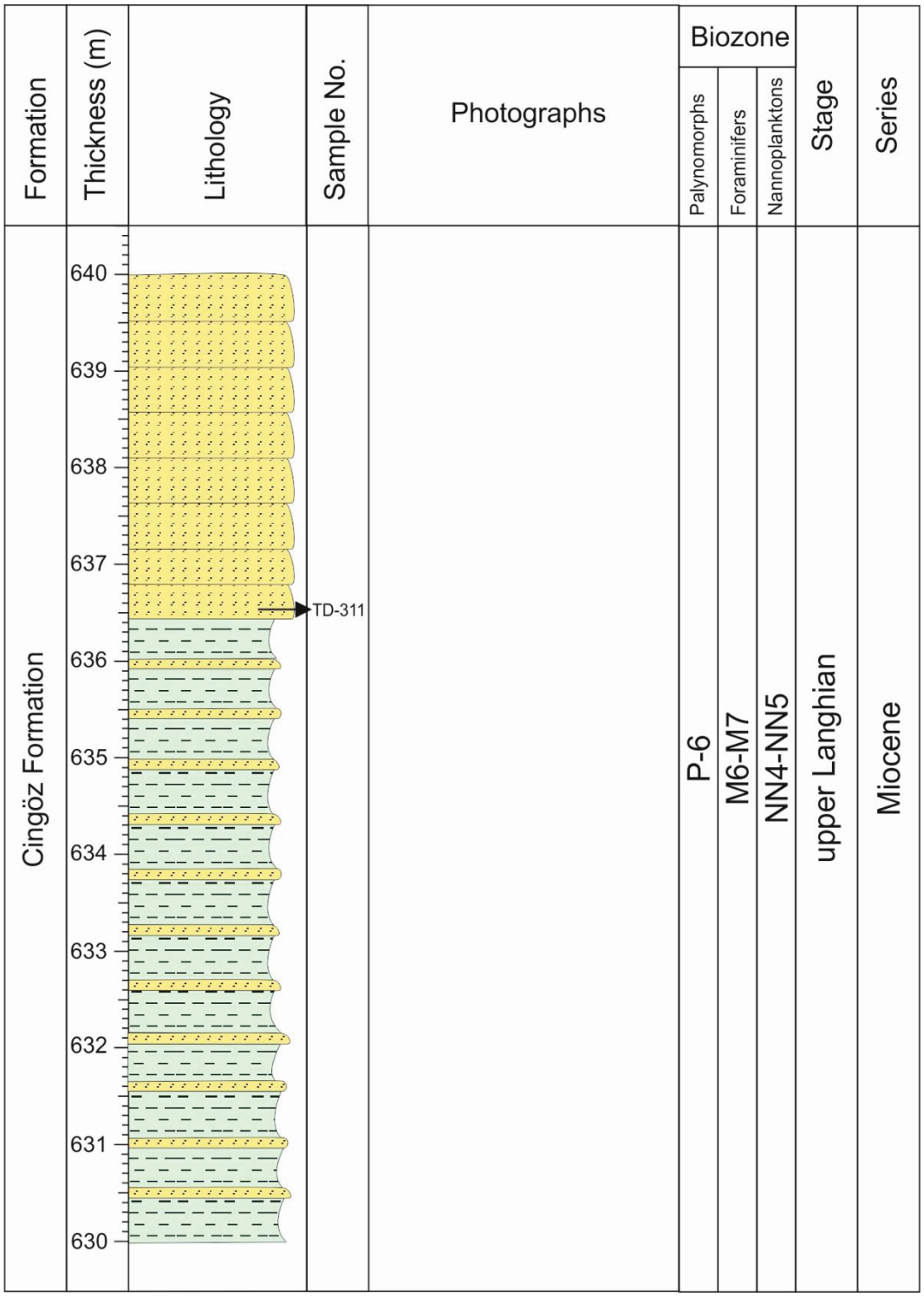

Figure 66. (cont'd)

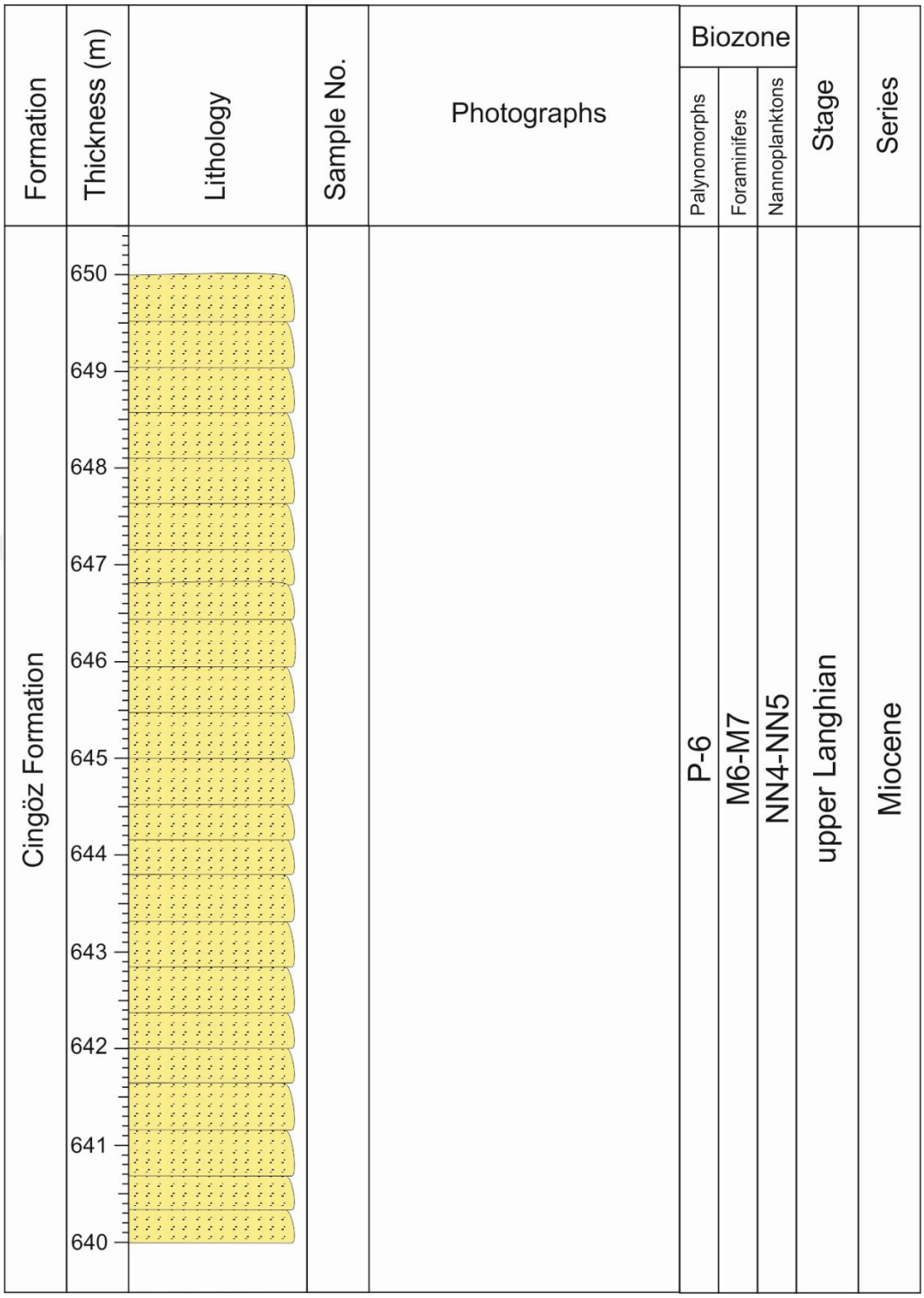

Figure 66. (cont'd)

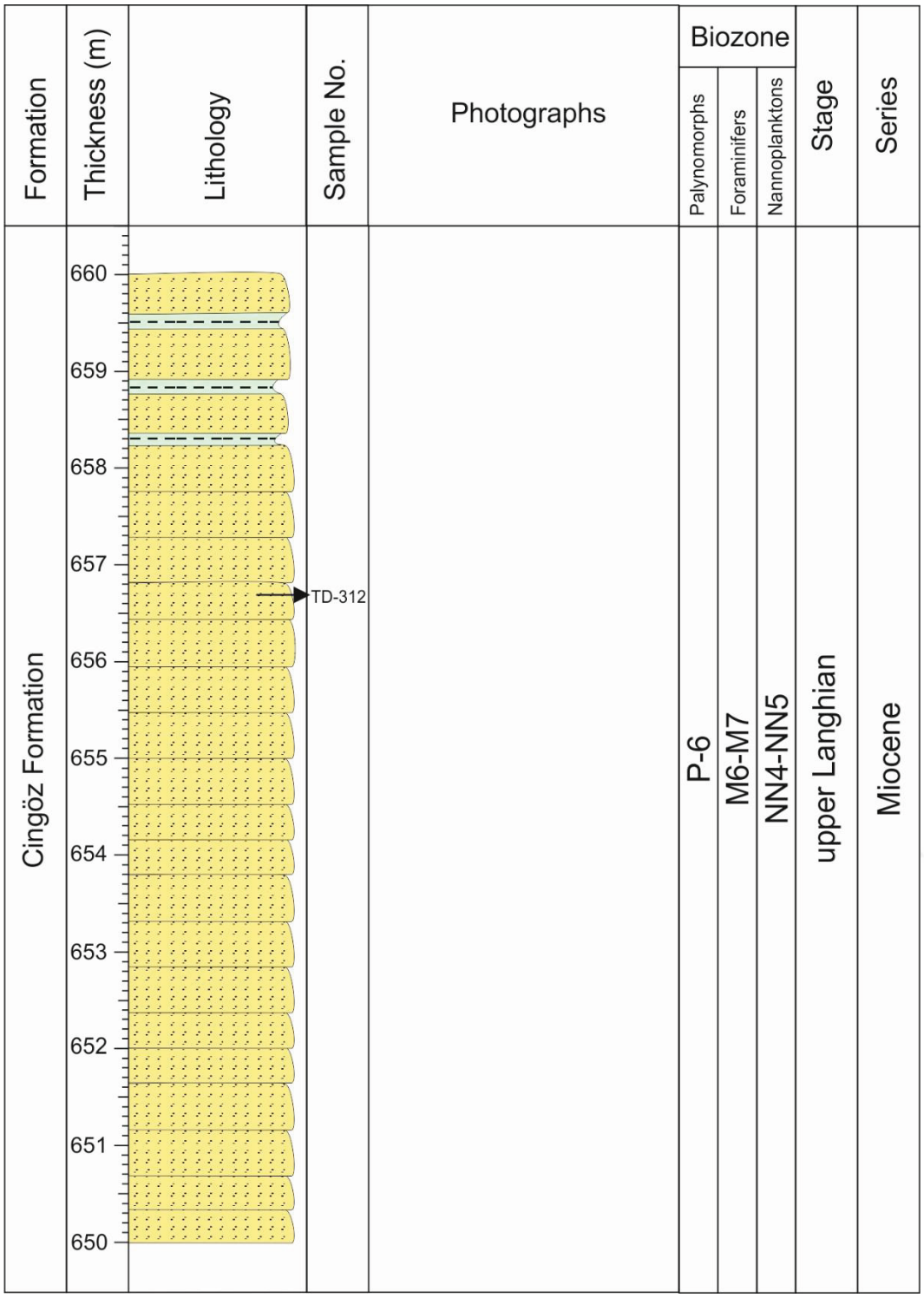

Figure 66. (cont'd)

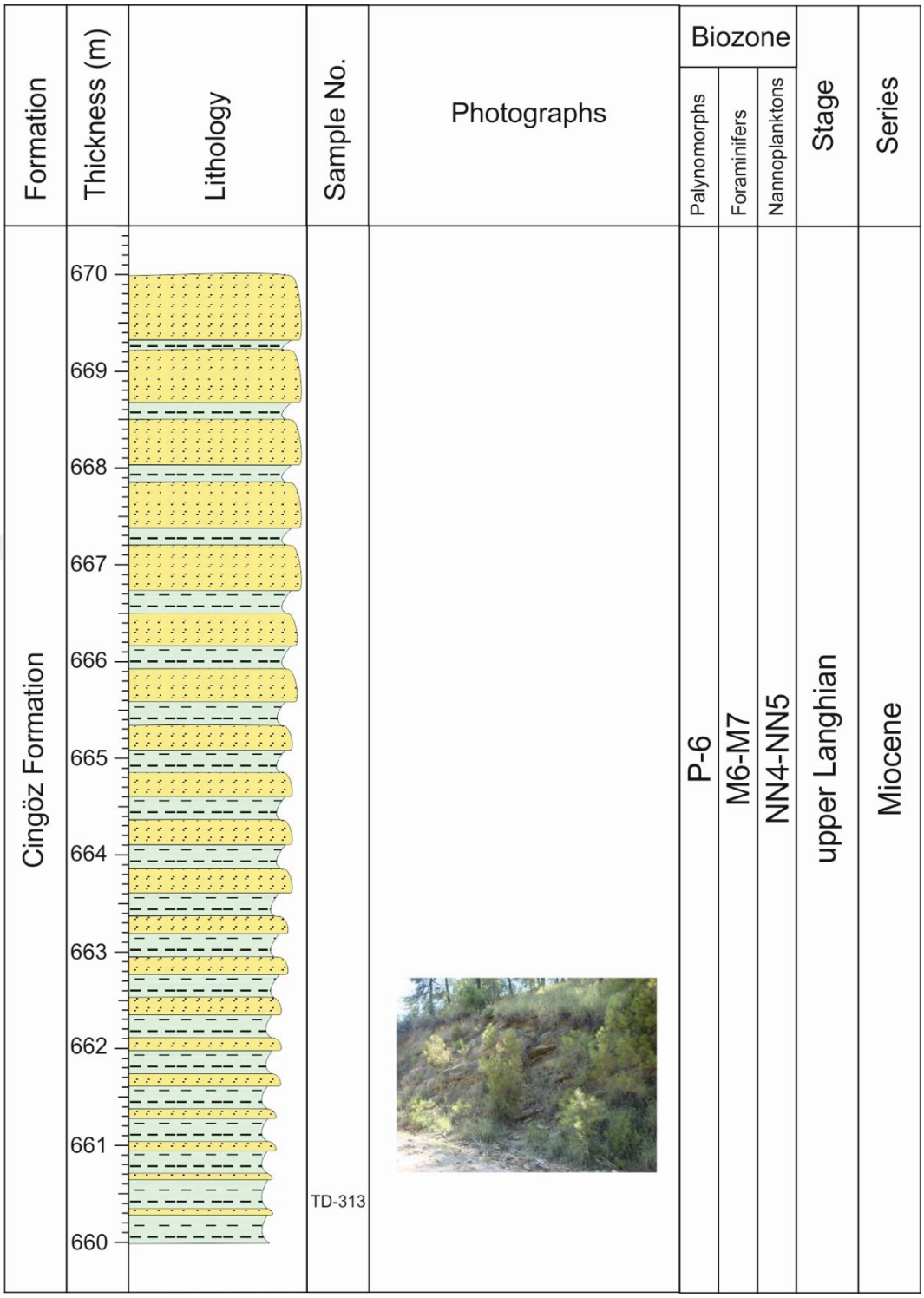

Figure 66. (cont'd)

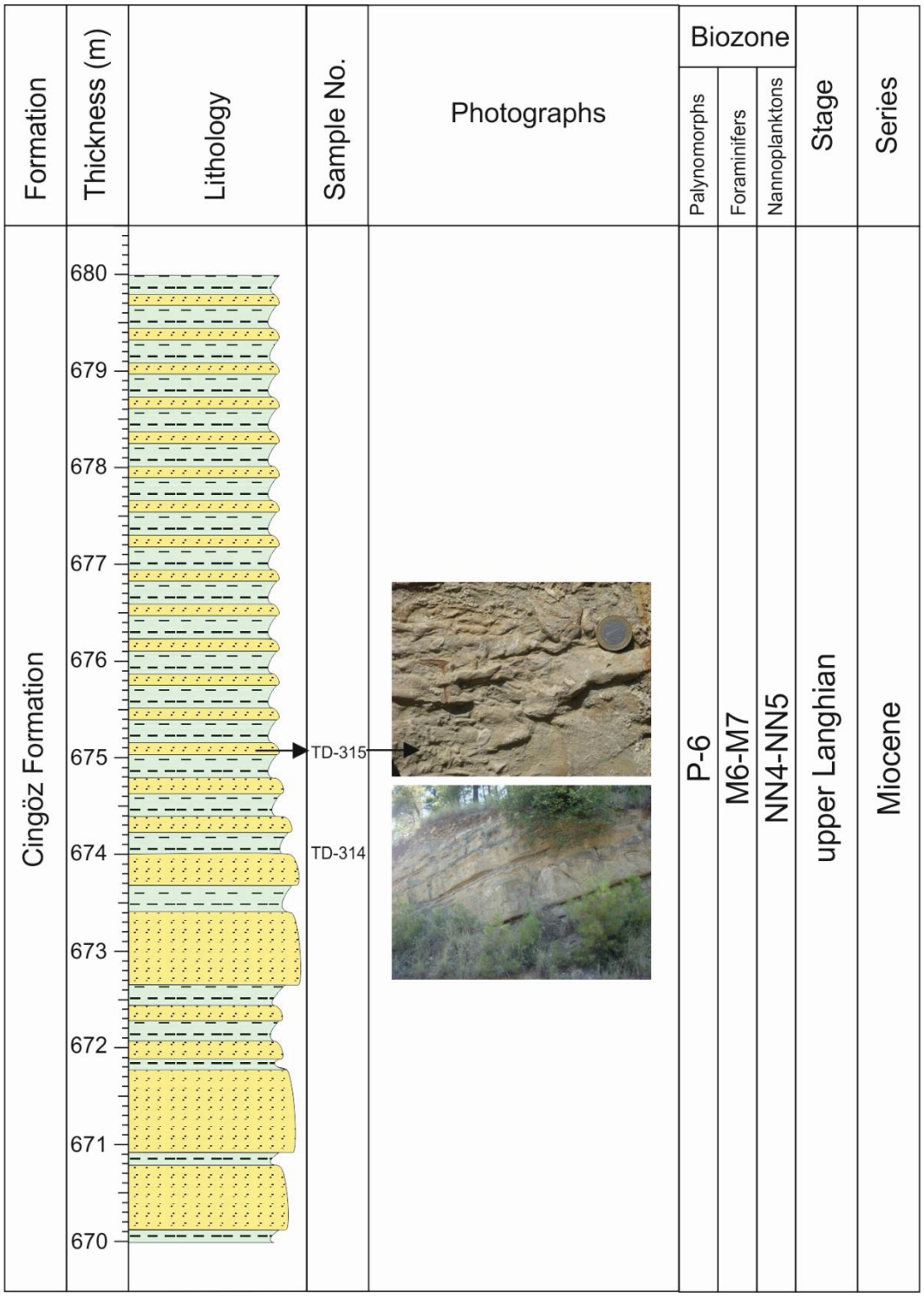

Figure 66. (cont'd)

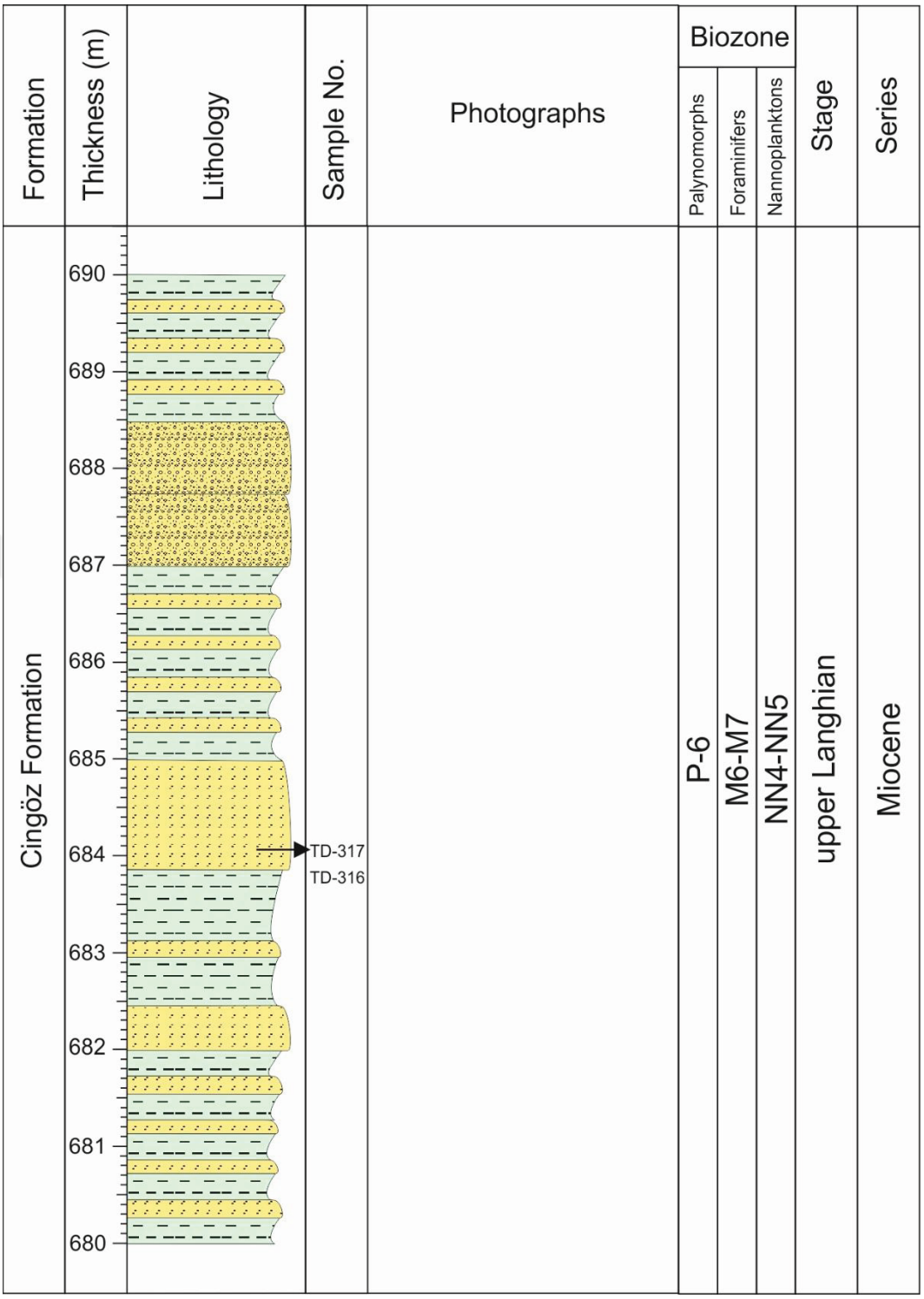

Figure 66. (cont'd)

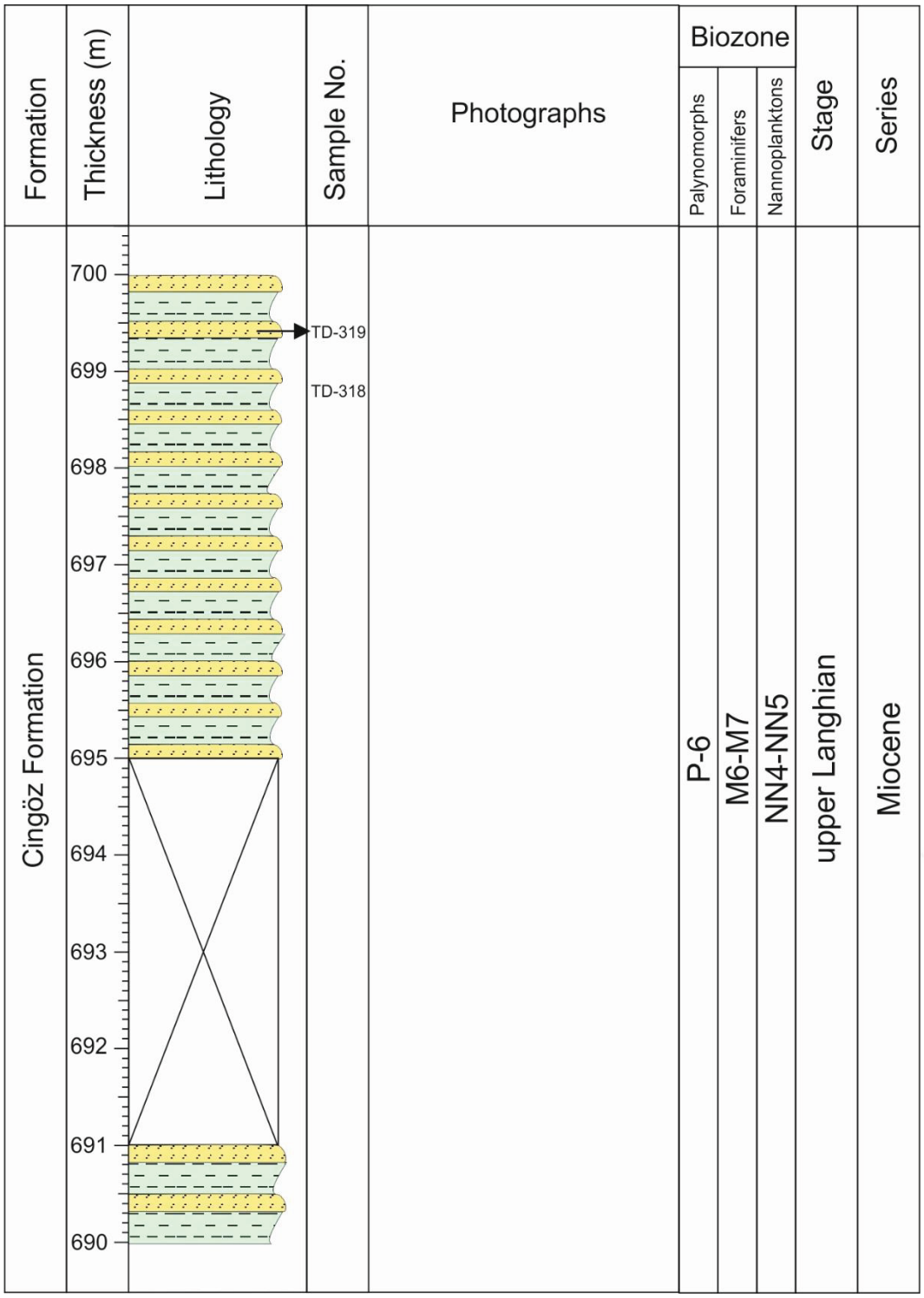

Figure 66. (cont'd)

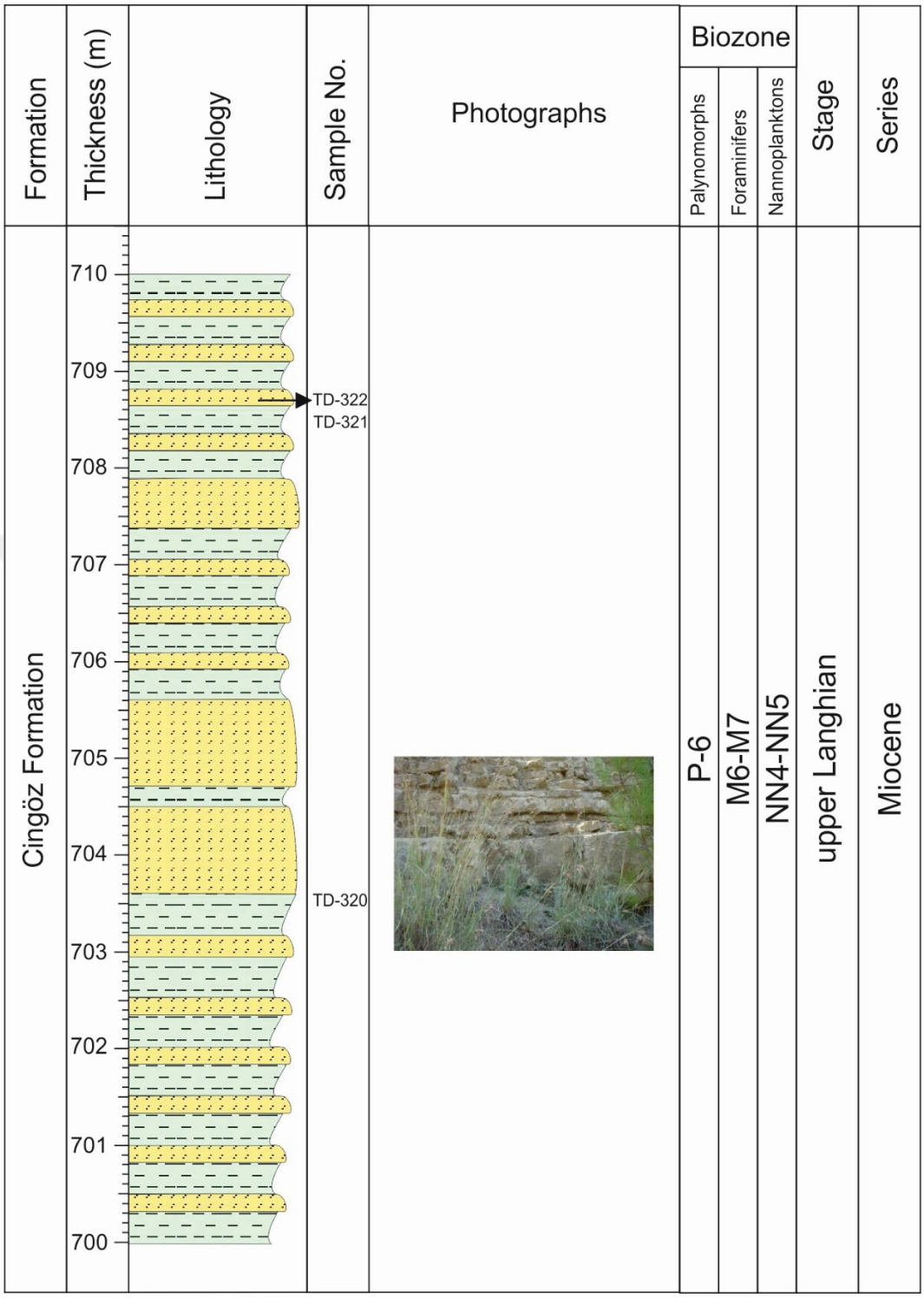

Figure 66. (cont'd)

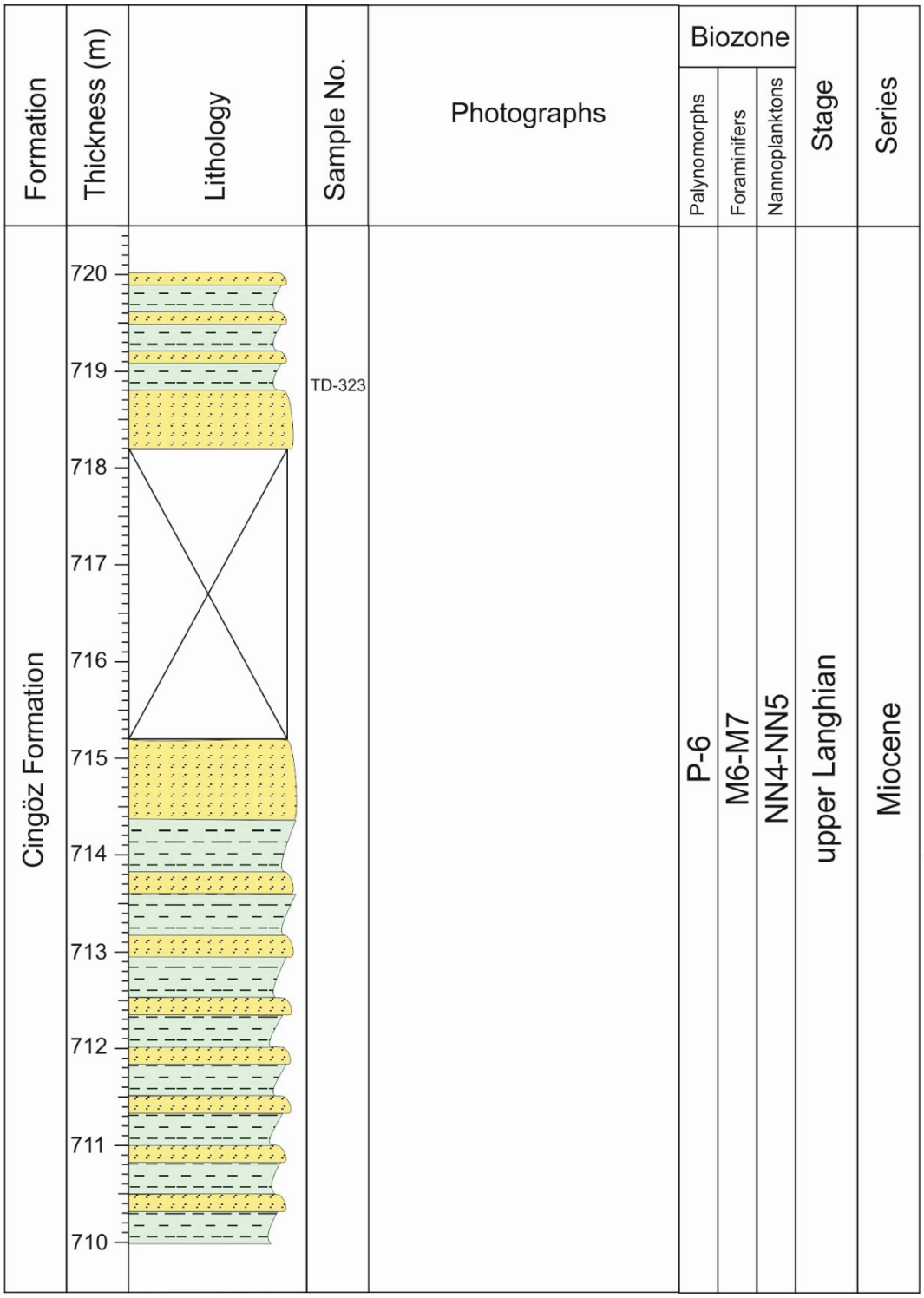

Figure 66. (cont'd)

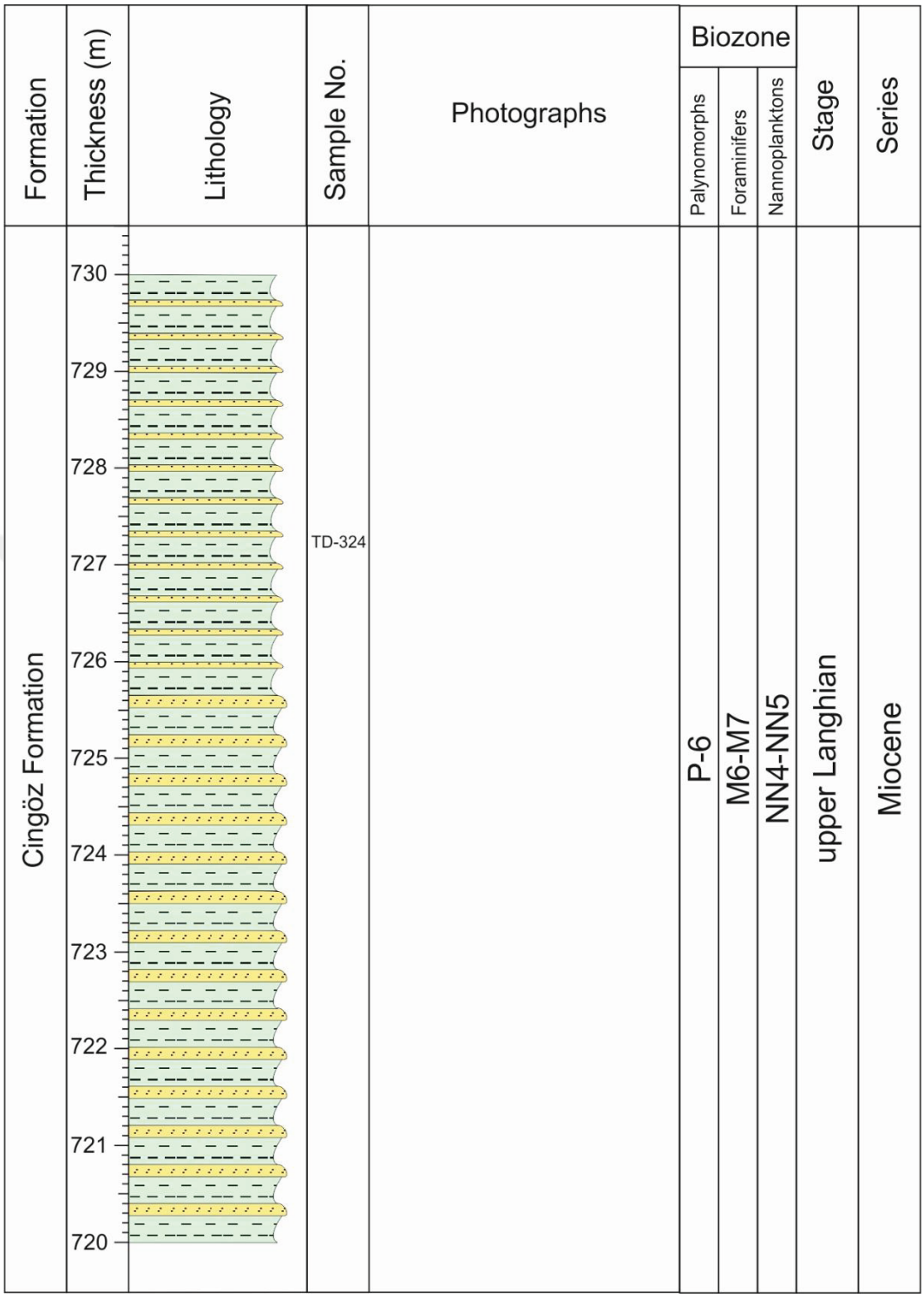

Figure 66. (cont'd)

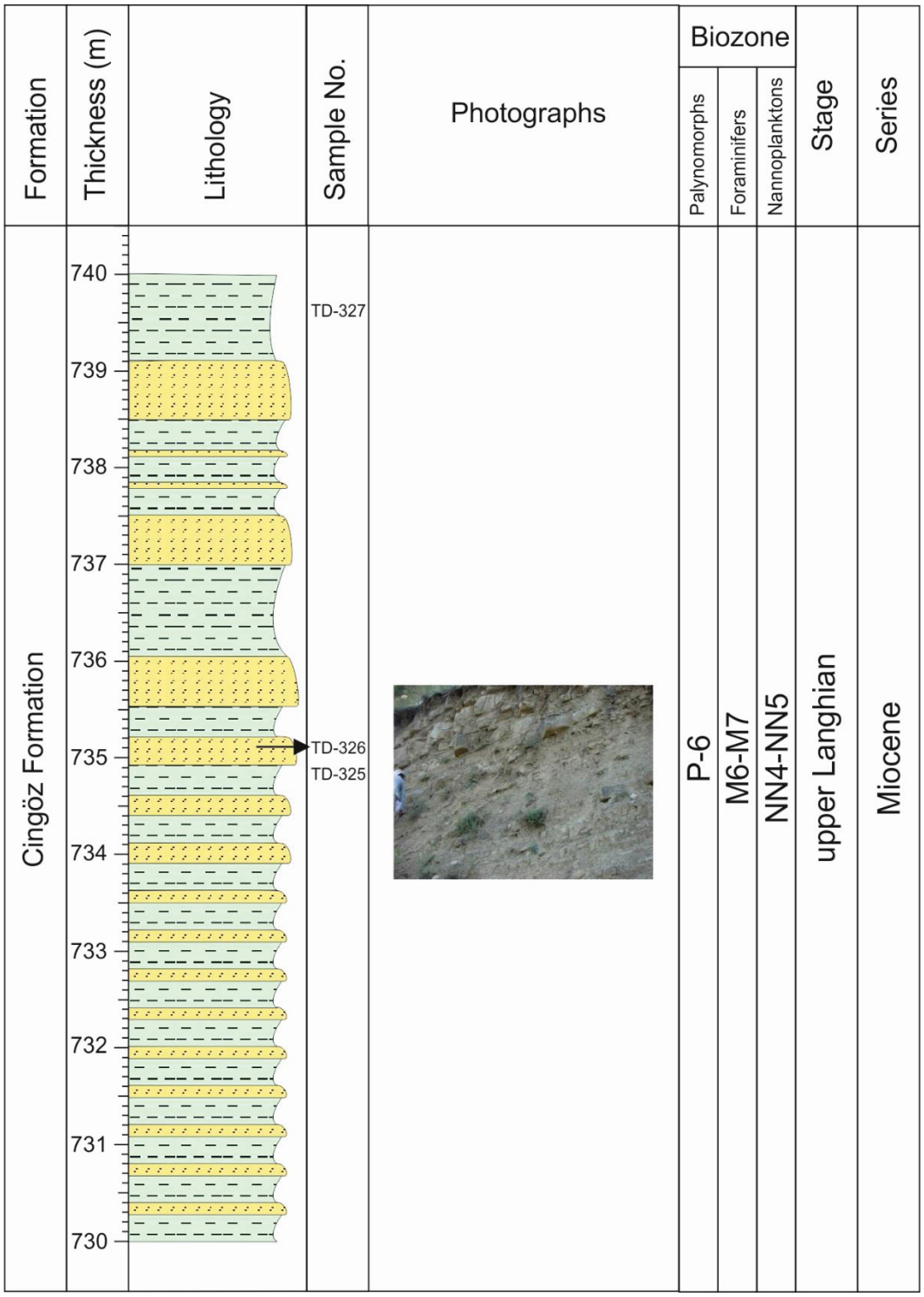

Figure 66. (cont'd)

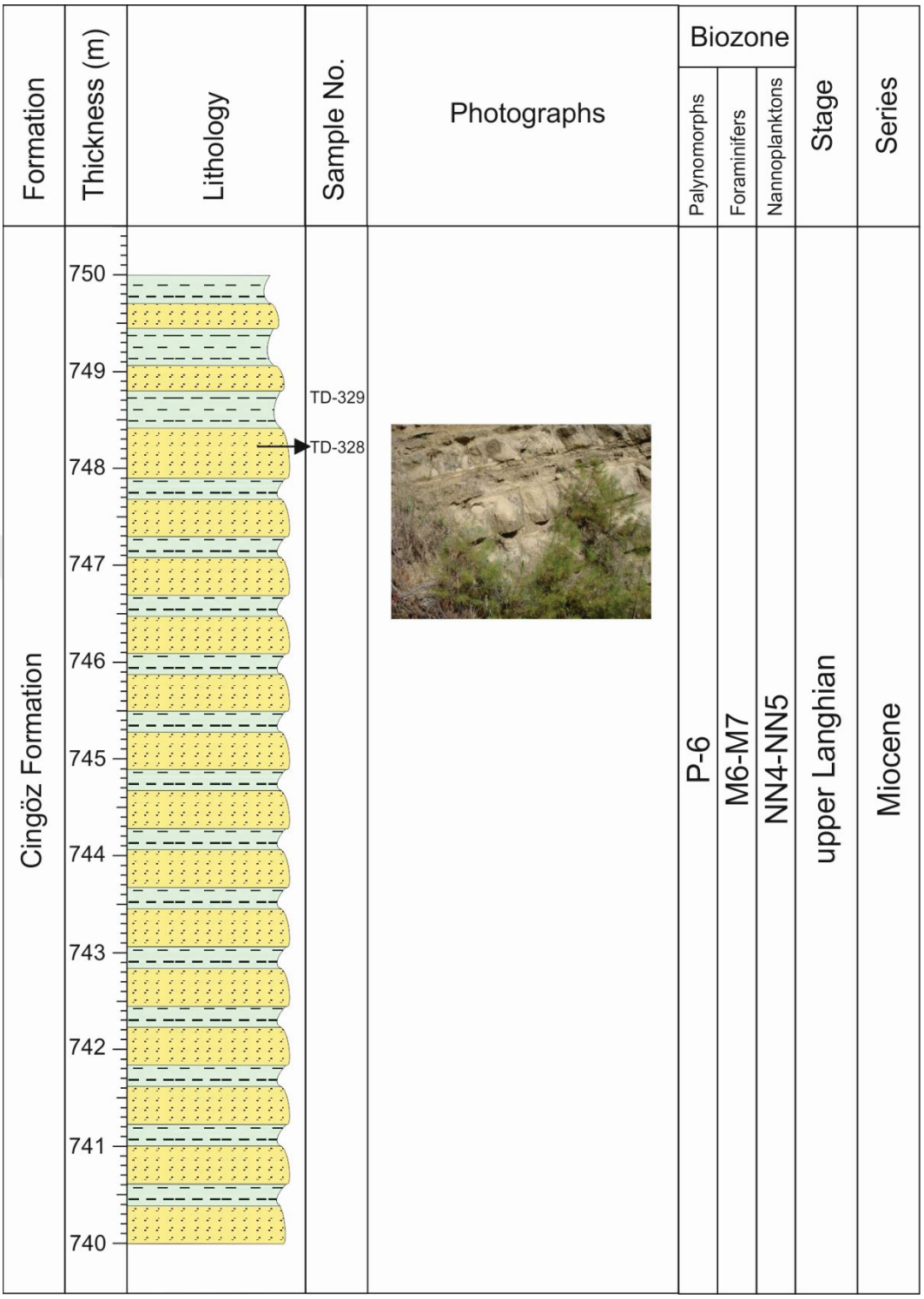

Figure 66. (cont'd)

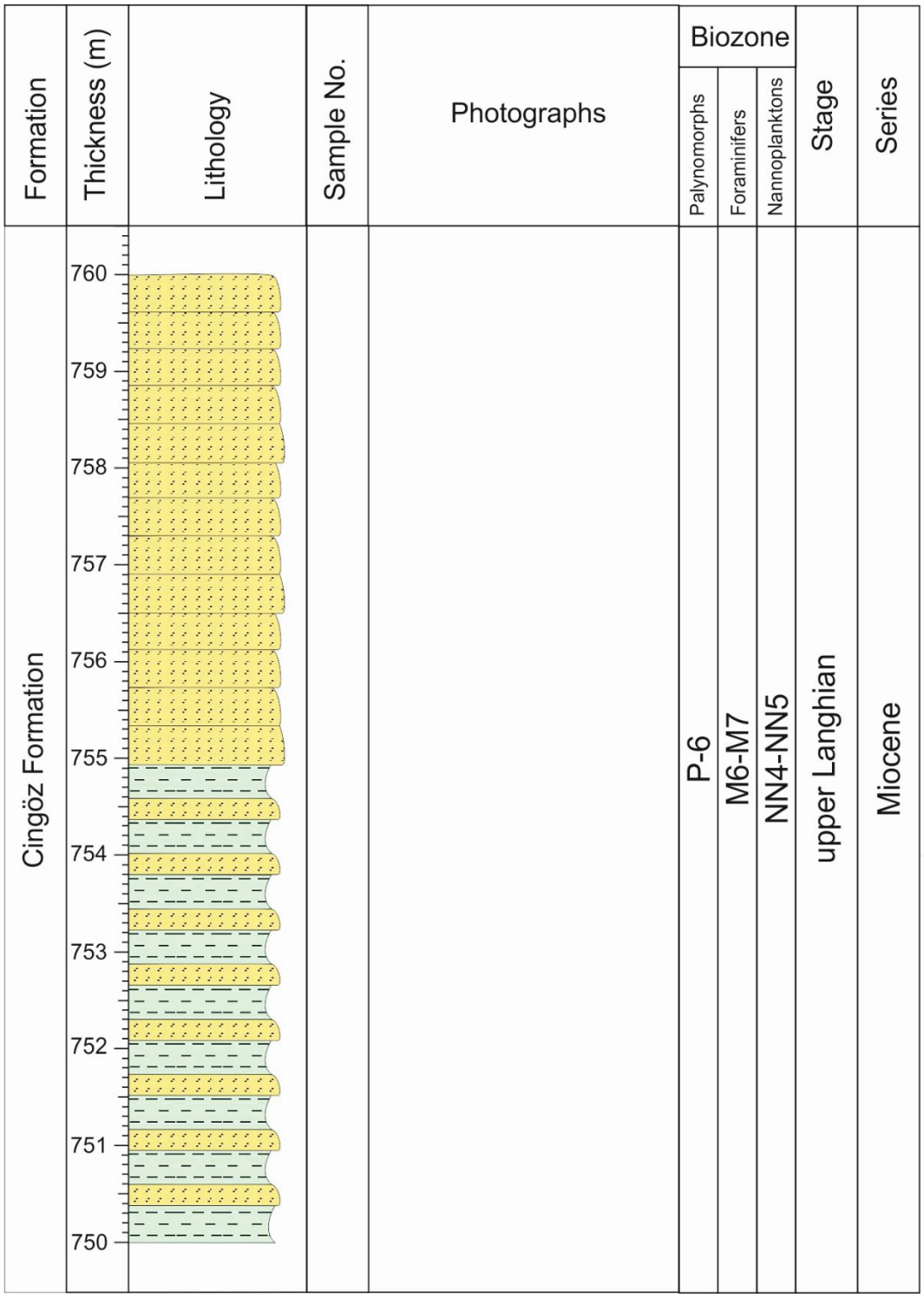

Figure 66. (cont'd)

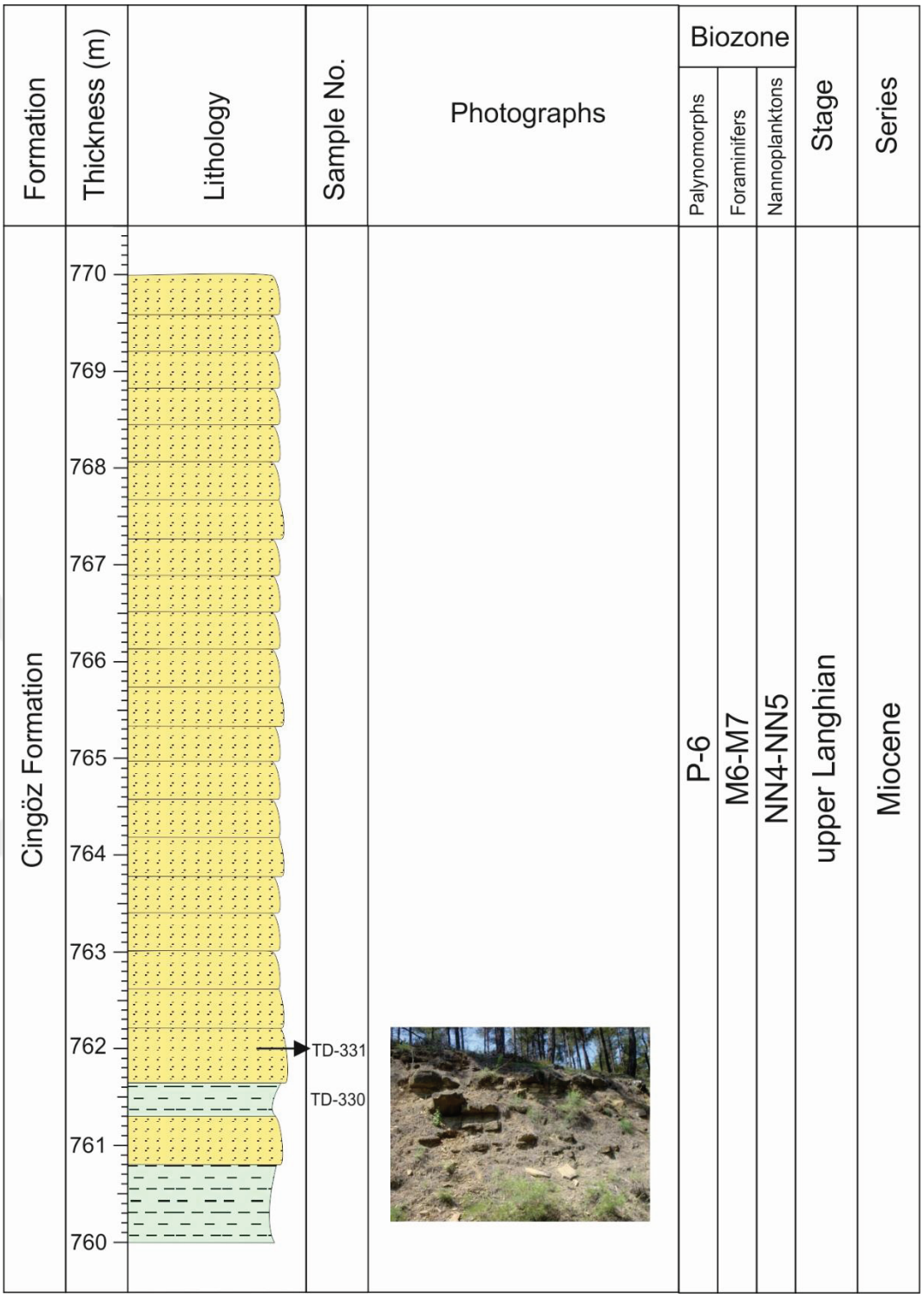

Figure 66. (cont'd)

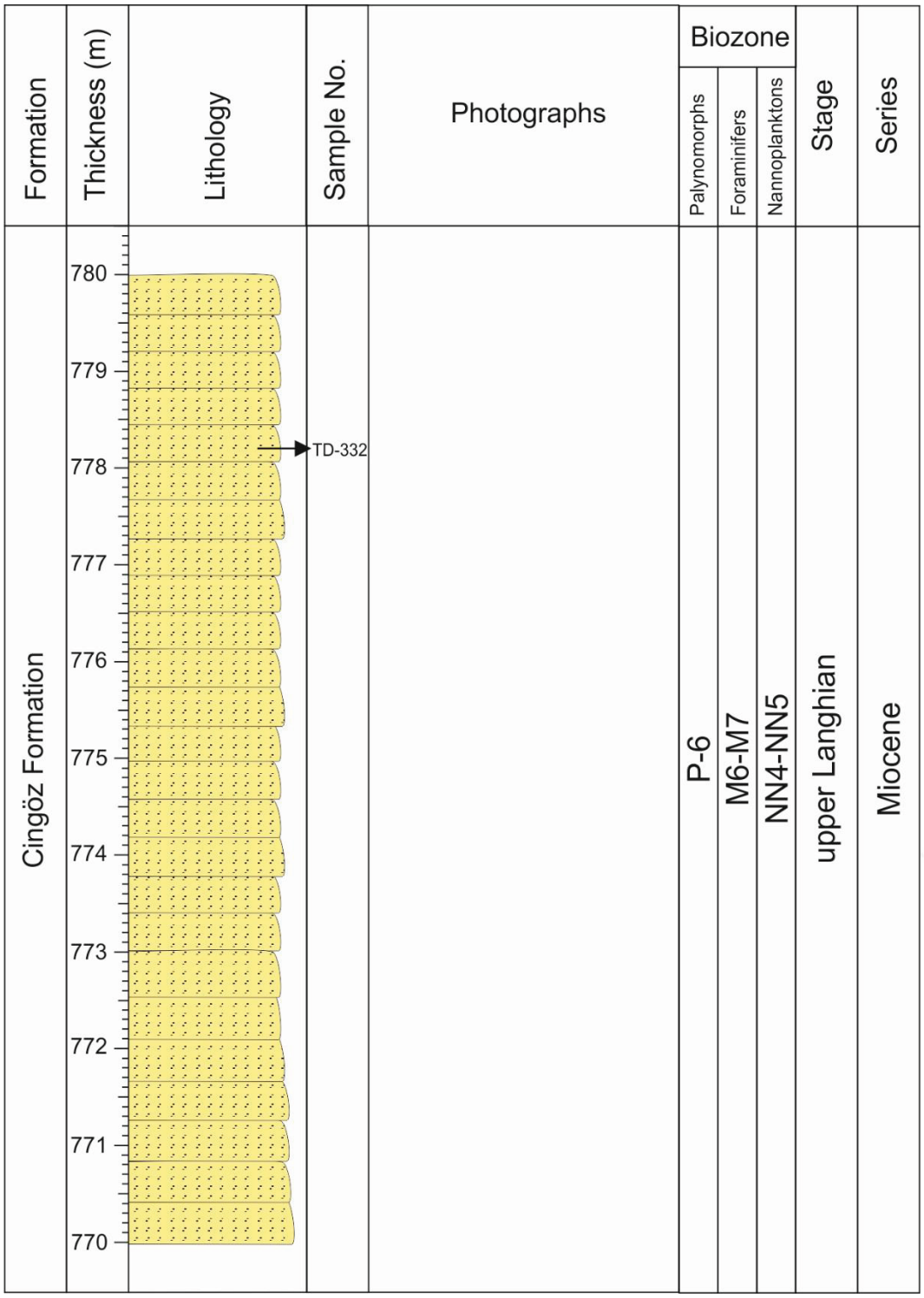

Figure 66. (cont'd)

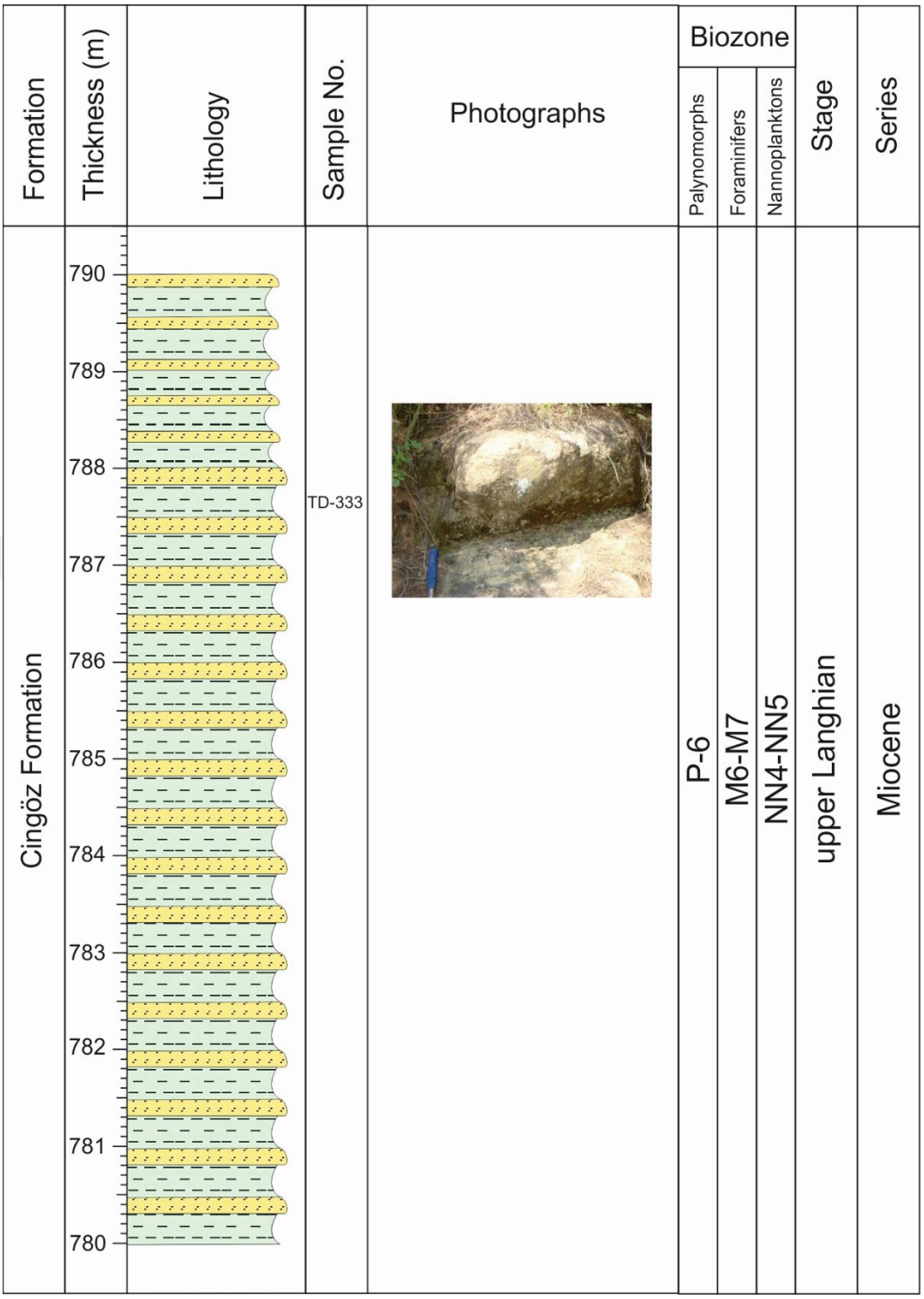

Figure 66. (cont'd)

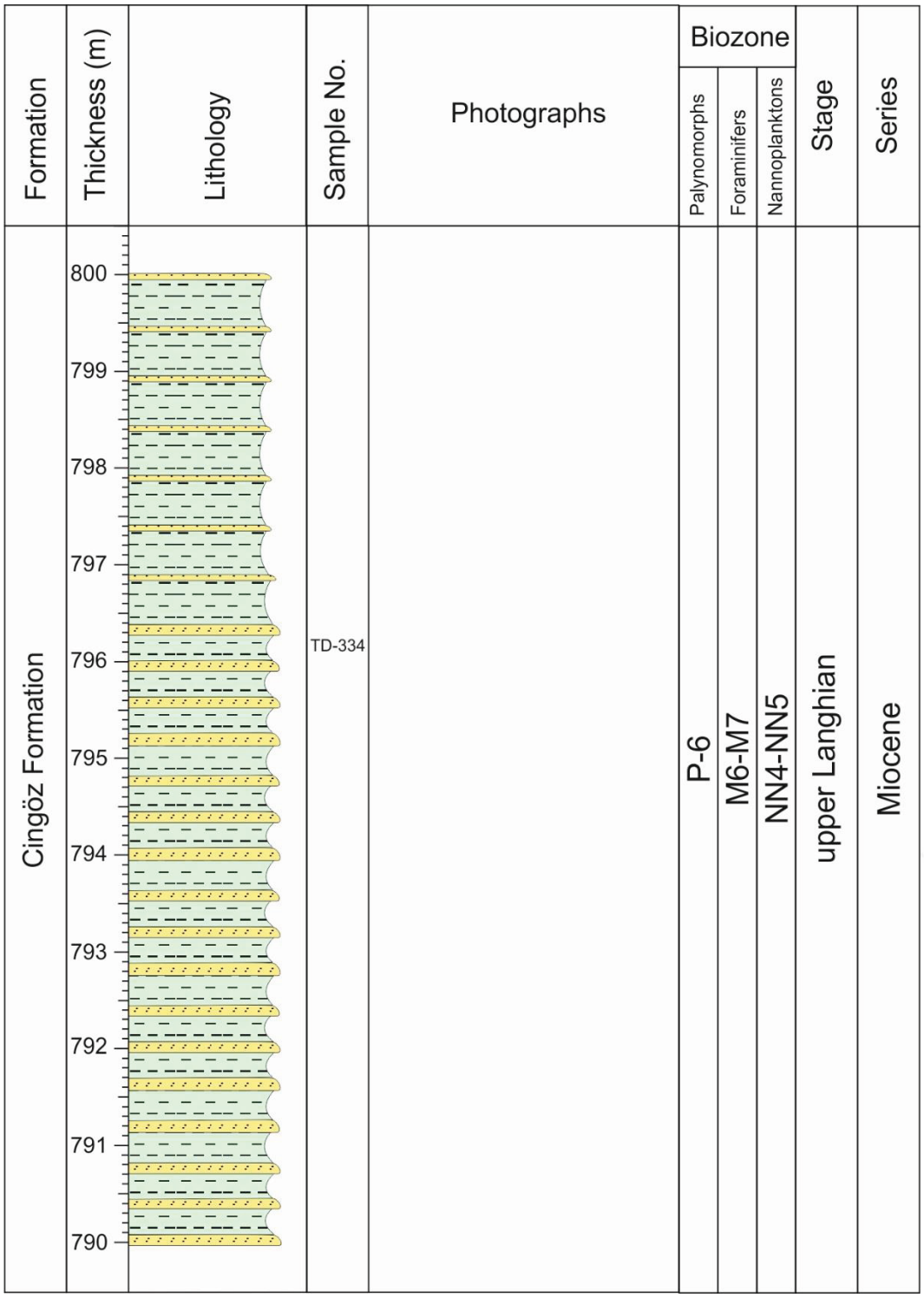

Figure 66. (cont'd)

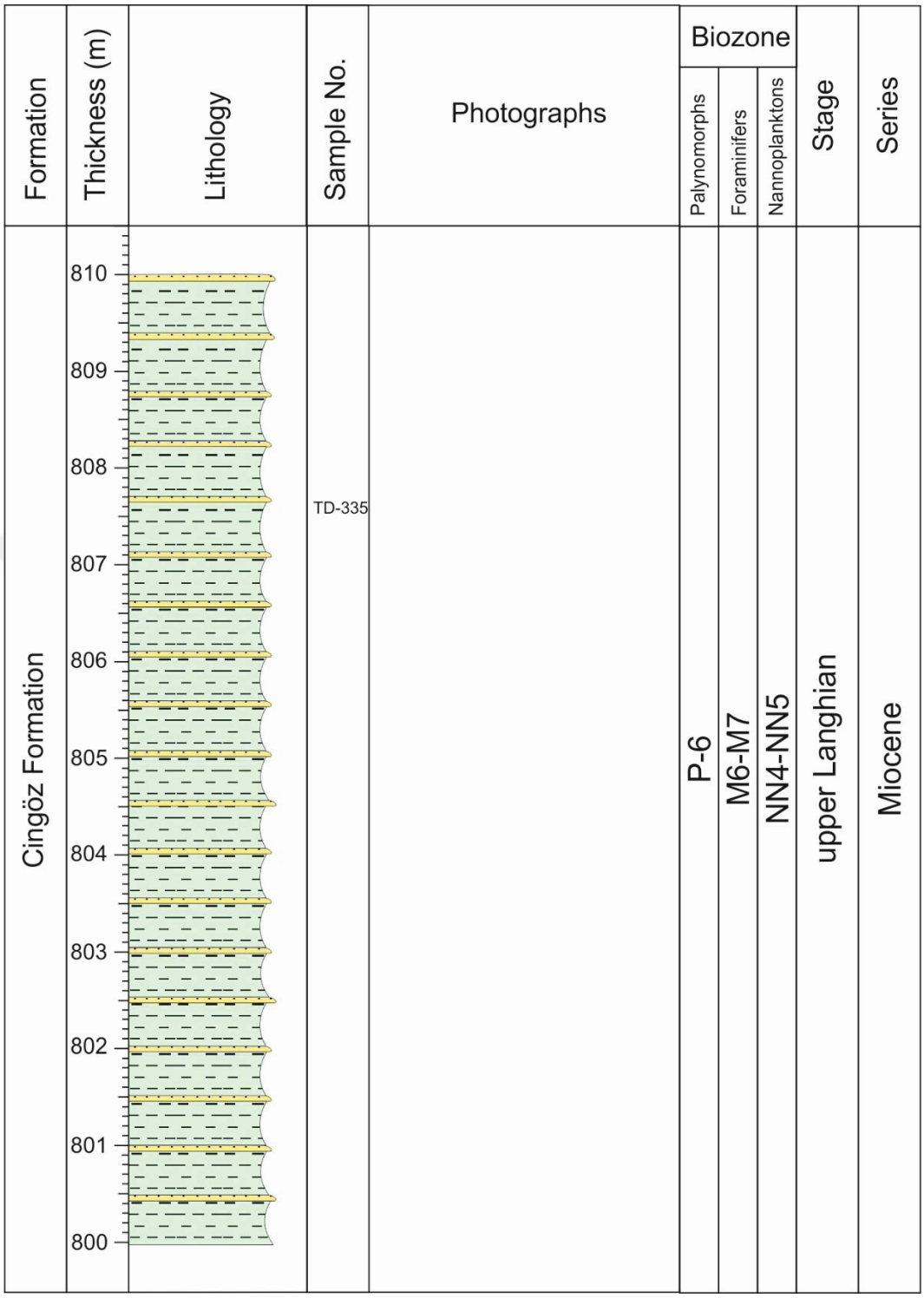

Figure 66. (cont'd)

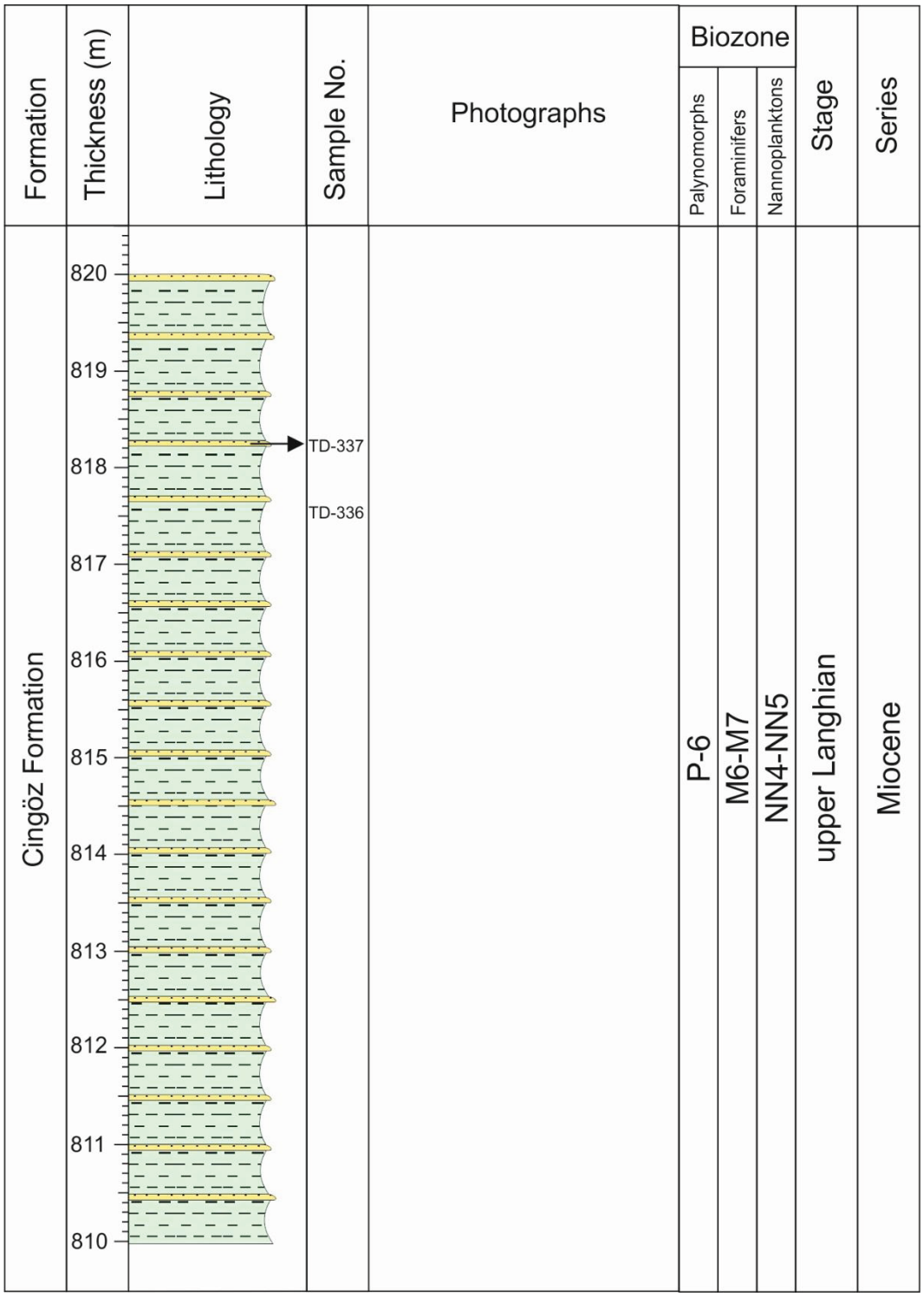

Figure 66. (cont'd)

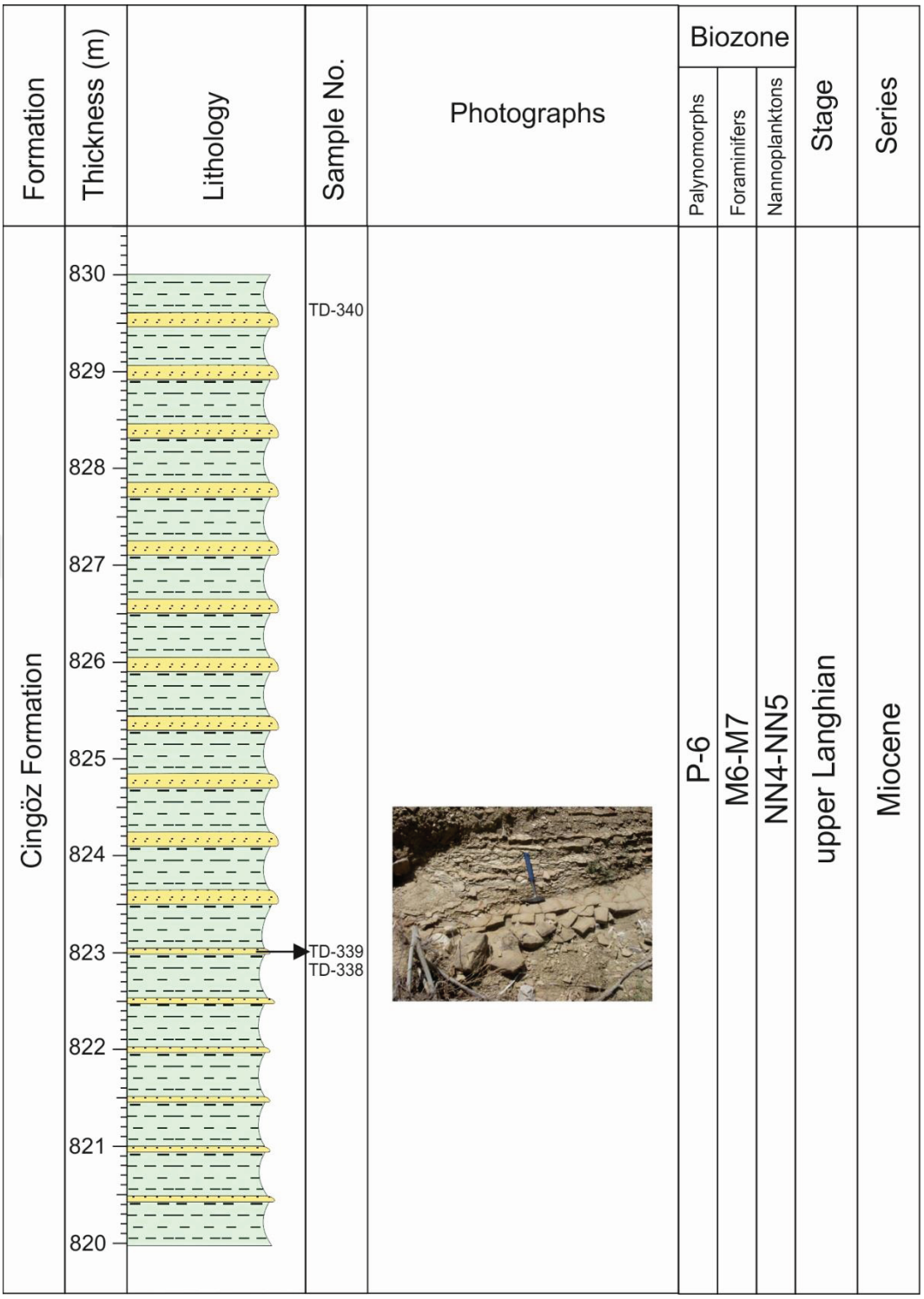

Figure 66. (cont'd)

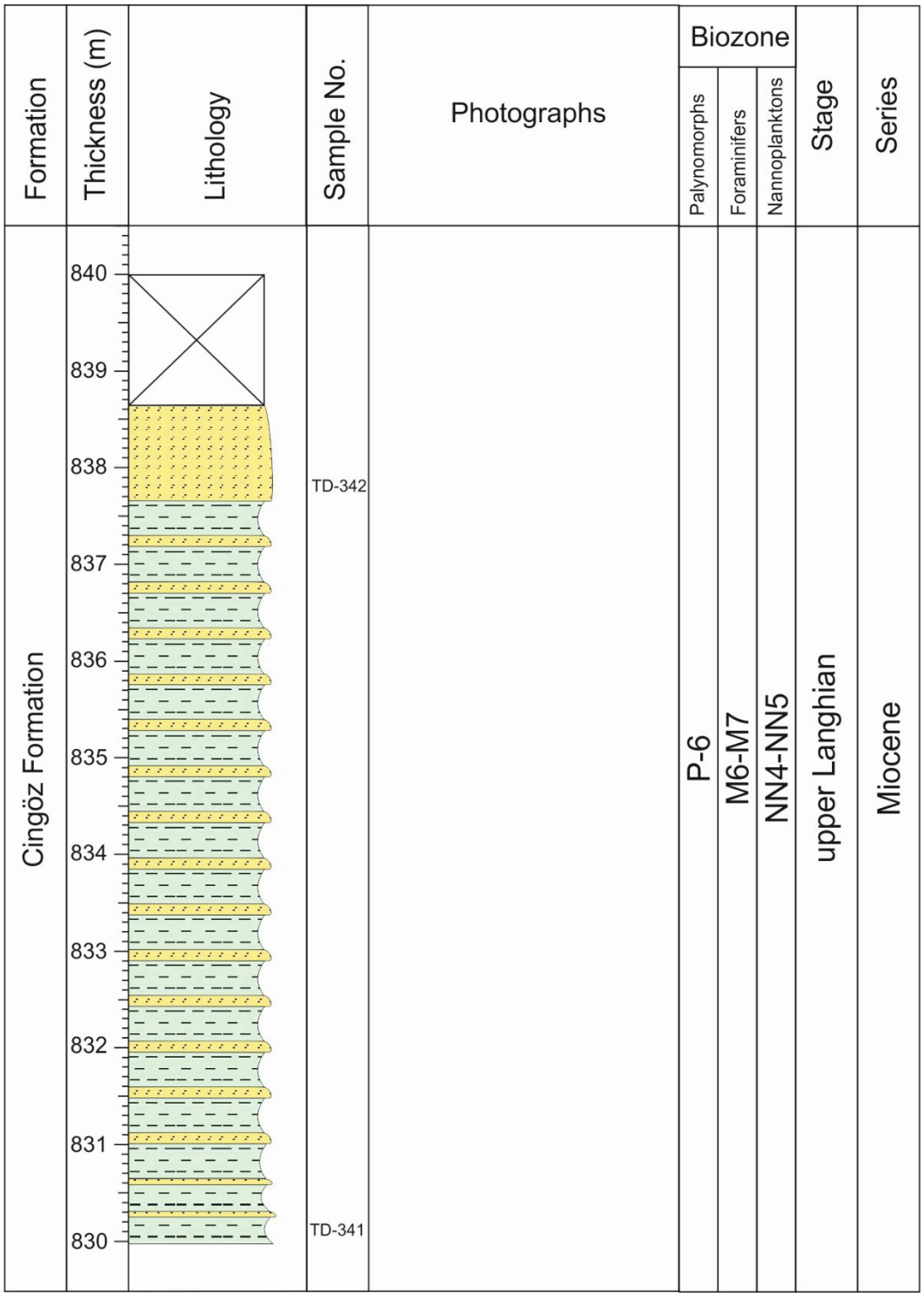

Figure 66. (cont'd)

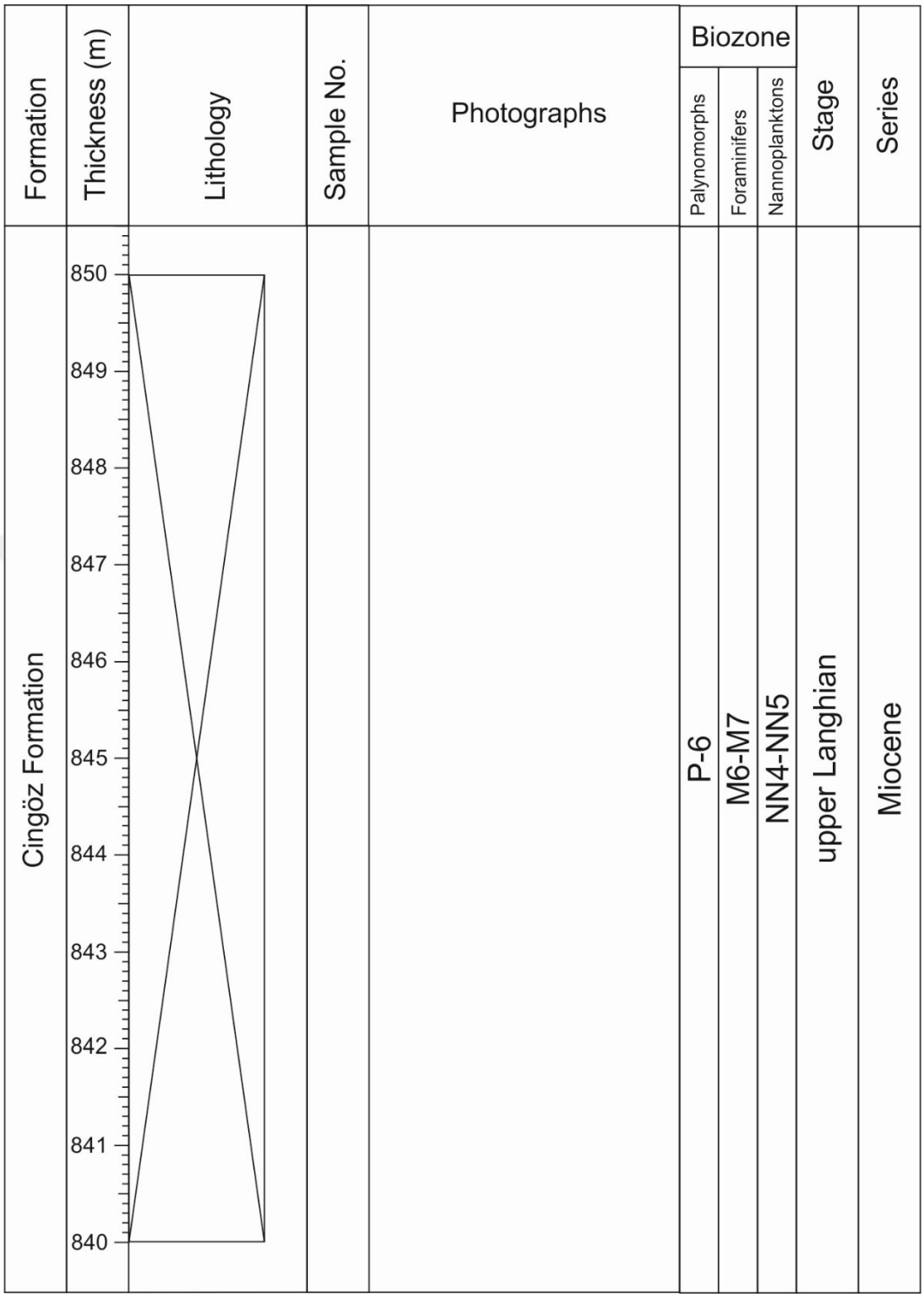

Figure 66. (cont'd)

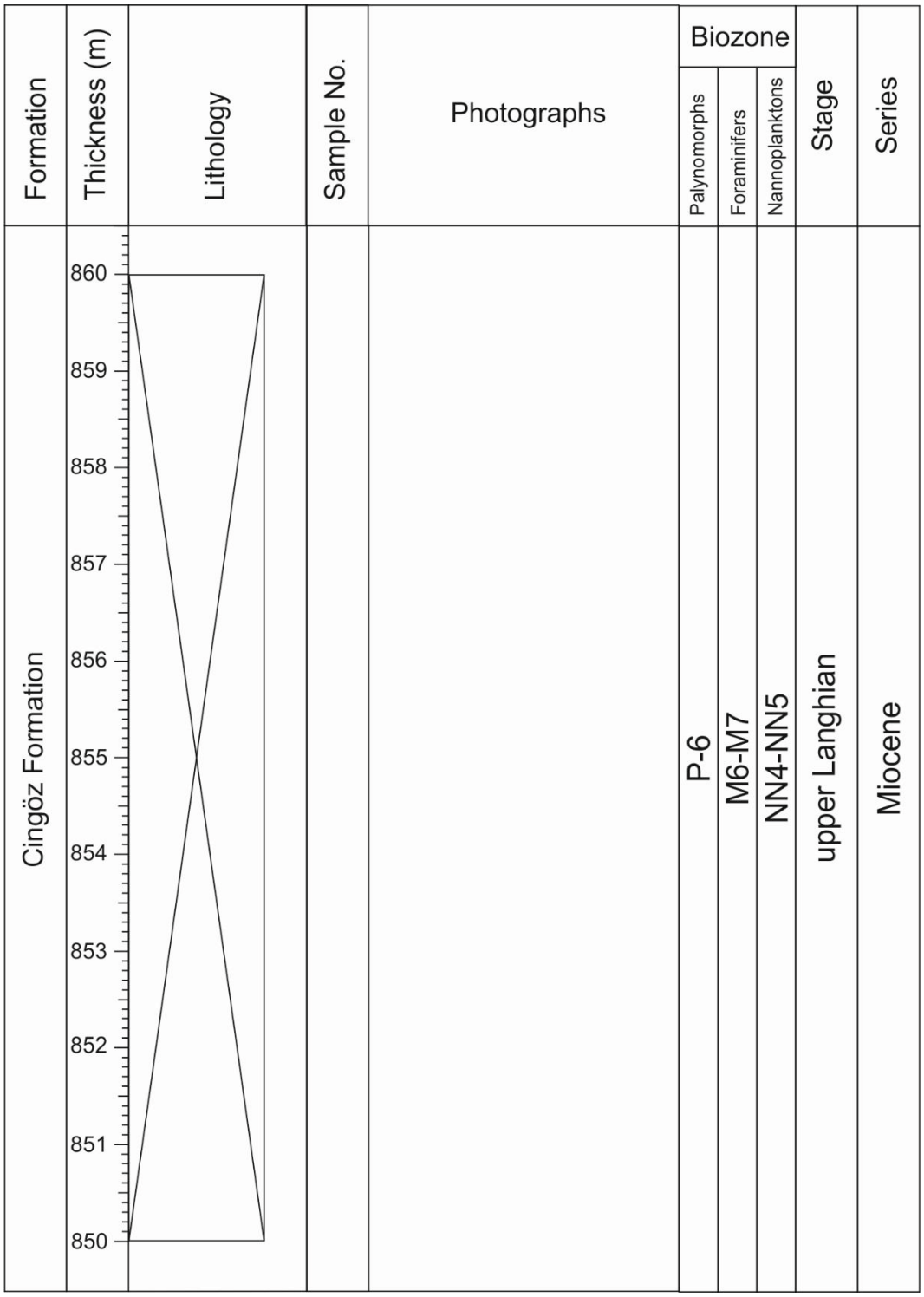

Figure 66. (cont'd)

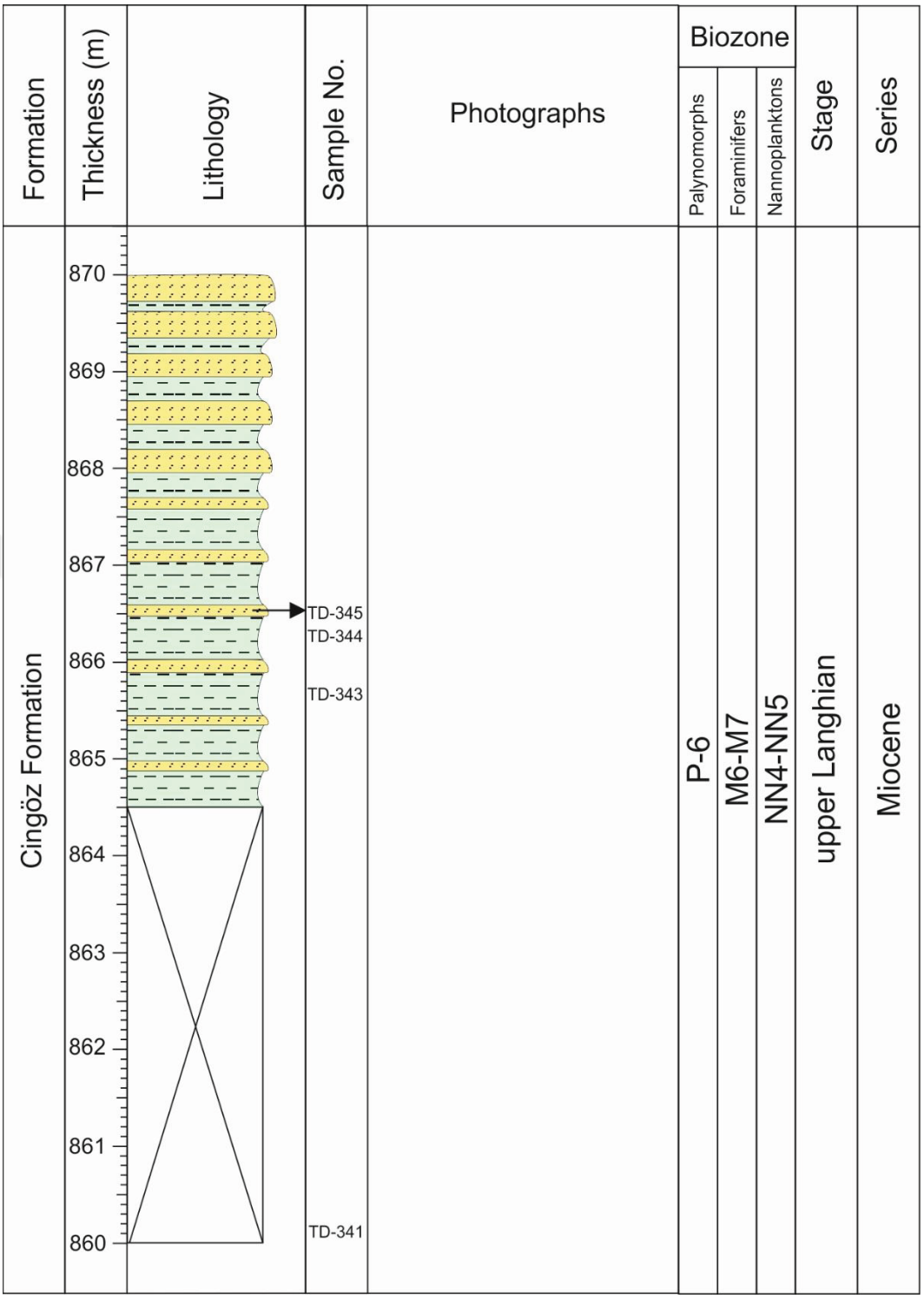

Figure 66. (cont'd)

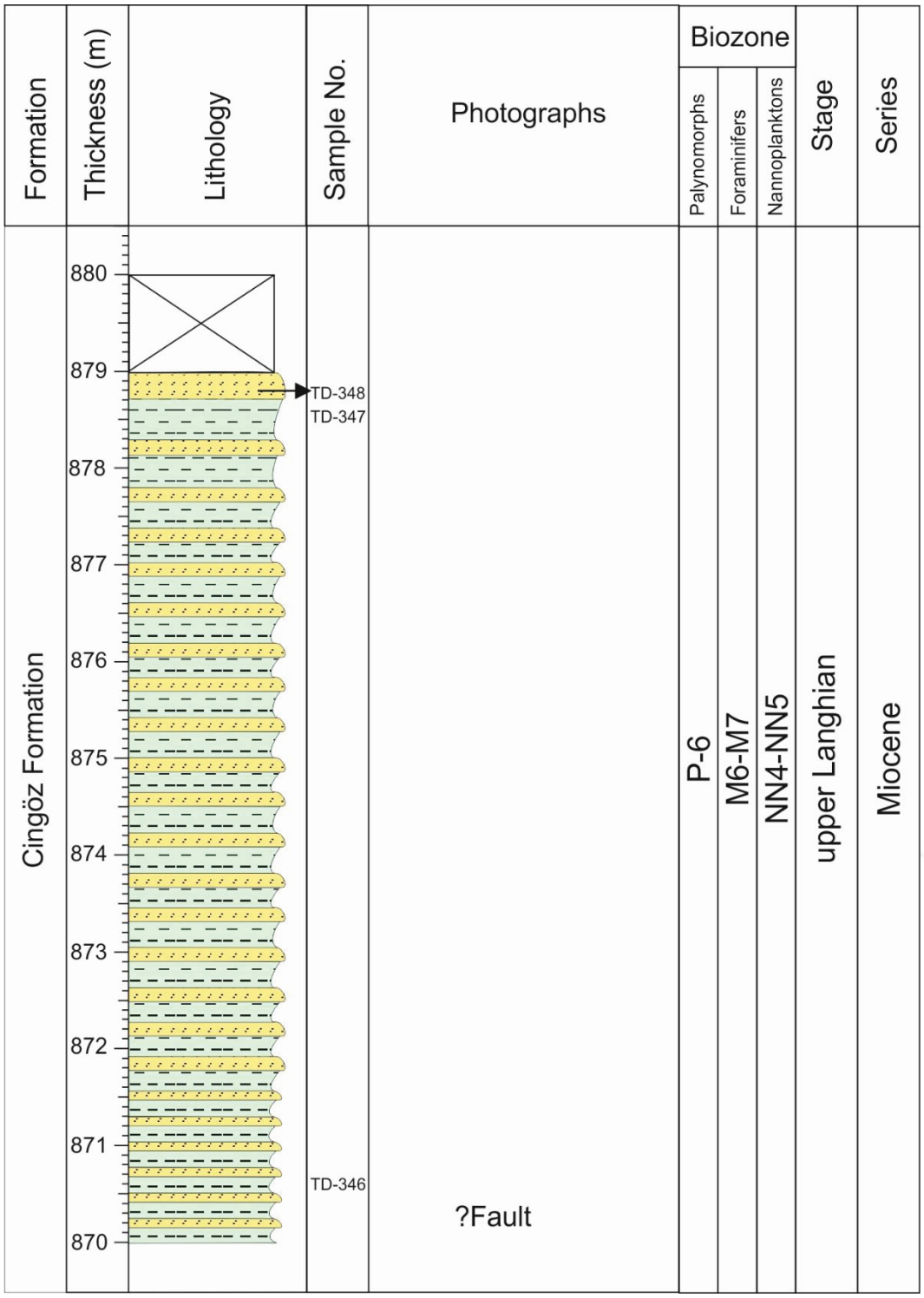

Figure 66. (cont'd)

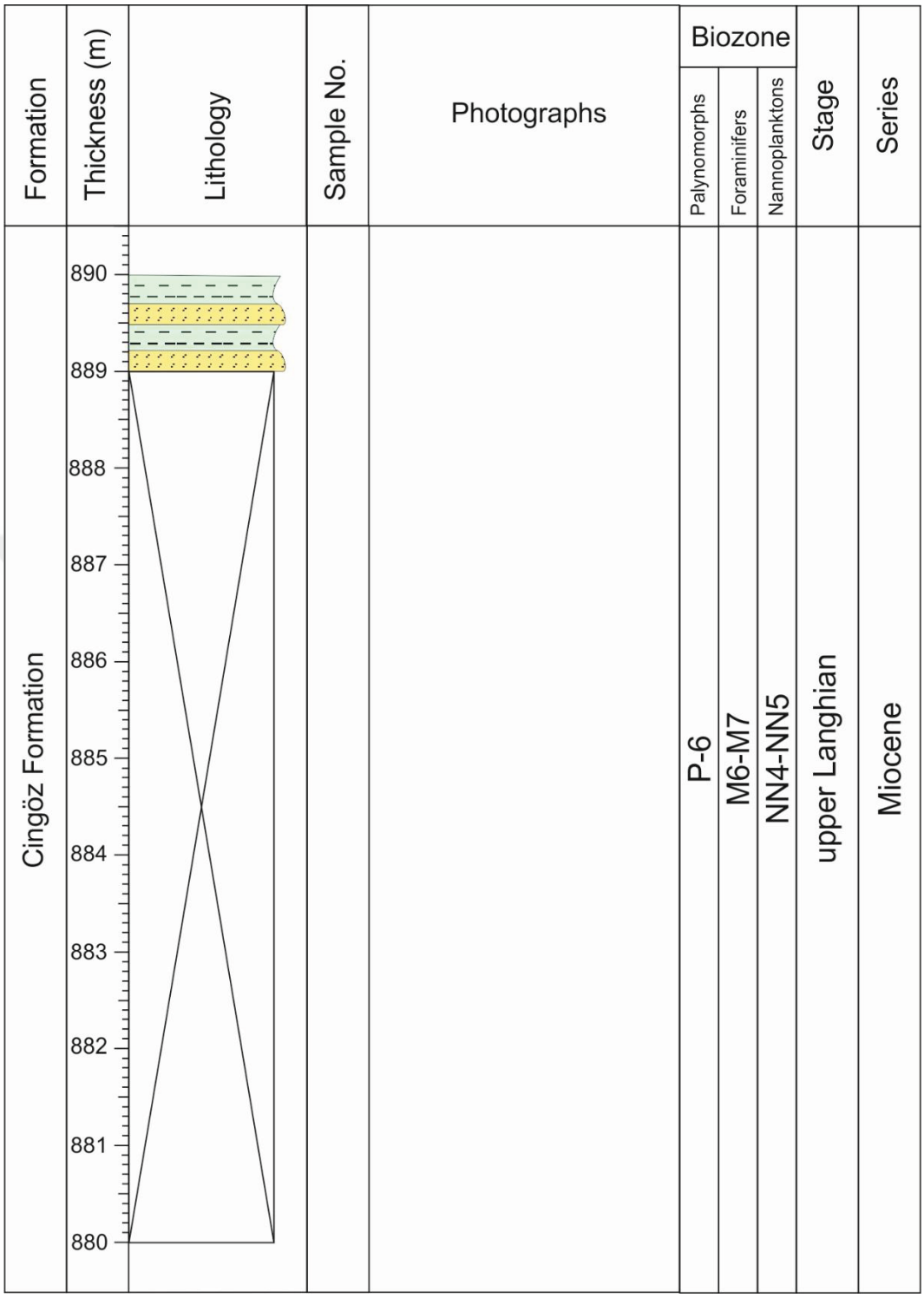

Figure 66. (cont'd)

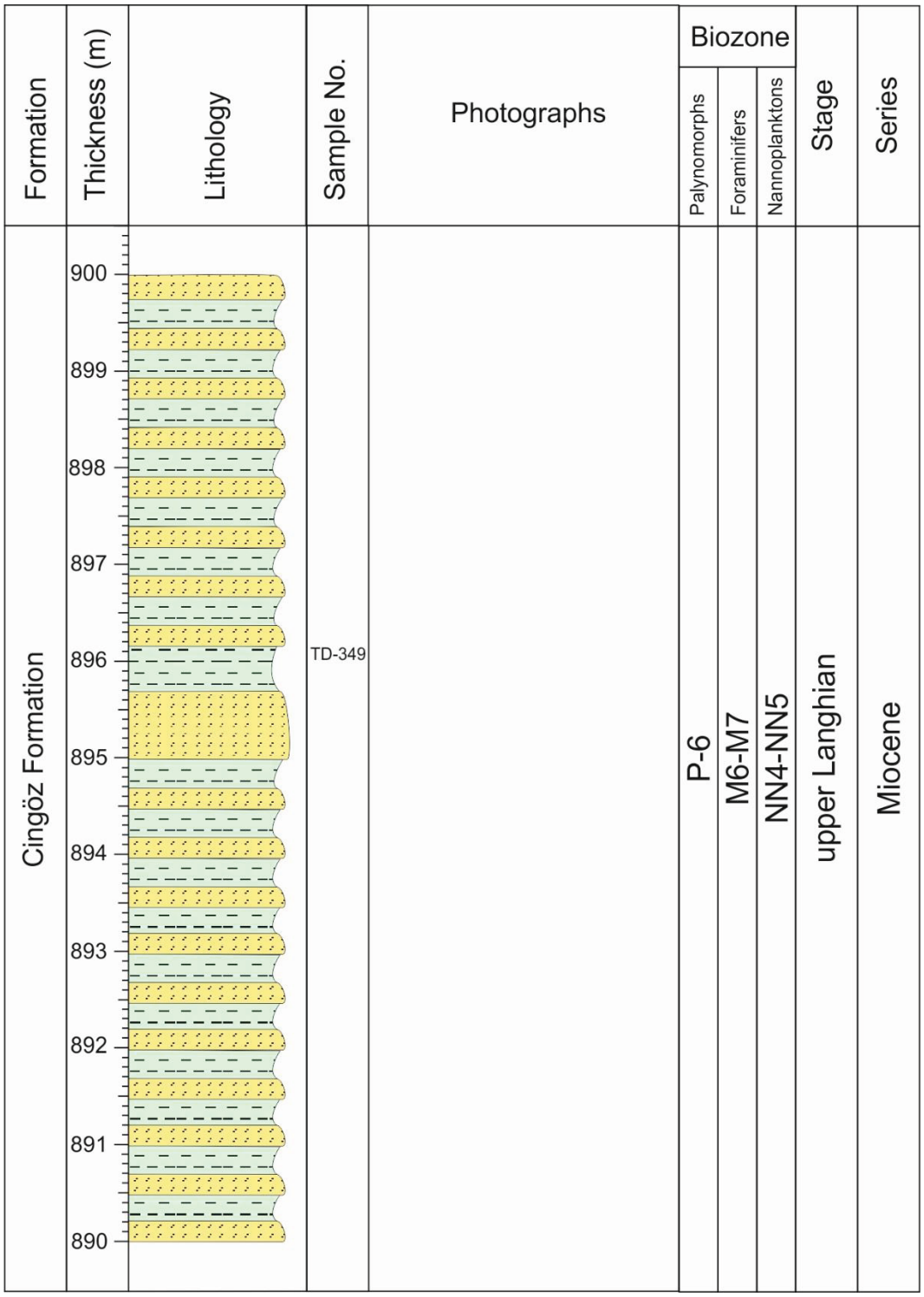

Figure 66. (cont'd)

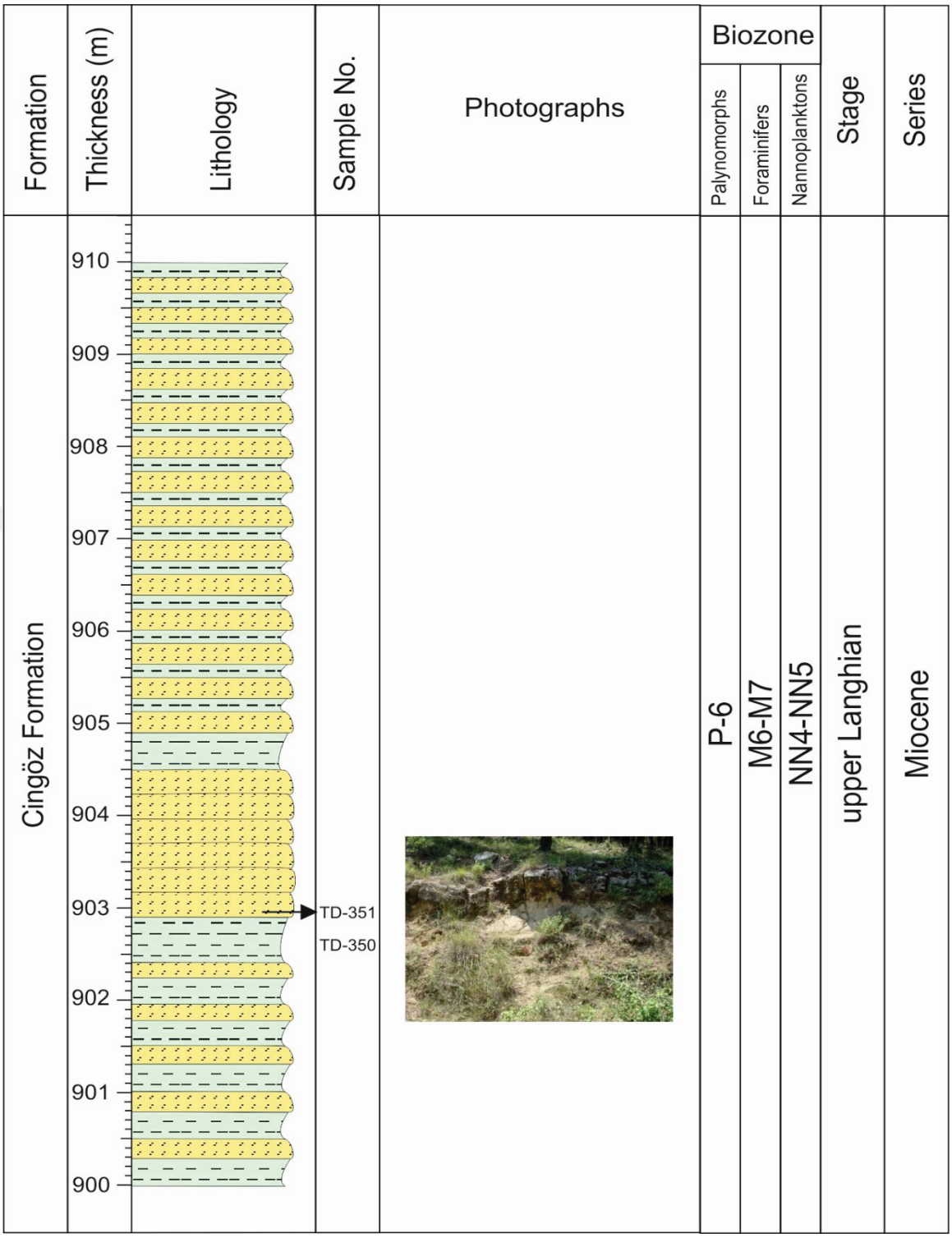

Figure 66. (cont'd)

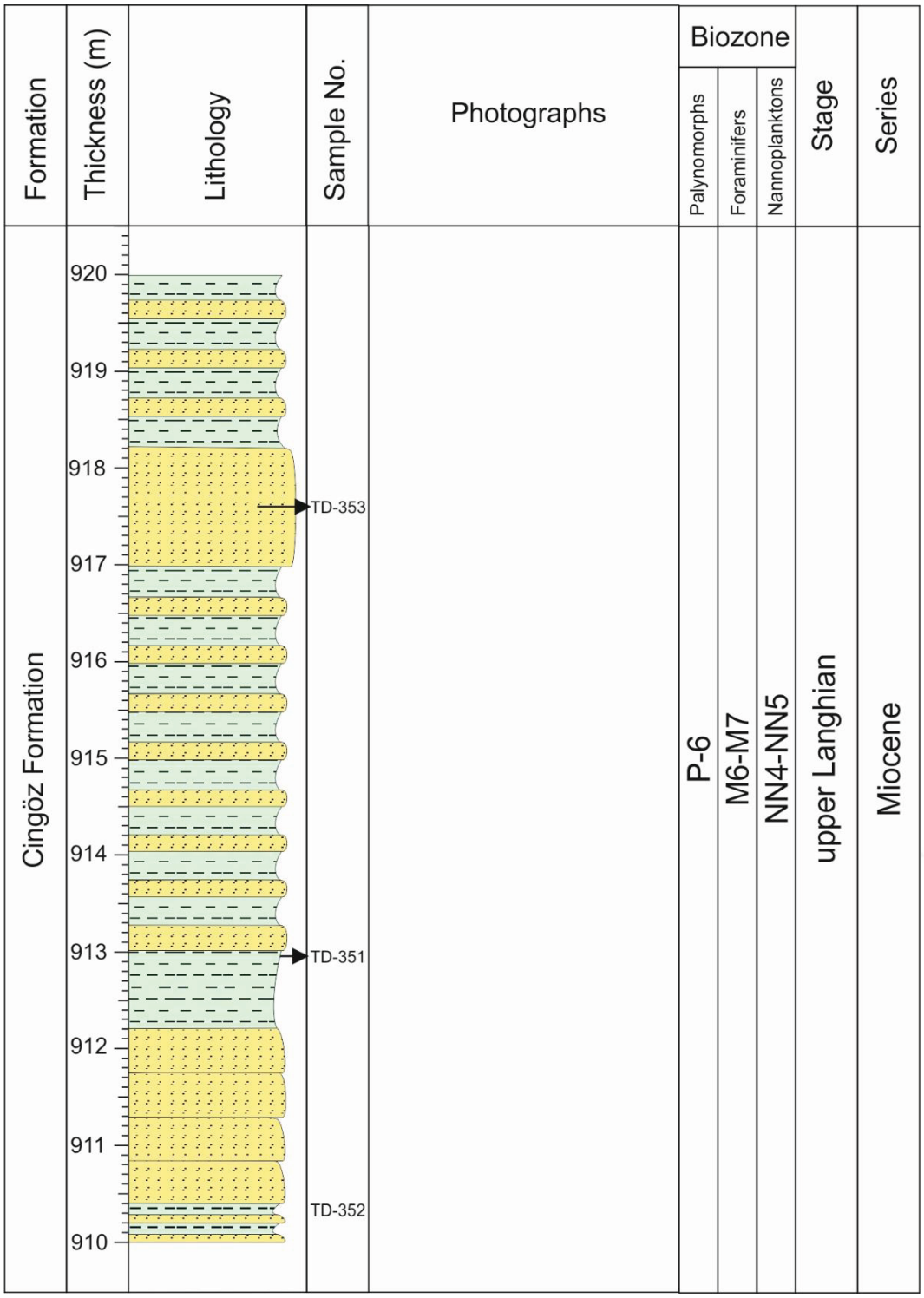

Figure 66. (cont'd)

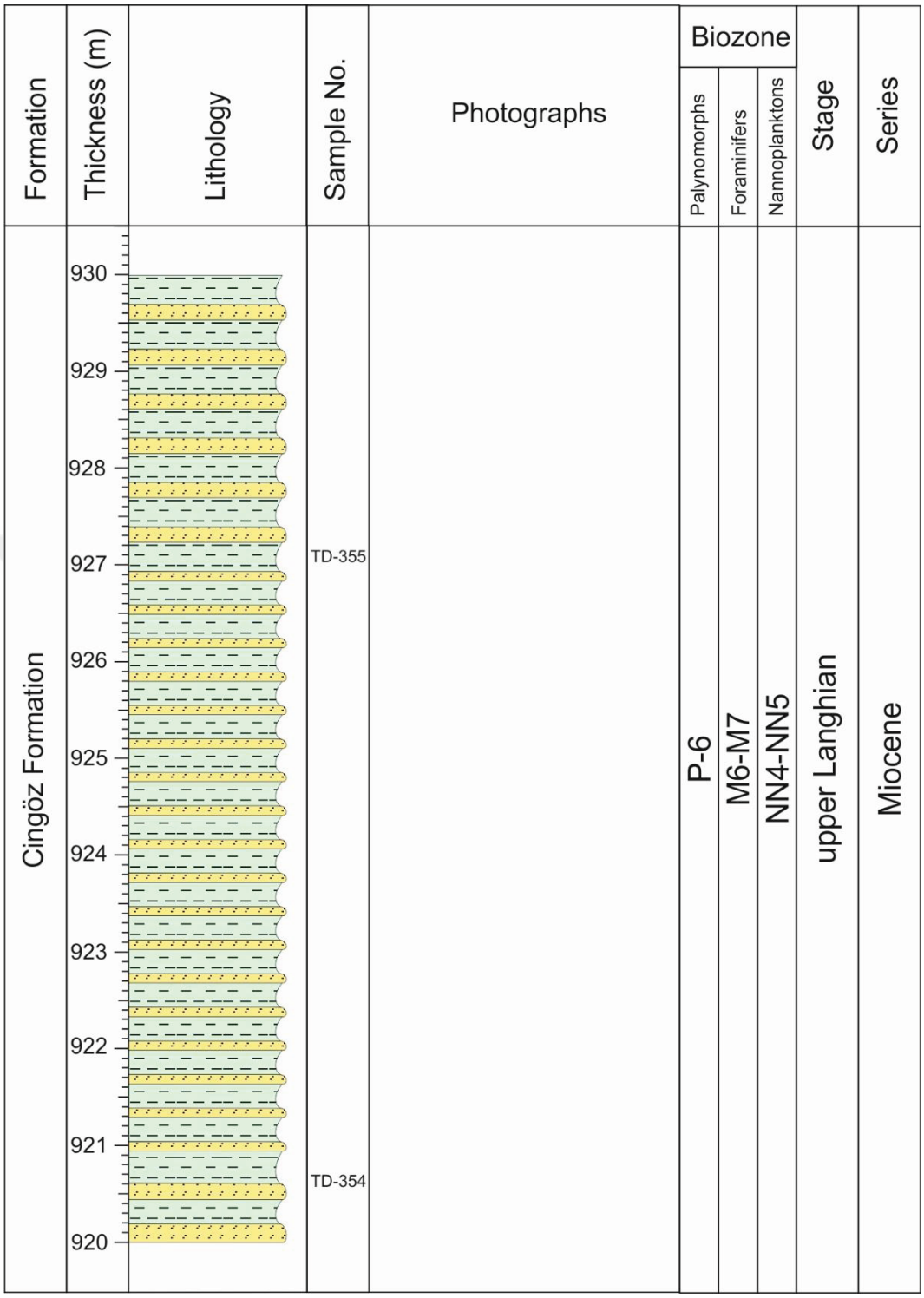

Figure 66. (cont'd)

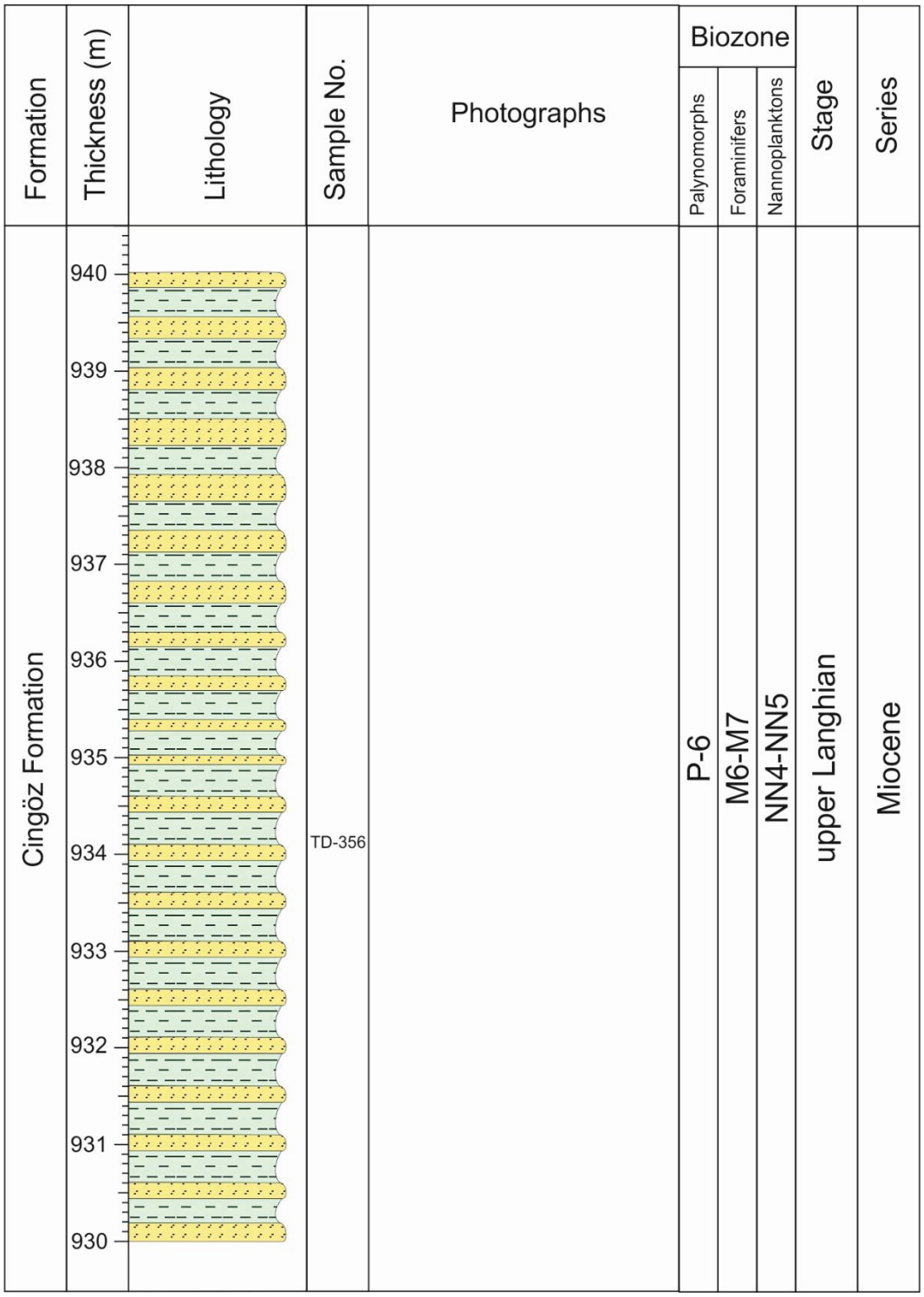

Figure 66. (cont'd)

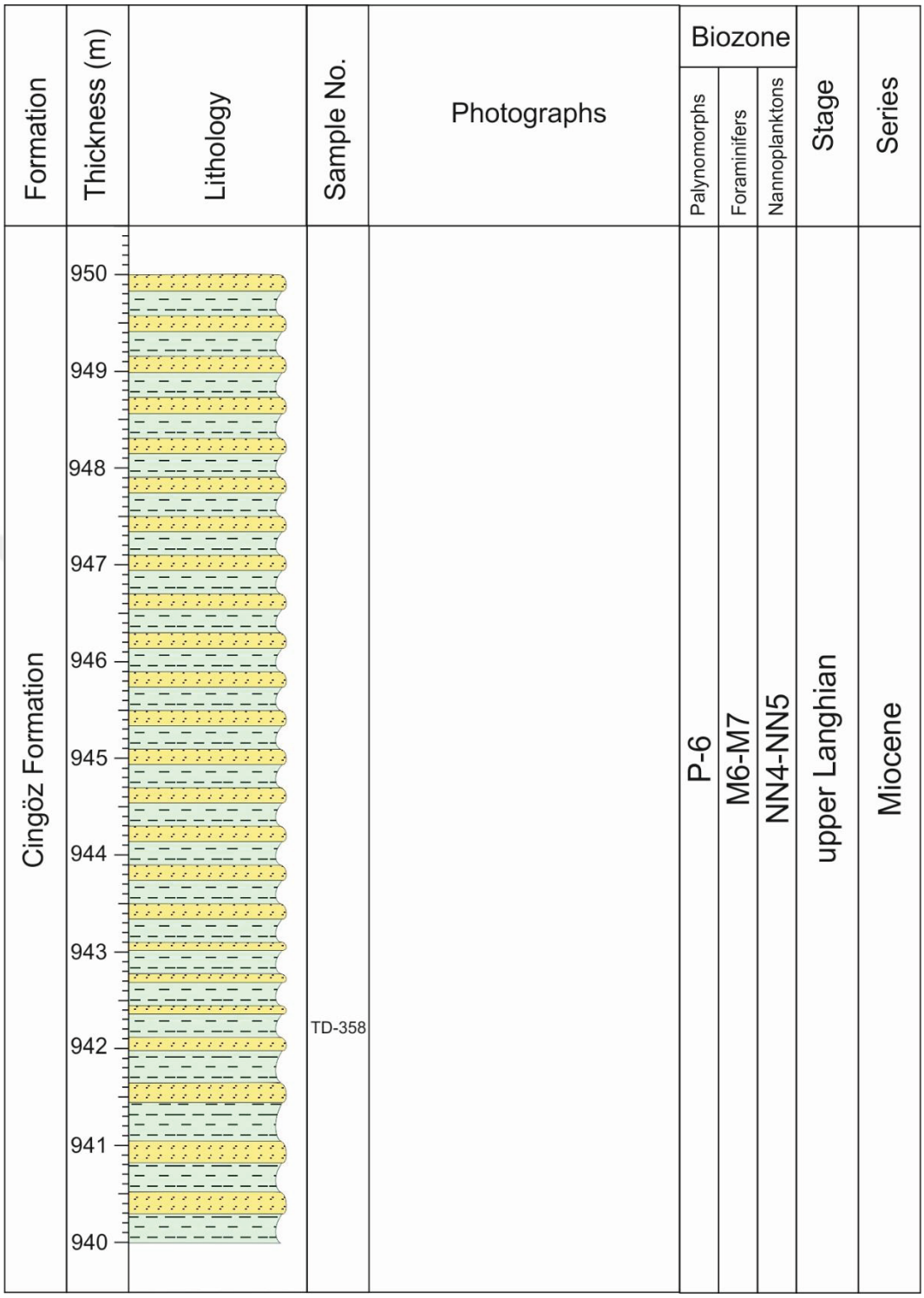

Figure 66. (cont'd)

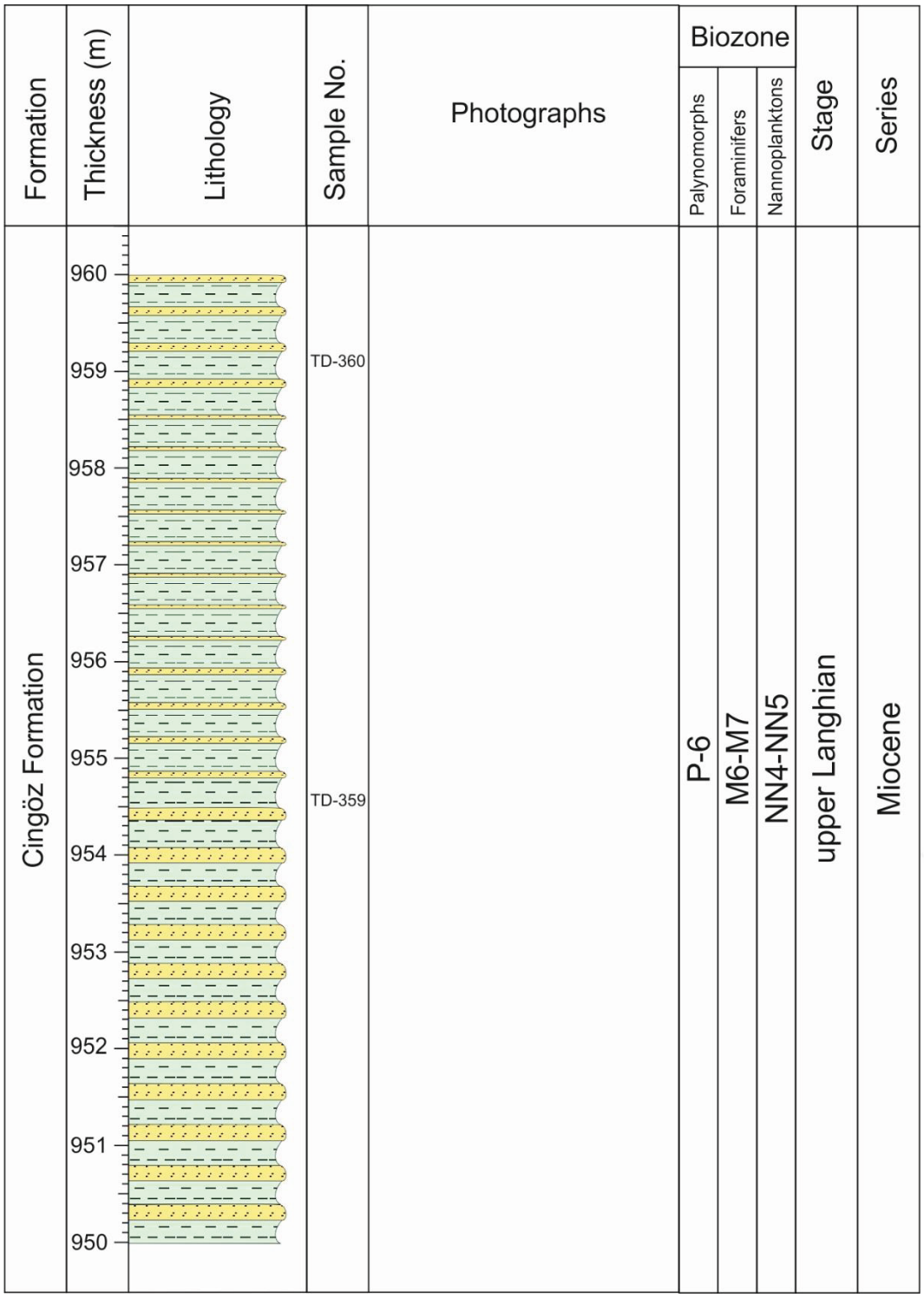

Figure 66. (cont'd)

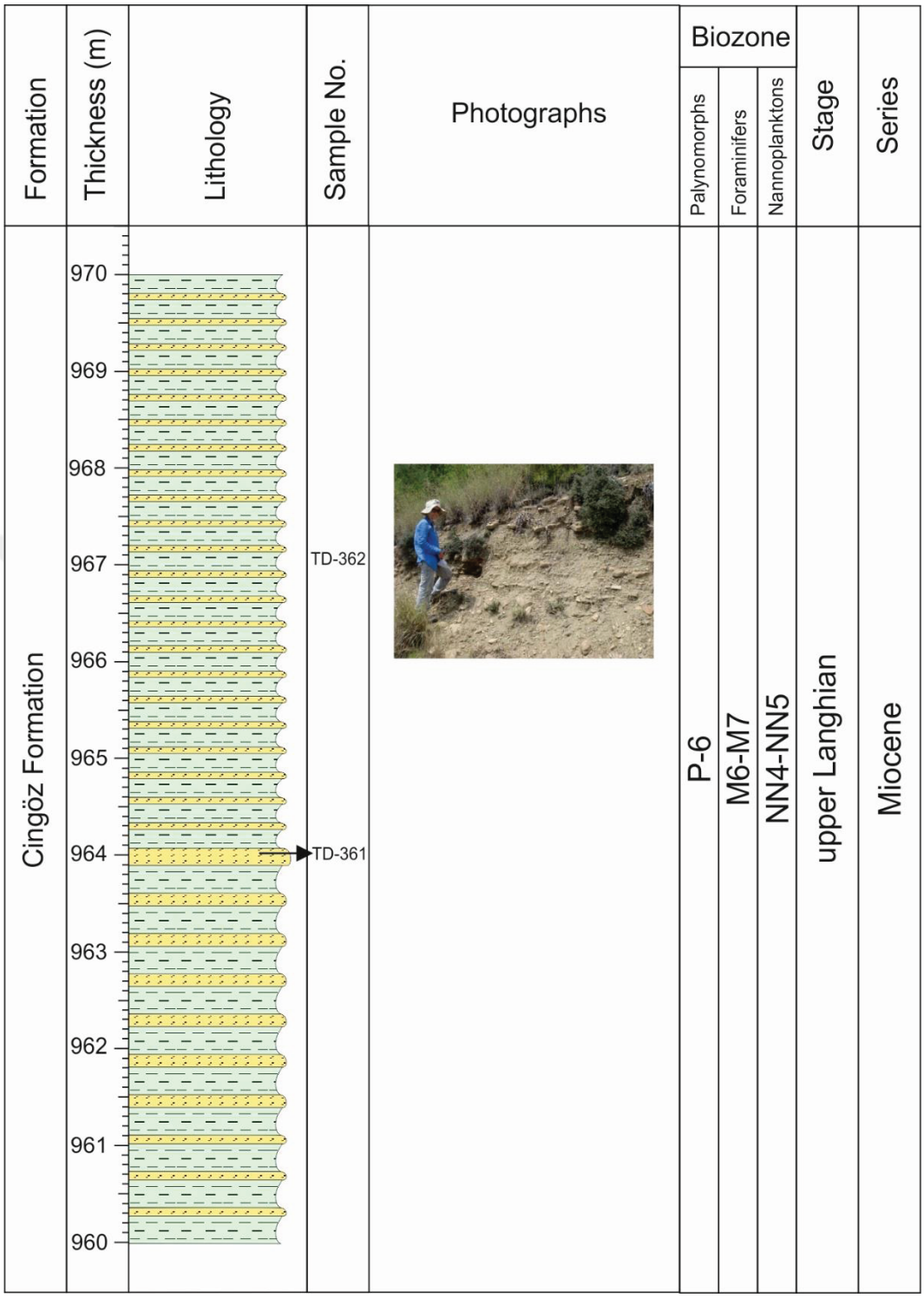

Figure 66. (cont'd)

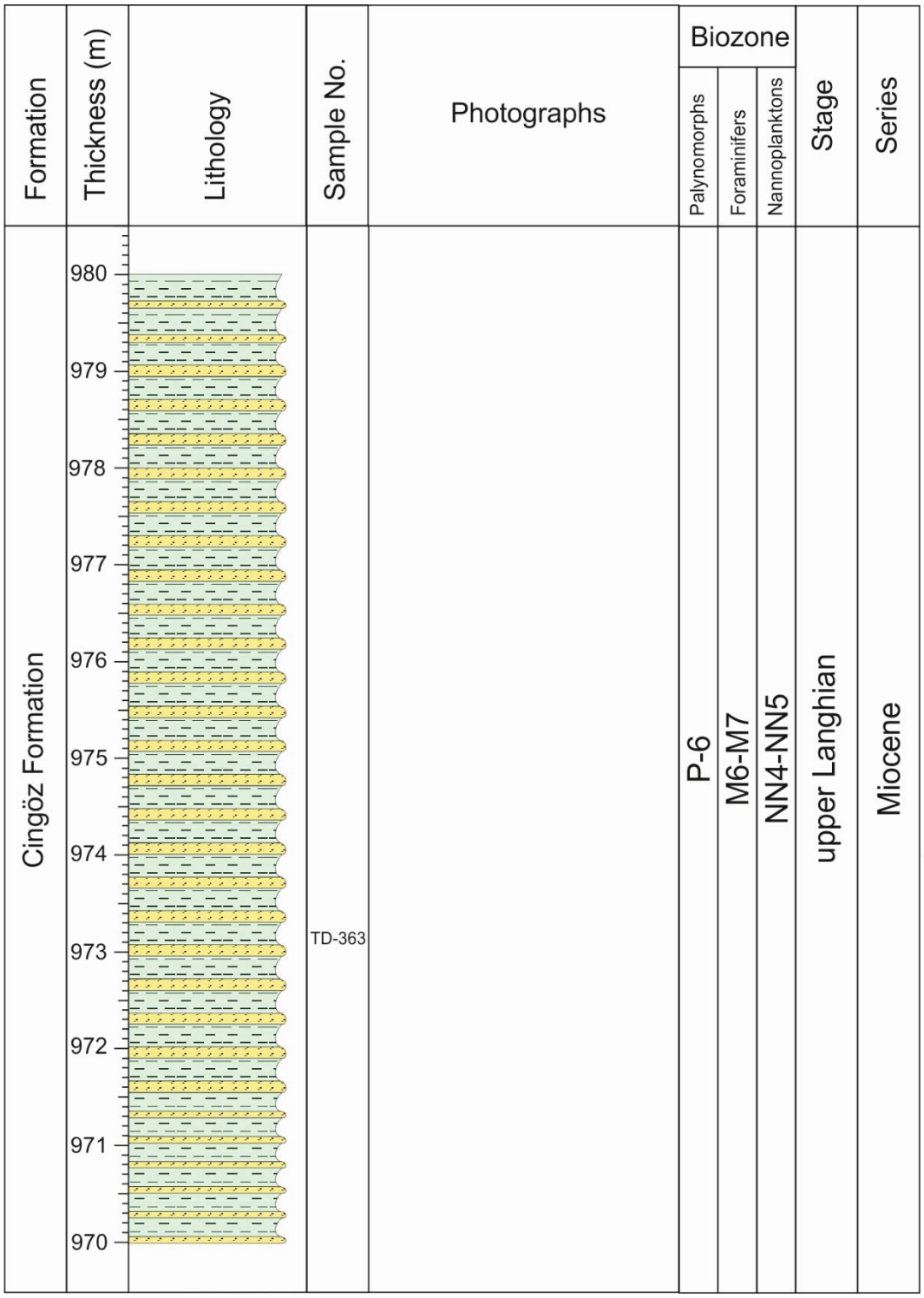

Figure 66. (cont'd)

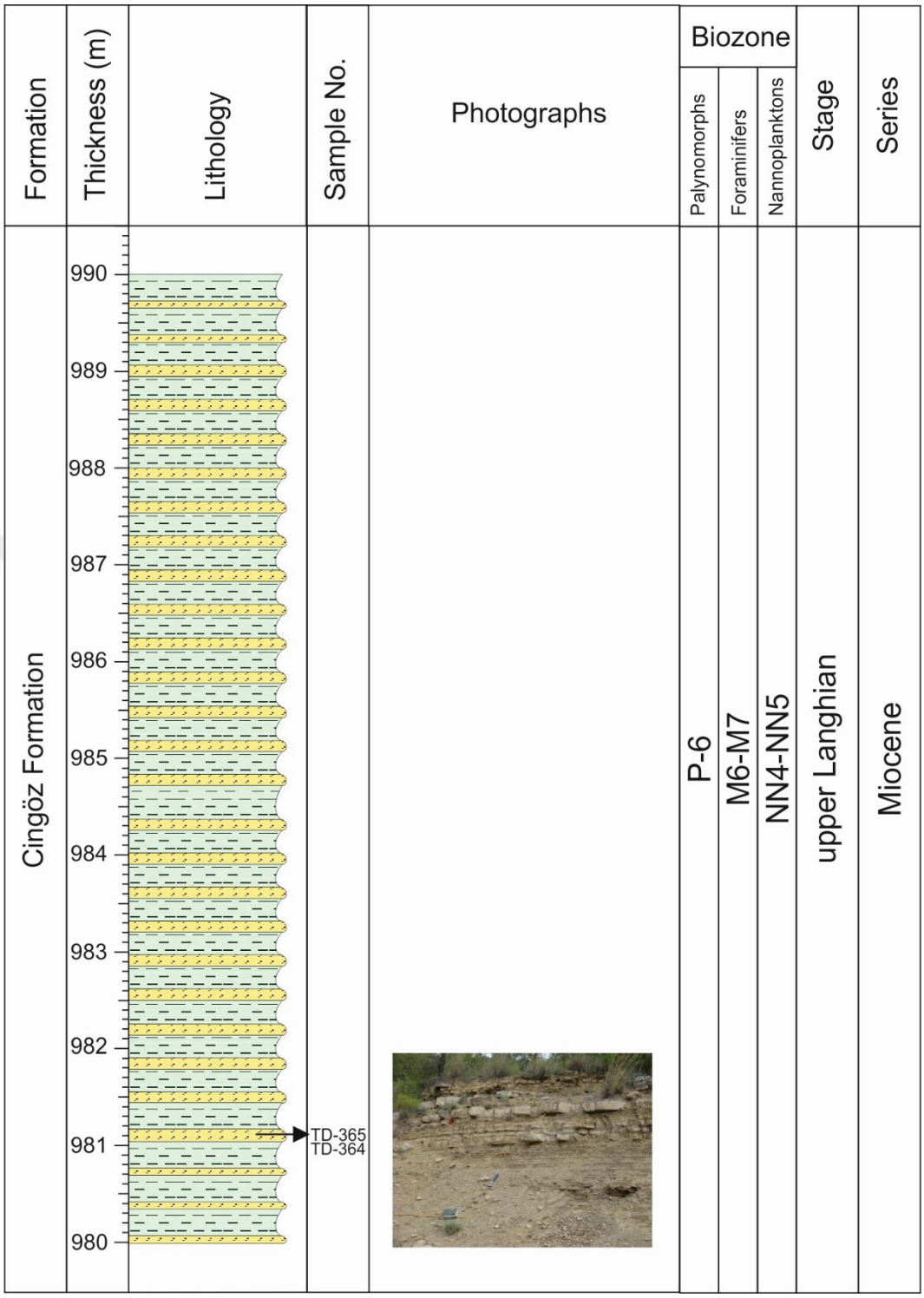

Figure 66. (cont'd)

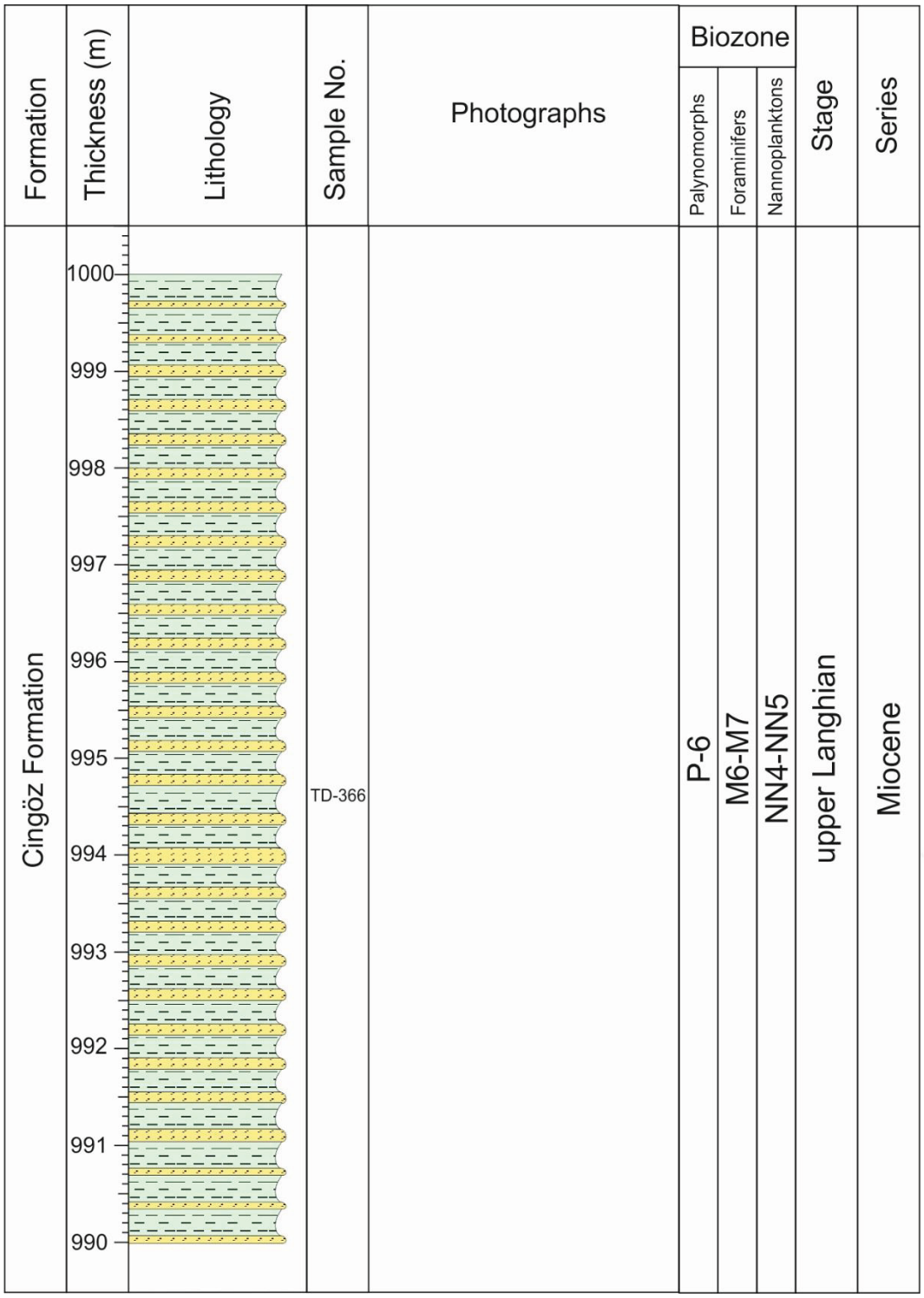

Figure 66. (cont'd)

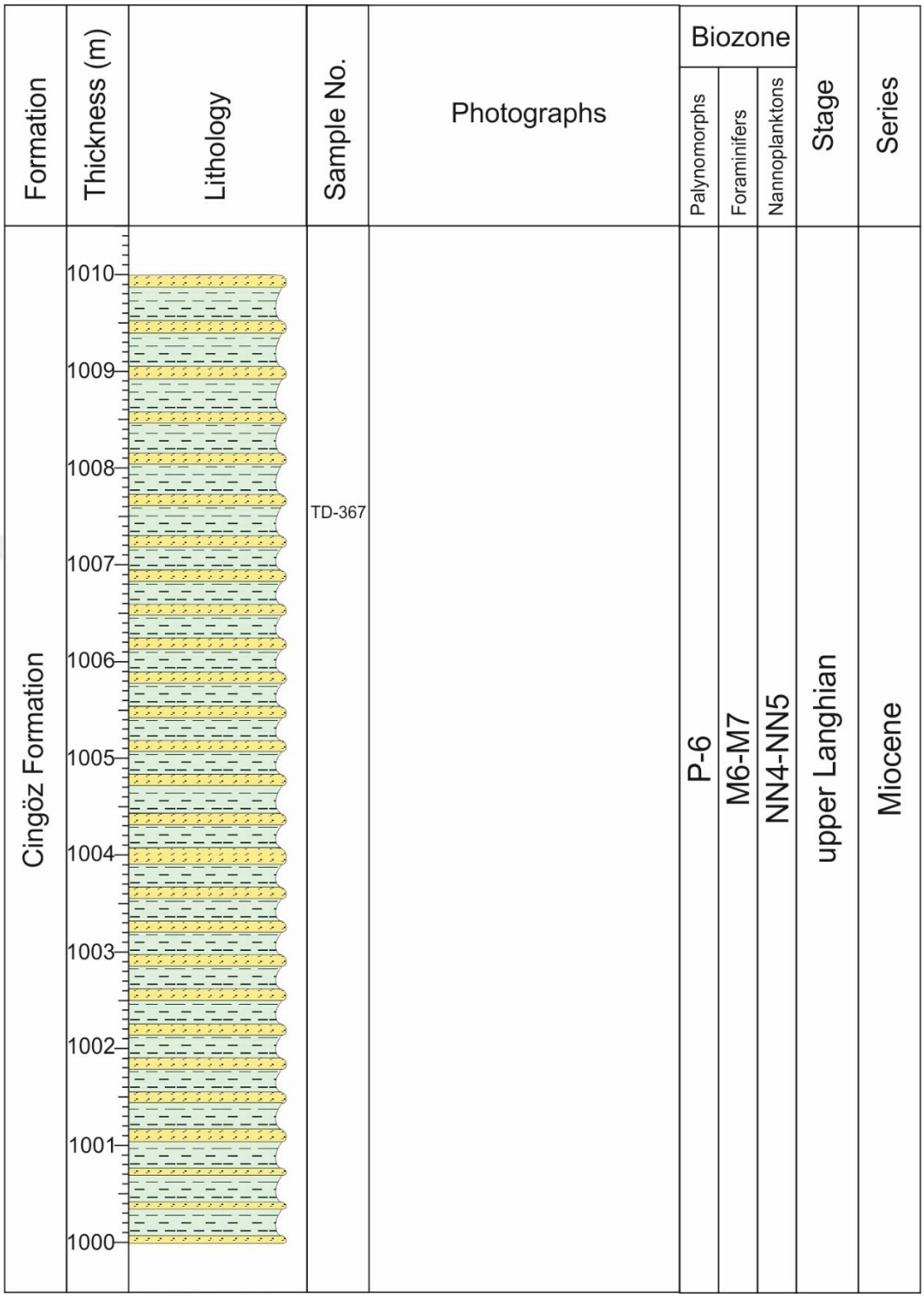

Figure 66. (cont'd)

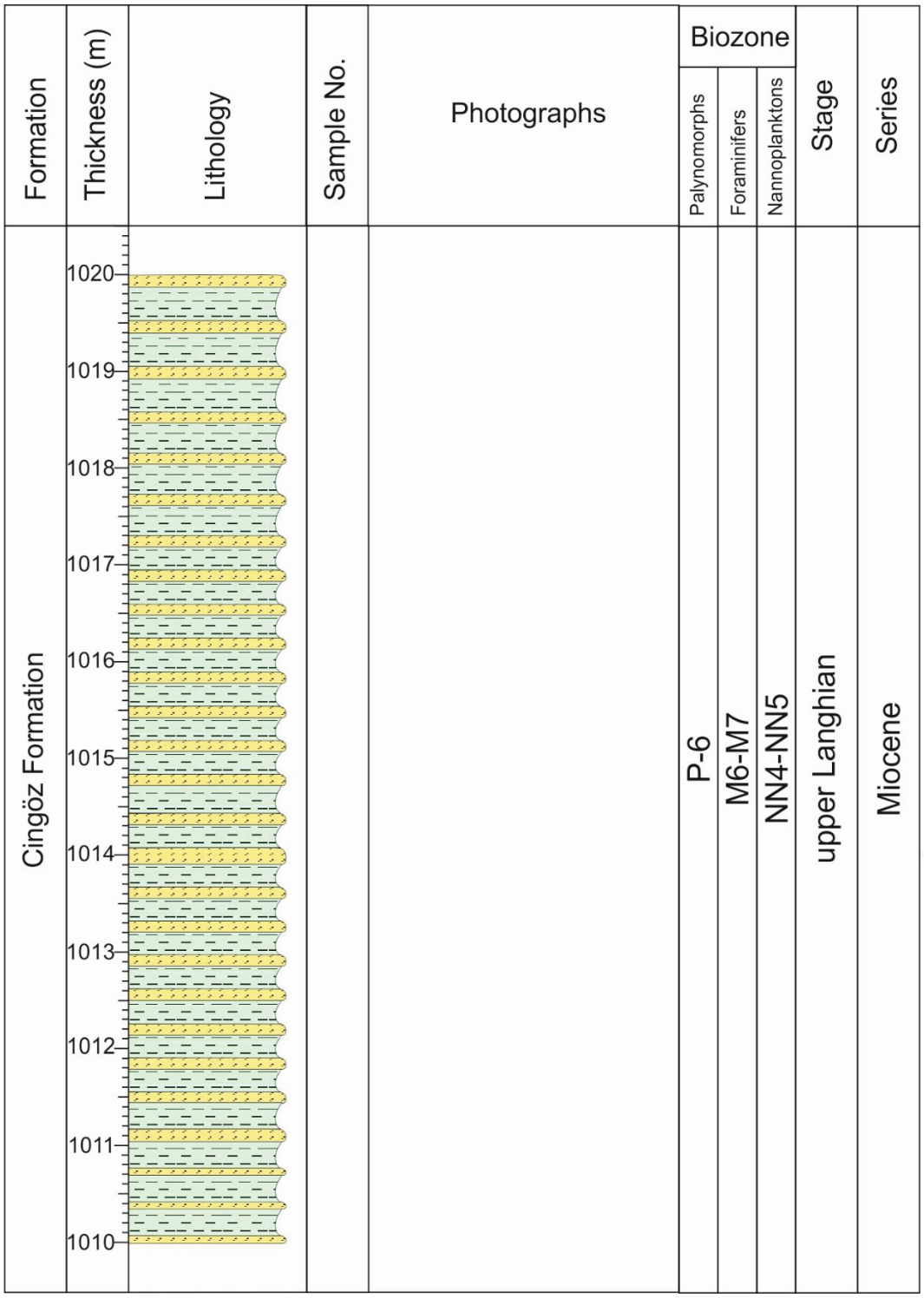

Figure 66. (cont'd)

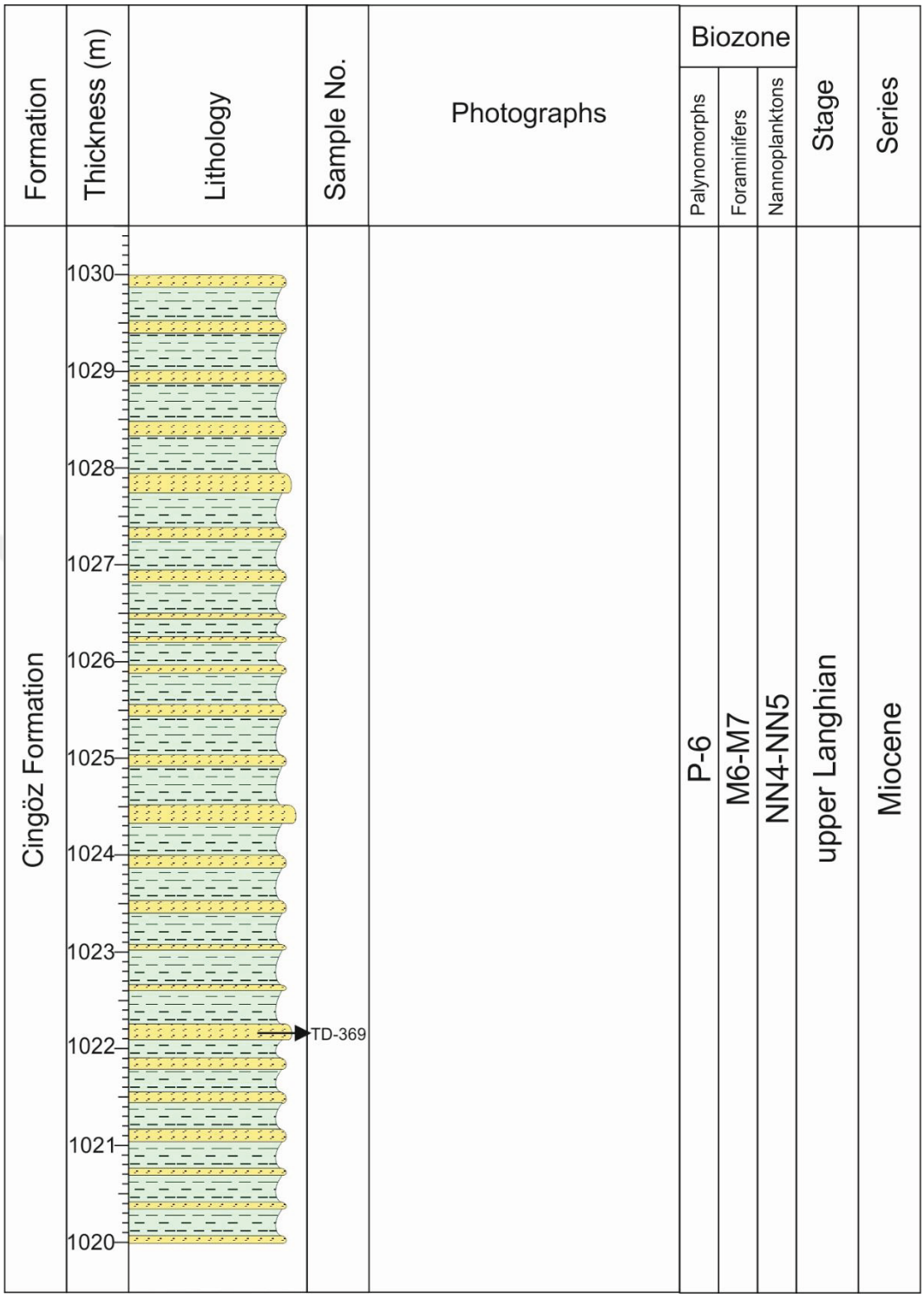

Figure 66. (cont'd)

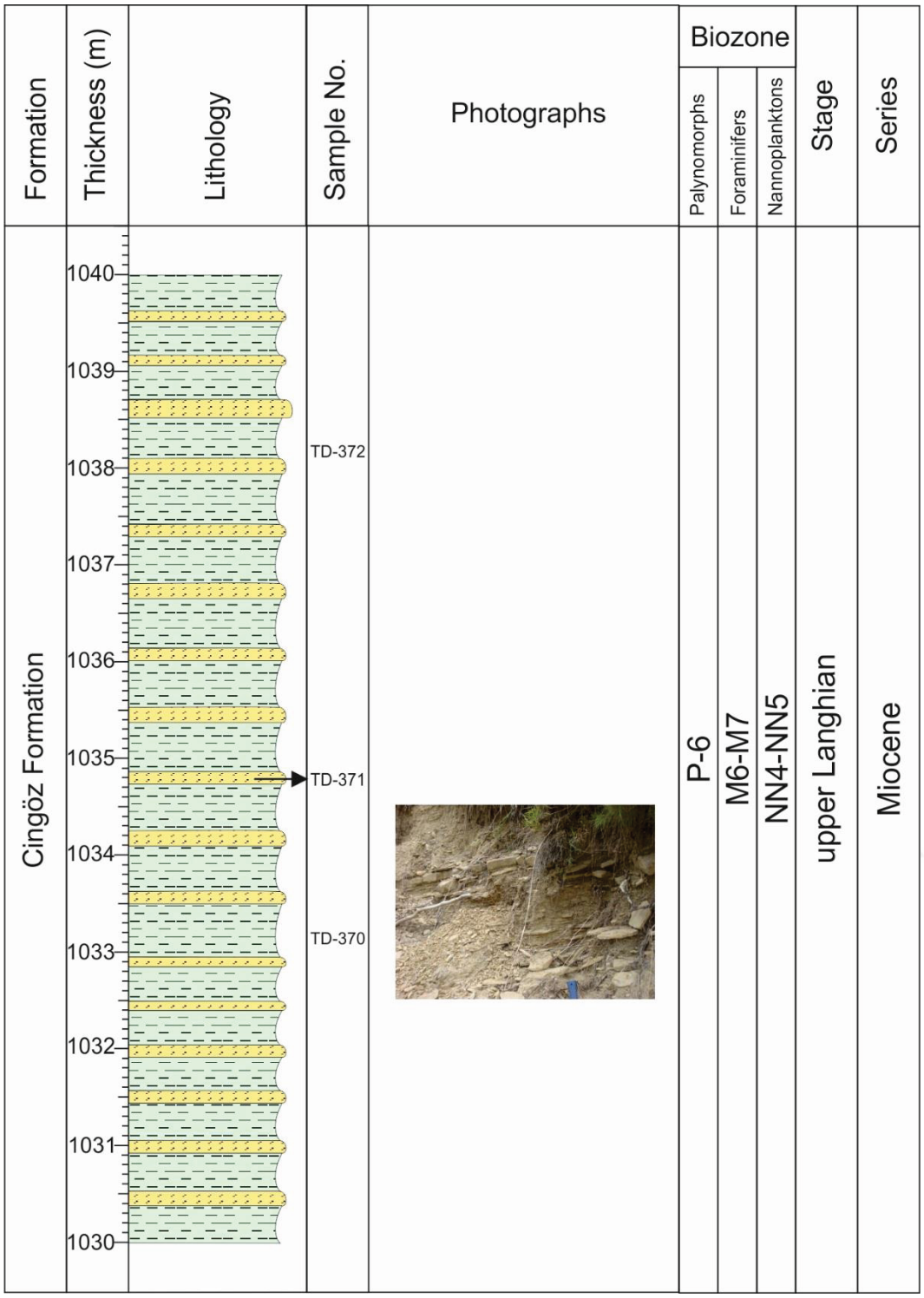

Figure 66. (cont'd)

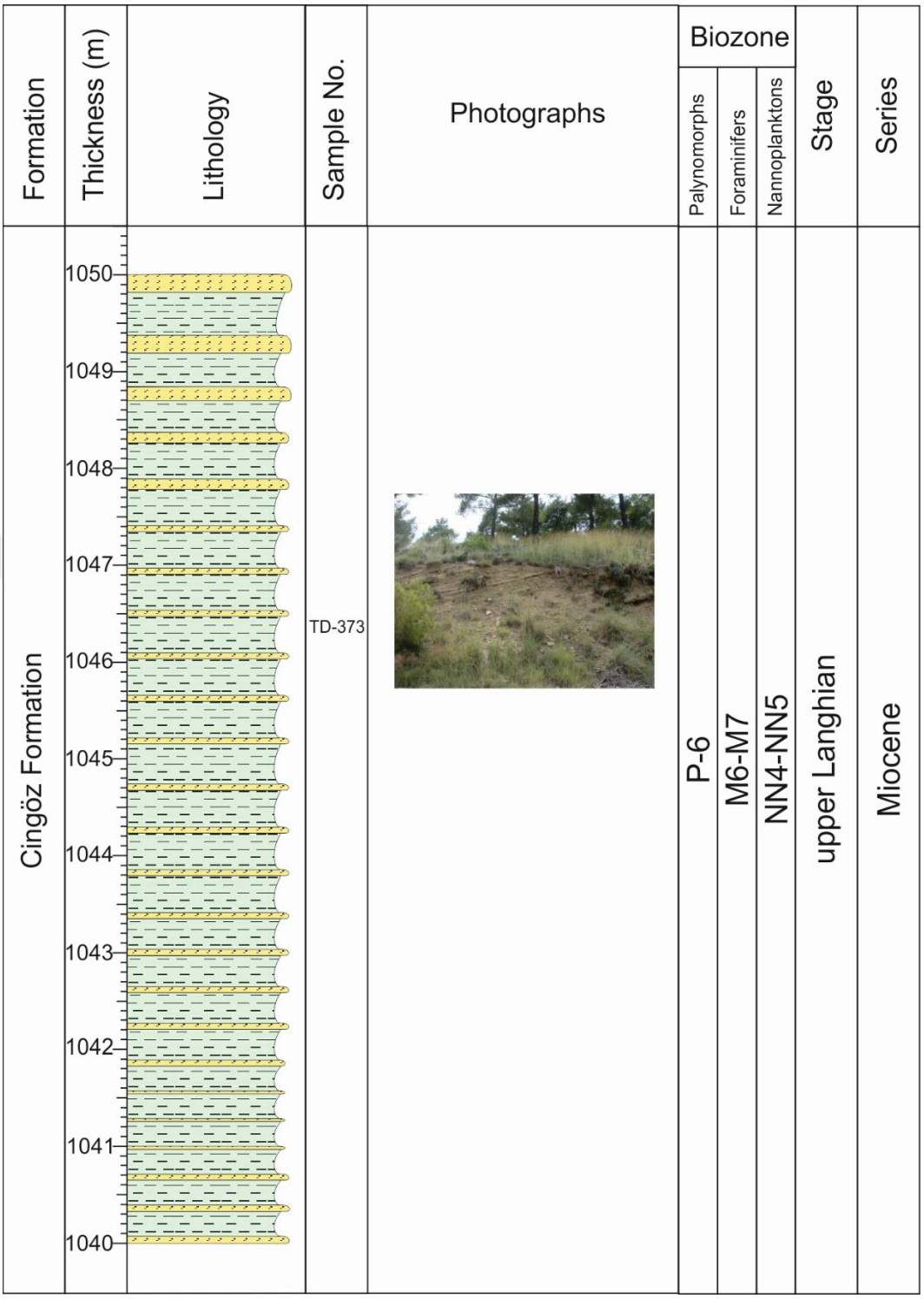

Figure 66. (cont'd)

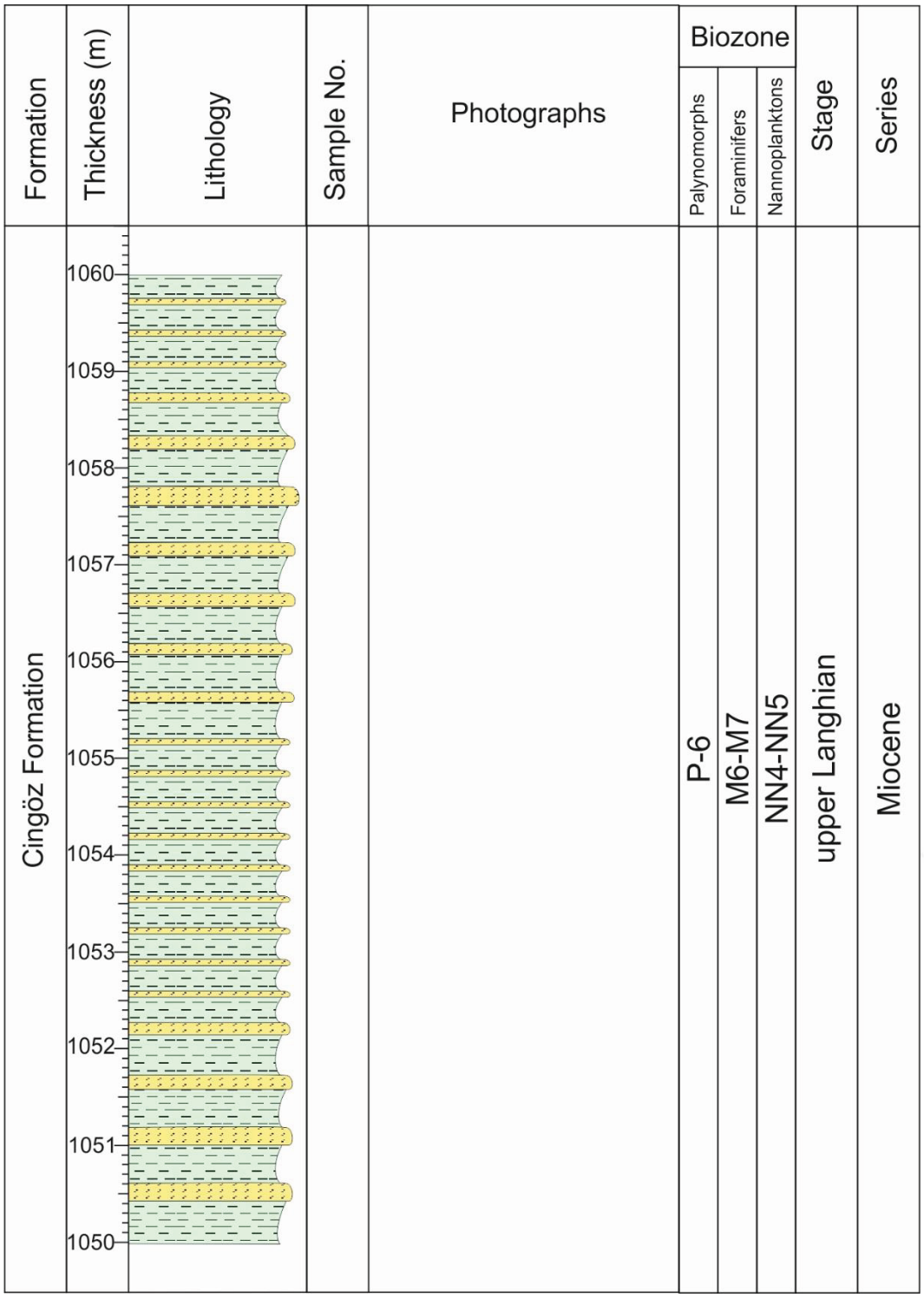

Figure 66. (cont'd)

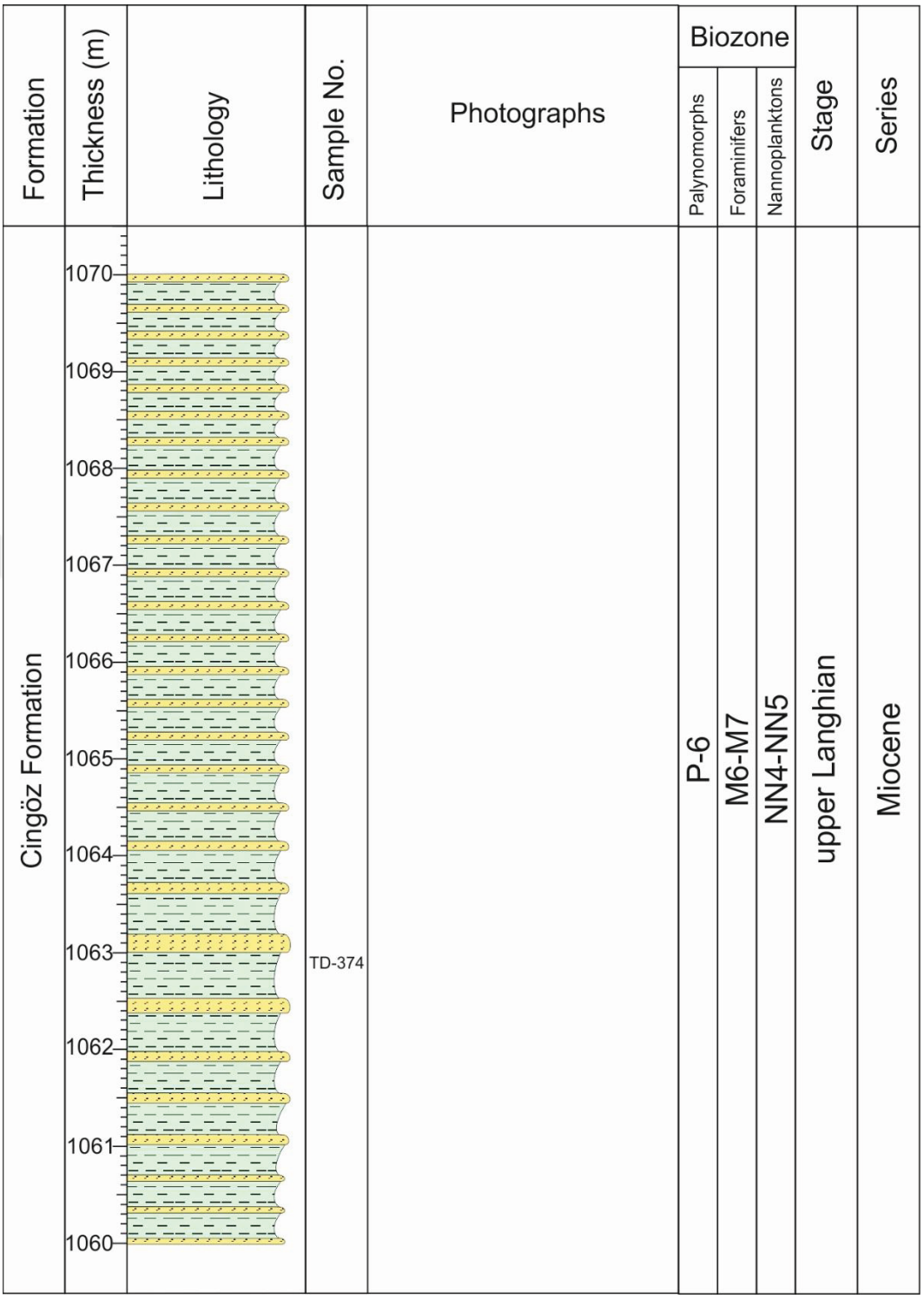

Figure 66. (cont'd)

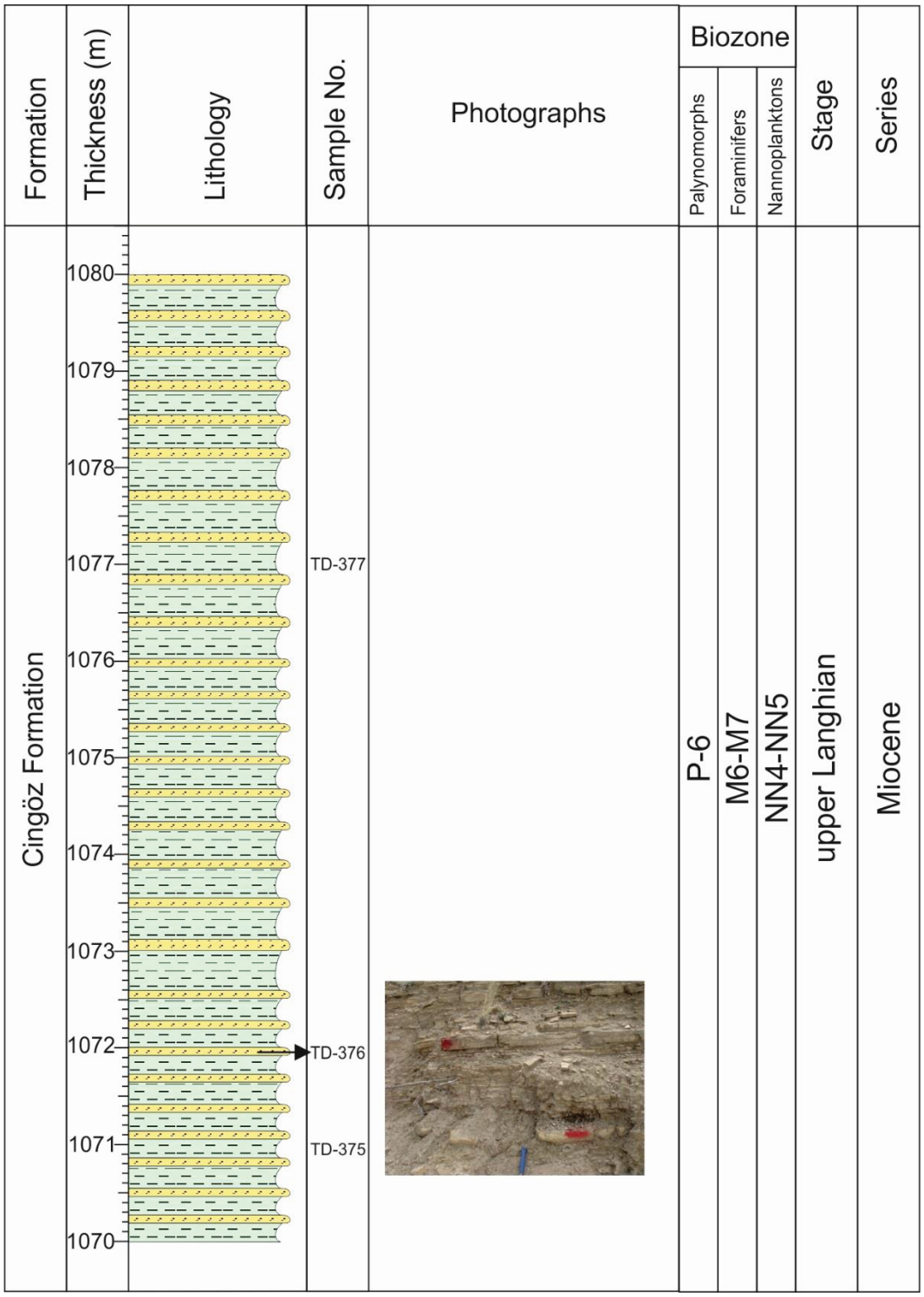

Figure 66. (cont'd)

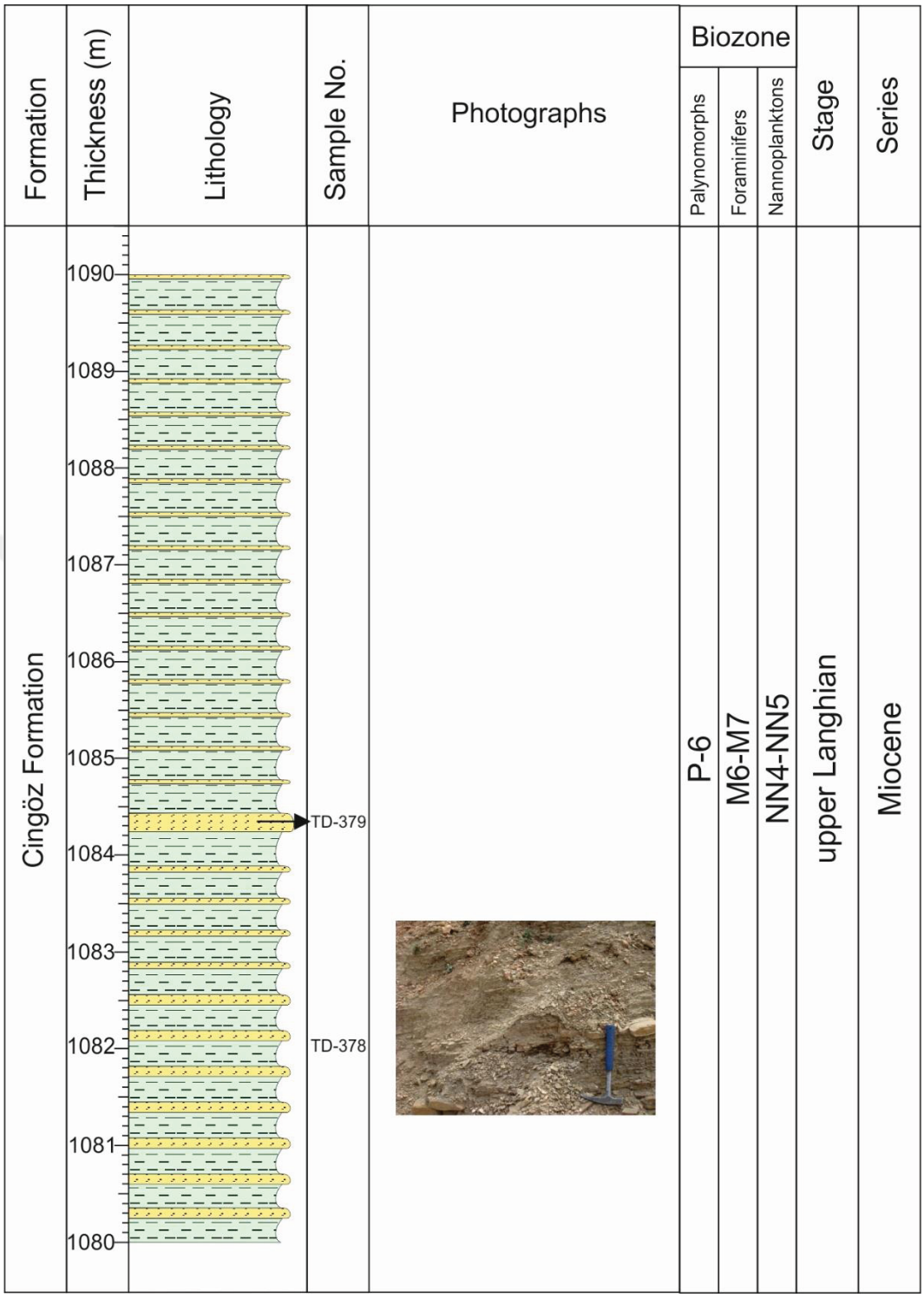

Figure 66. (cont'd)

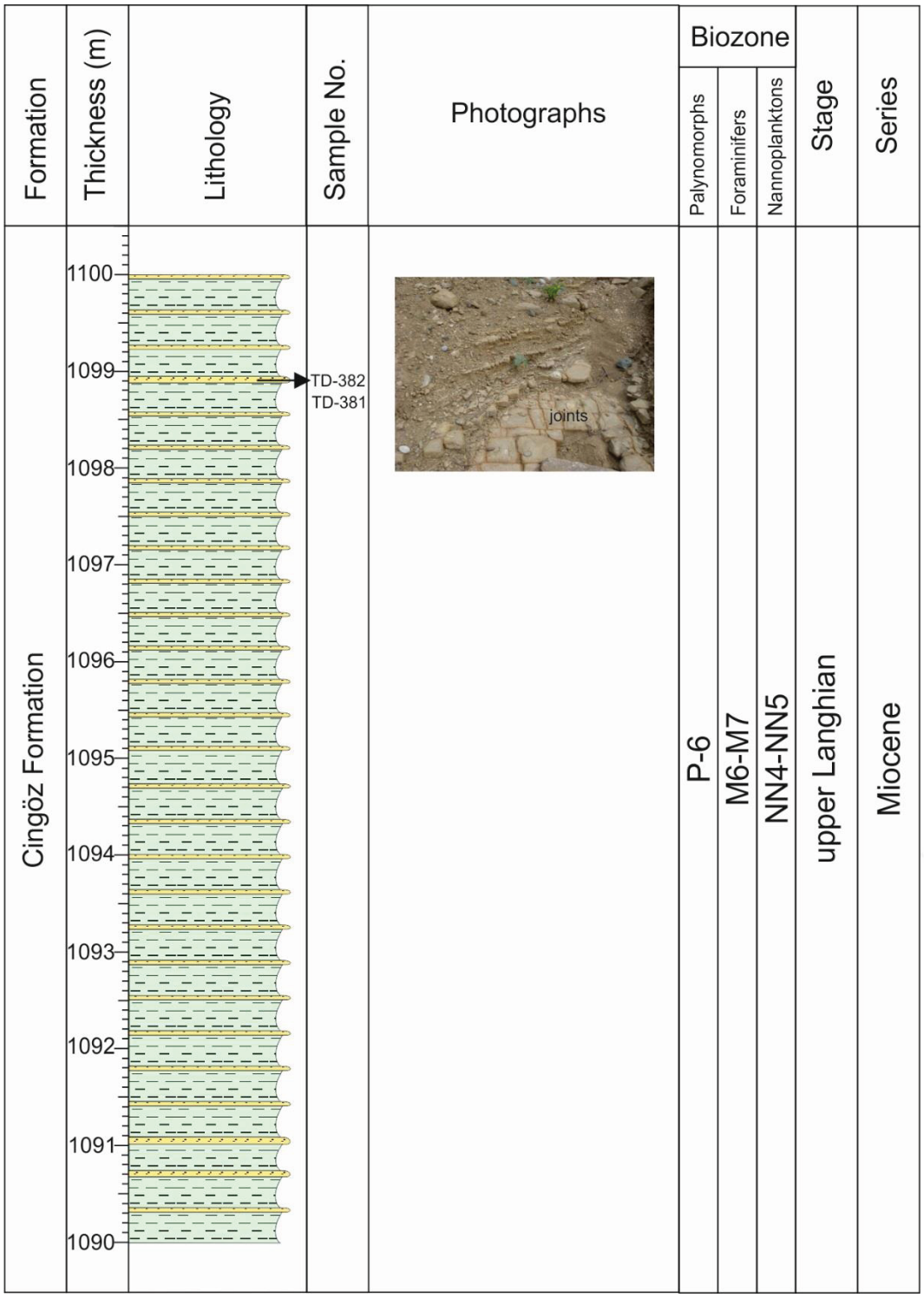

Figure 66. (cont'd)

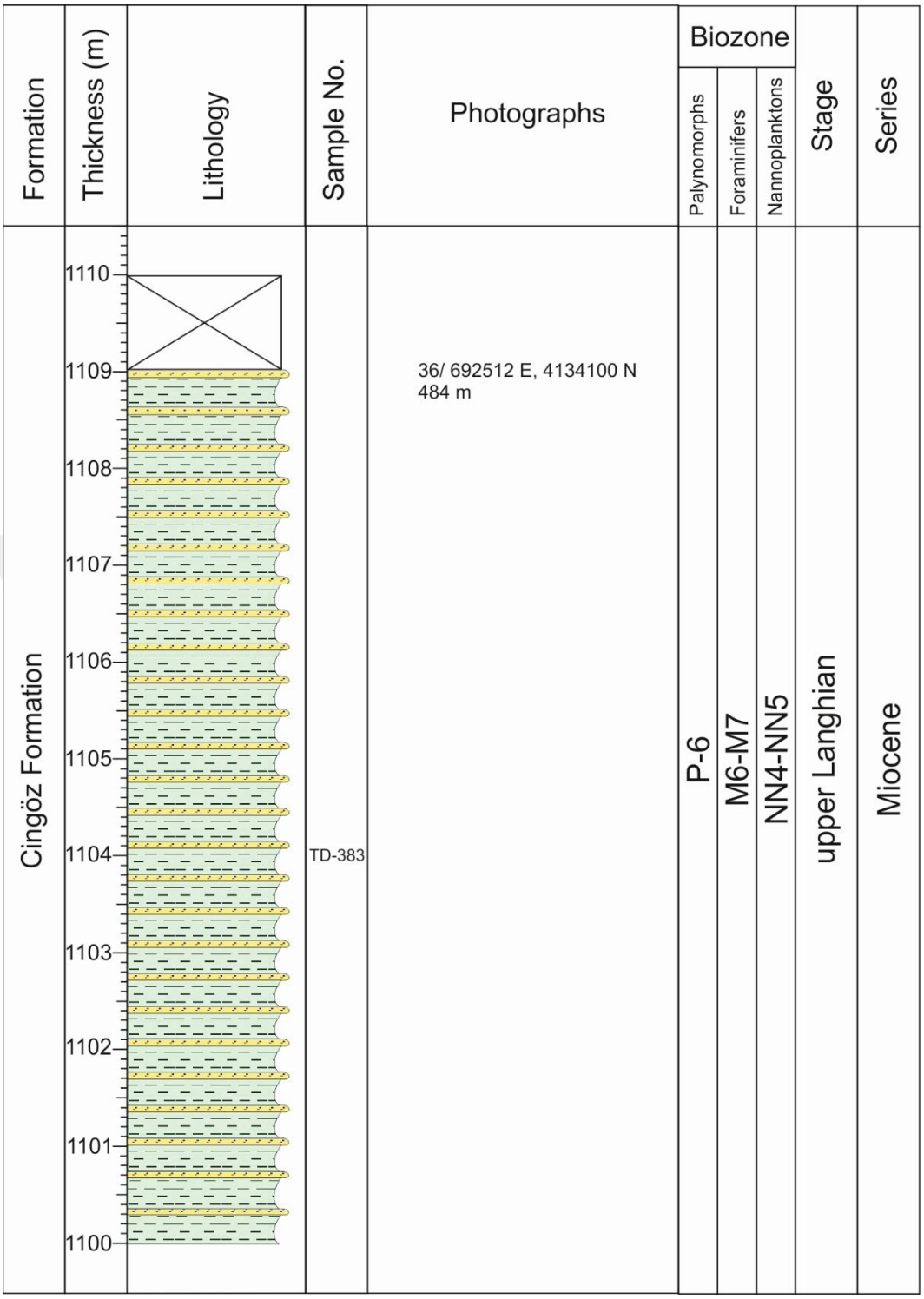

Figure 66. (cont'd)

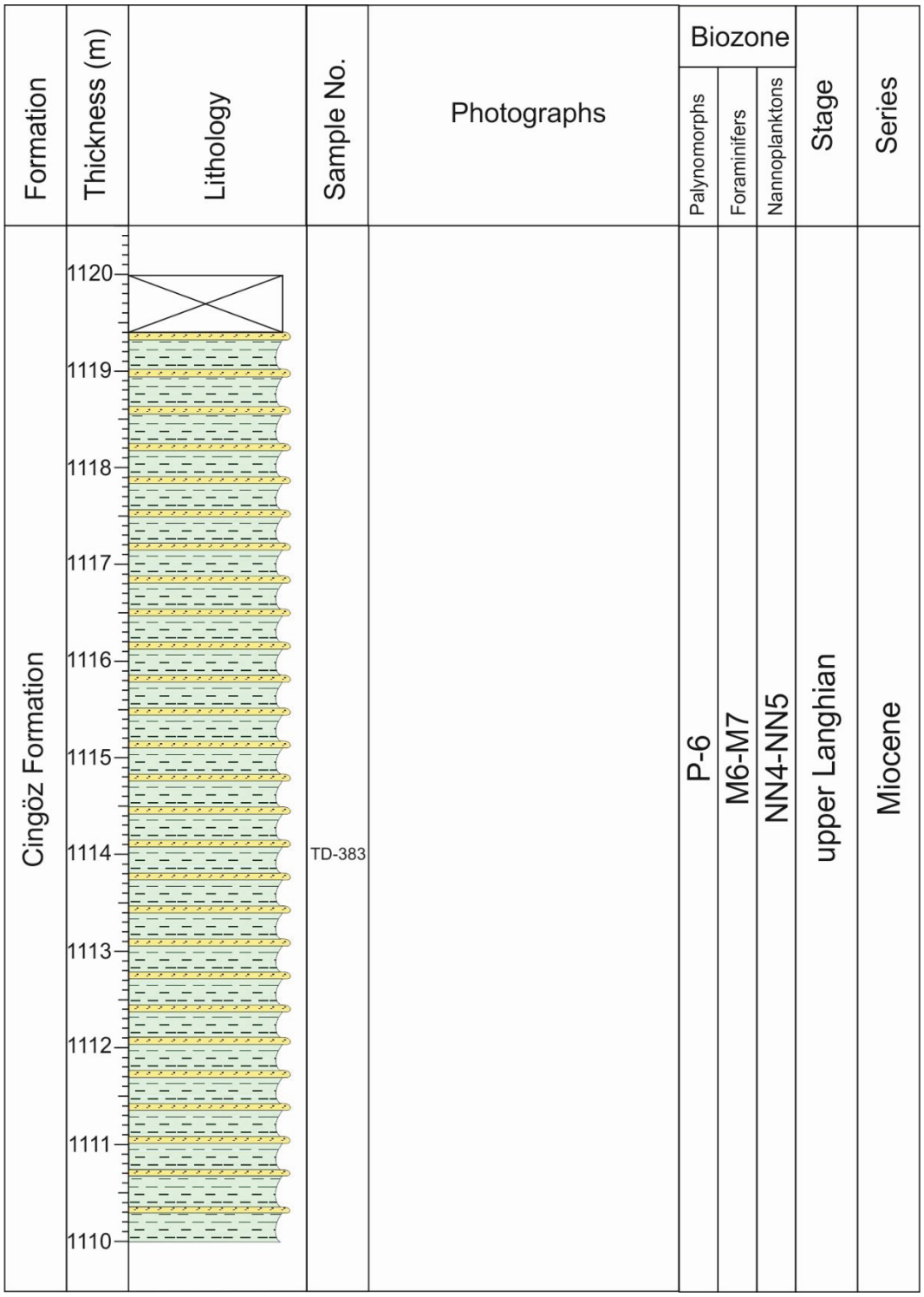

Figure 66. (cont'd)

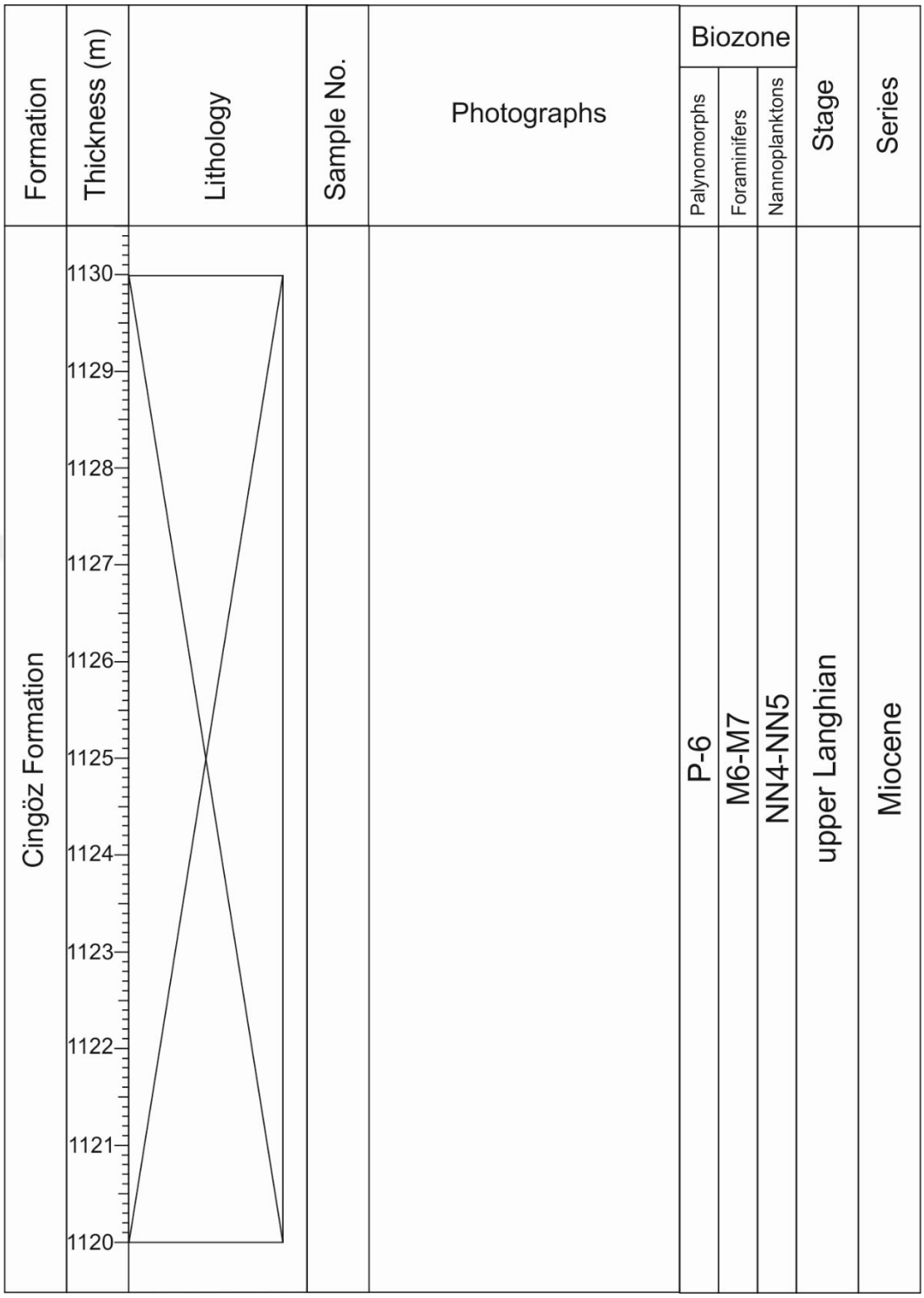

Figure 66. (cont'd)

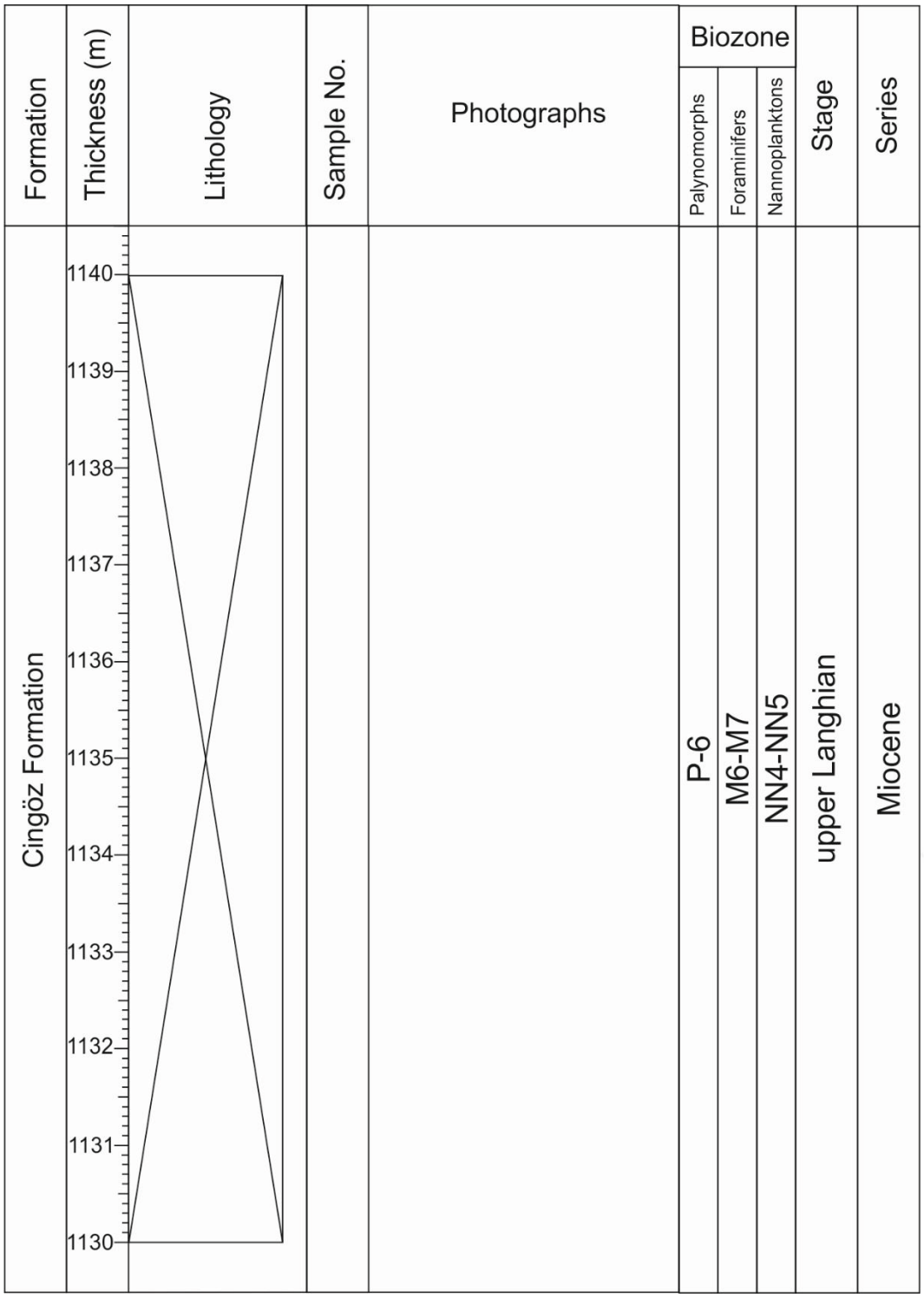

Figure 66. (cont'd)

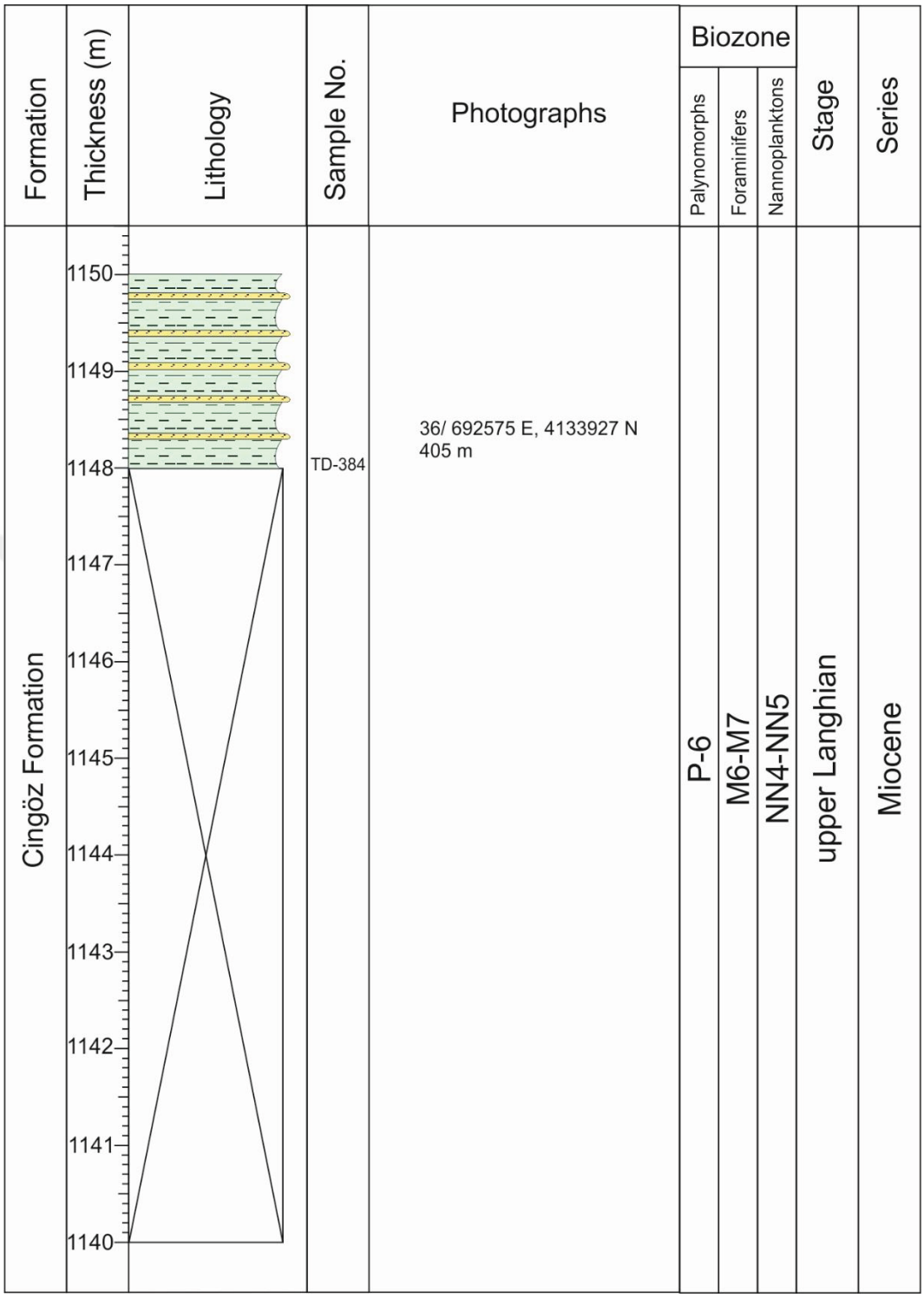

Figure 66. (cont'd)

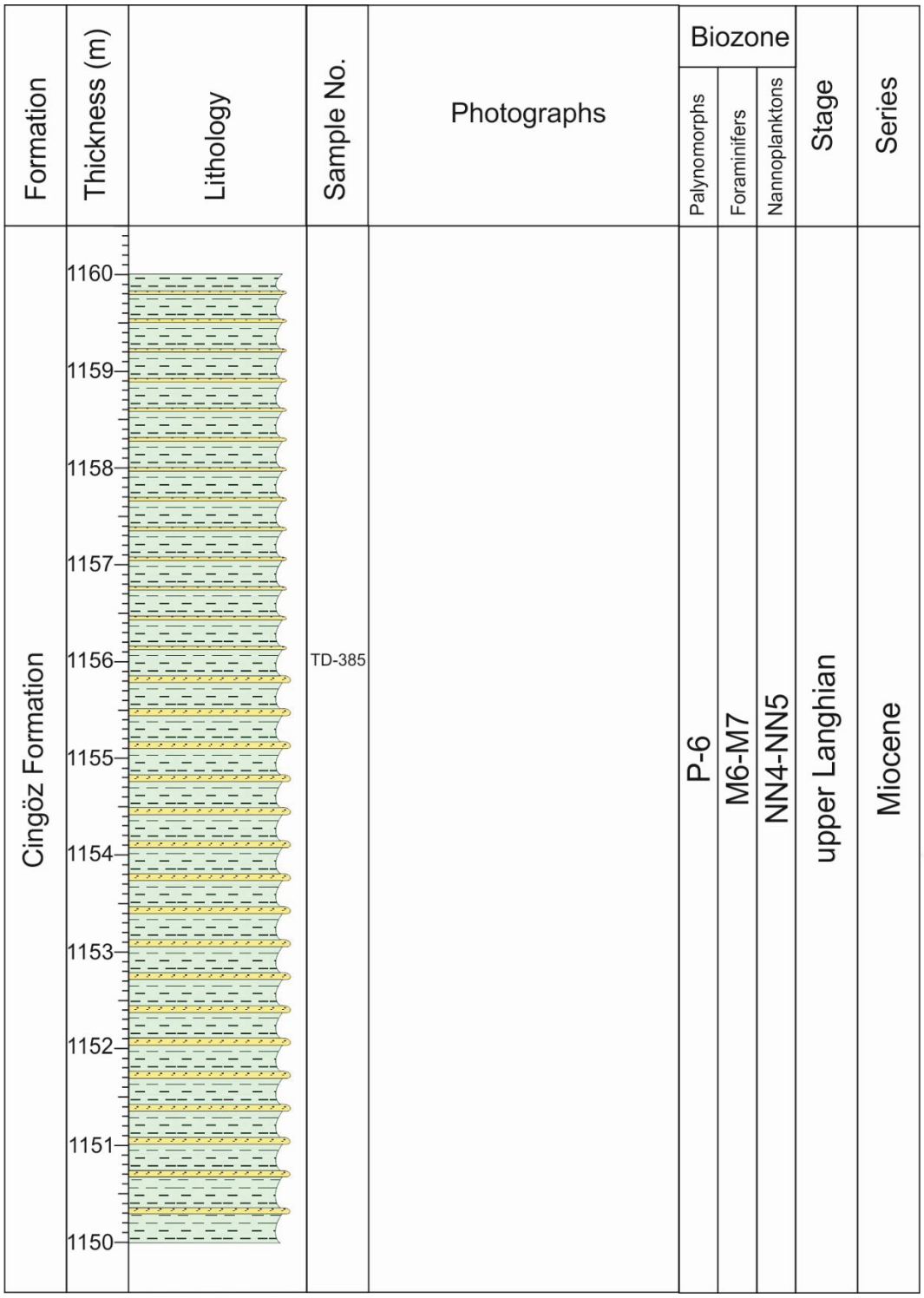

Figure 66. (cont'd)

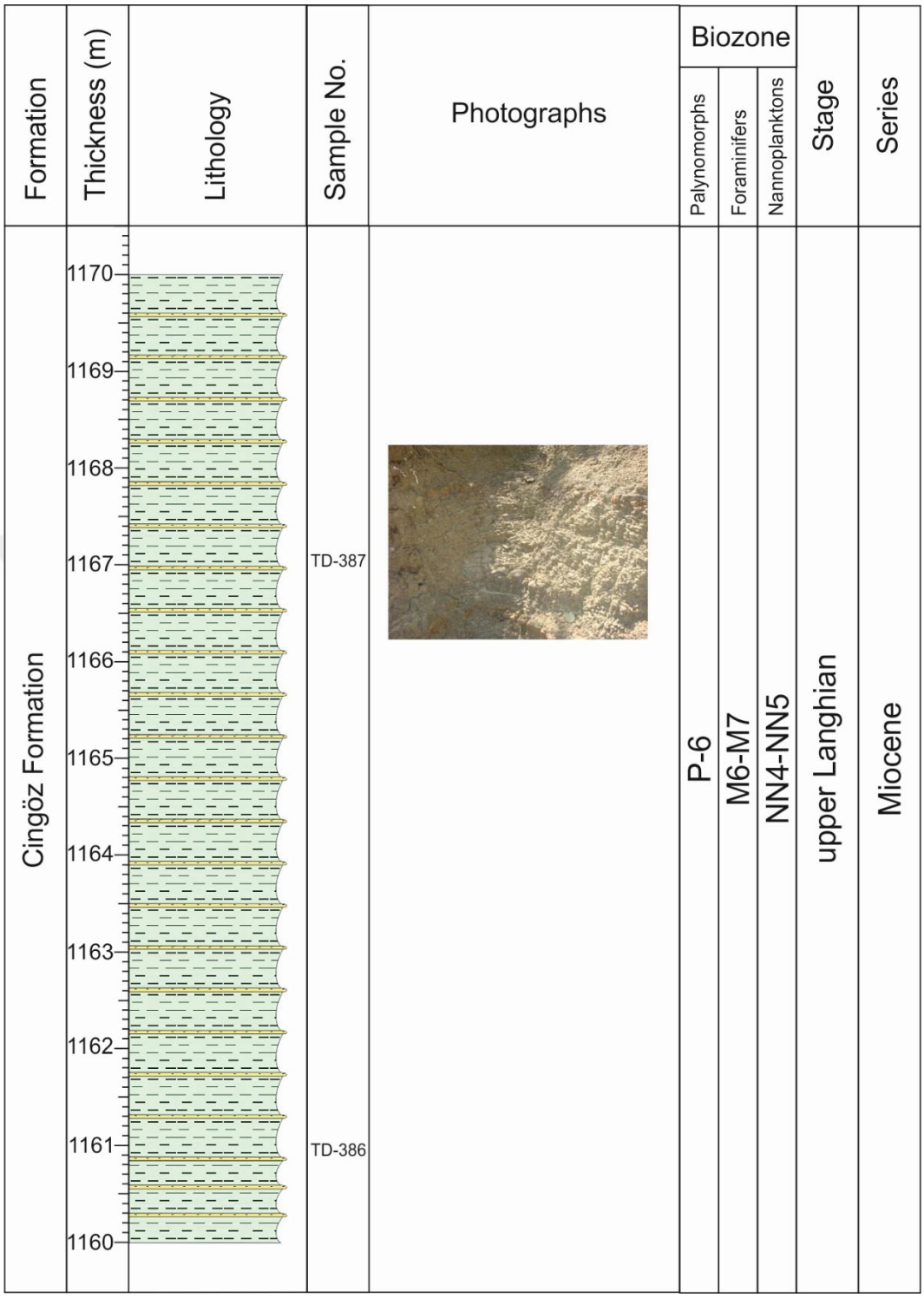

Figure 66. (cont'd)

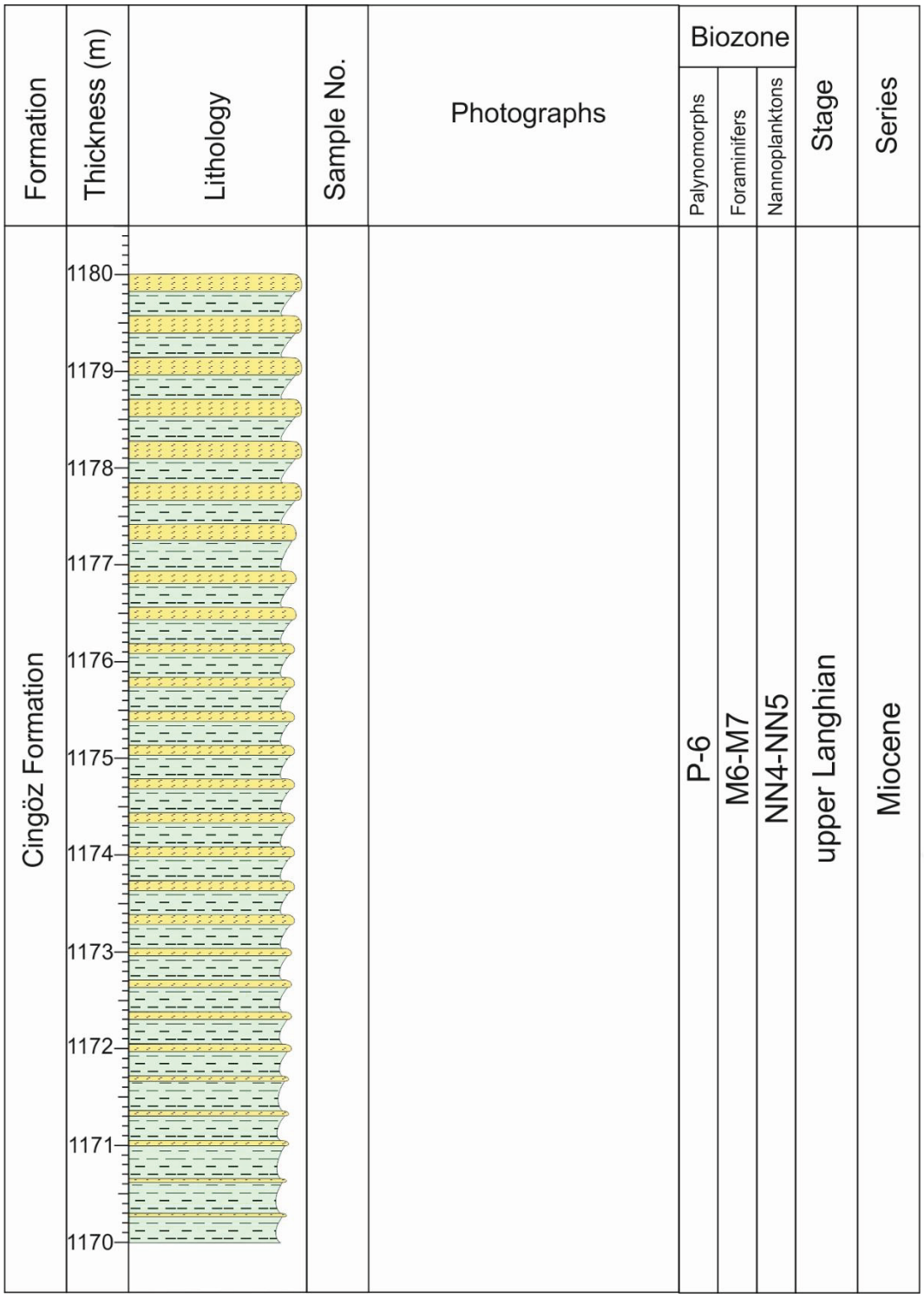

Figure 66. (cont'd)

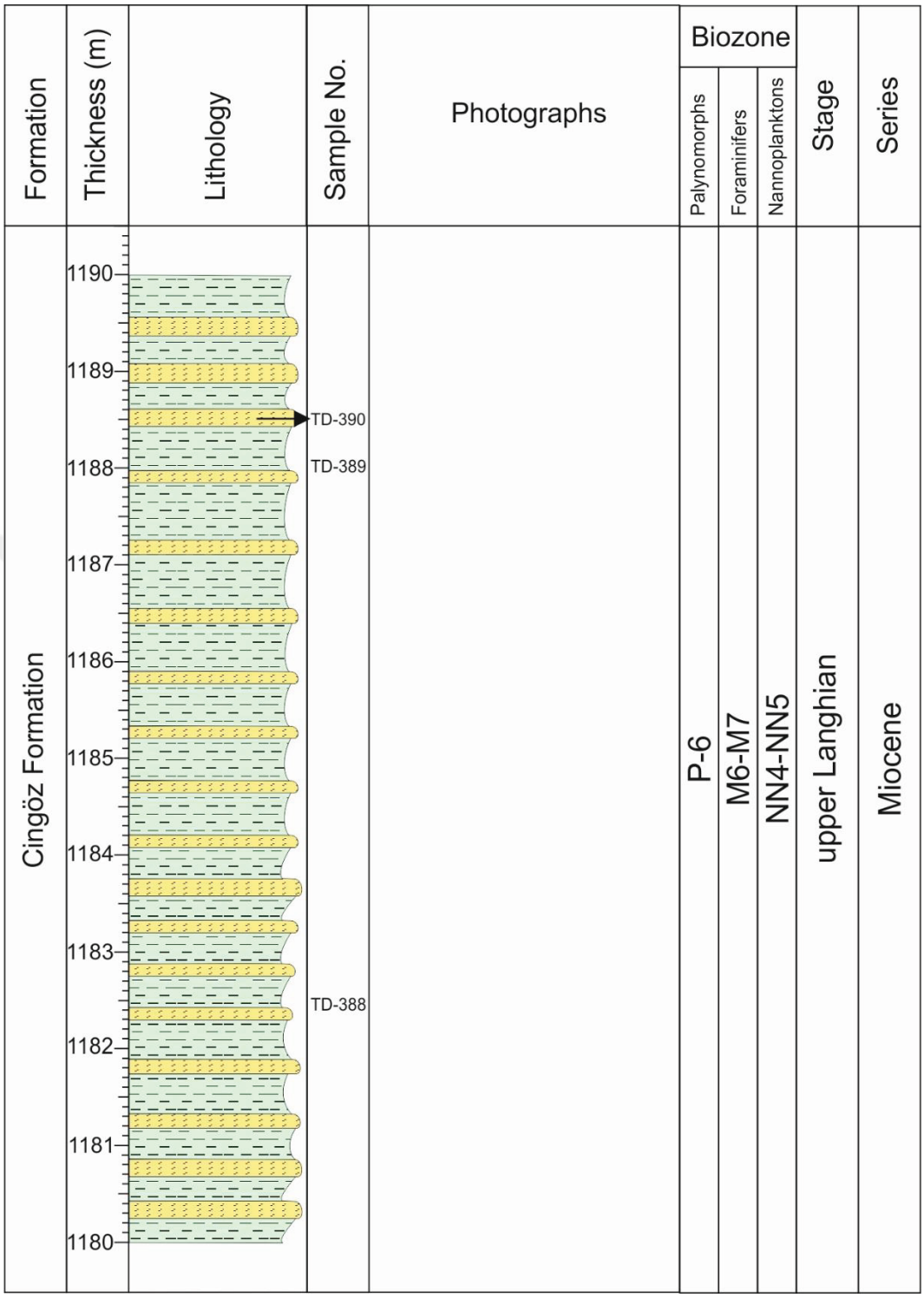

Figure 66. (cont'd)

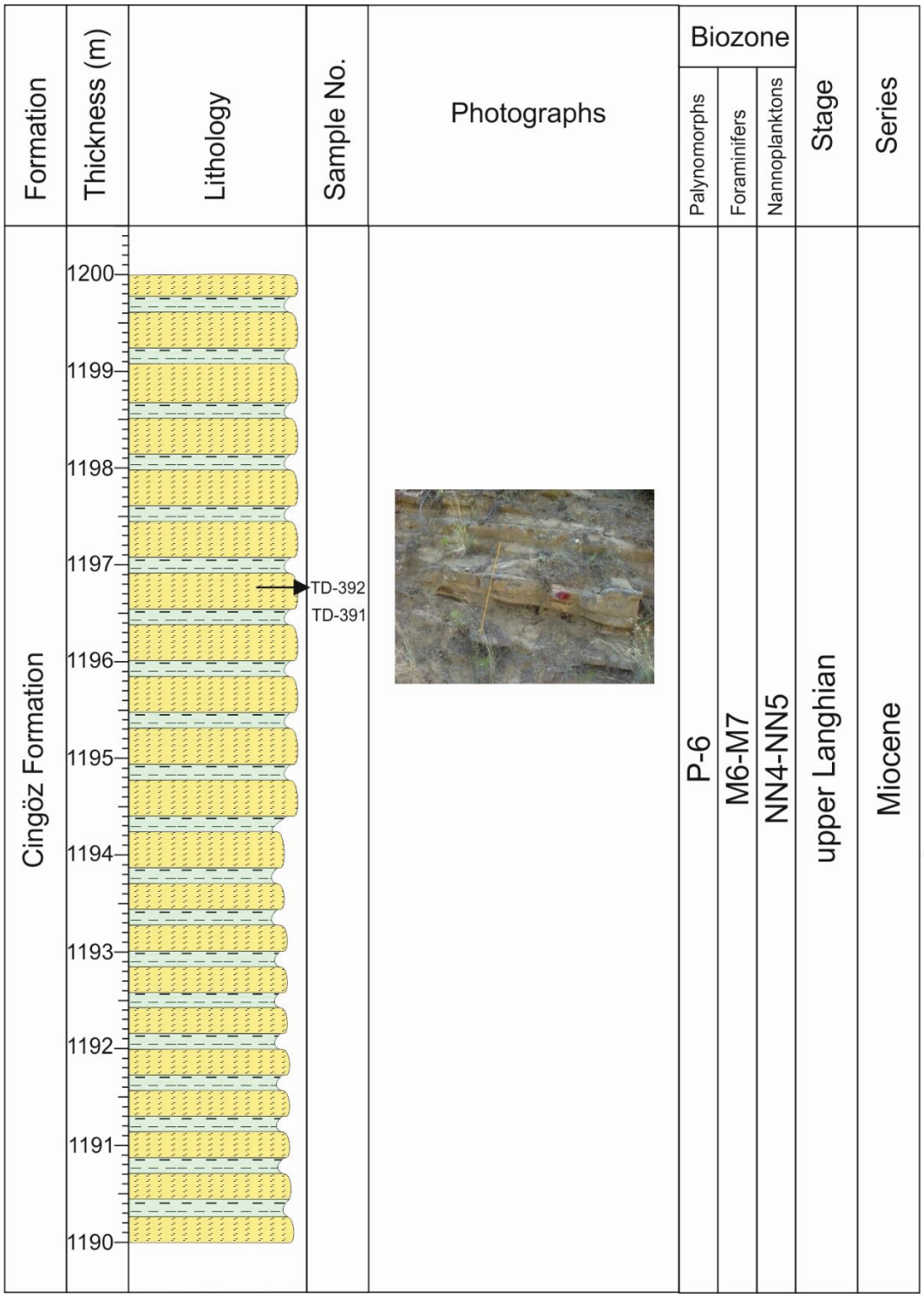

Figure 66. (cont'd)

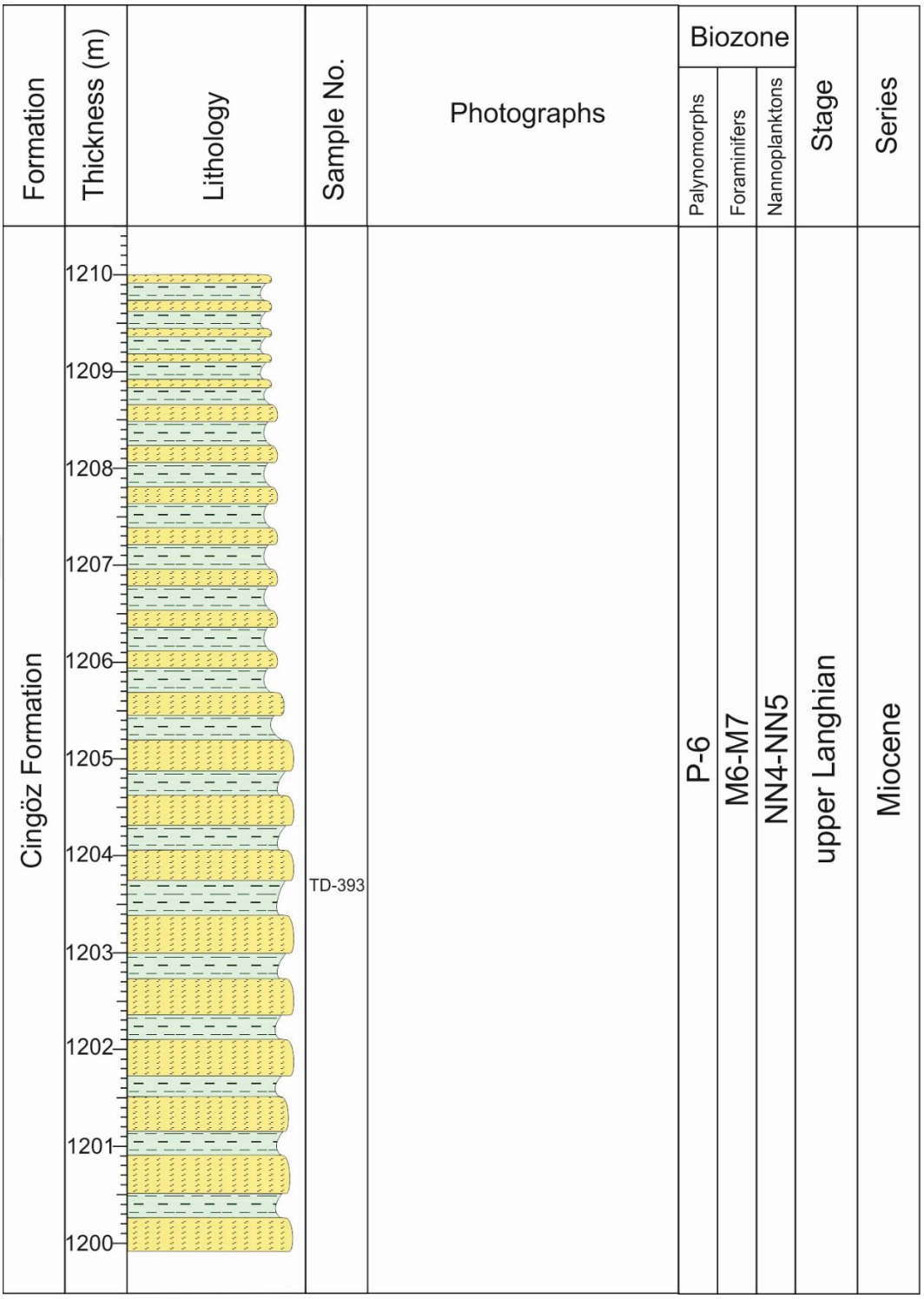

Figure 66. (cont'd)

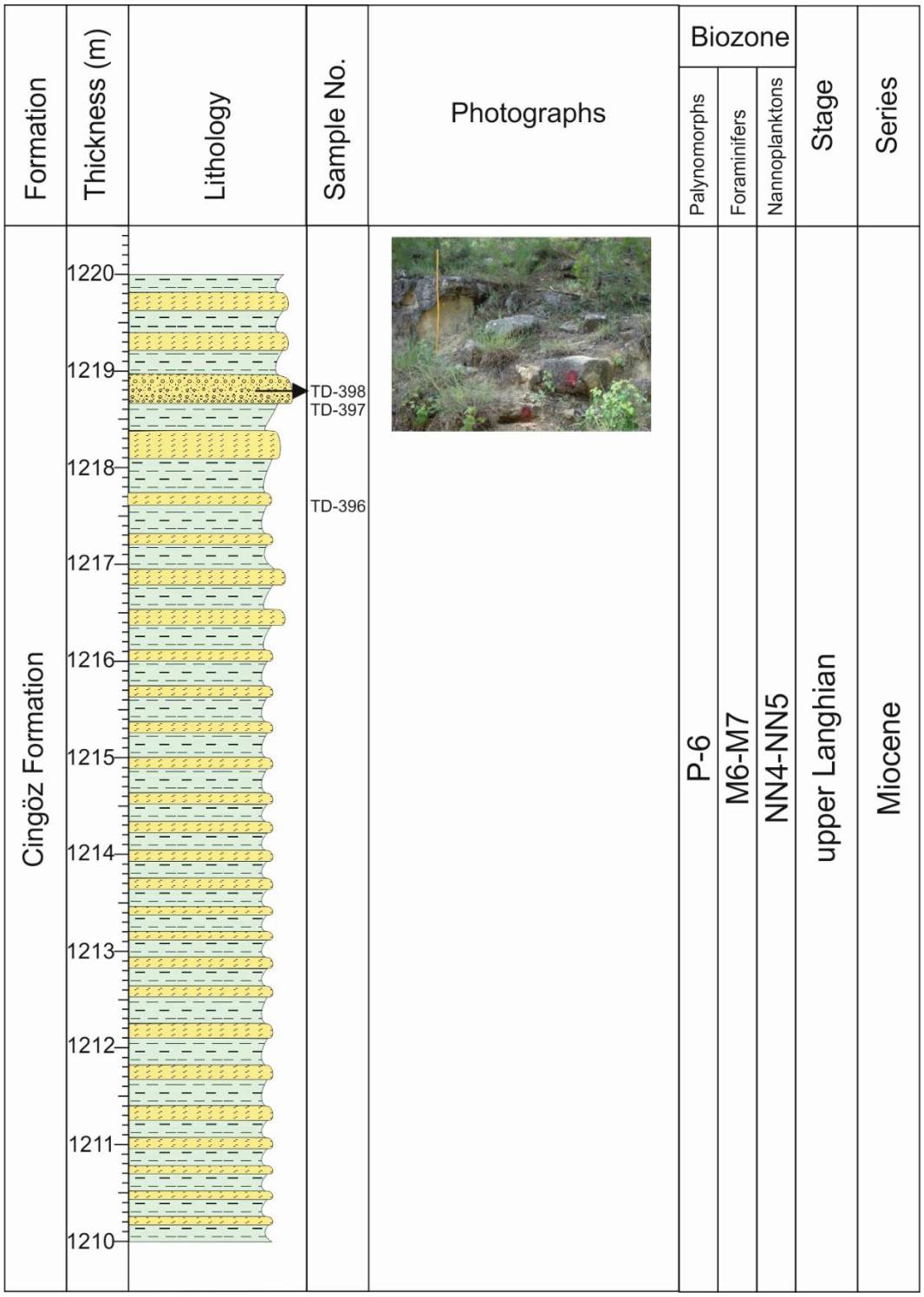

Figure 66. (cont'd)

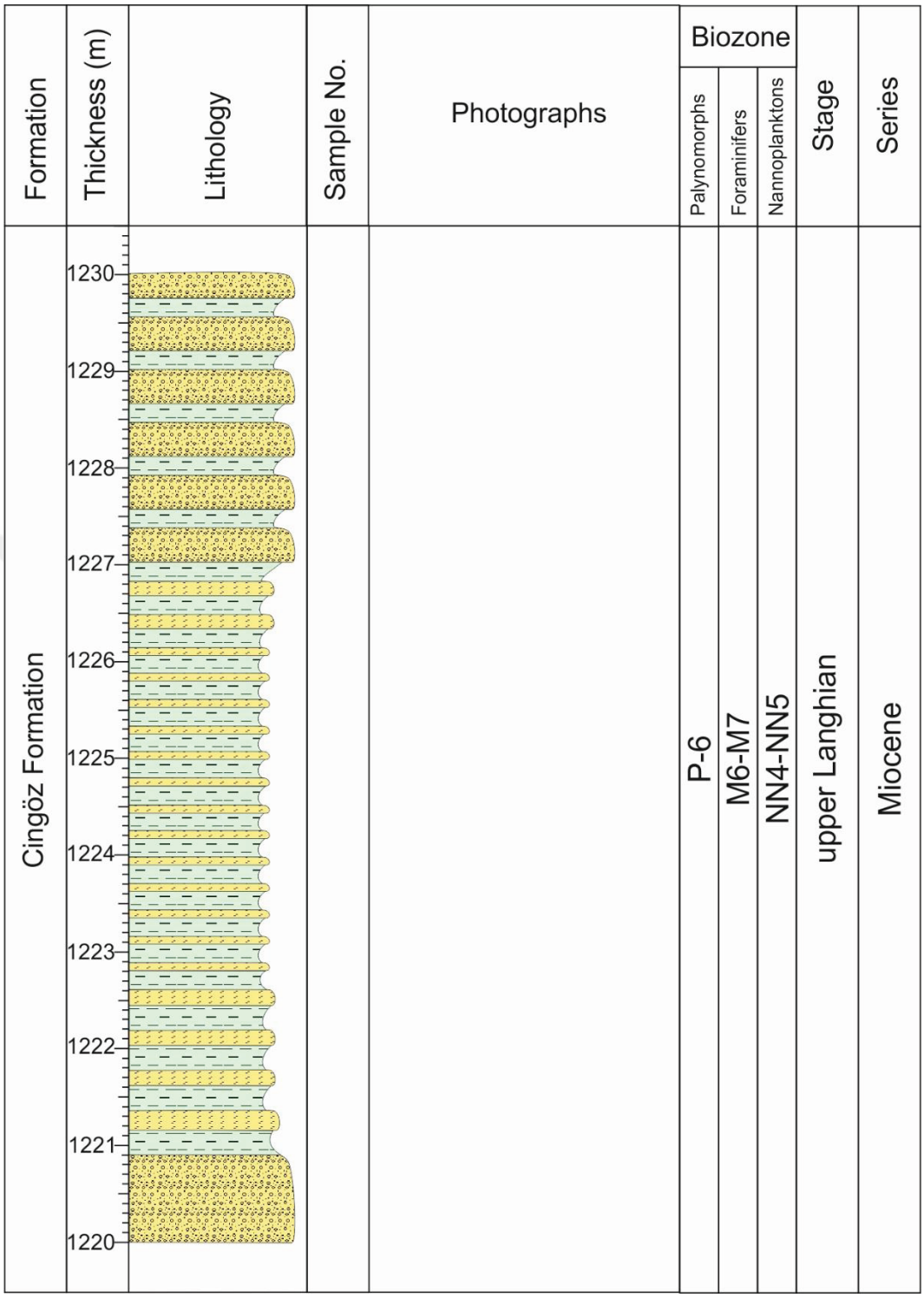

Figure 66. (cont'd)

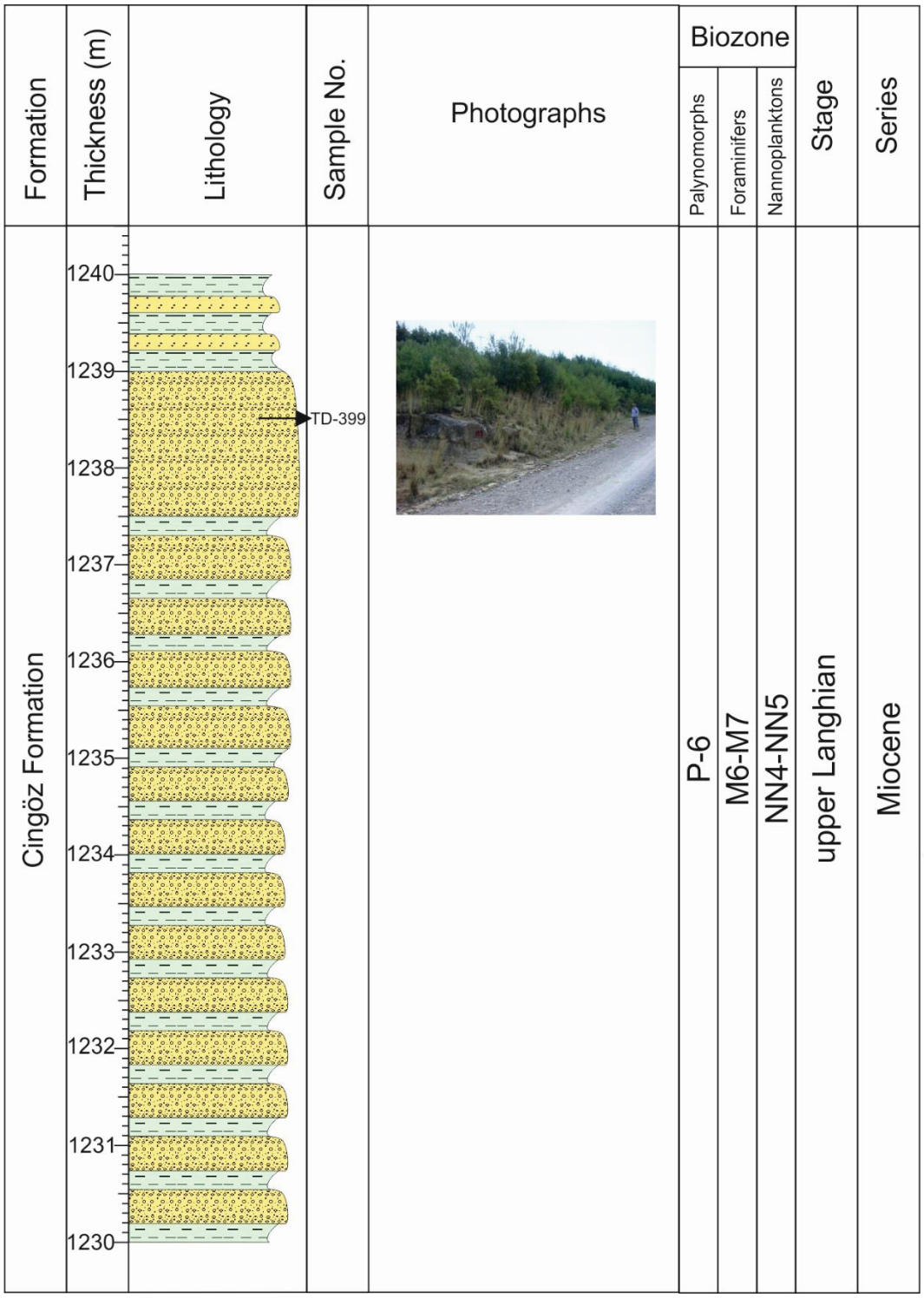

Figure 66. (cont'd)

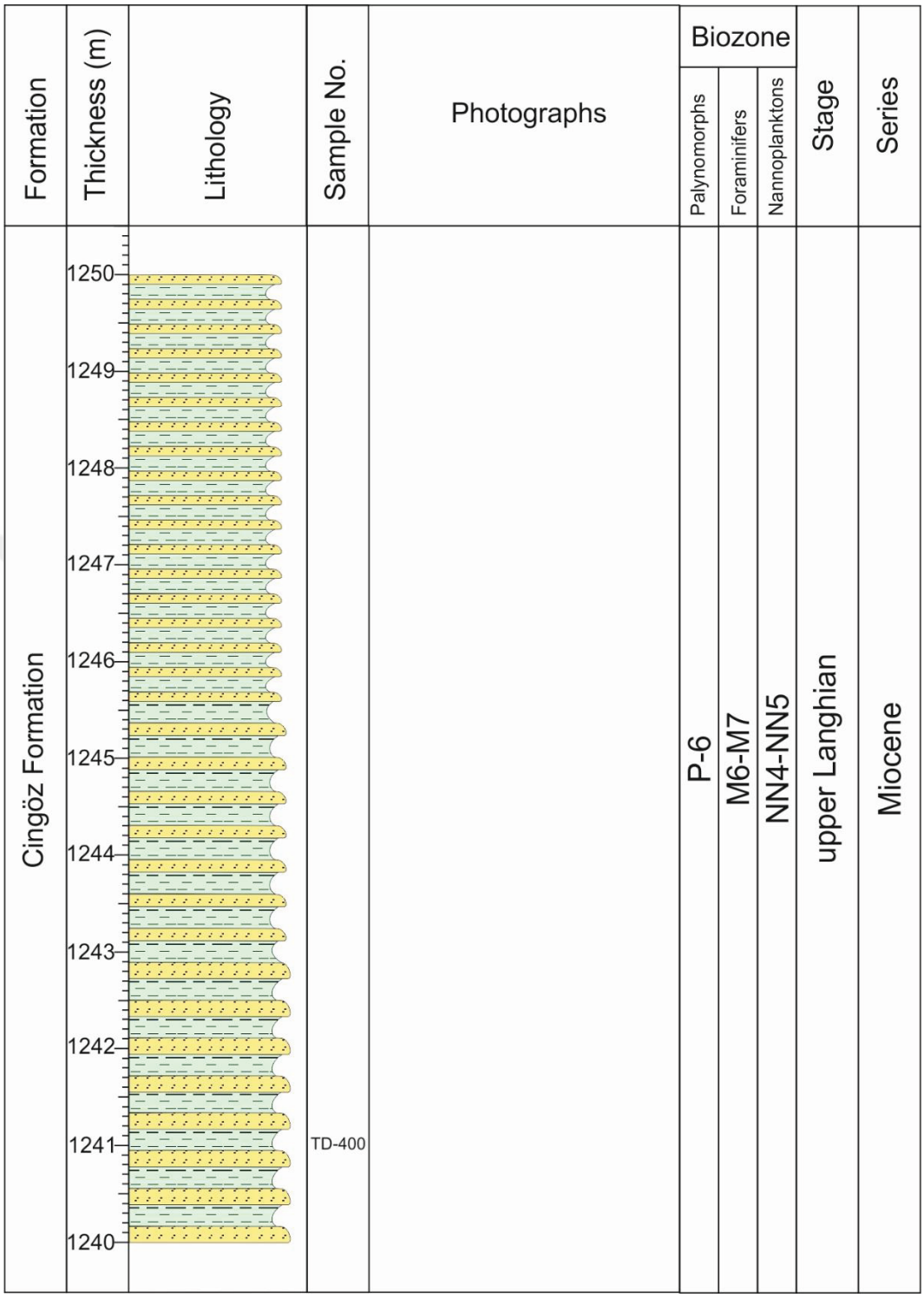

Figure 66. (cont'd)

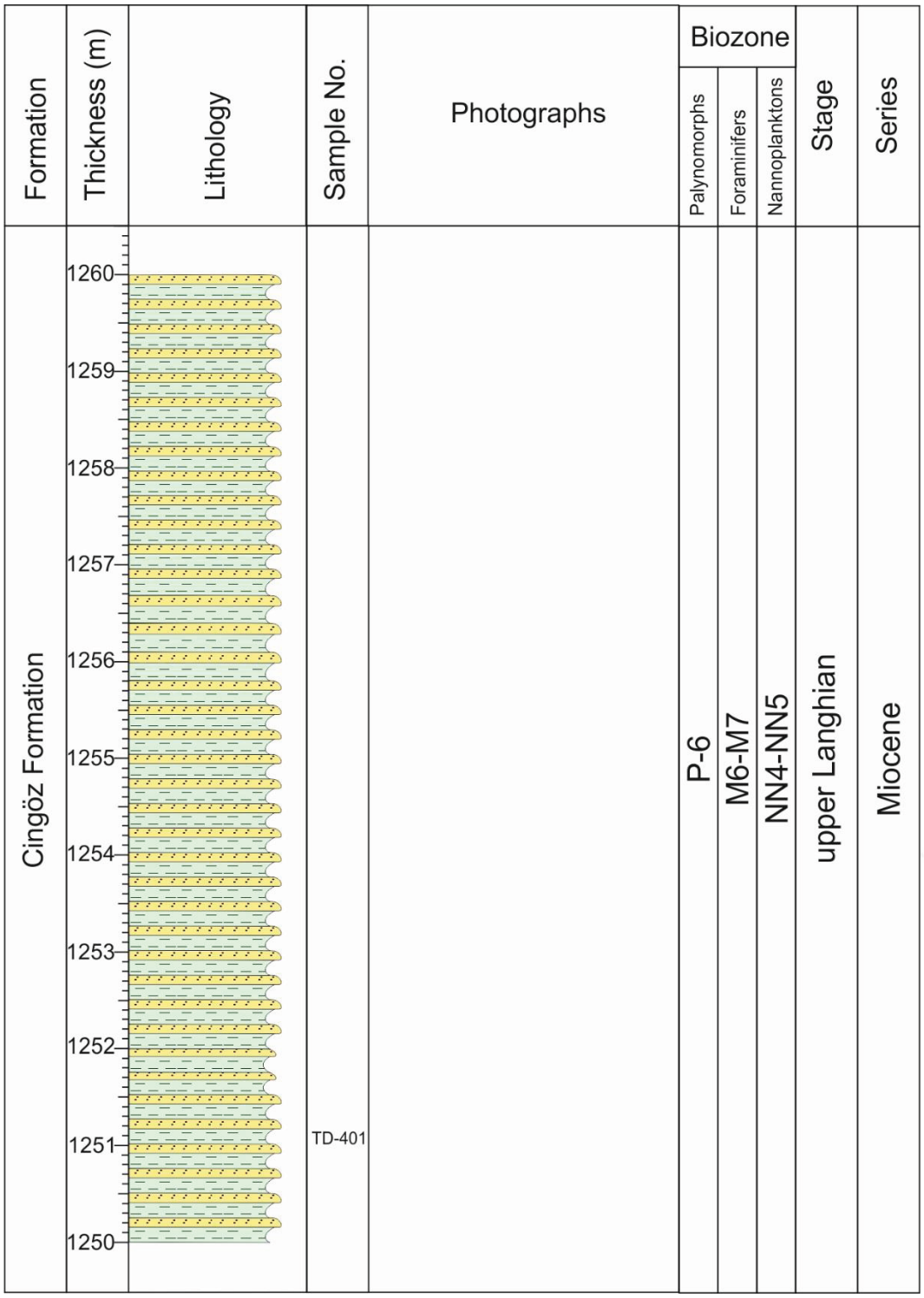

Figure 66. (cont'd)

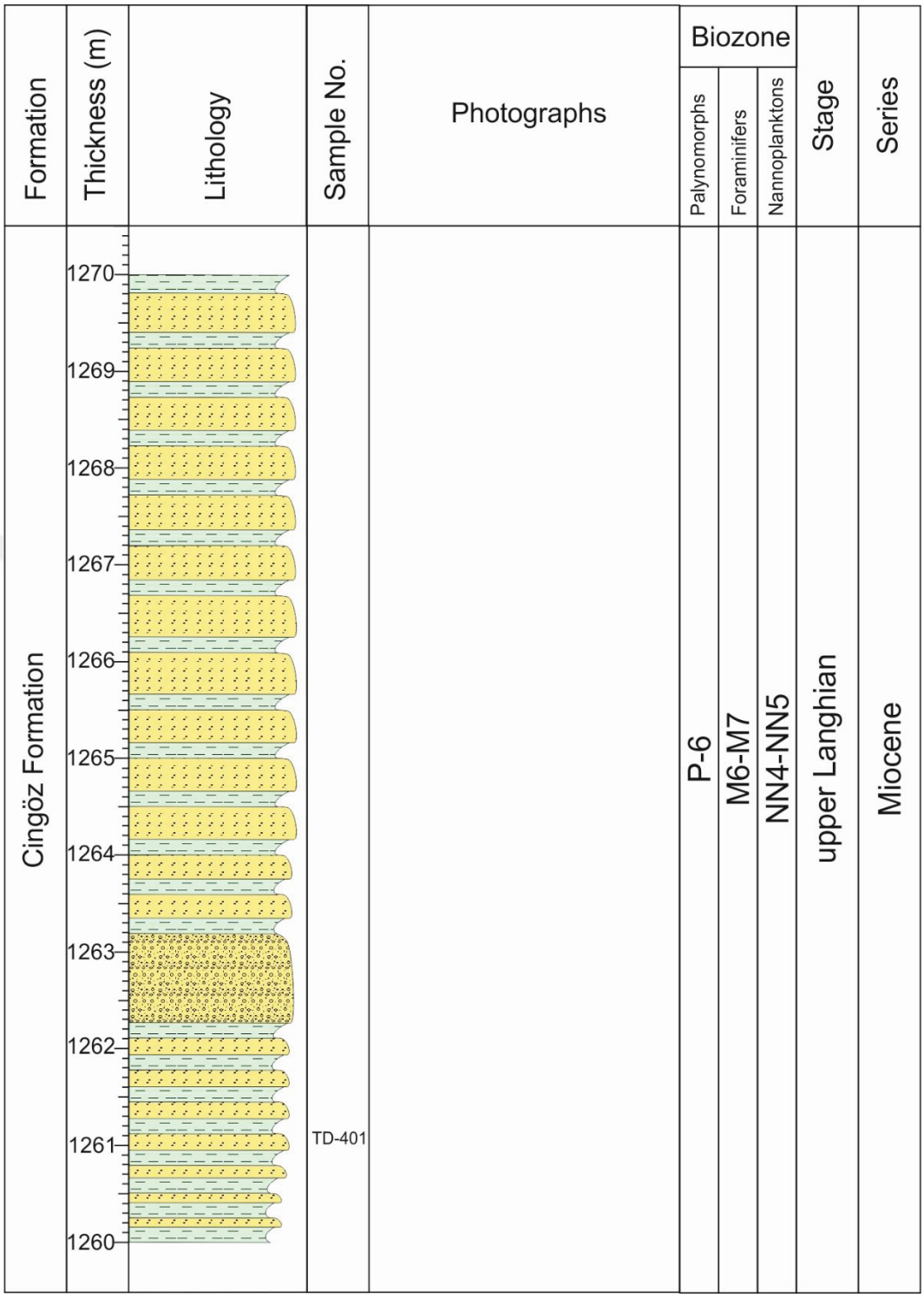

Figure 66. (cont'd)

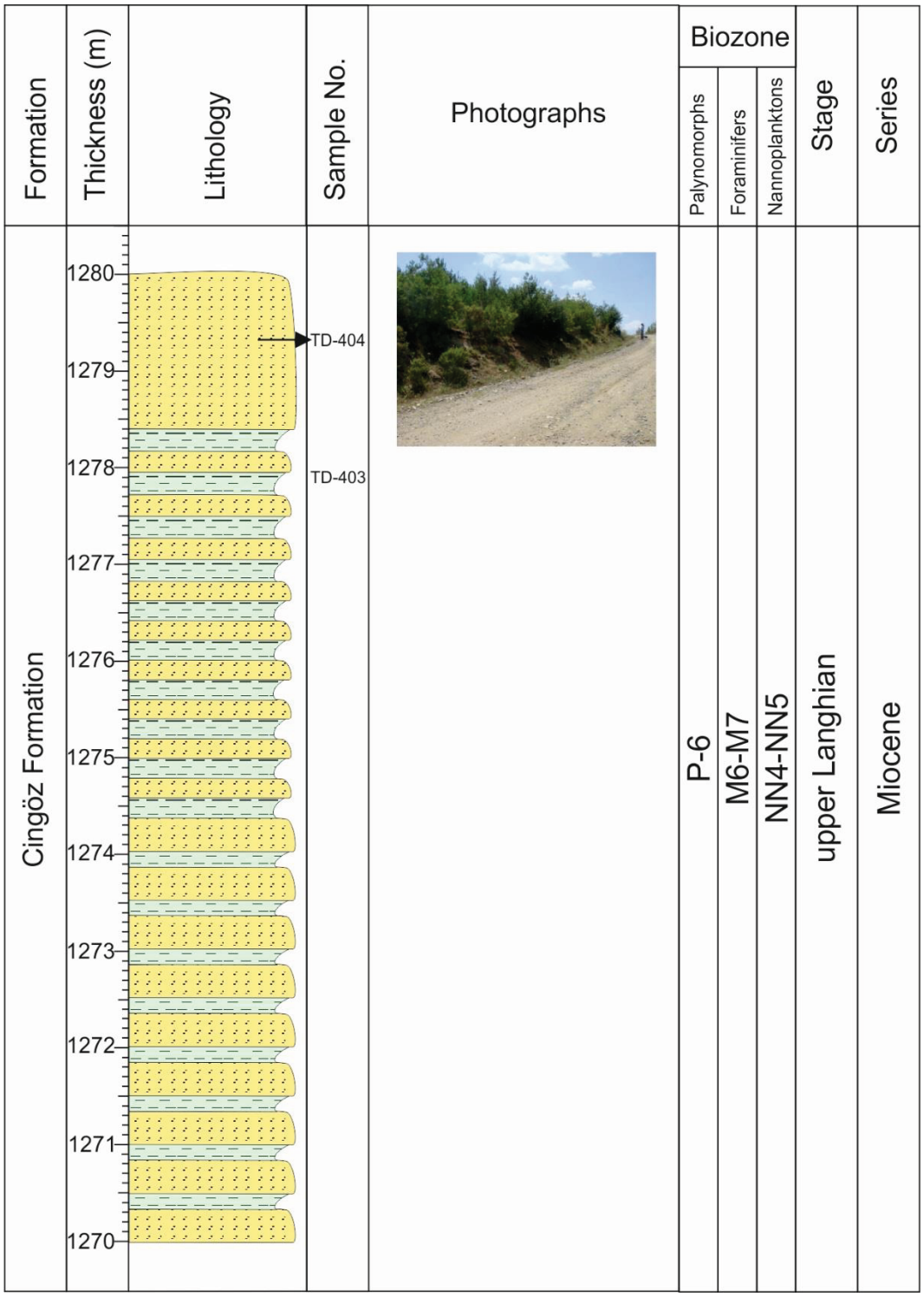

Figure 66. (cont'd)

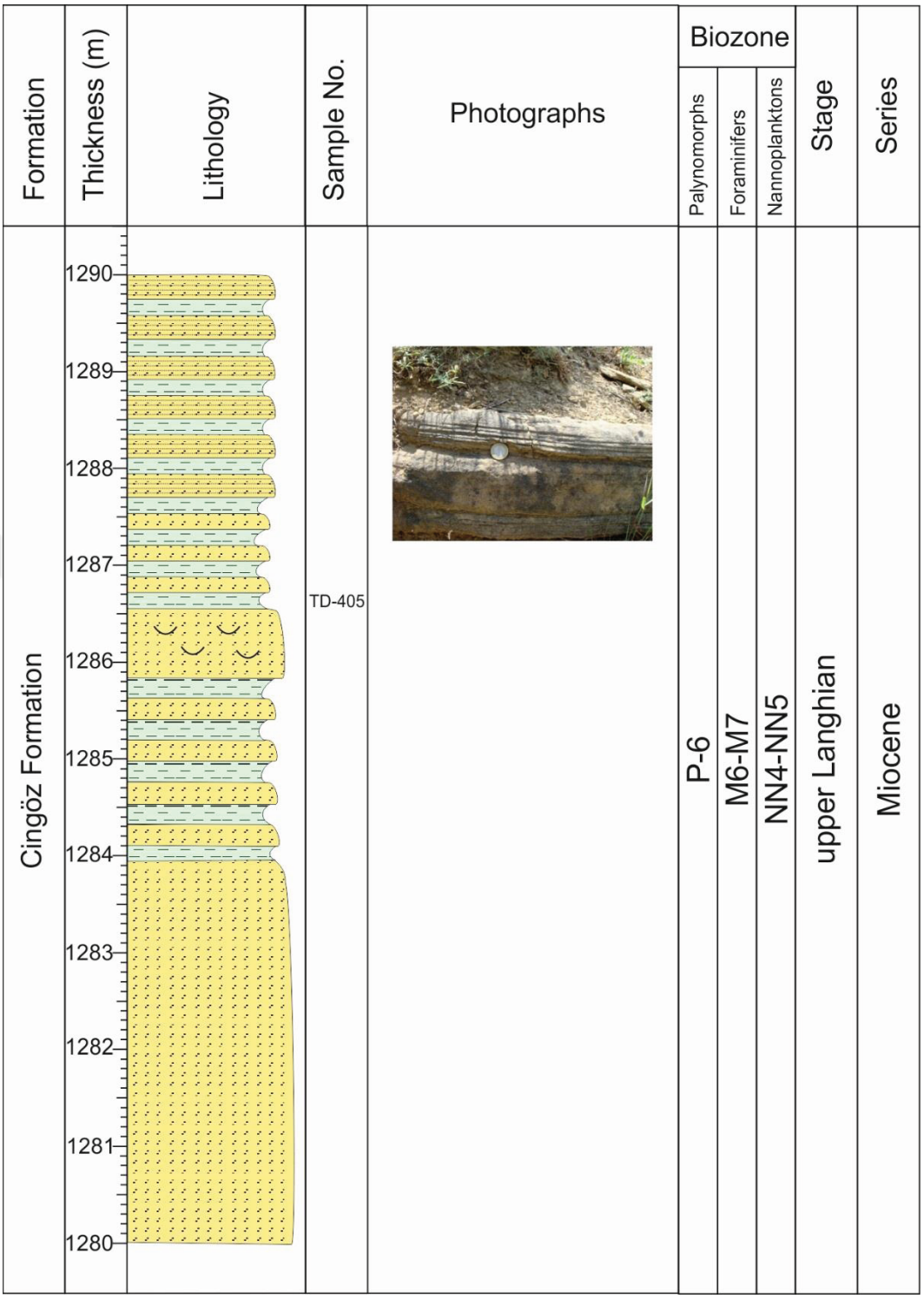

Figure 66. (cont'd)

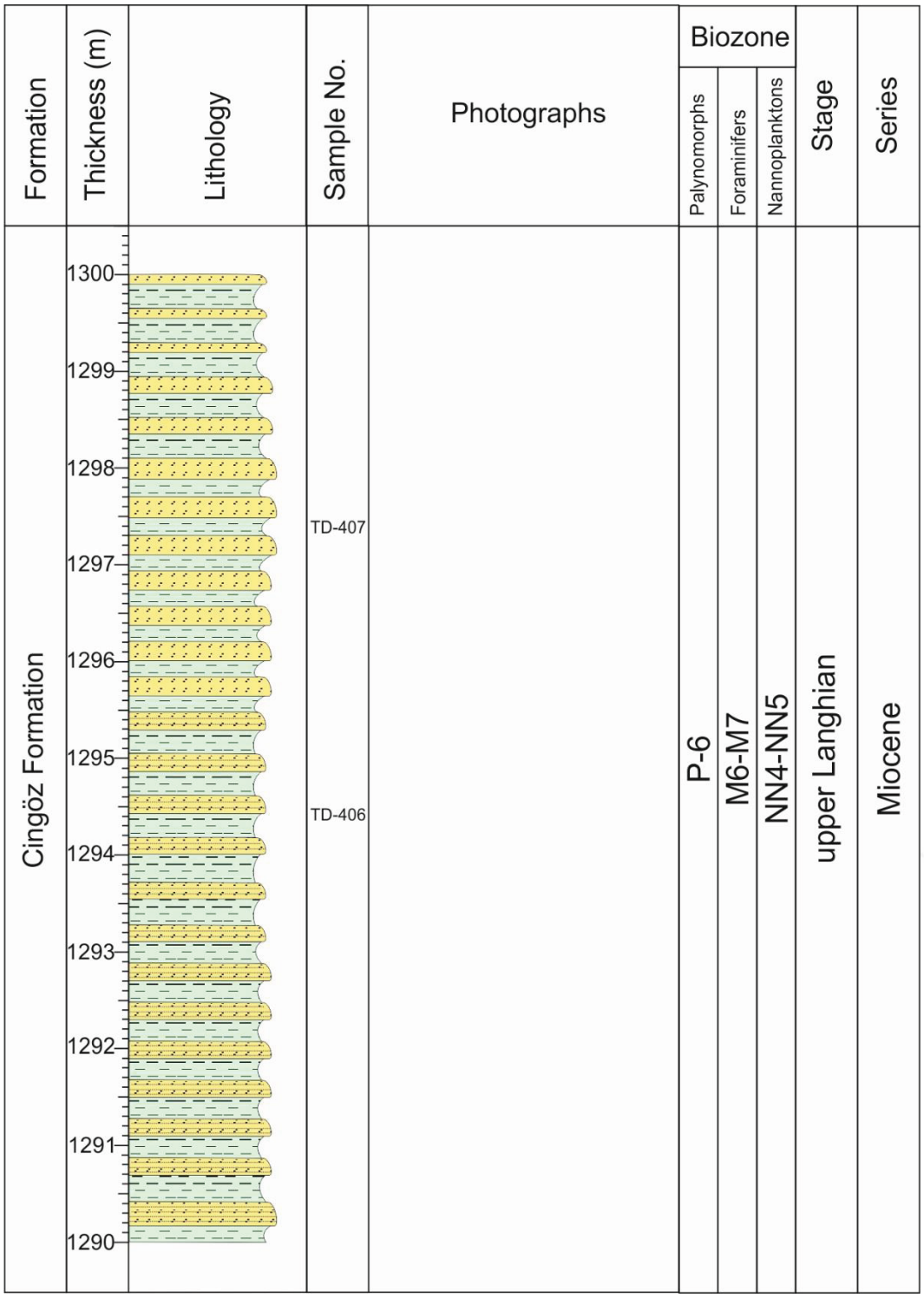

Figure 66. (cont'd)

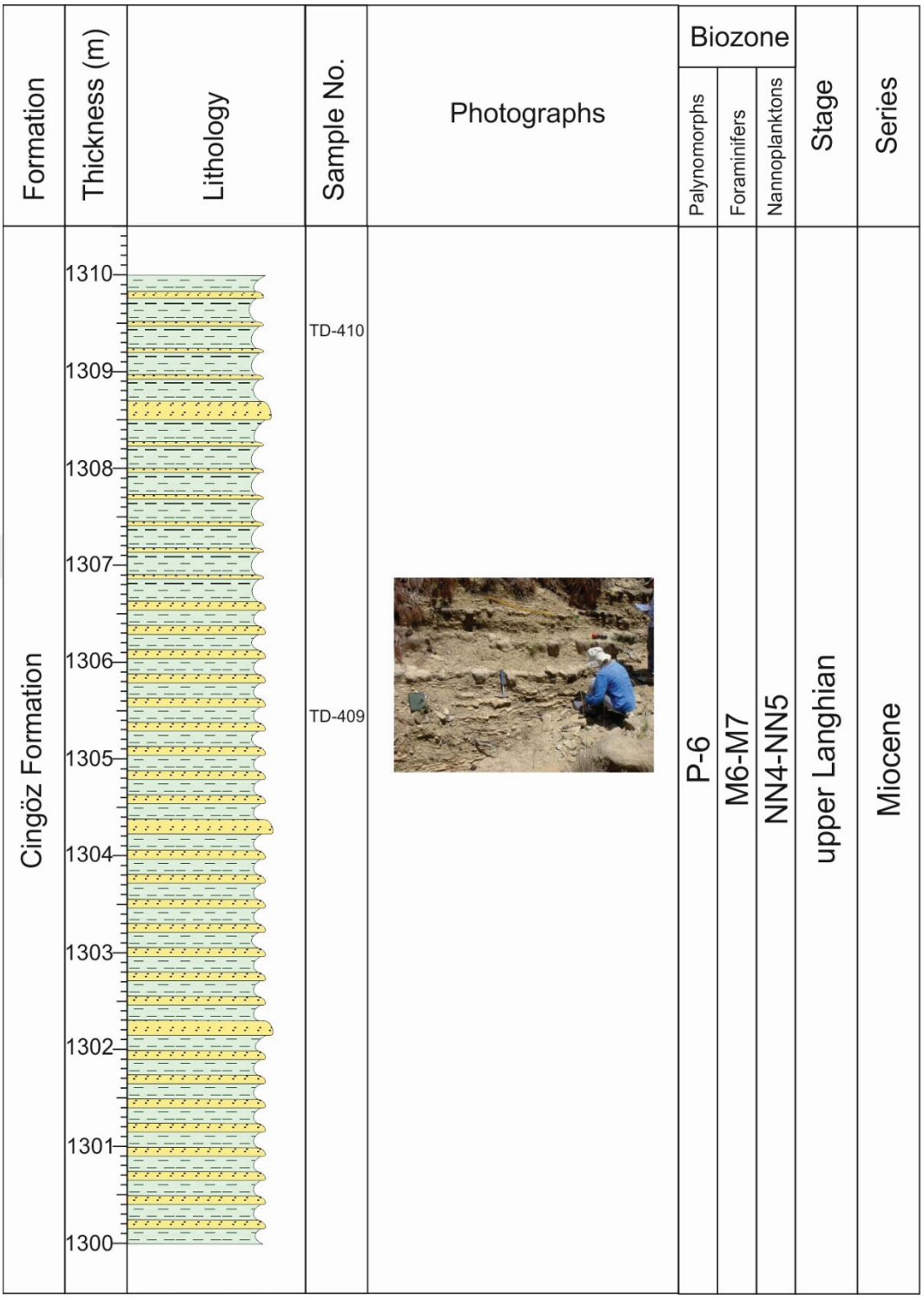

Figure 66. (cont'd)

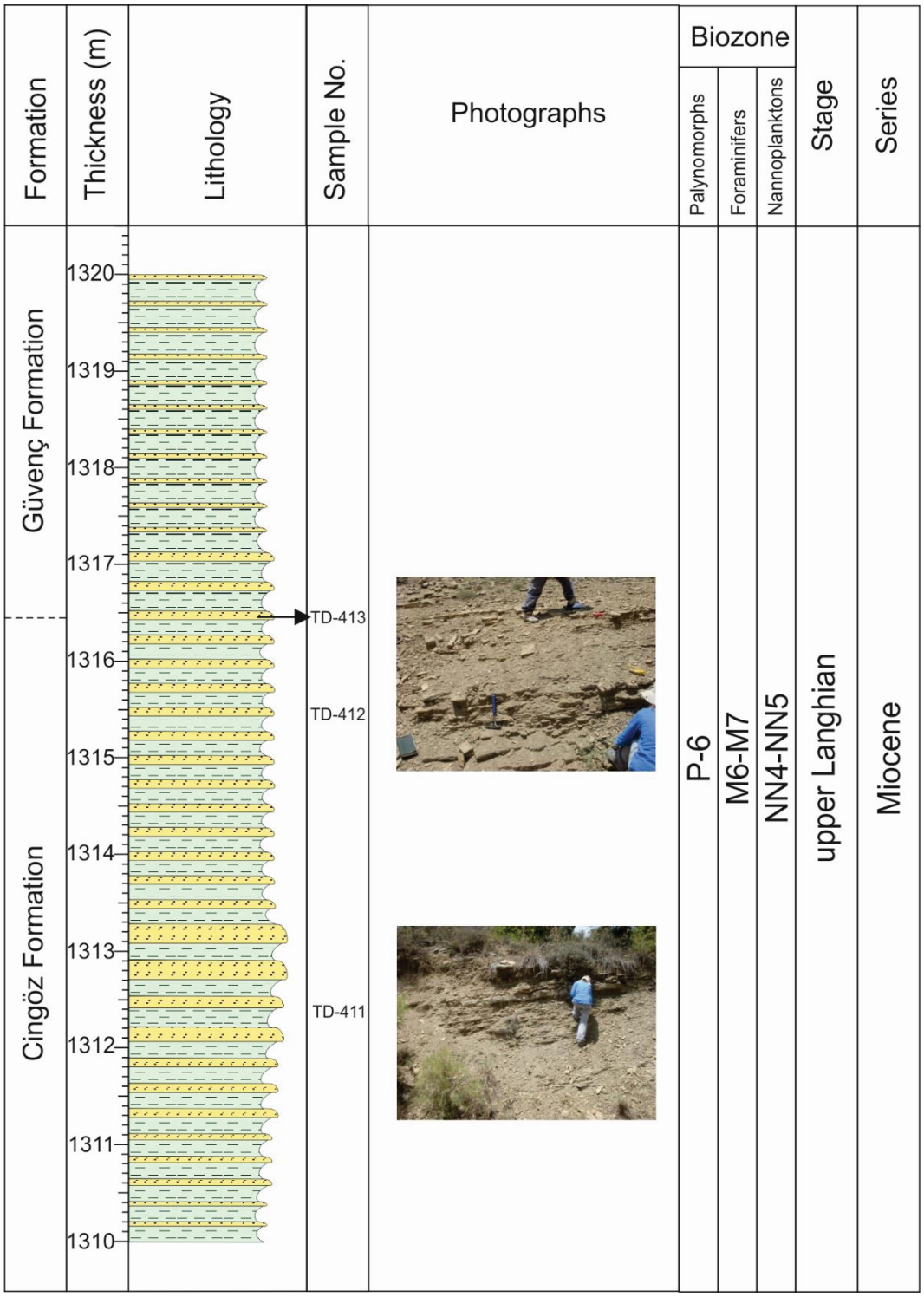

Figure 66. (cont'd)

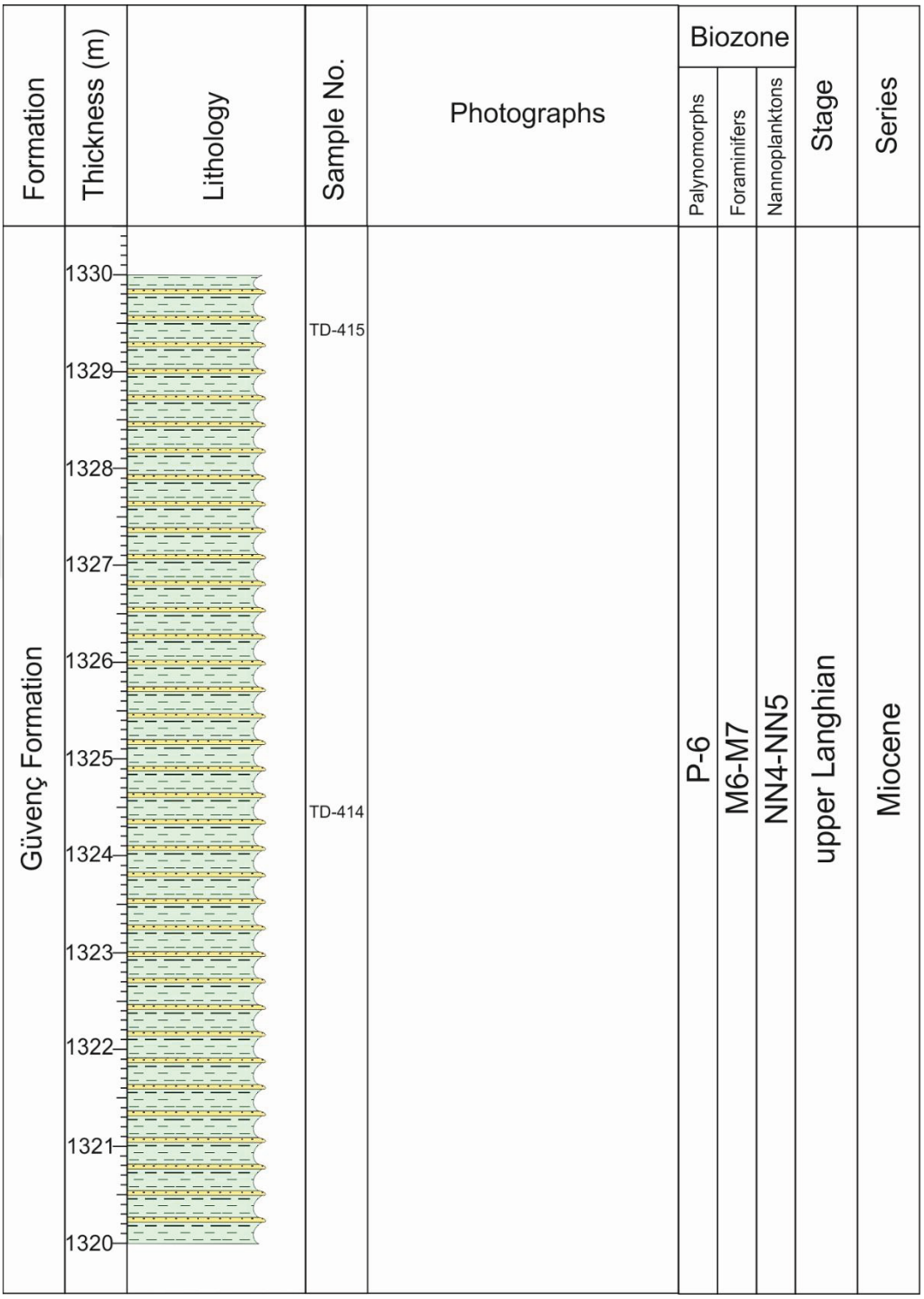

Figure 66. (cont'd)

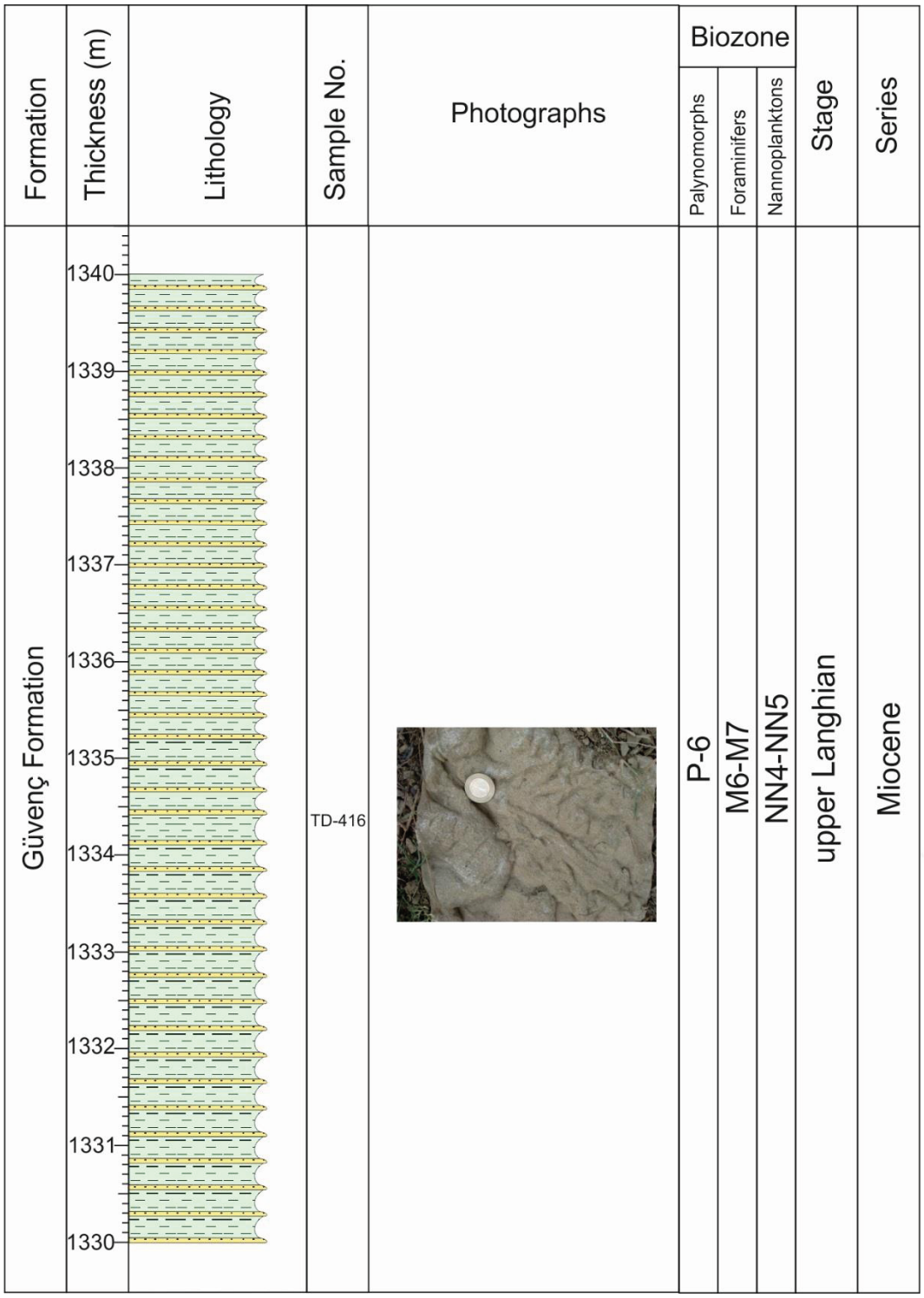

Figure 66. (cont'd)

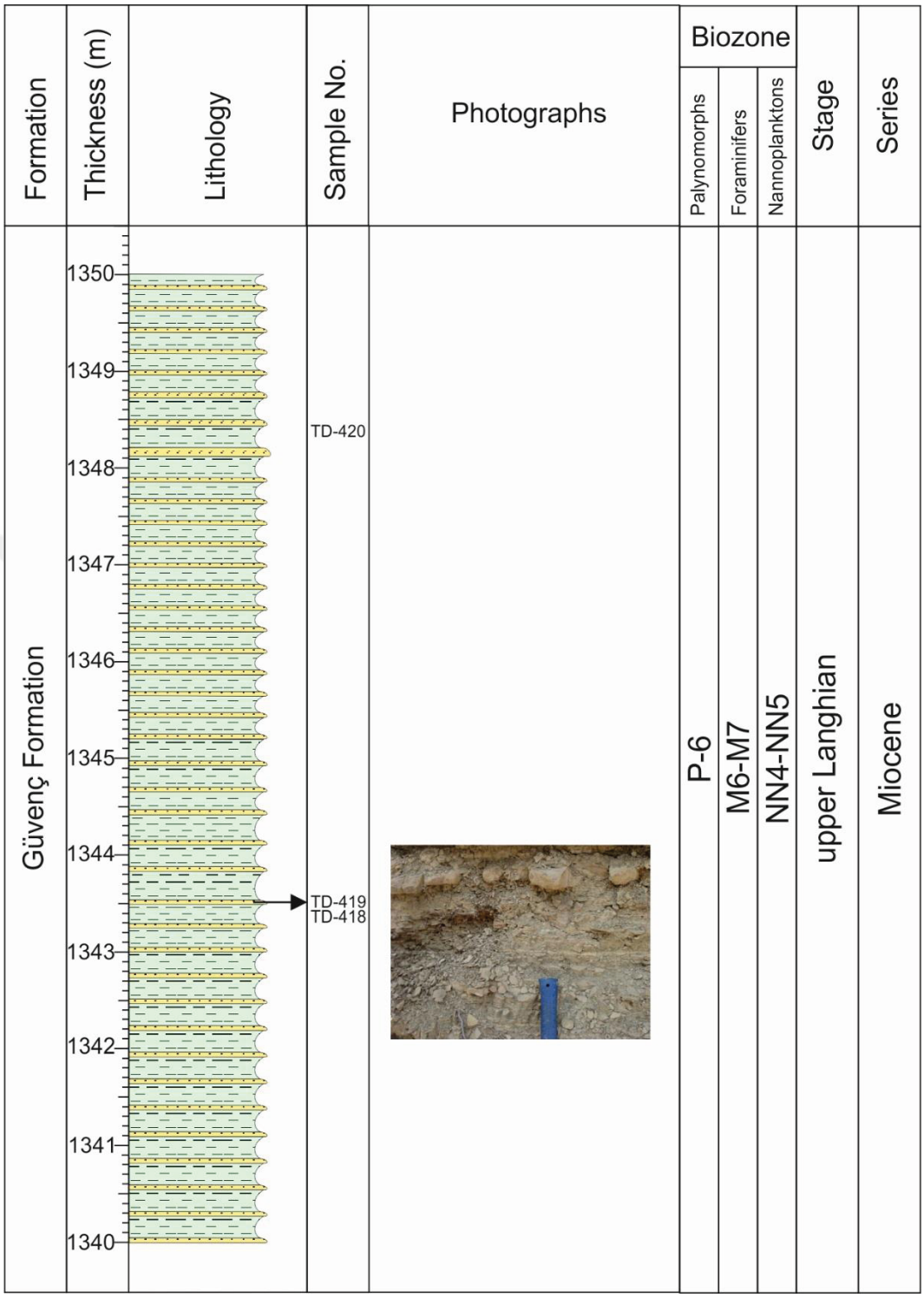

Figure 66. (cont'd)

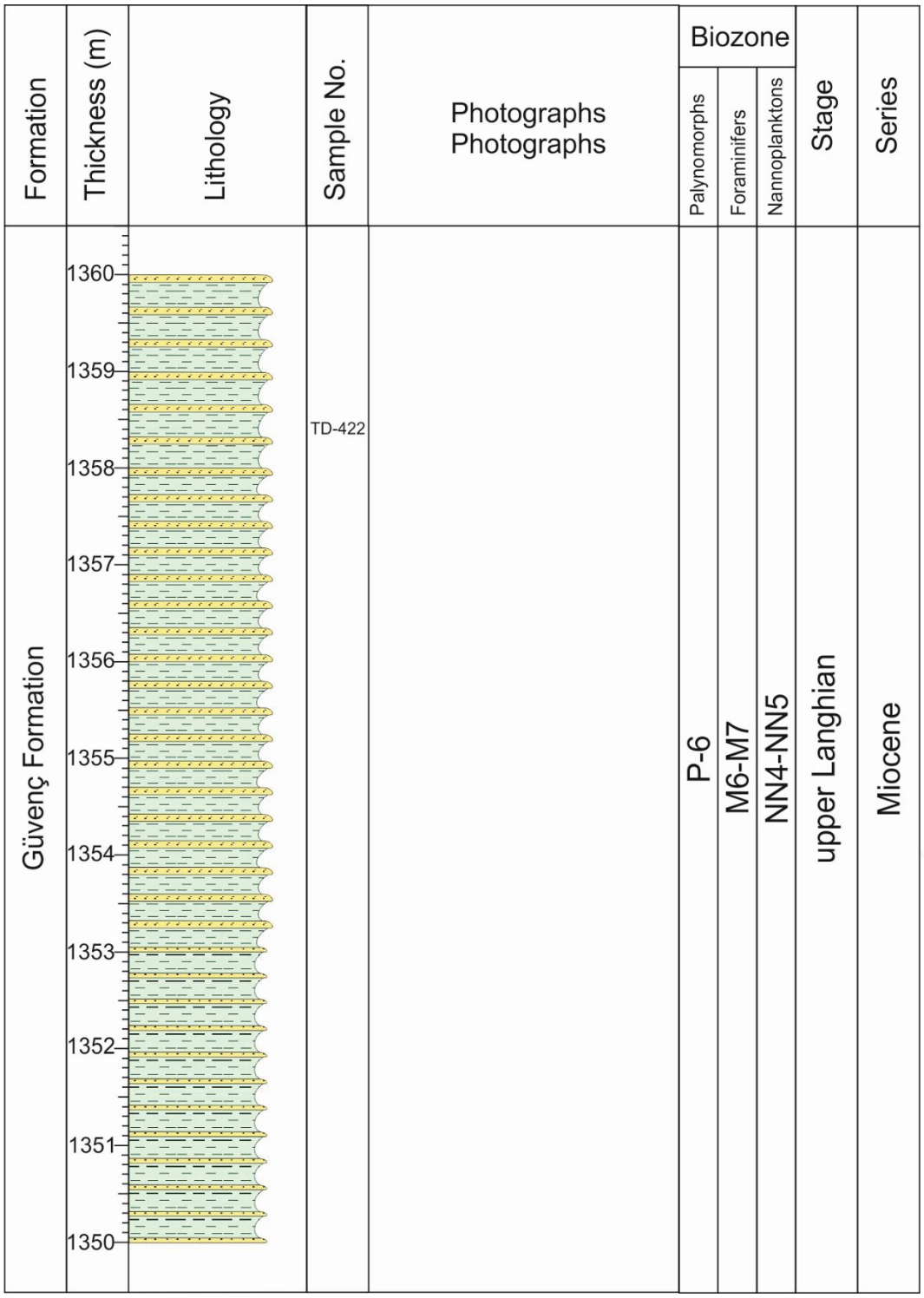

Figure 66. (cont'd)

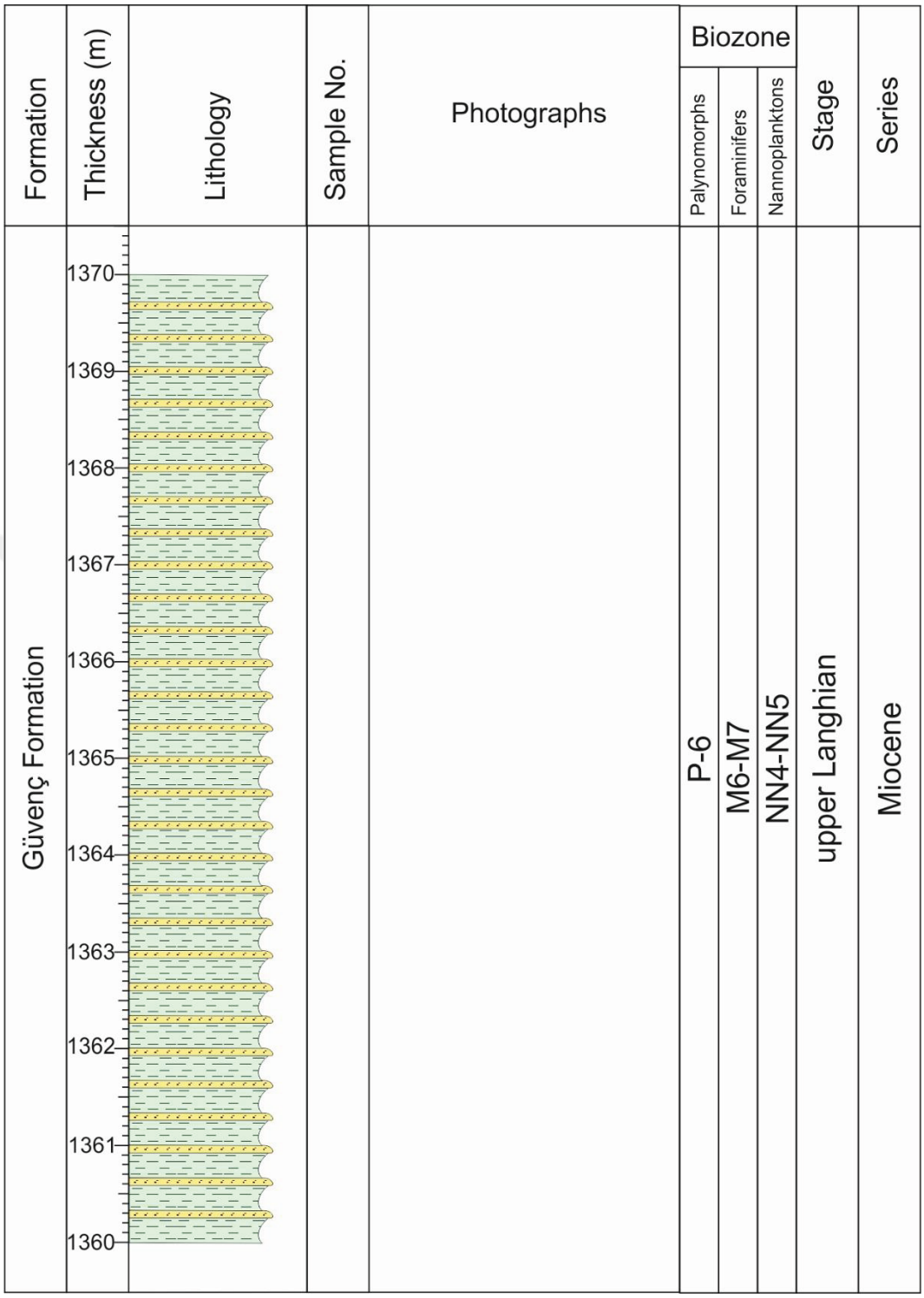

Figure 66. (cont'd)

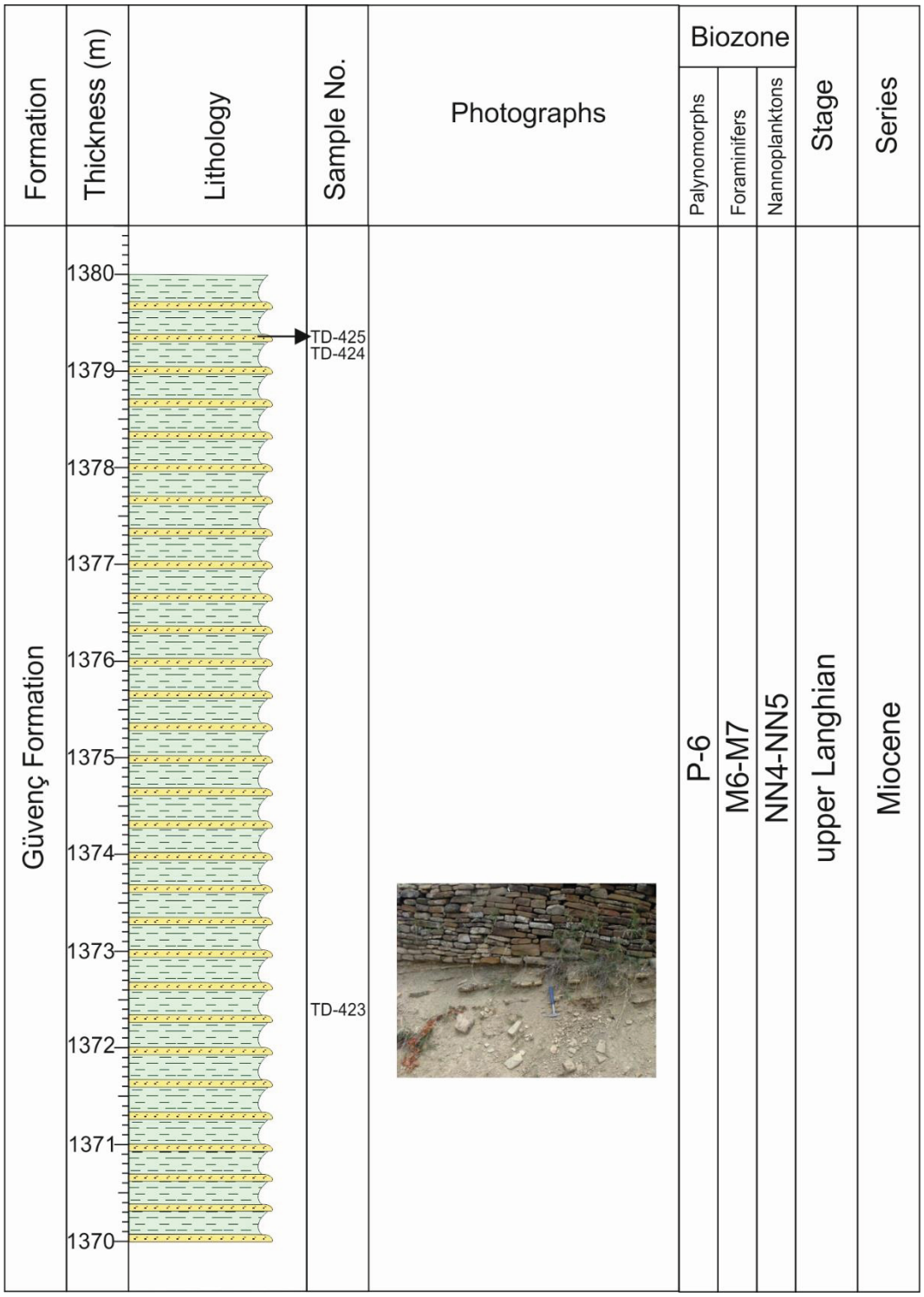

Figure 66. (cont'd)

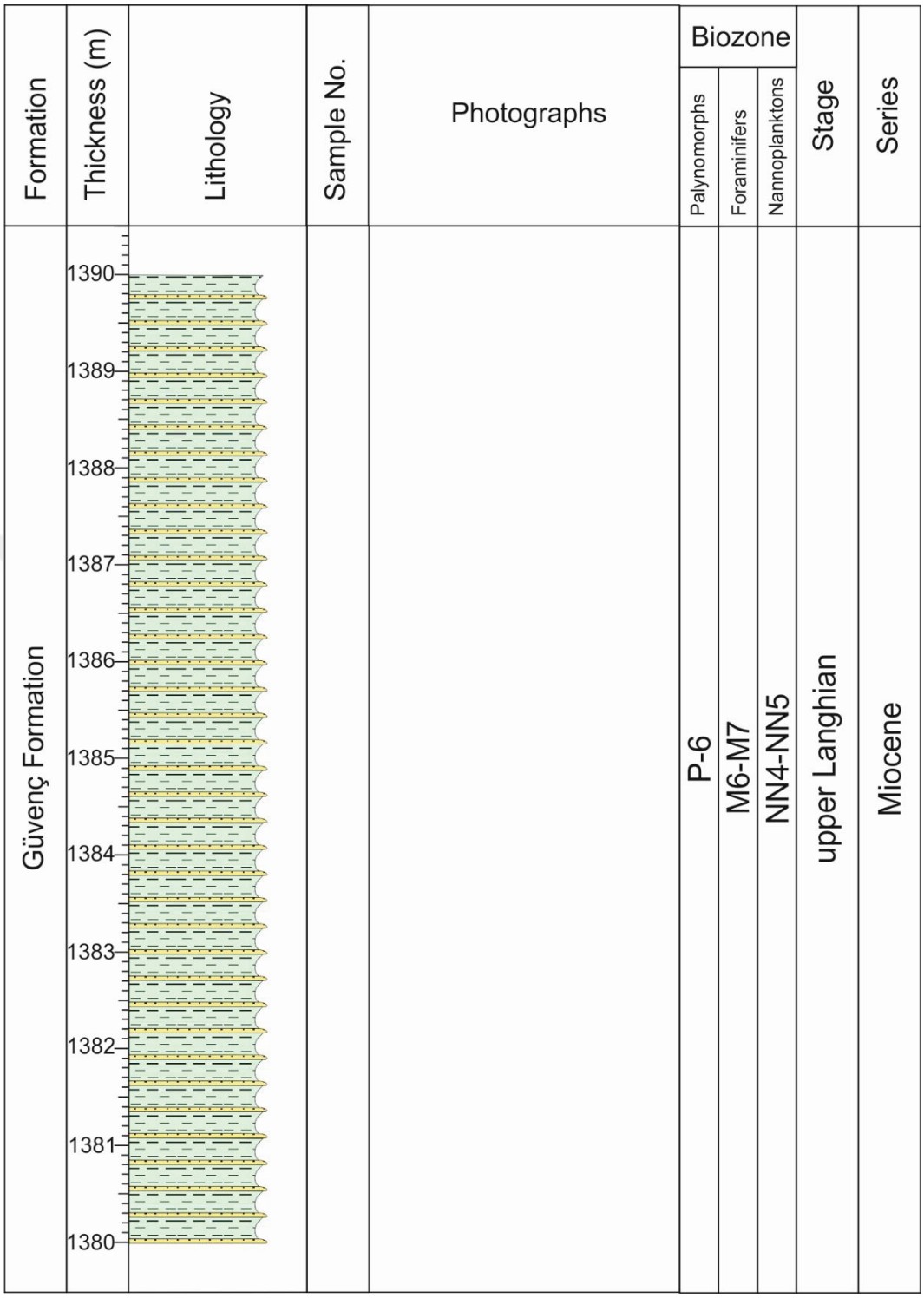

Figure 66. (cont'd)

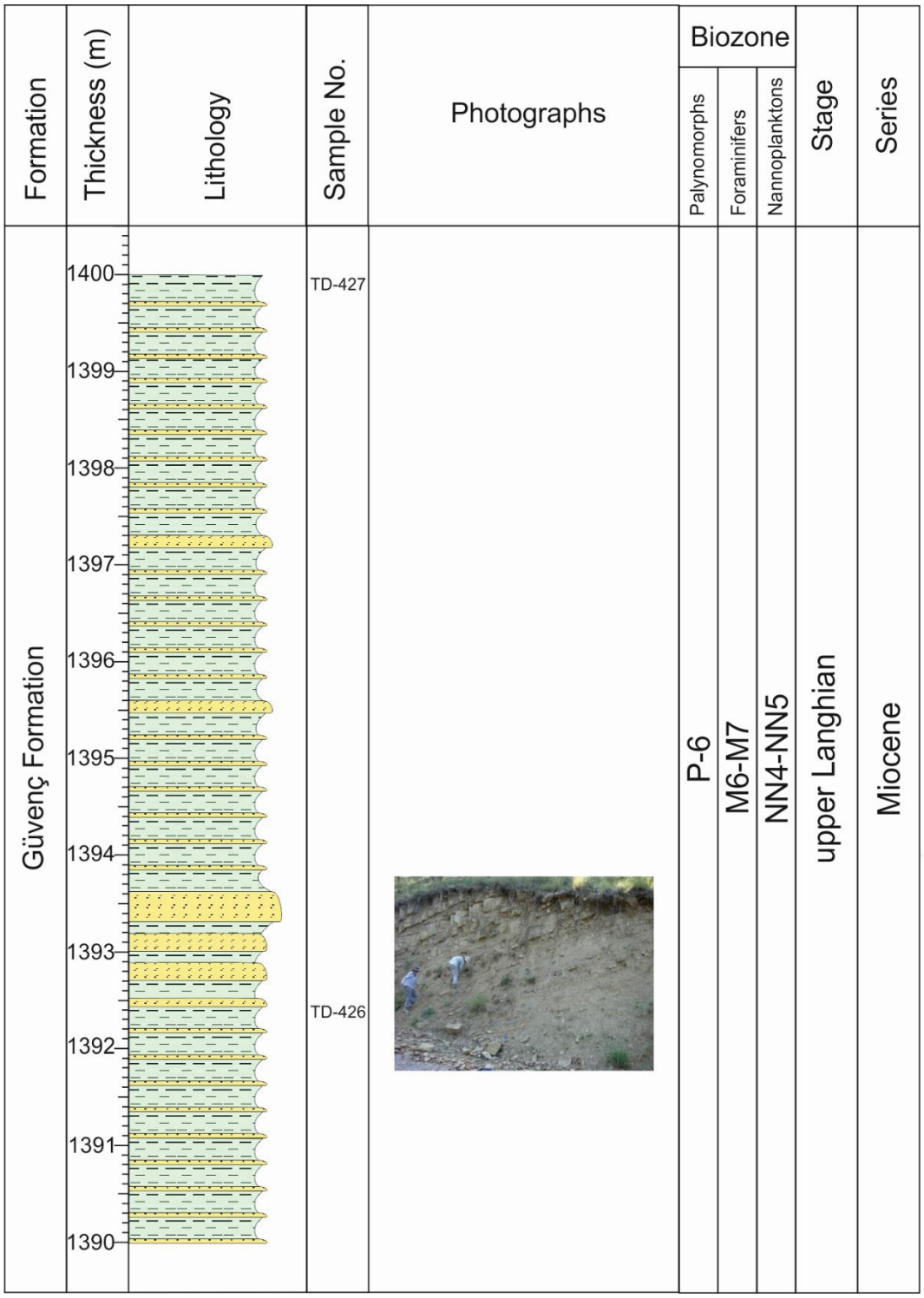

Figure 66. (cont'd)

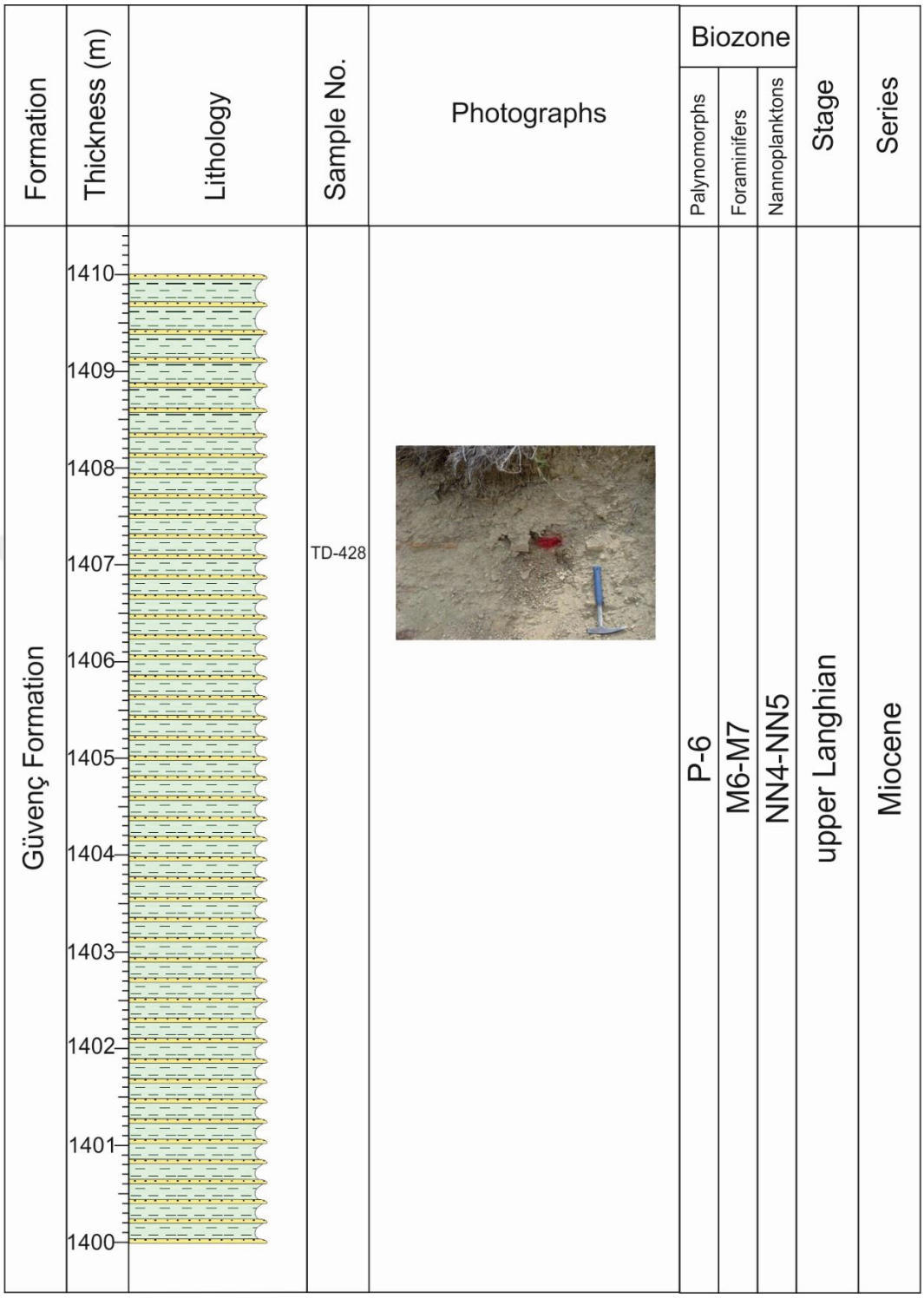

Figure 66. (cont'd)

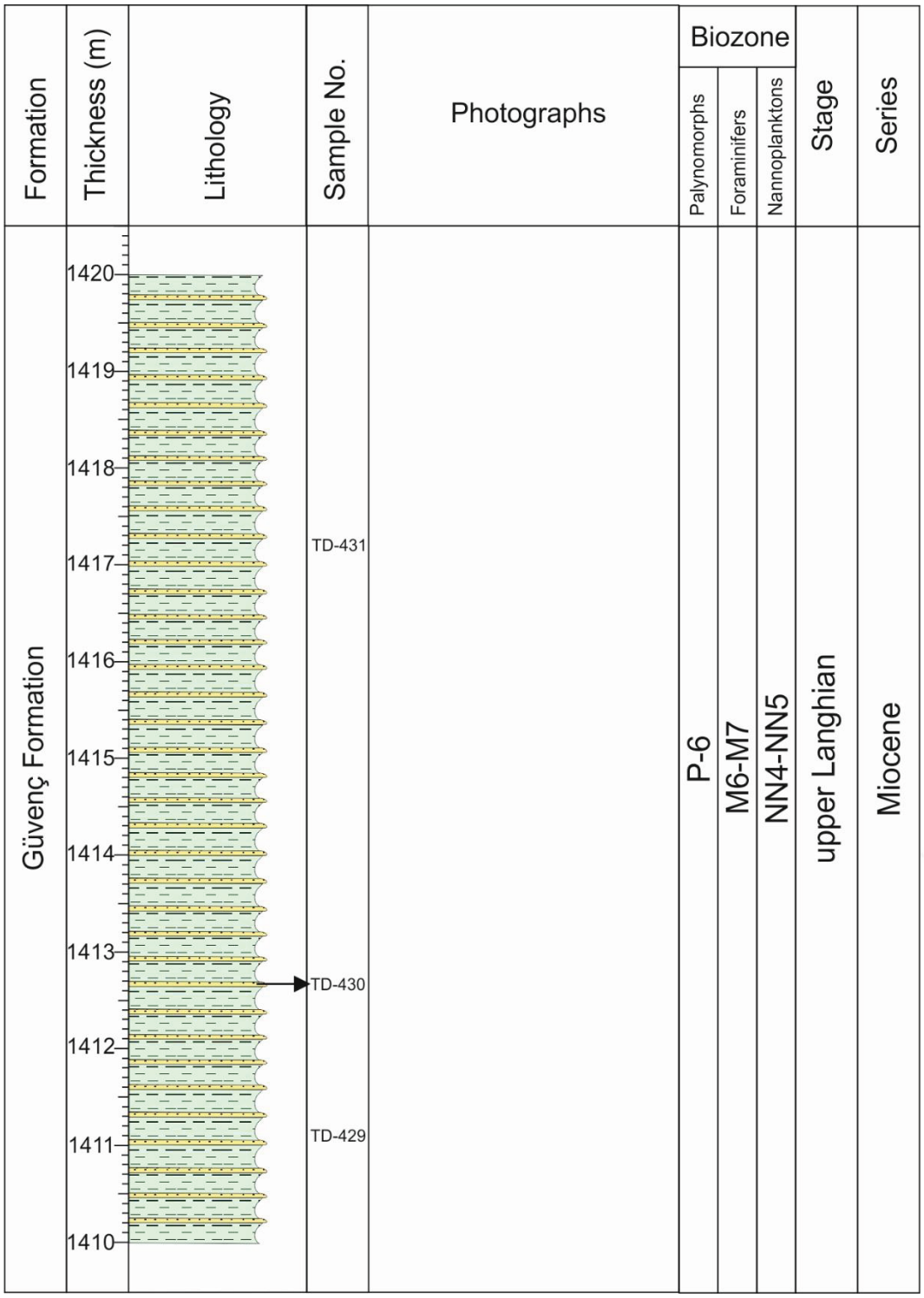

Figure 66. (cont'd)

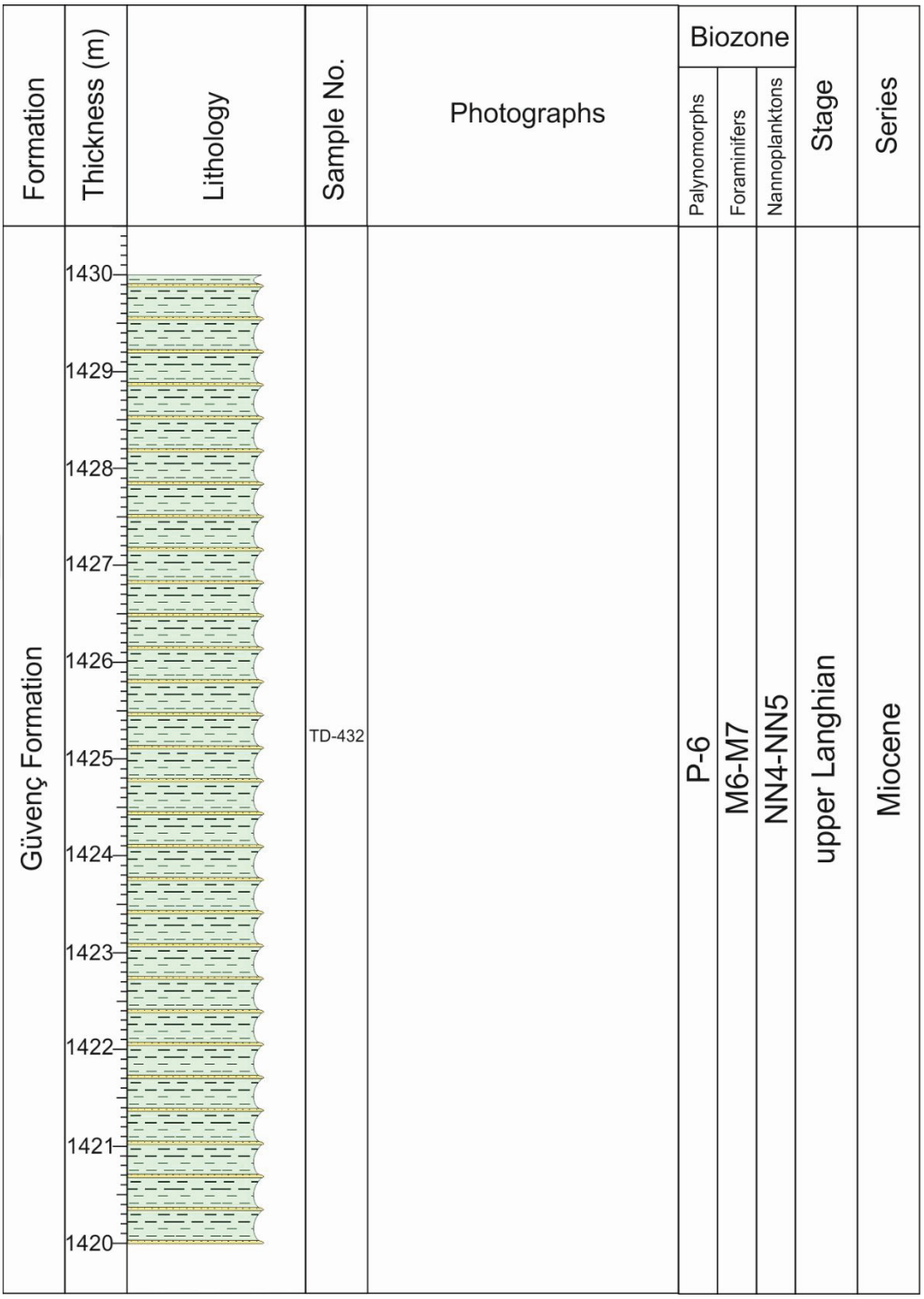

Figure 66. (cont'd)

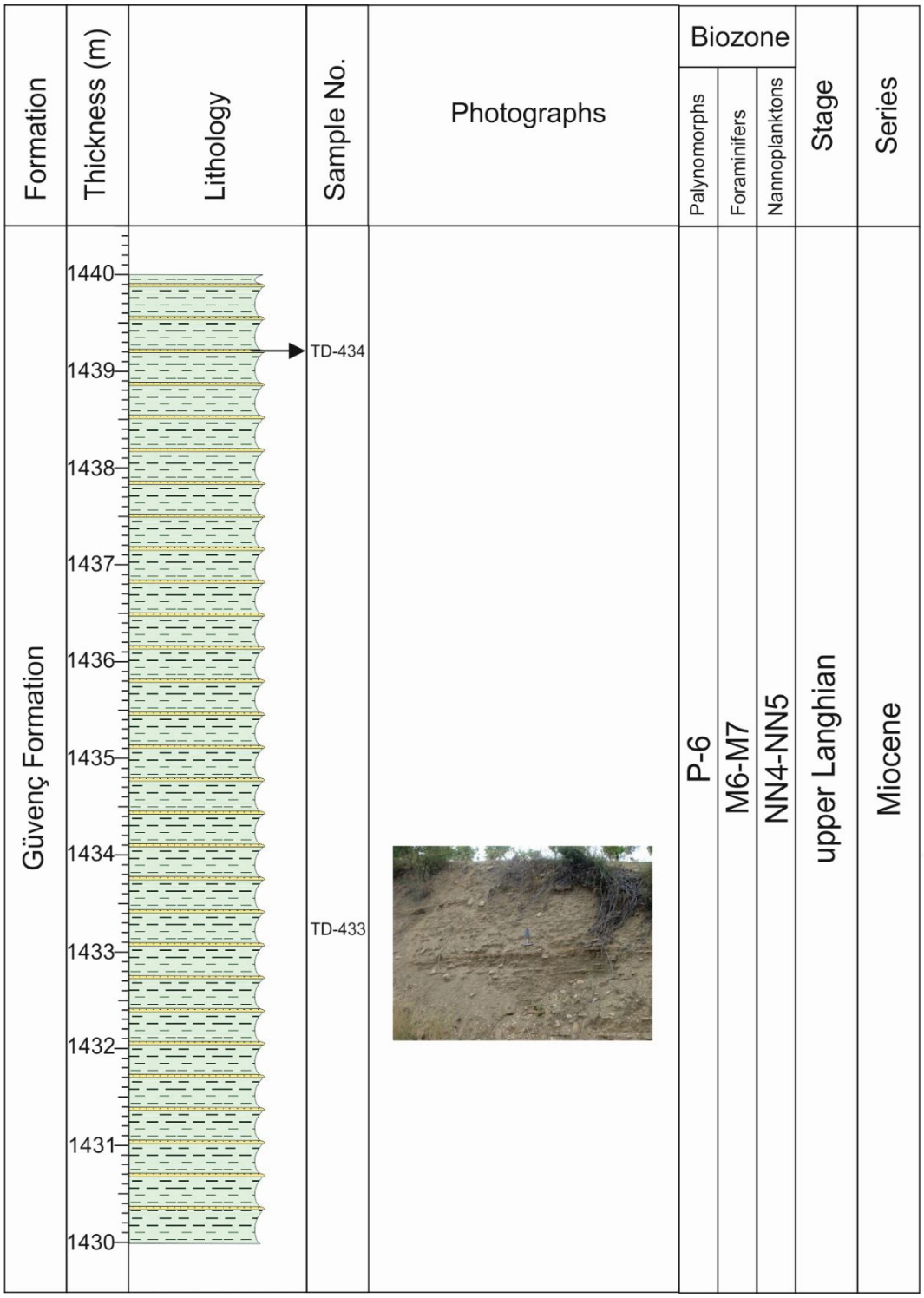

Figure 66. (cont'd)

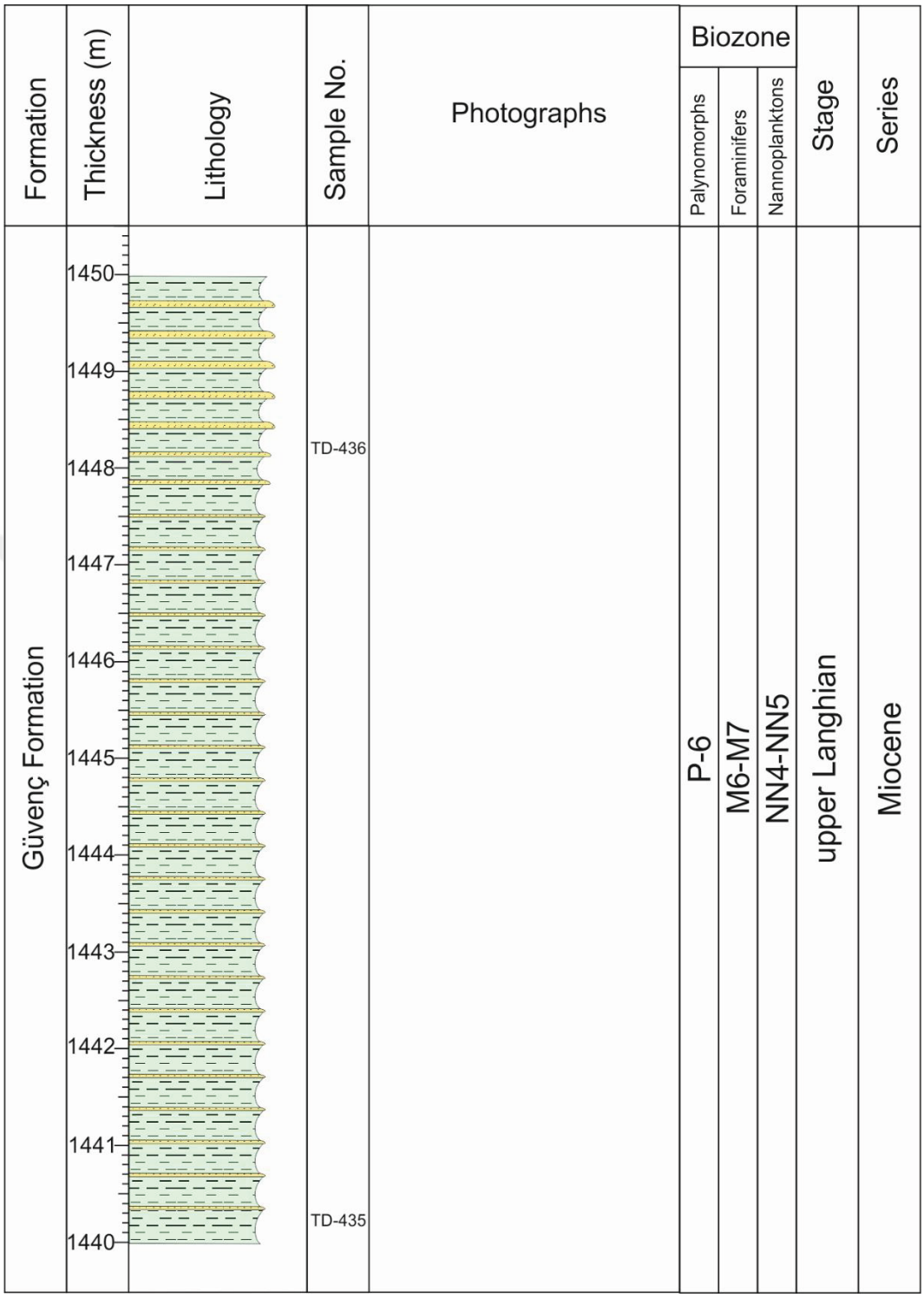

Figure 66. (cont'd)

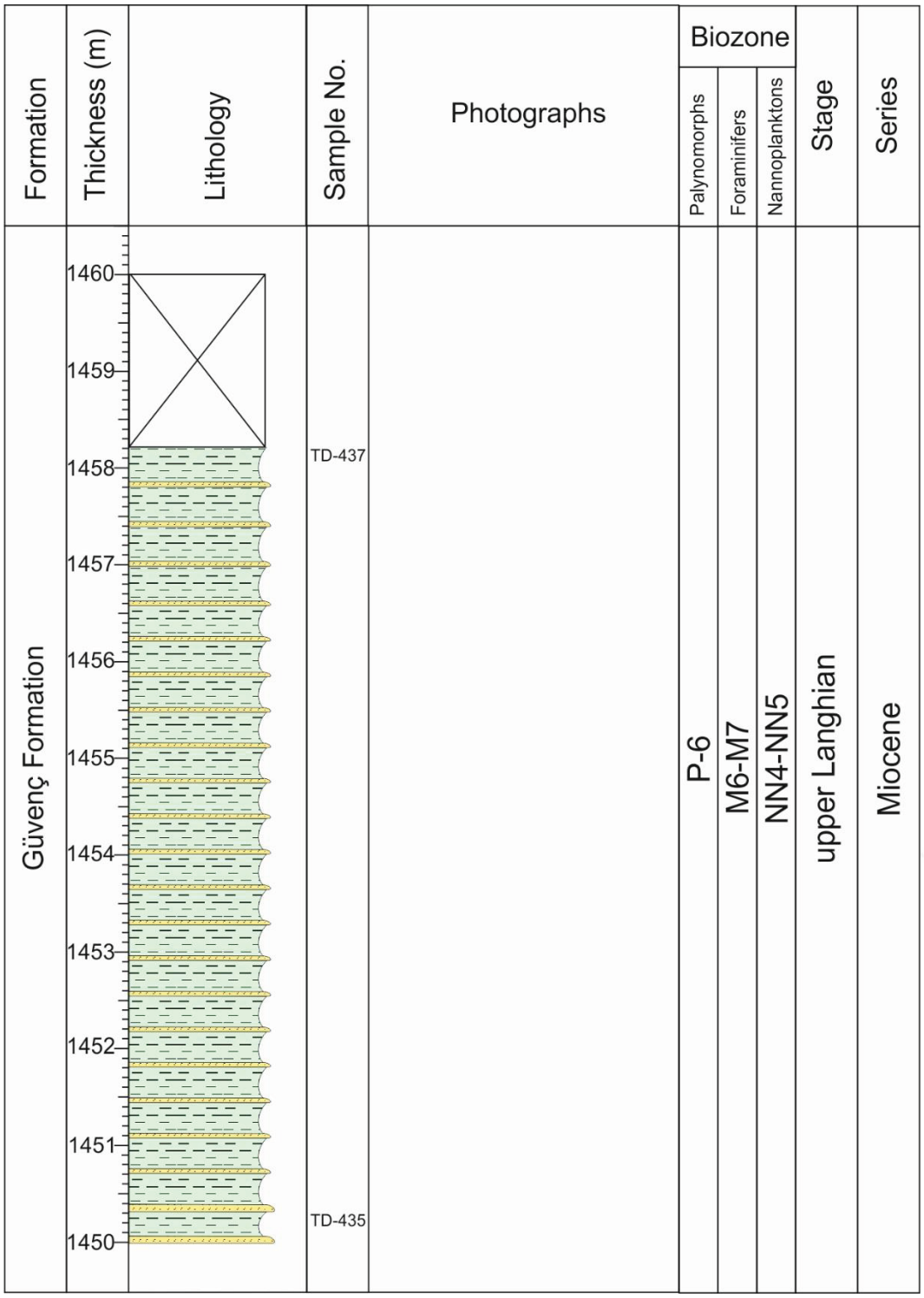

Figure 66. (cont'd)

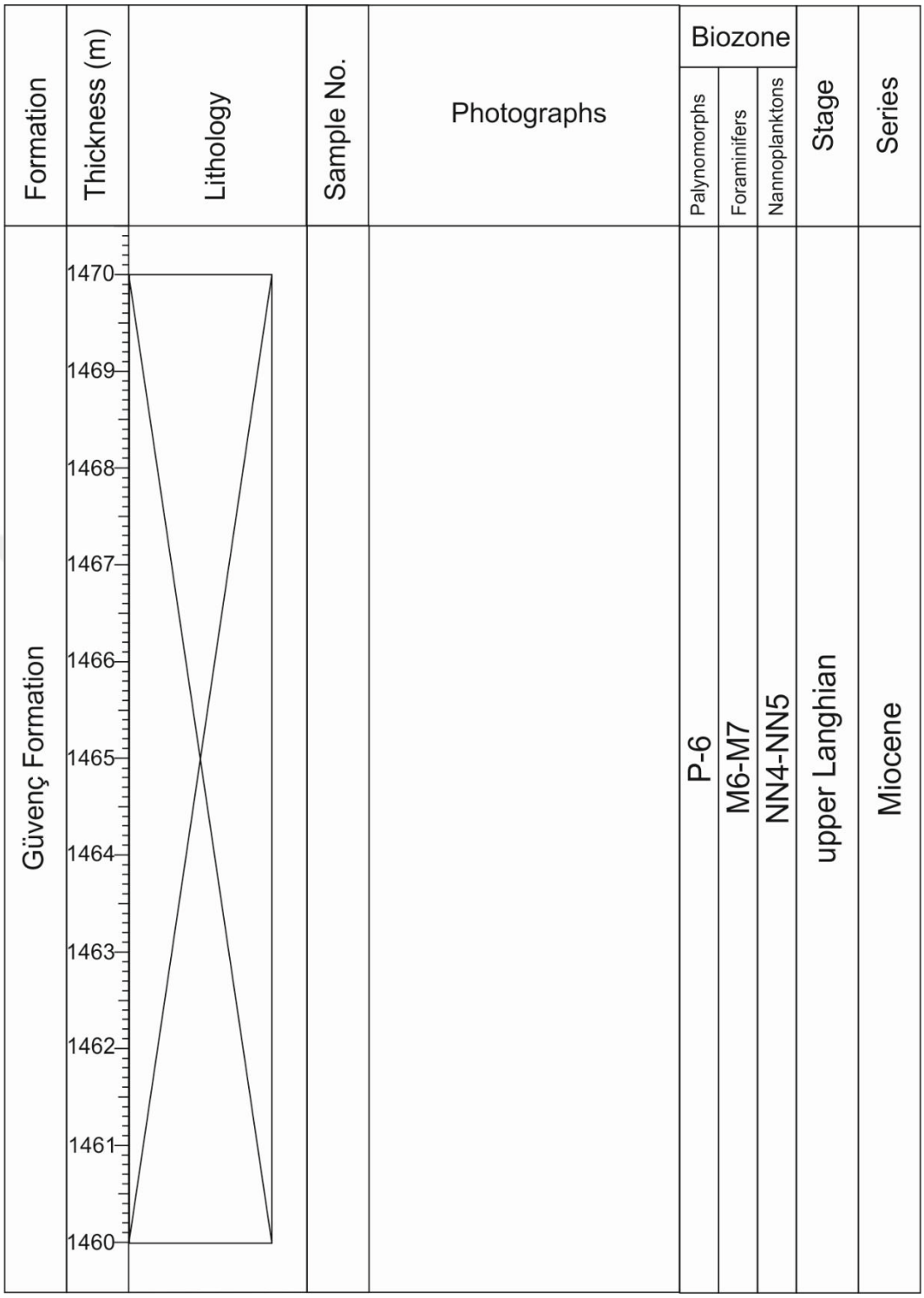

Figure 66. (cont'd)

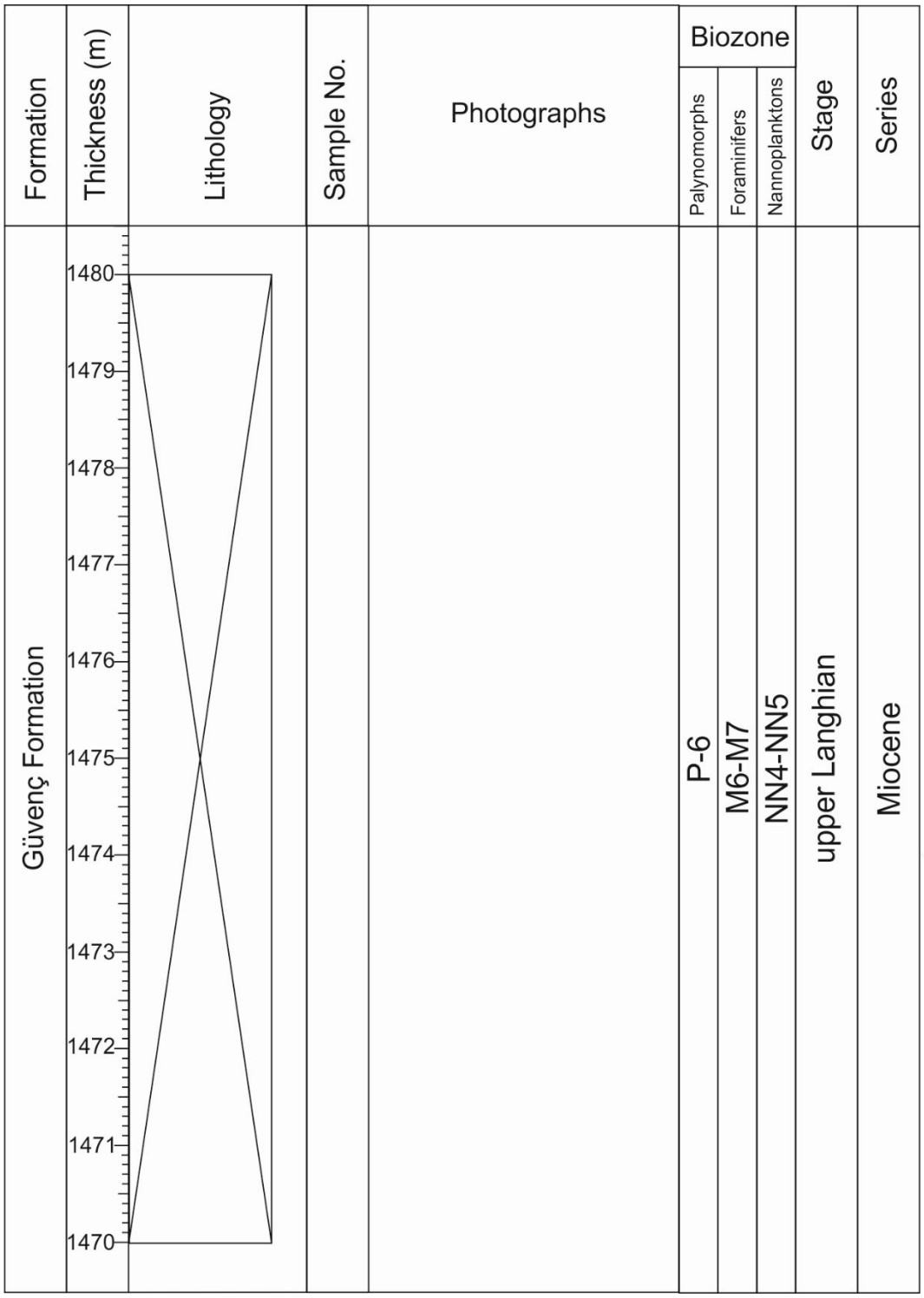

Figure 66. (cont'd)

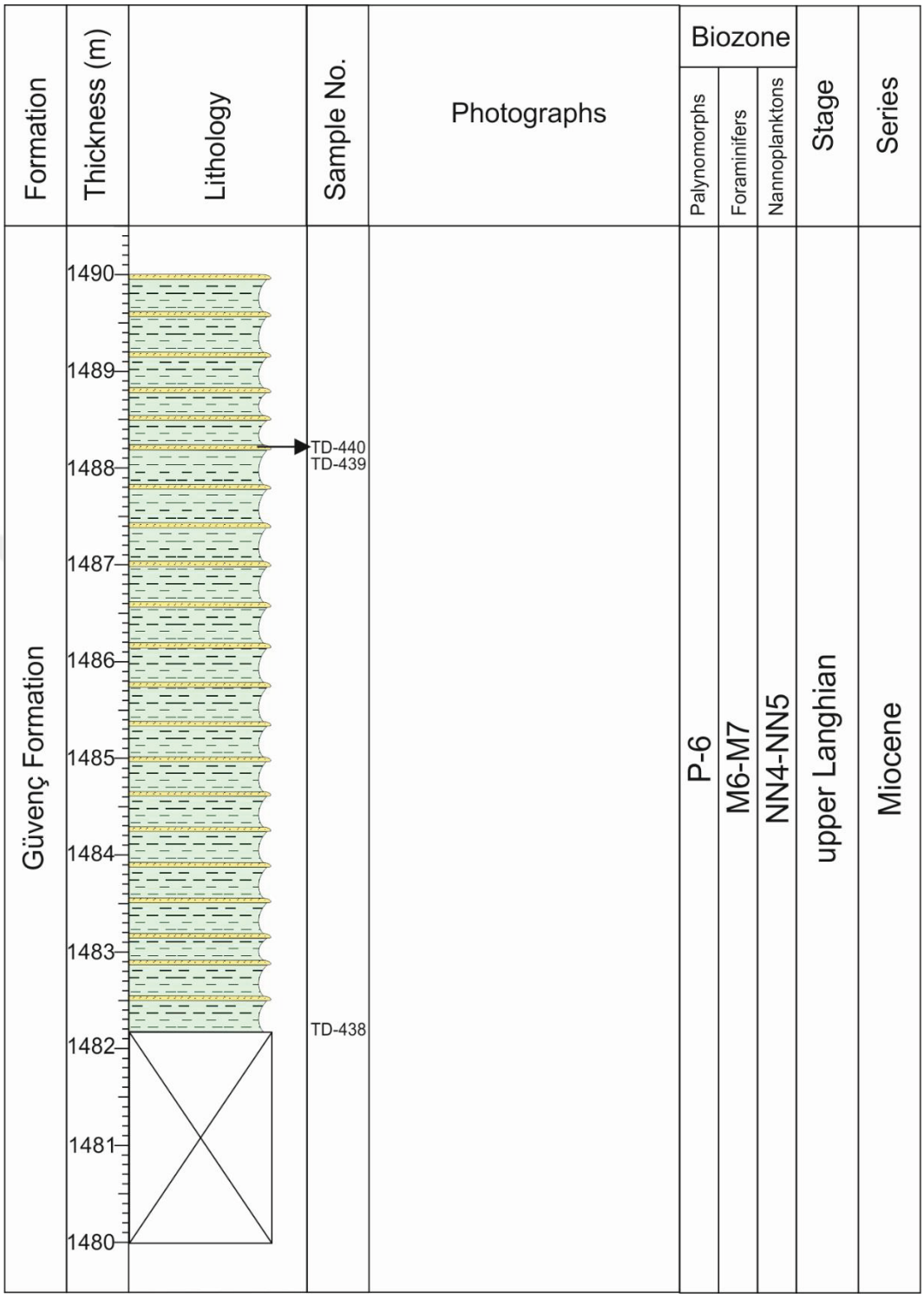

Figure 66. (cont'd)

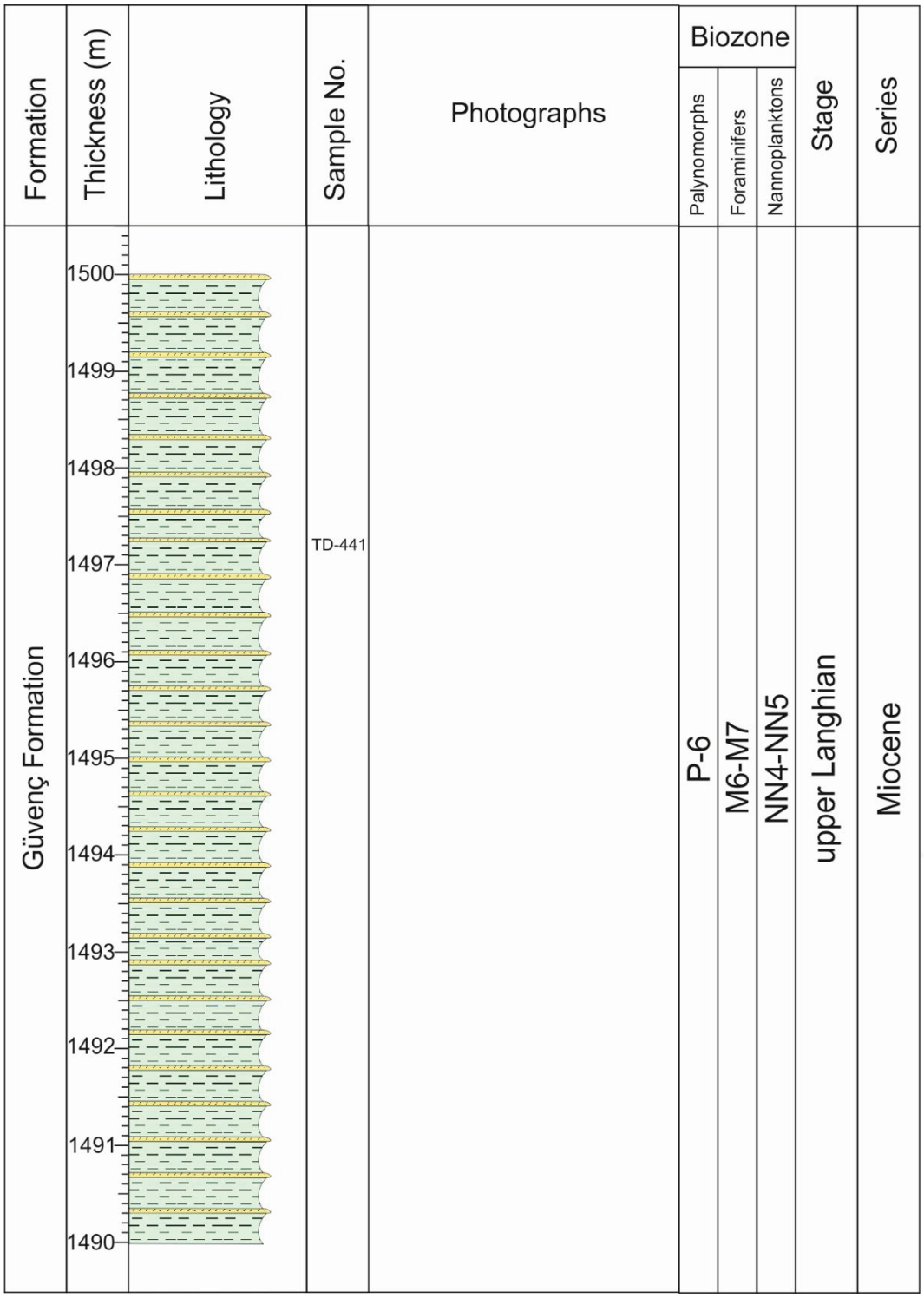

Figure 66. (cont'd)

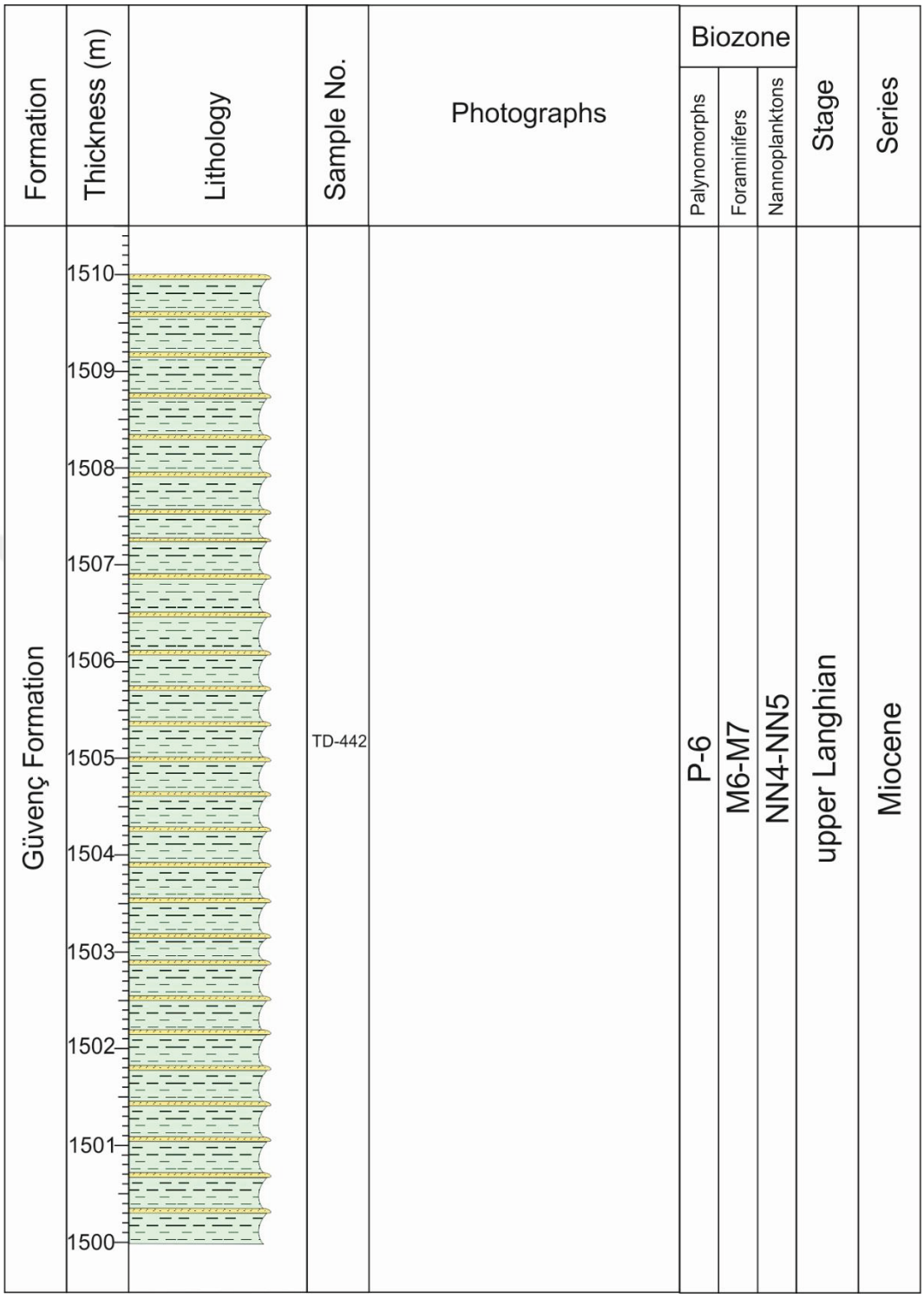

Figure 66. (cont'd)

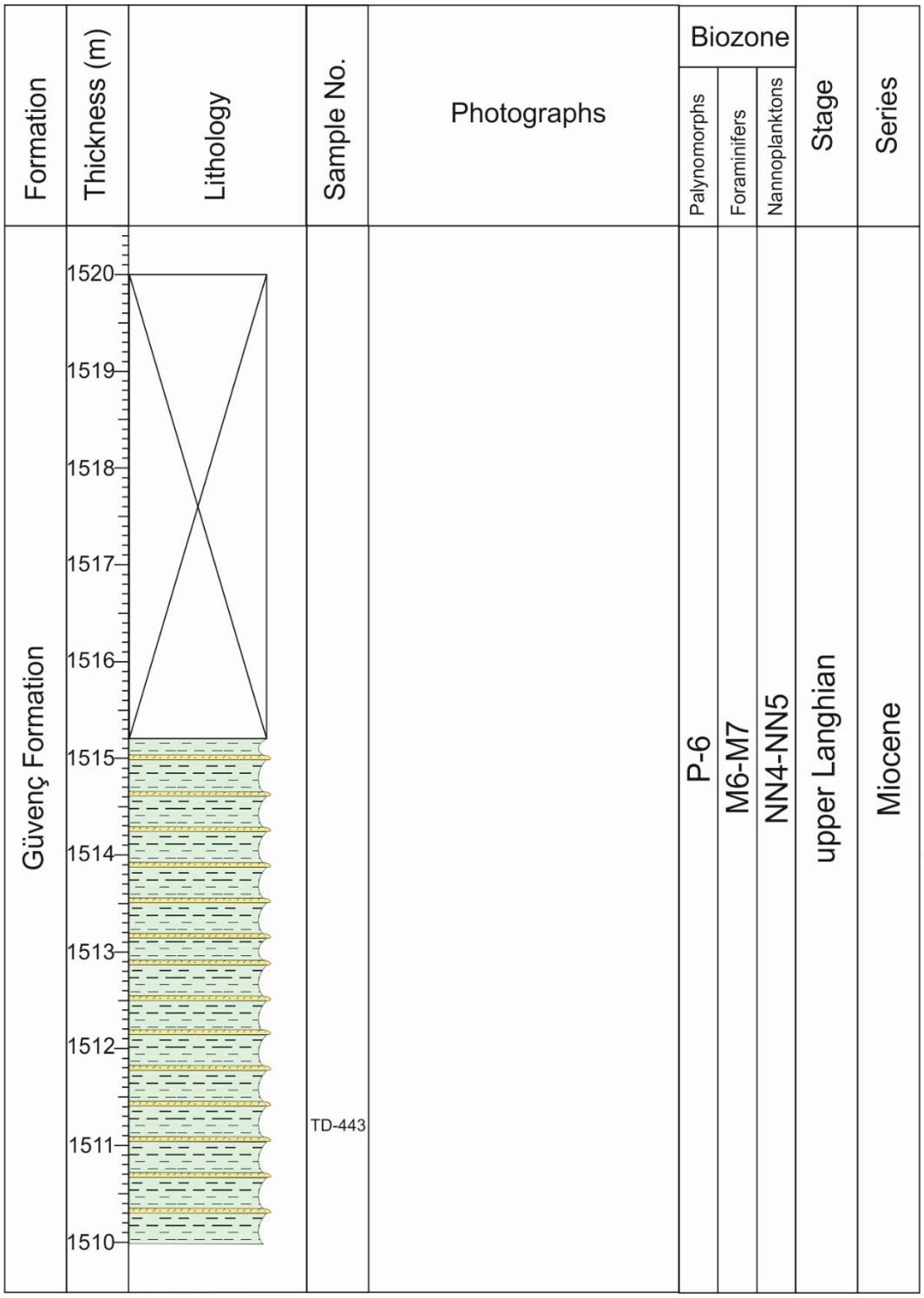

Figure 66. (cont'd)

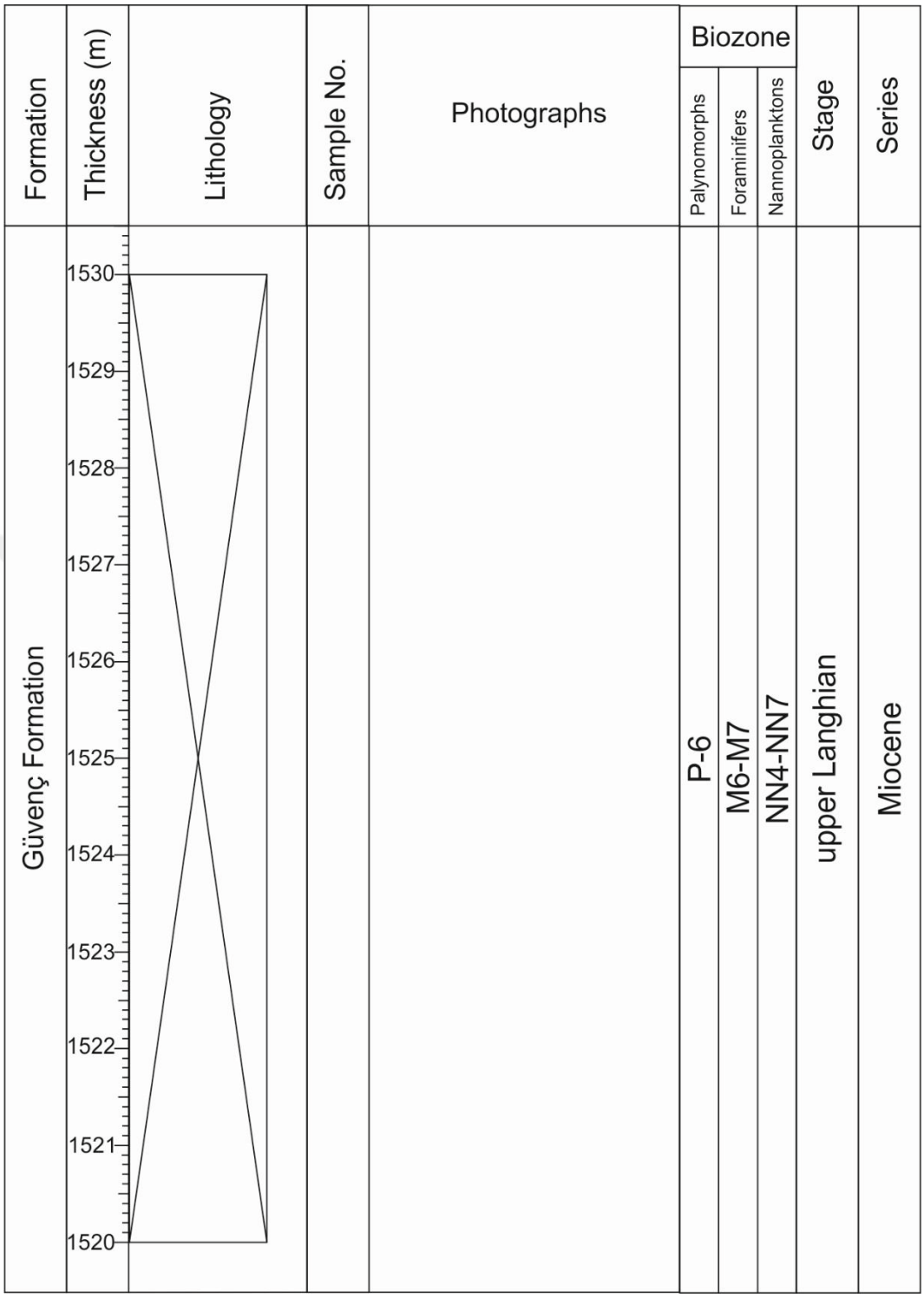

Figure 66. (cont'd)

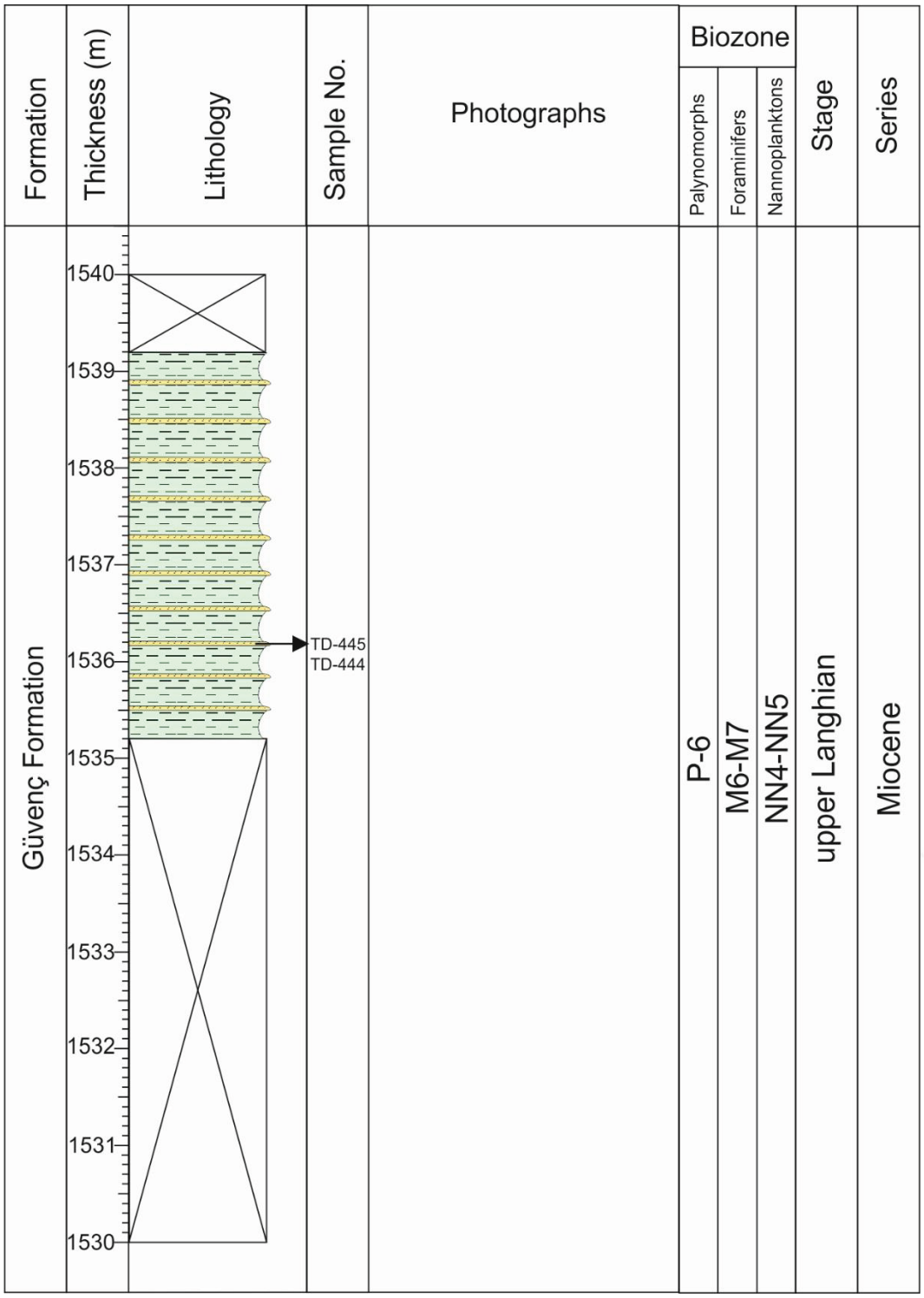

Figure 66. (cont'd)

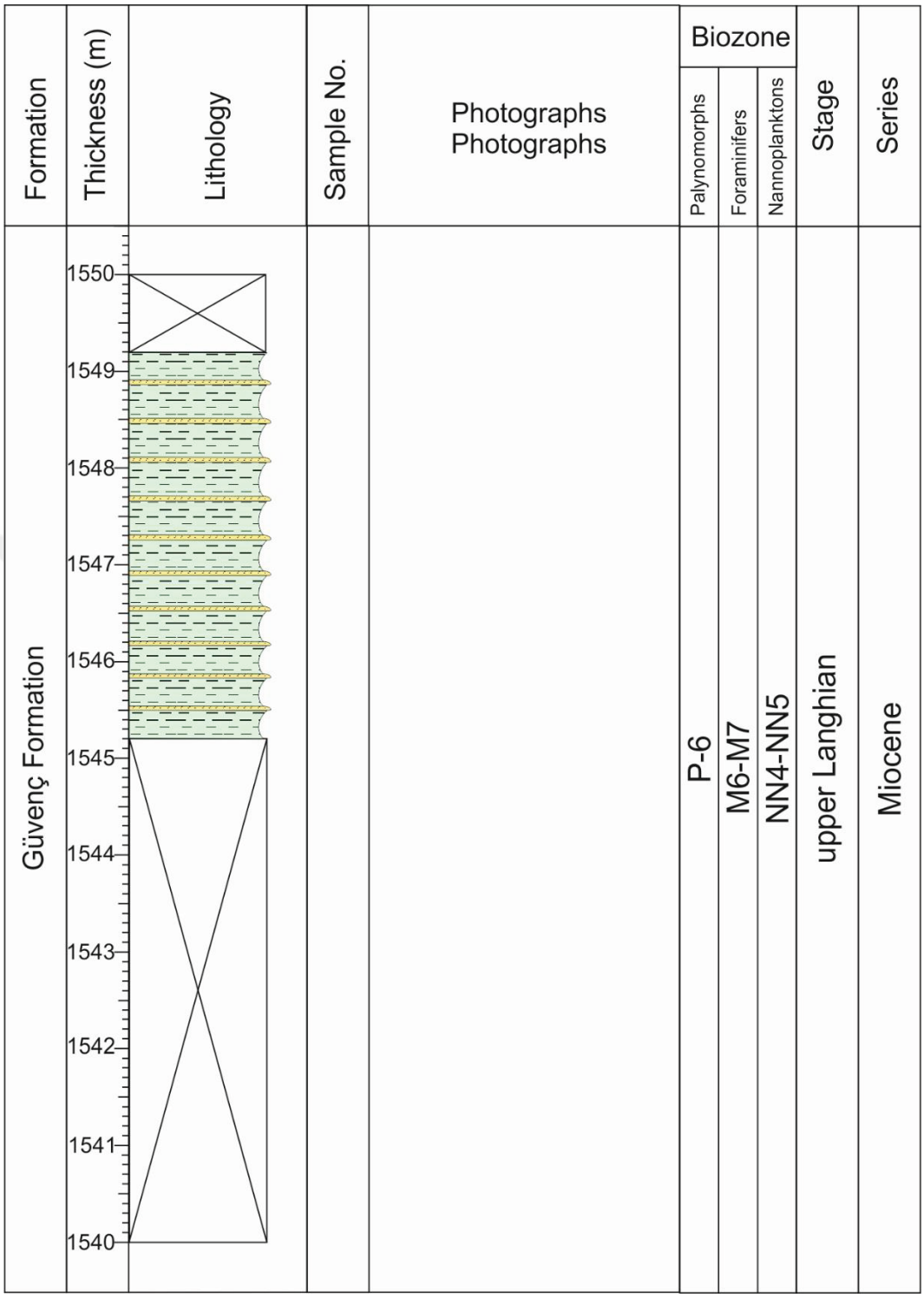

Figure 66. (cont'd)

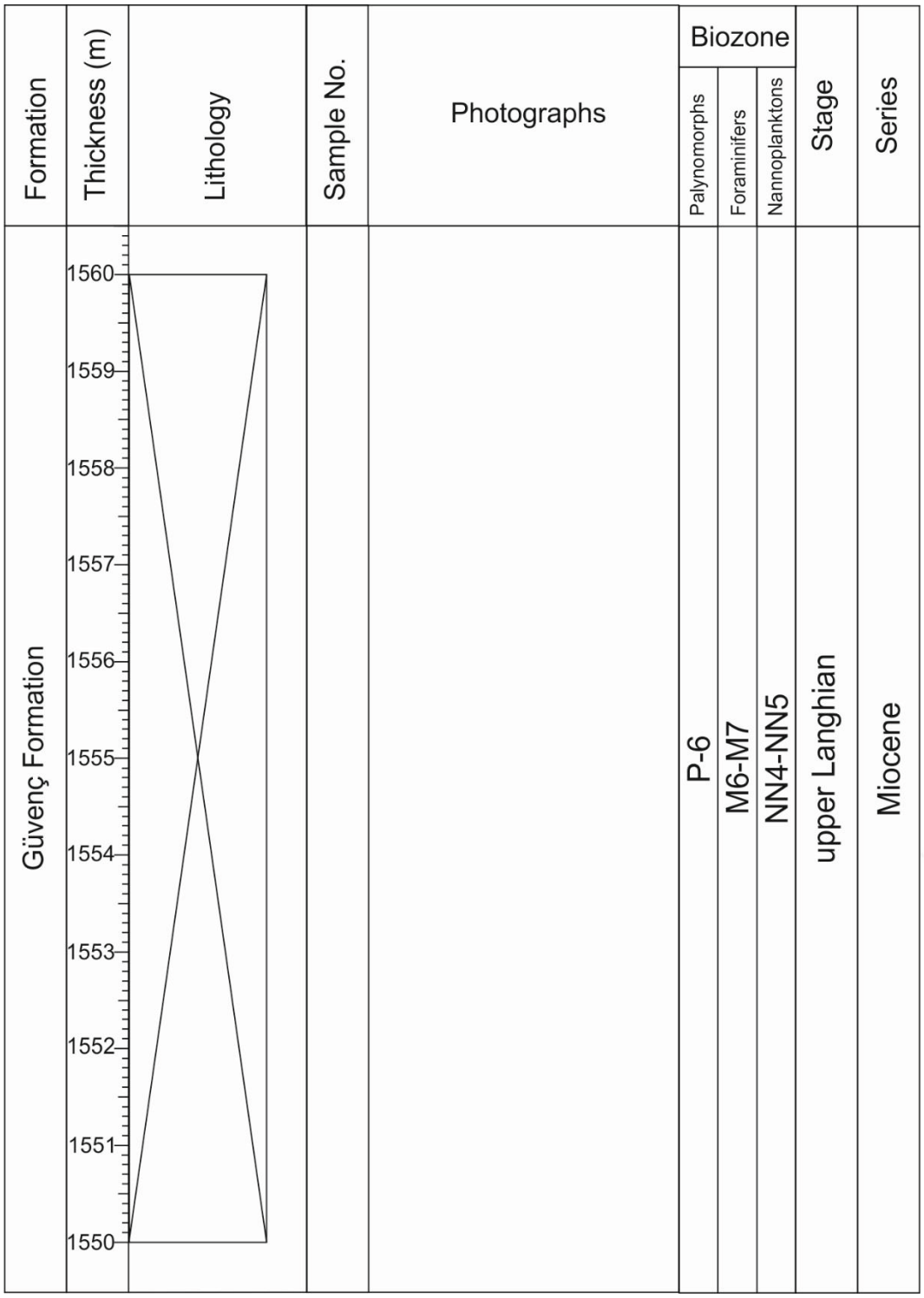

Figure 66. (cont'd)

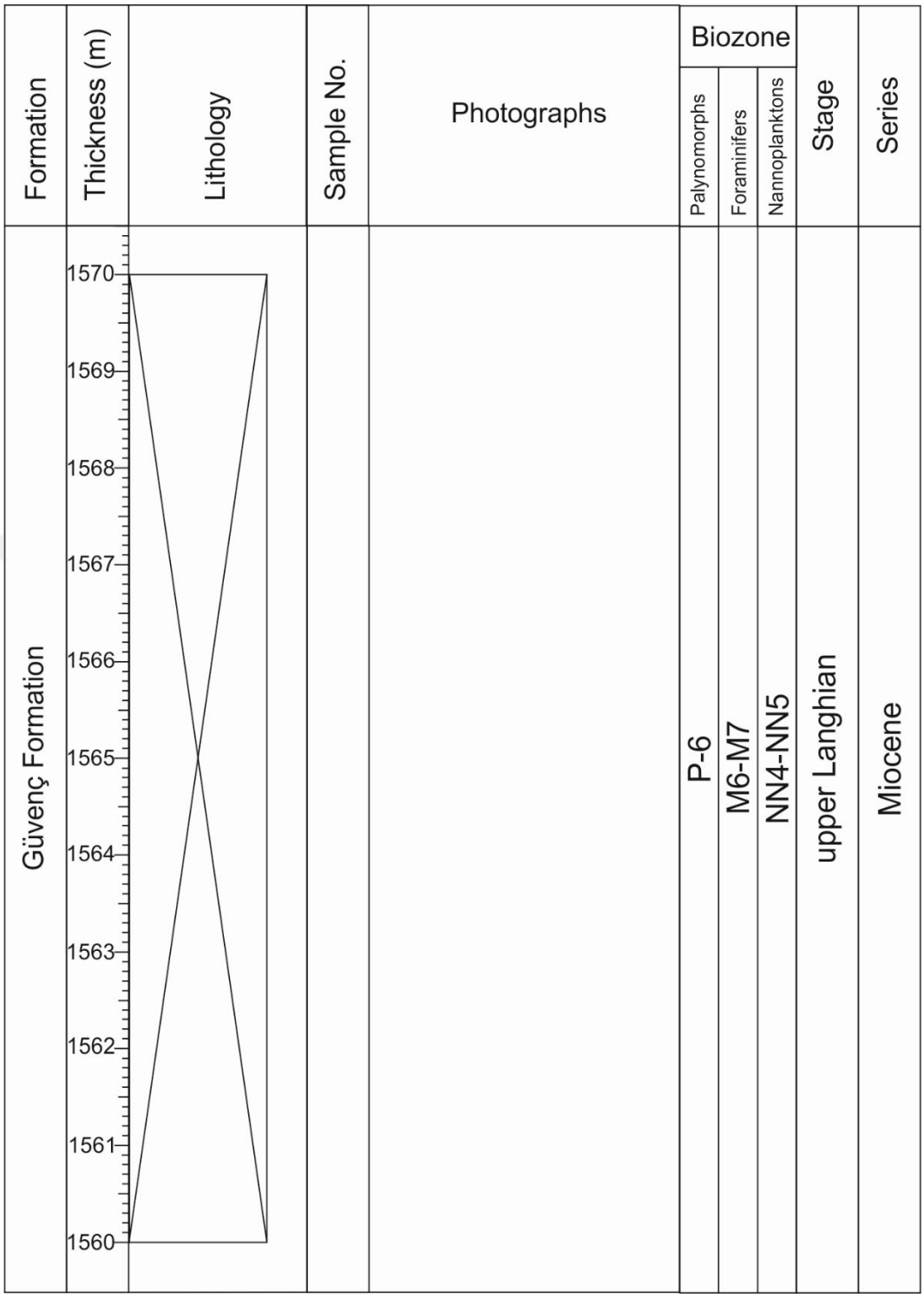

Figure 66. (cont'd)

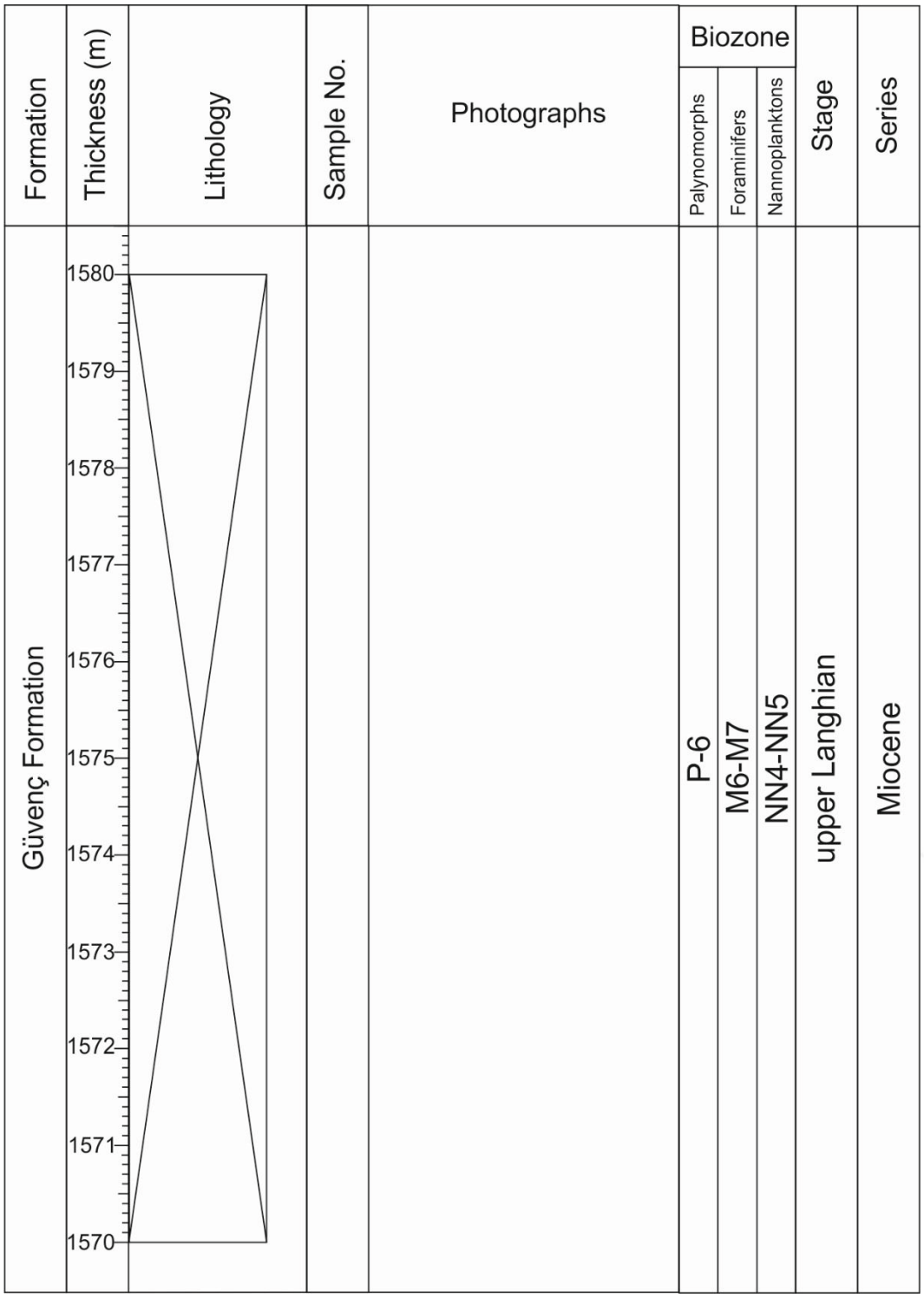

Figure 66. (cont'd)

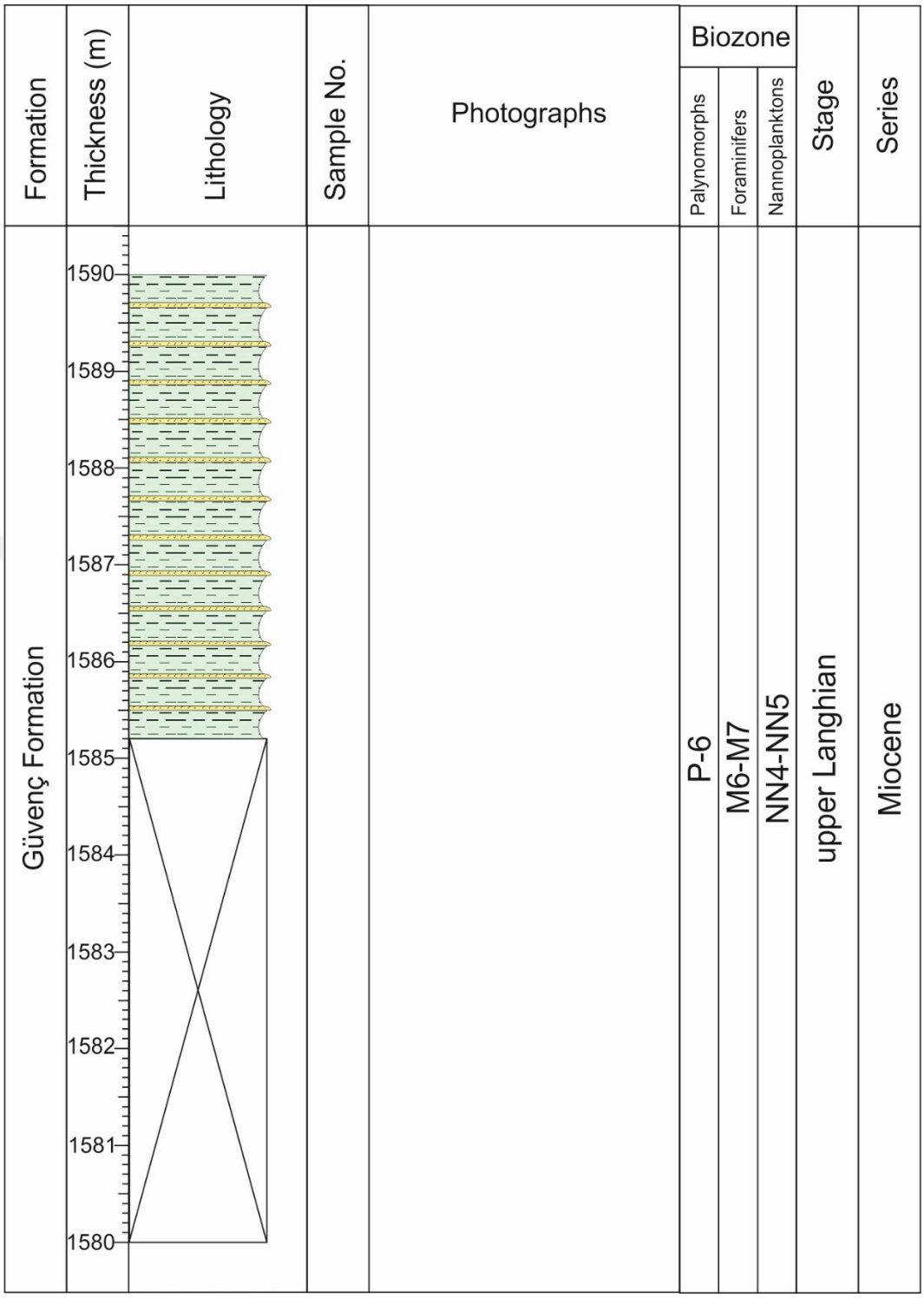

Figure 66. (cont'd)

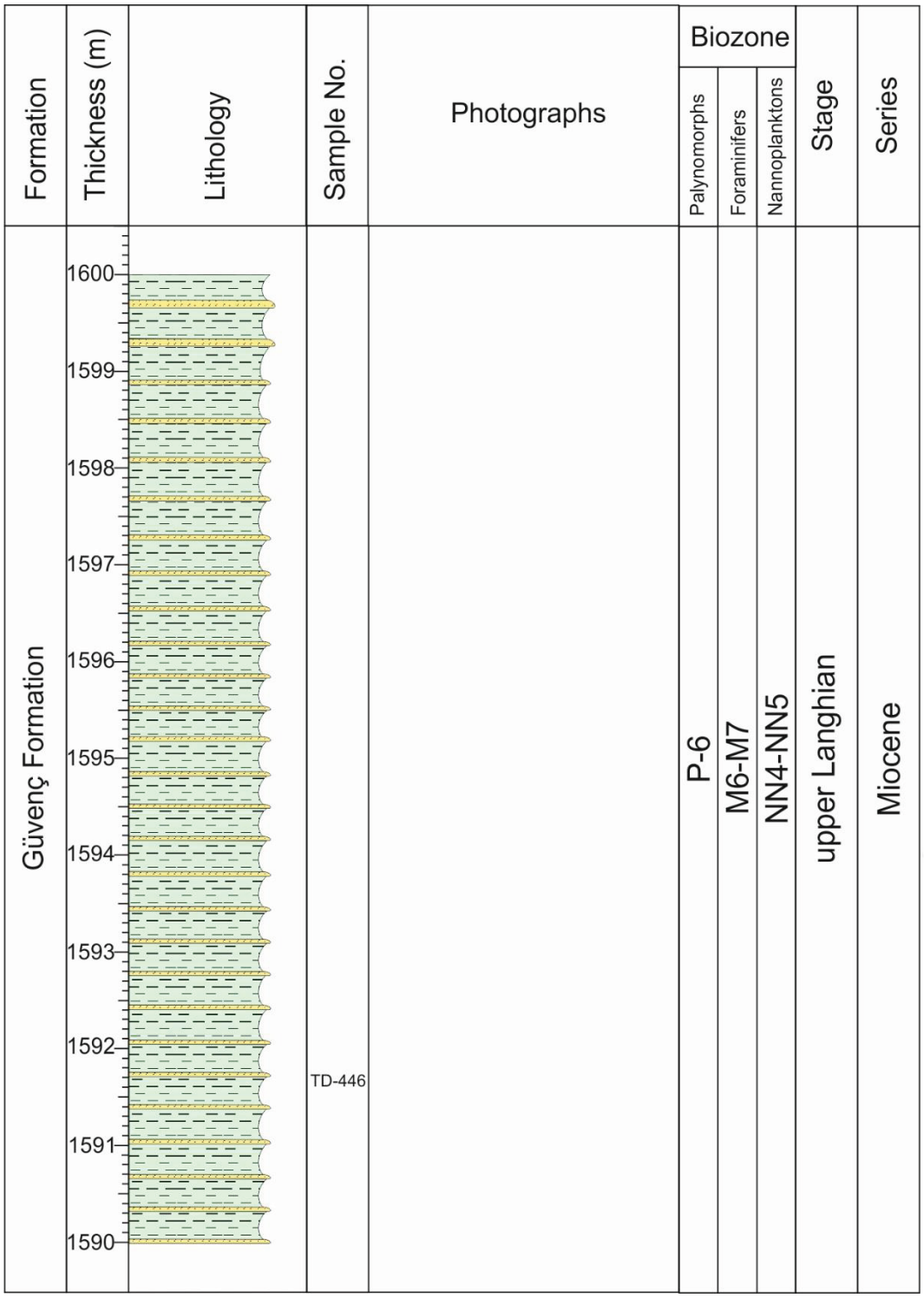

Figure 66. (cont'd)

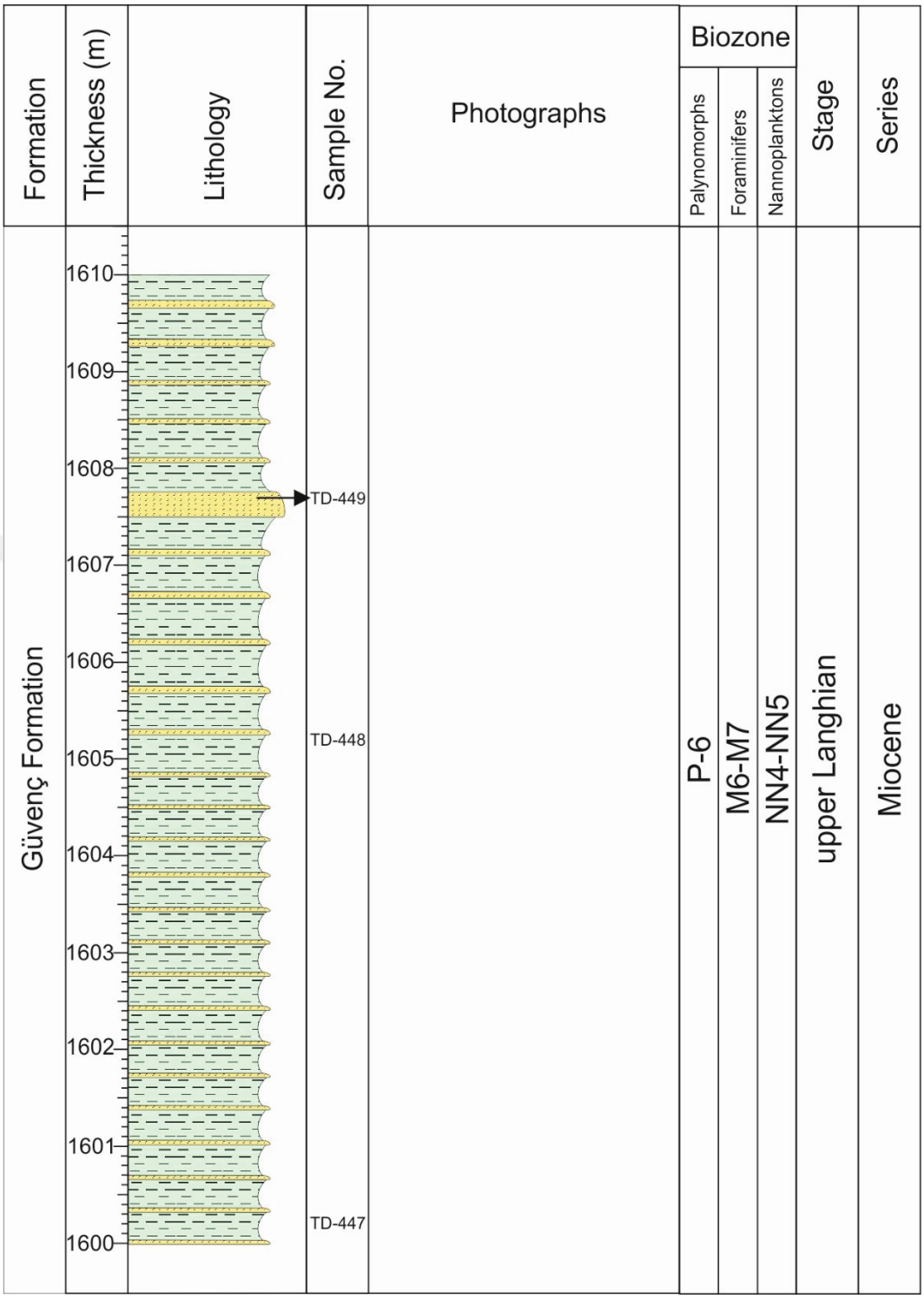

Figure 66. (cont'd)

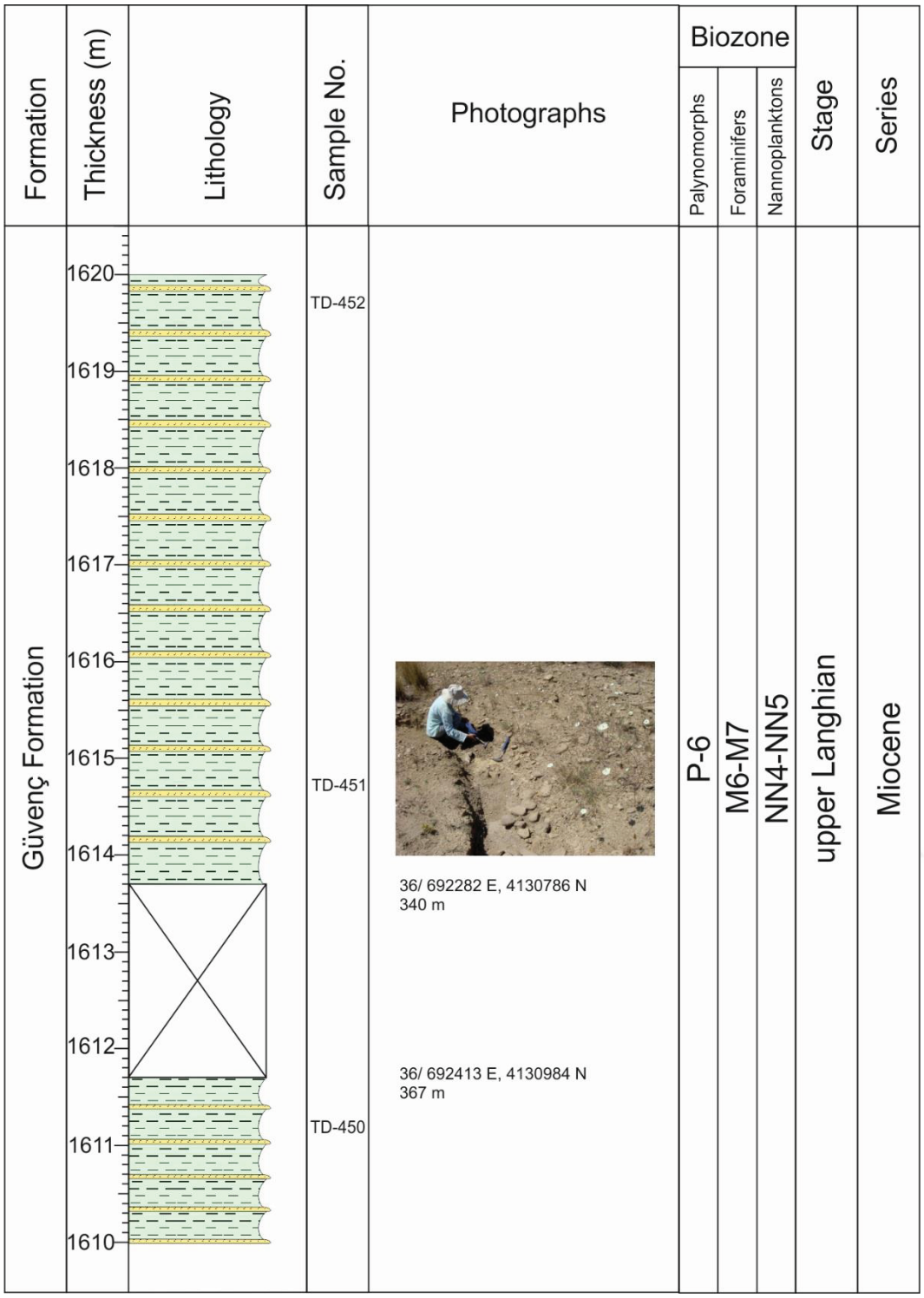

Figure 66. (cont'd)

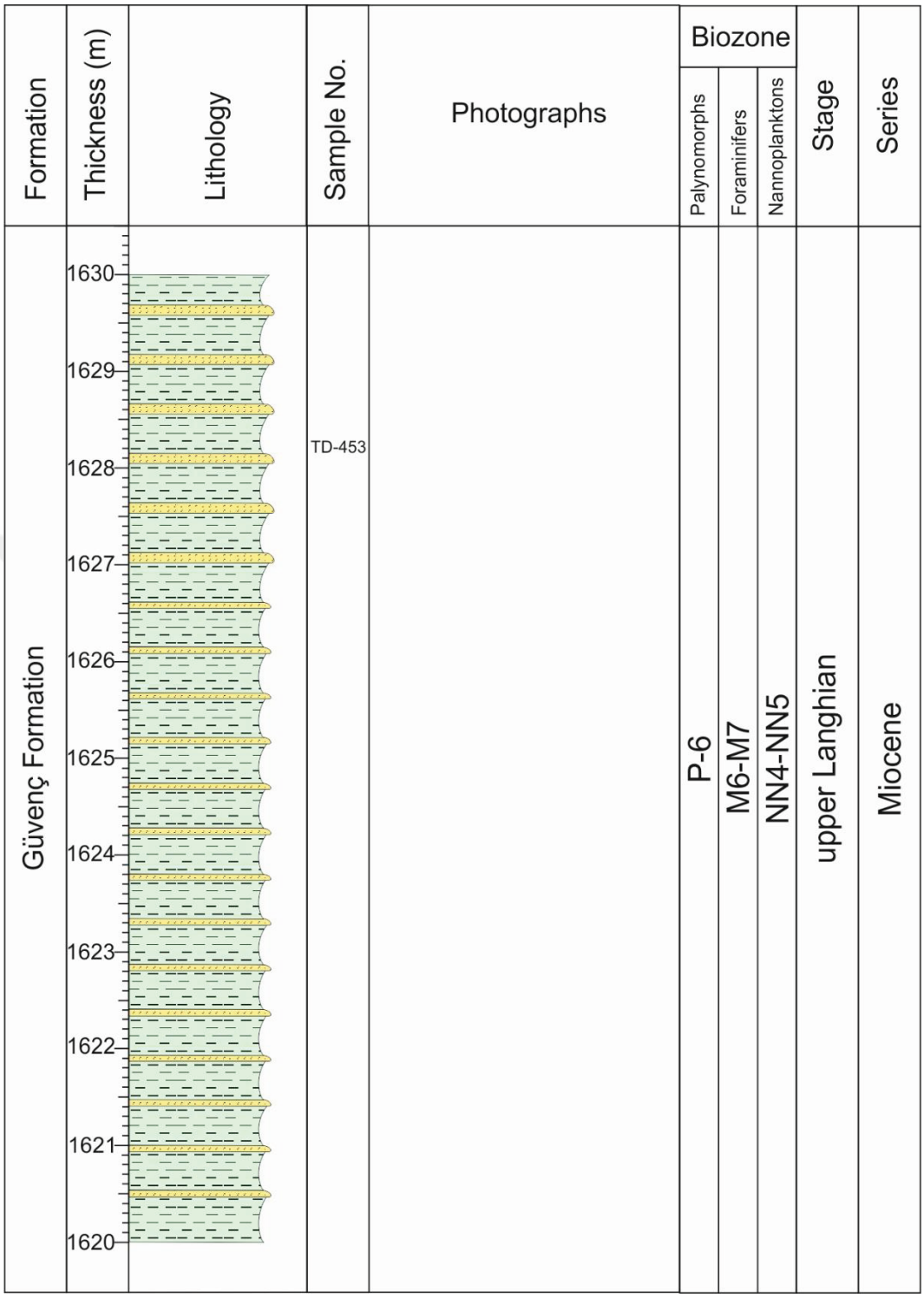

Figure 66. (cont'd)

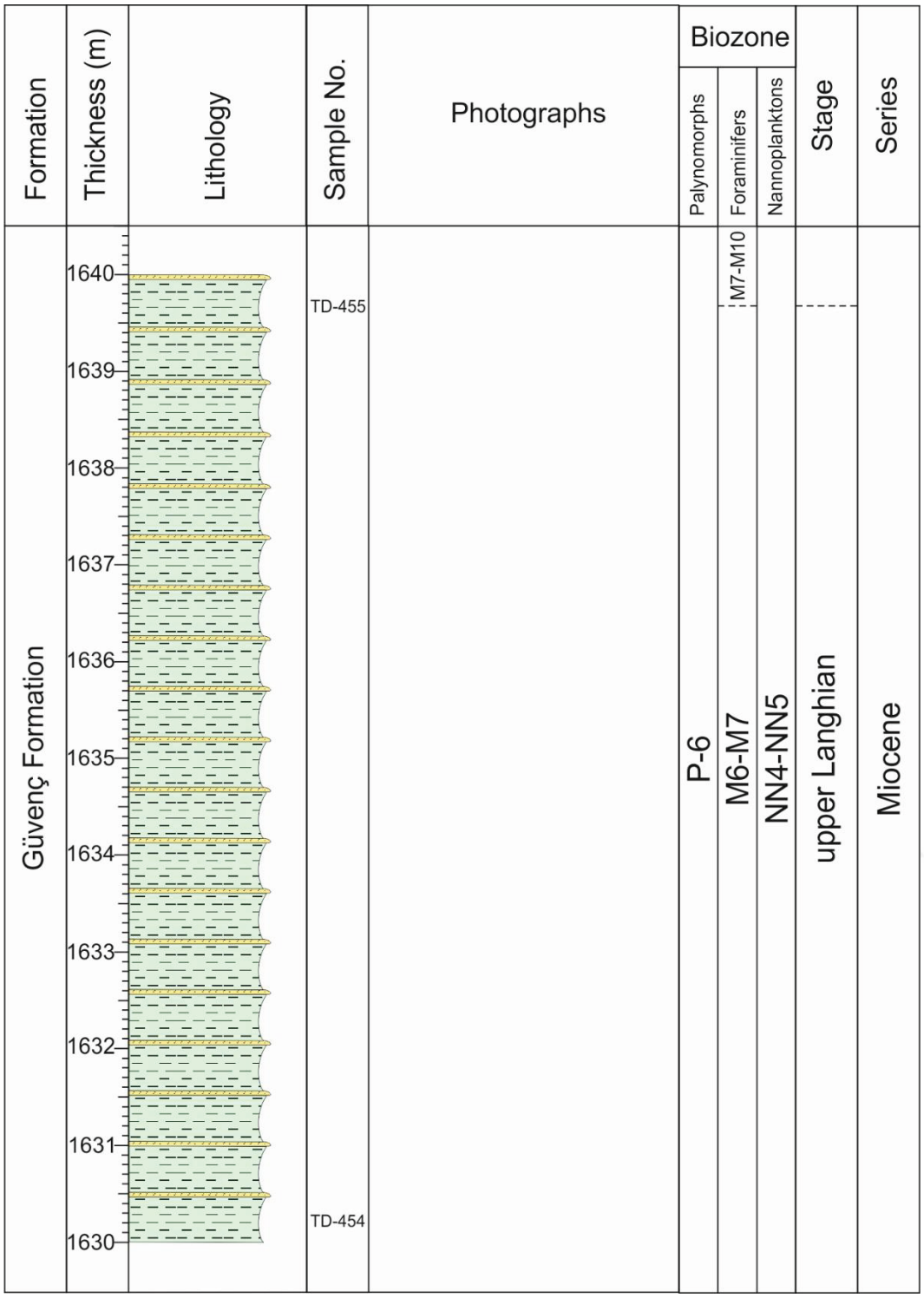

Figure 66. (cont'd)

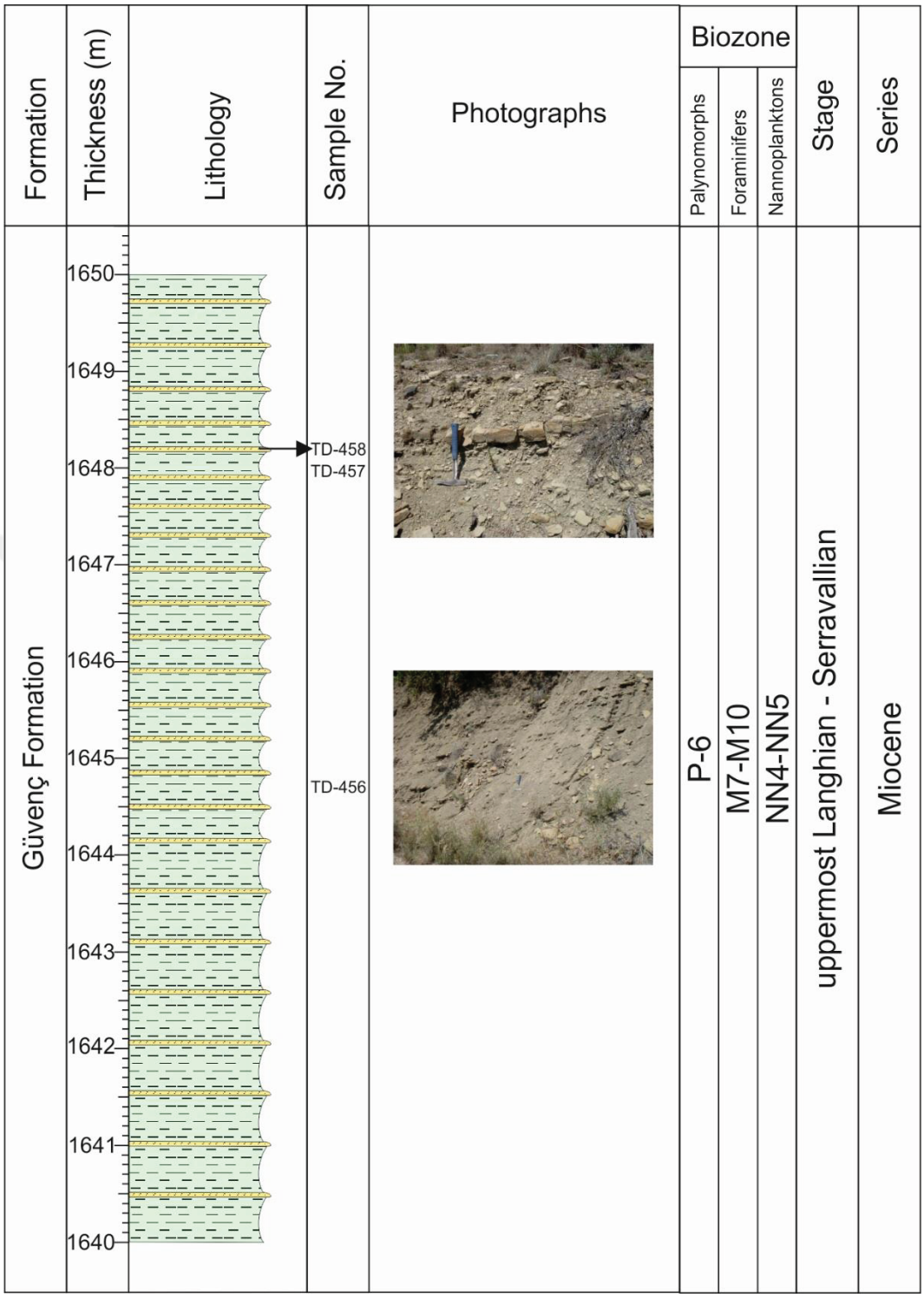

Figure 66. (cont'd)

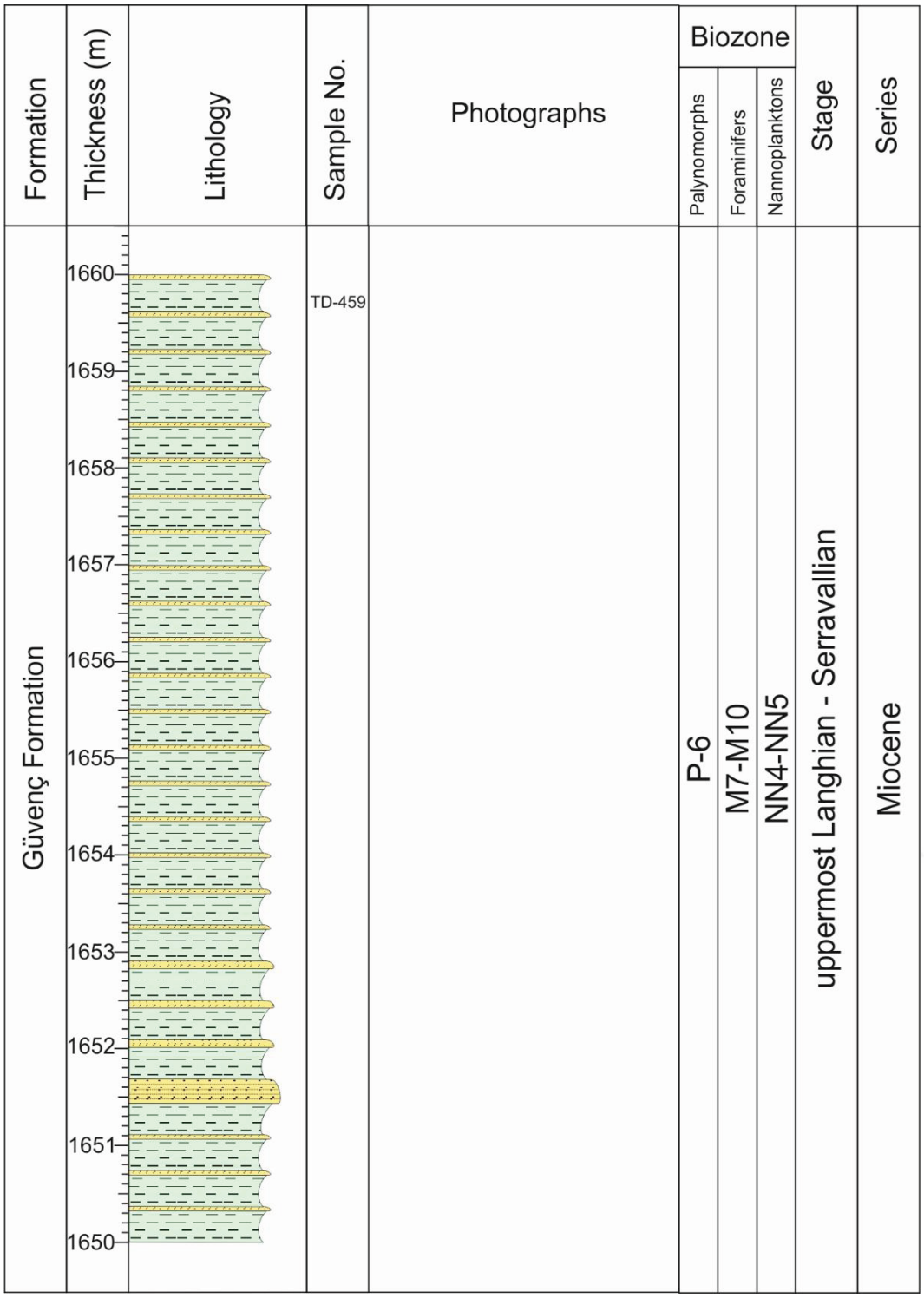

Figure 66. (cont'd)

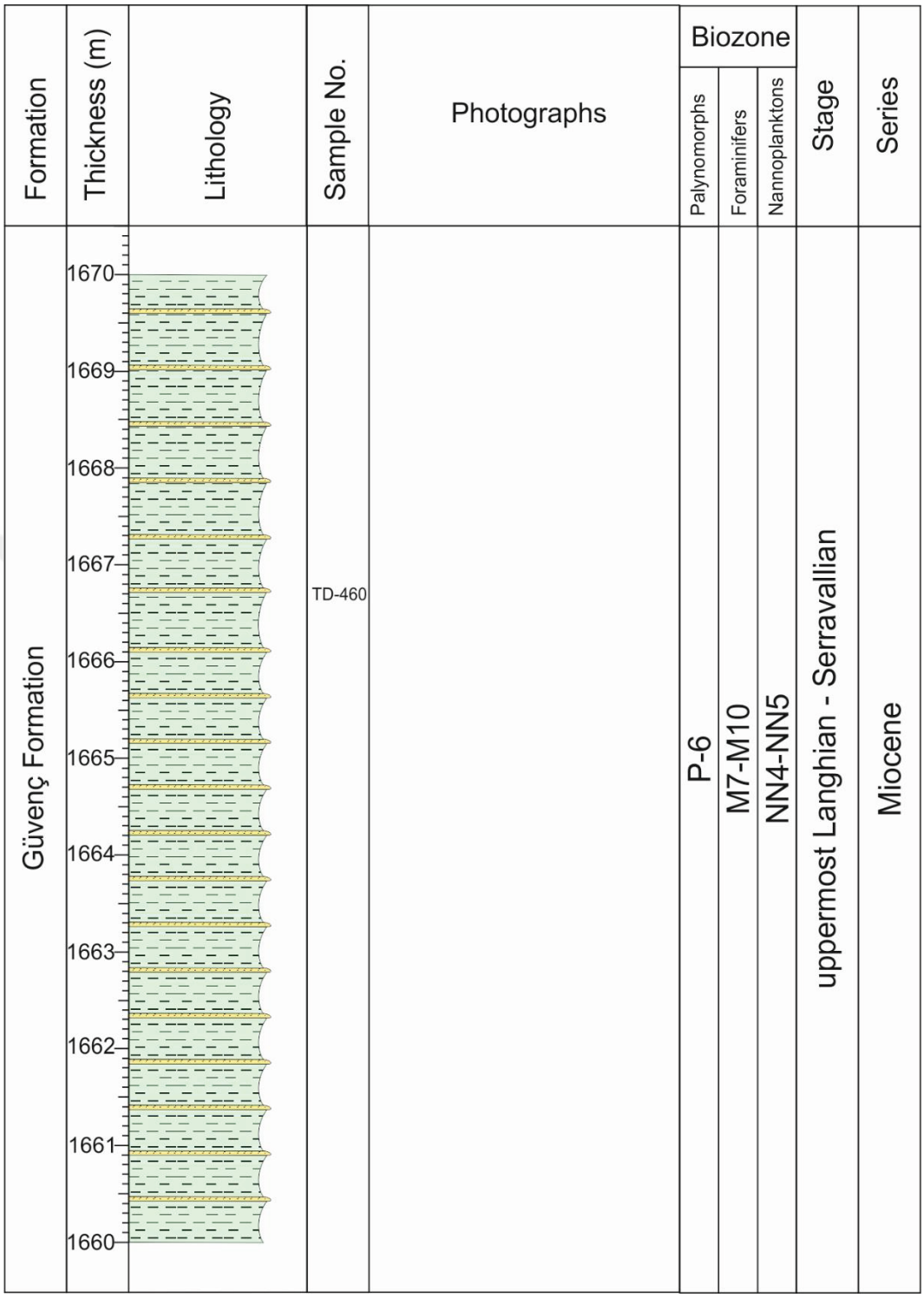

Figure 66. (cont'd)

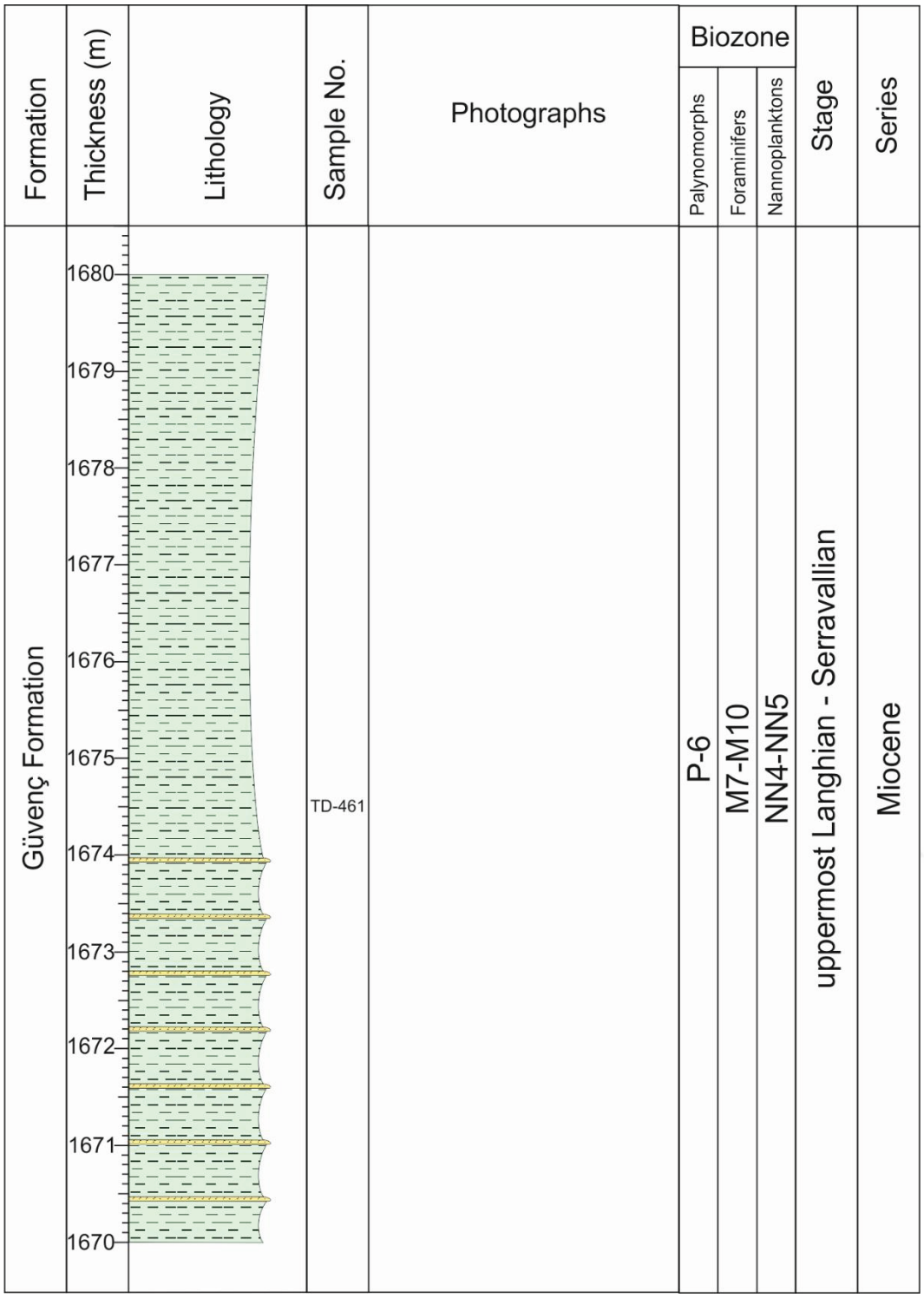

Figure 66. (cont'd)

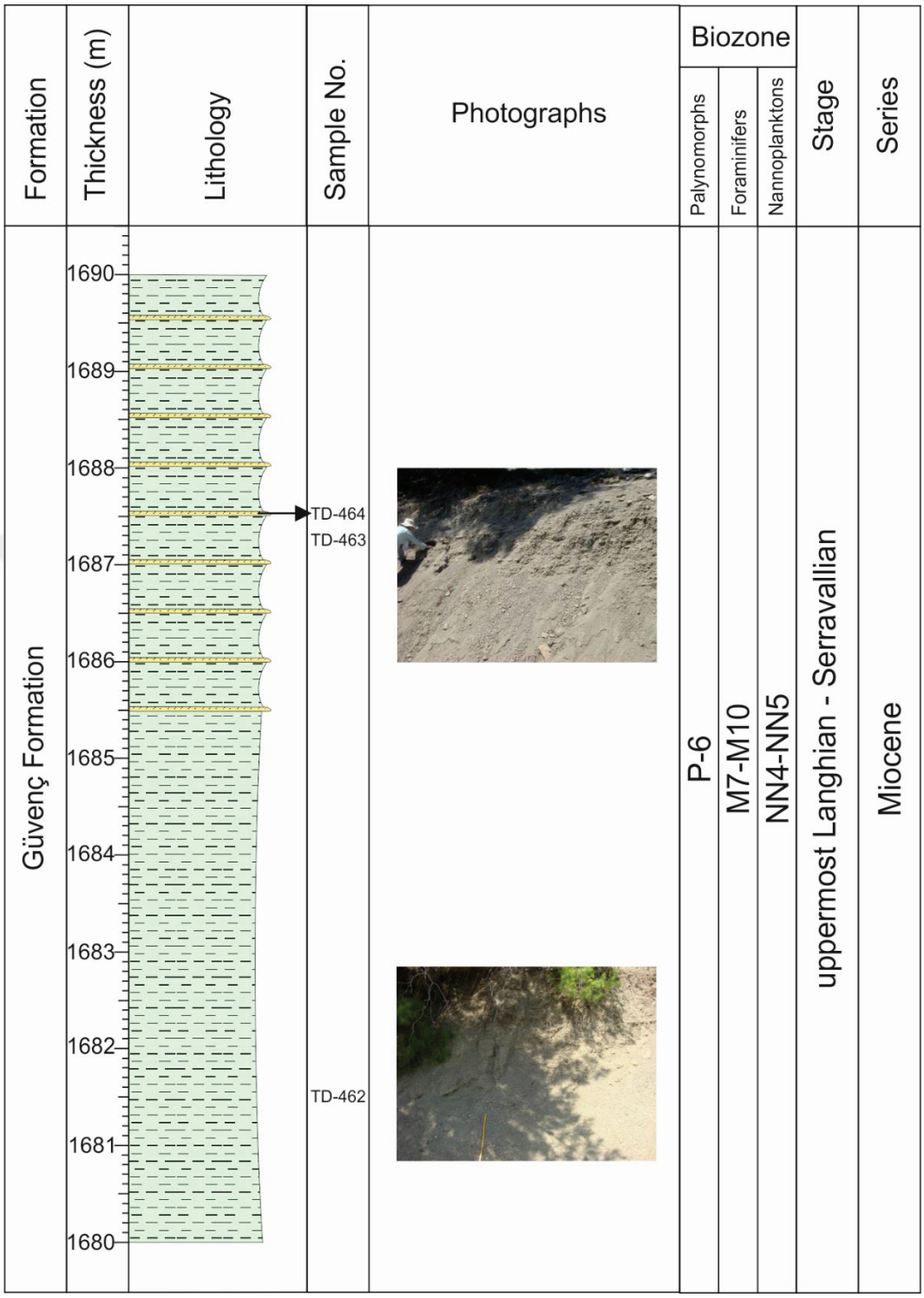

Figure 66. (cont'd)

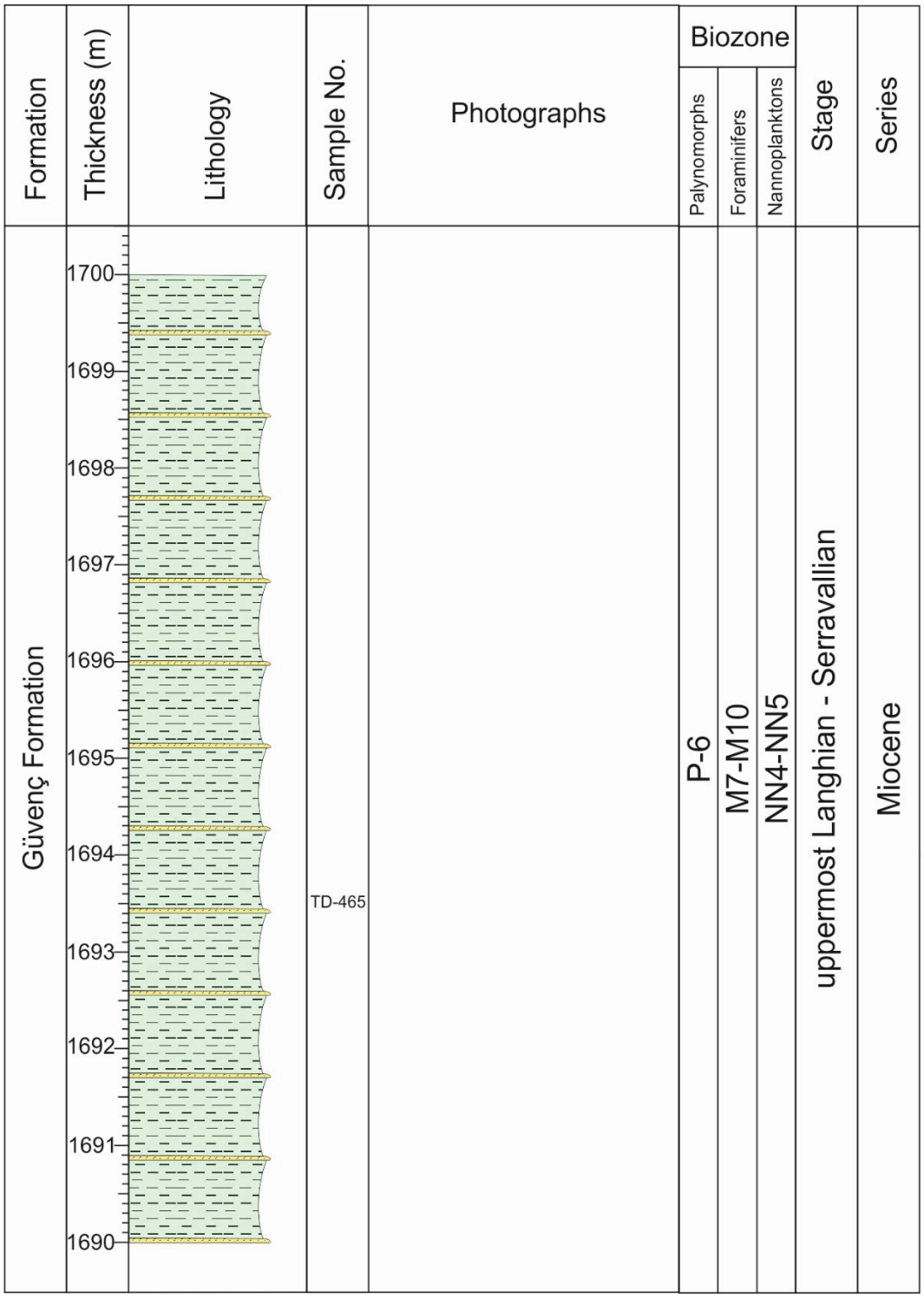

Figure 66. (cont'd)

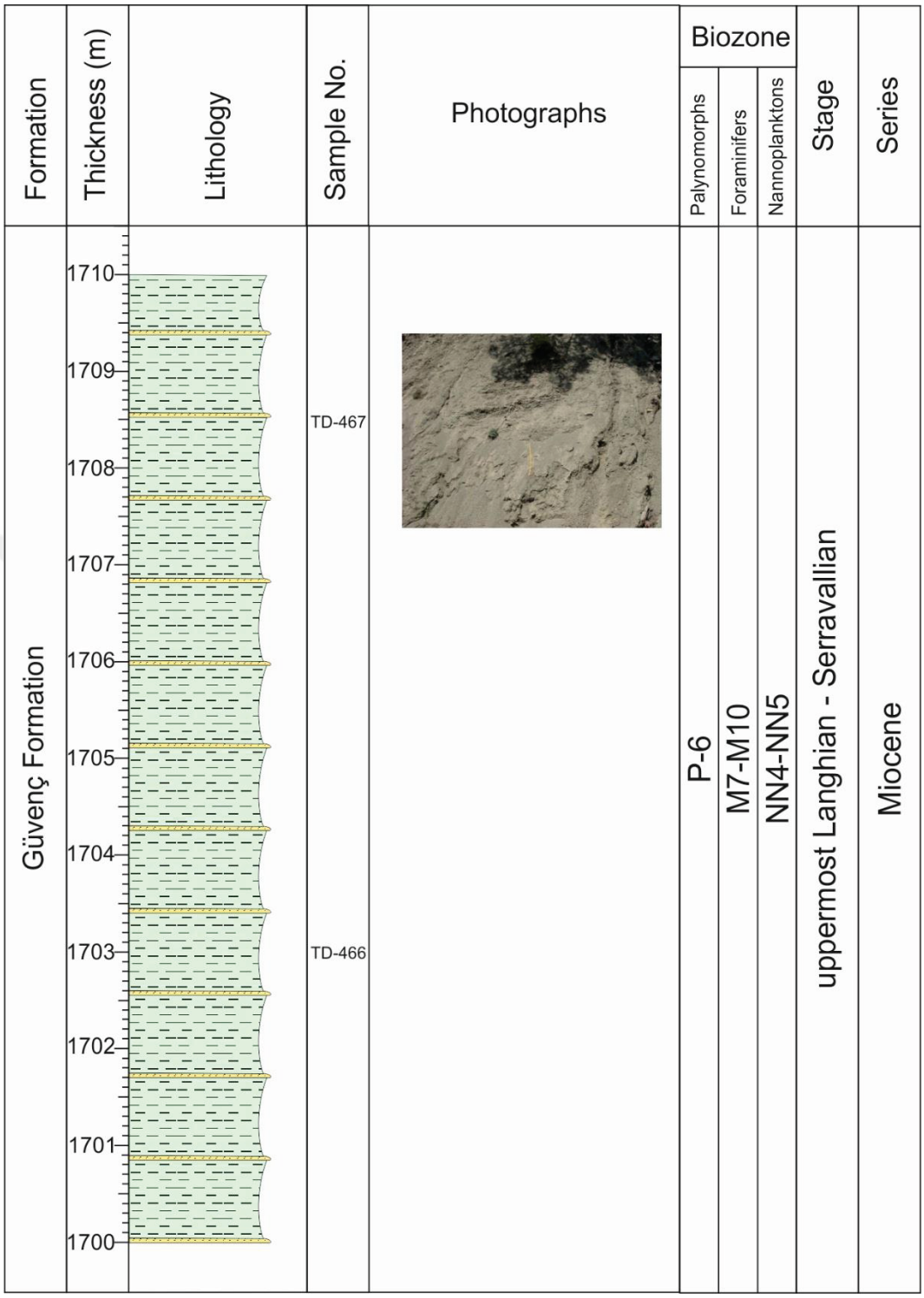

Figure 66. (cont'd)

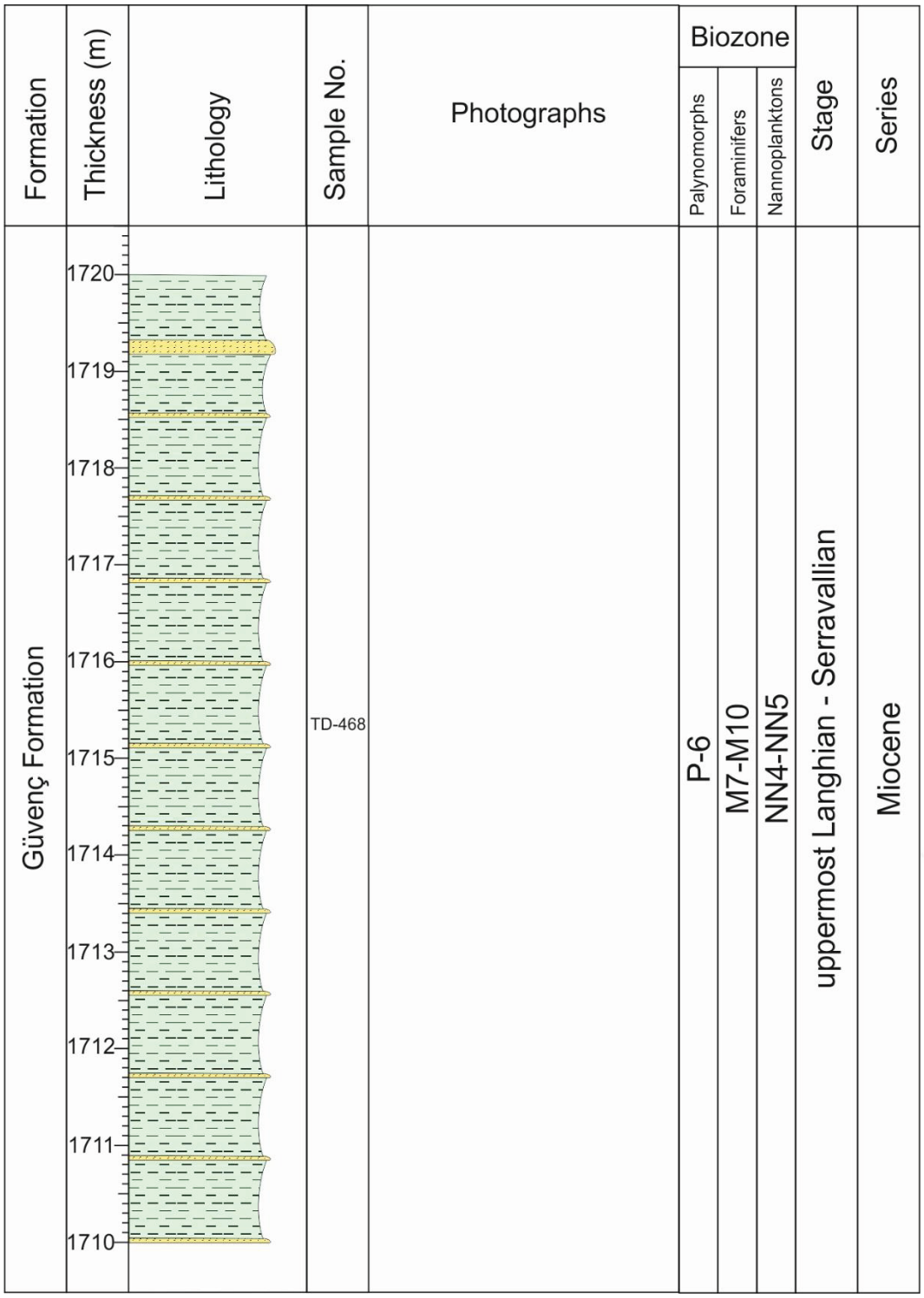

Figure 66. (cont'd)

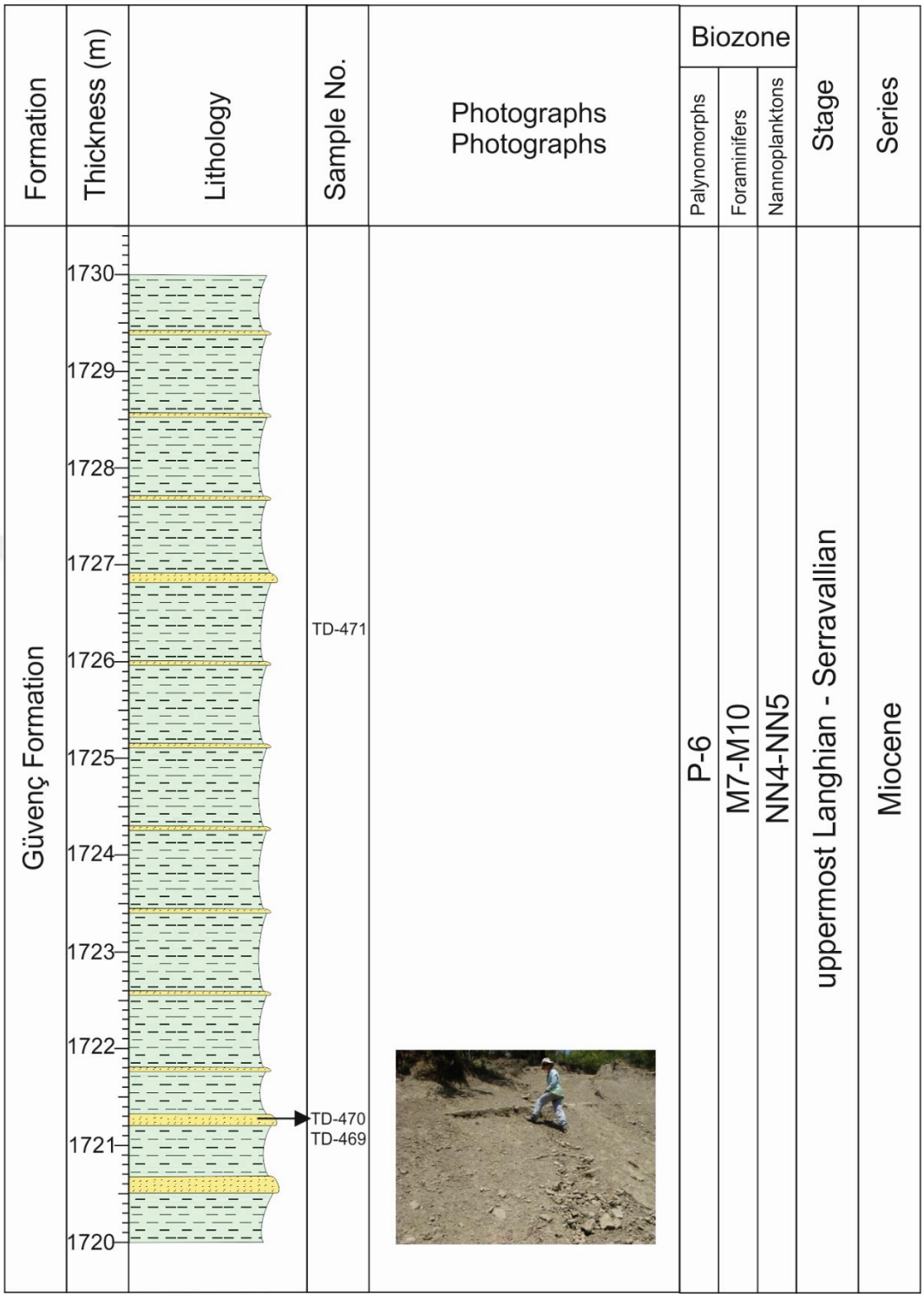

Figure 66. (cont'd)

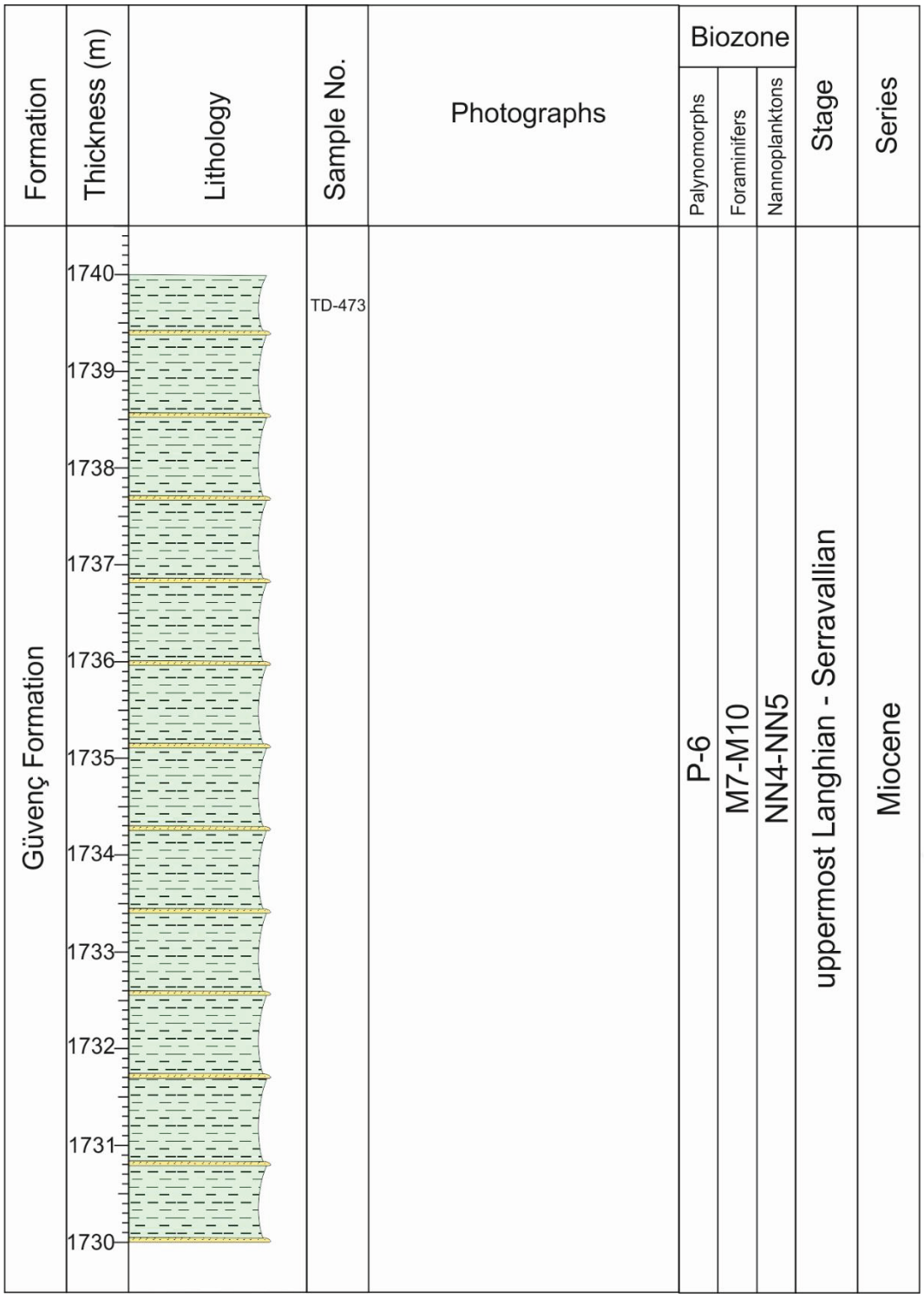

Figure 66. (cont'd)

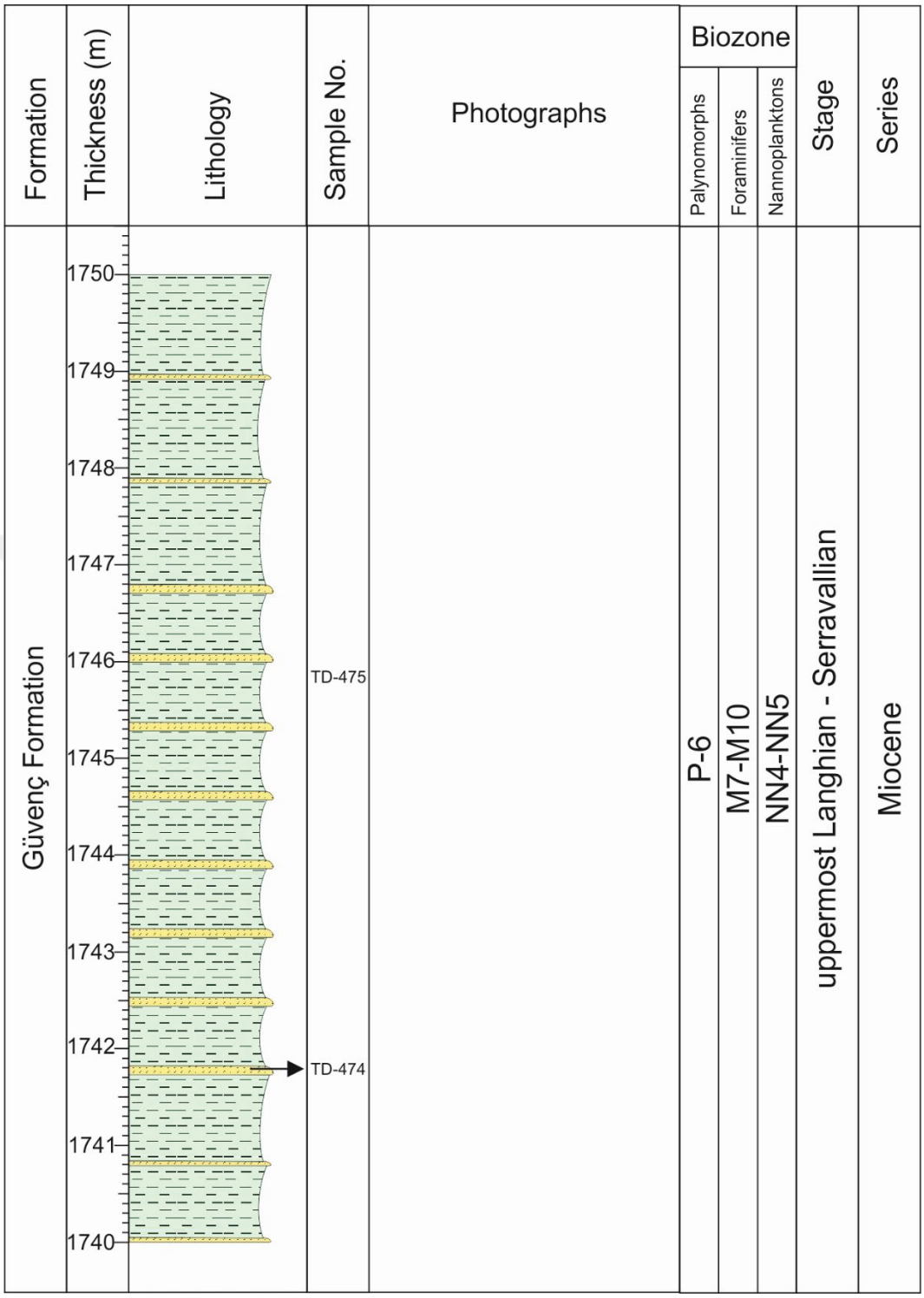

Figure 66. (cont'd)

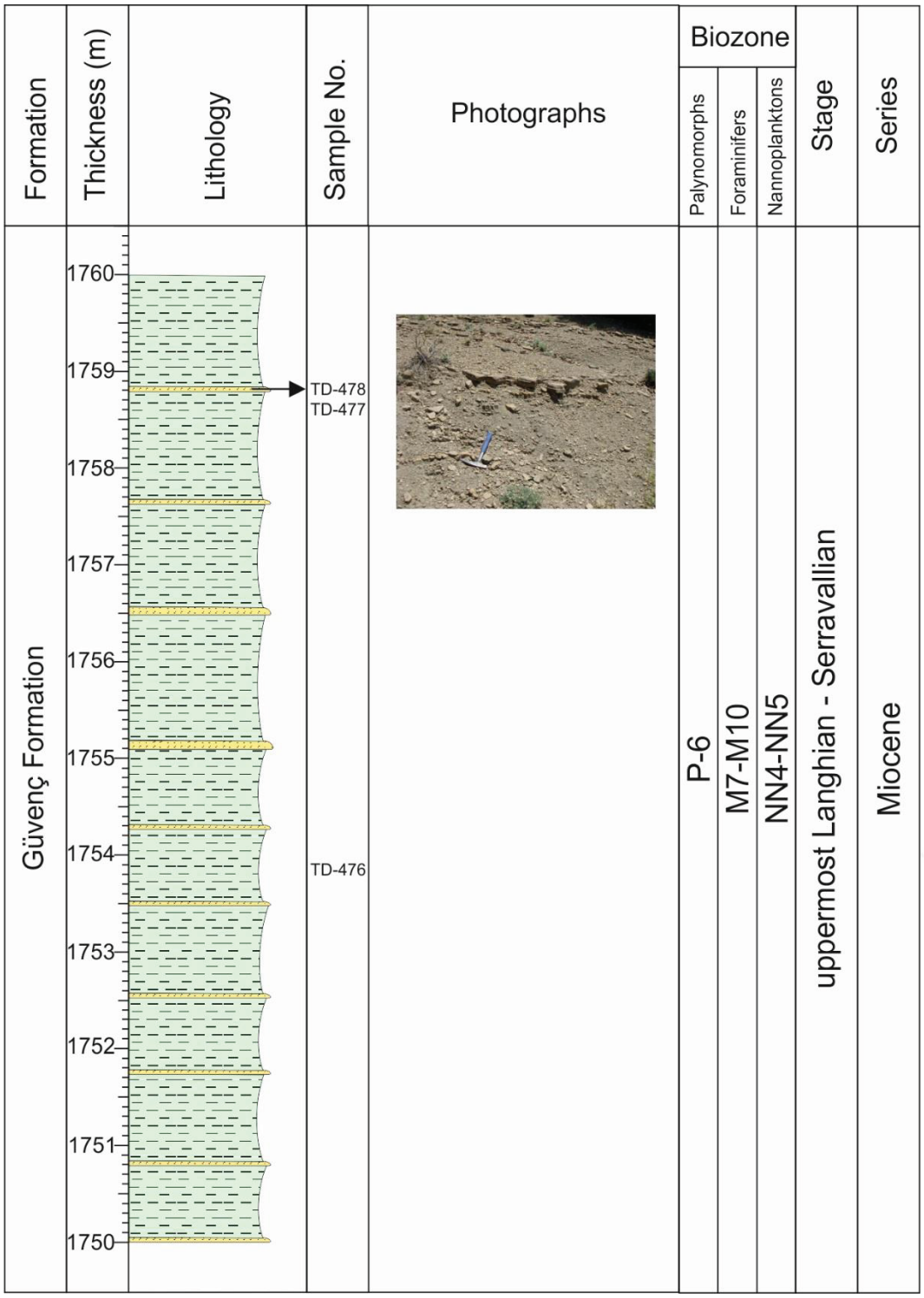

Figure 66. (cont'd)

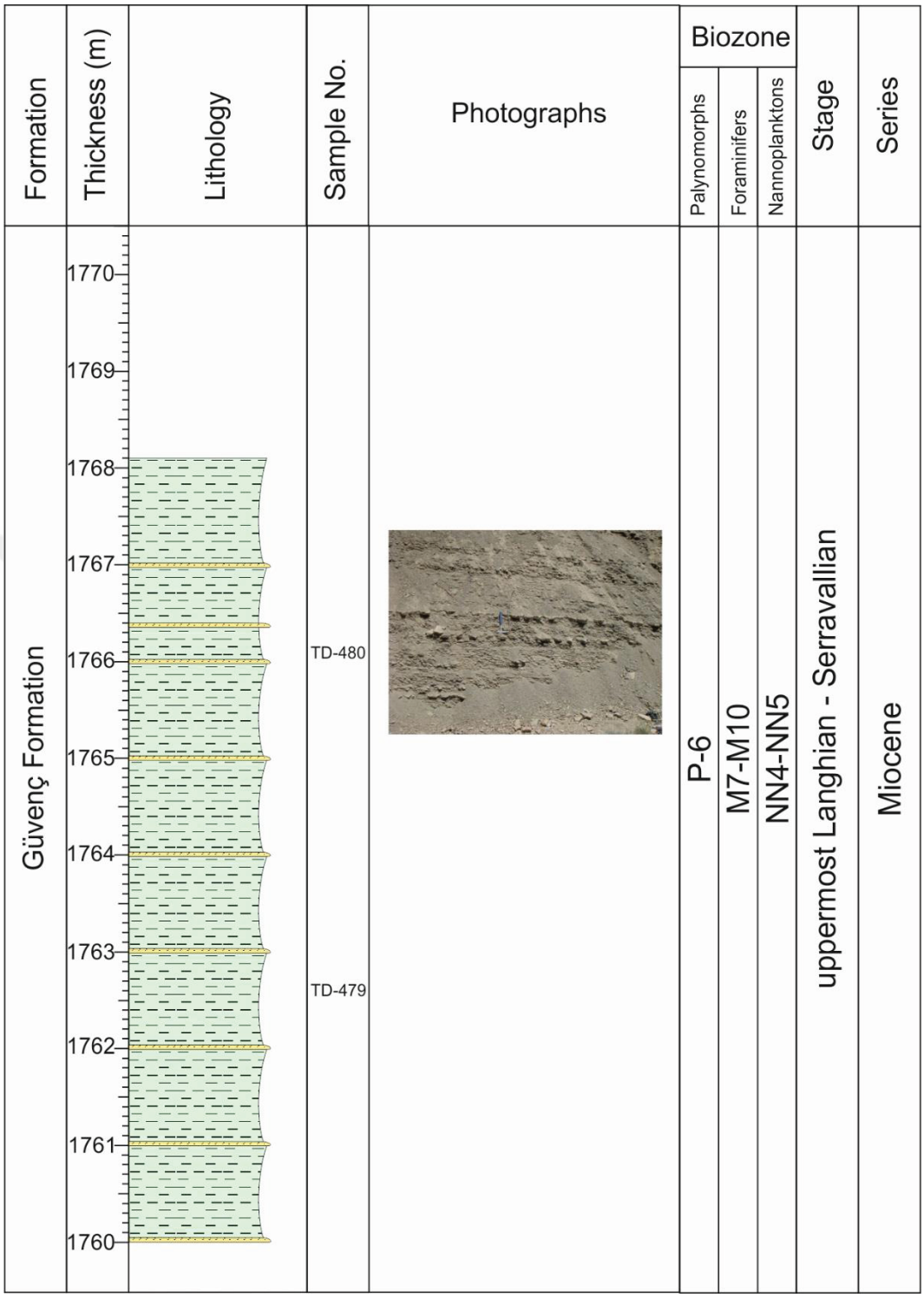

Figure 66. (cont'd)

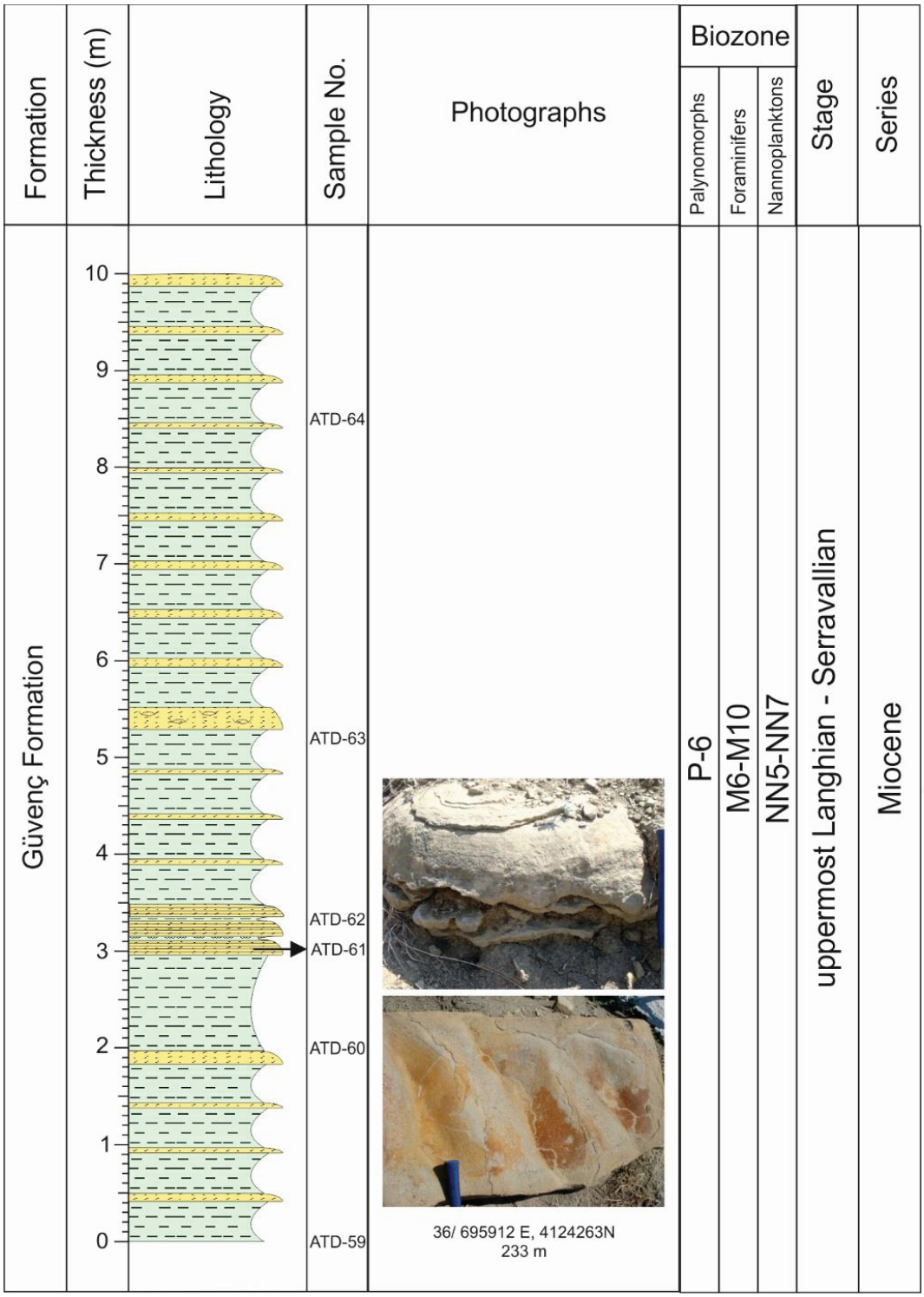

Figure 67. Koruklu Measured Stratigraphic Section.

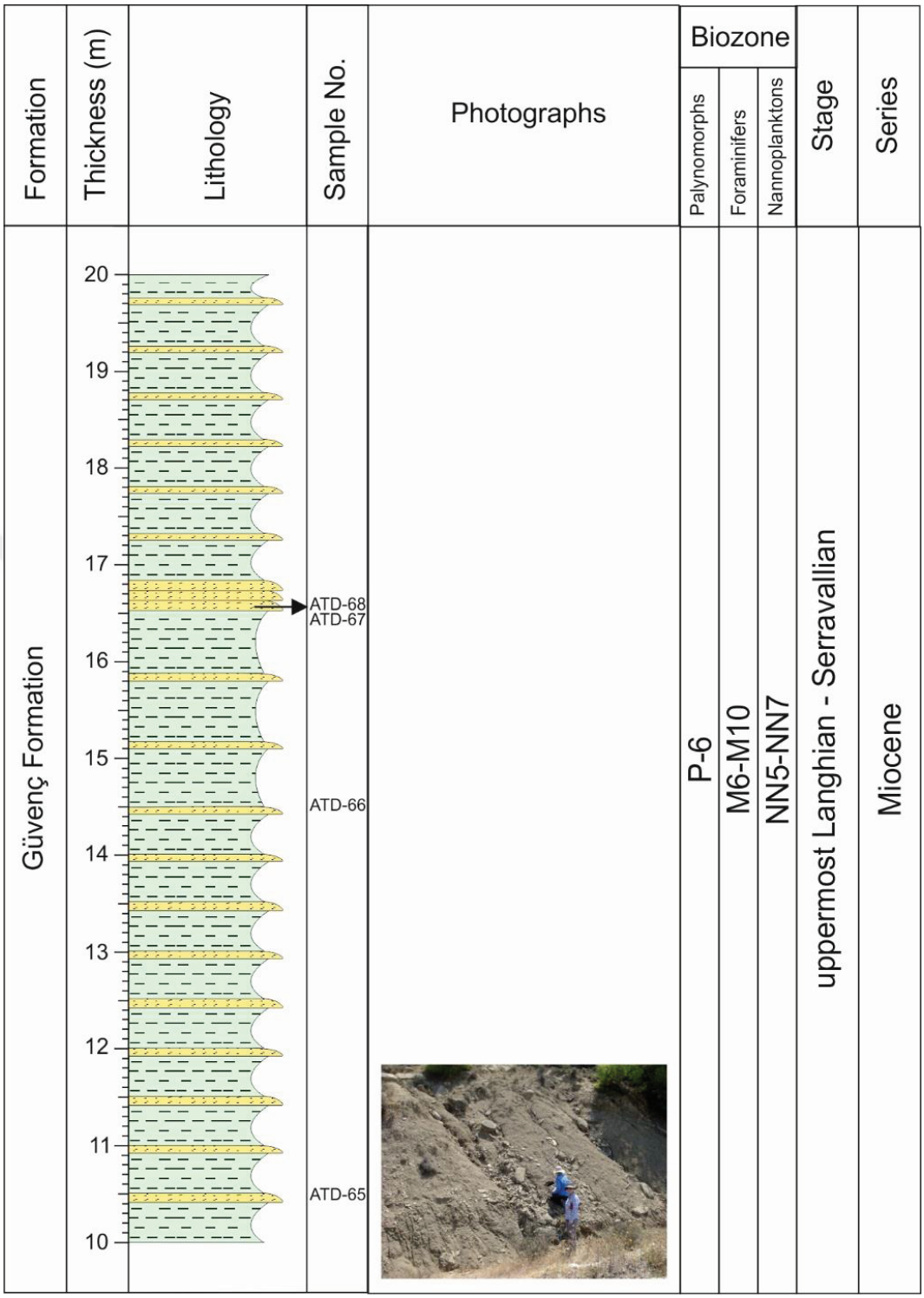

Figure 67. (cont'd)

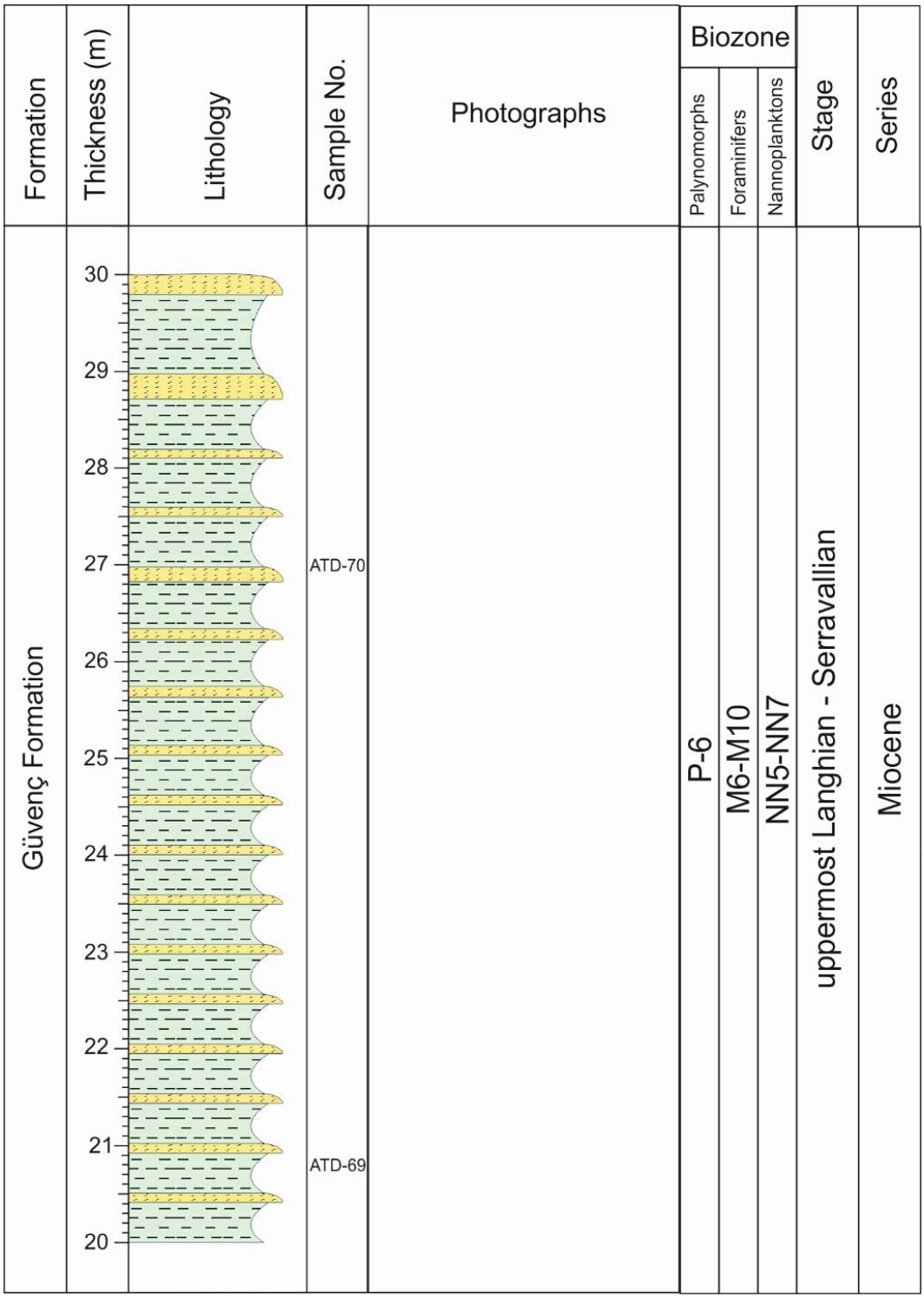

Figure 67. (cont'd)

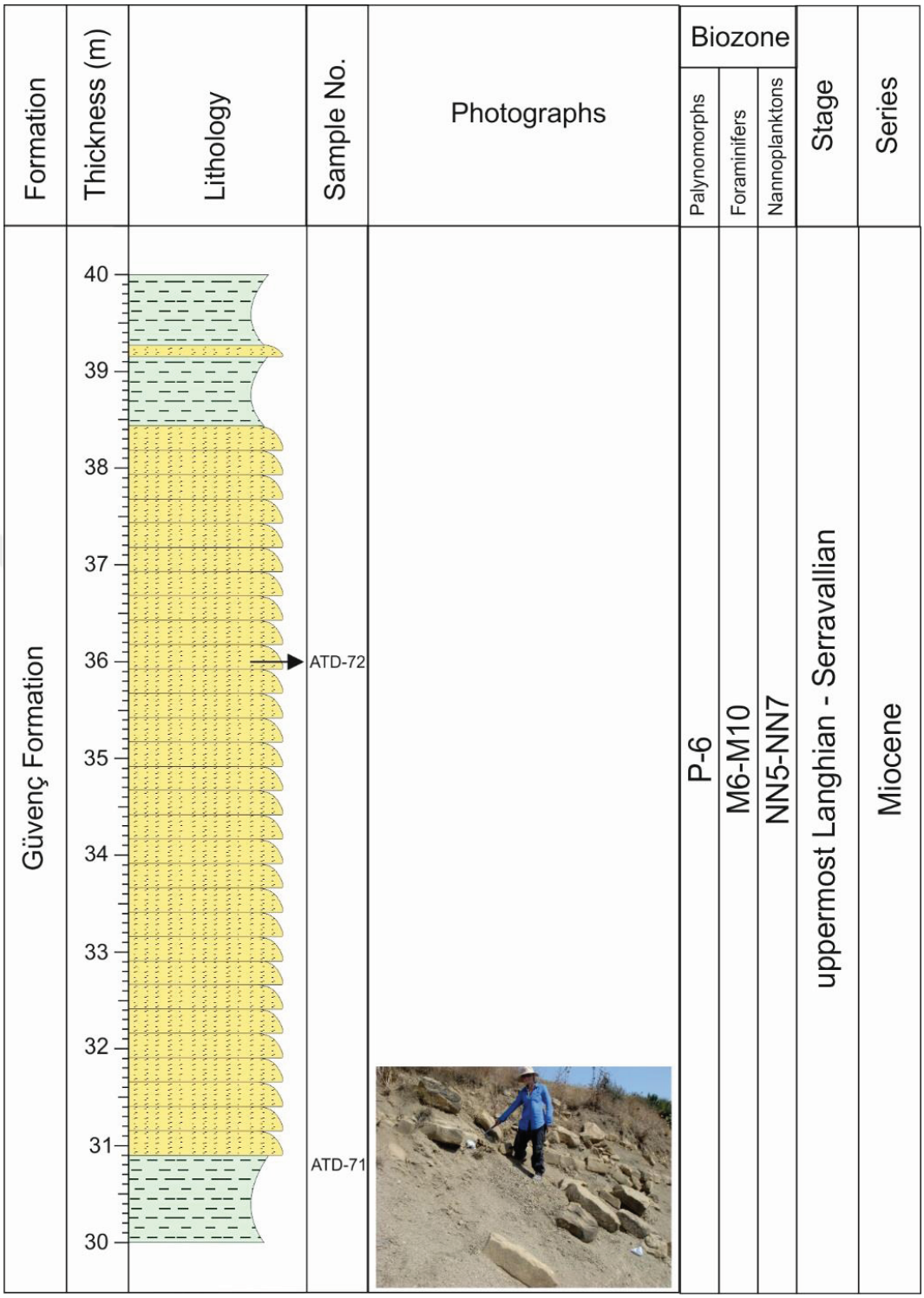

Figure 67. (cont'd)

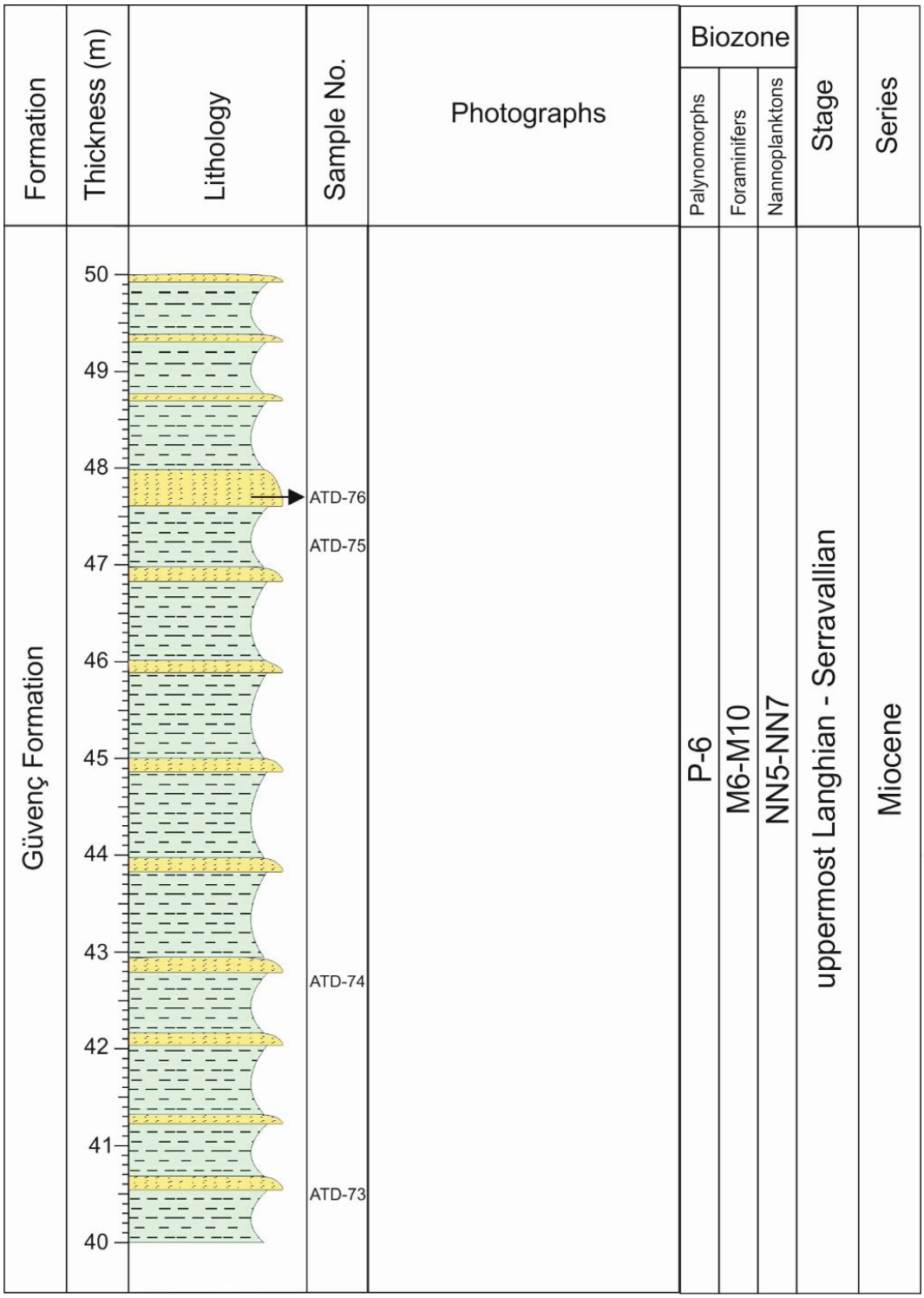

Figure 67. (cont'd)

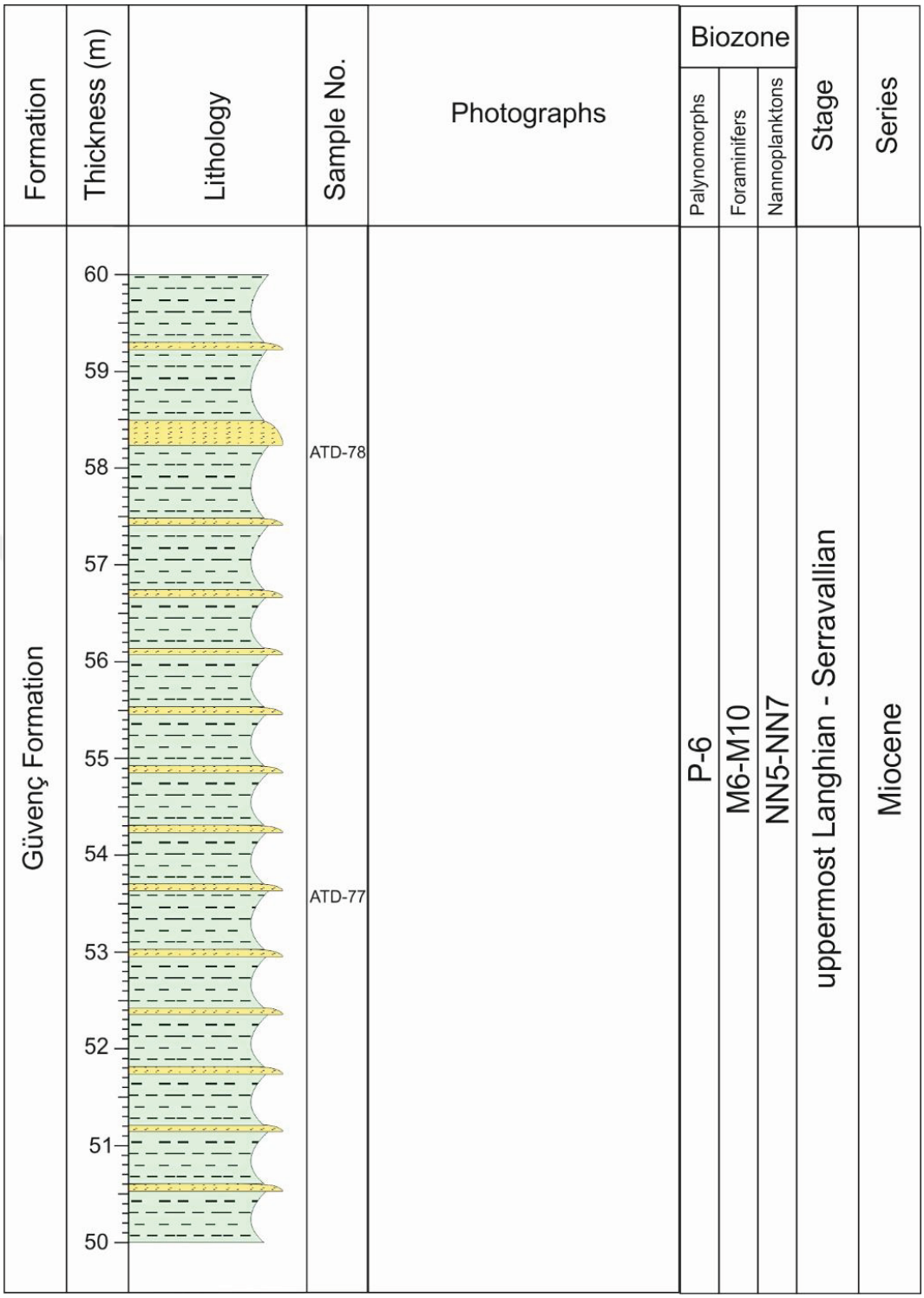

Figure 67. (cont'd)

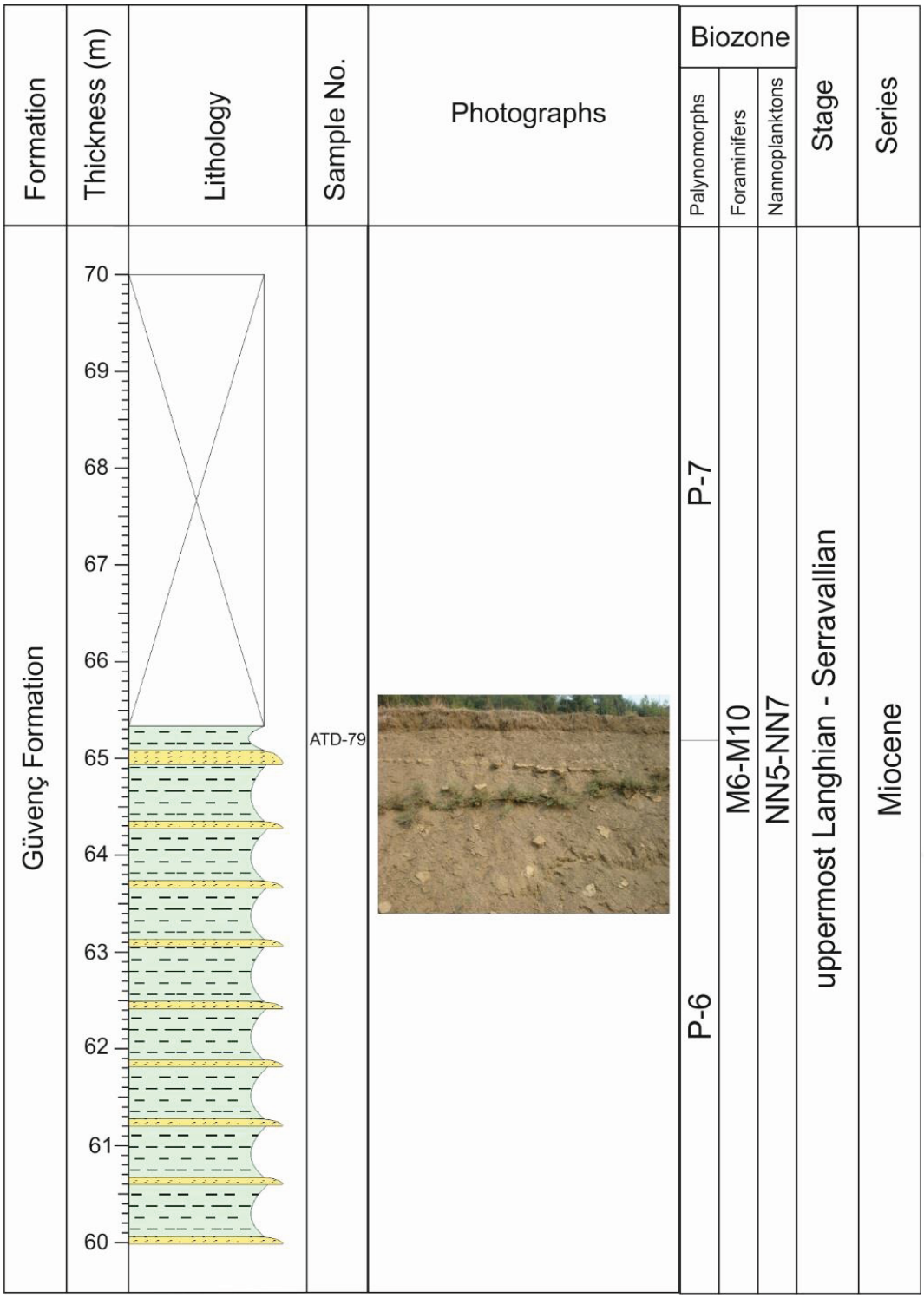

Figure 67. (cont'd)

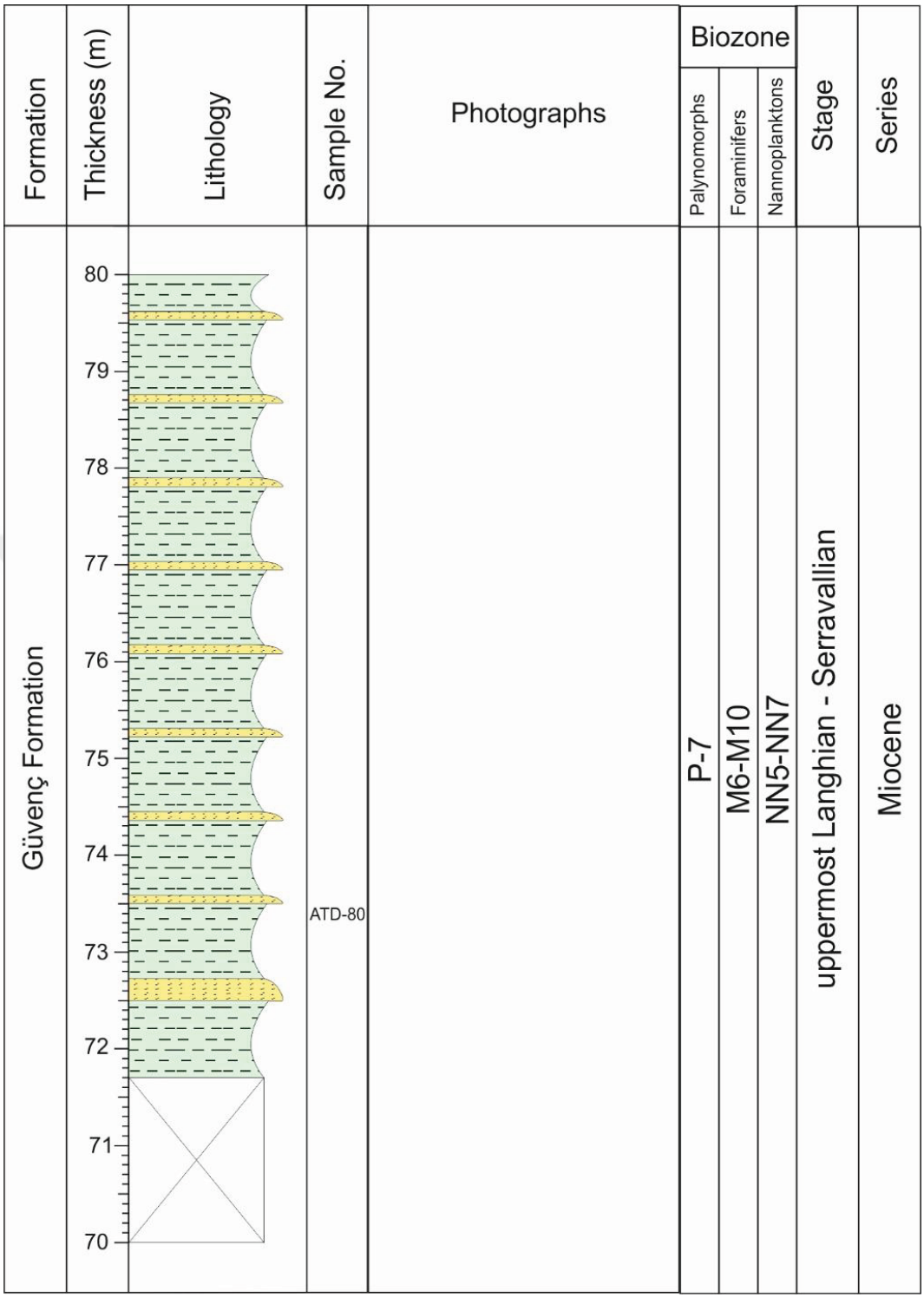

Figure 67. (cont'd)

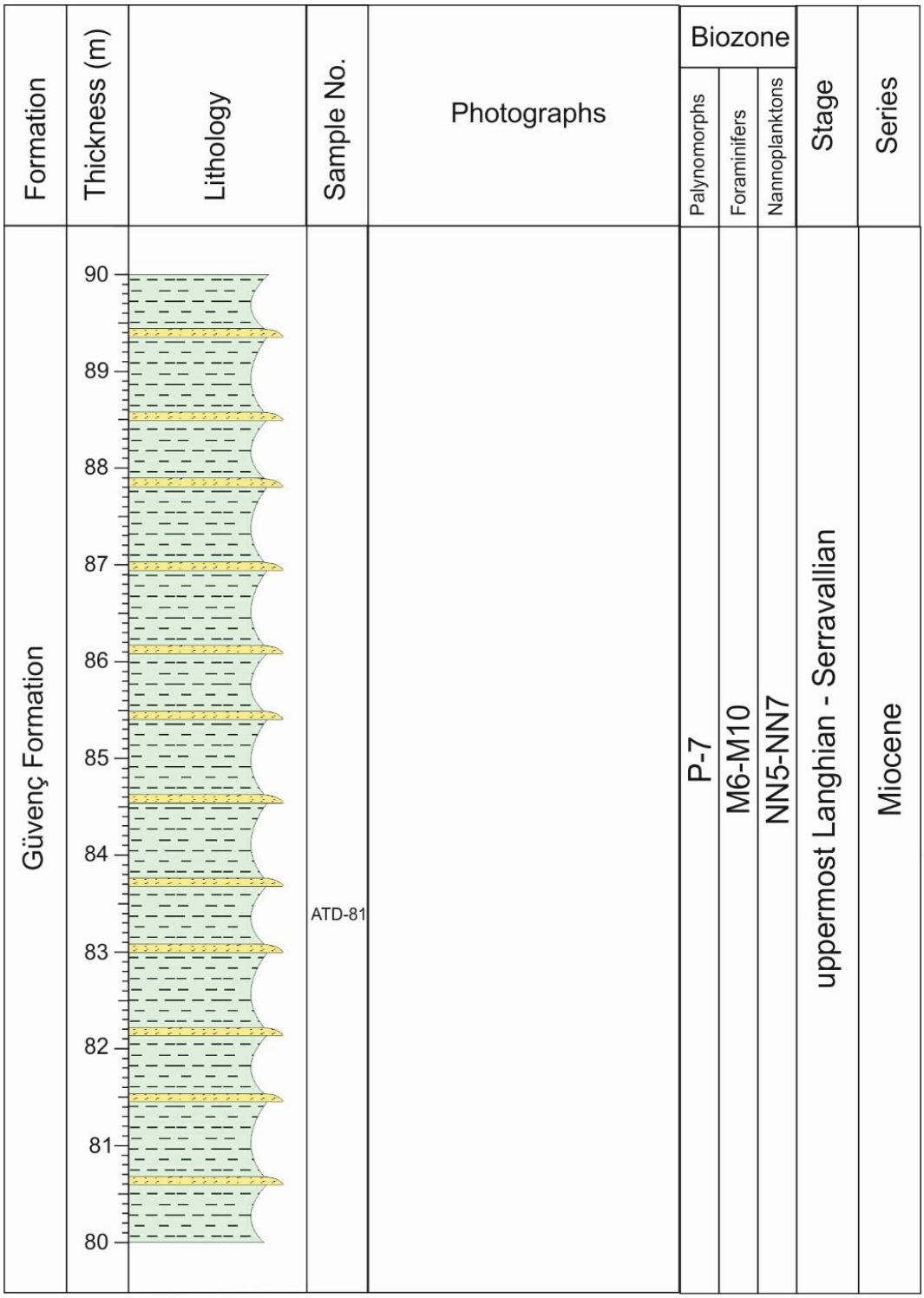

Figure 67. (cont'd)

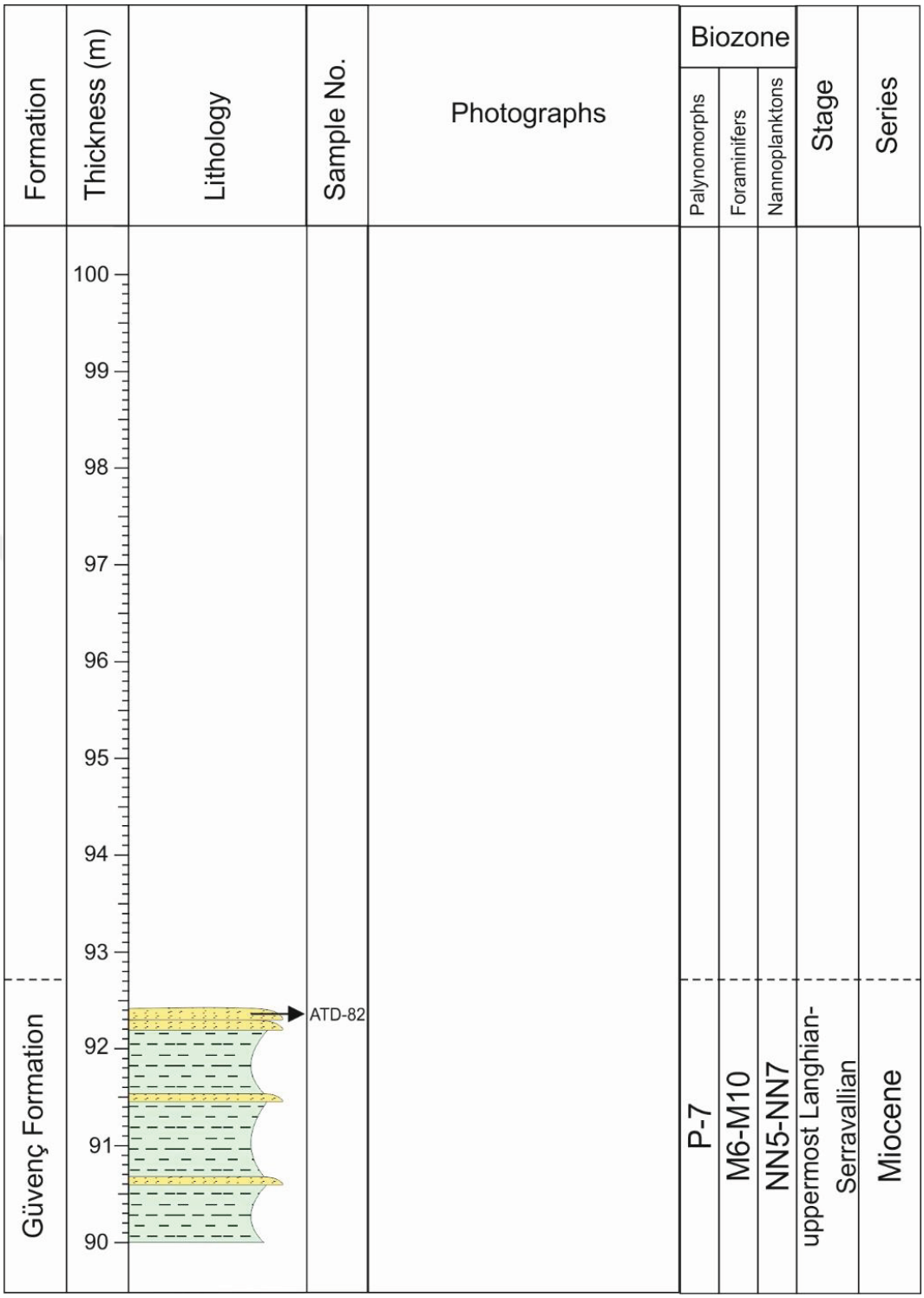

Figure 67. (cont'd)

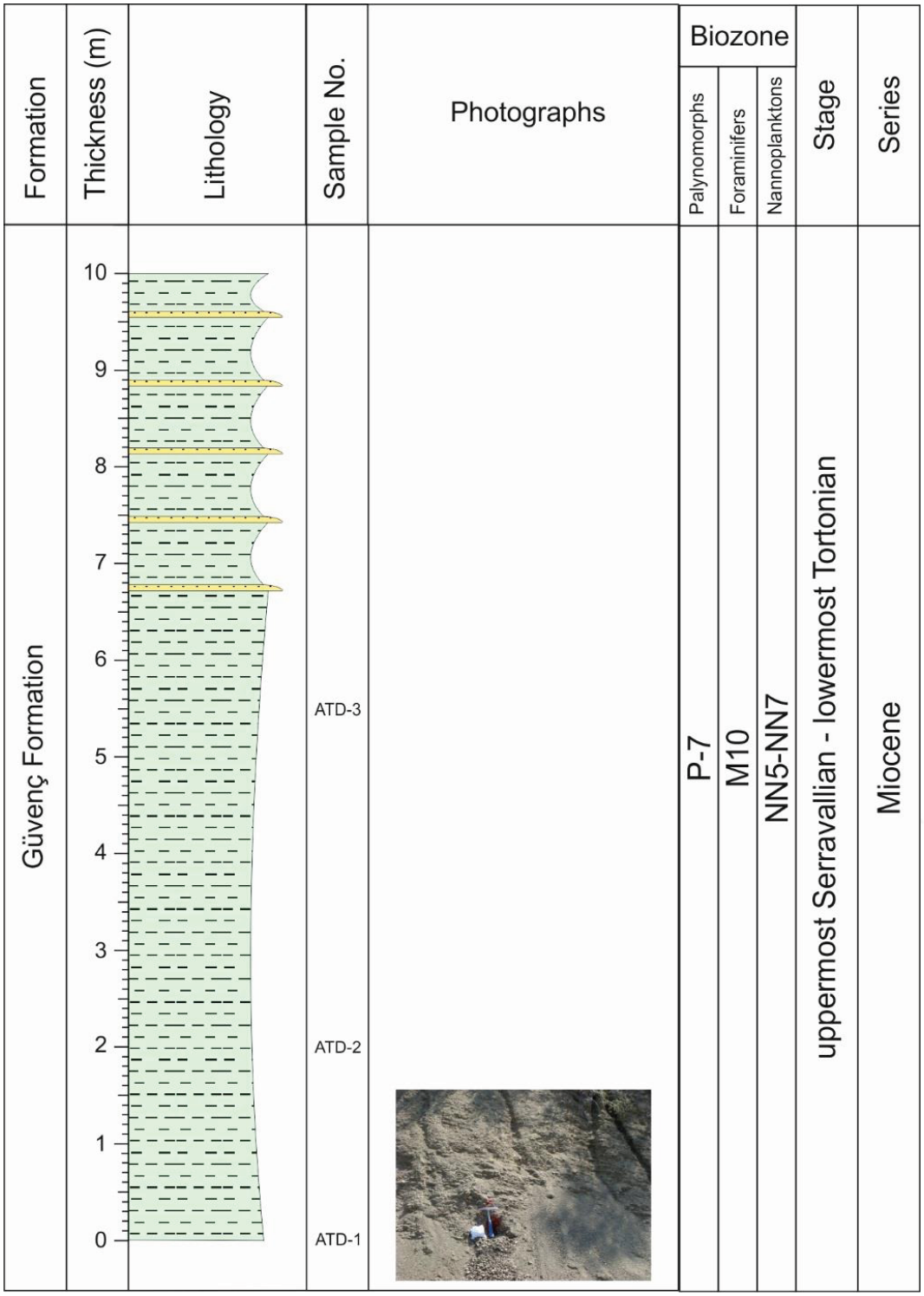

Figure 68. Bekirli Measured Stratigraphic Section.

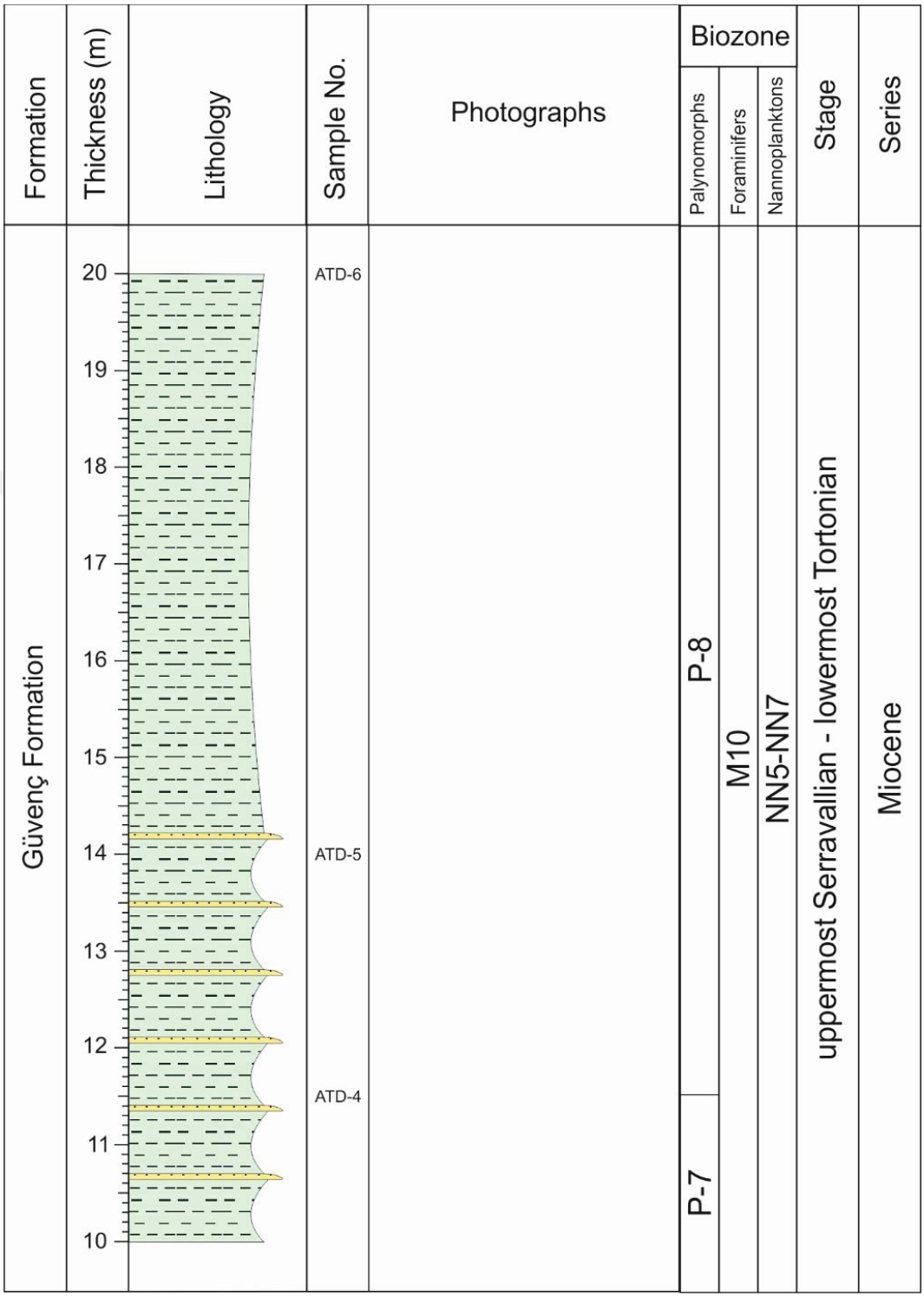

Figure 68. (cont'd)

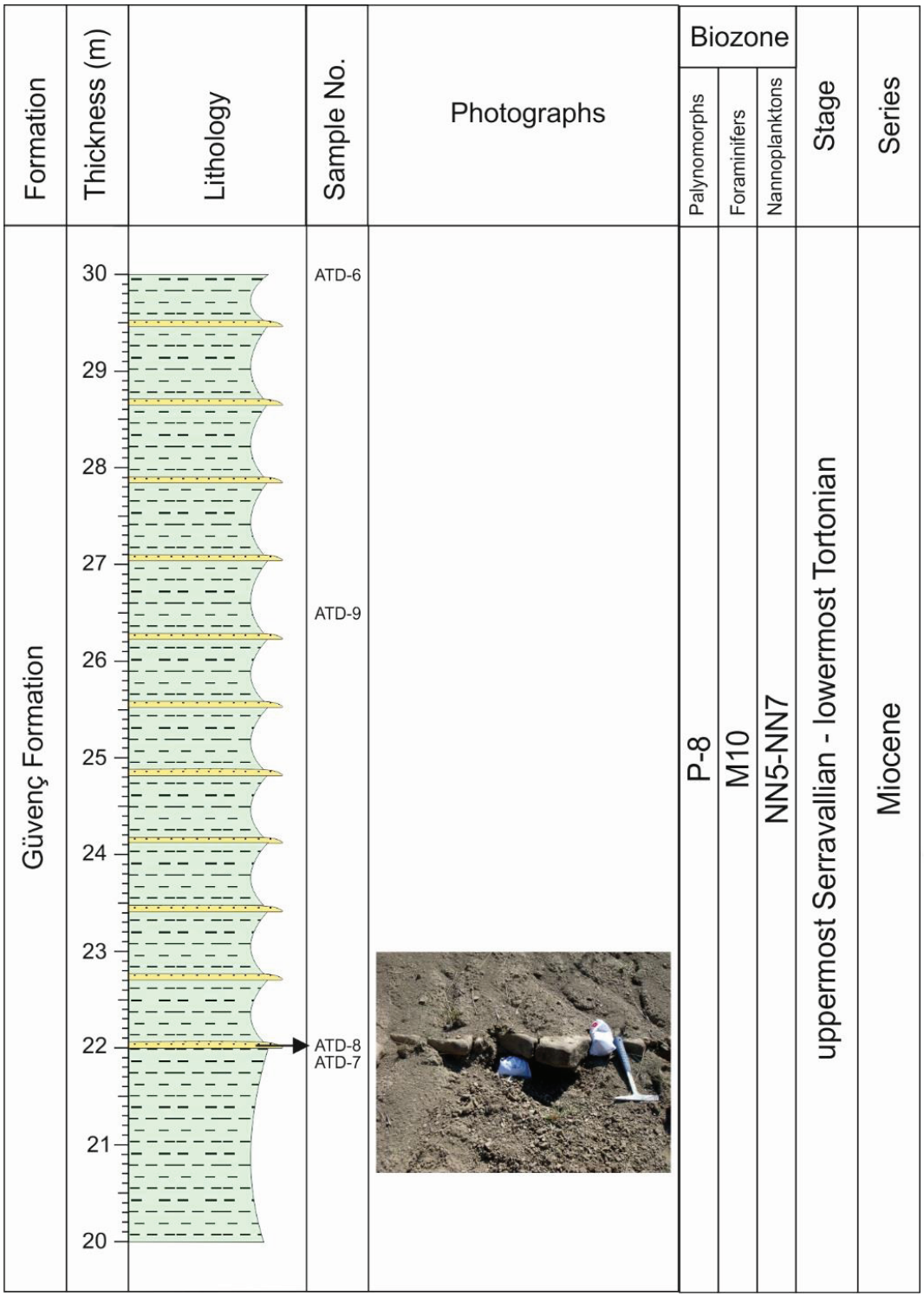

Figure 68. (cont'd)

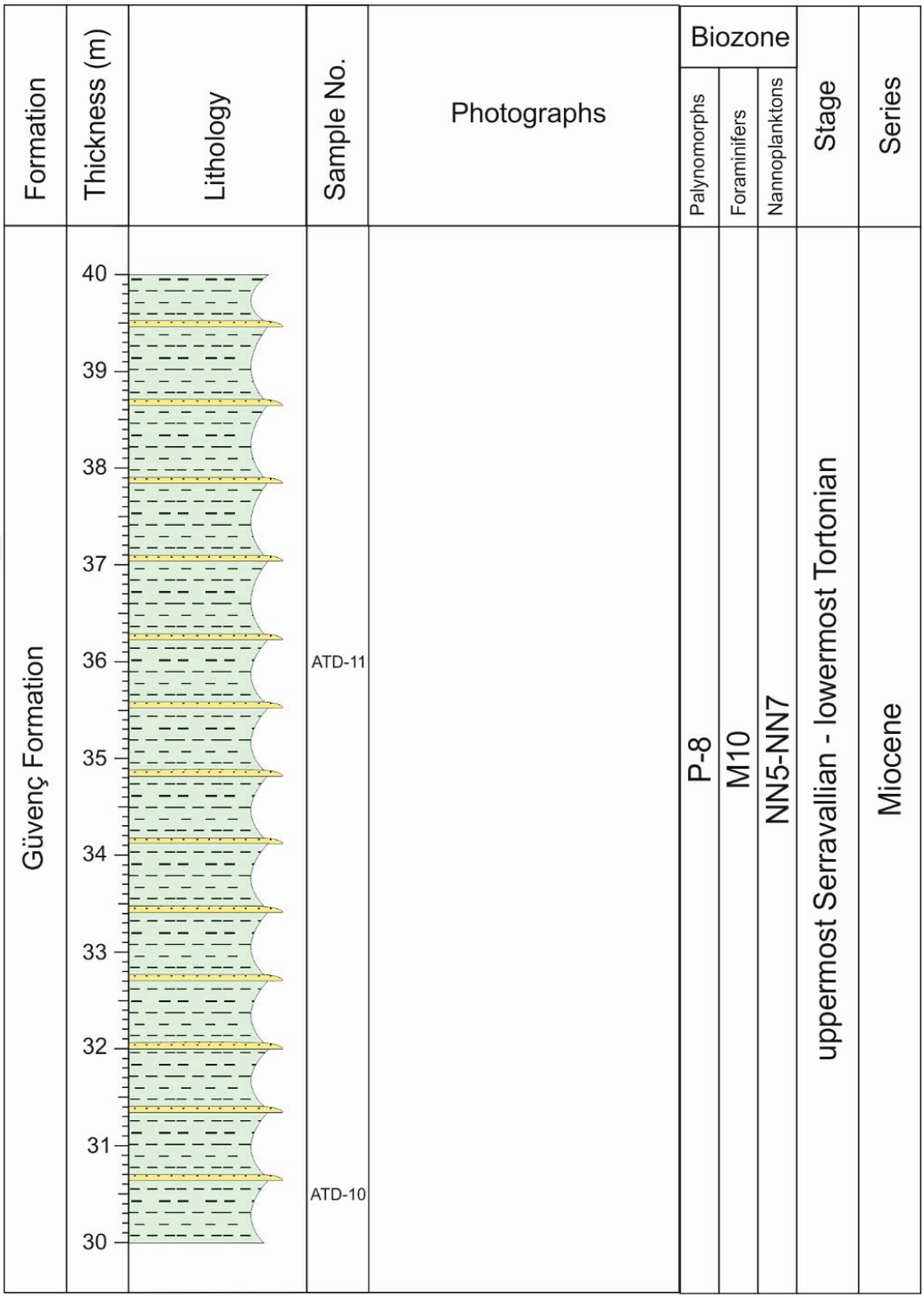

Figure 68. (cont'd)

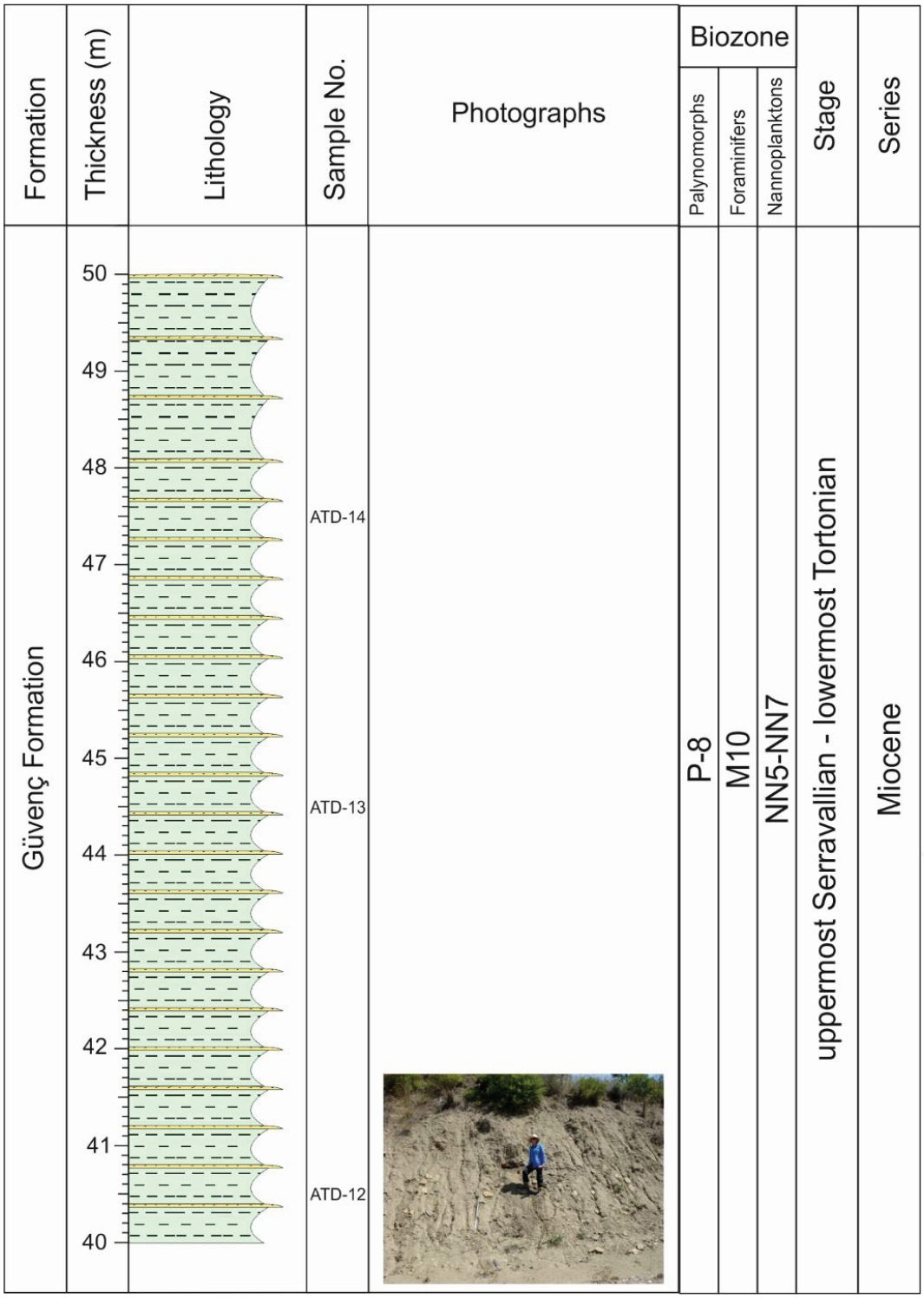

Figure 68. (cont'd)

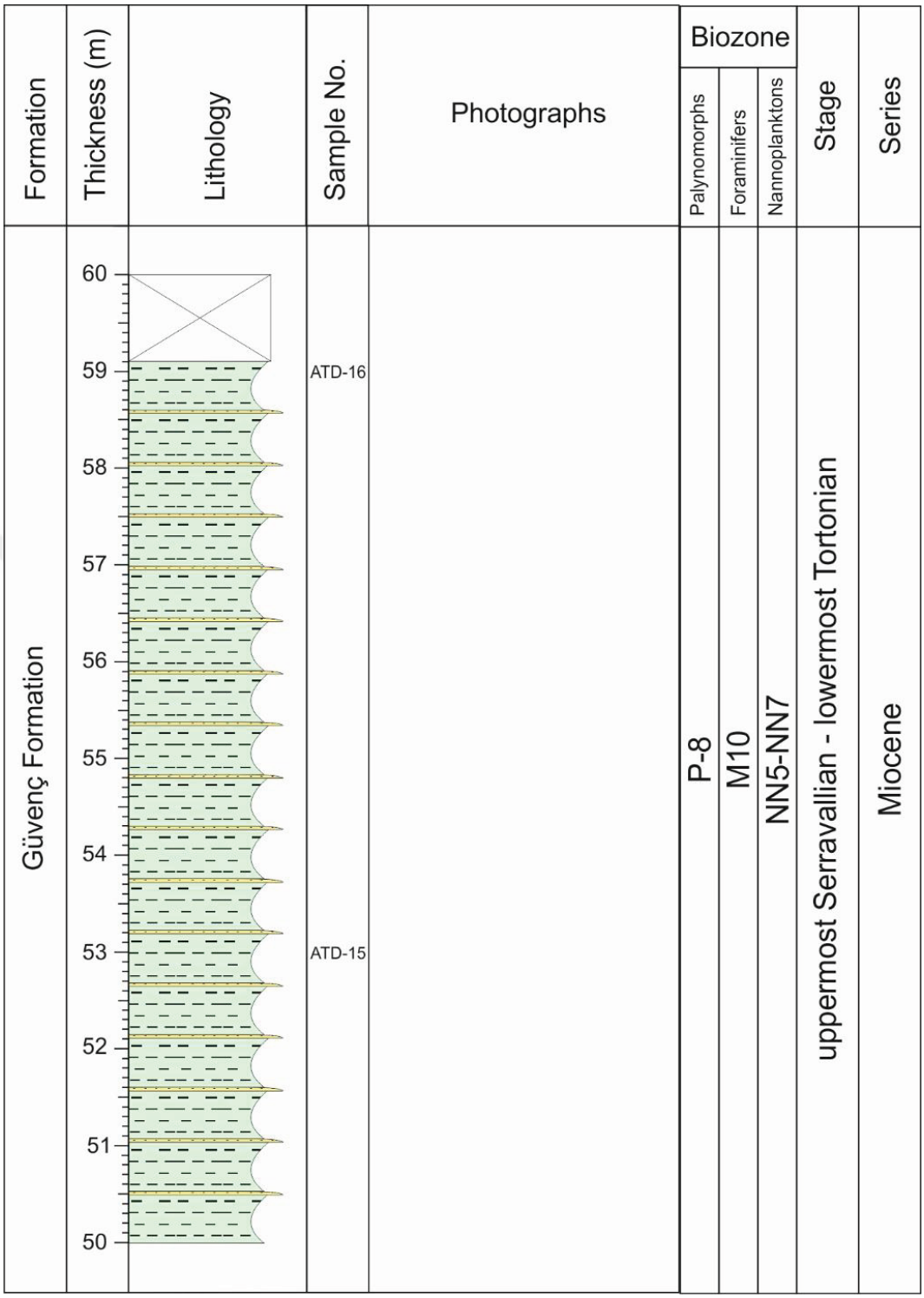

Figure 68. (cont'd)

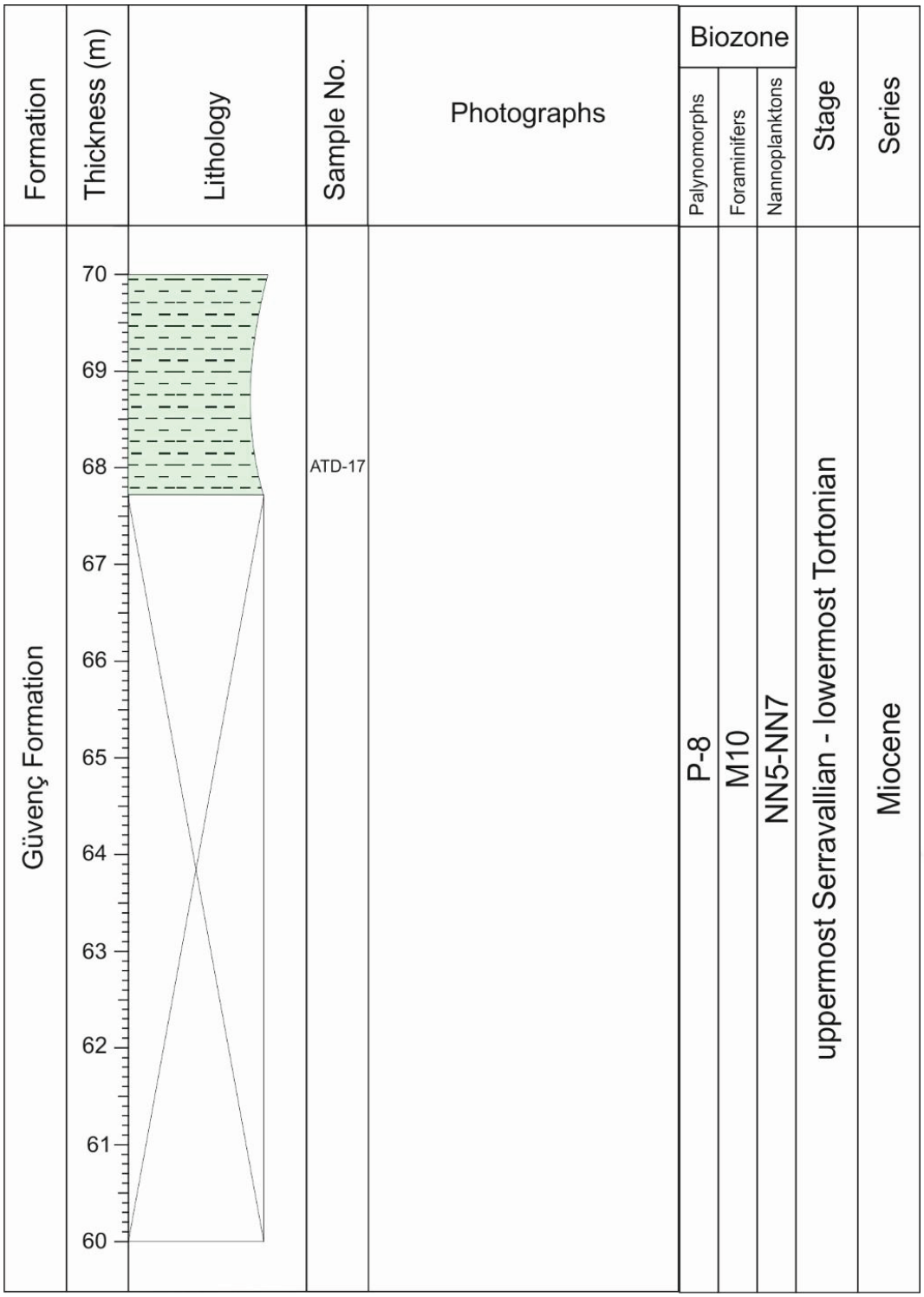

Figure 68. (cont'd)

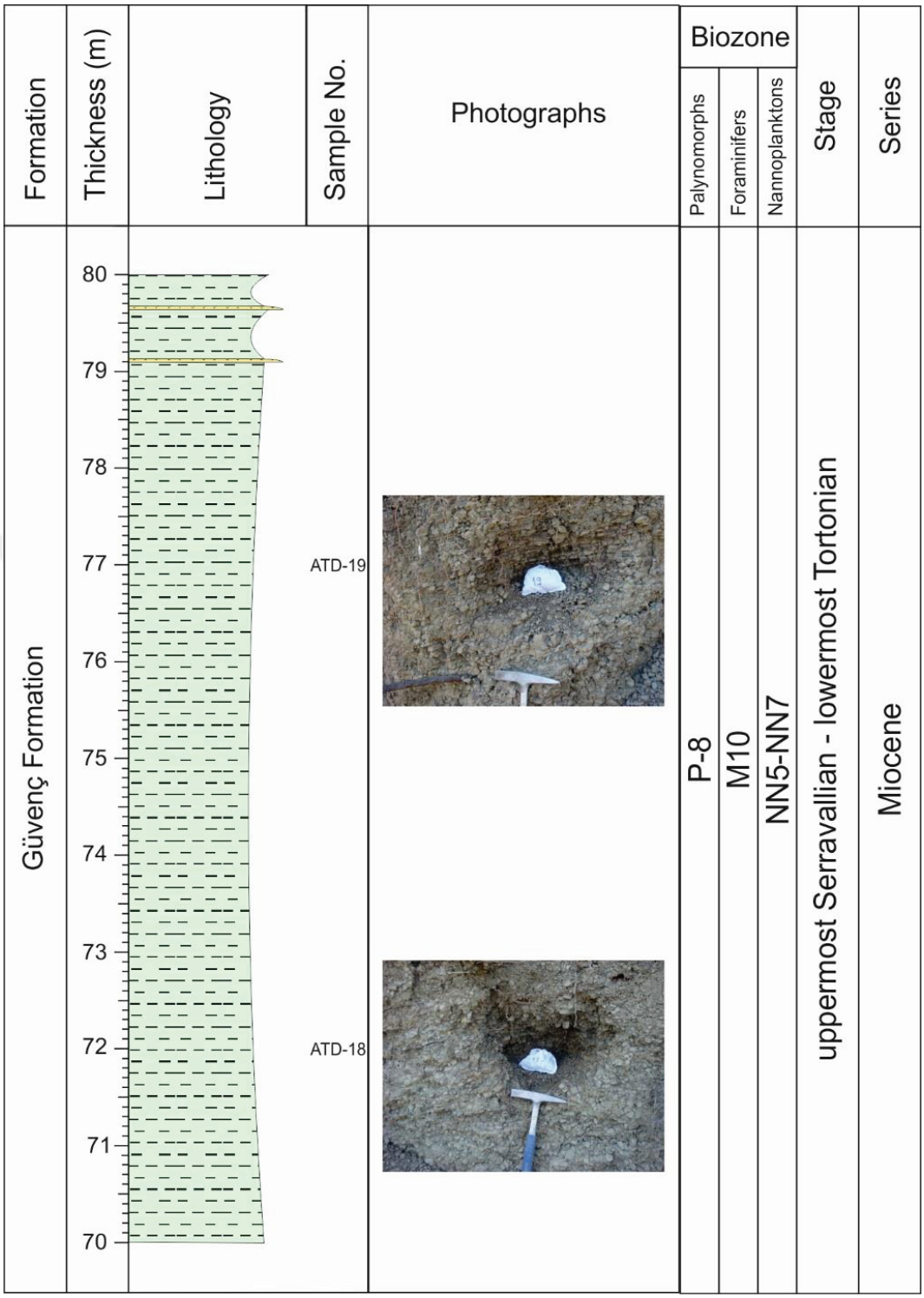

Figure 68. (cont'd)

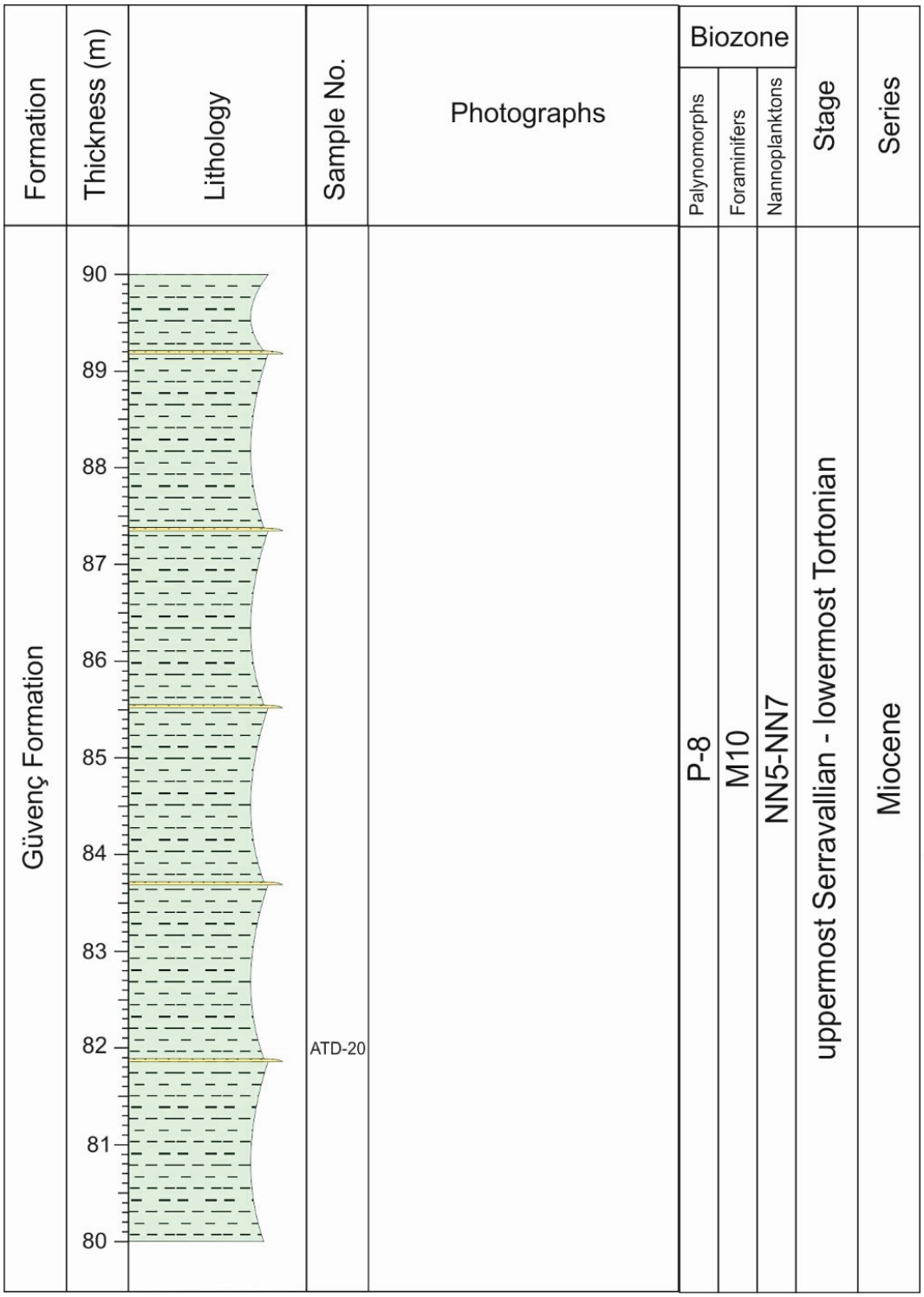

Figure 68. (cont'd)

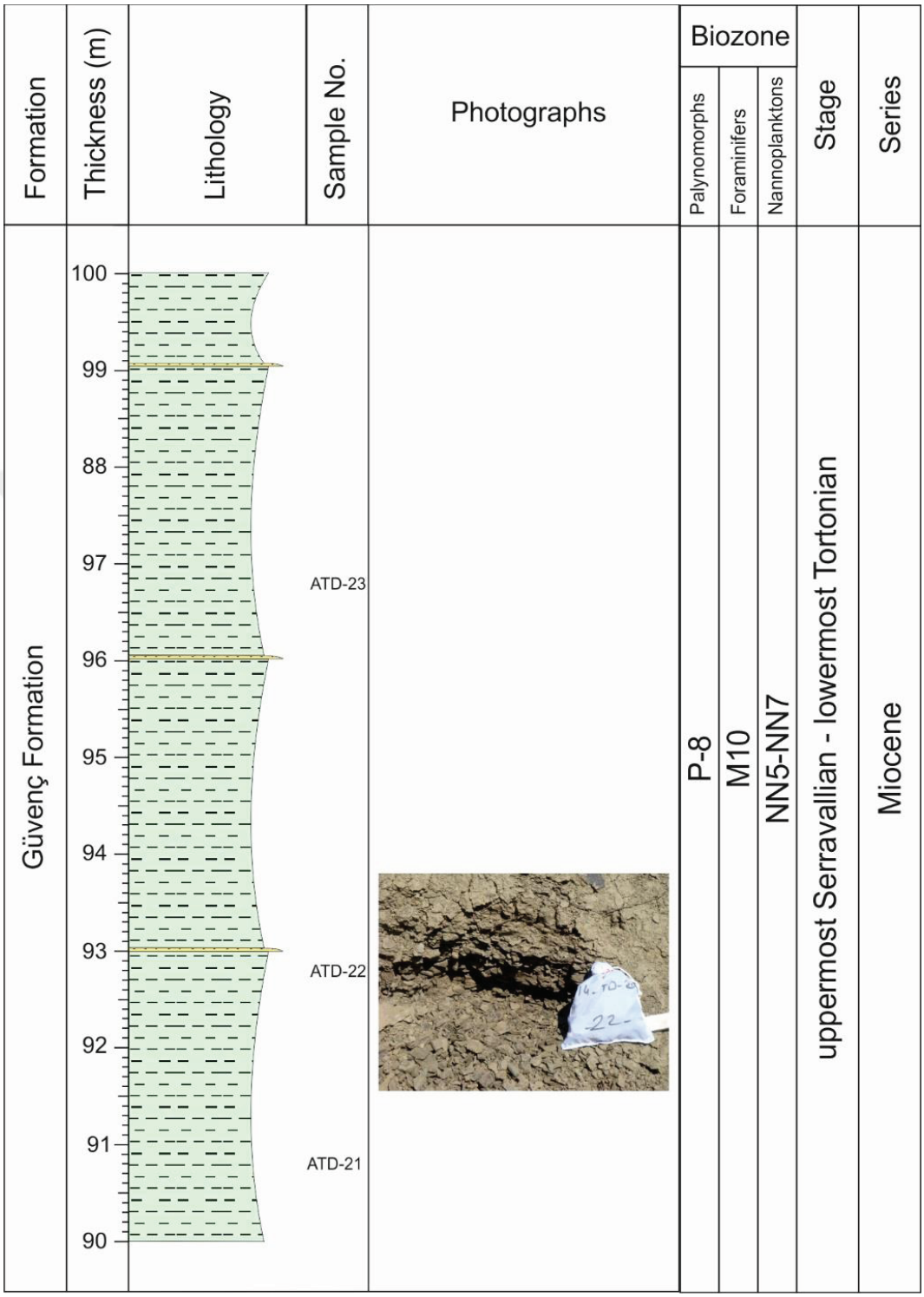

Figure 68. (cont'd)

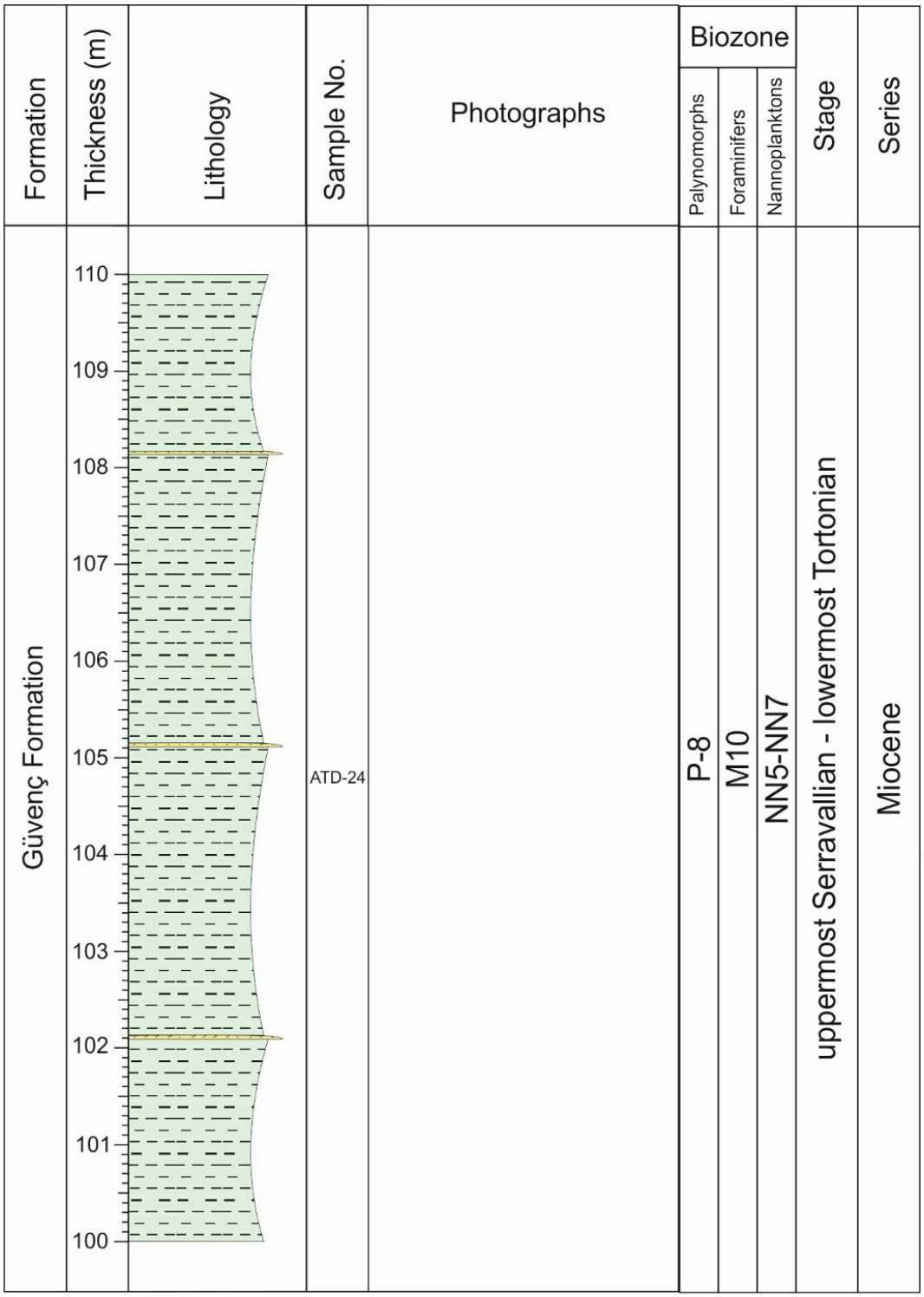

Figure 68. (cont'd)

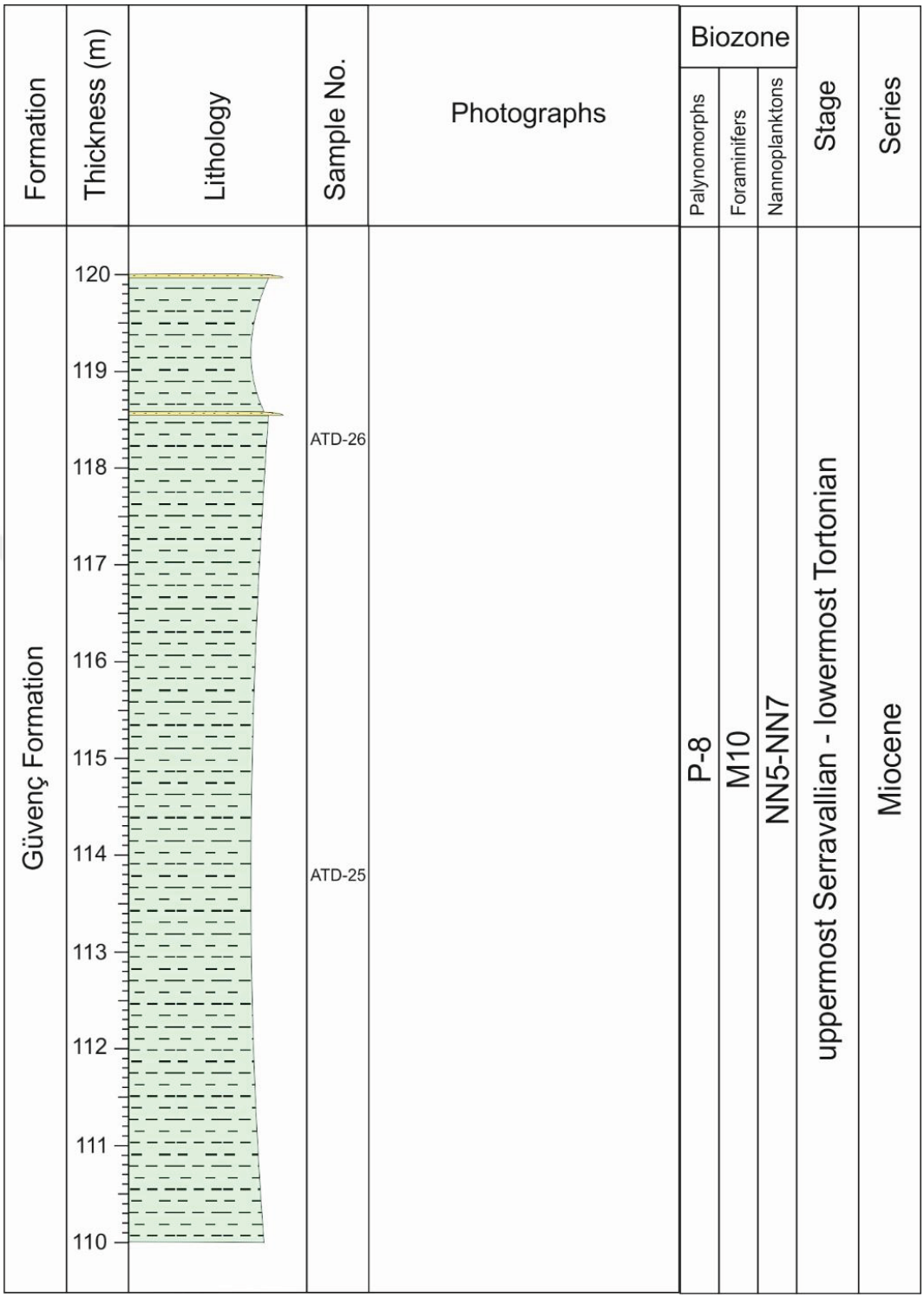

Figure 68. (cont'd)

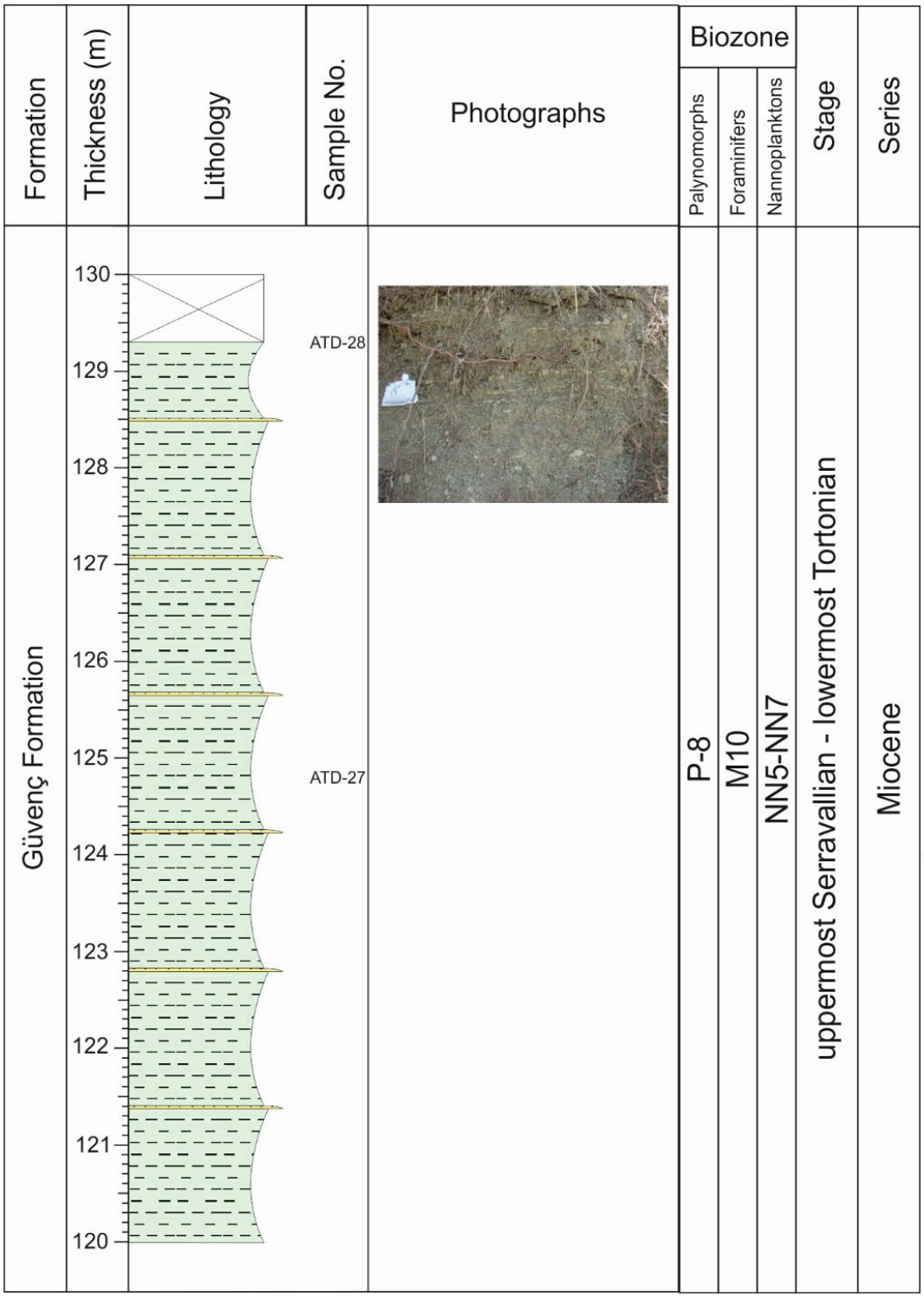

Figure 68. (cont'd)

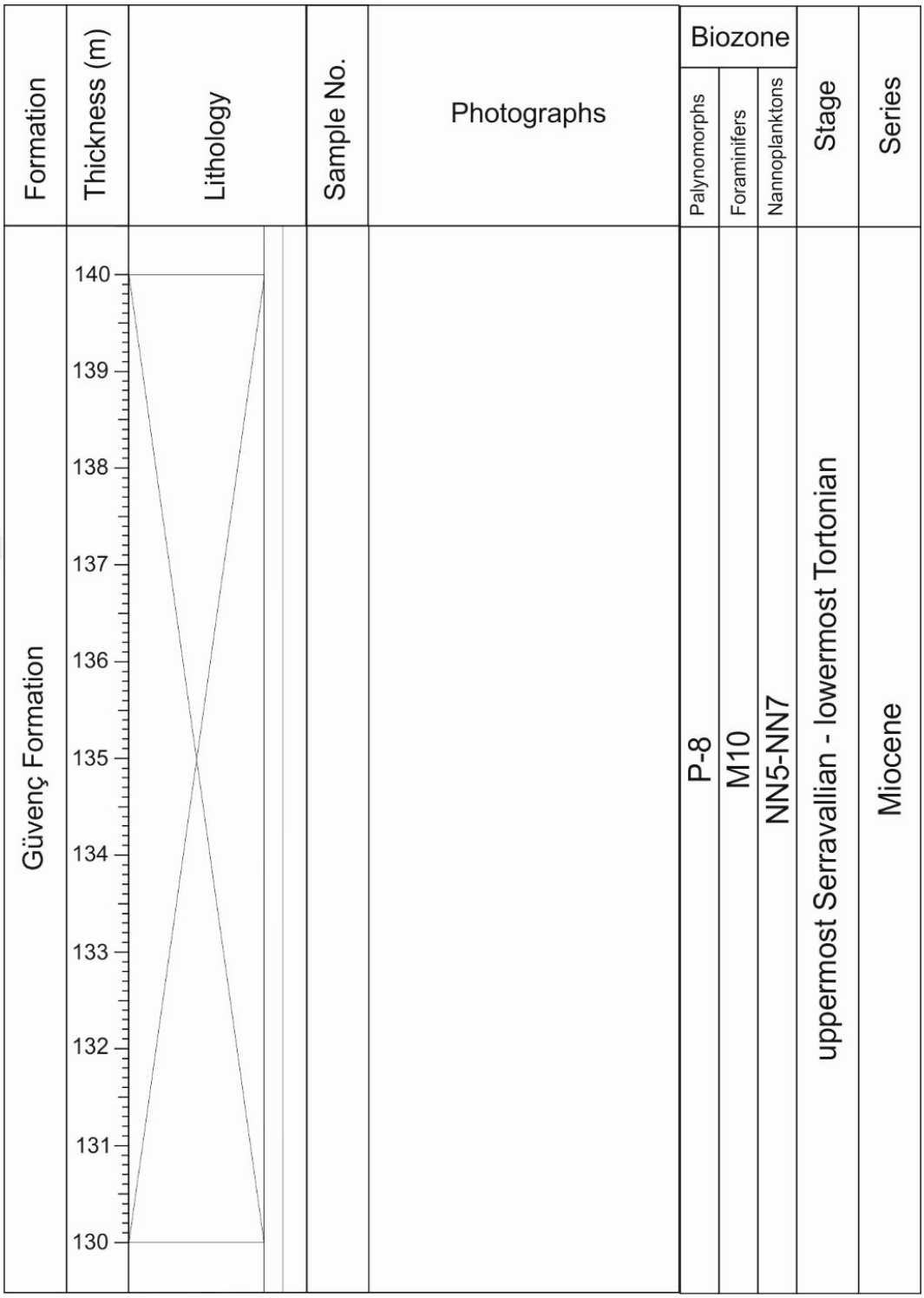

Figure 68. (cont'd)

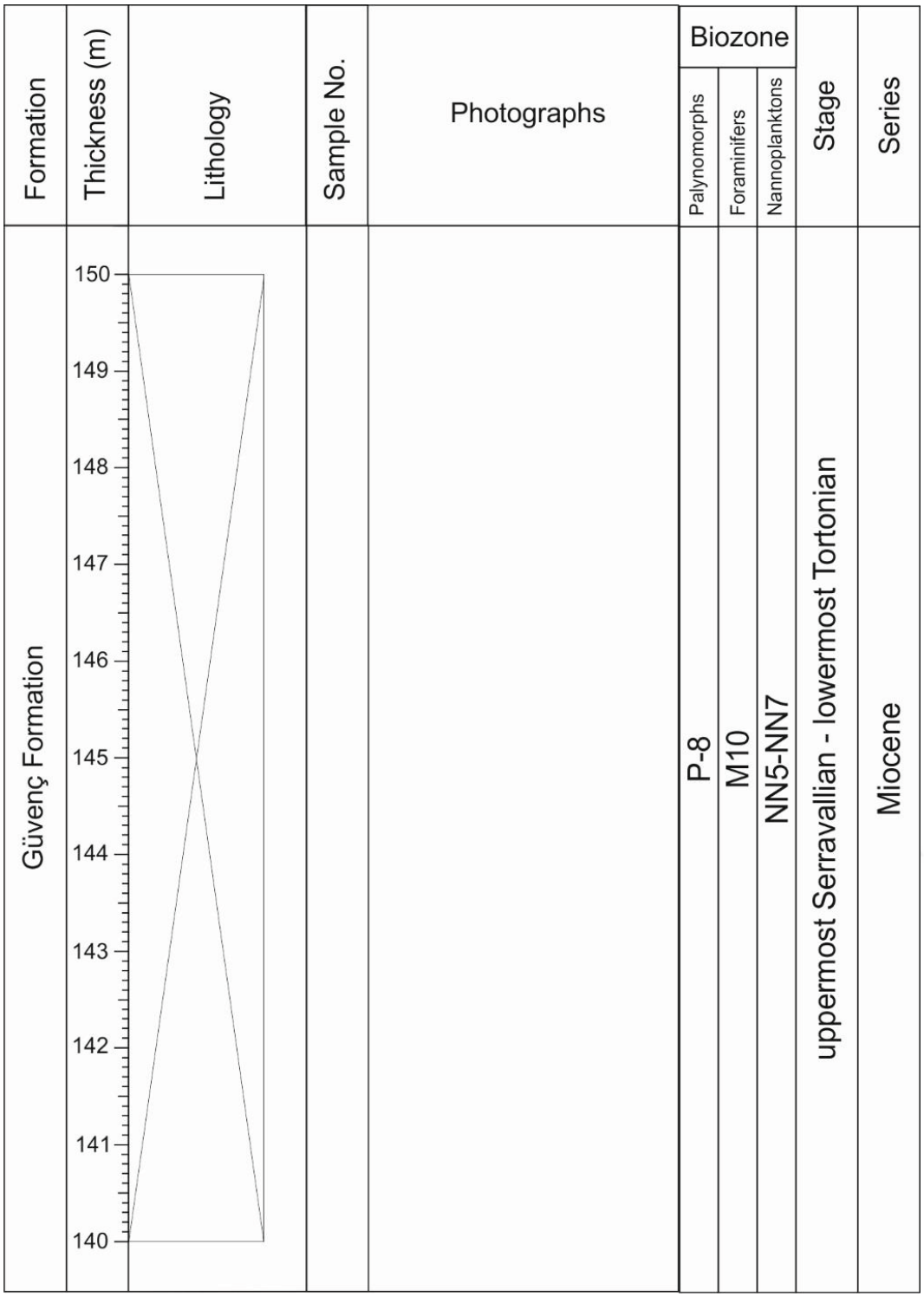

Figure 68. (cont'd)

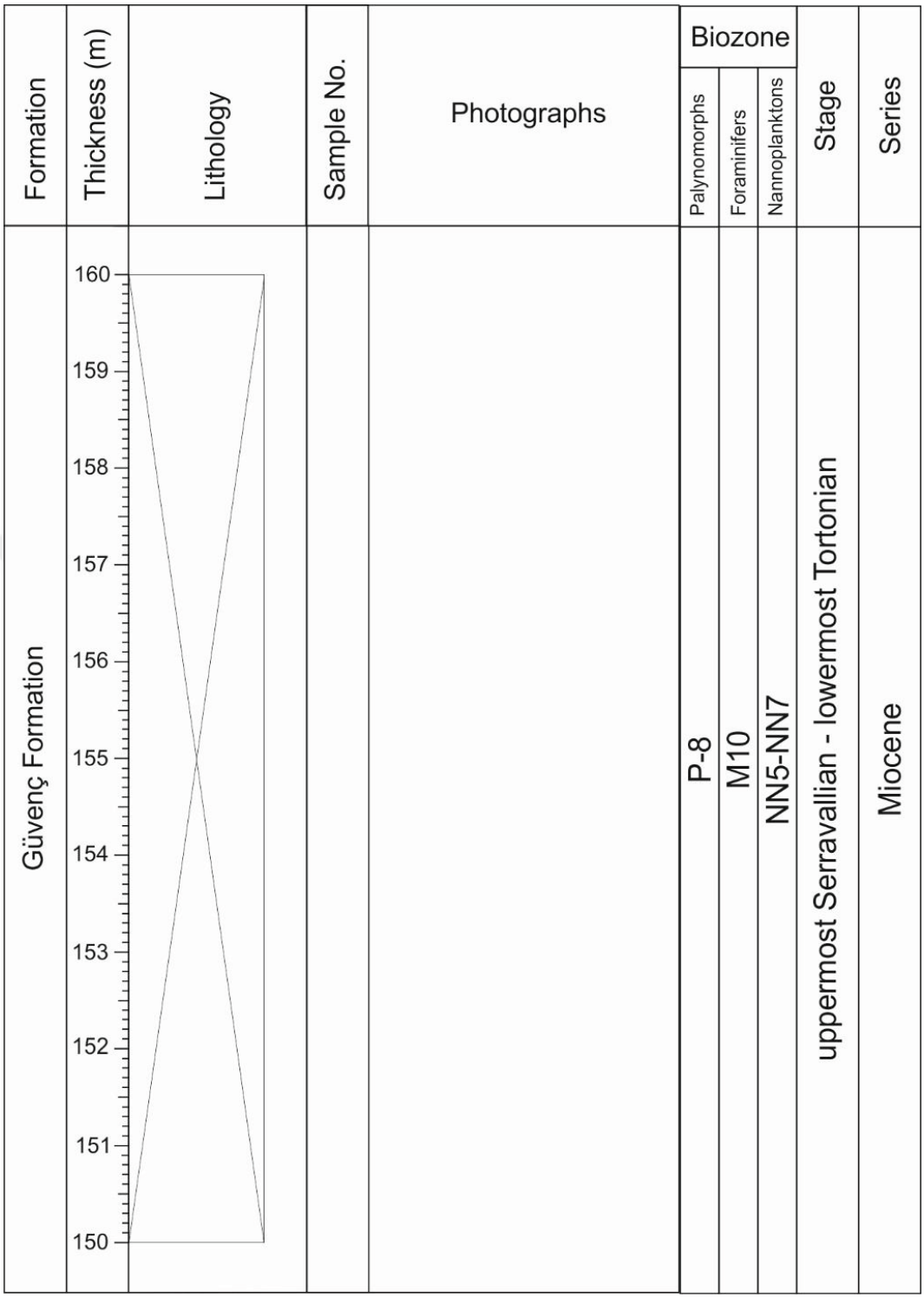

Figure 68. (cont'd)

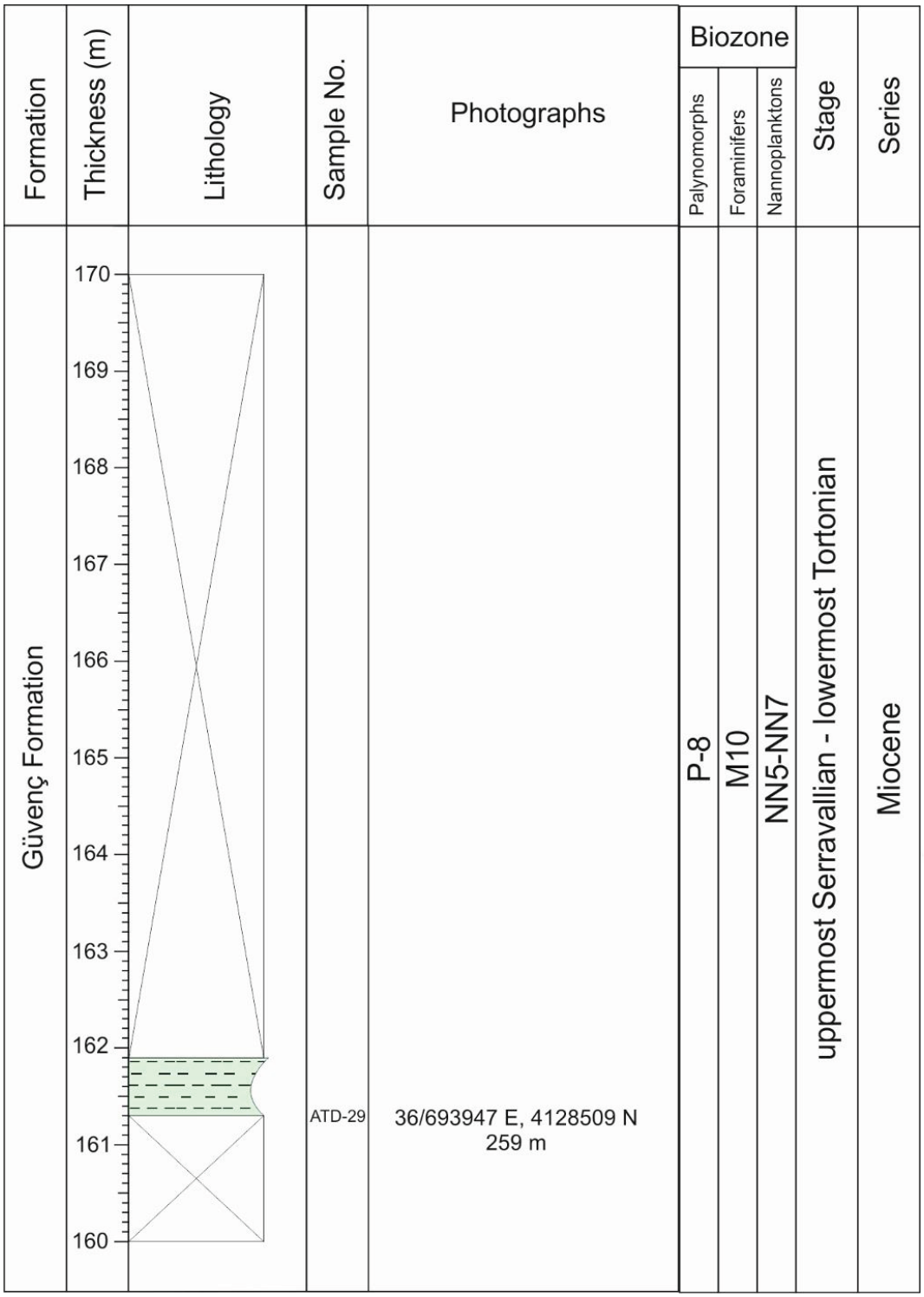

Figure 68. (cont'd)

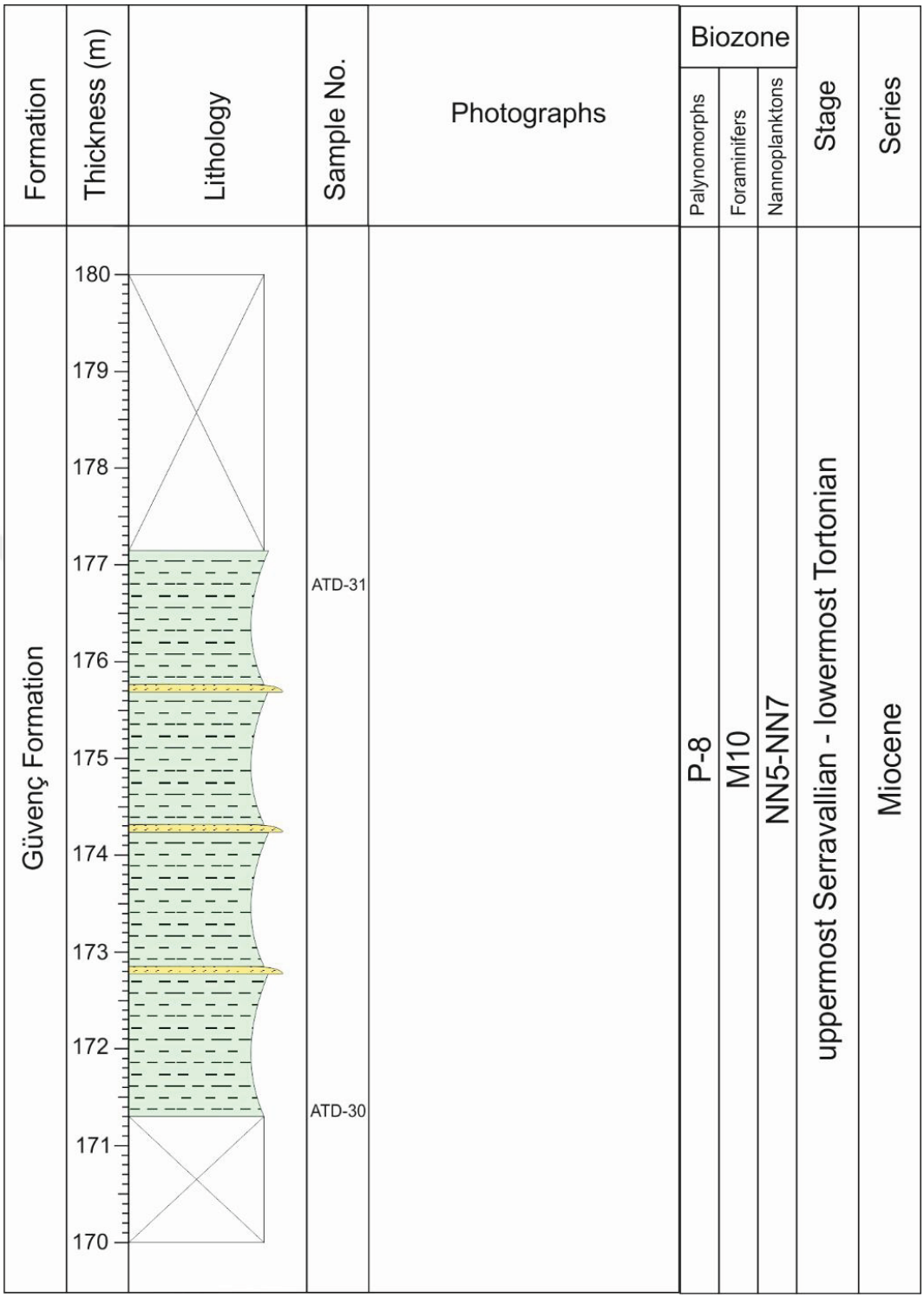

Figure 68. (cont'd)

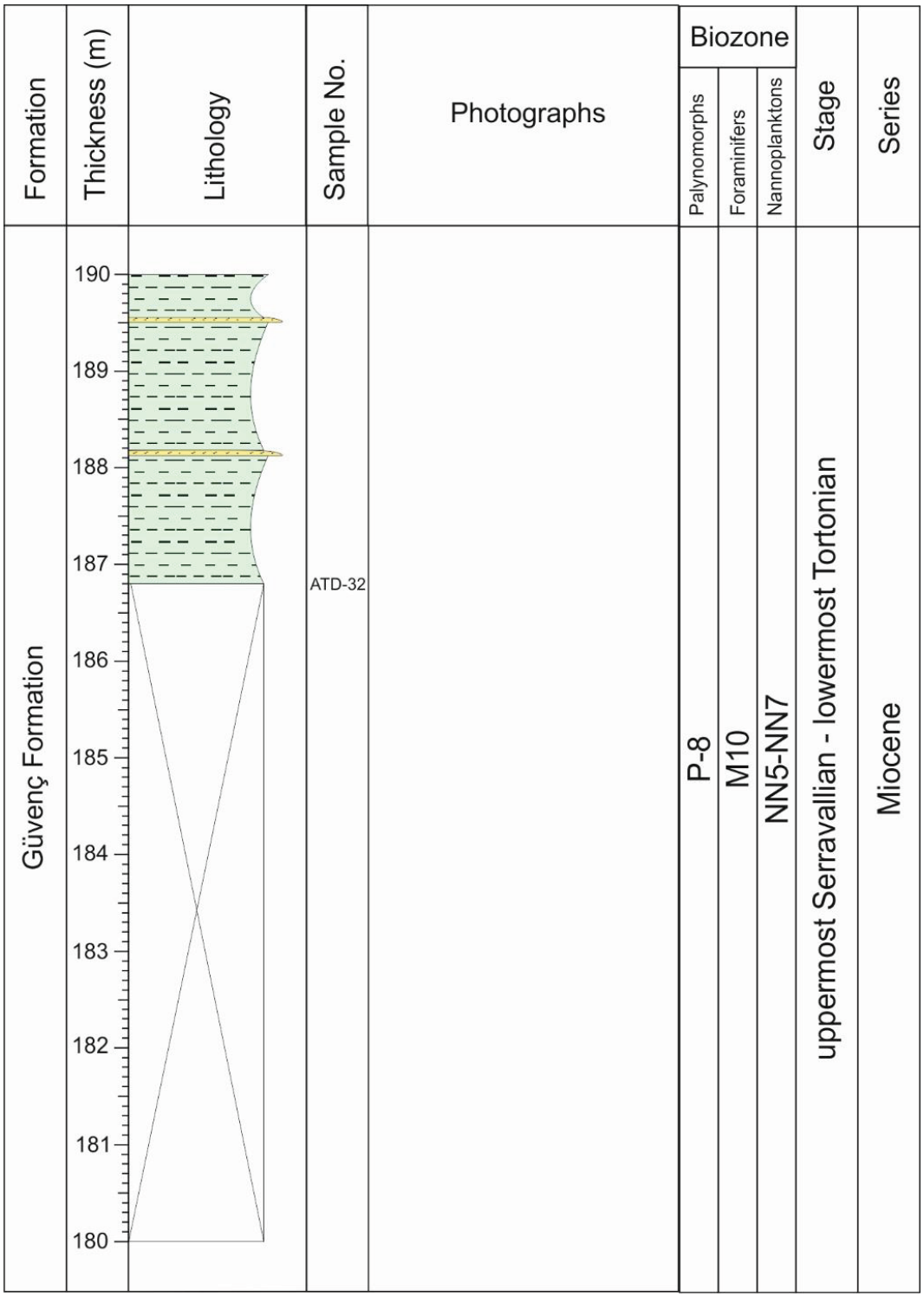

Figure 68. (cont'd)

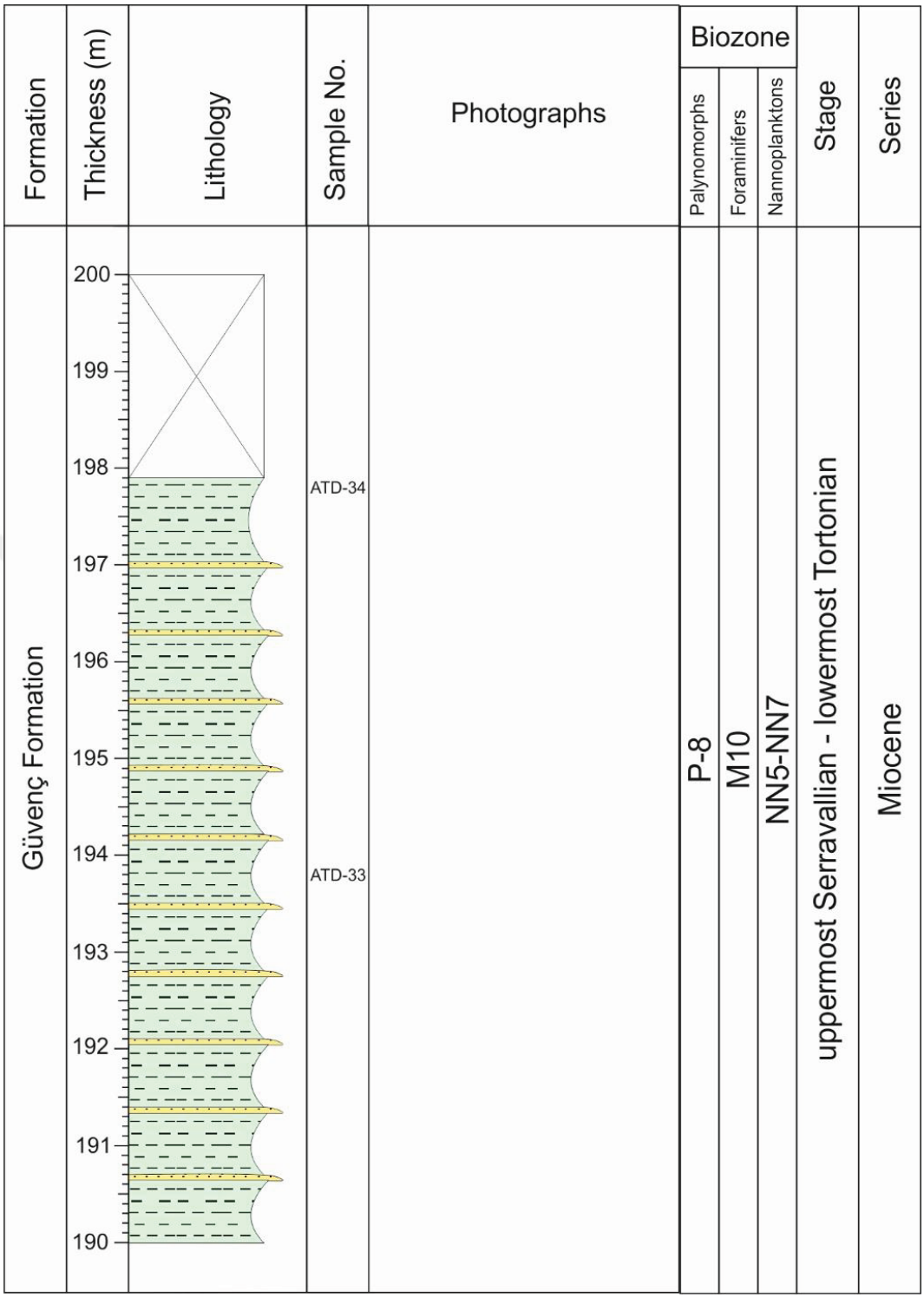

Figure 68. (cont'd)

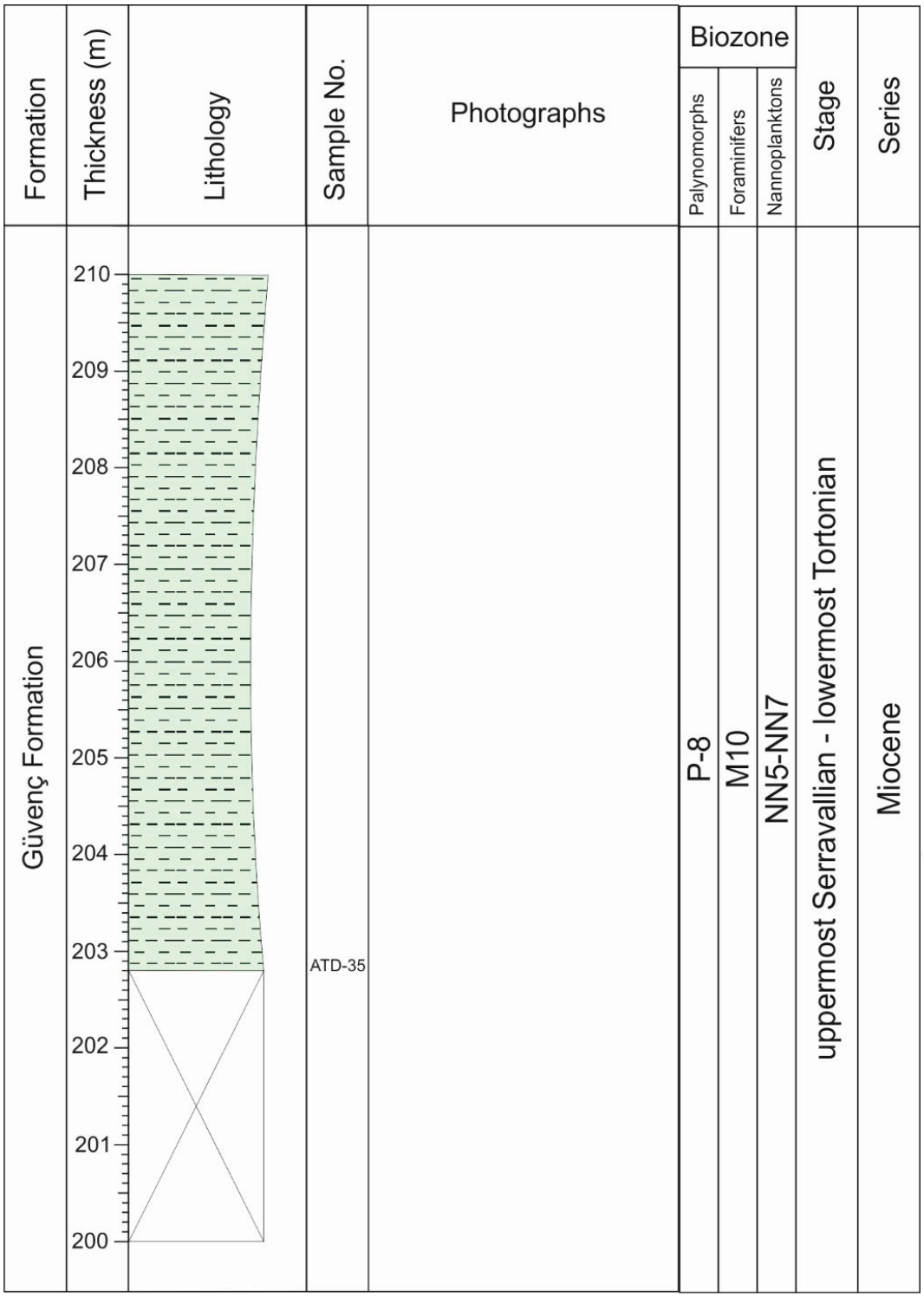

Figure 68. (cont'd)

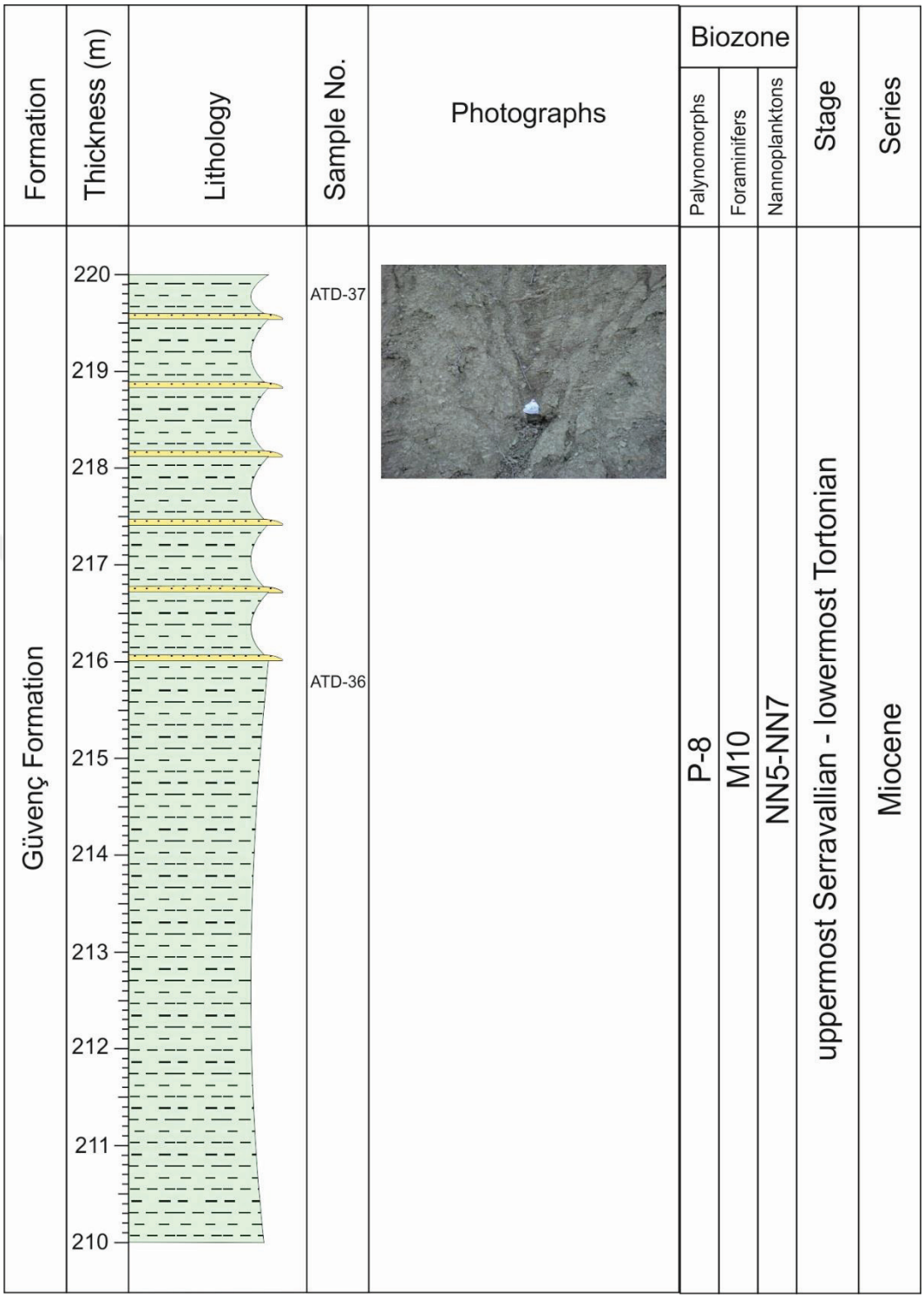

Figure 68. (cont'd)

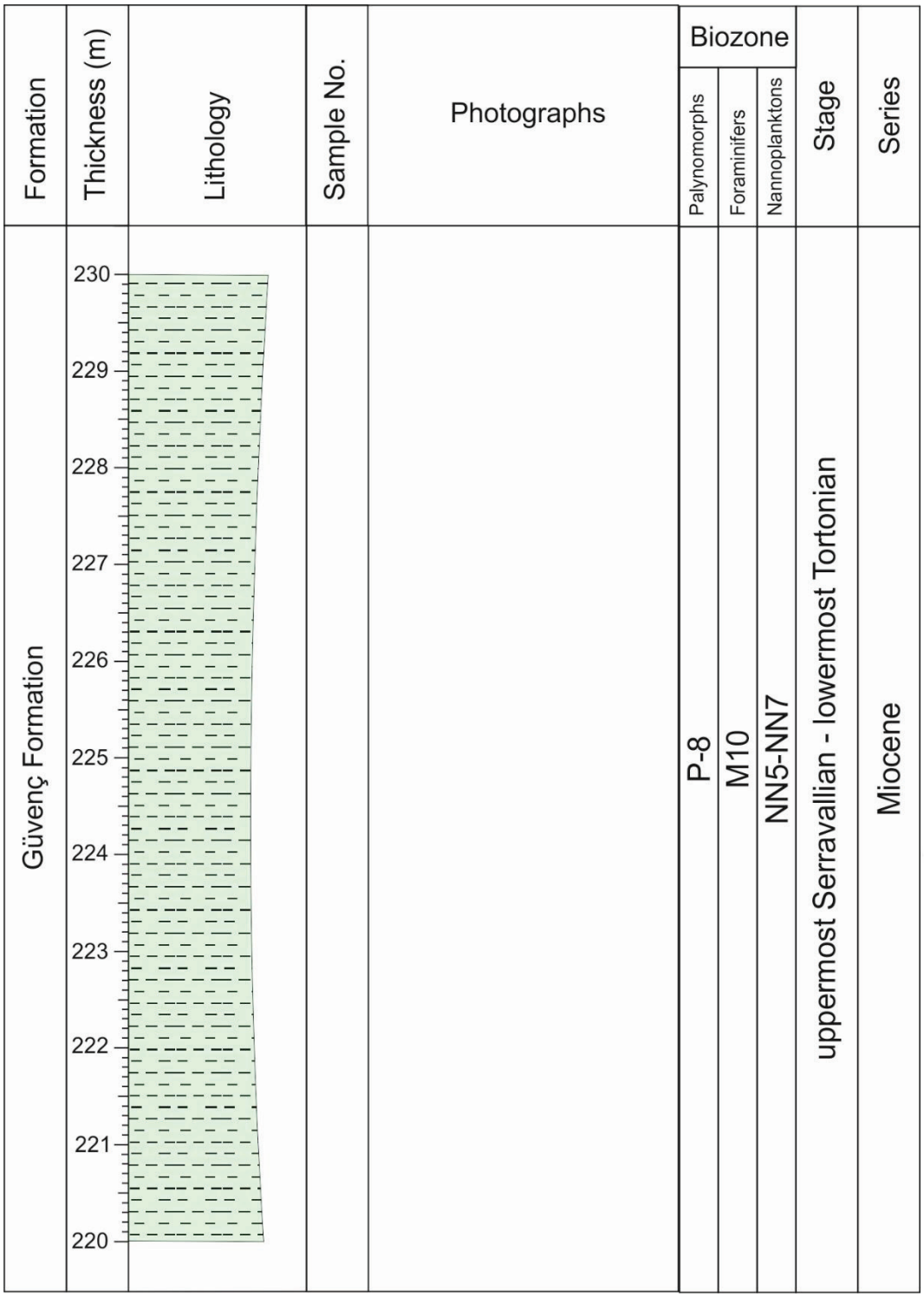

Figure 68. (cont'd)

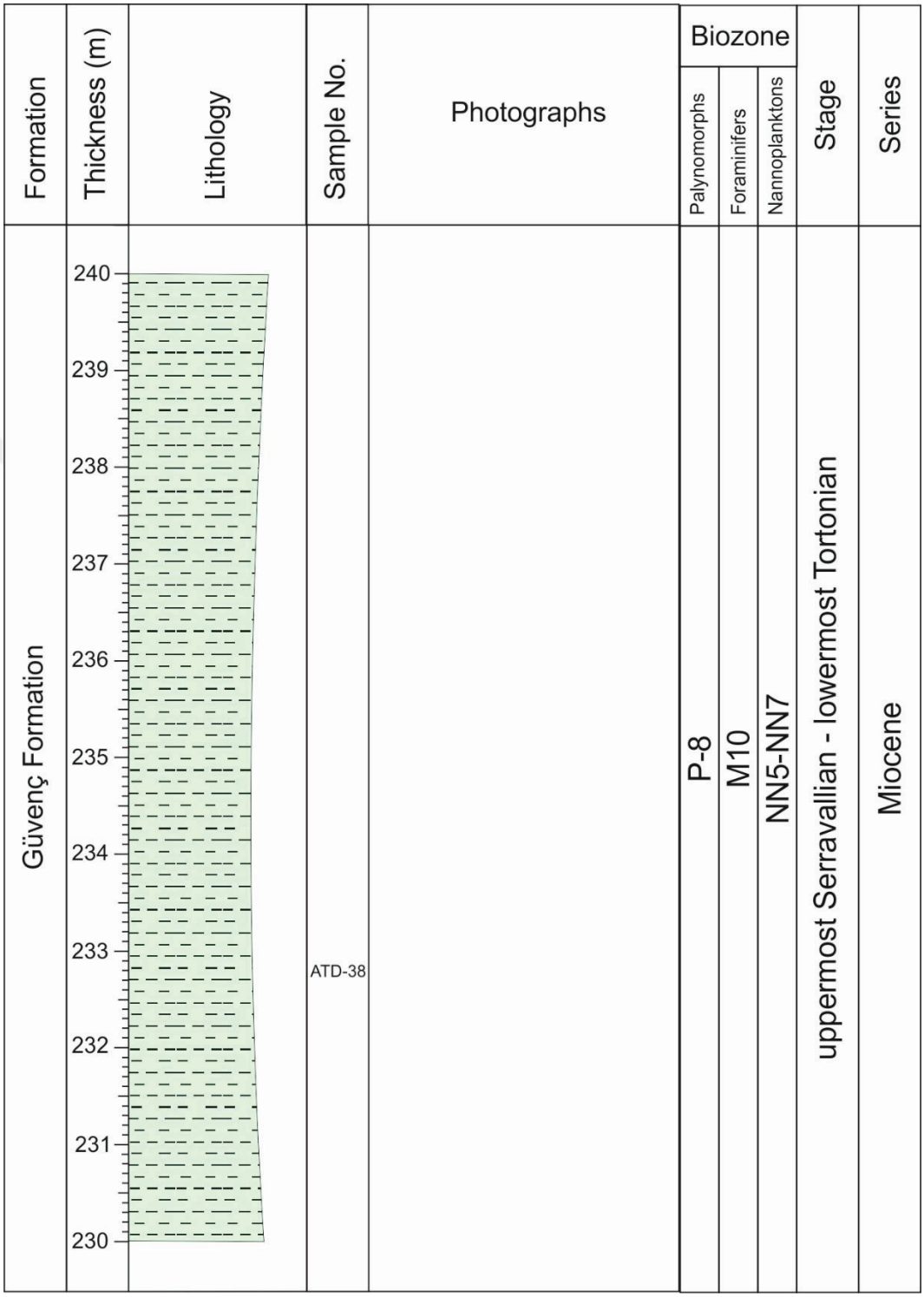

Figure 68. (cont'd)

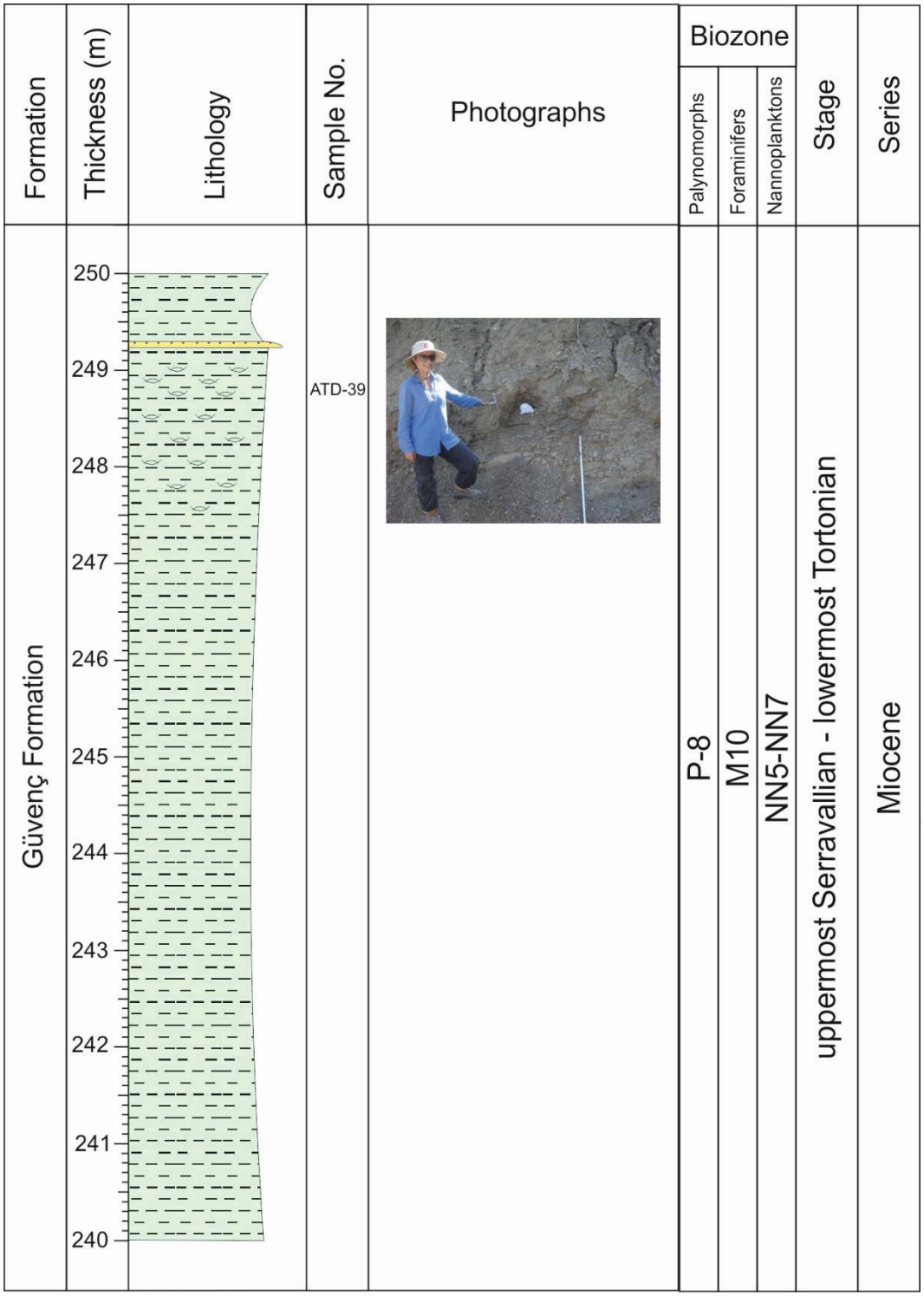

Figure 68. (cont'd)

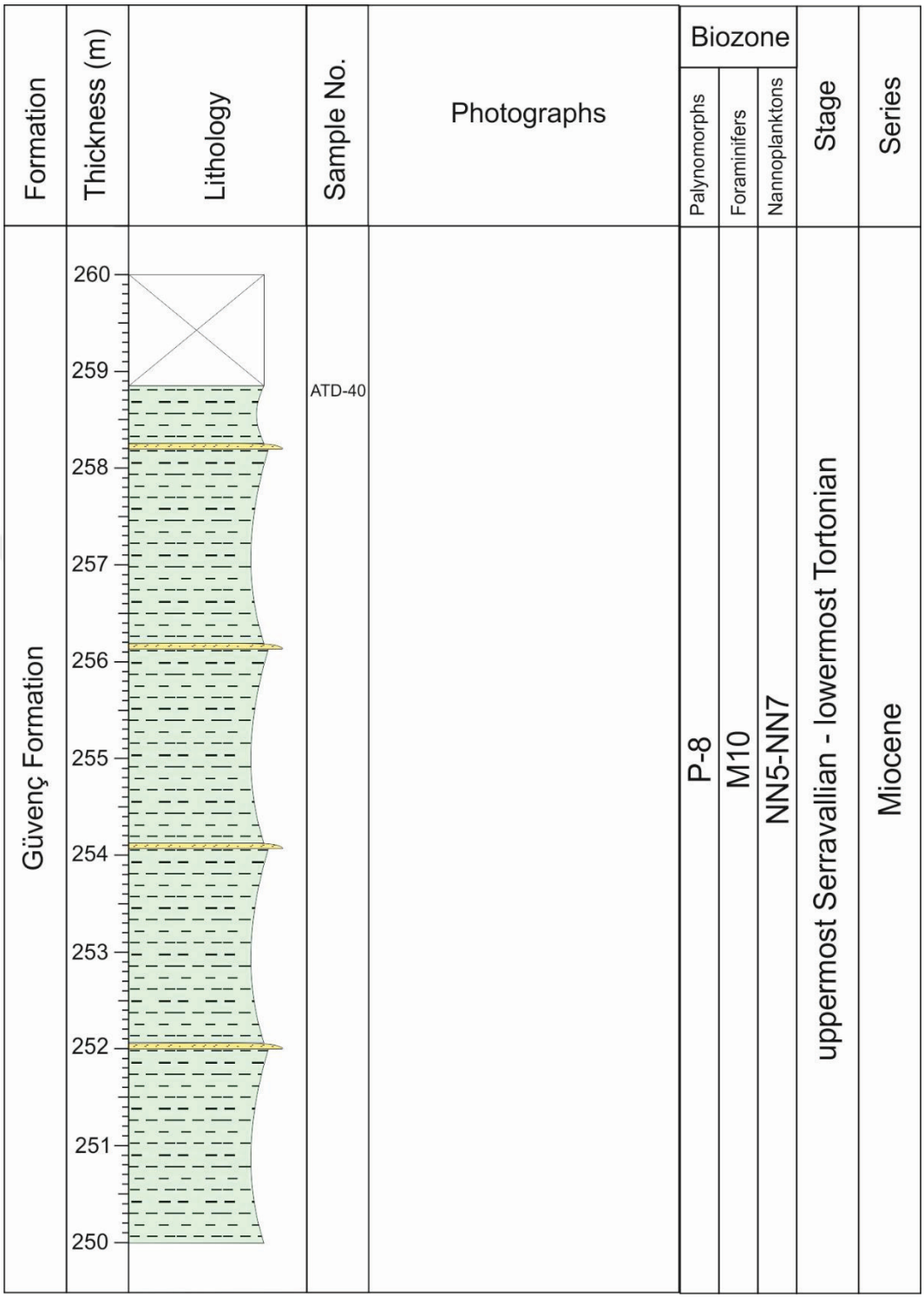

Figure 68. (cont'd)

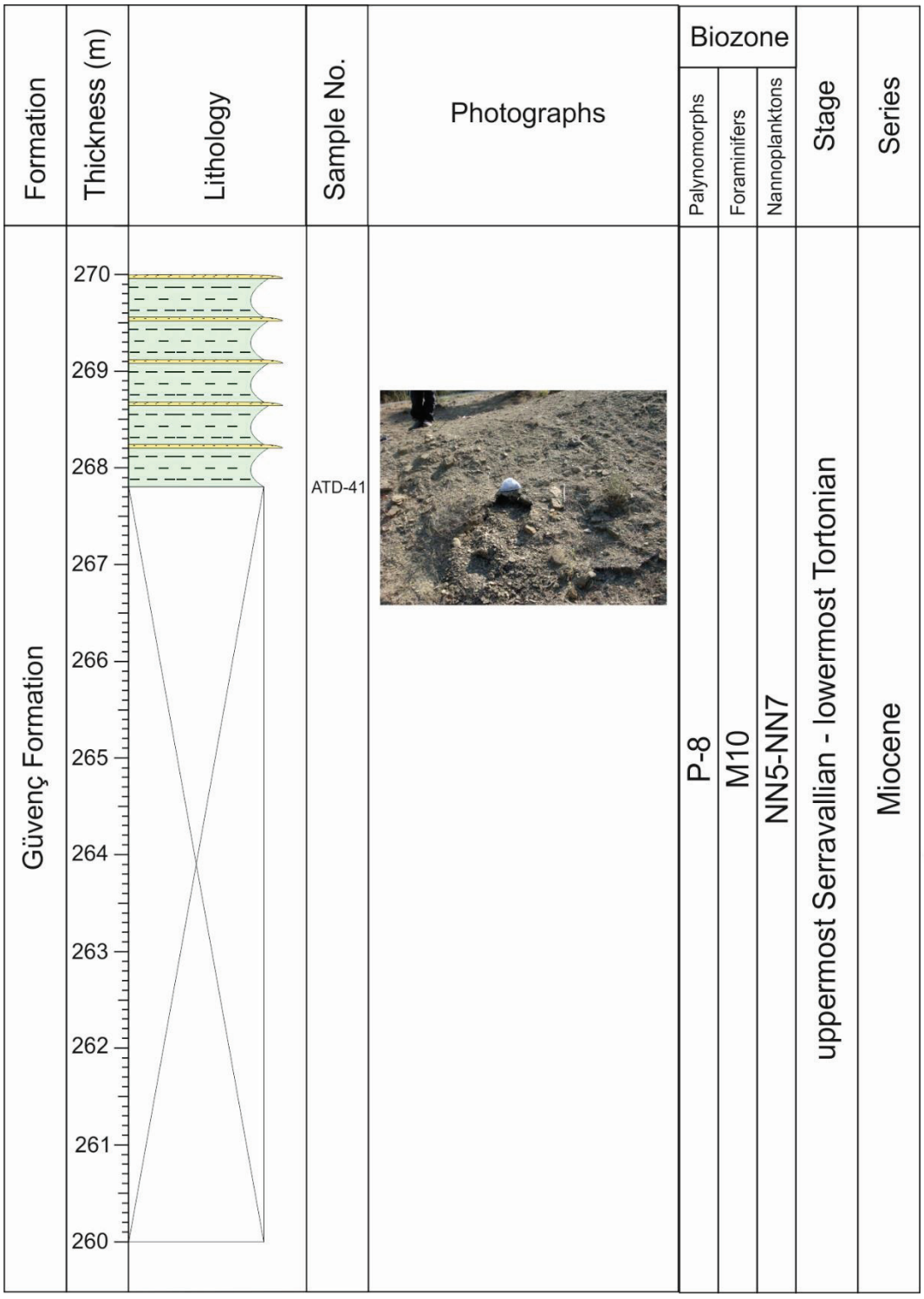

Figure 68. (cont'd)

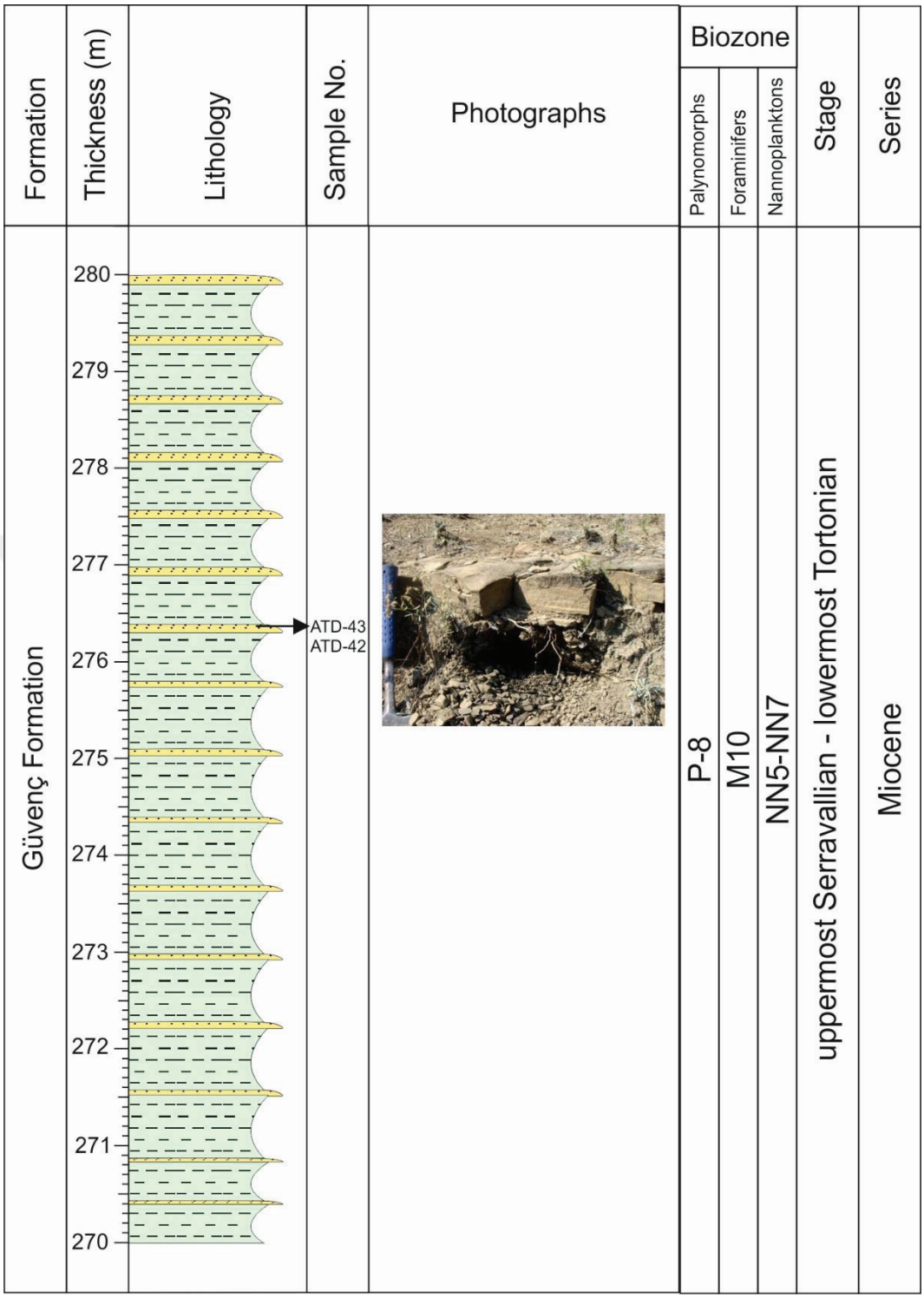

Figure 68. (cont'd)

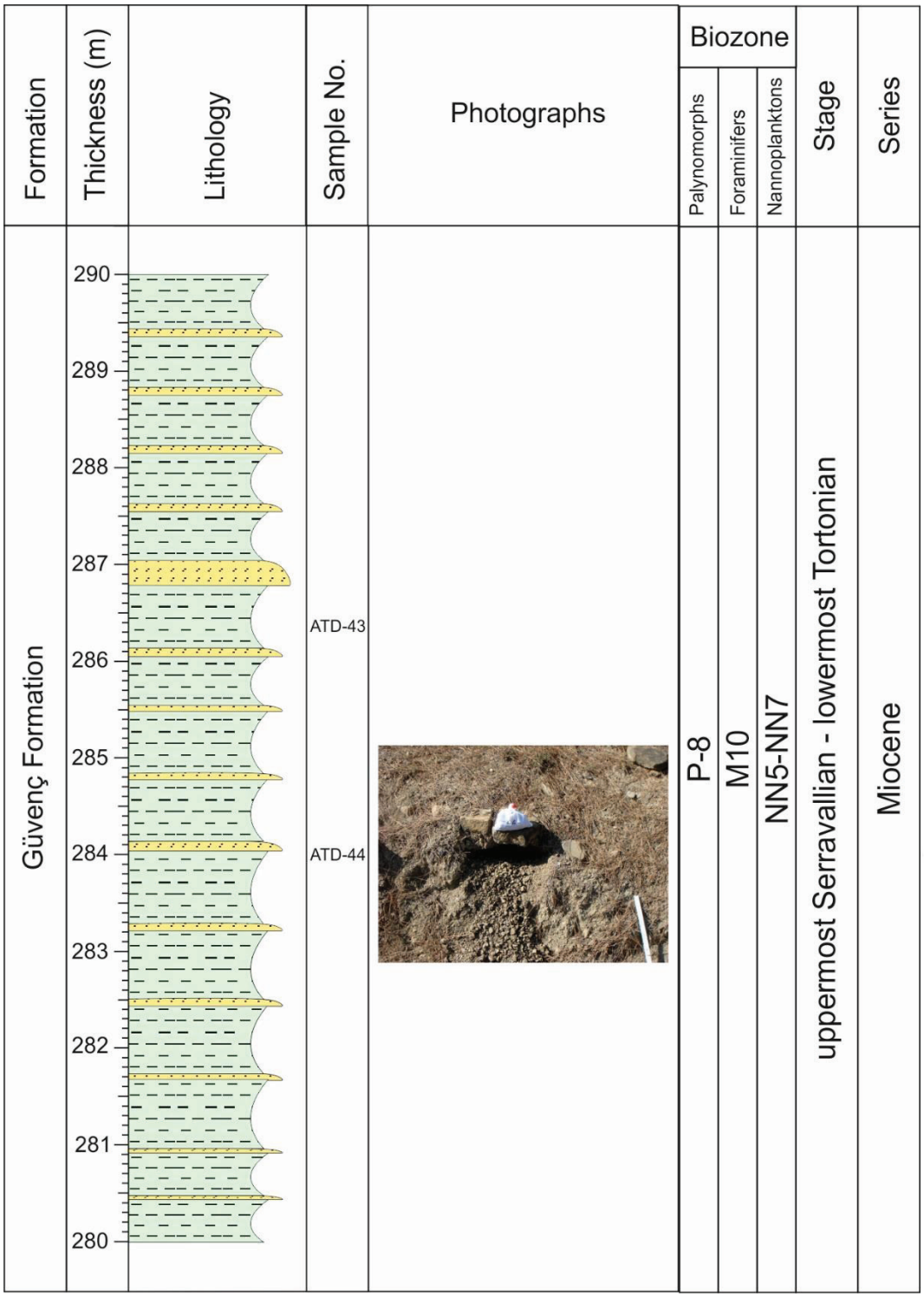

Figure 68. (cont'd)

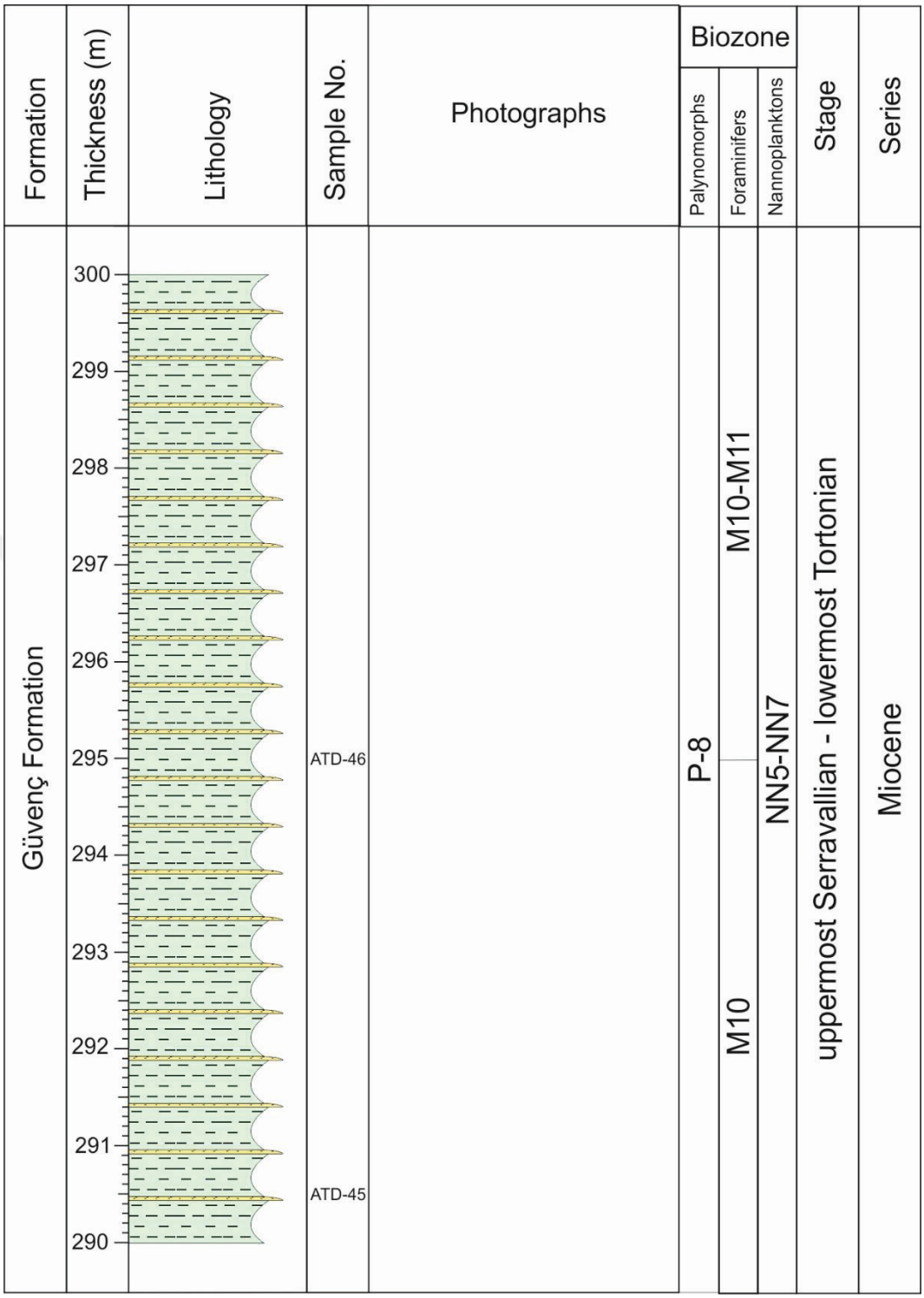

Figure 68. (cont'd)

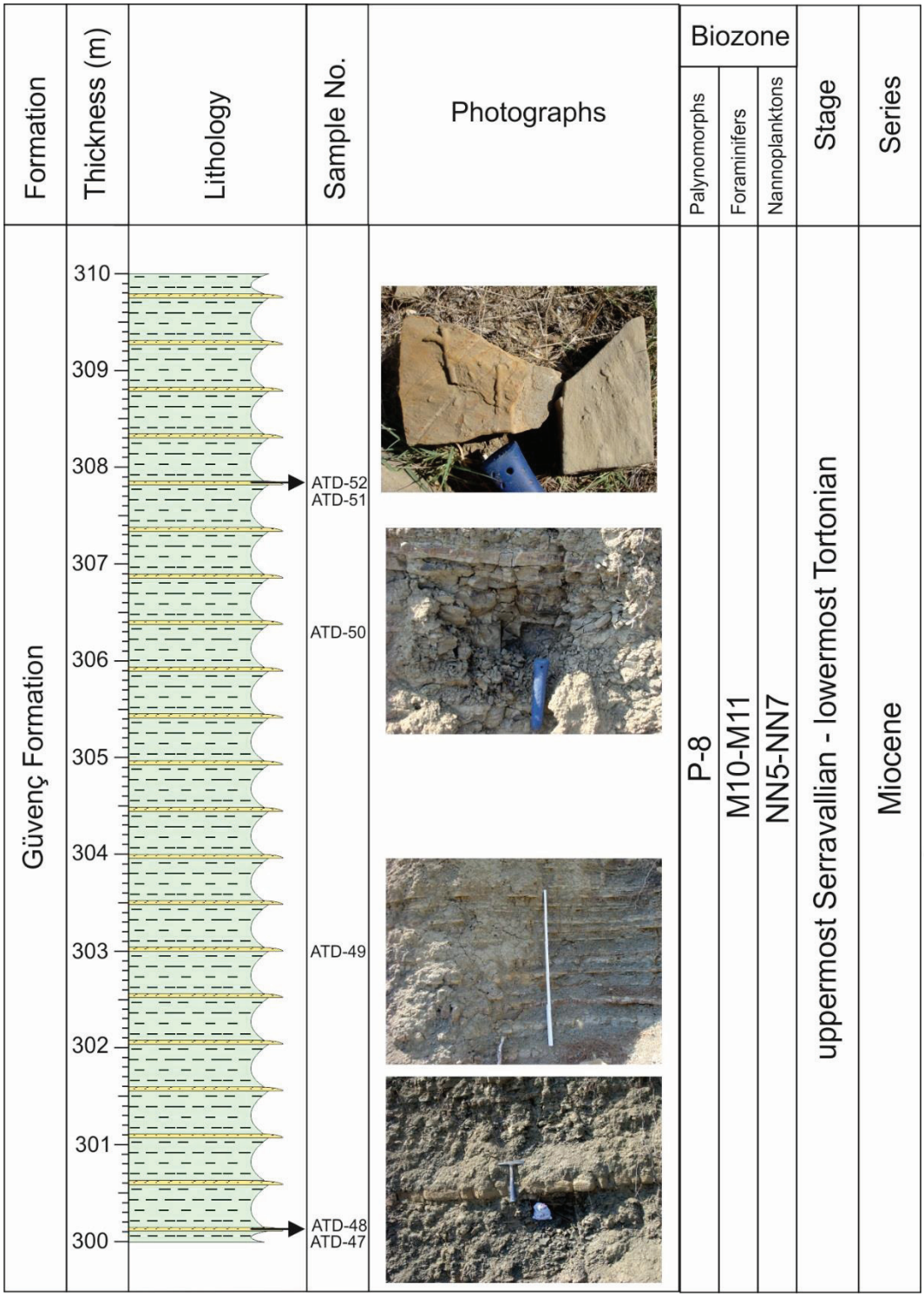

Figure 68. (cont'd)

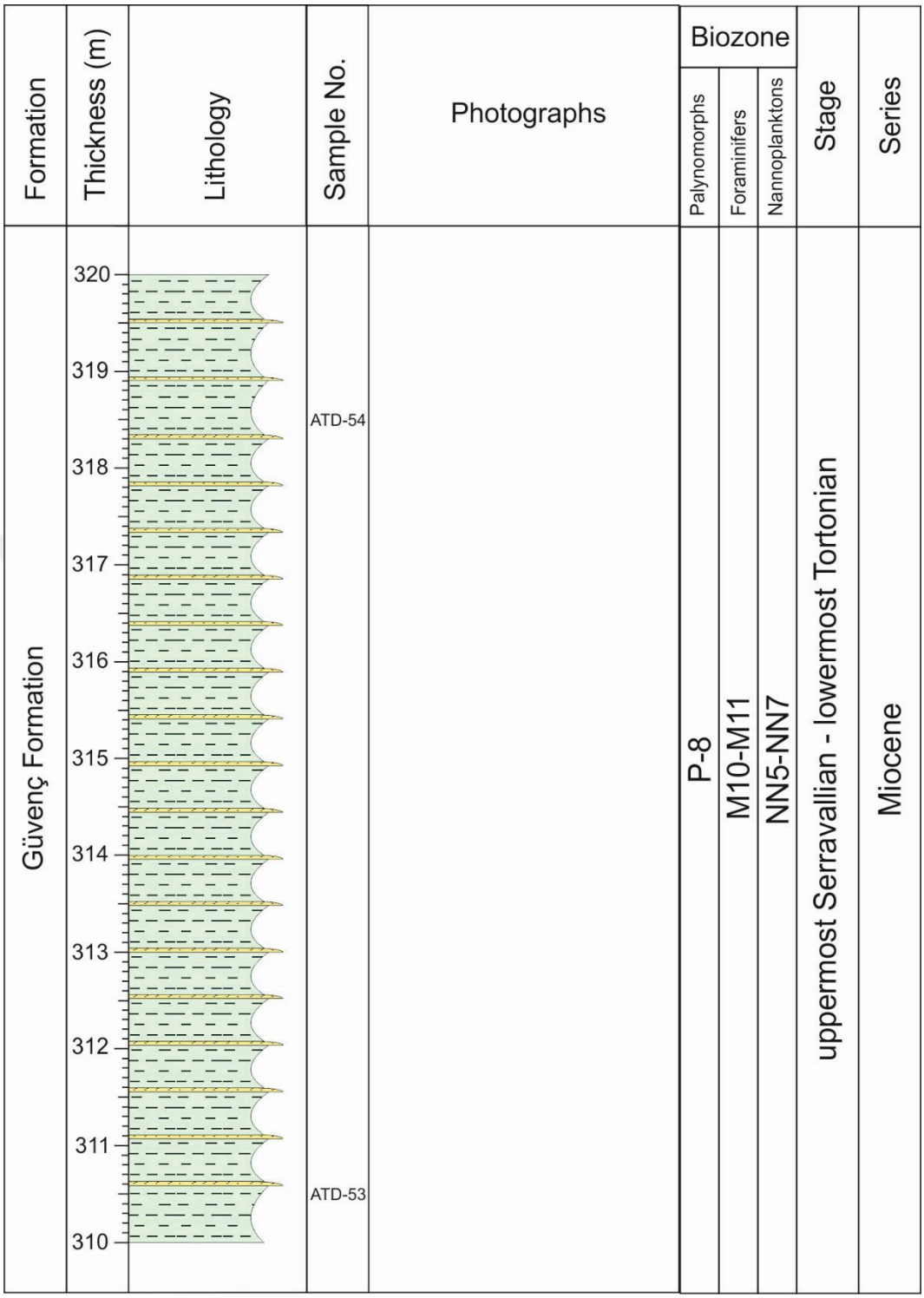

Figure 68. (cont'd)

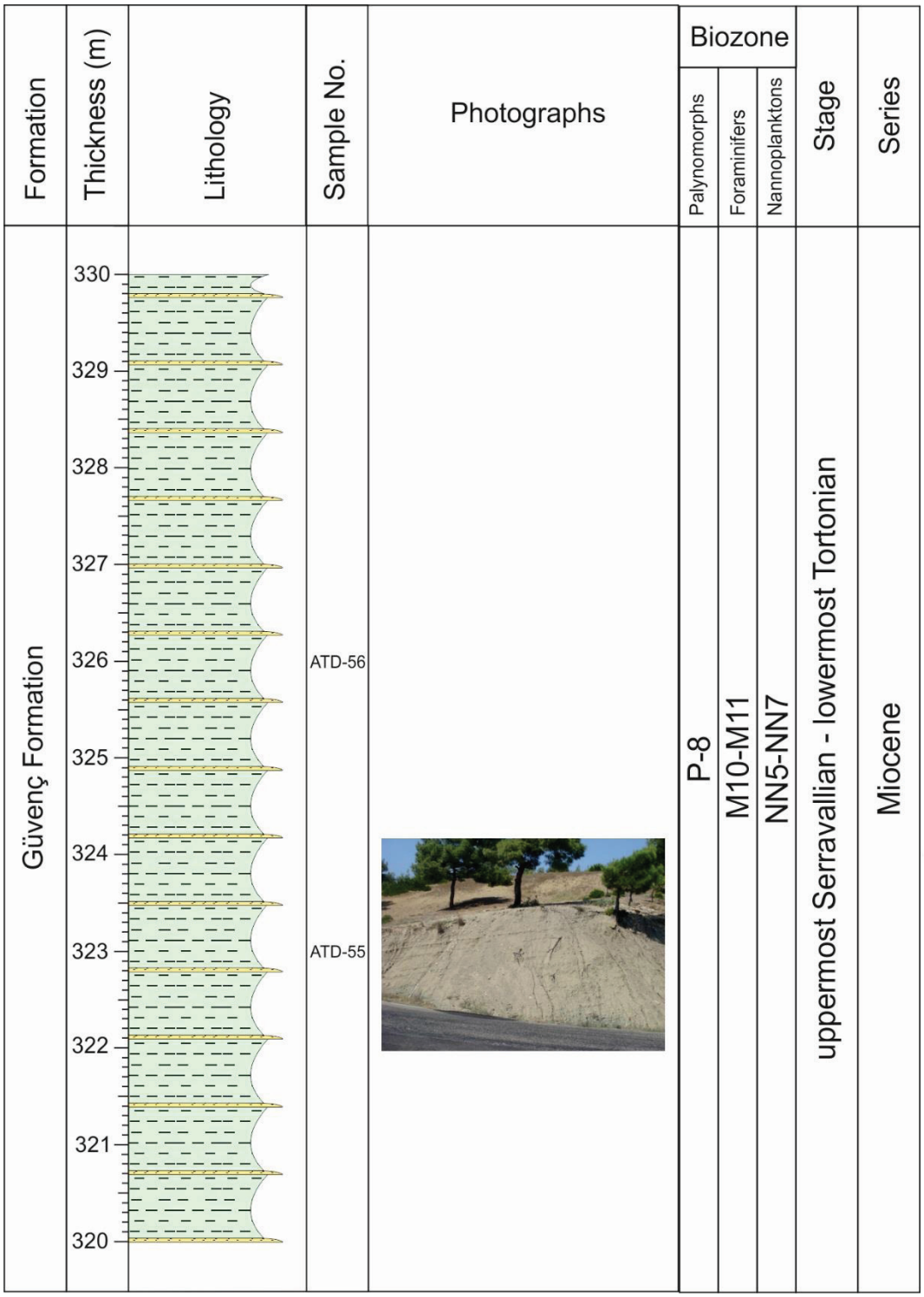

Figure 68. (cont'd)

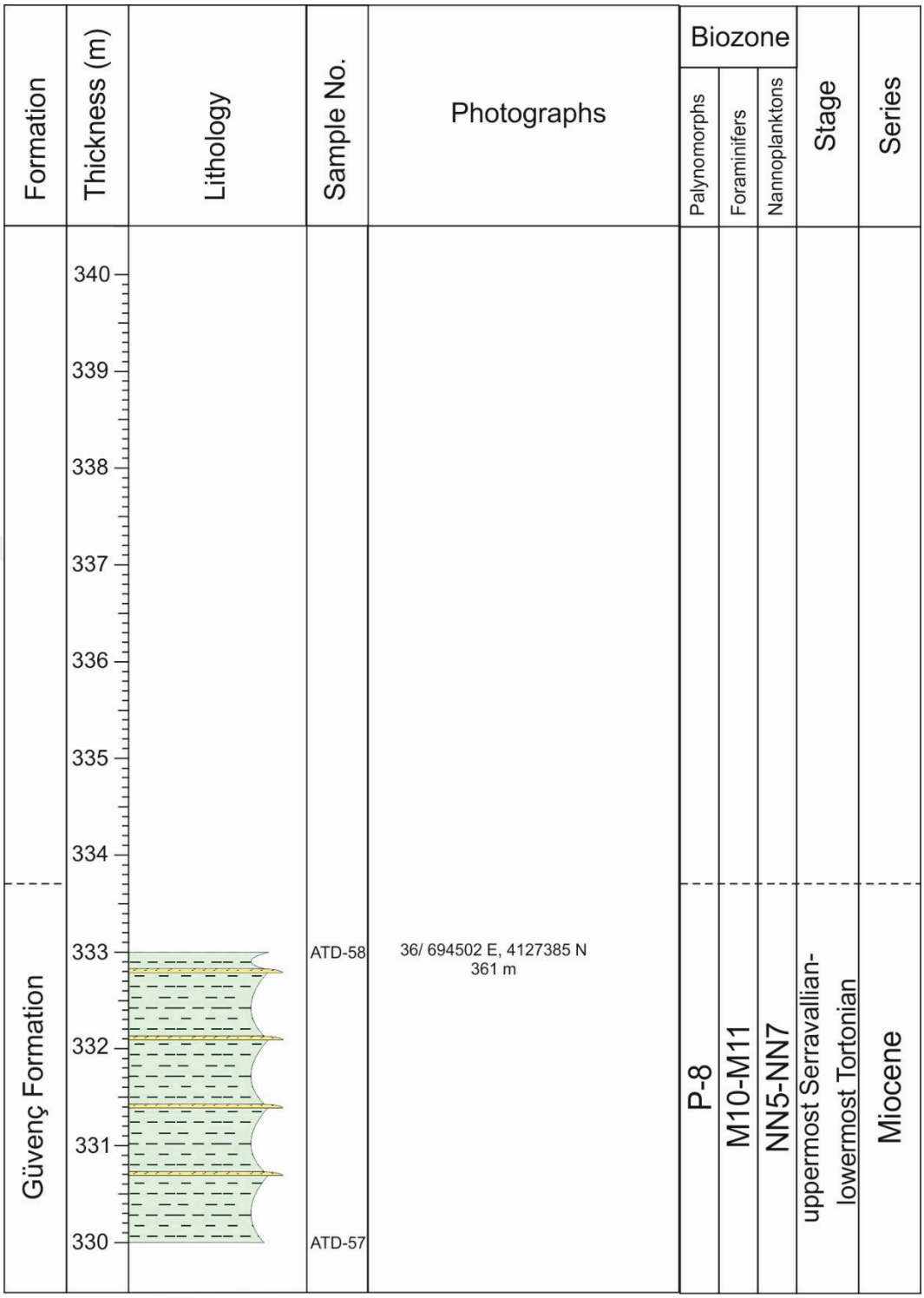

Figure 68. (cont'd)

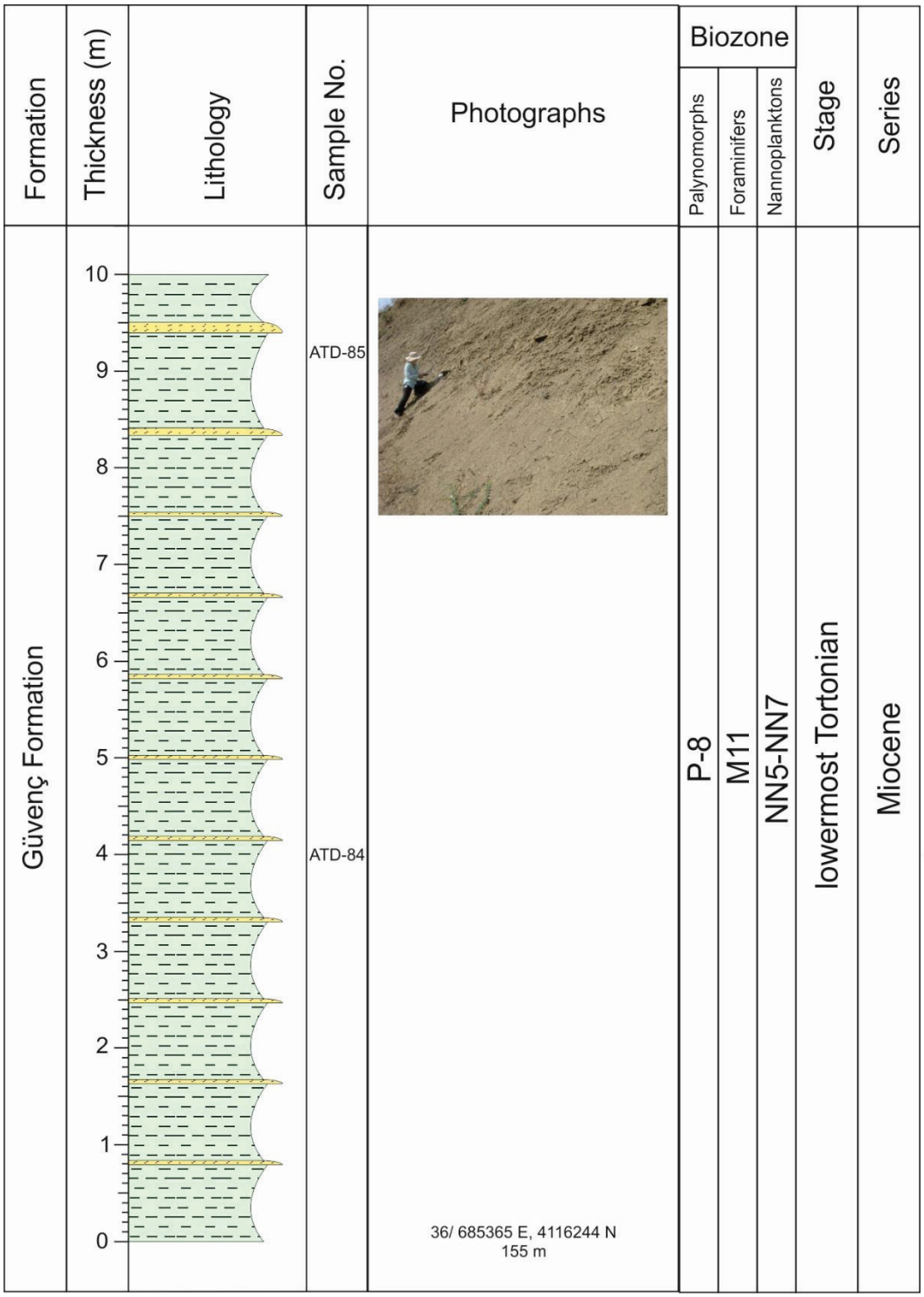

Figure 69. Güvenç Measured Stratigraphic Section.

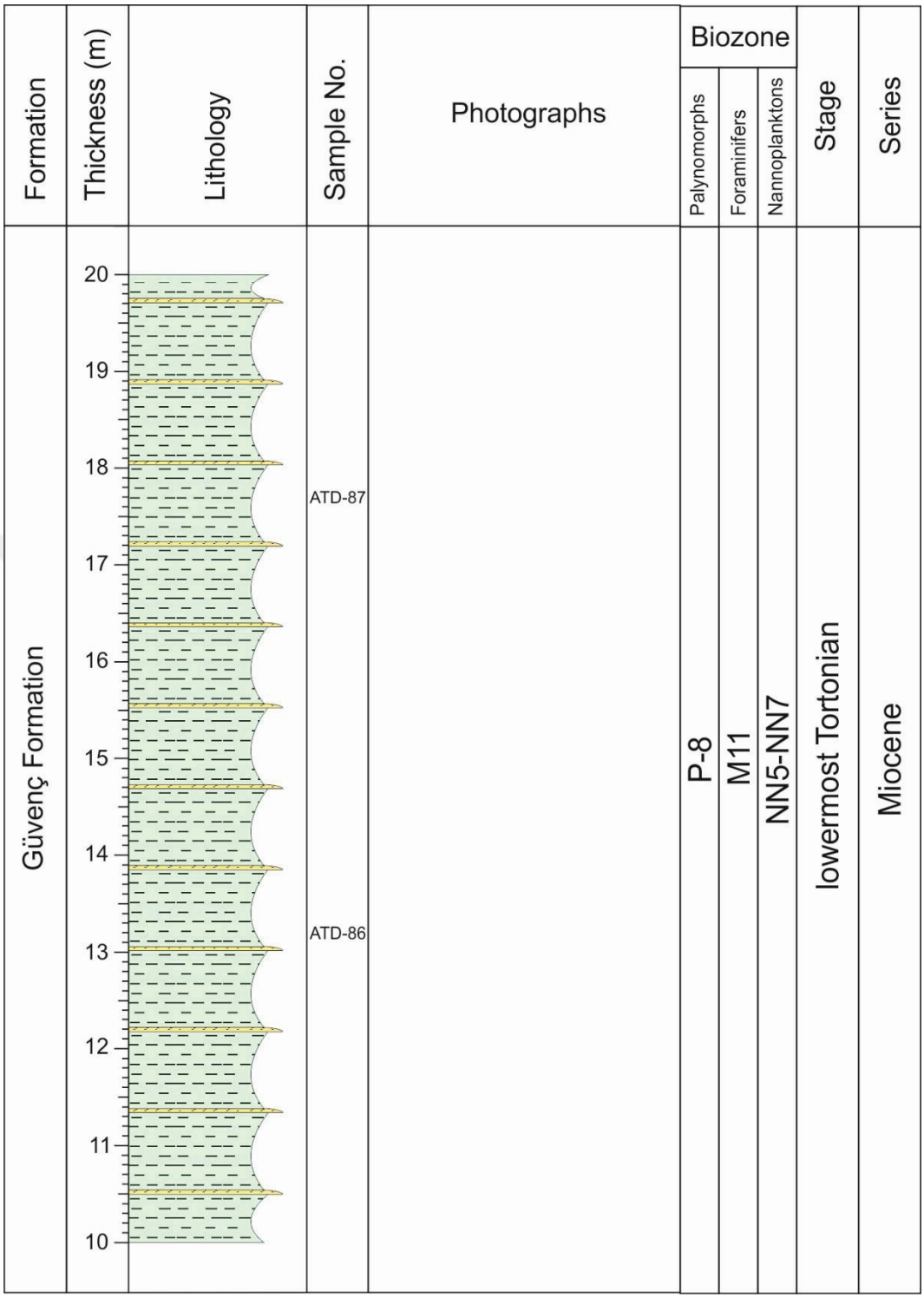

Figure 69. (cont'd)

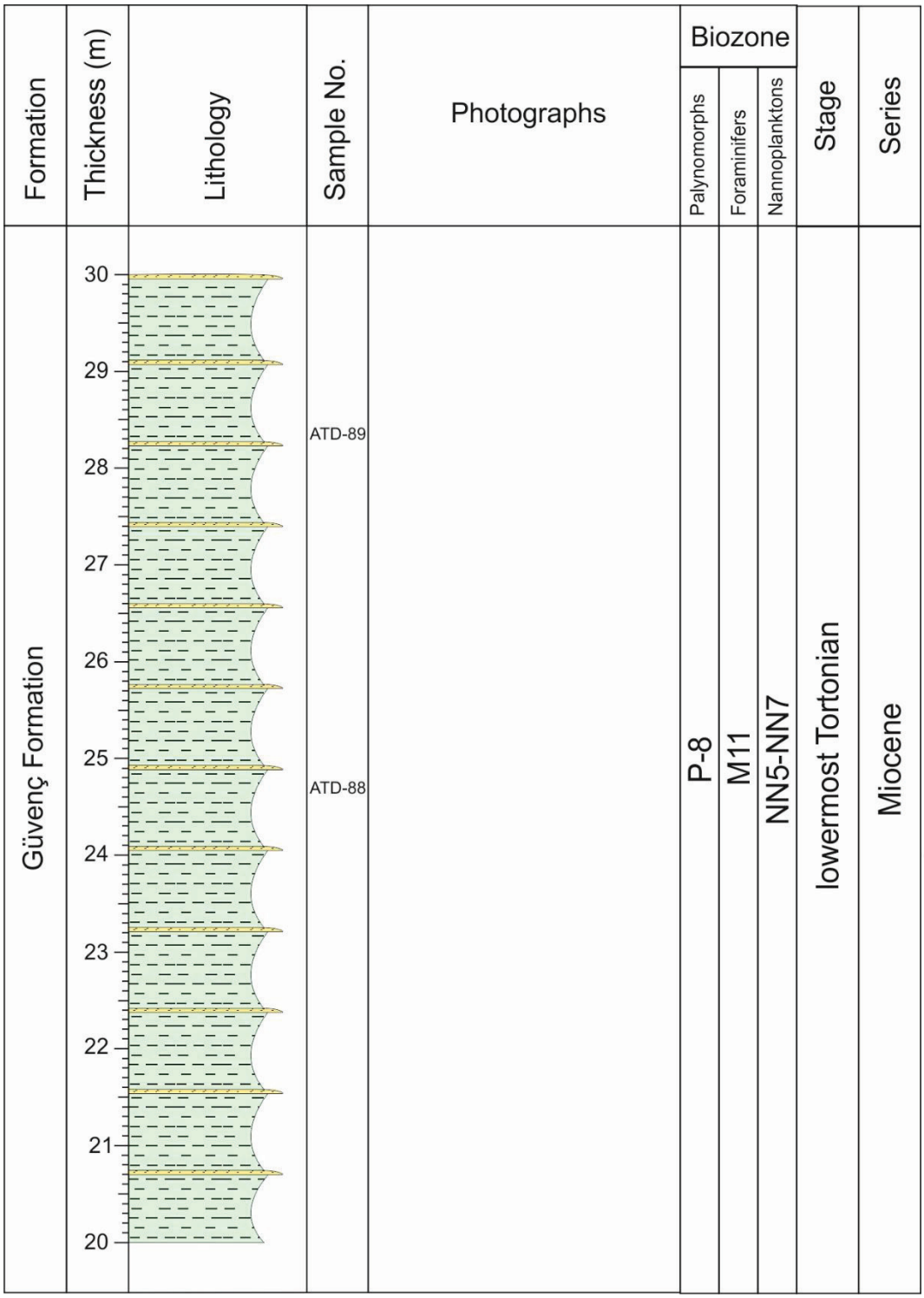

Figure 69. (cont'd)

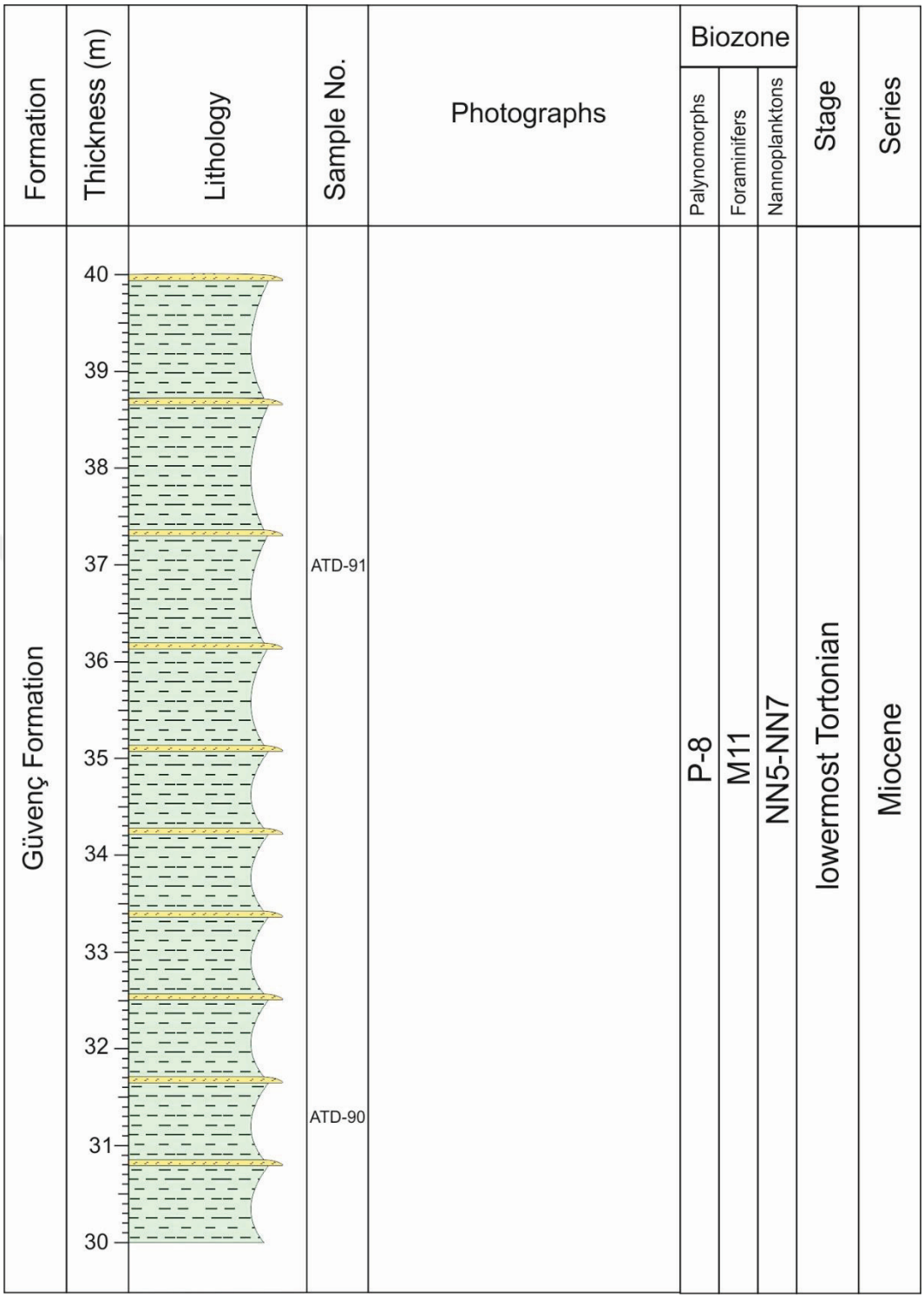

Figure 69. (cont'd)

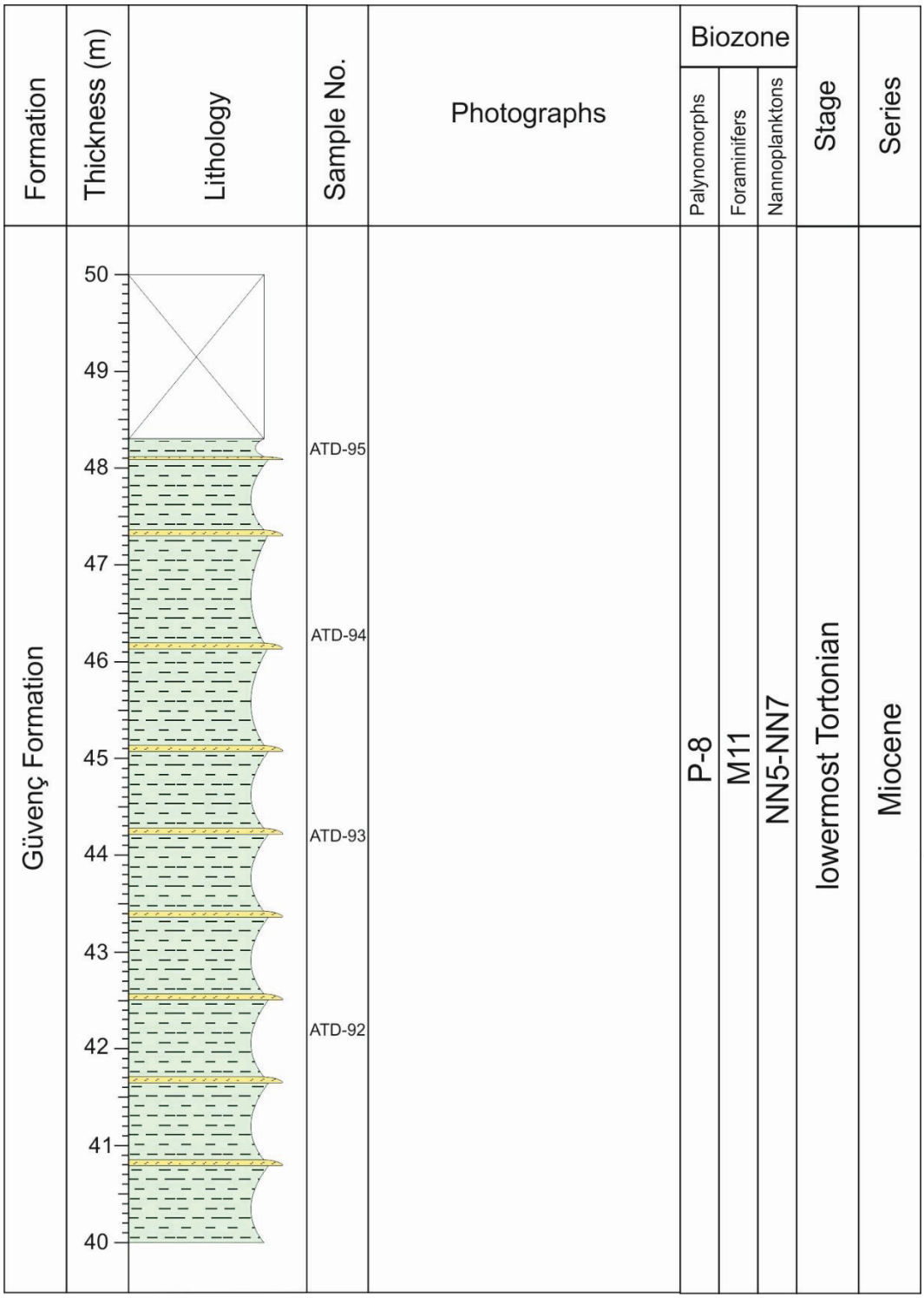

Figure 69. (cont'd)

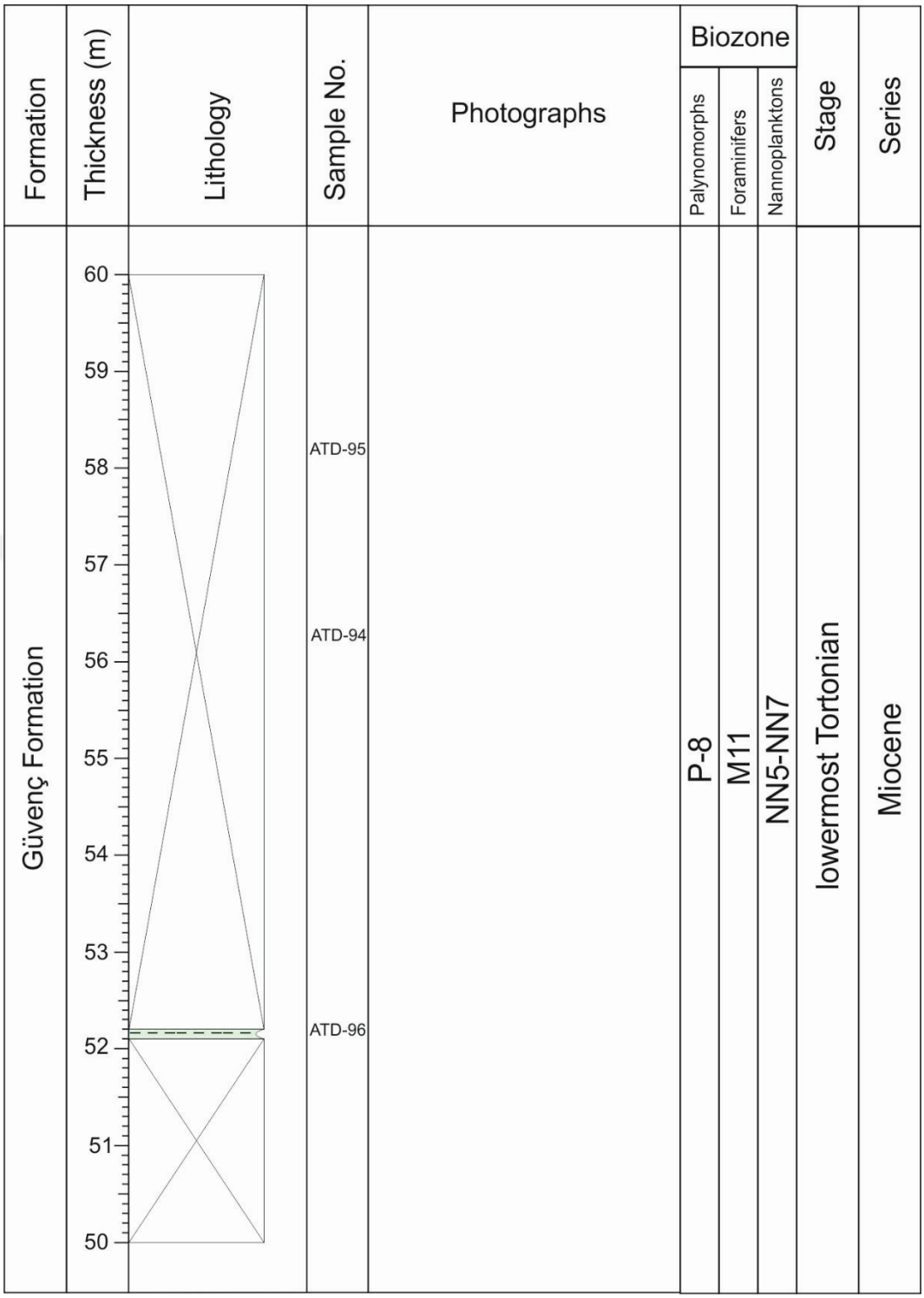

Figure 69. (cont'd)

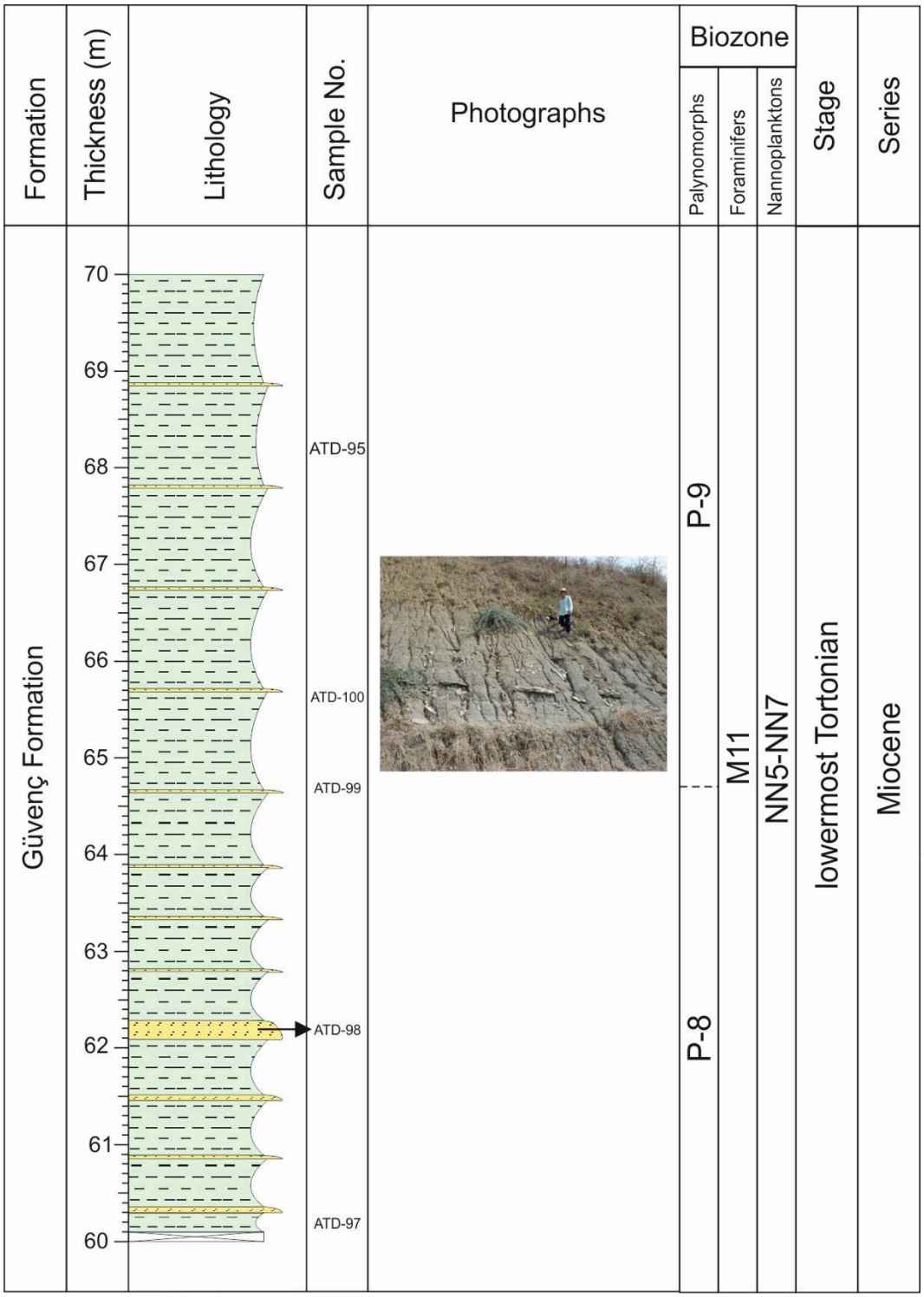

Figure 69. (cont'd)

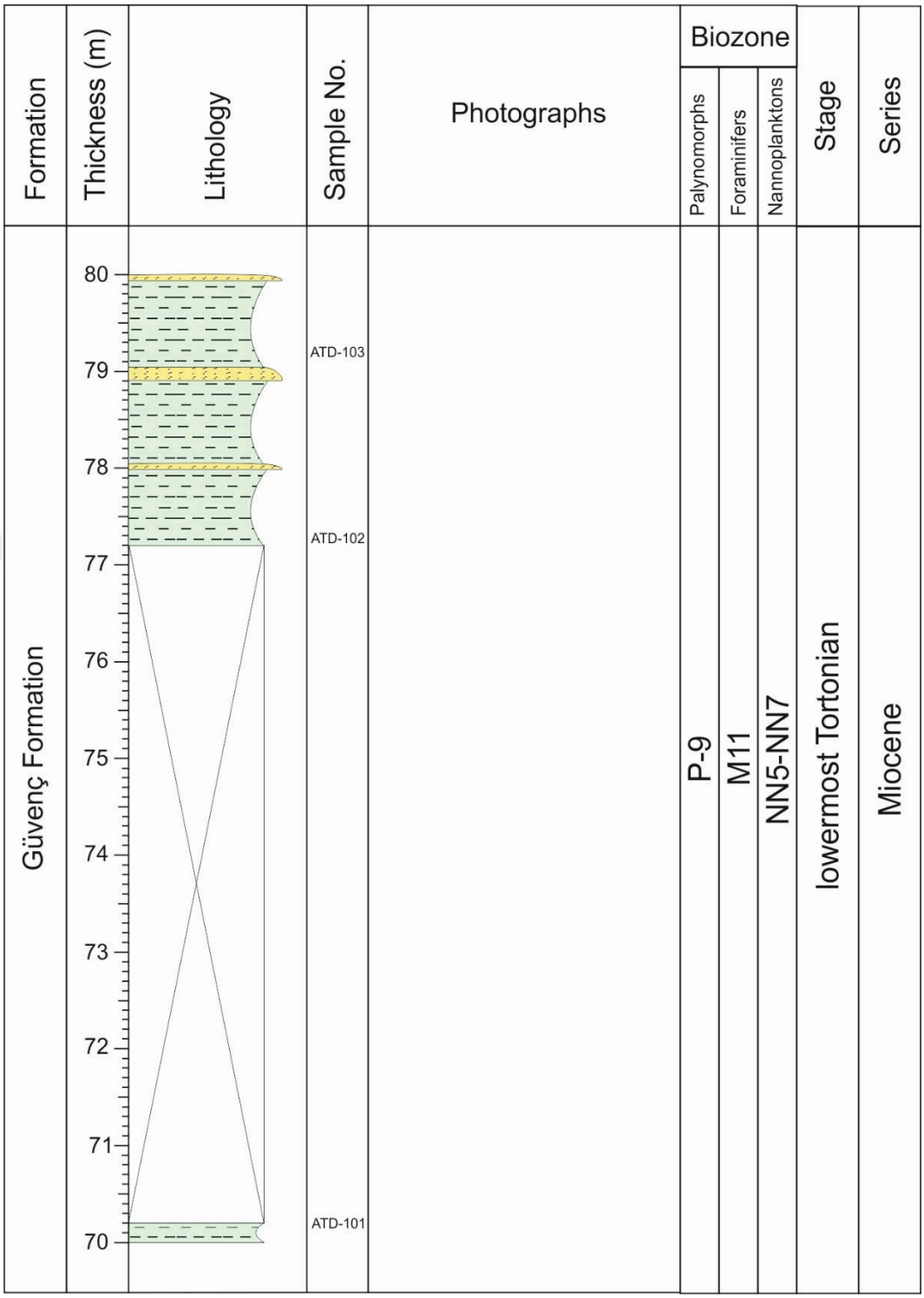

Figure 69. (cont'd)

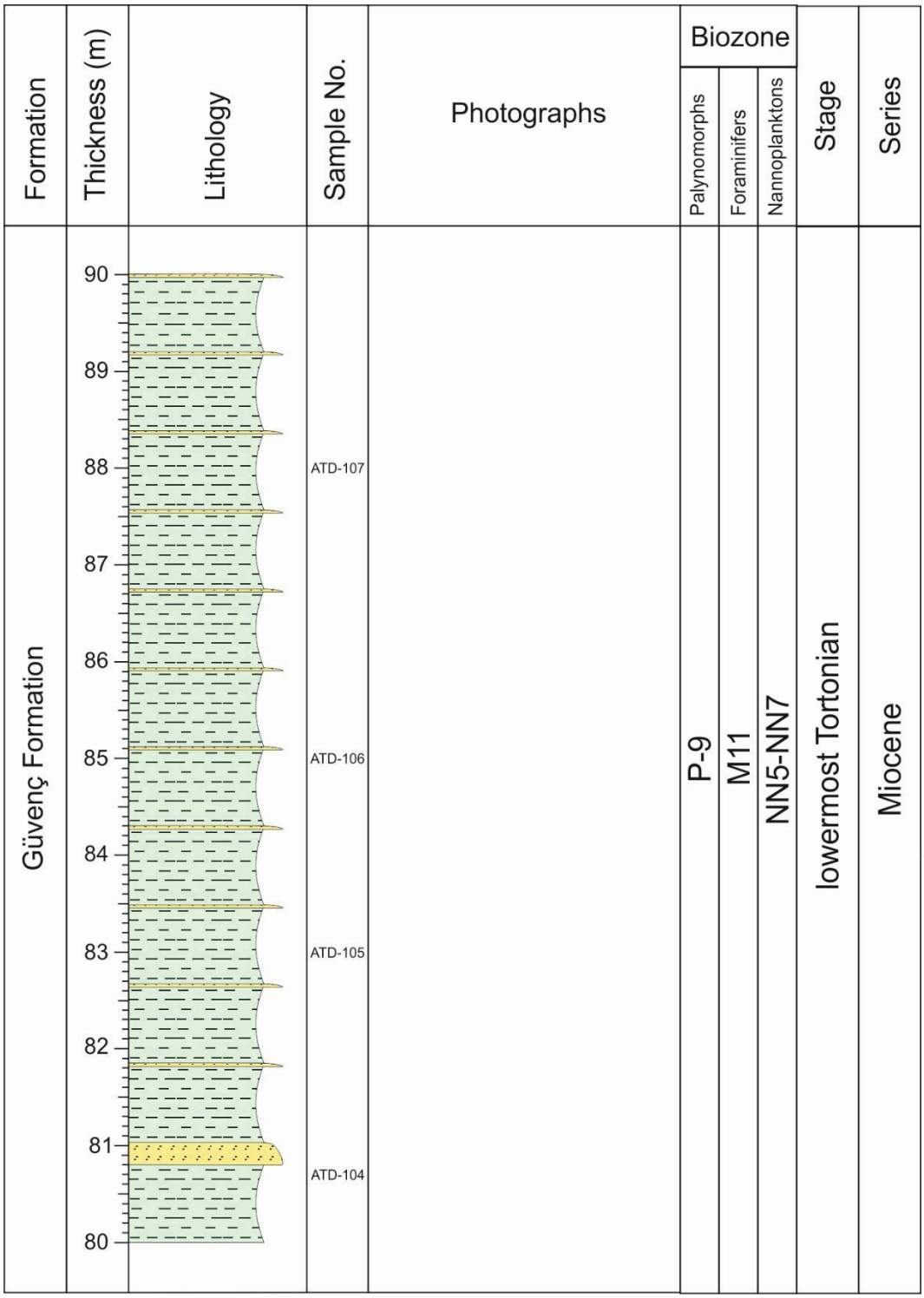

Figure 69. (cont'd)

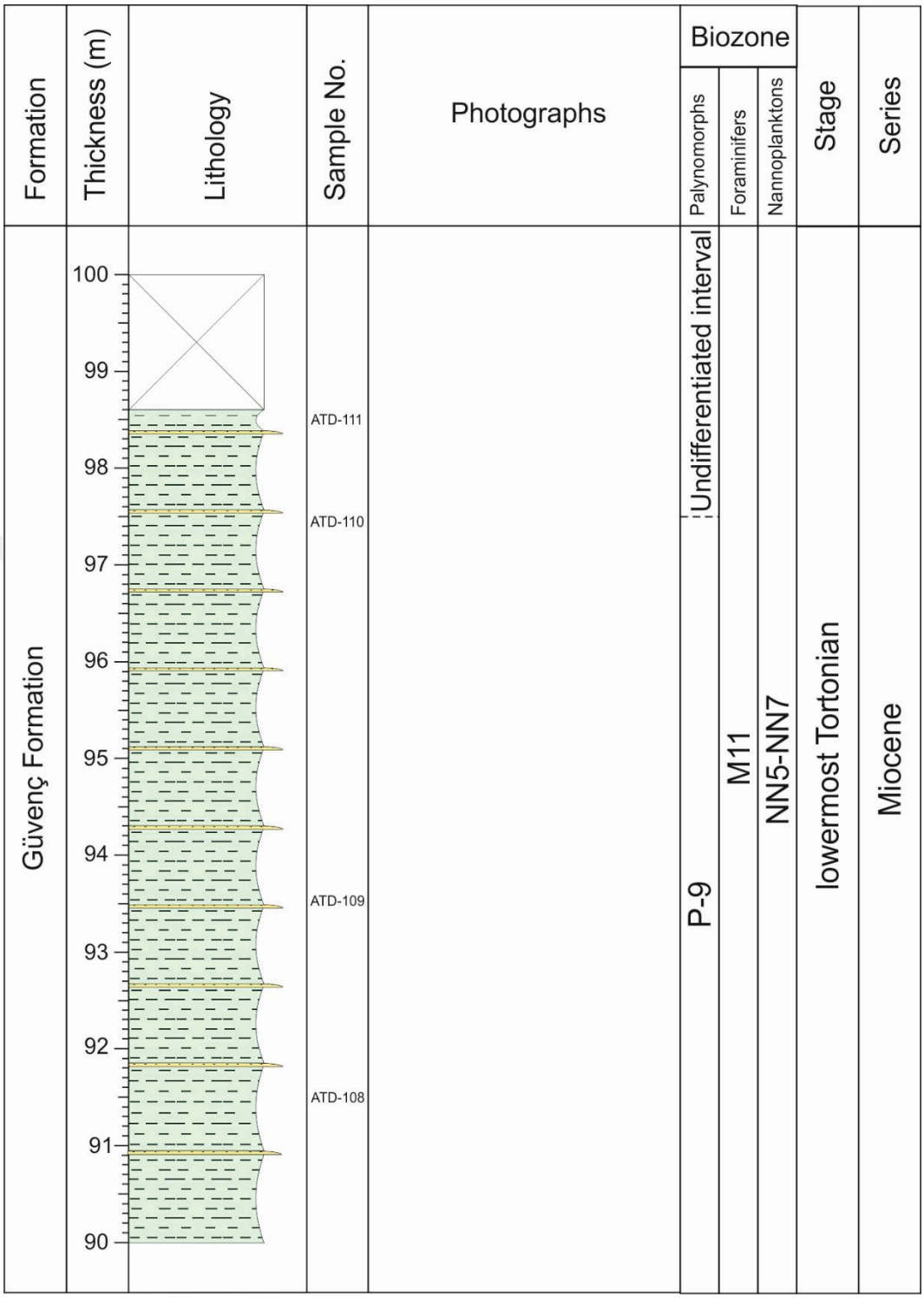

Figure 69. (cont'd)

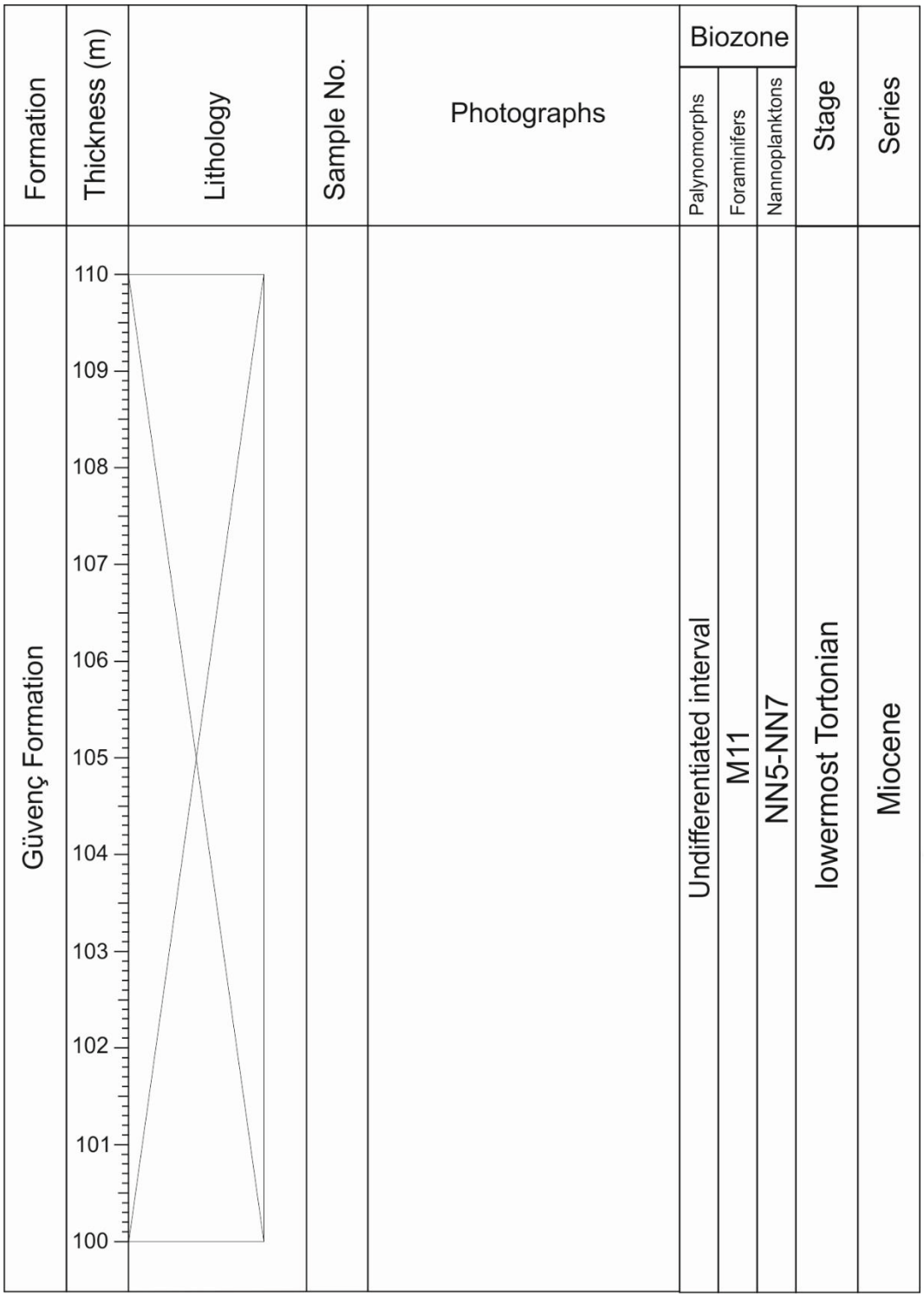

Figure 69. (cont'd)

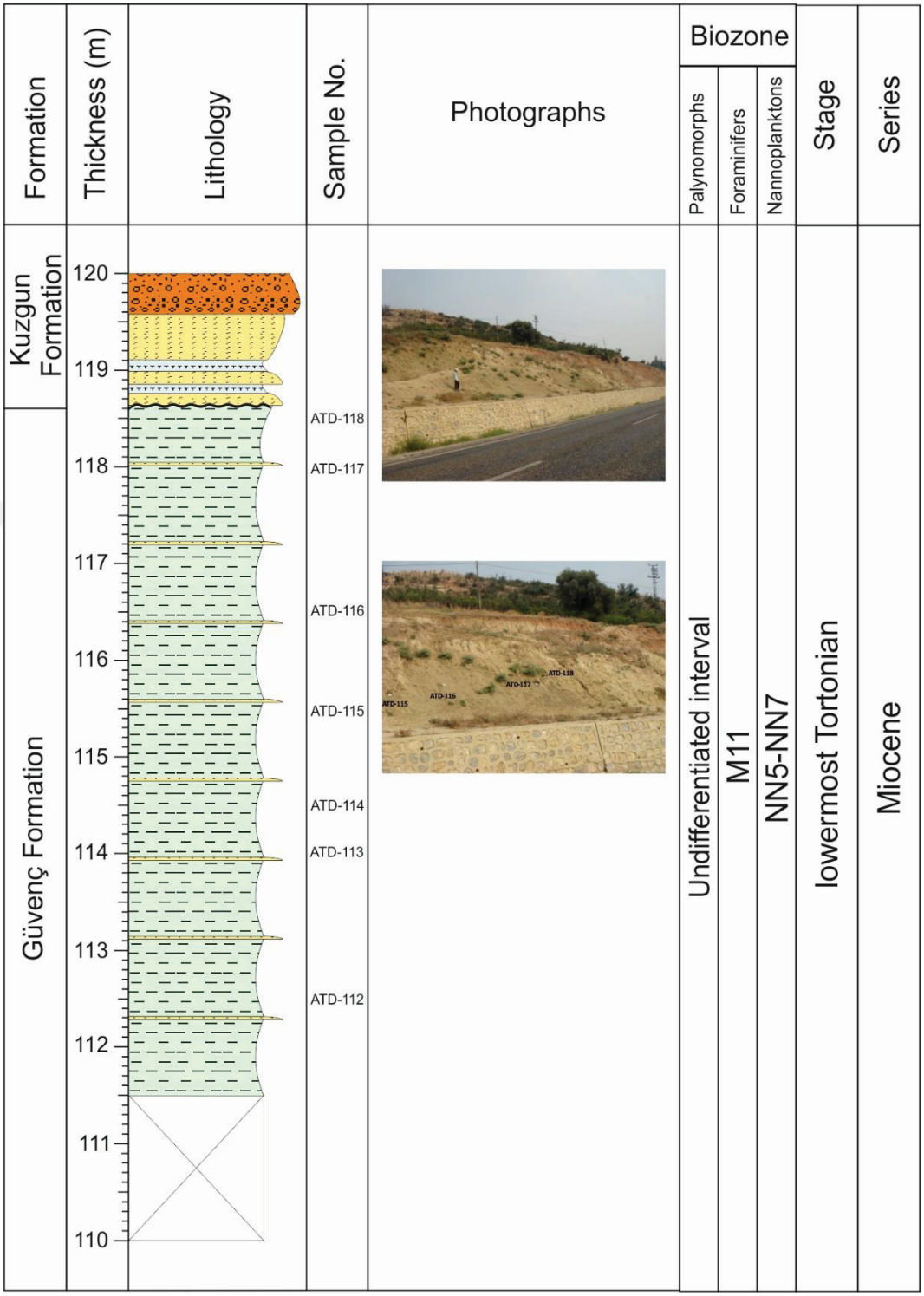

Figure 69. (cont'd)

C. ORGANIC MATTER DISTRIBUTION THROUGH THE MEASURED SECTIONS

Table 3. The organic matter distribution through the Köpekli Formation in the Çukurköy Section.

SAMPLE NO	AMORPHOUS (%)	HERBACEOUS (%)	WOODY (%)	COALY (%)	ABUNDANCE
ATD-138	15	30	50	5	LOW
ATD-139	20	25	50	5	LOW-MODERATE
ATD-141	30	20	45	5	LOW-MODERATE
ATD-142	25	15	55	5	LOW-MODERATE
ATD-143	50	15	30	5	VERY HIGH
ATD-145	60	15	20	5	HIGH-VERY HIGH
ATD-146	45	20	30	5	HIGH
ATD-147	20	25	45	10	VERY HIGH
ATD-148	25	25	45	5	HIGH
ATD-149	25	20	45	10	MODERATE-HIGH
ATD-150	20	25	45	10	MODERATE-HIGH
ATD-151	30	20	45	5	MODERATE-HIGH
ATD-152	35	20	40	5	HIGH
ATD-153	35	20	40	5	HIGH
ATD-154	45	20	30	5	HIGH-VERY HIGH
ATD-155	30	20	45	5	MODERATE-HIGH
ATD-156	35	20	40	5	MODERATE-HIGH
ATD-157	35	30	30	5	HIGH-VERY HIGH
ATD-158	30	30	35	5	HIGH-VERY HIGH
ATD-159	45	20	30	5	HIGH-VERY HIGH
ATD-160	45	15	35	5	MODERATE-HIGH
ATD-161	40	20	35	5	MODERATE-HIGH

Table 4. The organic matter distribution through the Köpekli Formation in the Köpekli Section.

SAMPLE NO	AMORPHOUS (%)	HERBACEOUS (%)	WOODY (%)	COALY (%)	ABUNDANCE
TD-158	30	25	40	5	HIGH
TD-160	40	30	25	5	HIGH
TD-161	45	30	20	5	HIGH-VERY HIGH
TD-162	35	25	35	5	HIGH-VERY HIGH
TD-163	40	25	30	5	HIGH-VERY HIGH
TD-164	30	20	40	10	MODERATE-HIGH
TD-165	40	30	25	5	HIGH
TD-166	35	30	30	5	HIGH
TD-167	40	30	25	5	HIGH
TD-168	40	30	25	5	HIGH-VERY HIGH
TD-169	40	30	25	5	HIGH-VERY HIGH
TD-170	35	30	30	5	HIGH
TD-171	35	25	35	5	MODERATE-HIGH
TD-172	30	20	40	10	HIGH
TD-173	35	20	35	5	HIGH-VERY HIGH
TD-174	40	30	25	5	HIGH-VERY HIGH

Table 5. The organic matter distribution through the Köpekli Formation in the Sofular Section.

SAMPLE NO	AMORPHOUS (%)	HERBACEOUS (%)	WOODY (%)	COALY (%)	ABUNDANCE
ATD-119	45	25	25	5	VERY HIGH
ATD-120	35	20	40	5	HIGH
ATD-121	20	15	55	10	MODERATE-HIGH
ATD-122	20	15	50	15	HIGH-VERY HIGH
ATD-123	25	15	50	10	VERY HIGH
ATD-124	25	20	50	5	MODERATE-HIGH
ATD-125	25	15	55	5	MODERATE-HIGH
ATD-126	40	20	35	5	MODERATE-HIGH
ATD-127	40	15	40	5	MODERATE-HIGH
ATD-128	20	10	60	10	MODERATE-HIGH
ATD-129	25	15	55	5	MODERATE-HIGH
ATD-130	25	20	50	5	MODERATE-HIGH
ATD-131	30	20	45	5	MODERATE-HIGH
ATD-132	35	25	35	5	HIGH

Table 6. The organic matter distribution through the Köpekli Formation in the Çorlu Section.

SAMPLE NO	AMORPHOUS (%)	HERBACEOUS (%)	WOODY (%)	COALY (%)	ABUNDANCE
TD-175	30	25	40	5	HIGH
TD-176	30	25	40	5	HIGH
TD-177	20	20	55	5	HIGH
TD-178	20	25	50	5	MEDIUM-HIGH
TD-179	25	20	50	5	MEDIUM-HIGH
TD-180	20	15	60	5	MEDIUM
TD-181	30	25	40	5	MEDIUM-HIGH
TD-183	35	20	40	5	VERY HIGH
TD-184	30	20	45	5	MEDIUM-HIGH
TD-185	40	25	30	5	HIGH-VERY HIGH
TD-186	30	20	45	5	MEDIUM-HIGH
TD-187	35	20	40	5	MEDIUM-HIGH
TD-188	30	20	45	5	HIGH
TD-189	25	20	50	5	MEDIUM
TD-190	15	15	65	5	LOW-MEDIUM
TD-191	10	15	70	5	LOW-MEDIUM
TD-192	15	15	65	5	LOW-MEDIUM
TD-193	25	20	50	5	MEDIUM
TD-194	15	10	70	5	LOW
TD-195	20	15	60	5	LOW-MEDIUM
TD-196	20	15	60	5	MEDIUM
TD-198	20	20	55	5	MEDIUM
TD-199	20	20	55	5	LOW-MEDIUM
TD-200	5	20	70	5	MEDIUM
TD-201	5	25	65	5	MEDIUM-HIGH
TD-203	10	25	60	5	MEDIUM-HIGH
TD-204	5	20	70	5	MEDIUM
TD-205	5	20	70	5	MEDIUM
TD-206	10	25	60	5	HIGH
TD-208	5	10	80	5	MEDIUM
TD-209	5	10	80	5	LOW-MEDIUM
TD-210	10	20	65	5	MEDIUM-HIGH

Table 6. (cont'd)

SAMPLE NO	AMORPHOUS (%)	HERBACEOUS (%)	WOODY (%)	COALY (%)	ABUNDANCE
TD-211	10	20	65	5	MEDIUM-HIGH
TD-213	15	15	65	5	LOW-MEDIUM
TD-214	5	15	75	5	LOW-MEDIUM
TD-215	10	15	65	10	HIGH
TD-216	5	10	80	5	LOW-MEDIUM
TD-218	10	10	75	5	MEDIUM
TD-219	10	15	70	5	LOW-MEDIUM
TD-220	10	10	75	5	VERY LOW
TD-221	5	10	80	5	LOW-MEDIUM
TD-222	5	10	80	5	LOW
TD-223	5	10	80	5	LOW
TD-224	5	15	70	10	LOW-MEDIUM
TD-226	5	15	70	10	LOW-MEDIUM
TD-227	10	10	75	5	LOW
TD-229	10	15	70	5	MEDIUM-HIGH
TD-231	10	10	75	5	MEDIUM
TD-232	5	10	80	5	LOW
TD-233	10	15	70	5	MEDIUM
TD-235	10	20	65	5	MEDIUM-HIGH
TD-236	10	20	65	5	MEDIUM
TD-237	15	20	60	5	HIGH
TD-238	15	15	65	5	LOW-MEDIUM
TD-240	10	10	75	5	LOW-MEDIUM
TD-241	15	25	55	5	MEDIUM-HIGH
TD-243	15	25	55	5	HIGH
TD-244	10	20	65	5	MEDIUM-HIGH

Table 7. The organic matter distribution through the Cingöz Formation in the Çorlu Section.

SAMPLE NO	AMORPHOUS (%)	HERBACEOUS (%)	WOODY (%)	COALY (%)	ABUNDANCE
TD-246	15	25	55	5	HIGH
TD-249	5	10	80	5	LOW
TD-250	10	10	75	5	LOW
TD-251	10	10	75	5	LOW-MEDIUM
TD-252	10	10	75	5	LOW
TD-253	10	10	75	5	LOW
TD-256	5	10	75	10	LOW-MEDIUM
TD-257	5	10	75	10	LOW-MEDIUM
TD-258	5	5	75	15	LOW
TD-260	10	10	75	5	LOW-MEDIUM
TD-262	15	10	65	10	LOW-MEDIUM
TD-264	10	5	75	10	LOW-MEDIUM
TD-266	10	15	70	5	LOW-MEDIUM
TD-267	10	15	70	5	LOW
TD-269	10	15	70	5	MEDIUM
TD-270	5	10	80	5	LOW
TD-272	10	15	70	5	LOW-MEDIUM
TD-274	10	10	75	5	VERY LOW
TD-275	10	15	70	5	LOW-MEDIUM
TD-276	10	10	75	5	LOW
TD-278	10	10	75	5	LOW-MEDIUM
TD-279	5	10	75	10	LOW-MEDIUM
TD-280	5	10	75	10	LOW-MEDIUM
TD-282	5	15	70	10	MEDIUM
TD-284	5	15	75	5	LOW-MEDIUM
TD-285	5	10	80	5	LOW-MEDIUM
TD-287	5	5	85	5	VERY LOW-LOW
TD-290	5	5	85	5	VERY LOW-LOW
TD-291	5	10	80	5	LOW-MEDIUM
TD-294	10	10	75	5	LOW

Table 7. (cont'd)

SAMPLE NO	AMORPHOUS (%)	HERBACEOUS (%)	WOODY (%)	COALY (%)	ABUNDANCE
TD-295	10	15	70	5	LOW-MEDIUM
TD-298	10	20	65	5	MEDIUM-HIGH
TD-300	5	10	80	5	VERY LOW-LOW
TD-304	5	10	80	5	VERY LOW-LOW
TD-305	5	10	80	5	LOW
TD-306	5	5	85	5	VERY LOW
TD-308	5	5	85	5	VERY LOW-LOW
TD-309	5	5	85	5	VERY LOW-LOW
TD-310	10	15	70	5	LOW-MEDIUM
TD-313	10	15	70	5	LOW-MEDIUM
TD-314	10	10	75	5	LOW-MEDIUM
TD-316	15	10	70	5	LOW-MEDIUM
TD-318	10	15	70	5	MEDIUM
TD-320	10	10	75	5	LOW
TD-321	10	15	70	5	LOW-MEDIUM
TD-323	15	10	70	5	LOW-MEDIUM
TD-324	15	10	70	5	LOW
TD-325	15	10	70	5	LOW-MEDIUM
TD-327	20	15	60	5	MEDIUM
TD-329	10	10	75	5	VERY LOW
TD-330	10	15	70	5	LOW-MEDIUM
TD-333	5	10	80	5	LOW-MEDIUM
TD-334	5	5	85	5	VERY LOW
TD-335	5	5	85	5	VERY LOW
TD-336	10	10	75	5	VERY LOW-LOW
TD-338	10	5	80	5	LOW-MEDIUM
TD-340	10	5	80	5	LOW-MEDIUM
TD-341	10	10	75	5	LOW-MEDIUM
TD-343	10	10	75	5	LOW-MEDIUM
TD-344	15	15	65	5	MEDIUM

Table 7. (cont'd)

SAMPLE NO	AMORPHOUS (%)	HERBACEOUS (%)	WOODY (%)	COALY (%)	ABUNDANCE
TD-346	10	10	75	5	LOW-MEDIUM
TD-347	10	15	70	5	LOW-MEDIUM
TD-349	20	15	60	5	MEDIUM
TD-350	15	10	70	5	MEDIUM
TD-352	25	15	55	5	MEDIUM-HIGH
TD-354	15	10	70	5	LOW
TD-355	25	15	55	5	MEDIUM
TD-356	10	10	75	5	LOW
TD-358	10	10	75	5	LOW-MEDIUM
TD-359	25	15	55	5	MEDIUM-HIGH
TD-360	30	15	50	5	MEDIUM-HIGH
TD-362	25	15	55	5	MEDIUM
TD-363	20	20	55	5	MEDIUM-HIGH
TD-364	20	25	50	5	MEDIUM-HIGH
TD-366	15	15	65	5	MEDIUM
TD-367	15	10	70	5	LOW-MEDIUM
TD-368	10	10	75	5	LOW
TD-370	20	25	50	5	MEDIUM-HIGH
TD-372	15	15	65	5	LOW-MEDIUM
TD-373	15	10	70	5	MEDIUM
TD-374	10	10	75	5	LOW-MEDIUM
TD-375	15	10	70	5	LOW-MEDIUM
TD-377	15	15	65	5	MEDIUM-HIGH
TD-378	20	15	60	5	MEDIUM-HIGH
TD-380	10	5	80	5	VERY LOW
TD-381	10	5	80	5	LOW
TD-383	25	20	50	5	MEDIUM
TD-384	20	20	55	5	LOW-MEDIUM
TD-385	25	20	50	5	MEDIUM
TD-387	20	15	60	5	LOW-MEDIUM

Table 7. (cont'd)

SAMPLE NO	AMORPHOUS (%)	HERBACEOUS (%)	WOODY (%)	COALY (%)	ABUNDANCE
TD-388	15	10	70	5	LOW-MEDIUM
TD-389	10	10	75	5	LOW
TD-391	15	10	70	5	LOW-MEDIUM
TD-393	30	25	40	5	MEDIUM-HIGH
TD-395	30	30	35	5	HIGH
TD-396	15	10	70	5	LOW
TD-397	20	10	65	5	LOW-MEDIUM
TD-400	20	15	60	5	LOW-MEDIUM
TD-401	25	15	55	5	MEDIUM
TD-402	20	20	55	5	MEDIUM
TD-403	35	20	40	5	HIGH
TD-405	25	20	50	5	MEDIUM
TD-406	25	20	50	5	MEDIUM
TD-407	20	15	60	5	MEDIUM-HIGH
TD-408	20	20	55	5	MEDIUM
TD-409	20	15	60	5	MEDIUM-HIGH
TD-410	15	10	70	5	LOW
TD-411	15	20	60	5	HIGH
TD-412	25	20	50	5	HIGH

Table 8. The organic matter distribution through the Güvenç Formation in the Çorlu Section.

SAMPLE NO	AMORPHOUS (%)	HERBACEOUS (%)	WOODY (%)	COALY (%)	ABUNDANCE
TD-414	10	5	80	5	LOW-VERY LOW
TD-415	15	10	70	5	MEDIUM
TD-416	15	10	70	5	MEDIUM
TD-417	15	10	70	5	MEDIUM
TD-418	20	25	50	5	MEDIUM-HIGH
TD-420	15	15	65	5	LOW-MEDIUM
TD-421	15	10	70	5	LOW
TD-422	20	10	65	5	MEDIUM
TD-423	15	10	70	5	LOW
TD-424	20	10	65	5	MEDIUM
TD-426	15	10	70	5	MEDIUM
TD-427	15	10	70	5	LOW-MEDIUM
TD-428	25	20	50	5	MEDIUM-HIGH
TD-429	20	20	55	5	HIGH
TD-431	20	15	60	5	MEDIUM
TD-432	30	10	55	5	MEDIUM
TD-433	35	20	40	5	HIGH
TD-435	35	25	35	5	HIGH
TD-436	25	20	50	5	MEDIUM
TD-437	20	20	55	5	MEDIUM-HIGH
TD-438	10	10	75	5	LOW
TD-439	10	5	80	5	VERY LOW
TD-441	10	10	75	5	LOW-MEDIUM
TD-442	10	10	75	5	LOW-MEDIUM
TD-443	15	10	70	5	MEDIUM-HIGH
TD-444	20	10	65	5	MEDIUM
TD-446	20	10	65	5	LOW-MEDIUM
TD-447	20	10	65	5	LOW-MEDIUM
TD-448	20	15	60	5	LOW-MEDIUM
TD-450	15	10	70	5	LOW
TD-451	20	10	65	5	MEDIUM
TD-452	20	25	50	5	HIGH

Table 8. (cont'd)

SAMPLE NO	AMORPHOUS (%)	HERBACEOUS (%)	WOODY (%)	COALY (%)	ABUNDANCE
TD-453	25	15	55	5	LOW-MEDIUM
TD-454	25	20	50	5	MEDIUM
TD-455	20	25	50	5	MEDIUM-HIGH
TD-456	20	15	60	5	MEDIUM
TD-457	25	30	40	5	MEDIUM
TD-459	40	25	30	5	MEDIUM-HIGH
TD-460	25	20	50	5	MEDIUM
TD-461	30	25	40	5	HIGH
TD-462	25	25	45	5	HIGH
TD-463	25	20	50	5	HIGH
TD-465	35	25	35	5	HIGH-VERY HIGH
TD-466	40	25	30	5	HIGH-VERY HIGH
TD-467	35	25	35	5	HIGH-VERY HIGH
TD-468	25	20	50	5	HIGH
TD-469	20	15	60	5	MEDIUM-HIGH
TD-471	20	15	60	5	HIGH
TD-472	15	10	70	5	LOW-MEDIUM
TD-473	25	30	40	5	HIGH-VERY HIGH
TD-475	30	25	40	5	HIGH
TD-476	25	20	50	5	MEDIUM-HIGH
TD-477	15	10	70	5	LOW-MEDIUM
TD-479	35	30	30	5	HIGH-VERY HIGH
TD-480	30	25	40	5	MEDIUM-HIGH

Table 9. The organic matter distribution through the Güvenç Formation in the Koruklu Section.

SAMPLE NO	AMORPHOUS (%)	HERBACEOUS (%)	WOODY (%)	COALY (%)	ABUNDANCE
ATD-59	15	10	70	5	LOW-MODERATE
ATD-60	15	15	65	5	MODERATE
ATD-62	10	15	65	10	MODERATE
ATD-63	10	15	65	10	MODERATE
ATD-64	25	20	50	5	MODERATE-HIGH
ATD-65	25	20	50	5	MODERATE-HIGH
ATD-66	20	20	55	5	MODERATE
ATD-67	35	15	45	5	MODERATE
ATD-69	25	20	50	5	MODERATE
ATD-70	20	20	55	5	MODERATE
ATD-71	20	15	60	5	LOW-MODERATE
ATD-73	25	20	50	5	MODERATE
ATD-74	25	20	50	5	MODERATE
ATD-75	20	20	50	10	MODERATE-HIGH
ATD-77	25	15	55	5	LOW-MODERATE
ATD-78	25	20	50	5	MODERATE
ATD-79	35	15	45	5	MODERATE
ATD-80	25	20	50	5	MODERATE
ATD-81	25	20	50	5	MODERATE

Table 10. The organic matter distribution through the Güvenç Formation in the Bekirli Section.

SAMPLE NO	AMORPHOUS (%)	HERBACEOUS (%)	WOODY (%)	COALY (%)	ABUNDANCE
ATD-1	15	20	55	10	HIGH
ATD-2	15	15	65	5	MODERATE-HIGH
ATD-3	15	20	60	5	MODERATE-HIGH
ATD-4	20	15	60	5	MODERATE-HIGH
ATD-5	20	30	45	5	MODERATE-HIGH
ATD-6	15	25	55	5	MODERATE
ATD-7	15	25	55	5	MODERATE-HIGH
ATD-9	20	25	50	5	MODERATE-HIGH
ATD-10	25	25	45	5	MODERATE-HIGH
ATD-11	25	20	50	5	MODERATE-HIGH
ATD-12	20	30	45	5	MODERATE
ATD-13	15	25	55	5	MODERATE
ATD-14	20	25	45	10	HIGH
ATD-15	20	20	55	5	MODERATE
ATD-16	20	25	45	10	HIGH
ATD-17	15	20	60	5	MODERATE-HIGH
ATD-18	20	20	55	5	MODERATE-HIGH
ATD-19	15	20	60	5	MODERATE
ATD-20	20	20	55	5	MODERATE-HIGH
ATD-21	25	15	50	10	HIGH
ATD-22	20	25	50	5	MODERATE-HIGH
ATD-23	15	15	65	5	MODERATE-HIGH
ATD-24	15	20	60	5	MODERATE
ATD-25	15	20	60	5	MODERATE-HIGH

Table 10. (cont'd)

SAMPLE NO	AMORPHOUS (%)	HERBACEOUS (%)	WOODY (%)	COALY (%)	ABUNDANCE
ATD-26	20	15	60	5	MODERATE-HIGH
ATD-27	20	25	50	5	MODERATE-HIGH
ATD-28	25	25	45	5	MODERATE-HIGH
ATD-29	20	20	55	5	MODERATE
ATD-30	25	25	45	5	LOW-VERY LOW
ATD-31	20	30	45	5	LOW-MODERATE
ATD-32	25	20	50	5	LOW-MODERATE
ATD-33	25	15	55	5	LOW
ATD-34	25	15	55	5	LOW
ATD-35	20	25	50	5	MODERATE
ATD-36	25	20	50	5	MODERATE
ATD-37	30	20	45	5	MODERATE
ATD-38	20	25	50	5	LOW-MODERATE
ATD-39	15	20	60	5	MODERATE
ATD-40	20	20	55	5	LOW-MODERATE
ATD-41	20	25	50	5	LOW-MODERATE
ATD-42	25	30	40	5	MODERATE
ATD-44	20	25	50	5	MODERATE
ATD-45	25	25	45	5	MODERATE
ATD-46	30	25	40	5	MODERATE-HIGH
ATD-47	30	20	45	5	HIGH
ATD-49	20	25	50	5	MODERATE
ATD-50	20	20	55	5	MODERATE
ATD-52	20	35	40	5	MODERATE

Table 10. (cont'd)

SAMPLE NO	AMORPHOUS (%)	HERBACEOUS (%)	WOODY (%)	COALY (%)	ABUNDANCE
ATD-53	30	25	40	5	MODERATE-HIGH
ATD-54	25	35	35	5	HIGH
ATD-55	45	20	30	5	HIGH
ATD-56	35	20	40	5	LOW-MODERATE
ATD-57	20	15	60	5	LOW
ATD-58	20	15	60	5	LOW

Table 11. The organic matter distribution through the Güvenç Formation within the Güvenç Section.

SAMPLE NO	AMORPHOUS (%)	HERBACEOUS (%)	WOODY (%)	COALY (%)	ABUNDANCE
ATD-83	15	15	60	10	LOW-MODERATE
ATD-84	20	15	60	5	LOW-MODERATE
ATD-85	20	15	55	10	HIGH
ATD-86	15	15	65	5	LOW
ATD-87	25	20	50	5	MODERATE
ATD-88	20	15	60	5	LOW-MODERATE
ATD-89	25	15	55	5	MODERATE
ATD-90	25	20	45	10	HIGH
ATD-91	20	15	55	10	MODERATE
ATD-92	20	15	60	5	MODERATE-HIGH
ATD-93	25	20	50	5	MODERATE-HIGH
ATD-94	15	15	60	10	LOW-MODERATE
ATD-95	20	15	60	5	MODERATE
ATD-96	20	20	55	5	MODERATE
ATD-97	30	15	50	5	LOW-MODERATE
ATD-99	40	20	35	5	HIGH
ATD-100	30	25	40	5	MODERATE-HIGH
ATD-101	25	20	50	5	MODERATE
ATD-102	30	20	45	5	MODERATE
ATD-103	20	20	50	10	HIGH
ATD-104	25	15	55	5	MODERATE-HIGH
ATD-105	20	15	60	5	MODERATE-HIGH
ATD-106	30	15	50	5	MODERATE
ATD-107	30	20	45	5	MODERATE

Table 11. (cont'd)

SAMPLE NO	AMORPHOUS (%)	HERBACEOUS (%)	WOODY (%)	COALY (%)	ABUNDANCE
ATD-108	20	15	60	5	LOW-MODERATE
ATD-109	65	20	10	5	HIGH-MODERATE
ATD-110	50	20	25	5	MODERATE
ATD-111	20	15	60	5	LOW-MODERATE
ATD-112	15	20	60	5	LOW-MODERATE
ATD-113	15	20	60	5	LOW
ATD-114	10	15	65	10	LOW
ATD-116	10	10	75	5	VERY LOW
ATD-117	10	10	75	5	VERY LOW
ATD-118	10	10	75	5	VERY LOW

CURRICULUM VITAE

PERSONAL INFORMATION

Surname, Name: Türkecan, Aksel Tuğba
Nationality: Turkish (TC)
Date and Place of Birth: 17 October1982, Rize
Marital Status: Maried
Phone: +90 312 207 24 62
Fax: +90 312 286 90 00
email: atdinc@tp.gov.tr

EDUCATION

Degree	Institution	Year of Graduation
MS	METU Geological Engineering	2006
BS	METU Geological Engineering	2009
High School	Trabzon Yomra Science High School,	2000

WORK EXPERIENCE

Year	Place	Enrollment
2010-	Turkish Petroleum (TP)	Geological Engineer
2009-2010	Teck Resources Limited	Geological Engineer
2006-2008	Fronteer Development Group	Geological Engineer

FOREIGN LANGUAGES

Advanced English

HOBBIES

Bridge, Painting, Swimming, Movies